

NASA Contractor Report 3267

Application of Advanced Computational Procedures for Modeling Solar-Wind Interactions With Venus - Theory and Computer Code

Stephen S. Stahara, Daniel Klenke,
Barbara C. Trudinger, and John R. Spreiter

CONTRACT NASW-3182
MAY 1980

FOR REFERENCE

NOT TO BE TAKEN FROM THIS ROOM

LIBRARY COPY

MAY 20 1980

LANGLEY RESEARCH CENTER
LIBRARY, NASA
HAMPTON, VIRGINIA



NF02112

NASA

NASA Contractor Report 3267

Application of Advanced Computational
Procedures for Modeling Solar-Wind
Interactions With Venus -
Theory and Computer Code

Stephen S. Stahara, Daniel Klenke,
Barbara C. Trudinger, and John R. Spreiter
Nielsen Engineering & Research, Inc.
Mountain View, California

Prepared for
NASA Headquarters
under Contract NASW-3182



National Aeronautics
and Space Administration

**Scientific and Technical
Information Office**

1980

TABLE OF CONTENTS

<u>Section</u>	<u>Page No.</u>
LIST OF ILLUSTRATIONS	iv
SUMMARY	1
INTRODUCTION	2
LIST OF SYMBOLS	4
ANALYSIS	8
The Mathematical Model - Formulation of the Fluid Representation	8
<u>Governing equations</u>	8
<u>Conditions at discontinuities</u>	10
<u>Frozen-field approximation</u>	12
Determination of the Ionosphere Boundary	14
Calculation of the Gasdynamic Flow Properties	20
<u>Nose region solution - implicit unsteady Euler equation method</u>	21
<u>Downstream region solution - shock capturing marching method</u>	25
<u>Calculation of the streamlines</u>	27
Calculation of the Magnetic Field	27
Calculation of the Contour Lines	30
Solar-Ecliptic/Solar-Wind Coordinate Transformations	31
Properties Along a Spacecraft Trajectory	33
RESULTS	36
CONCLUDING REMARKS	47
ACKNOWLEDGEMENTS	48
APPENDIX A - COMPUTER PROGRAM USER'S MANUAL	49
APPENDIX B - LISTING OF COMPUTER PROGRAM	131
APPENDIX C - CATALOG OF TEST CASES	177
REFERENCES	287
TABLE 1	289
FIGURES 1 THROUGH 20	291

LIST OF ILLUSTRATIONS

<u>Figure</u>	<u>Page No.</u>
1. Illustration of ionopause shapes for atmospheres with various (i) constant scale heights H/R_0 and (ii) gravitational variation included in the scale height \bar{H}/R_0 .	291
2. Comparison of former and present computational procedures for determining the gasdynamic flow properties of solar wind-magneto/ionopause interactions	292
3. Transformation from physical domain to rectangular computational domain	293
4. Illustration of capability for providing an additional flow-field segment to the obstacle nose solution in the computational procedure for determining the gasdynamic flow properties of solar wind-ionopause interactions	294
5. Illustration of quantities used for streamline calculation	295
6. Illustration of quantities used for magnetic field-line calculation in the plane of magnetic symmetry	295
7. Illustration of the components of the three-dimensional magnetic field	296
8. Illustration of the sun-planet (x_s, y_s, z_s) and solar wind (x, y, z) coordinate systems and the azimuthal (Ω) and polar (ϕ_p) solar-wind angles, both shown in a positive sense	297
9. Illustration of solar-wind (x, y, z) and (X, Y, Z) coordinate systems and the interplanetary magnetic field and magnetic-field angles (α_p, α_n)	298
10. Bow shock locations for $M_\infty = 8.0$, $\gamma = 5/3$ flow past constant scale-height ionopause shapes with $H/R_0 = 0.5$ and 1.0	299
11. Bow shock shapes for flow past an ionopause shape with gravitational variation included in scale height with $H/R_0 = 0.25$, $\gamma = 5/3$ and $M_\infty = 2.0$ and 3.0	300
12. Overall features of Pioneer-Venus Orbiter trajectory crossings of solar-wind/Venus-ionosphere interaction region	301
13. Illustration of typical flow-field grid density for gasdynamic solution; $M_\infty = 3.0$, $\gamma = 5/3$	302
14. P-V Orbit 6 trajectories and observational bow shock crossings as viewed in solar-wind coordinates based on inbound and outbound interplanetary solar-wind directions; also, various bow shock shapes for different interplanetary solar-wind conditions	303

LIST OF ILLUSTRATIONS (Concluded)

<u>Figure</u>	<u>Page No.</u>
15. Comparison of observed (OPA) and theoretical time histories of ionosheath plasma properties for P-V Orbit 6 based on inbound and outbound interplanetary solar-wind conditions using a gasdynamic solution for $M_{\infty} = 13.3$, $\gamma = 2.0$	304
16. Comparison of observed (OMAG) and theoretical time histories for the magnitude of the magnetic field for P-V Orbit 6 based on inbound and outbound interplanetary conditions using gasdynamic solution for $M_{\infty} = 13.3$, $\gamma = 2$	305
17. P-V Orbit 3 trajectories and observational bow shock crossings as viewed in solar-wind coordinates based on inbound and outbound interplanetary solar-wind directions; also, various bow shock shapes for different interplanetary solar wind conditions	307
18. Comparison of observed and theoretical time histories of ionosheath plasma properties for P-V Orbit 3 based on inbound and outbound interplanetary solar-wind conditions	308
19. Comparison of observed (OMAG) and theoretical time histories for the magnetic field for P-V Orbit 3 based on inbound and outbound interplanetary solar-wind conditions using gasdynamic solutions $M_{\infty} = 7.38$, $\gamma = 2.0$ for inbound and $M_{\infty} = 5.96$, $\gamma = 2.0$ for outbound calculations	309
20. Comparison of observed (OMAG) and theoretical time histories of the magnetic field for P-V Orbit 3 based on inbound solar wind interplanetary conditions using a gasdynamic solution for $M_{\infty} = 3.0$, $\gamma = 5/3$	311

APPLICATION OF ADVANCED COMPUTATIONAL PROCEDURES FOR
MODELING SOLAR-WIND INTERACTIONS WITH VENUS - THEORY
AND COMPUTER CODE

by

Stephen S. Stahara, Daniel Klenke,
Barbara C. Trudinger, and John R. Spreiter

SUMMARY

Advanced computational procedures are developed and applied to the prediction of solar-wind interaction with nonmagnetic terrestrial-planet atmospheres, with particular emphasis to Venus. The theoretical method is based on a single-fluid, steady, dissipationless, magnetohydrodynamic continuum model, and is appropriate for the calculation of axisymmetric, supersonic, super-Alfvénic solar-wind flow past terrestrial planets. The procedures, which consist of finite-difference codes to determine the gasdynamic properties and a variety of special-purpose codes to determine the frozen magnetic field, streamlines, contours, plots, etc. of the flow, are organized into one computational program which has been extensively documented and is presented in a general user's manual included as part of this report.

Theoretical results based upon these procedures are reported for a wide variety of solar-wind conditions and ionopause obstacle shapes. Plasma and magnetic-field comparisons in the ionosheath are also provided with actual spacecraft data obtained by the Pioneer-Venus Orbiter. These results have verified the appropriateness of the basic theoretical model, and have indicated the importance of accounting for the variable oncoming direction of the interplanetary solar wind.

INTRODUCTION

The magnetohydrodynamic models (refs. 1-9) of solar-wind interaction with planetary magneto/ionospheres and their associated calculations of the detailed flow and magnetic-field properties provide the basis of the theoretical understanding and interpretation of phenomena occurring in space around terrestrial planets from the viewpoint of a fluid rather than particle description of the flow. The general value and usefulness of results based on these models are now well established, and have advanced to the point where theoretical calculations can be used to predict important planetary and magnetic-field characteristics.

Prior to the previous work reported in reference 9, the utility of calculations based on these models was severely restricted due both to the fact that the original solution techniques employed bordered on what was barely possible at the time, as well as that considerable hand computation and intervention was required. Moreover, reported results were carried out for only a limited set of solar-wind conditions such as obstacle shape, oncoming Mach number, interplanetary magnetic field, etc., and were presented in archival publications only in the form of plots from which results for other conditions had to be determined by interpolation. The importance of the preliminary work of reference 9 was that advanced computational methods, based on current state-of-the-art algorithms, were introduced to this problem to provide the basic gas-dynamic solutions. The frozen-in magnetic-field was then solved for on the high-resolution flow-field grid, and the entire computational procedure was assembled into a user-oriented program providing the detailed flow-field and magnetic-field properties in a convenient output format.

In the current work reported here, those basic procedures have been extended and generalized in several important directions. These include the capability for treating very low oncoming interplanetary gasdynamic Mach numbers ($M_\infty \approx 2.0$), as well as quite general ionopause shapes. A new family of ionopause shapes has been developed which accounts for the effect of gravitational variation in scale height. Additionally, the capability for determining the plasma gasdynamic and magnetic-field properties along an arbitrary spacecraft trajectory, simultaneously accounting

for an arbitrary oncoming direction of the solar wind, has been developed. Moreover, a large number of sample calculations have been performed for typical solar-wind conditions and, using the output contour-plot capability, a catalog of these cases were established and are archived here for convenient quick-look use. Finally, a number of successful comparisons were made by the present computational model with actual spacecraft observations obtained from initial orbits of the Pioneer-Venus Orbiter. These comparisons have both provided a verification of the basic theoretical model as well as demonstrated its value as a convenient research tool capable of routinely providing details of the solar-wind/planetary atmosphere interaction process not previously attainable--at modest computational cost and in a format directly compatible with observational data.

LIST OF SYMBOLS

a	speed of sound, $(\gamma p/\rho)^{1/2}$
A	Alfvén speed, $(B^2/4\pi\rho)^{1/2}$
\bar{A}	Jacobian matrix associated with IMP code, equal to $\partial\hat{E}/\partial\hat{U}$
\underline{B}	magnetic field vector
\bar{B}	Jacobian matrix associated with IMP code, equal to $\partial\hat{F}/\partial\hat{U}$
C_p	specific heat at constant pressure
C_v	specific heat at constant volume
D	distance defined by eq. (59)
e	internal energy, eq. (3)
e_t	total energy, eq. (44)
E	column matrix defined by eq. (42)
\hat{E}	column matrix associated with IMP code, equal to $(\xi_T U + \xi_X E + \xi_R F)/J$
F	column matrix defined by eq. (42)
\hat{F}	column matrix associated with IMP code, equal to $(\eta_T U + \eta_X E + \eta_R F)/J$
g	acceleration due to gravity
g_k	gravitational component, eq. (5)
G	column matrix defined by eq. (42)
h	enthalpy, eq. (47)
h_t	total enthalpy, eq. (47)
H	local scale height of atmosphere, $\bar{RT}/\bar{M}g$
\bar{H}	local scale height with gravitational variation, $H(R_R/R_S)^2$
J	Jacobian matrix, eq. (43)
K	constant defined by eq. (34)
$\Delta\ell$	vector length of elemental magnetic flux tube
M	local Mach number, $ \underline{v} /a$
\bar{M}	nondimensional mean molecular mass, equal to 1/2 for ionized atomic hydrogen

LIST OF SYMBOLS (Continued)

M_A	local Alfven Mach number, $ v /A$
P	pressure
q	shock velocity
Q	dummy parameter
r	spherical radial distance
R	cylindrical radial distance
\bar{R}	gas constant, $8.315 \times 10^7 \text{ ergs/gm}^\circ\text{K}$
R_i	spherical radius of ionopause, eq. (39)
R_O	spherical distance from center of planet to ionopause nose
S_k	Poynting vector component
ΔS	incremental distance along streamline
t, T	time
(u, v, w)	velocity components associated with the (X, Y, Z) coordinate directions, respectively
U	column matrix defined by eq. (42)
\hat{U}	column matrix associated with IMP code, equal to U/J
\underline{v}	velocity vector
(x, y, z) or (x_w, y_w, z_w)	solar-wind oriented Cartesian coordinates with origin at planetary center, x positive upstream and z positive northward
(x_s, y_s, z_s)	sun-planet oriented Cartesian coordinates with origin at planetary center, x_s positive toward sun, y_s positive opposite to planetary orbital motion, and z_s positive northward
(x', y', z')	solar-wind oriented Cartesian coordinates defined by an azimuthal rotation given by eq. (70)
(X, Y, Z)	solar-wind oriented Cartesian coordinates with origin at planetary center, X positive downstream and Z positive northward
α_p	interplanetary magnetic-field angle between perpendicular and parallel components, eq. (62)
α_n	interplanetary magnetic-field angle between normal and in-plane components, eq. (63)

LIST OF SYMBOLS (Continued)

β	spherical polar angle, measured with origin at planet center, from subsolar point away from undisturbed solar wind direction; varies from 0 in upstream direction to π in downstream direction; eq. (39)
γ	ratio of plasma specific heats
δ	angle defined by eq. (59)
δ_{ik}	Kronecker delta
δ_S	local angle of bow shock wave
$(\delta_\xi, \delta_\eta)$	second-order difference operators in (,) direction
ϵ	smoothing coefficient in IMP code
η	transformation variable, eqs. (40), (48)
θ	azimuthal rotation angle in solar-wind (X,Y,Z) system, eq. (69); also shock tangency angle, eq. (59)
Λ	quantity defined by eq. (36)
ξ	transformation variable, eqs. (40), (48)
ρ	density
σ	conductivity
τ	transformed time, eq. (40)
Φ	gravitational potential, eq. (5)
ϕ_p	solar-wind polar angle
ψ	angle between outward normal to magneto/ionosphere boundary and oncoming undisturbed solar wind, eq. (32); also, angle of magnetic component $(\underline{B}/B_\infty)_\perp$, eq. (58)

Subscripts

b	obstacle body
i	ionopause
n	normal direction
P	arbitrary point
R	reference quantity
s	planetary surface; also streamline
S	shock surface

LIST OF SYMBOLS (Concluded)

s_t	stagnation conditions
t	tangential direction
o	reference quantity at subsolar point
1	conditions upstream of a discontinuity
2	conditions downstream of a discontinuity
∞	interplanetary undisturbed quantity
(\parallel, \perp, n)	parallel, perpendicular, and normal magnetic-field components as defined in eq. (56)

Superscripts

\wedge	unit vector
$*$	relative to shock

ANALYSIS

The Mathematical Model - Formulation of the Fluid Representation

The fundamental assumption underlying the present work and that reported in all of the references cited above is that the average bulk properties of solar-wind flow around a planetary magneto/ionosphere can be adequately described by the continuum equations of magnetohydrodynamics for a single-component perfect gas having infinite electrical conductivity and zero viscosity and thermal conductivity. Theoretical justification of this point has not yet been established, and proof remains essentially qualitative at present. The primary justification for use of the continuum fluid model is the outstanding agreement of the qualitative results predicted on this basis with those actually measured in space. It appears that the continuum model is capable of accounting both for many of the details as well as the broad features of the observations.

Governing equations.- The equations which express the conservation of the average bulk mass, momentum, energy, and magnetic field of the solar-wind plasma are given by the following expressions:

$$\frac{\partial \rho}{\partial t} + \frac{\partial}{\partial x_k} (\rho v_k) = 0 \quad (1)$$

$$\frac{\partial}{\partial t} (\rho v_i) + \frac{\partial}{\partial x_k} \left(\rho v_i v_k + p \delta_{ik} - \frac{B_i B_k}{4\pi} + \frac{B^2}{8\pi} \delta_{ik} + \frac{g_i g_k}{4\pi G} - \frac{g^2}{8\pi G} \delta_{ik} \right) = 0 \quad (2)$$

$$\frac{\partial}{\partial t} \left(\frac{\rho v^2}{2} + \rho e + \rho \phi + \frac{B^2}{8\pi} \right) + \frac{\partial}{\partial x_k} \left[\rho v_k \left(\frac{v^2}{2} + e + \frac{p}{\rho} + \phi \right) + S_k \right] = 0 \quad (3)$$

$$\frac{\partial B_i}{\partial t} = \frac{\partial}{\partial x_k} (v_i B_k - v_k B_i) , \quad \frac{\partial B_i}{\partial x_i} = 0 \quad (4)$$

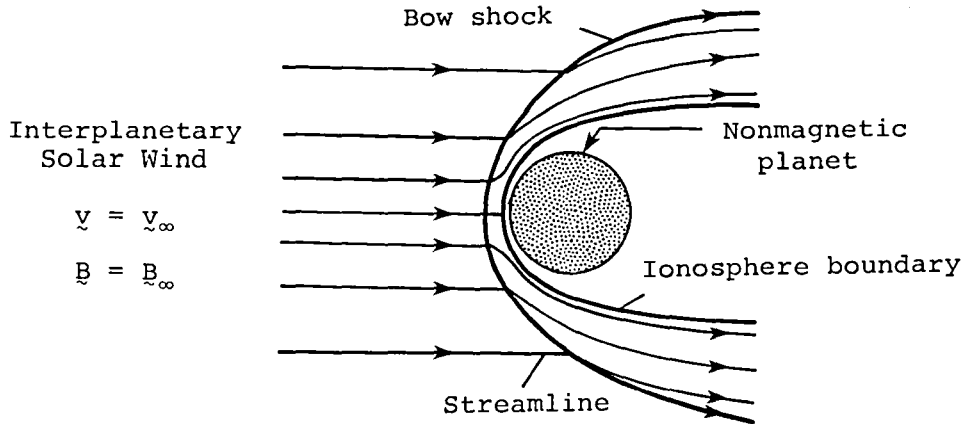
where

$$g_i = - \frac{\partial \Phi}{\partial x_i} , \quad S_k = \frac{1}{4\pi} \left(v_k B^2 - B_k v_i B_i \right) \quad (5)$$

and the equation of state of a perfect gas is given by

$$p = \frac{\rho \bar{R} T}{\bar{M}} \quad (6)$$

In these equations and those to follow, the symbols ρ , p , \underline{v} , T , $e = C_v T$, and $h = C_p T$ refer to the density, pressure, velocity, temperature, internal energy and enthalpy, and C_v and C_p refer to the specific heats at constant volume and pressure. We define the symbol $\bar{R} = (C_p - C_v) \bar{M} = 8.31 \times 10^7$ ergs/gm°K as the universal gas constant, and \bar{M} as the mean molecular weight nondimensionalized so that $\bar{M} = 16$ for atomic oxygen. For fully ionized hydrogen, \bar{M} is thus 1/2. The magnetic field \underline{B} and the Poynting vector \underline{S} for the flux of electromagnetic energy are expressed in terms of gaussian units. The gravitational potential Φ and acceleration \underline{g} are assumed to be due to massive fixed bodies so that their time derivatives are zero. These equations apply in the region exterior to the ionosphere boundary, as shown in the sketch below, and also in a degenerate sense in the ionosphere.



Conditions at discontinuities.— Because of the omission of dissipative terms in these equations, surfaces of discontinuity may develop in the solution, across which the fluid and magnetic properties change abruptly, but in such a way that mass, momentum, magnetic flux, and energy are conserved. These are approximations to comparatively thin surfaces across which similar but continuous changes in the fluid and magnetic properties occur in the corresponding theory of a dissipative gas, and correspond physically to the bow wave, ionosphere boundary, and possibly other thin regions of rapidly changing properties. Across these surfaces, continuous solutions of the dissipationless differential equations cease to exist. The flow is no longer governed solely by the differential equations (1) to (4), but must be supplemented by additional considerations. The conservation of mass, momentum, magnetic flux, and energy lead to the following conditions which relate quantities on the two sides of any such discontinuity:

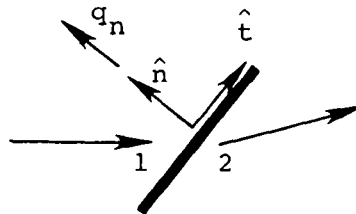
$$[\rho v_n^*] = 0 \quad (7)$$

$$[\rho \underline{v} \cdot \underline{v}_n^* + (p + B^2/8\pi)\hat{n} - B_n \underline{B}_t/4\pi] = 0 \quad (8)$$

$$[\underline{B}_t \cdot \underline{v}_n^* - B_n \cdot \underline{v}_t] = 0 \quad (9)$$

$$\left[v_n^* \left(\frac{1}{2} \rho v^2 + \rho e + p + \frac{B^2}{4\pi} \right) + q_n \cdot \left(p + \frac{B^2}{8\pi} \right) - \frac{B_n (\underline{v} \cdot \underline{B})}{4\pi} \right] = 0 \quad (10)$$

Here, (\hat{n}, \hat{t}) denote unit vectors normal and tangential to the discontinuity surface, as sketched below,



where q_n represents the local normal velocity of the discontinuity surface, and $v_n^* = v_n - q_n$ is the fluid normal velocity component relative to the normal velocity q_n of the discontinuity surface. The square brackets are used to indicate the difference between the enclosed quantities on the two sides of the discontinuity, as in $[Q] = Q_2 - Q_1$ where subscripts 1 and 2 refer to conditions on the upstream and downstream sides, respectively, of the discontinuity.

Five classes of discontinuities are described by Eqs. (7-10). Those with $v_n^* = 0$ are called tangential discontinuities or contact discontinuities according to whether or not B_n vanishes. Discontinuities across which there is flow ($v_n^* \neq 0$) are divided into three categories called rotational discontinuities, and fast and slow shock waves. Some properties which distinguish the various discontinuities are indicated by the following relationships:

Tangential:

$$v_n^* = B_n = 0, [\underline{v}_t] \neq 0, [\underline{B}_t] \neq 0, [\rho] \neq 0, [p + B^2/8\pi] = 0 \quad (11)$$

Contact:

$$v_n^* = 0, B_n \neq 0, [\underline{v}] = [\underline{B}] = [p] = 0, [\rho] \neq 0 \quad (12)$$

Rotational:

$$v_n^* = \pm B_n / \sqrt{4\pi\rho}, [\underline{v}_t] = \pm [\underline{B}_t] / \sqrt{4\pi\rho} \quad (13)$$

$$[\rho] = [p] = [v_n] = [v^2] = [B^2] = [B_n] = 0$$

Fast and Slow Shock Waves:

$$v_n^* \neq 0, [\rho] > 0, [p] > 0, [B_n] = 0$$

$$\left(\rho v_n^* \right)_{\text{fast}} \geq \left(\rho v_n^* \right)_{\text{rot.}} \geq \left(\rho v_n^* \right)_{\text{slow}} \quad (14)$$

$$B_t \text{ and } B^2 \begin{matrix} \text{increase} \\ \text{decrease} \end{matrix} \text{ through } \begin{matrix} \text{fast} \\ \text{slow} \end{matrix} \text{ shock waves}$$

Of the five classes of discontinuities possible, two of these, the fast shock wave and the tangential discontinuity, are of concern in the present applications. The first relates conditions on the two sides of the bow shock wave, and any other shock waves present, while the latter has properties required to describe a boundary surface (ionopause) that separates the flowing solar wind and the planetary ionosphere. More detailed consideration of the tangential discontinuity condition leads to a determination of the ionopause shape, as described in the following sections.

With regard to conditions at the bow wave, for solar-wind flows past Venus, as well as Mars and the Earth, that discontinuity can only be represented by a fast shock wave since the mass flux through each of the other possible choices is too small. With regard to conditions at the ionopause, of the various possibilities, only the tangential discontinuity has properties compatible with those required to describe a boundary surface that separates the externally flowing solar wind and the planetary atmosphere; that is, the condition $v_n^* = 0$ prohibits flow across the boundary, while the condition $B_n = 0$ must hold since by assumption no magnetic field exists interior to the ionopause and the solenoidal jump condition $[B_n] = 0$ always holds.

Frozen-field approximation.— Two important parameters characterize the solar-wind flow at any field point as described by eqs. (1-5). These are the Mach number $M = v/a$ and the Alfvén Mach number $M_A = v/A$. The former is the ratio of the flow velocity to the speed of sound $a = (\gamma p/\rho)^{1/2}$, while the latter is the ratio of the flow velocity to the speed $A =$

$(B^2/4\pi\rho)^{1/2}$ of a rotational or Alfvén wave propagating along the direction of the magnetic field.

For typical solar-wind conditions (refs. 5,6), both the oncoming Mach number and the Alfvén Mach number are high ($M_\infty \approx M_A \approx 0(10)$). In this instance, an important simplification of the magnetohydrodynamic equations occurs. This is so because the order of magnitude of the inertia term in differential equation (2) for the momentum is related to that of the magnetic terms by the square of the Alfvén Mach number. When the latter is large, therefore, the magnetic terms in eqs. (2), (3), (8), and (10) decouple from the gasdynamic portions of those equations. Furthermore, for Earth, Venus, or Mars, the strong interactive nature of the flow permits the terms involving g and ϕ to be disregarded because of the relative smallness of their effect on the fluid motion (ref. 5). The equations for the fluid motion thereby reduce to those of gasdynamics, while the magnetic field B can be determined subsequently by solving the remaining equations using the values for y already determined. The magnetic field, determined in this fashion, is usually interpreted as being "frozen-in" or moving with the fluid (ref. 5).

This then results in the following differential and conservation equations; for the flow field

$$\frac{\partial \rho}{\partial t} + \frac{\partial}{\partial x_k} (\rho v_k) = 0 \quad (15)$$

$$\frac{\partial}{\partial t} (\rho v_i) + \frac{\partial}{\partial x_k} (\rho v_i v_k + p \delta_{ik}) = 0 \quad (16)$$

$$\frac{\partial}{\partial t} \left(\frac{\rho v^2}{2} + \rho e \right) + \frac{\partial}{\partial x_k} \left[\rho v_k \left(\frac{v^2}{2} + e + p/\rho \right) \right] = 0 \quad (17)$$

$$[\rho v_n^*] = 0 \quad (18)$$

$$[\rho \underline{v} \cdot \underline{v}_n^* + p] = 0 \quad (19)$$

$$\left[\mathbf{v}_n^* \cdot \left(\frac{1}{2} \rho v^2 + \rho e + p \right) \right] = 0 \quad (20)$$

and for the magnetic field

$$\frac{\partial B_i}{\partial t} + \frac{\partial}{\partial x_k} (v_k B_i - v_i B_k) = 0 \quad (21)$$

$$\frac{\partial B_i}{\partial x_i} = 0 \quad (22)$$

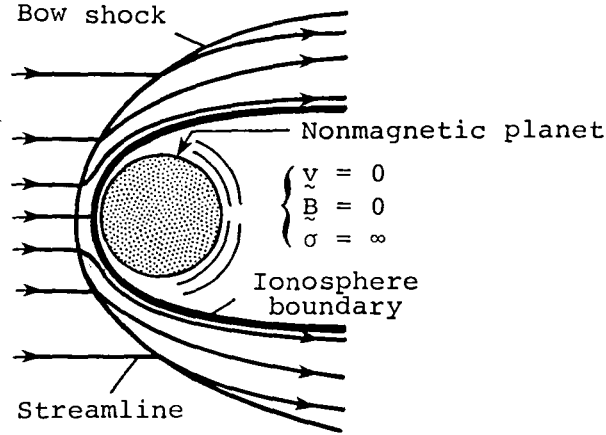
$$[B_n] = 0 \quad (23)$$

$$[B_n \cdot \mathbf{v}_t - B_t \cdot \mathbf{v}_n^*] = 0 \quad (24)$$

Equations (15) to (24) provide the governing equations which form the basis of the mathematical representation of the solar wind-magneto/ionosphere interaction problem considered here. For all of the results as well as the computer codes presented herein, we are interested exclusively in the steady-state solution to these equations which are obtained by setting $\partial/\partial t = 0$ and $\mathbf{v}_n^* = \mathbf{v}_n$, i.e. $q_n = 0$. We have presented the unsteady equations, however, since one of the computational methods used to determine the gasdynamic solution employs an unsteady procedure, integrating in time until the steady-state solution is asymptotically obtained.

Determination of the Ionosphere Boundary

The determination of the ionosphere boundary initiates from the assumptions that the ionosphere, or at least the outer part of it that participates in the interaction with the solar wind, is idealized as a spherically-symmetric and hydrostatically-supported plasma having infinite electrical conductivity, effectively bound to the planet and incapable of mixing with the solar wind, as indicated in the sketch below:



This interior plasma is separated from the flowing solar plasma by a tangential discontinuity across which the relations

$$v_n = B_n = [p + B^2/8\pi] = 0 \quad (25)$$

$$[\tilde{v}_t] \neq 0; [\tilde{B}_t] \neq 0; [\rho] \neq 0$$

given previously (eq. (11)) must hold. The basis for important simplifying approximations to these conditions, which can be assumed to apply at the Venusian ionosphere boundary and possibly for that at Mars as well, is that the gas pressure p is much larger than the magnetic pressure $B^2/8\pi$ on both sides of the ionopause. Therefore, the discontinuity pressure balance relation $[p + B^2/8\pi] = 0$ of eq. (25) reduces to a simple equality between the ionosphere pressure and the static pressure of the flowing solar plasma adjacent to the ionopause, i.e.

$$(p)_{\text{atm.}} = (p)_{\text{flow}} \quad (26)$$

Determination of the ionospheric pressure in the vicinity of the ionopause for the ionosphere models chosen in this study proceeds from the assumption of hydrostatic support, which implies a quiescent ionosphere where the bulk motions of the gas with respect to the planet are sufficiently small ($\tilde{v} = 0$) that equilibrium exists between the pressure gradient and gravity, viz.

$$dp/dr = -\rho g \quad (27)$$

where p and ρ are the gas pressure and density, r is the radial distance measured from the center of the planet, and g is the acceleration due to gravity. The variation of g is inversely proportional to r_s , so that $g = g_s(r_s/r)^2$ where the subscript s denotes values at the surface of the planet. Since the density ρ is related to the pressure according to the perfect gas law eq. (6), eq. (27) can be integrated to yield

$$p = p_R \exp \left[- \int_{R_R}^r \frac{dr}{H} \right] \quad (28)$$

where p_R is the pressure at some reference radius R_R and H is the local scale height of the atmosphere given by $H = \bar{R}T/\bar{M}g$.

If H is regarded as constant; that is, if variations of g and T with r are neglected, eq. (27) can be integrated directly to yield

$$p = p_R \exp \left[- \frac{r - R_R}{H} \right] \quad (29)$$

In view of uncertainties associated with measurements of the atmospheric properties of Venus and Mars, the variation of p with r as given by eq. (29) was adopted in the initial solar wind/ionosphere applications (ref. 6) and was also used in the previous study (ref. 9) involving the initial application of advanced computational methods to this problem. With preliminary ionospheric data now available from the Pioneer-Venus spacecraft (refs. 10 and 11), some of these uncertainties for Venus have been removed. It has been found that the assumption of an isothermal ($T = \text{constant}$) atmosphere at typical ionopause heights is quite reasonable. Consequently, there is no need to neglect the variation of gravity in the scale height in eq. (28). Including this effect leads to the following result for the pressure

$$p = p_R \exp \left[- \frac{R_R \cdot (r - R_R)}{\bar{H} \cdot r} \right] \quad (30)$$

where

$$\bar{H} = H_s \cdot (R_R/R_s)^2 \quad (31)$$

and R_s is the planetary radius and $H_s = \bar{R}T/\bar{M}g_s$. Equations (29) and (30) provide the two models employed in this study for the ionosphere pressure variation which is required in eq. (26) for the pressure balance condition at the ionopause.

For the a priori determination of the static pressure of the flowing solar-wind plasma on the exterior boundary of the ionosphere - $(p)_{\text{flow}}$ in eq. (26) - we use, as in all previous applications, the Newtonian approximation

$$p = p_{\text{st}} \cos^2 \psi \quad (32)$$

where ψ is the angle between the outward normal to the magnetosphere boundary and the flow direction of the oncoming undisturbed solar wind, and p_{st} is the stagnation or ram pressure exerted on the nose of the ionopause and is given by

$$p_{\text{st}} = K \rho_{\infty} v_{\infty}^2 \quad (33)$$

In this relation, K is a constant usually taken as one, but whose actual value is

$$K = \frac{1}{\gamma} \left[\frac{[(\gamma + 1)/2](\gamma + 1)}{\gamma - (\gamma - 1)/2M_{\infty}^2} \right]^{\frac{1}{\gamma - 1}} \quad (34)$$

For the high Mach number flows typical of solar-wind conditions, K approaches 0.844 for $\gamma = 2$ and 0.881 for $\gamma = 5/3$. Modification of the product $K \rho_{\infty}$ in eq. (33) to account for the presence of minor constituents such as ionized helium in the solar wind, as well as a discussion of the differences in that product between a fluid and collisionless representative, is provided in reference 8. The important implication associated with the introduction of the Newtonian approximation is that the calculation of the shape of the ionosphere boundary decouples from the calcula-

tion of the external flow. We then arrive at the following equation for the pressure balance at the ionopause locations R_i :

$$K\rho_\infty v_\infty^2 \cos^2 \psi = p_R \Lambda(R_i) \quad (35)$$

where

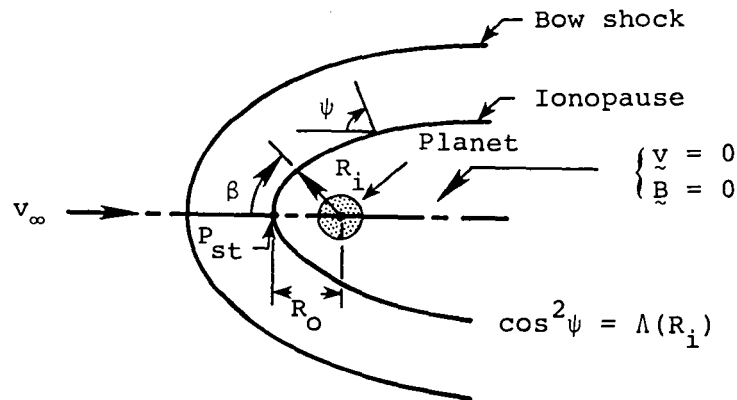
$$\Lambda(R_i) = \begin{cases} \exp \left[- \frac{(R_i - R_R)}{H} \right] & g, T = \text{Const.} \\ \exp \left[- R_R \frac{(R_i - R_R)}{H \cdot R_i} \right] & g = g_s \left(\frac{r_s}{r} \right)^2, T = \text{Const.} \end{cases} \quad (36a)$$

$$(36b)$$

depending upon whether the gravitational variation is included in scale height or not. It is convenient to choose as the reference radius and location the stagnation point on the ionopause; that is, $R_R = R_O$ where R_O is the distance from the center of the planet to the nose of the ionopause. This implies that $p_R = p_O = K\rho_\infty v_\infty^2$ and that at all points along the ionosphere boundary

$$\cos^2 \psi = \Lambda(R_i) \quad (37)$$

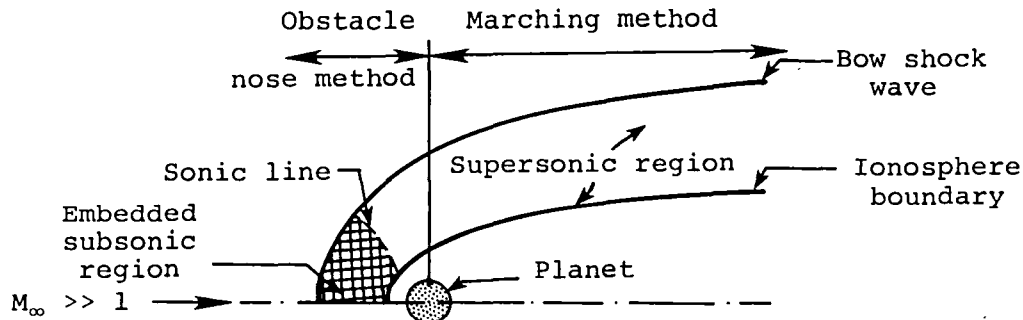
The final mathematical statement of the free-boundary problem for determining the shape of the ionosphere boundary then is summarized in the sketch below:



In order to proceed to a final determination of the ionopause shape, it is necessary to relate the local angle ψ to the local coordinates (R_i, β) of the boundary. This is accomplished with the help of the following sketch

Calculation of the Gasdynamic Flow Properties

Determination of the gasdynamic flow properties is, both conceptually and computationally, the most difficult and time-consuming portion of the total calculation of the solar-wind/terrestrial-planet interaction; and represents the heart of the present modeling effort insofar as the application of advanced computational procedures is concerned. The calculation consists of determining solutions to the differential equations and discontinuity conservation equations given by eqs. (15-20). Since in solar-wind/terrestrial-planet interactions, both the downstream tail region (far field) as well as the region in the vicinity of the obstacle nose (near field) are generally of interest, the computational methods selected must be capable of efficiently determining this entire flow field. In view of the need to carry the flow calculation to an arbitrary downstream distance, the most computationally-expedient procedure is to subdivide the flow field into two regions, as indicated in the sketch below:



This sketch illustrates the essential features of the high-supersonic Mach number flow typical of solar-wind flows past terrestrial planets. Of particular note is the embedded subsonic pocket located at the nose of the ionopause. The presence of this subsonic pocket necessitates use of a computational method capable of treating mixed subsonic/supersonic flows. Downstream of this region, the flow becomes supersonic and remains so for the convex shapes typical of solar-wind/ionosphere boundaries. In that region, a more computationally-economical procedure than that required near the nose can be employed. Such a subdivision of both flow field and solution procedures is common practice for calculating such flows and was employed in the previous solar-wind applications as well as in a related application to space shuttle reentry flows (ref. 12). The precise surface on which the solutions are joined is relatively

arbitrary; in our procedure it was convenient to place it along a plane through the planet center and normal to the free-stream direction of the solar wind, i.e. the dawn-dusk terminator. As illustrated in fig. 2, this position is further downstream than used in the former work in which an inverse iteration method was used for the nose region and the method of characteristics was used for the remaining supersonic region. In light of recent advances, both of the techniques used in the former procedures, particularly the inverse method, are now considered obsolete and much inferior to more current methods. In the new code, those two methods have been superceded by: (1) a new axisymmetric implicit unsteady Euler-equation solver (IMP) specifically developed for the present application, which determines the steady-state solution in the nose region by an asymptotic time-marching procedure, and (2) a shock-capturing marching solution (SCT) which spatially advances the solution downstream as far as required by solving the steady Euler equations.

Nose region solution - implicit unsteady Euler equation method.- The partial differential equations employed in the implicit (IMP) code are the unsteady gasdynamic Euler eqs. (15-20) for axisymmetric flow. These equations may be written in conservation-law form under the generalized independent variable transformation

$$\tau = T, \quad \xi = \xi(T, X, R), \quad \eta = \eta(T, X, R) \quad (40)$$

as follows

$$(U/J)_{\tau} + \left[(\xi_T U + \xi_X E + \xi_R F) / J \right]_{\xi} + \left[(\eta_T U + \eta_X E + \eta_R F) / J \right]_{\eta} + G = 0 \quad (41)$$

where

$$U = \begin{bmatrix} \rho \\ \rho u \\ \rho v \\ \rho e_t \end{bmatrix} \quad E = \begin{bmatrix} \rho u \\ p + \rho u^2 \\ \rho uv \\ (\rho e_t + p)u \end{bmatrix} \quad (42)$$

$$F = \begin{bmatrix} \rho v \\ \rho uv \\ p + \rho v^2 \\ (\rho e_t + p)v \end{bmatrix} \quad G = \frac{1}{RJ} \begin{bmatrix} \rho v \\ \rho uv \\ \rho v^2 \\ (\rho e_t + p)v \end{bmatrix}$$

and the Jacobian

$$J = \xi_X \eta_R - \xi_R \eta_X \quad (43)$$

In eqs. (40) through (43), T denotes time, X is the axial downstream coordinate, and R the cylindrical radial distance; u and v the velocity components in the X and R directions; and e_t is the total energy per unit mass, which for a perfect gas is related to the other quantities by

$$e_t = p/[\rho(\gamma - 1)] + (u^2 + v^2)/2 \quad (44)$$

The subscripts in eqs. (41) and (43) denote partial derivatives with respect to the indicated variable.

The analysis commences by introducing a computational mesh in polar (r, β) coordinates such that one family of coordinates consists of rays from the planetary center spaced at equal increments of β measured from the obstacle nose, and the other of curved lines intersecting each ray so as to divide the portion of it between the ionopause and the shock wave into a fixed number of equal segments. The coordinate transformation eq. (40) is then used to map the portion of the X, R, T physical space bounded by (1) the bow wave, (2) the downstream outflow boundary at $\beta = \pi/2$, (3) the obstacle surface, and (4) the stagnation streamline at $\beta = 0$ into a rectangle in the ξ, η, τ computational space as illustrated in fig. 3. Generally, the transformation metrics at each time step are not known beforehand, and must be determined numerically as part of the solution. Integration step size is established by using the eigenvalues of the Jacobian matrices \bar{A} and \bar{B} , where $\bar{A} = \partial \hat{E} / \partial \hat{U}$, $\bar{B} = \partial \hat{F} / \partial \hat{U}$, and $\hat{U} = U/J$, $\hat{E} = (\xi_T U + \xi_X E + \xi_R F)/J$, and $\hat{F} = (\eta_T U + \eta_X E + \eta_R F)/J$.

Boundary conditions necessary for the specification of a properly-posed mathematical problem are that the flow (a) satisfy the axisymmetric Rankine-Hugoniot shock relations derivable from eq. (41) along (1), (b) be entirely supersonic along (2), (c) be parallel to boundaries (3) and (4), and (d) be symmetric about boundary (4). Initial flow-field conditions are determined by use of an approximating formula for the coordinates of the bow shock wave which is dependent on γ , M_∞ and the shape of the obstacle, and by prescribing a Newtonian pressure

distribution on the obstacle. Since the maximum entropy streamline wets the obstacle surface, that fact plus the known flow direction on the obstacle serve to determine the remainder of the flow properties on that surface. A linear variation for the flow properties between the bow shock and the obstacle is then prescribed. This provides the initial flow field which is then integrated in a time-asymptotic fashion until the steady-state solution is obtained.

The basic numerical algorithm used in the IMP code was developed by Beam and Warming (ref. 13) and is second-order accurate, noniterative, and spatially factored. In particular, the "delta form" with Euler time differencing is employed. When applied to eq. (41), the algorithm assumes the form

$$(I + \Delta\tau\delta_{\xi}\bar{A}^n)(I + \Delta\tau\delta_{\eta}\bar{B}^n)(\hat{U}^{n+1} - \hat{U}^n) = -\Delta\tau(\delta_{\xi}\hat{E}^n + \delta_{\eta}\hat{F}^n + G) \quad (45)$$

where \bar{A} and \bar{B} are the Jacobian matrices, I is the identity matrix, δ_{ξ} and δ_{η} are second-order, central-difference operators, $\hat{U}^{n+1} = \hat{U}(n\Delta\tau)$ and $\Delta\tau$ is the integration step size.

Equation (45) is solved at the interior points only. It requires two 4x4 block tridiagonal inversions at each time step of the integration. The solution proceeds as follows:

1. Define $\Delta\hat{U} = \hat{U}^{n+1} - \hat{U}^n$
2. Form the right-hand side of eq. (45) and store results in the \hat{U}^{n+1} array.
3. Apply smoothing $\hat{U}^{n+1} = \hat{U}^{n+1} - (\epsilon/8)S/J$.
4. Define $\bar{U} = (I + \Delta\tau\delta_{\eta}\bar{B}^n)\Delta\hat{U}$ and solve the matrix equation $(I + \Delta\tau\delta_{\xi}\bar{A}^n)\bar{U} = \hat{U}^{n+1}$ for \bar{U} storing the result in the \hat{U}^{n+1} array.
5. Solve the matrix equation $(I + \Delta\tau\delta_{\eta}\bar{B}^n)\Delta\hat{U} = \hat{U}^{n+1}$ for $\Delta\hat{U}$.
6. Obtain the values of \hat{U}^{n+1} from the relation $\hat{U}^{n+1} = \Delta\hat{U} + \hat{U}^n$.

7. Transfer contents of \hat{U}^{n+1} to \hat{U}^n and repeat all steps until satisfactory convergence is attained.

In step 3 a fourth-order smoothing term S is used to eliminate non-linear instabilities that may arise since the use of central differences in the spatial directions results in a neutrally stable algorithm. This smoothing term is given by

$$\begin{aligned}
 S_{jk} = & (\hat{U}_J)^{n+1}_{j+2,k} - 4 \left[(\hat{U}_J)^{n+1}_{j+1,k} + (\hat{U}_J)^{n+1}_{j-1,k} \right] + 12 (\hat{U}_J)^{n+1}_{j,k} + (\hat{U}_J)^{n+1}_{j-2,k} \\
 & + (\hat{U}_J)^{n+1}_{j,k+2} - 4 \left[(\hat{U}_J)^{n+1}_{j,k+1} + (\hat{U}_J)^{n+1}_{j,k-1} \right] + (\hat{U}_J)^{n+1}_{j,k-2}
 \end{aligned}
 \tag{46}$$

and ϵ , the smoothing coefficient, chosen from the range $0 \leq \epsilon \leq 0.4$ depending upon the size of the time step. The j and k indices correspond to the ξ and η directions, respectively. At the points adjacent to the boundaries a special form of the smoothing term is used.

At the boundaries, modification of the differencing algorithm to account for the particular conditions described above is accomplished as follows. The obstacle-surface flow-tangency condition is incorporated through the use of Kentzer's scheme (ref. 14), while at the symmetry plane, the variables are reflected according to whether they are odd or even. At the outflow boundary where the flow is entirely supersonic, the dependent variables are determined by extrapolation from the adjacent interior points. For the upstream boundary formed by the bow shock wave, the sharp discontinuity approach of reference 15 is used. The interior flow field bounded by these various boundaries is treated in shock-capturing fashion and, therefore, allows for the correct formation of secondary internal shocks.

In the initial development of the nose-region solution procedure (ref. 9), it was found that for certain ionopause obstacle shapes which have a significant amount of lateral flaring at the dawn-dusk terminator, for example, constant scale-height shapes for $H/R_0 \geq 0.5$, and/or cases involving low free-stream Mach numbers $M_\infty \leq 3$, the axial component of velocity at some points on the terminator plane $\beta = \pi/2$ may become

subsonic. Although this has no effect whatsoever on the nose-region solver, for these cases the downstream solution cannot be obtained since the marching-region solver which determines the solution downstream of this starting plane, and which is described in detail in the following section, requires supersonic axial velocities in order to proceed. Under the work reported here, this limitation has been removed by developing the capability for adding an additional portion of the flow field, located downstream of the terminator, to the blunt-body solution as illustrated in figure 4. This effectively generalizes the capability of the present procedures to treat a wide variety of ionopause shapes - including all of the shapes of interest described by the constant scale-height and scale-height with gravitational variation atmospheric models found from eqs. (36a,b) - as well as to treat relatively low free-stream Mach numbers, $M_\infty \approx 2.0$. Details of this capability are provided in the Computer Program Users Manual, Section A.2.1.1 of this report.

Downstream region solution - shock capturing marching method.- Since the shock-capturing technique employed has been described previously in references 16-18, only an outline of the salient features is provided here. The analysis is based on the conservation-law form of the gasdynamic Euler equations for steady axisymmetric flow, which can be readily obtained from eqs. (40) through (44) by setting the τ derivatives to zero. The fourth of this set of equations representing conservation of energy ρe_t can be integrated for steady flow to yield the following relation for the total enthalpy

$$h_t = h + (u^2 + v^2)/2 = \text{constant} \quad (47)$$

where $h = e + p/\rho = C_p T$ is the enthalpy per unit mass.

The computational mesh is defined by lines of constant X and $(R-R_b)/(R_s-R_b)$, where R_s and R_b are functions of X that describe the radial cylindrical coordinates of the ionopause and bow shock wave at the same X as the field point (X,R) . The three remaining partial differential equations for conservation of mass and of axial and radial momentum are then transformed to a rectangular computational space by the transformation

$$\xi = X, \quad \eta = \frac{R - R_b}{(R_s - R_b)} \quad (48)$$

to obtain

$$\partial \tilde{E} / \partial \xi + \partial \tilde{F} / \partial \eta + \tilde{G} = 0 \quad (49)$$

$$\tilde{E} = E, \quad \tilde{F} = \left\{ F - \left[\frac{\partial}{\partial \xi} R_b + \eta \frac{\partial}{\partial \xi} (R_s - R_b) \right] \right\} / (R_s - R_b)$$

$$\tilde{G} = G + \frac{E}{R_s - R_b} \frac{\partial}{\partial \xi} (R_s - R_b) \quad (50)$$

The finite-difference counterpart of eq. (49) is integrated with respect to the hyperbolic coordinate ξ to yield values of the conservative variable E . Subsequent to each integration step, the physical flow variables p , ρ , u , and v must be decoded from the components e_i of E . This necessitates the solution of four simultaneous, nonlinear equations consisting of eq. (47) together with the three elements e_i . This can be done readily by using the relations $v = e_3/e_1$, $p = e_2 - e_1 u$, and $\rho = e_1/u$ together with the expression $h = \gamma/(\gamma-1)(p/\rho)$ for a perfect gas to determine the following quadratic equation for u

$$\begin{aligned} \frac{u^2}{2} + \frac{\gamma}{\gamma-1} \left(\frac{e_2 - e_1 u}{e_1} \right) u - h_t + \left(\frac{e_3}{e_1} \right)^2 \\ = - \frac{\gamma+1}{2(\gamma-1)} u^2 + \left(\frac{\gamma}{\gamma-1} \right) \frac{e_2}{e_1} u - h_t + \left(\frac{e_3}{e_1} \right)^2 = 0 \end{aligned} \quad (51)$$

Two roots exist; one corresponds to subsonic flow and is discarded since u is always supersonic in the present application, while the other corresponds to supersonic flow and gives the desired solution.

Since only the bow shock wave is treated as a sharp discontinuity and any others that may be present are "captured" by the difference algorithm, selection of the appropriate finite difference scheme to advance the calculation in the ξ direction is of prime importance. Following the analysis of refs. 16-18, the numerical integration of eq. (49) is accomplished using the finite-difference predictor-corrector

scheme of MacCormack (ref. 19), the most efficient second-order algorithm for shock-capturing calculations. General descriptions of the method can be found in the references cited.

Calculation of the streamlines.— The streamlines are determined by integrating fluid particle trajectories through the known velocity field since this procedure was found to be more accurate than the alternative mass-flow calculation. The calculation of a particular streamline is initiated at the point where the streamline crosses the bow shock, as illustrated in figure 5. At that point, exact values of the streamline slope dR_S/dX are known in terms of the local shock angle δ_S and free-stream quantities according to the relation

$$\frac{dR_S}{dX} = \frac{(2\cot \delta_S)(M_\infty^2 \sin^2 \delta_S - 1)}{2 + M_\infty^2(\gamma + 1 - 2\sin^2 \delta_S)} \quad (52)$$

which is contained implicitly in both the blunt-body (IMP) and marching (SCT) code solutions. At other points in the flow field, the local streamline slope is given by the ratio of radial to downstream velocity, i.e.,

$$dR_S/dX = v/u \quad (53)$$

and the streamline determination is made by stepwise integration in X using a modified third-order Euler predictor-corrector method. Bivariate linear interpolation from the flow-field grid points is employed to obtain the velocity components (u,v) required at the stepwise points along the streamline trajectory. Separate streamline calculations are made for the nose region (IMP results) and downstream region (SCT results) because of the different coordinate systems employed in those two regions.

Calculation of the Magnetic Field

With the flow properties known from the gasdynamic calculations, determination of the steady magnetic field B proceeds by integrating the

remaining magnetohydrodynamic equations not employed in the gasdynamic analysis, that is eqs. (21-24) with $\partial/\partial t = 0$:

$$\begin{aligned}\text{curl } (\underline{B} \times \underline{v}) &= 0, \quad \text{div } \underline{B} = 0 \\ [B_n v_t - B_t v_n] &= 0, \quad [B_n] = 0\end{aligned}\tag{54}$$

These equations are commonly interpreted as indicating the field lines move with the fluid. The analysis associated with eqs. (54) leads to a straightforward calculation in which the vector distance from each point on an arbitrarily-selected field line to its corresponding point on an adjacent field line in the downstream direction is determined by numerically integrating $\int \underline{v} dt$ over a fixed time interval Δt . Once the coordinates of the field lines are determined, the magnetic field at any point may be calculated from the relation

$$\frac{\underline{B}}{|\underline{B}_\infty|} = \frac{\rho}{\rho_\infty} \frac{\Delta \underline{\ell}}{|\Delta \underline{\ell}_\infty|}\tag{55}$$

where $\Delta \underline{\ell}$ is the vector length of a small element of a flux tube. Figure 6 clarifies these quantities for the plane of magnetic symmetry defined by the plane containing the axis of symmetry of the obstacle and the magnetic-field lines upstream of the bow wave for the special case when the latter is perpendicular to the flow. In that figure the open symbol \bigcirc denotes locations of points on the streamlines corresponding to the fixed-time interval $\Delta t = \Delta S_\infty/v_\infty$.

Such a procedure is valid generally, but its use in the present calculations is confined to only the component of the magnetic field $(\underline{B})_\perp$ just described. The remainder of the magnetic-field calculation makes use of a decomposition due to Alksne and Webster (ref. 20) in which the axisymmetric properties of the gasdynamic solution and the linearity of the magnetic-field eqs. (54) are employed to derive the following relationship for the magnetic field \underline{B}_P at any point P:

$$\underline{B}_P = \left(\frac{\underline{B}_P}{\underline{B}_\infty} \right)_n \underline{B}_{\infty n} + \left(\frac{\underline{B}_P}{\underline{B}_\infty} \right)_\perp \underline{B}_{\infty \perp} + \hat{e}_n \left(\frac{\underline{B}_P}{\underline{B}_\infty} \right)_n \underline{B}_{\infty n}\tag{56}$$

As illustrated in figure 7, subscripts ∞ , \perp , and n refer to contributions associated with the components $B_{\infty\infty}$ of B_{∞} parallel to \underline{v}_{∞} ; the component $B_{\infty\perp}$ perpendicular to \underline{v}_{∞} in the plane that contains the point P, the center of the planet, and the vector \underline{v}_{∞} ; and the component $B_{\infty n}$ normal to the latter plane, and \hat{e}_n is a unit vector in the latter direction. The unit ratios $(B_P/B_{\infty})_{\infty}$ and $(B_P/B_{\infty})_n$ can be calculated directly from the gas-dynamic solution by the expressions

$$\left(\frac{B_P}{B_{\infty}}\right)_{\infty} = \frac{\rho_P \underline{v}_P}{\rho_{\infty} |\underline{v}_{\infty}|}, \quad \left(\frac{B_P}{B_{\infty}}\right)_n = \frac{R_P \rho_P}{R_P \rho_{\infty}} \quad (57)$$

where R_P is the radial cylindrical coordinate of the streamline through P, as indicated in figure 7.

In carrying out the determination of $(B_P/B_{\infty})_{\perp}$ using eq. (55), values for $|\Delta \underline{\ell}|/|\Delta \underline{\ell}_{\infty}|$ are determined initially at the points where the streamlines and perpendicular-component field lines intersect. A generalized quadrilateral interpolation scheme followed by a fifth-order smoothing is then employed to determine the corresponding values at the computational grid points where values for ρ/ρ_{∞} are available for calculation of $(B_P/B_{\infty})_{\perp}$. At the bow shock, an exact formula is used

$$\begin{aligned} (|\Delta \underline{\ell}|/|\Delta \underline{\ell}_{\infty}|)^2 &= 1 + \cot^2 \theta (1+D^2) - 2D \times \csc \theta \times \cot \theta \times \cos (\theta-\delta) \\ \psi &= \theta + \sin^{-1} \left\{ [D \times \cot \theta \times \sin (\theta-\delta)] / (|\Delta \underline{\ell}|/|\Delta \underline{\ell}_{\infty}|) \right\} \end{aligned} \quad (58)$$

where

$$\begin{aligned} D^2 &= 1 - 4(M_{\infty}^2 \sin^2 \theta - 1)(\gamma M_{\infty}^2 \sin^2 \theta + 1) / [(\gamma + 1)^2 M_{\infty}^4 \sin^2 \theta] \\ \cot \delta &= \tan \theta \times \left\{ (\gamma + 1) M_{\infty}^2 / [2(M_{\infty}^2 \sin^2 \theta - 1)] - 1 \right\} \\ \theta &= \tan^{-1} \left(\frac{dR_S}{dX} \right) \end{aligned} \quad (59)$$

Finally, the resultant magnetic field can then be expressed in components relative to any orthogonal (X,Y,Z) coordinate system. For convenience of illustration, we have chosen the point P to lie in the (X,Y) plane. Relative to this reference frame, the magnetic components are

$$\begin{aligned}
B_X/B_\infty &= \left[(|B|/B_\infty)_n \cos \phi \cos \alpha_p + (|B|/B_\infty)_\perp \cos \psi \sin \alpha_p \right] \cos \alpha_n \\
B_Y/B_\infty &= \left[(|B|/B_\infty)_n \sin \phi \cos \alpha_p + (|B|/B_\infty)_\perp \sin \psi \sin \alpha_p \right] \cos \alpha_n \\
B_Z/B_\infty &= (B/B_\infty)_n \sin \alpha_n
\end{aligned} \tag{60}$$

where ϕ is the local flow angle given by

$$\phi = \tan^{-1} \left(\frac{v}{u} \right) \tag{61}$$

and the interplanetary magnetic field angles α_p and α_n indicated in figure 7 are defined by

$$\alpha_p = \tan^{-1} \left[\frac{B_{\infty\perp}}{B_{\infty n}} \right] = \tan^{-1} \left[\frac{B_{Y_\infty}}{B_{X_\infty}} \right] \tag{62}$$

$$\alpha_n = \tan^{-1} \left[\frac{B_{\infty n}}{\sqrt{(B_{\infty n})^2 + (B_{\infty\perp})^2}} \right] = \tan^{-1} \left[\frac{B_{Z_\infty}}{\sqrt{(B_{X_\infty})^2 + (B_{Y_\infty})^2}} \right] \tag{63}$$

The generalizations of these results when the point P is at some arbitrary (Y,Z) location, i.e. not in the (X,Y) plane, are provided below in the spacecraft trajectory section.

Calculation of the Contour Lines

Contours are calculated for nondimensionalized velocity $|v|/v_\infty$, density ρ/ρ_∞ , magnetic field components $(|B|/B_\infty)_n$, $(|B|/B_\infty)_\perp$, and $(B/B_\infty)_n$ by application of a modified version of a contour procedure developed at NASA/Ames Research Center. After specifying a value for the contour line, the boundary is searched for intervals which bracket the selected value. After locating one such point by interpolation, the remainder of the contour is determined by 'walking' around the contour, searching at each step for the interval and then interpolating to find the point through which the contour line next passes. This is repeated until a boundary

point is reached. Then closed contours are found in a similar manner. Linear interpolation is used throughout the process. Since the temperature is a function of $|\underline{v}|/v_\infty$ only for a specified M_∞ and γ ,

$$T/T_\infty = 1 + \left[\left(\frac{\gamma - 1}{2} \right) M_\infty^2 \right] \left[1 - \left(\frac{|\underline{v}|}{v_\infty} \right)^2 \right] \quad (64)$$

velocity contours may also be considered as temperature contours with only a relabeling required. The coordinates of the contour lines are output either or both as listings and pen plots.

Solar-Ecliptic/Solar-Wind Coordinate Transformations

In order to facilitate comparison of results from the current theoretical model with actual observational data obtained by a spacecraft, it is necessary to consider the appropriate transformations between the spacecraft and solar-wind coordinate systems. Part of the data required as input to the theoretical model consists of oncoming interplanetary values of solar-wind temperature, density, and velocity and magnetic-field vector components. These are naturally obtained in the spacecraft coordinate system, and are usually reported in a sun-planet or solar-ecliptic reference frame. The key coordinate system for the theoretical model is one which aligns the axial direction with the oncoming solar wind, since the gasdynamic calculation is assumed to be axisymmetric about this direction. Thus, the interplanetary input data must be transformed to the solar-wind system to initiate the theoretical determination. Once the gasdynamic and magnetic-field calculations in the solar-wind system are complete, those results must then be transformed back to the sun-planet system to allow direct comparison with spacecraft data obtained at arbitrary locations in the solar-wind/ionosphere interaction region. Consequently, direct and inverse transformations for both spatial coordinates as well as vector quantities between these reference frames are required.

For the measurements of the oncoming interplanetary solar-wind velocity we have assumed that the velocity is obtained with reference to a

sun-planet (x_s, y_s, z_s) system with origin at planetary center and in which the x_s -axis points to the sun, the y_s -axis is opposite to the planetary orbital motion, and the z_s -axis points northward. The direction of the oncoming solar wind is such that the total aberration or azimuthal angle, including planetary orbital motion, of the solar-wind velocity vector in the plane of the ecliptic is Ω and the out-of-ecliptic plane or polar angle is ϕ_p . The positive sense of the azimuthal angle is for east-to-west flow and for the polar angle for north-to-south flow, as indicated in figure 8. In that figure we have also indicated the solar-wind (x, y, z) coordinate system so defined by (Ω, ϕ_p) . For the gas-dynamic calculation, the (x, y, z) system is somewhat inconvenient since the direction of solar-wind flow is in the negative x -direction. Hence, the internal gasdynamic and magnetic-field calculations are performed in an (X, Y, Z) system as shown in figure 9.

The coordinate and vector transformations from the ecliptic sun-planet (x_s, y_s, z_s) system to the (X, Y, Z) solar-wind system are given by

$$\begin{pmatrix} Q_X \\ Q_Y \\ Q_Z \end{pmatrix} = \begin{pmatrix} -\cos \Omega \cos \phi_p & -\sin \Omega \cos \phi_p & \sin \phi_p \\ \sin \Omega & -\cos \Omega & 0 \\ -\cos \Omega \sin \phi_p & \sin \Omega \sin \phi_p & \cos \phi_p \end{pmatrix} \begin{pmatrix} Q_{x_s} \\ Q_{y_s} \\ Q_{z_s} \end{pmatrix} \quad (65)$$

where (Q_X, Q_Y, Q_Z) represents the Cartesian components of any vector referred to the solar-wind (X, Y, Z) coordinate system, and $(Q_{x_s}, Q_{y_s}, Q_{z_s})$ represents the corresponding vector in the sun-planet ecliptic (x_s, y_s, z_s) system. Thus, for a transformation of coordinates

$$\begin{aligned} (Q_X, Q_Y, Q_Z) &= (X, Y, Z) \\ (Q_{x_s}, Q_{y_s}, Q_{z_s}) &= (x_s, y_s, z_s) \end{aligned} \quad (66)$$

while for a vector transformation of, say, the magnetic field

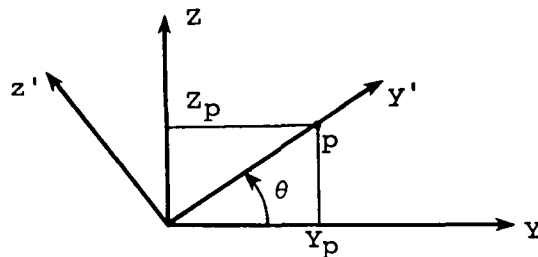
$$\begin{aligned} (Q_X, Q_Y, Q_Z) &= (B_X, B_Y, B_Z) \\ (Q_{x_s}, Q_{y_s}, Q_{z_s}) &= (B_{x_s}, B_{y_s}, B_{z_s}) \end{aligned} \quad (67)$$

The inverse transformation from the solar-wind to the sun-ecliptic system is given by

$$\begin{pmatrix} Q_{X_S} \\ Q_{Y_S} \\ Q_{Z_S} \end{pmatrix} = \begin{pmatrix} -\cos \Omega \cos \phi_p & \sin \Omega & -\cos \Omega \sin \phi_p \\ \sin \Omega \cos \phi_p & -\cos \Omega & \sin \Omega \sin \phi_p \\ \sin \phi_p & 0 & \cos \phi_p \end{pmatrix} \begin{pmatrix} Q_X \\ Q_Y \\ Q_Z \end{pmatrix} \quad (68)$$

Properties Along a Spacecraft Trajectory

One of the primary aims of the present effort has been the development of the capability to determine plasma and magnetic-field properties, as predicted by the present theoretical model, at locations specified along an arbitrary spacecraft trajectory, and in such a form as to enable comparisons to be made directly with actual spacecraft data. To this end, the following procedure has been developed and implemented in the associated computer code. First, from the known oncoming interplanetary conditions provided in a sun-planet reference frame, the azimuthal and polar solar-wind angles (Ω, ϕ_p) are employed to establish both the location of the trajectory point in the solar-wind (X, Y, Z) frame as well as the interplanetary magnetic-field components $(B_{X_\infty}, B_{Y_\infty}, B_{Z_\infty})$ using the transformation eq. (65). Next, the axisymmetric gasdynamic and unit magnetic-field calculations are carried out. Because the gasdynamic flow is axisymmetric in the (X, Y, Z) system, the internal coordinate system in which the trajectory calculations are actually performed may be rotated about the X axis into the most convenient orientation. If we consider a point P located at (X_p, Y_p, Z_p) , then the rotation most appropriate for the present application is indicated in the sketch below



where the angle θ is given by

$$\theta = \tan^{-1} \left[\frac{z_p}{y_p} \right] \quad (69)$$

This rotation defines a new coordinate system (x', y', z') where

$$\begin{pmatrix} x' \\ y' \\ z' \end{pmatrix} = \begin{pmatrix} 1 & 0 & 0 \\ 0 & \cos \theta & \sin \theta \\ 0 & -\sin \theta & \cos \theta \end{pmatrix} \begin{pmatrix} x \\ y \\ z \end{pmatrix} \quad (70)$$

in which

$$\begin{aligned} x' &= x_p \\ y' &= \sqrt{y_p^2 + z_p^2} \\ z' &= 0 \end{aligned} \quad (71)$$

Thus, the (x', y') plane which contains the X axis and the arbitrary point P corresponds directly to the plane $(X, R) = (x_p, \sqrt{y_p^2 + z_p^2})$ in which the axisymmetric gasdynamic flow properties are calculated. In particular, the velocity magnitude v , density ρ , and flow angle ϕ at the point P are found by bilinear interpolation through the (X, R) flow-field grid. The vector velocity in the (X, Y, Z) system is then given by the transformation

$$\begin{pmatrix} v_x \\ v_y \\ v_z \end{pmatrix} = \begin{pmatrix} 1 & 0 & 0 \\ 0 & \cos \theta & -\sin \theta \\ 0 & \sin \theta & \cos \theta \end{pmatrix} \begin{pmatrix} v \cos \phi \\ v \sin \phi \\ 0 \end{pmatrix} \quad (72)$$

and then in the sun-ecliptic system by the transformation given in eq. (68)

$$\begin{pmatrix} v_{x_s} \\ v_{y_s} \\ v_{z_s} \end{pmatrix} = \begin{pmatrix} -\cos \Omega \cos \phi_p & \sin \Omega & -\cos \Omega \sin \phi_p \\ \sin \Omega \cos \phi_p & -\cos \Omega & \sin \Omega \sin \phi_p \\ \sin \phi_p & 0 & \cos \phi_p \end{pmatrix} \begin{pmatrix} v_x \\ v_y \\ v_z \end{pmatrix} \quad (73)$$

Calculation of the magnetic field at an arbitrary point is somewhat more complicated since these components are dependent upon the orientation of the incident interplanetary magnetic field. With the known $(B_{X_\infty}, B_{Y_\infty}, B_{Z_\infty})$ components, the corresponding components $(B'_{X_\infty}, B'_{Y_\infty}, B'_{Z_\infty})$ in the rotated (x', y', z') system are given by

$$\begin{pmatrix} B'_{X_\infty} \\ B'_{Y_\infty} \\ B'_{Z_\infty} \end{pmatrix} = \begin{pmatrix} 1 & 0 & 0 \\ 0 & \cos \theta & \sin \theta \\ 0 & -\sin \theta & \cos \theta \end{pmatrix} \begin{pmatrix} B_{X_\infty} \\ B_{Y_\infty} \\ B_{Z_\infty} \end{pmatrix} \quad (74)$$

In this reference frame, the perpendicular, parallel, and normal interplanetary components are identified as

$$\begin{aligned} B_{\infty_{\parallel}} &= B'_{X_\infty} \\ B_{\infty_{\perp}} &= B'_{Y_\infty} \\ B_{\infty_n} &= B'_{Z_\infty} \end{aligned} \quad (75)$$

Then, the magnetic field angles α'_p and α'_n in the rotated system are given by

$$\alpha'_p = \tan^{-1} \left[\frac{B_{\infty_{\perp}}}{B_{\infty_{\parallel}}} \right] = \tan^{-1} \left[\frac{B'_{Y_\infty}}{B'_{X_\infty}} \right] \quad (76)$$

$$\alpha'_n = \tan^{-1} \left[\frac{B_{\infty_n}}{\sqrt{(B_{\infty_{\parallel}})^2 + (B_{\infty_{\perp}})^2}} \right] = \tan^{-1} \left[\frac{B'_{Z_\infty}}{\sqrt{(B'_{X_\infty})^2 + (B'_{Y_\infty})^2}} \right] \quad (77)$$

The magnetic angle ψ associated with the incident perpendicular component and the unit magnetic-field ratios $(|B|/B_\infty)_{\parallel}$, $(|B|/B_\infty)_{\perp}$, $(B/B_\infty)_n$ in the rotated system are next determined by bilinear interpolation through the flow-field grid. Then, the magnetic-field components (B'_x, B'_y, B'_z) in the rotated system are calculated from

$$B'_x = \cos \alpha'_n \left[\cos \phi \cdot \cos \alpha'_p \cdot \left| \frac{B}{B_\infty} \right|_{\parallel} + \cos \psi \cdot \sin \alpha'_p \cdot \left| \frac{B}{B_\infty} \right|_{\perp} \right] \cdot B_\infty \quad (78)$$

$$B'_Y = \cos \alpha'_n \left[\sin \phi \cdot \cos \alpha'_p \cdot \left| \frac{B}{B_\infty} \right|_{\parallel} + \sin \psi \cdot \sin \alpha'_p \cdot \left| \frac{B}{B_\infty} \right|_{\perp} \right] \cdot B_\infty \quad (79)$$

$$B'_Z = \sin \alpha'_n \cdot \left(\frac{B}{B_\infty} \right)_n \cdot B_\infty \quad (80)$$

The magnetic-field components in the solar-wind (X,Y,Z) system are then determined from the rotational transformation.

$$\begin{pmatrix} B_X \\ B_Y \\ B_Z \end{pmatrix} = \begin{pmatrix} 1 & 0 & 0 \\ 0 & \cos \theta & -\sin \theta \\ 0 & \sin \theta & \cos \theta \end{pmatrix} \begin{pmatrix} B'_X \\ B'_Y \\ B'_Z \end{pmatrix} \quad (81)$$

and finally in the sun-planet system from

$$\begin{pmatrix} B_{X_s} \\ B_{Y_s} \\ B_{Z_s} \end{pmatrix} = \begin{pmatrix} -\cos \Omega \cos \phi_p & \sin \Omega & -\cos \Omega \sin \phi_p \\ \sin \Omega \cos \phi_p & -\cos \Omega & \sin \Omega \sin \phi_p \\ \sin \phi_p & 0 & \cos \phi_p \end{pmatrix} \begin{pmatrix} B_X \\ B_Y \\ B_Z \end{pmatrix} \quad (82)$$

RESULTS

Using the computational procedures developed under the current modeling effort, a large variety and number of different solar-wind/planetary-ionosphere interaction results were systematically obtained. These results were directed toward the following specific objectives: (1) verification of the correctness of the procedures, (2) demonstration of their flexibility and generality for a variety of cases covering ranges typical of solar-wind conditions, (3) establishment of a catalog of flow and magnetic-field results for a large number of solar-

wind flows, and (4) comparisons of theoretical predictions with data obtained from spacecraft measurements. The results obtained associated with these objectives are discussed below.

Verification of the correctness of the procedures developed under the current effort primarily involved testing the computational extensions developed regarding both the gasdynamic and magnetic-field calculation methods reported in ref. 9. For the gasdynamic solver, this consists of demonstrating the extended blunt-body capability. As discussed previously in the section describing the nose-region solution and also in section A.2.1.1 of the computer manual, that extension involves the addition to the nose-region flow field of a region downstream of the dawn-dusk terminator - which is the usual plane terminating the nose-region solution. This added capability effectively removes any restriction with regard to obstacle shape and interplanetary gasdynamic Mach number of the previous procedures (ref. 9); and permits the calculation of ionopause shapes which have significant flaring in the radial direction at the dawn-dusk terminator, as well as flows at very low ($M_\infty \approx 2.0$) free-stream Mach numbers. In figure 10, we present results for the bow shock locations for $M_\infty = 8.0$, $\gamma = 5/3$ flow past constant scale-height ionopause shapes (see eq. (36a) with $H/R_0 = 0.5$ and 1.0). The downstream solutions for neither of these shapes could be determined with the previous procedures (ref. 9), whereas with the present method they present no problem. The downstream locations to which the nose-region solutions were extended were $X/R_0 = (0.54, 0.67)$, respectively, for the $H/R_0 = (0.5, 1.0)$ ionopause shapes - indicating that the addition of an extensive downstream region to the nose solution for such flows is unnecessary. This is important, as the nose-region solver requires significantly more computational time for a given flow-field region than the marching solver. Hence, minimization of the nose-region flow field is essential in minimizing the total computational time.

In figure 11, we display additional results using the extended nose-region grid capability to demonstrate the ability of the current method for calculating very low interplanetary gasdynamic Mach number flows. Bow shock locations are shown for $M_\infty = 2.0$ and 3.0 , $\gamma = 5/3$ flows past an

ionopause obstacle shape with gravitational variation included in scale-height having $\bar{H}/R_0 = 0.25$ (see eq. (36b)). This particular obstacle is a relatively blunt shape, as can be observed from the ionopause profiles presented previously in figure 1, and, computationally, presents a more difficult flow to determine than flows for shapes having less flaring. For applications to terrestrial planets, such as Mars and Venus, typical ionopause shapes occurring in nature appear to lie in the range $0.01 \leq \bar{H}/R_0 \leq 0.10$. Consequently, demonstration of the ability of the current procedures to treat successfully such flows as shown in figures 10 and 11 - which lie at the limits of interest as far as applications to nonmagnetic terrestrial planets, indicates that these procedures will not be restricted insofar as ionopause geometry and interplanetary solar-wind conditions are concerned.

Corresponding verification of the extensions to the procedures for the magnetic-field calculation has involved demonstration of the correctness of the magnetic-field prediction at any arbitrary point in the solar-wind flow field. This was accomplished by consideration of a variety of special test cases in which the location in the flow field and the incident interplanetary magnetic-field orientation were systematically changed so as to produce both symmetric and antisymmetric changes in the resultant ionosheath magnetic field, as well as to reverse the roles of the perpendicular and normal components. All of these various permutations of the magnetic-field calculation procedure were successfully verified.

One of the primary objectives of the present work was to demonstrate the flexibility and generality of the present procedures by exercising them over a wide range of ionopause geometries and solar wind oncoming conditions so as to cover, insofar as possible, the entire range of practical interest of these parameters. These calculations were to be summarized in a convenient format and then archived so as to provide at-a-glance information regarding the variation of the flow-field and unit magnetic-field quantities. The output format selected was the automatic pen-plot output option of the program involving plots of the flow-field streamlines, and contours of the velocity magnitude $|\underline{v}|/v_\infty$, temperature T/T_∞ , density ρ/ρ_∞ , and the field-line locations and contours of the unit magnetic-field ratios $(|\underline{B}|/B_\infty)_n$ and $(|\underline{B}|/B_\infty)_t$.

The test cases selected for this catalog involved a ratio of specific heats $\gamma = 5/3$ and the following matrix of free-stream Mach numbers M_∞ and ionopause shapes:

$$\begin{aligned} M_\infty &= \{2.0, 3.0, 5.0, 8.0, 12.0, 25.0\} \\ H/R_O &= \{0.01, 0.10, 0.25\} \\ \bar{H}/R_O &= \{0.10, 0.20, 0.25\} \end{aligned}$$

Thus, a total of 36 separate cases were calculated. The plot output for these cases is provided in Appendix B, which also presents a convenient page index to the individual results. These archived results provide an very convenient means of determining the overall dependence of flow-field and magnetic-field quantities with M_∞ and obstacle shape, in particular the variation of bow shock location and flow-field contour changes. We note that the range of free-stream Mach numbers selected easily spans the entire range of solar-wind conditions usually encountered, while the different obstacle shapes provide a wide variation as well, as can be observed from figure 1.

The final and ultimate check of the current procedures lies in the comparison of the results predicted by the present model with data actually measured by a spacecraft. To that end, we have made a number of preliminary comparisons with data obtained from orbits 3 and 6 of the Pioneer-Venus Orbiter spacecraft.

The overall features of the spacecraft trajectory crossings of the solar-wind/Venus-ionosphere interaction region are provided in the sketch given in figure 12. In that figure, which is referred to the sun-Venus solar-ecliptic coordinate system, we note in particular the highly elliptic spacecraft orbit (periapsis ≈ 200 Km, apoapsis $\approx 66,000$ Km) and the crossings of the bow shock and ionopause surfaces. The oncoming solar-wind direction, with arbitrary azimuthal (aberration) and polar angles (Ω, ϕ_p) is as indicated, with the ionopause and bow shock surfaces symmetric about that direction. The oncoming arbitrary interplanetary magnetic field \vec{B} is also as indicated.

The procedural outline employed for the theoretical comparisons is as follows:

I. Orbital data selection

Select data from an orbit when solar-wind conditions are relatively steady.

II. Theoretical calculations

Input:

Ionospheric ρ and T versus altitude from orbiter retarding potential analyzer (ORPA)

Solar wind v_∞ , ρ_∞ , T_∞ from orbiter plasma analyzer (OPA)

Solar wind B_∞ from orbiter magnetometer (OMAG)

Trajectory coordinates

Output: (Contours and/or time histories along orbital trajectory)

Ionosheath ρ , T , y , B and their scalar components in solar ecliptic coordinates

III. Comparisons with Spacecraft data

Observational ionosheath data for ρ , $|y|$, T from OPA and for B from OMAG with two sets of theoretical predictions based on $\left\{ \begin{smallmatrix} \text{last} \\ \text{first} \end{smallmatrix} \right\}$ interplanetary solar-wind properties (v_∞ , T_∞ , ρ_∞ , B_∞) measured $\left\{ \begin{smallmatrix} \text{before} \\ \text{after} \end{smallmatrix} \right\}$ bow shock $\left\{ \begin{smallmatrix} \text{inbound} \\ \text{outbound} \end{smallmatrix} \right\}$ crossings.

First, the selection of the particular orbit for which theoretical calculations and data comparisons will be carried out must be made. This choice is based on spacecraft observations of the oncoming interplanetary solar wind, and for the cases reported here, the selections were made when conditions appeared relatively steady. In particular, the interplanetary conditions regarding solar-wind velocity, density, temperature and magnetic field based on the orbiter solar-wind plasma analyzer (OPA) and fluxgate magnetometer (OMAG) measurements just prior

to inbound bow shock crossing and immediately after outbound bow shock crossing were analyzed by the Pioneer-Venus investigators responsible for these instruments for a number of the initial orbits of the Pioneer-Venus spacecraft, and on this basis the selection of Orbits 3 and 6 were made.*

To initiate the theoretical calculations, information regarding both the ionospheric obstacle shape and the oncoming interplanetary conditions are required. The determination of the obstacle shape is based on measurements of atmospheric density and temperature as a function of altitude made by the orbiter retarding potential analyzer at (ORPA) locations interior to the ionopause boundary.** These measurements yield the variation of atmospheric pressure with altitude in the vicinity of ionopause altitudes. From this information, the value of the scale-height parameter from the atmospheric pressure model given by either eq. (29) or (30) can be determined. For Venus, it appears that the ionosphere/solar-wind interaction is such that the ionopause wraps tightly about the planet (ref. 10). Our calculations based on ORPA data for Orbits 3 and 6 indicate scale heights of approximately 200 Km, which yield a corresponding range of values for H and \bar{H} of $0.02 \leq H/R_0, \bar{H}/R_0 \leq 0.05$. We note that for such small values of scale height, the two ionospheric pressure models eqs. (29) and (30) yield essentially the same obstacle shape, as can be seen from figure 1. For the comparisons reported here for both Orbits 3 and 6, we have selected a value of $\bar{H}/R_0 = 0.03$. With regard to oncoming interplanetary conditions, we require as input the solar-wind bulk velocity v_∞ , density ρ_∞ , temperature T_∞ , and magnetic field B_∞ . The first three are provided by the orbiter plasma analyzer (OPA), while the magnetic field is given by the orbiter fluxgate magnetometer (OMAG). We note that the OPA provides either ion density and temperature or electron density and temperature, but not both simultaneously. For orbits 3 and

* Special thanks are due to J. H. Wolfe and J. P. Mihalov who provided information regarding the solar-wind plasma from OPA measurements (refs. 21,22) and to C. T. Russell, R. C. Elphic, and J. A. Slavin for magnetic-field information from OMAG measurements (refs. 23,24).

** Special thanks are due to W. C. Knudsen and K. Spenner for providing the ionospheric plasma information from ORPA measurements (refs. 10,11).

6, ion measurements were available and have been employed. Information regarding the oncoming direction of the solar wind, as given by the angles (Ω, ϕ_p) , defines the requisite coordinate rotations required to align the gasdynamic calculation in the oncoming solar-wind direction; while information of solar-wind speed, density, and temperature serve to define the oncoming gasdynamic Mach number required to initiate the gasdynamic calculations.

With this information, the detailed gasdynamic and unit magnetic-field calculations in the ionosheath region can be carried out. In order to provide an idea of the detail obtained by the present computational procedures in these calculations, we have displayed in figure 13 the flow-field grid for one of the gasdynamic flow solutions used in the data comparisons discussed below. The result shown is for $M_\infty = 3.0$, $\gamma = 5/3$ flow past an ionopause obstacle shape with $\bar{H}/R_O = 0.03$, and is shown carried to a downstream location of $X/R_O = 3.0$. The flow field properties $[\underline{v}/v_\infty, \rho/\rho_\infty, T/T_\infty]$ and the unit frozen magnetic-field ratios $[(B/B_\infty)_n, (B/B_\infty)_\perp, (B/B_\infty)_\parallel]$ are determined at each intersection of the grid lines, including the bow shock, stagnation streamline, and ionopause boundaries. The final output of the calculation consists of detailed flow-field and magnetic-field properties in the ionosheath region, both in terms of tabular output and plotted contours and time histories along the orbital trajectory of the velocity magnitude and components, density, temperature, and magnetic-field magnitude and components. Complete details are provided in section A.4 of the Computer User's Manual.

For the comparisons with spacecraft data, the most convenient portion of the output format are the time-history predictions along the spacecraft orbit. The observational data used for comparisons with the theoretical predictions in the ionosheath region include plasma density, velocity, and temperature from OPA measurements and magnetic field from OMAG measurements. For the theoretical predictions, two sets of results are usually generated based on $\begin{Bmatrix} \text{last} \\ \text{first} \end{Bmatrix}$ interplanetary solar-wind properties $(\underline{v}_\infty, T_\infty, \rho_\infty, B_\infty)$ measured $\begin{Bmatrix} \text{before} \\ \text{after} \end{Bmatrix}$ bow shock $\begin{Bmatrix} \text{inbound} \\ \text{outbound} \end{Bmatrix}$ crossing.

In figure 14, we have displayed some overall flow-field results for Orbit 6. Indicated in that figure are bow shock locations for the three combinations of free-stream Mach number M_∞ and plasma specific heat ratio γ , i.e. $(M_\infty, \gamma) = (13.3, 5/3), (13.3, 2), (3.0, 5/3)$ for flow about an ionopause with $\bar{H}/R_\odot = 0.03$. Also indicated are two sets of points $(-\odot-, -\square-)$ representing the spacecraft trajectory for orbit 6 as viewed in two solar-wind oriented coordinate systems. The trajectory indicated by the solid lines and circles $(-\odot-)$ is that based on the last measured direction $(\Omega, \phi_p) = (6.5^\circ, -1.4^\circ)$ of the interplanetary solar wind just prior to crossing the bow shock on the inbound leg, while the dashed line and squares $(--\square--)$ denotes the trajectory based on the first measured direction $(\Omega, \phi_p) = (4.9^\circ, 7.6^\circ)$ of the solar wind immediately after crossing the bow shock on the outbound leg. We note that the spatial location of the spacecraft trajectory in solar-wind coordinates depends only on the direction (Ω, ϕ_p) of the oncoming solar wind, but not on its magnitude. With regard to the results indicated in figure 14 for the spacecraft trajectory, we observe the extremely large dependence of spatial position of a trajectory point, as viewed in solar-wind coordinates, on solar-wind direction. For the particular inbound and outbound solar-wind angles indicated, the shift in X-coordinate of a trajectory point can be as high as a quarter of the Venusian planetary radius, which obviously results in substantial differences in predicted flow and magnetic-field properties. In previous work, the influence of the angular shift in the solar wind was generally considered to be small and negligible. The current results, however, indicate that this purely geometrical effect can be surprisingly large, even for directional shifts of less than 5° , and must be accounted for in any realistic theoretical comparison with data. See reference 7 for another example of the importance of this effect.

Finally, with regard to the three sets of bow shock results displayed in figure 14, these calculations represent an attempt to resolve the uncertainty in the oncoming free-stream Mach number and ratio of specific heats of the plasma. Because only solar-wind ion temperatures from the OPA were available for Orbit 6, the initial calculation of the free-stream Mach number was based on the assumption that $T_e = T_i$, which leads to $M_\infty = 13.3$. A ratio of specific heats $\gamma = 5/3$ was assumed, and these interplanetary values result in the bow shock indicated by the

dot-dash line. That shock location is in poor agreement with the observational shock crossings, indicated as occurring between the pairs of solid circles and squares. A separate uncertainty arises from the possibility that the magnetic field may act to align the plasma particle motion in its direction, thus effectively reducing the number of degrees of translational freedom from 3 to 2 and thereby increasing the ratio of specific heats from $5/3$ to 2. To investigate this possibility, we have repeated the $M_\infty = 13.3$ calculation using $\gamma = 2$. That result is indicated by the dashed line, and is in better but still not completely satisfactory agreement with the observed shock locations. Finally, if it is assumed that the oncoming interplanetary electron temperature is not equal to the ion temperature, but is substantially higher, we are lead to low Mach numbers of the order of $M_\infty \approx 3-5$. We have displayed bow shock results of a $M_\infty = 3.0$, $\gamma = 5/3$ calculation in figure 14 as the solid line, and observe that based on this Mach number and the inbound solar-wind direction, the observational shock crossings display very good agreement with the theoretical results.

Figure 15 displays the time-history comparisons of the theoretically-predicted bulk plasma density, speed and temperature in the ionosheath region with OPA measurements of these quantities. These theoretical results were based on a gasdynamic flow solution with $M_\infty = 13.3$, $\gamma = 2.0$. In these results, the solid lines with circles correspond to results based on inbound interplanetary conditions, while the dashed lines with squares correspond to outbound conditions. We note that while the few data points available are in general agreement with the theoretical calculations, the lack of more detailed plasma measurements in the ionosheath prevents a definitive conclusion. The OPA instrument requires approximately 9 minutes to acquire sufficient data to enable predictions of the bulk plasma quantities. While this time lag presents no problem when the spacecraft is in the interplanetary solar wind, the large resolution time effectively averages the plasma quantities in the ionosheath over such a large spatial range that only overall comparisons of the bulk plasma properties are possible.

The situation is quite different for the magnetic field, as the OMAG instrument provides essentially instantaneous magnetic-field measurements. Comparisons of the frozen magnetic-field predictions with data

are displayed in figures 16(a,b). These comparisons employ the gas-dynamic solution $M_\infty = 13.3$, $\gamma = 2$ for which plasma properties were given in figure 15. In figure 16a, we display two sets of theoretical calculations for the magnitude of the magnetic field, based on the inbound and outbound interplanetary magnetic field conditions as indicated on the figure. In these comparisons, we observe very good agreement with both sets of predictions. In particular, on the inbound leg, the theoretical predictions based on the inbound interplanetary conditions are in very good agreement with the data, while the outbound-condition predictions are clearly not as favorable. On the other hand, as we proceed in time along the outbound leg, the opposite is true. Here, the outbound-condition predictions are in very good agreement with the data, while the inbound-condition predictions are notably inferior, particularly with regard to shock crossing. Corresponding results for the magnetic-field components are provided in figure 16b, and display a similar behavior. The agreement of the theoretical results with data for the individual components is remarkable, confirming the accuracy of the frozen-field model, as well as the shift of the ionosheath magnetic field from a solution related to inbound interplanetary conditions to one related to outbound conditions.

For Orbit 3, similar comparisons as those shown in figures 14-16 for Orbit 6 are given in figures 17 to 19. In figure 17, we have provided the bow shock locations for five different combinations of M_∞ and γ as indicated. The Mach numbers $M_\infty = 7.38, 5.96$ correspond, respectively, to the inbound and outbound interplanetary conditions for $|\underline{v}_\infty|$, ρ_∞ , T_∞ as measured by the OPA, while the two values of $\gamma = 5/3, 2$ used in the calculations represent our uncertainty of the ratio of plasma specific heats. We have also indicated for reference the bow shock location for $M_\infty = 3.0$, $\gamma = 5/3$ as given previously in figure 14 for Orbit 6. Note that the observational shock crossings are again closest to the $M_\infty = 3.0$, $\gamma = 5/3$ shock. Also provided in figure 17 are the orbital trajectories as viewed in solar-wind coordinates for the inbound $(\Omega, \phi_p) = (3.3^\circ, 0.15^\circ)$ and outbound $(\Omega, \phi_p) = (3.7^\circ, 4.9^\circ)$ solar-wind directions.

The comparisons for the bulk plasma properties for Orbit 3 are provided in figure 18. Again we note an overall agreement for bulk plasma speed and density, but note an observable discrepancy in the temperature.

This is thought to be indicative of the manner in which the bulk properties from the theoretical model are being interpreted in relation to the observational measurements; i.e. the theoretical values correspond to those for a single-component plasma, while the measurements are in terms of a multi-component plasma. Whether the theoretical plasma properties require rescaling or reformulation, or whether their present formulation is appropriate for comparison with the multi-component data, appears to be a necessary and important subject for future study.

Results for the magnetic-field comparisons are displayed in figures 19(a,b), which provide time-histories of both the magnitude and the individual magnetic-field components based on both inbound and outbound interplanetary conditions. We note again, although the shock crossing comparisons are somewhat in disagreement since the gasdynamic flow fields used in these results were for $M_\infty = 7.56, 5.96$ and $\gamma = 2$, the reasonable comparisons are obtained for the ionosheath magnetic field. In particular, we observe the drift with time along the trajectory of the trajectory of the agreement of theory with data from the predictions based on inbound interplanetary conditions on the inbound leg, to those based on outbound conditions on the outbound leg.

In order to demonstrate the improvement obtained in magnetic-field results when a gasdynamic flow-field solution is employed which more closely agrees with the observational bow shock location, we have displayed in figure 20(a,b) the analogous time-history magnetic-field comparisons when using a $M_\infty = 3.0$, $\gamma = 5/3$ gasdynamic result. In this case, results were computed for only the inbound direction $(\Omega, \phi_p) = (3.3^\circ, 0.15^\circ)$ of the solar wind. As can be seen, there is a marked improvement in the agreement near the bow shock, and quite good agreement throughout the ionosheath as well as, for both the magnitude and the individual magnetic-field components. We note that the general agreement of theory and observation of the individual components demonstrates both the accuracy of the calculation and, in particular, the need for accounting in the theoretical results of the variable direction of the interplanetary solar wind.

CONCLUDING REMARKS

The application of advanced computational procedures was undertaken for the purpose of modeling the interaction of the solar wind with non-magnetic planets, with particular emphasis on Venus. Based on the successful theoretical model employed previously (ref. 9), i.e., the steady, dissipationless, magnetohydrodynamic model for axisymmetric, supersonic, super-Alfvénic solar-wind flow, a number of important theoretical extensions have been developed and included in the computational procedures. These include the capability for treating very low oncoming interplanetary gasdynamic Mach numbers ($M_\infty \approx 2.0$), as well as quite general ionopause shapes. A new family of ionopause shapes has been developed which includes the effect of gravitational variation in scale height, and has been incorporated in the computational program. Additionally, the capability for determining the plasma gasdynamic and magnetic-field properties along any arbitrary spacecraft trajectory, accounting for an arbitrary oncoming direction of the solar wind, has been developed. All of these developments have been incorporated into an assemblage of computer codes to enable detailed calculations of the solar-wind interaction with planetary atmospheres. The computer codes have been extensively documented and are described in a computer user's manual included as part of this report.

Comparisons are reported which verify the correctness of these new procedures, and which demonstrate their capability for computing a wide range of flows encompassing those typical of solar-wind conditions about terrestrial planetary atmospheres. A catalog of sample solar-wind flows covering a large number of flow conditions and ionopause geometries was established, and reported in summary format in the forms of contour plots of important flow-field and magnetic-field properties. Finally, successful comparisons of results from the theoretical model were made with actual spacecraft data obtained from initial orbits of the Pioneer-Venus Orbiter. These results have indicated the importance, heretofore largely neglected, of the directional variability of the oncoming solar wind. All of these results, taken in toto, serve to verify the basic theoretical model which underlies the present procedures. Furthermore, it demonstrates the value of the present computational procedures as a research tool capable of routinely providing - at small computation cost

and in a format directly compatible with experimental observations - details of the solar-wind/planetary atmosphere interaction process not previously attainable.

With regard to future uses as well as improvements of the present model, the obvious need for a detailed study involving comparisons between theory and observations for a large number of orbits of the Pioneer-Venus Orbiter is clear. Based on the preliminary comparisons for orbits 3 and 6, the frozen magnetic-field model appears to be remarkably accurate for relatively quiet-time conditions. Similar comparisons of the plasma properties indicate a need for an improved interpretation of the results from the single-fluid theory in terms of multi-component measurements. Questions regarding the possible suppression by the interplanetary magnetic field of the number of degrees of freedom of the plasma require further study and could be clarified through systematic comparisons with data. Additionally, observations from the Pioneer-Venus Orbiter of the nightside ionosphere of Venus have indicated a more complex and dynamic structure than suspected. These observations point, in particular, toward the need for improvement of the simple model used in the present method for the determination of the ionosphere boundary. This improved determination would involve an iterative procedure in which a balance of the sum of the solar-wind gasdynamic plus magnetic pressure along the ionopause surface would be maintained against the ionospheric pressure. The present method, which balances the Newtonian pressure distribution against the ionospheric pressure, represents the first step in this iteration.

ACKNOWLEDGEMENTS

Support for the research reported in this investigation was provided by National Aeronautics and Space Administration, Headquarters under Contract NASW-3182 with Robert Murphy as Technical Monitor. Special thanks are given to J. H. Wolfe and J. D. Mihalov for generously providing solar-wind plasma information from Pioneer-Venus Orbiter plasma analyzer measurements, to C. T. Russell and J. A. Slavin for magnetic field information from Pioneer-Venus Orbiter fluxgate magnetometer measurements, and W. C. Knudsen for ionosphere plasma information from Pioneer-Venus Orbiter retarding potential analyzer measurements.

APPENDIX A
COMPUTER PROGRAM USER'S MANUAL

APPENDIX A
COMPUTER PROGRAM USER'S MANUAL

TABLE OF CONTENTS

<u>Section</u>	<u>Page No.</u>
A.1 INTRODUCTION	53
A.2 PROGRAM DESCRIPTION	54
A.2.1 Calculation Procedure	56
A.2.1.1 Blunt-body calculation	56
A.2.1.2 Marching calculation	58
A.2.1.3 Streamline calculation	59
A.2.1.4 Magnetic-field calculation	61
A.2.1.5 Contour calculation and plot generation	64
A.2.1.6 Trajectory calculation	65
A.2.2 Rerun Option	70
A.2.3 Program Limitations and Precautions	70
A.2.4 Convergence Criteria for Blunt-Body Calculation	71
A.3 DESCRIPTION OF INPUT	72
A.3.1 Dictionary of Input Variables	72
A.3.2 Preparation of Input Data	77
A.3.3 Format of Input Data	81
A.4 DESCRIPTION OF OUTPUT	85
A.5 PROGRAM ERROR MESSAGES	87
A.6 SAMPLE CASE	90
FIGURES A.1 THROUGH A.6	92

This Page Intentionally Left Blank

APPENDIX A

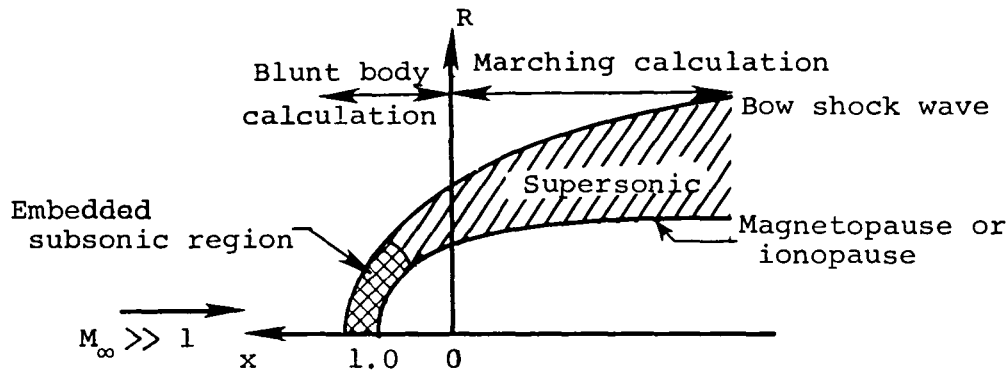
A.1 INTRODUCTION

The purpose of this appendix is to describe the operation of the assemblage of computer codes which were developed in conjunction with the theoretical work presented in this report and organized into one program, and to provide sufficient detail to permit understanding and use of the program. The program computes the flow field of the solar wind about a terrestrial planet, using a procedure for the calculation of supersonic/hypersonic flow about an axisymmetric blunt body. The corresponding frozen-in magnetic field is calculated from the previously-determined velocity and density fields. Streamlines and contour lines of various flow-field properties and magnetic-field components are also determined. Next, these flow-field and magnetic-field values are calculated for points along a user-specified trajectory.

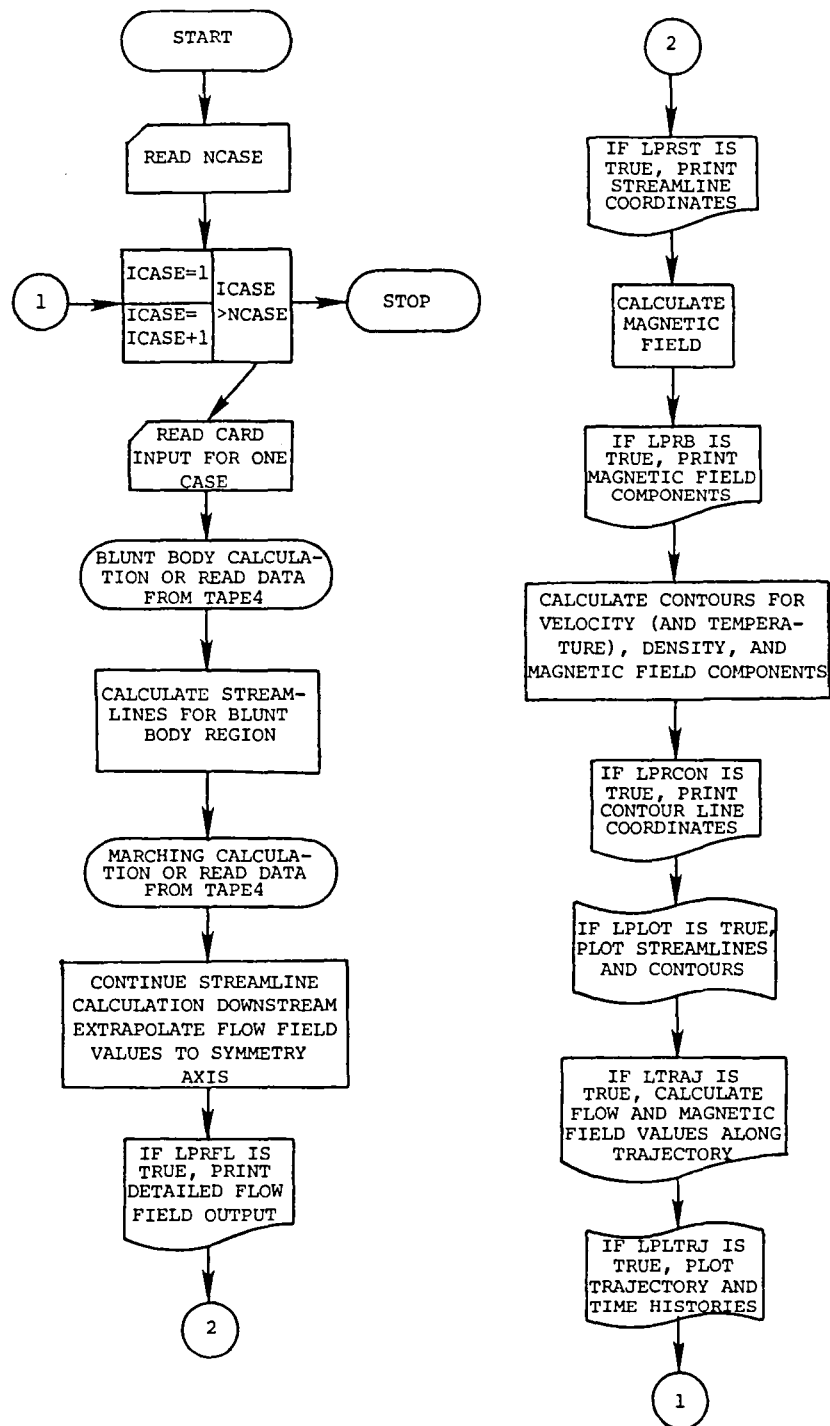
A description of the general operating procedure of the program is given, with descriptions of input and output. The program is written in FORTRAN IV and has been developed on a CDC 7600 computer. University Computing Company (UCC) Standard Plotting Software and Functional Software packages are used to produce automated plots. Files used, besides TAPE5 for INPUT and TAPE6 for OUTPUT, are TAPE1 for the plot file (system default), TAPE4 for input file for rerun option, and TAPE9 for storing data for rerun. Typical run times for cases using the default parameters are 110 to 120 seconds, using the OPT=2 compiler. For a case using the rerun option, which employs a previously-calculated flow field, the run time is approximately 15 seconds. The storage requirements are 146K₈ for small core memory and 273K₈ for large core memory.

A.2 PROGRAM DESCRIPTION

For computational purposes, the flow is subdivided into two regions, as indicated in the sketch below, with the center of the planet as origin.



The region near the nose of the magnetopause/ionopause includes all of the imbedded subsonic flow and part of the supersonic flow. An axisymmetric implicit unsteady Euler equation solver is used to calculate this part of the flow field. Using the solution plane at $x = 0.0$ to provide starting conditions, the flow field in the purely supersonic downstream region is determined by integrating the steady Euler equations using a spatial-marching procedure. Streamlines, the magnetic field, and contours are calculated using the entire flow field, distinguishing between the two regions as required by the different forms of the computational grids. A rerun capability is provided, where flow-field data is read from a file written on a previous run, rather than repeating the blunt-body and marching calculations. The computations proceed as shown in the sketch below, which provides an overall flow chart of the complete program. The program provides for several cases to be run consecutively.



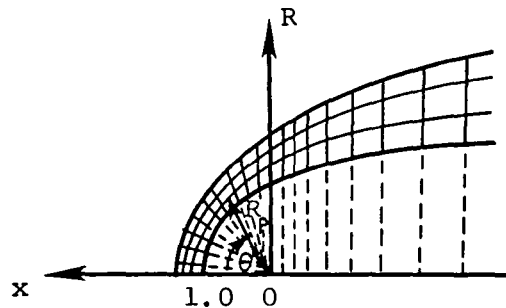
Program Flow Chart

A.2.1 Calculation Procedure

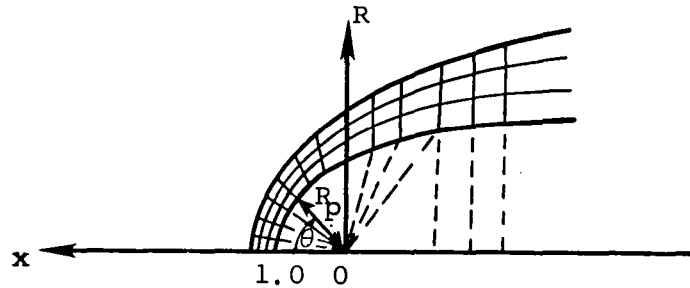
After reading in the number of cases in the run, each case is calculated independently. Subroutine INPUT reads in all card input required for one case, viz. a title, flow conditions, obstacle geometry, calculation and print control parameters, and desired contour values. The user may supply the obstacle geometry in the form of a shape table for an axisymmetric body, or use one of the default shapes which are calculated internally by the program. These default shapes are the magnetopause equatorial trace, constant scale-height ionopauses, and ionopauses having gravitational variation in scale-height. The input is printed as the first item of output.

A.2.1.1 Blunt-body calculation

A computational mesh in polar (R_p, θ) coordinates is established for the blunt-body calculation; then, for the marching calculation, this is extended into a cylindrical (x, R) system, as indicated below:



This method has proven effective except for certain obstacle shapes which have a significant amount of flaring at the terminator and/or cases involving low free-stream Mach numbers $M_\infty \leq 3$. Under such conditions, the axial component of velocity may become subsonic at the starting plane of a marching calculation (terminator) and the calculation cannot proceed. In this case the blunt-body grid must be extended past $\theta = 90^\circ$ as shown below:



The number of rays added to the blunt-body mesh is controlled by the input variable NXADD, and are limited by the requirement, $\text{NBLUNT} + \text{NXADD} \leq 39$.

All lengths, x , R , R_p , are normalized so that the nose of the obstacle is at $x = 1.0$. For the default shapes, rays at equal angular increments of $\Delta\theta$ are used, starting at $-\Delta\theta/2$, up to $90^\circ + \Delta\theta$, where $\Delta\theta = 90^\circ/(\text{NBLUNT}-1.5)$, and NBLUNT is an input parameter describing the number of angular mesh points to be used in the blunt-body calculation. Program default value is $\text{NBLUNT} = 24$, so that for the default mesh, $\Delta\theta = 4^\circ$. The obstacle shape is determined by integrating the appropriate differential equation by a trapezoidal predictor-corrector method. For a user-supplied shape, the θ grid is determined by rays from the origin through the first NBLUNT points, and the reflection of the first ray about the x -axis. Values for R_p are determined by dividing the line segments between the body and bow shock wave into $\text{NR}-1$ equal intervals. Thus, including the obstacle and bow shock wave, the grid forms NR arcs around the obstacle. A starting solution for the blunt-body calculation is obtained by guessing a bow shock shape and by prescribing a Newtonian pressure distribution on the body. Noting that the maximum entropy streamline wets the body, other flow properties on the body surface can then be calculated. An initial flow field is then established by linear interpolation between the obstacle and the guessed bow shock, where the Rankine-Hugoniot relations hold. The integration proceeds in time for ITER steps. The initial bow shock shape used for the magnetopause equatorial trace and for an

ionopause with $H/R_O \geq 0.1$ is a correlation shape depending on $(M_\infty, \gamma, H/R_O)$ and given by the parabola $R_p = \delta_1 \sqrt{\delta_O - x/\sqrt{\delta_O}}$ where

$$\delta_O = 1.0 + 1.1 \{[(\gamma-1)M_\infty^2 + 2]/(\gamma+1)M_\infty^2\} \times (0.9 + 0.5 H/R_O)$$

$$\delta_1 = \Delta_O \{ (1.273 + 0.009 M_\infty^2) (0.904 + 0.655 H/R_O) \\ \times [3.95 - 5.3 H/R_O + 3.85 (H/R_O)^2] \} + (R_{body})_{x=0.0}$$

$$\Delta_O = [(\gamma-1)M_\infty^2 + 2]/[(\gamma+1)M_\infty^2] \times 0.78$$

For a user-supplied obstacle shape and for an ionopause with $H/R_O < 0.1$, the initial shock shape used is the curve $R_p = \sqrt{[1 + \Delta_O (1 + 0.68 \theta^2 + 0.16 \theta^4)]}$. Information on convergence, the final sonic line locations, and the body and final bow shock shape are printed from this calculation.

The flow chart for the blunt-body code is shown in Figure A.1(a).

A.2.1.2 Marching calculation

The results at the $\theta = 90^\circ$ plane of the blunt-body calculation are used as starting conditions for the marching calculation, after proper variable normalization for the internal marching calculation. For default geometries, the obstacle shape is determined by integration of the appropriate differential equation proceeding from the nose downstream at equal θ increments to form a body-shape table. The stepsize along the x-axis is recalculated at every ICONST(49) with ICONST(49) being set to 10. At each x-location, R_{body} is determined by linear interpolation. The computational mesh is extended by adding the line perpendicular to the x-axis at each step, divided in the same manner as for the blunt nose. The calculation marches downstream with a maximum stepsize of 1.0 until the terminal location specified

by the user has been passed. However, the number of steps is limited to 75, after which the calculation will end regardless of the x-location. The coordinates of the obstacle and bow shock are printed at each step.

The grid coordinates and flow-field values are written to a file, TAPE9, which may be saved to use as input for a later run. This rerun option, which replaces construction of the computational mesh and performance of the blunt-body and marching calculations with the reading of the rerun input file TAPE4, is described in section A.2.2. The flow chart for the marching calculation is provided in figure A.1(b).

A.2.1.3 Streamline calculation

The streamlines are calculated in two sections, following each of the flow-field calculations. Using the results of the blunt-body calculation, i.e. the (x,R) grid coordinates, (R_p, θ) grid coordinates, density ρ/ρ_∞ , and velocity components v_X/v_∞ and v_R/v_∞ , the velocity magnitude $|v|/v_\infty$ and flow angle ϕ are calculated. Density ρ/ρ_∞ and velocity magnitude $|v|/v_\infty$ are first smoothed along the rays of constant- θ , using a third-degree least-squares fit with respect to R_p . Streamlines are then calculated downstream to $x = 0.0$, using the trajectory method and integrating through the velocity field by means of a third-order modified Euler integration procedure with the grid locations on the bow shock used as starting positions. The flow angle $\phi = \tan^{-1}(v_R/v_X)$ at each point is determined using bivariate linear interpolation first in θ , then R_p . Points for which $\theta < 0^\circ$ or $\theta > 90^\circ$ are discarded in the interpolation.

The marching calculation provides (x,R) grid coordinates, and values of density ρ/ρ_t , and velocity components v_X/v_t and v_R/v_t , where t denotes free-stream stagnation conditions. For compatibility with the blunt-body solution, the flow-field values are converted to ρ/ρ_∞ , v_X/v_∞ , v_R/v_∞ before calculating the resultant velocity magnitude

$|y|/v_\infty$ and flow angle ϕ . The streamline calculation is continued downstream, employing the same method as in the nose region. Starting positions on the shock wave for the streamline calculation in the marching zone are set at equal R-increments, with a maximum of 50 streamlines calculated. The flow angle is determined using bivariate linear interpolation first in x , then in R .

Along the symmetry axis, values of x , ρ/ρ_∞ , and $|y|/v_\infty$ are determined by extrapolation, using a third-order Lagrangian polynomial in θ on each arc of the computational grid. Exact values for the stagnation streamline are used where possible, viz. at the bow shock

$$\rho/\rho_\infty = (\gamma+1)M_\infty^2 / [(\gamma-1)M_\infty^2 + 2]$$

$$|y|/v_\infty = 1/(\rho/\rho_\infty)$$

at the body surface

$$\begin{aligned} \rho/\rho_\infty &= (\rho/\rho_\infty)_{\text{shock}} \cdot \left\{ \left[\left[(\gamma+1)M_\infty^2 \right]^2 / \left[4\gamma M_\infty^2 - 2(\gamma-1) \right] \right]^{1/(\gamma-1)} \right\} \\ |y|/v_\infty &= 0.0 \\ x &= 1.0 \end{aligned}$$

Detailed flow-field output may now be printed by subroutine FLOUT, with LPRFL as print control variable. In addition to grid coordinates, density, velocities and flow angle, values of temperature T/T_∞ and pressure P/P_∞ are output, where

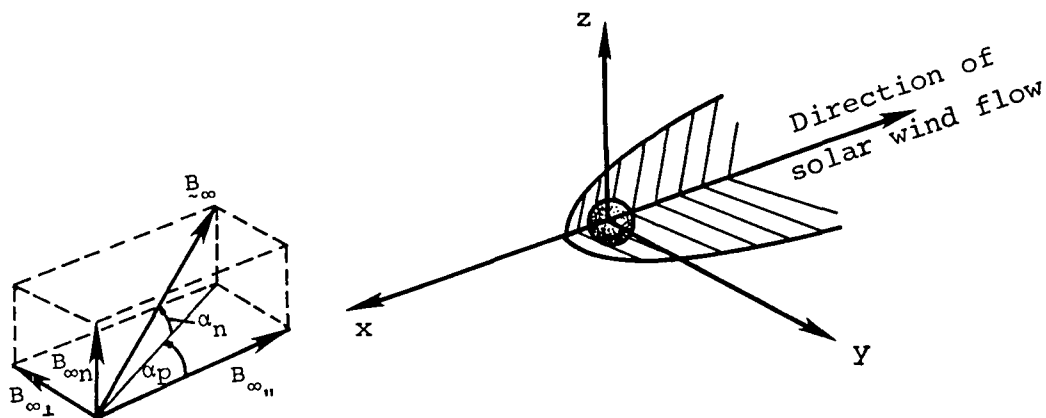
$$T/T_\infty = 1 + [(\gamma-1)/2] \cdot M_\infty^2 \cdot [1 - (|y|/v_\infty)^2]$$

$$P/P_\infty = (\rho/\rho_\infty) (T/T_\infty)$$

Streamline coordinates may also be printed by subroutine STOUT, with LPRST as print control variable. A plot of the streamlines is generated if the variable LPLLOT is true. A flow chart of the streamline calculation is shown in figure A.1(c).

A.2.1.4 Magnetic-field calculation

The magnetic field is determined by separately calculating the unit components whose directions are parallel, perpendicular, and normal to the flow, in the undisturbed solar wind. These components are then added vectorially, the resultant being expressed in orthogonal (x,y,z) components. The angles in the free stream α_p and α_n between the magnetic field and the flow, as shown in the sketch below, are either input or, in the case of a trajectory calculation, are calculated internally from the input interplanetary magnetic field.



The magnetic-field components are calculated using the following formulae in which \underline{e} signifies a vector of magnitude e in the direction of the component field line, and \hat{n} the unit normal vector.

$$\left(\frac{\underline{B}}{\underline{B}_\infty}\right)_{\parallel} = \left(\frac{\underline{v}}{v_\infty}\right)\left(\frac{\rho}{\rho_\infty}\right); \quad \left(\frac{\underline{B}}{\underline{B}_\infty}\right)_{\perp} = \left(\frac{\Delta\ell}{\Delta\ell_\infty}\right)\left(\frac{\rho}{\rho_\infty}\right); \quad \left(\frac{\underline{B}}{\underline{B}_\infty}\right)_n = \left(\frac{R}{R_\infty}\right)\left(\frac{\rho}{\rho_\infty}\right)$$

$$\left(\frac{\underline{B}}{\underline{B}_\infty}\right) = \left(\frac{\underline{B}}{\underline{B}_\infty}\right)_{\parallel} \left(\frac{\underline{B}_\infty}{\underline{B}_\infty}\right)_{\parallel} + \left(\frac{\underline{B}}{\underline{B}_\infty}\right)_{\perp} \left(\frac{\underline{B}_\infty}{\underline{B}_\infty}\right)_{\perp} + \hat{n} \left(\frac{\underline{B}}{\underline{B}_\infty}\right)_n \left(\frac{\underline{B}_\infty}{\underline{B}_\infty}\right)_n$$

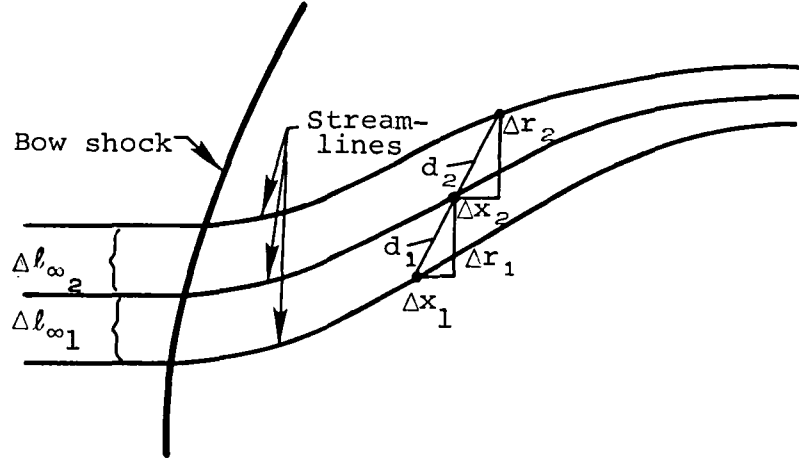
The magnetic-field line vector component $\underline{B}_{\parallel}$ which results from the interplanetary component $\underline{B}_{\infty\parallel}$ that is parallel to the undisturbed solar flow has local magnitude given by $(|\underline{v}|/v_\infty)(\rho/\rho_\infty)$, and the same local direction ϕ as the fluid flow. Determination of the normal magnetic-field component \underline{B}_n requires calculation of R/R_∞ , where R_∞ is the free-stream cylindrical R-ordinate of the streamline through the point under consideration. This is calculated by linearly interpolating in the local radial cylindrical coordinate R between the streamlines, with $R/R_\infty = 1.0$ along the x-axis. The magnetic-field vector component \underline{B}_{\perp} resulting from the interplanetary component $\underline{B}_{\infty\perp}$ which is perpendicular to the undisturbed solar-wind flow requires the distance vector $\Delta\ell/\Delta\ell_\infty$, whose magnitude is $|\Delta\ell|/\Delta\ell_\infty$ and direction is ψ , where $|\Delta\ell|/\Delta\ell_\infty$ is the stretching factor of the perpendicular field at the point, and ψ is the direction of the field line through the point. The magnitude and direction of $\Delta\ell/\Delta\ell_\infty$ are calculated according to

$$\frac{|\Delta\ell|}{\Delta\ell_\infty} = \frac{d_1 \cdot d_2}{d_1 + d_2} \cdot \frac{1}{\Delta\ell_{\infty 1} + \Delta\ell_{\infty 2}}$$

and

$$\psi = \frac{\tan^{-1} \left(\frac{\Delta r_1}{\Delta x_1} \right) \cdot d_2 + \tan^{-1} \left(\frac{\Delta r_2}{\Delta x_2} \right) \cdot d_1}{(d_1 + d_2)}$$

where the quantities d_1 , d_2 , Δx_1 , Δx_2 , Δr_1 , Δr_2 , $\Delta \ell_{\infty 1}$, and $\Delta \ell_{\infty 2}$ are described by the sketch below. The points marked (•) on the streamlines represent equal-time intervals in the flow.



The perpendicular field lines are determined by integrating $\int \underline{v} dt$ along each streamline, using trapezoidal integration to locate points along the streamline at regular increments in time, Δt , starting at a perpendicular field line ahead of the bow shock. Values for $|\Delta \underline{\ell}|/\Delta \ell_{\infty}$ and ψ are calculated at the points where the perpendicular field lines and streamlines intersect, interpolating only along the field lines. A generalized quadrilateral interpolation scheme is then employed to determine $|\Delta \underline{\ell}|/\Delta \ell_{\infty}$ and ψ at the computational grid points, using the quadrilateral containing the point formed by the intersection of pairs of adjacent streamlines and perpendicular field lines. At the bow shock, an exact formula is used, viz.

$$(|\Delta \underline{\ell}|/\Delta \ell_{\infty})^2 = 1 + \cot^2 \theta (1+D^2) - 2D \times \csc \theta \times \cot \theta \times \cos(\theta-\delta)$$

$$\psi = \theta + \sin^{-1}[D \times \cot \theta \times \sin(\theta-\delta)/(|\Delta \underline{\ell}|/\Delta \ell_{\infty})]$$

where

$$D^2 = 1 - 4(M_\infty^2 \sin^2 \theta - 1)(\gamma M_\infty^2 \sin^2 \theta + 1) / [(\gamma + 1)^2 M_\infty^4 \sin^2 \theta]$$

$$\cot \delta = \tan \theta \times \{(\gamma + 1) M_\infty^2 / [2(M_\infty^2 \sin^2 \theta - 1)] - 1\}$$

$$\theta = \tan^{-1} \left(\frac{dR_{\text{shock}}}{dx} \right)$$

The values of $|\Delta \underline{\ell}|/\Delta \ell_\infty$ at the grid points are smoothed using fifth-order least-squares fit with respect to arc length along the arcs of the grid. The resultant magnetic field can then be expressed in orthogonal (x,y,z) components. The code determines these components for the case when the field point is located in the (x,y) plane, i.e., z = 0. These components are given by

$$B_x/B_\infty = \cos \alpha_n \times [\cos \phi \times \cos \alpha_p \times (|\underline{B}|/B_\infty)_n + \cos \psi \times \sin \alpha_p \times (|\underline{B}|/B_\infty)_\perp]$$

$$B_y/B_\infty = \cos \alpha_n \times [\sin \phi \times \cos \alpha_p \times (|\underline{B}|/B_\infty)_n + \sin \psi \times \sin \alpha_p \times (|\underline{B}|/B_\infty)_\perp]$$

$$B_z/B_\infty = \sin \alpha_n \times (B/B_\infty)_n$$

Magnetic-field components may now be printed by subroutine BOUT, with LPRB as print control parameter. The magnetic field is not calculated when LPRB = .FALSE. and KBCON=0. A flow chart of the magnetic-field calculation is shown in figure A.1(d).

A.2.1.5 Contour calculation and plot generation

Contours are calculated for velocity $|\underline{v}|/v_\infty$, density ρ/ρ_∞ , and magnetic components $(|\underline{B}|/B_\infty)_n$, $(|\underline{B}|/B_\infty)_\perp$, and $(|\underline{B}|/B_\infty)_n$. The method used is a modified version of a procedure developed by R. Sorenson

of NASA/Ames Research Center. The boundary is searched for intervals which bracket a contour point. Having found one point, the remainder of the contour is determined by 'walking' around the contour, searching at each step for the interval through which the contour line next passes, until a boundary point is reached. Then closed contours are found in a similar manner. Linear interpolation is used throughout the process. Note that since T/T_∞ is a function of $|\underline{v}|/v_\infty$ only, velocity contours may also be considered as temperature contours. Temperature and velocity are related by the following function.

$$T/T_\infty = 1 + \frac{\gamma-1}{2} M_\infty^2 \left[1 - \left(\frac{|\underline{v}|}{v_\infty} \right)^2 \right]$$

The coordinates of the contour lines can be printed by subroutine CONOUT, with LPRCON as print control parameter.

The program segment which controls the generation of contour plots is accessed only when LPLOT = .TRUE. The UCC Plot Routines used to produce these plots are AXIS, CHAR, DASH, DOTLN, ENPLT, GREEK, MATH, NUMPLT, PLOT, PLTLN, POLAR, RESET, SCALF, and VECTOR. A flow chart of the contour calculation and plot generation in figure A.1(e).

A.2.1.6 Trajectory calculation

This segment of the program provides theoretical plasma and magnetic-field properties in an output form that is useful for direct comparison with actual spacecraft data. Given a sequence of coordinates describing the spacecraft trajectory, the program calculates the density, temperature, and velocity and magnetic-field components at each point. Generation of trajectory plots is controlled by the logical variable LPLTRJ. The trajectory calculation proceeds as follows.

Input to this calculation includes interplanetary values of temperature, density, velocity, and magnetic field together with

the trajectory coordinates. The trajectory input is required as a function of time and normalized by planetary radius. If the logical variable LSUN is TRUE, then it is assumed that the trajectory coordinates and vector quantities are expressed in terms of a sun-planet (ecliptic) coordinate system. In this case, these quantities are converted by the program into a solar-wind coordinate system by the transformation

$$\begin{pmatrix} x_w \\ y_w \\ z_w \end{pmatrix} = \begin{pmatrix} \cos \Omega \cos \phi_p & -\sin \Omega \cos \phi_p & \sin \phi_p \\ \sin \Omega & \cos \Omega & 0 \\ -\cos \Omega \sin \phi_p & \sin \Omega \sin \phi_p & \cos \phi_p \end{pmatrix} \begin{pmatrix} x_s \\ y_s \\ z_s \end{pmatrix}$$

where (x_w, y_w, z_w) are coordinates in the solar-wind system and (x_s, y_s, z_s) are coordinates in the sun-planet system. The angles Ω and ϕ_p are the azimuthal (total aberration) and polar angles, respectively. The azimuthal angle, Ω , is the angle in the plane of the ecliptic between the sun-planet line and the oncoming solar-wind, i.e., the x_s -axis and the x_w -axis as shown in figure A.2. The angle ϕ_p , positive for southward solar-wind flow, measures the deviation of the solar-wind from the plane of the ecliptic. Figure A.2 illustrates the transformation from sun-planet ecliptic coordinates to solar-wind coordinates. In this case the azimuthal and polar angles indicated are both positive.

If LSUN is FALSE, it is assumed that all input data are referenced to the solar-wind coordinate system and this transformation is not performed.

In order to conform with the internal flow-field and magnetic-field calculations, the signs of the x and y components of the trajectory and vector quantities are reversed. This is, in effect, another coordinate transformation which is defined by

$$\begin{pmatrix} x_c \\ y_c \\ z_c \end{pmatrix} = \begin{pmatrix} -1 & 0 & 0 \\ 0 & -1 & 0 \\ 1 & 0 & 1 \end{pmatrix} \begin{pmatrix} x_w \\ y_w \\ z_w \end{pmatrix} = \begin{pmatrix} -\cos \Omega \cos \phi_p & -\sin \Omega \cos \phi_p & \sin \phi_p \\ \sin \Omega & -\cos \Omega & 0 \\ -\cos \Omega \sin \phi_p & \sin \Omega \sin \phi_p & \cos \phi_p \end{pmatrix} \begin{pmatrix} x_s \\ y_s \\ z_s \end{pmatrix}$$

where (x_c, y_c, z_c) are coordinates referenced to the internal calculation system. This transformation is illustrated in figure A.3. Also shown in figure A.3 is the relationship of the interplanetary parallel, perpendicular, and normal magnetic field components to the internal calculation system. Specifically,

$$B_{\infty_{\parallel}} = B_{x_c}, \quad B_{\infty_{\perp}} = B_{y_c}, \quad \text{and} \quad B_{\infty_n} = B_{z_c}$$

The angles α_p and α_n are now calculated from the relationships

$$\alpha_p = \tan^{-1} \left(\frac{B_{y_c}}{B_{x_c}} \right)$$

and

$$\alpha_n = \tan^{-1} \left(\frac{B_{y_c}}{\sqrt{(B_{x_c})^2 + (B_{y_c})^2}} \right)$$

At this point, all data is in a form compatible with the internal calculations and the program can interpolate for flow and magnetic-field values along the trajectory. The following procedure is repeated at each trajectory point. Noting that the flow is axisymmetric, the coordinate system may be rotated to the most convenient orientation for the calculation. The present (x_c, y_c, z_c) coordinates are converted to (x_c, R) coordinates by a rotation in the (y_c, z_c) plane about the x_c -axis through the angle $\theta = \tan^{-1}[z_c/y_c]$. This rotation defines a new coordinate system (x', y', z') in which $z' = 0$. Subroutine IJRAJ now locates the point with reference to the computational flow-field grid. The point is either within the ionopause, in the grid

region, or beyond the bow shock. If the point is within the ionopause, all values are set to zero. If the point lies beyond the bow shock, all quantities assume their free-stream values. For points within the grid, the velocity magnitude, density, and flow angle ϕ are found by interpolation using function FTRAJ. From the flow angle ϕ and the rotation angle θ , velocity components in the (x_c, y_c, z_c) system can be calculated according to

$$\begin{aligned}v_{x_c} &= v \cos \phi \\v_{y_c} &= v \sin \phi \cos \theta \\v_{z_c} &= v \sin \phi \sin \theta\end{aligned}$$

Calculation of the magnetic field is complicated somewhat because the components are dependent on the incident magnetic field. Using α_p and α_n , B'_{x_∞} , B'_{y_∞} , and B'_{z_∞} are calculated in the rotated (x', y', z') system by

$$\begin{aligned}B'_{x_\infty} &= B_{x_{c_\infty}} \\B'_{y_\infty} &= B_{y_{c_\infty}} \cos \theta + B_{z_{c_\infty}} \sin \theta \\B'_{z_\infty} &= -B_{y_{c_\infty}} \sin \theta + B_{z_{c_\infty}} \cos \theta\end{aligned}$$

Then α'_p and α'_n are defined by

$$\alpha'_p = \tan^{-1} \left(\frac{B'_{y_\infty}}{B'_{x_\infty}} \right) \text{ and } \alpha'_n = \tan^{-1} \left[\frac{B'_{z_\infty}}{\sqrt{(B'_{x_\infty})^2 + (B'_{y_\infty})^2}} \right]$$

Interpolation is then carried out to determine the magnetic angle ψ and the ratios $\left| \frac{\tilde{B}}{B_\infty} \right|_{\parallel}$, $\left| \frac{\tilde{B}}{B_\infty} \right|_{\perp}$, and $\left(\frac{B}{B_\infty} \right)_n$ in the rotated system again using the function FTRAJ. Next, the magnetic-field components B'_x , B'_y , B'_z in the rotated system are calculated from

$$B'_x = \cos \alpha'_n \left[\cos \phi \cdot \cos \alpha'_p \cdot \left| \frac{\tilde{B}}{B_\infty} \right|_{\parallel} + \cos \psi \cdot \sin \alpha'_p \cdot \left| \frac{\tilde{B}}{B_\infty} \right|_{\perp} \right] \cdot B_\infty$$

$$B'_y = \cos \alpha'_n \left[\sin \phi \cdot \cos \alpha'_p \cdot \left| \frac{\tilde{B}}{B_\infty} \right|_{\parallel} + \sin \psi \cdot \sin \alpha'_p \cdot \left| \frac{\tilde{B}}{B_\infty} \right|_{\perp} \right] \cdot B_\infty$$

$$B'_z = \sin \alpha'_n \cdot \left(\frac{B}{B_\infty} \right)_n \cdot B_\infty$$

Finally, these magnetic-field components are rotated back through the angle θ to yield magnetic-field components referenced to the internal calculation system (x_c, y_c, z_c) by

$$\begin{pmatrix} B_{x_c} \\ B_{y_c} \\ B_{z_c} \end{pmatrix} = \begin{pmatrix} 1 & 0 & 0 \\ 0 & \cos \theta & -\sin \theta \\ 0 & \sin \theta & \cos \theta \end{pmatrix} \begin{pmatrix} B'_x \\ B'_y \\ B'_z \end{pmatrix}$$

Subroutine TROUT now prints the trajectory output in both the solar-wind (x_c, y_c, z_c) and the sun-planet (x_s, y_s, z_s) coordinate systems using the transformation below to obtain sun-planet magnetic-field vector components from solar-wind magnetic-field vector components.

$$\begin{pmatrix} B_{x_s} \\ B_{y_s} \\ B_{z_s} \end{pmatrix} = \begin{pmatrix} -\cos \Omega \cos \phi_p & \sin \Omega & -\cos \Omega \sin \phi_p \\ \sin \Omega \cos \phi_p & -\cos \Omega & \sin \Omega \sin \phi_p \\ \sin \phi_p & 0 & \cos \phi_p \end{pmatrix} \begin{pmatrix} B_{x_c} \\ B_{y_c} \\ B_{z_c} \end{pmatrix}$$

The transformation of the solar-wind velocity components (v_{x_c} , v_{y_c} , v_{z_c}) into sun-planet components (v_{x_s} , v_{y_s} , v_{z_s}) is also done using the same transformation.

Finally, if LPLTRJ is true, a file of trajectory plots is created. A flow chart for this program segment is shown in figure A.1(f).

A.2.2 Rerun Option

The rerun option is used when LRERUN = .TRUE. The blunt-body and marching calculations are replaced with the reading of grid coordinates and flow-field values from the rerun file, TAPE4, which contains data written to TAPE9, then saved, on a previous run. Different values for any parameter not used in the flow-field calculations may be specified, viz. contour values, plot length, magnetic-field angles, and output options. Values of AMACH, GAMMA, and HRO are required input, to ensure that the input rerun file does contain the case desired for rerun. If the geometry is user-supplied, the body-shape table will be read from TAPE4, and should not be input from cards.

After reading the card input, MACH, GAMMA, and HRO are tested against values from TAPE4. The grid coordinates and flow-field values from the blunt-body calculation are read in, then smoothed, and streamlines calculated for this region, as previously described. The results of the marching calculation are then read, and the streamline calculation continued downstream. The calculations then proceed as described in section A.2.1.

A run must not contain more than one case which uses the rerun option.

A.2.3 Program Limitations and Precautions

The program makes some assumptions about the geometry of the obstacle shape around which flow is to be calculated, and about the

flow field. The obstacle shape is assumed to be monotonically increasing in cylindrical radius R , going downstream. The nose of the obstacle is at $x = 1.0$. The origin of the (x,R) coordinate system is the center of the planet. Obstacle shapes with sharp corners should be avoided. In the magnetic-field calculation, the first streamline is assumed to be inside the arc described by the grid points immediately off the body, downstream of $x = 0.0$. To reduce computational costs, a grid using $NR = 10$ may be used, in which case a lower value of CN may be required. This would reduce the running time by approximately 40 percent. A free-stream Mach number less than 2.0 is not advised.

A.2.4 Convergence Criteria for Blunt-Body Calculation

The output provides two measures of the convergence of the blunt-body calculation. The RMS of shock speed and maximum shock speed are printed at each iteration. These quantities should both tend to zero as the iterations proceed. A value for q_{RMS} , RMS of shock speed, of

$$q_{RMS} < \sqrt{\gamma} \times M_{\infty} \times 10^{-3}$$

where γ is the specific heat ratio, and M_{∞} is the free-stream Mach number, usually indicates a converged solution. The RMS of error in enthalpy, HT , should be less than 1 percent, with the maximum enthalpy error also of that order.

The Courant number, CN , determines the time step size used by the calculation. A value not greater than the default of 3.0 should be used. For low Mach numbers or a coarser mesh than the default grid, a lower value may be preferable. If the default value does not generate a converged solution, or if the error message from subroutine SHOCK is printed, try lowering CN in increments of 0.5 to find a better value of CN . User-supplied bodies may also require a lower Courant number.

A.3 DESCRIPTION OF INPUT

This section describes the card input for the program. An alphabetized dictionary of input variables is provided, defining the variables, listing default values and limitations. A discussion of the preparation of the card input is then presented, followed by a description of the input card format.

A.3.1 Dictionary of Input Variables

- AMACH free-stream Mach number; $3.0 \leq \text{AMACH} \leq 25.0$ is recommended
- ANGN the angle, in degrees, measuring the deviation of the free-stream magnetic field from the plane in which $B_{\infty n}$ and $B_{\infty \perp}$ lie; equal to $\tan^{-1} \left(B_{\infty n} / \sqrt{|B_{\infty n}|^2 + |B_{\infty \perp}|^2} \right)$; see figure A.3, measured in the (x_c, y_c, z_c) coordinate system; only specified when interplanetary magnetic-field components not specified.
- ANGP the angle, in degrees, measuring the deviation of the in-plane magnetic component ($B_{\infty n} + B_{\infty \perp}$) from the direction of flow; equal to $\tan^{-1} (B_{\infty n} / B_{\infty \perp})$; see figure A.3, measured in the (x_c, y_c, z_c) coordinate system; only specified when interplanetary magnetic-field components not specified.
- AZANG angle in the ecliptic plane between the sun-planet line and the direction of solar-wind flow. See figure A.2 for positive direction.
- BCON(I) KBCON-dimensional array specifying values to be used for magnetic field strength contours
- BINF magnetic field strength free-stream value; set to 1.0 if plots desired in nondimensionalized units.

BX1	x_s -component of interplanetary magnetic field; referred to sun-planet coordinates
BY1	y_s -component of interplanetary magnetic field; referred to sun-planet coordinates
BZ1	z_s -component of interplanetary magnetic field; referred to sun-planet coordinates
CN	Courant number used for blunt-body calculation; program default value is 3.0
GAMMA	ratio of plasma specific heats
HRO	obstacle geometry indicator: HRO > 0. - ionopause with $H/R_o = HRO$ HRO = 0. - magnetopause equatorial trace HRO < 0. - geometry is user-supplied
ITER	integer, number of iterations for blunt-body calculation; program default value is 300
KBCON	integer, number of values specified for magnetic-field contours; $0 \leq KBCON \leq 20$
KRCON	integer, number of values specified for density contours; $0 \leq KRCON \leq 20$
KVCON	integer, number of values specified for velocity magnitude contours; $0 \leq KVCON \leq 20$
LGRAV	logical variable indicating whether default ionopause is calculated with gravitational variation in scale height FALSE - no TRUE - yes

LPLOT	logical variable indicating whether to create plots or plot file FALSE - no TRUE - yes
LPLTRJ	logical variable indicating whether to create trajectory and time history plots FALSE - no TRUE - yes
LPRB	logical variable indicating whether to print magnetic field output FALSE - no TRUE - yes
LPRCON	logical variable indicating whether to print coordinates of contours lines FALSE - no TRUE - yes
LPRFL	logical variable indicating whether to print detailed flow- field output FALSE - no TRUE - yes
LPRST	logical variable indicating whether to print coordinates of streamlines FALSE - no TRUE - yes
LRERUN	logical variable indicating whether this case uses rerun option FALSE - perform blunt-body and marching calculations TRUE - read results of a previous calculation from TAPE4

LRSTRT logical variable indicating whether to use previous shock shape as initial guess for blunt body
 TRUE - use shock shape from previous solution.
 (Must have a full solution as an earlier run in same job.)
 FALSE - use default initial guess for shock shape

LSUN logical variable indicating whether trajectory input is referenced to sun-planet coordinate system
 FALSE - trajectory input in solar-wind coordinates
 TRUE - trajectory input in sun-planet coordinates

LTRAJ logical variable indicating whether to perform a trajectory calculation
 TRUE - trajectory calculation, data provided
 FALSE - no trajectory calculation

MARKT(I) NMARKT - dimensional array specifying points to be marked for cross reference. If $K = \text{NMARKT}(I)$, the K th point of the trajectory is to be marked.

NBLUNT integer, number of angular mesh points for blunt-body calculation; for user-supplied geometry, $\text{XX}(\text{NBLUNT}-1)=0.0$; program default value, and maximum, is 24

NBOD integer, number of points in body-shape table when geometry is user-supplied; $1 \leq \text{NBOD} \leq 100$

NCASE integer, number of cases to be run consecutively; $\text{NCASE} > 1$

NMARKT integer, numbered values specified for cross reference points; $0 \leq \text{NMARKT} \leq 12$.

NR integer, number of radial mesh points; program default value, and maximum, is 19

NTRAJ	integer, number of points specified in trajectory table
NXADD	integer, number of points to be added to blunt-body grid past $\theta = 90^\circ$, default value is 0.
POLANG	angle, measured in degrees, between the plane of the ecliptic and direction of solar-wind flow; positive for southward flow; see figure A.2
RCON(I)	KRCON - dimensional array specifying values to be used for density contours
RHOINF	density-free stream value; set to 1.0 if plots desired in nondimensional units
RPLNT	radius of planet in units of nose radius, R_{PLNT}/R_O
RR(I)	NBOD - dimensional array representing the R-locations, in cylindrical (x,R) coordinates, of the user-supplied body shape; in units of nose radius
TITLE	descriptive heading of the case, to be printed on the first page of output; may contain up to 80 characters, including blanks
TMPINF	free-stream temperature; set to 1.0 if plots desired in nondimensional units
TTRAJ(I)	NTRAJ - dimensioned array specifying time locations of trajectory points
VCON(I)	KVCON - dimensional array specifying values to be used for velocity contours

VINF free-stream velocity; set to 1.0 if plots desired in non-dimensional units

XCALC terminal downstream x-location for marching calculation of flow field; $XCALC < 0.0$; program default value is -1.0

XPLOT terminal downstream x-location for calculation of streamlines, magnetic field, and contours; $XCALC \leq XPLOT \leq 0.0$; program default value is -1.0

XTRAJ(I) NTRAJ - dimensioned array specifying x_s -locations of trajectory points; in units of planetary radius; when (ANGP,ANGN) are specified, XTRAJ(I) is referred to solar-wind x_c -locations; see figures A.2 and A.3

XX(I) NBOD - dimensional array representing the x-locations, in cylindrical (x,R) coordinates, of the user-supplied body shape; in units of nose radius. See figures A.2 and A.3

YTRAJ(I) NTRAJ - dimensioned array specifying y_s -locations of trajectory points; in units of planetary radius; when (ANGP,ANGN) are specified, YTRAJ(I) is referred to solar-wind y_c -locations; see figures A.2 and A.3

ZTRAJ(I) NTRAJ - dimensioned array specifying z_s -locations of trajectory points; in units of planetary radius; when (ANGP,ANGN) are specified, ZTRAJ(I) is referred to solar-wind z_c -locations; see figures A.2 and A.3

A.3.2 Preparation of Input Data

The card input for a run consists of one card containing the number of cases to be run consecutively, Item 0, followed by a set of input for each case, Item 1 through Item 7, and Item 8 if required. Where a default value is to be used, the input field should be left blank.

For each case, all required variables which do not assume their default values should be specified. The input format for all cards is described in section A.3.3.

Item 0 - This item consists of one card, containing the number of cases in this run, NCASE.

Item 1 - This card provides identification of the case, TITLE, which is printed on the first page of the output for this case.

Item 2 - This card contains information on the flow conditions and body geometry, and parameters required for the blunt-body and marching calculations. AMACH, GAMMA, and HRO must be specified for each case. For the rerun option, the values are tested against the values from the rerun file. The parameters XCALC, NR, NBLUNT, CN, ITER are used only when the flow field is to be calculated. These variables each assume a default value if the input field is blank.

Item 3 - This item consists of one card containing the rerun indicator, LRERUN, the output control variables LPRFL, LPRST, LPRCON, LPRB, and LPLOT, the trajectory indicator LTRAJ, and the restart indicator LRSTRT.

Item 4 - This card contains the variables XPLOT, ANGP, ANGN, NXADD, and LGRAV. The value for XPLOT is changed by the program to be the x-location of the marching calculation immediately upstream of the input value for XPLOT. The angles describing the deviation of the magnetic field from the flow, ANGP and ANGN, are not required when LPRB = .FALSE; KBCON = 0, and LTRAJ = .FALSE. since the magnetic field is not calculated under these conditions. ANGP is the angle between the vectors $(\underline{B}_{\infty n} + \underline{B}_{\infty \perp})$ and \underline{v}_{∞} , while ANGN is the angle between \underline{B}_{∞} and $(\underline{B}_{\infty n} + \underline{B}_{\infty \perp})$, where $\underline{B}_{\infty n}$, $\underline{B}_{\infty \perp}$, $\underline{B}_{\infty n}$ are the components of the free-stream magnetic field, \underline{B}_{∞} , which are parallel, perpendicular, and normal to \underline{v}_{∞} , and are as indicated in figure A.3. The two angles ANGP and ANGN fully determine the half plane for which the magnetic field

is to be calculated. The magnetic field for the other half of the plane may be calculated by rerunning with the sign of ANGP reversed. When $(B_{\infty n} + B_{\infty 1}) = 0$, $ANGN = \pm 90^\circ$, $ANGP = 0^\circ$; and, when $B_{\infty n} = 0$, $ANGN = 0^\circ$. Note that ANGP and ANGN are referenced to the (x_c, y_c, z_c) system and are specified only when the interplanetary magnetic-field components are not specified.

If both LTRAJ = .TRUE. and LSUN = .TRUE., then ANGP and ANGN are calculated internally from the interplanetary magnetic-field components BX1, BY1, and BZ1.

Item 5 - This item contains the values for the velocity contours. The first card contains KVCON, the number of values specified for VCON. If KVCON > 0, the contour values are then read. Up to three cards may be required to accommodate the values, eight per card, maximum of 20. The contour values should be monotonically increasing, with at least one value within the range of the magnitude of the velocity in the region for which contours are to be calculated.

Item 6 - This item contains the values for the density contours. The description is similar to that for Item 5, with KRCON being the number of values specified, and RCON the array of values.

Item 7 - This item contains the values for the magnetic-field contours. The description is similar to that for Item 5, with KBCON being the number of values specified, and BCON the array of values. Note that the same contour values are used for the parallel and perpendicular components.

Item 8 - This optional item is required when HRO < 0.0 and LRERUN = .FALSE., and contains the body-shape table for the user-supplied geometry. The first card contains NBOD, the number of points in the shape table. The next NBOD cards contain the cylindrical (x,R) coordinates of these points, [XX(I), RR(I)], one point per card. The points supplied by the user determine the θ -spacing of the mesh used for the

blunt-body calculation. The first point should be near, but not on, the x-axis. A suggested location is such that the θ -spacing between the first point and the x-axis is half the θ -spacing between the first two points. The blunt-body calculation adds a point which is the reflection about the x-axis of the first point in the body-shape table. The (NBLUNT-1)th point should be at $x = 0.0$. The BLUNTth point is also used to create the grid for the blunt-body calculation. The coordinates must be normalized so that the planet center is at (0.,0.) and the nose of the body at (1.,0.).

Item 9 - This optional item is read only when LTRAJ is TRUE. The first card contains NTRAJ, the number of points in the trajectory. Then follows NTRAJ cards, each containing the time T, and location (x_s, y_s, z_s) of one point. The time values should be monotonically increasing. At present, $NTRAJ \leq 100$ is required. Note that when ANGP and ANGN are specified, the trajectory is specified in (x_c, y_c, z_c) coordinates.

Item 10 - This item is read only when LTRAJ is TRUE. The variable LPLTRJ indicates whether plots are to be produced of the trajectory and time histories. The relative size of the planet to the ionopause is given by RPLNT, which may be 0.0, in which case, a value of 1.0 is assumed in the calculations, but the planet is not drawn on the plots. Next are the four free-stream values $v_\infty, T_\infty, \rho_\infty, B_\infty$. If the plots are desired to be in nondimensional units, any or all of these values may be input as 1.0. Each quantity must have a value, zero is not permissible.

Item 11 - This item is read only when LTRAJ is TRUE. The first card contains NMARKT, the number of values specified for MARKT, (presently maximum of 12). If NMARKT = 0, only this card is required. If NMARKT > 0, the values of MARKT are read, 8 per card.

Item 12 - This item, which includes the variables LSUN, AZANG, POLANG, BX1, BY1, and BZ1, is read only when LTRAJ is true.

A.3.3 Format of Input Data

Four format types are used for the input data. For real numbers (F-format), a decimal point is required. Integers (I-format) should be right-adjusted in the field. For logical variables (L-format), the first non-blank character in the field, which should be 'T' or 'F', determines the value. Note that a blank input field is interpreted as 'FALSE'. The title, which is in A-format, may contain any valid character.

A description of the card format of the input data follows, with item numbers corresponding to those in section A.3.2:

Item No. 0: 1 card

Variable	NCASE
Card Column	10
Format type	I

Item No. 1: 1 card

Variable	Title
Card Column	80
Format type	A

Item No. 2: 1 card

Variable	AMACH	GAMMA	HRO	XCALC	NR	NBLUNT	CN	ITER
Card column	10	20	30	40	50	60	70	80
Format type	F	F	F	F	F	F	F	F

Item No. 3: 1 card

Variable	LRERUN	LPRFL	LPRST	LPRCON	LPRB	LPLOT	LTRAJ	LRSTRT
Card column	10	20	30	40	50	60	70	80
Format type	L	L	L	L	L	L	L	L

Item No. 4: 1 card

Variable	XPLOT	ANGP	ANGN	NXADD	LGRAV
Card column	10	20	30	40	50
Format type	F	F	F	N	L

Item No. 5: a) 1 card

Variable	KVCON
Card column	10
Format type	I

b) 0 to 3 cards as needed for up to 20 values, 8 per card

Variable	VCON(1)	VCON(2)			VCON(KVCON)			
Card column	10	20	30	40	50	60	70	80
Format type	F	F	F	F	F	F	F	F

Item No. 6: a) 1 card

Variable	KRCON
Card column	10
Format type	I

b) 0 to 3 cards

Variable	RCON(1)	RCON(2)			RCON(KRCON)			
Card column	10	20	30	40	50	60	70	80
Format type	F	F	F	F	F	F	F	F

Item No. 7 a) 1 card

Variable	KBCON
Card column	10
Format type	I

b) 0 to 3 cards

Variable	BCON(1)	BCON(2)			BCON(KBCON)			
Card column	10	20	30	40	50	60	70	80
Format type	F	F	F	F	F	F	F	F

Item No. 8 a) 1 card (this item required only when HRO < 0.0 and LRERUN = .FLASE.)

Variable	NBOD
Card column	10
Format type	I

b) NBOD cards

XX(I)	RR(I)
10	20

Item No. 9: a) 1 card (this item read only when LTRAJ is TRUE)

Variable	NTRAJ
Card column	10
Format type	I

b) NTRAJ cards

Variable	TTRAJ(I)	XTRAJ(I)	YTRAJ(I)	ZTRAJ(I)
Card column	10	20	30	40
Format type	F	F	F	F

Item No. 10: 1 card (this item read only when LTRAJ is TRUE)

Variable	LPLTRJ	RPLNT	VINF	RHOINF	TMPINF	BINF
Card column	10	20	30	40	50	60
Format type	L	F	F	F	F	F

Item No. 11: a) 1 card (this item read only when LTRAJ is TRUE)

Variable	NMARKT
Card column	10
Format type	I

b) 0-2 cards

Variable	MARKT(1)	MARKT(2)			MARKT(NMARKT)		
Card column	10	20	30	40	50	60	70
Format type	I	I	I	I	I	I	I

Item No. 12: 1 card (this item read only when LTRAJ is TRUE)

Variable	LSUN	AZANG	POLANG	BX1	BY1	BZ1
Card column	10	20	30	40	50	60
Format type	L	F	F	F	F	F

A.4 DESCRIPTION OF OUTPUT

This section describes the output of the computer program. The contents of each output item are specified and discussed. The printed output consists of seven items, five of which are optional and are controlled with input parameters. Plotted output is also optional.

The first output item consists of a banner page and the input data. The input is presented in two forms: first, as images of the input cards, and then with identification of each variable. Default values are printed as if they were input. Parameters CN, NR, NBLUNT, ITER for the blunt-body calculation and XCALC, the terminal location for the marching calculation, are printed only when the flow field is to be calculated. When the obstacle geometry is user-supplied, the input body-shape table is printed. For a default geometry, the body shape is indicated by the description "default ionopause shape for constant scale height with $H/R_0 =$ ", or "default ionopause shape with gravitational variation in scale height, $H/R_0 =$ ". Trajectory input is printed only when LTRAJ is true.

The second output item is not printed when LRERUN = .TRUE. From the blunt-body calculation, the shock speed at each iteration, the final enthalpy error, final sonic-line location, and body and final bow-shock shape are printed. For the marching calculation, the downstream x-location and body and shock ordinates are output. There is no control variable allowing the user to suppress this item of output when the flow field is calculated.

Detailed flow-field output is the third item, and is printed only when LPRFL = .TRUE. Coordinates are labeled as X/D, R/D, RP/D, or X/R₀, R/R₀, RP/R₀, to emphasize that distances are normalized by the distance from the center of the planet to the nose of the body, D for the magnetopause, R₀ for an ionopause. Along the symmetry axis, the values printed are velocity magnitude V/V_{INF}, density RHO/RHO_{INF},

temperature T/T_{INF} , and pressure P/P_{INF} . Over the rest of the flow field, values are also given for velocity components VX/V_{INF} , VR/V_{INF} , and flow angle ϕ . Note that the flow angle is the deviation of the flow about the obstacle, and so $0^\circ \leq \phi \leq 90^\circ$.

The next output item is the (x,R) coordinates of the streamlines. For blunt-body region, the (R_p, θ) coordinates of the starting position on the bow shock wave are also given. This item is printed only when $LPRST = .TRUE.$

The magnetic-field components are then printed, if $LPPRB = .TRUE.$ The location of each point is defined in (R_p, θ) coordinates for the blunt-body region, and (x,R) coordinates for the downstream marching region. The components along field lines parallel, perpendicular, and normal to the flow in the free stream are printed as $B/B_{INF}(PARALLEL)$, $B/B_{INF}(PERP)$, $B/B_{INF}(NORMAL)$. The orthogonal (x_c, y_c, z_c) components of the resultant are printed as $BX/B_{INF}(RESULTANT)$, $BY/B_{INF}(RESULTANT)$, $BZ/B_{INF}(RESULTANT)$. The magnetic field in the symmetry (x_c, y_c) plane, defined by the vector sum $[(\underline{B}/B_\infty)_\parallel + (\underline{B}/B_\infty)_\perp]$, is also printed, and is given by the magnitude $B/B_{INF}(IN-PLANE)$ and direction $B-ANGLE(IN-PLANE)$ of the vector. We note, as pointed out in the text, that the orthogonal magnetic-field components printed here correspond to those in the (x_c, y_c) plane, i.e., $z_c = 0$.

The next item printed is the (x_c, R) coordinates of the contours, for which $LPRCON$ is the logical control variable. Noting that temperature and velocity contours coincide, the corresponding value of T/T_{INF} is printed along with V/V_{INF} for the velocity contours. There are three nonfatal error messages which may occur - see section A.5.

Trajectory output is the last item to be printed. This output is presented first in terms of the solar-wind coordinate system (x_c, y_c, z_c) , and then in terms of sun-planet coordinates (x_s, y_s, z_s) .

The trajectory coordinates are printed as a function of time and are shown normalized by both R_0 and the planetary radius. Next, flow and magnetic-field components are printed for each trajectory point. This output is presented in both nondimensional and dimensionalized forms and includes $|\underline{v}|$, v_x , v_y , v_z , density, temperature, $|\underline{B}|$, B_x , B_y , and B_z .

The program also has the capability to produce two sets of plotted output using UCC plot routines AXIS, CHAR, DASH, DOTLN, ENPLT, GREEK, MATH, NUMPLT, PLOT, PLTLN, POLAR, SCALE, and VECTOR. The first set of plots is generated when $LPLT = .TRUE.$ and provides a pictorial representation of the streamlines and contours with a maximum of seven frames produced. The first frame is a plot of the streamlines followed by contour plots of velocity magnitude, temperature, and density. The next three frames are contour plots of the unit parallel, perpendicular, and normal magnetic-field components. These plots are referred to the solar-wind (x,R) coordinate system.

The second set of plots is produced according to the value of the logical variable $LPLTRJ$. This set consists of twelve plots. The first frame is a projection of the trajectory rotated onto the $x-R$ plane. The second frame is a plot of the trajectory projected onto the y_c-z_c plane. The remaining frames are time-history plots of density, temperature, velocity, and magnetic field. The velocity plots include magnitude and three components as do the magnetic field plots. The vector components are referred to the sun-planet ecliptic (x_s, y_s, z_s) coordinates.

A.5 PROGRAM ERROR MESSAGES

This section lists the messages printed by the program, and indicates what action should be taken by the user.

(1) ***** EXECUTION TERMINATED *****
RERUN DATA ON TAPE4 DOES NOT AGREE
WITH CASE SPECIFIED ON CARD INPUT:
MACH NO. GAMMA H/RO

FROM CARDS
FROM TAPE4

The first three parameters of item 2 of the input for a case using the rerun option should agree with those used when creating the file. The tolerance used in comparing the values is 10^{-5} . For a user-supplied geometry, it is sufficient for both values of H/R_0 to be negative.

(2) ***** EXECUTION TERMINATED *****
ARRAY OF CONTOUR VALUES IMPROPERLY SPECIFIED

When specified, the contour values should be monotonically increasing with at least one value in the range of the velocity, density, or magnetic-field strength for the region under consideration. This error does not inhibit generation of the rerun file.

(3) CONTOUR SEARCH ABORTED - TABLE OVERFLOW IN NAD

The program allows for 29 contour lines to be found, storing the starting address of each contour line in array NAD. This message indicates that at least one more contour line could be found. If the user requires all the contours of the levels specified, the case should be rerun in two parts. Otherwise, reduce the number of contour levels specified.

(4) CONTOUR SEARCH ABORTED - TABLE OVERFLOW IN (X,Y)

The contour lines may be described by up to 1000 points, stored in arrays X and Y. This message indicates that more points would be

required for the contour lines requested. The last contour line found will be incomplete. As with (3), either reduce the number of contour levels or run as two cases.

(5) NEGATIVE PRESSURE DETECTED BY SHOCK AT J=
 PN= PO= PTAU=

This message is printed by the blunt-body code when a negative pressure has been calculated at the shock on this iteration, at radial locations J. The quantities printed are: PN, the pressure calculated on this step; PO, the pressure from the previous step; and PTAU, the partial derivative of pressure with respect to time. This condition indicates that the shock wave motion is too extreme. Lowering the value of CN, and thus reducing the time step, may remove the problem.

The following messages (6)-(10) usually result from using an obstacle geometry which is in some way too severe for the program to handle in its present form. The obstacle slope may be sufficiently high at $x = 0.0$ that the axial Mach number becomes subsonic in the starting solution for the marching calculation, or there may be a sharp corner in the profile. Check input, particularly free-stream Mach number and body geometry.

(6) NEGATIVE PRESSURE ON BODY DETECTED BY BNDRY, PB= AT J=

This message indicates that a negative pressure on the body, PB, has been calculated at radial location J.

(7) NEGATIVE PRESSURE OR DENSITY ON BODY DETECTED BY BNDRYM AT X=
 PB= RHOB= VXB= VRB=

The program makes internal corrections when this condition occurs, resulting pressure PB, density RHOB, and velocity components VXB and VRB.

(8) NEGATIVE SIGMA-BAR-1 IN EIGENM INDICATES SUBSONIC FLOW AT I=

(9) NEGATIVE SIGMA-BAR-2 IN EIGENM INDICATES SUBSONIC FLOW AT I=

These messages are printed when subsonic flow is detected by the marching calculation. The computed stepsize for this region will be quite small.

(10) -----BODY TURN STOPPED AT M2=100-----

This message indicates that the body has a sharp corner, which has been limited to 100° when being transformed.

A.6 SAMPLE CASE

The sample case presented in this section is based on actual interplanetary conditions as measured by the solar-wind plasma analyzer, the fluxgate magnetometer, and retarding potential plasma analyzer on the Pioneer-Venus Orbiter for orbit 3.

The sample case is run alone and is set up to produce all possible output. The gasdynamic solution is to be calculated about a default ionopause shape with $H/R_O = 0.03$, $M_\infty = 3.0$, and $\gamma = 5/3$. The value of H/R_O is based on measurements of ionospheric density and temperature by the retarding potential plasma analyzer. Streamlines, magnetic-field components, and contours are desired to a downstream location of $-5.5 x/R_O$. Contour values are specified for all quantities. Interplanetary values for velocity magnitude and direction, density, and temperature were provided by the solar-wind plasma analyzer and for the magnetic field by the fluxgate magnetometer.

The input data is tabulated in figure A.4, with item numbers corresponding to those in sections A.3.2 and A.3.3. The first card, item 0, indicates that there is one case to run. The remaining

fifty-five cards provide the data for this case. Item 1 contains the identifying title. On the next card, item 2, values are specified for AMACH, GAMMA, HRO, and XCALC. The other data fields are left blank to indicate that the default values will be used. The values of the logical variables of item 3 specify that the flow field is to be calculated and that full printed and plotted output is to be produced. Item 4 defines the plot length to be $-5.5 x/R_o$. The fields for ANGP and ANGN are left blank as they are to be calculated internally by the program. Items 5, 6, and 7 specify the contour levels to be used - 14 for velocity and temperature, 11 for density, and 13 for magnetic-field strength. Item 8 is omitted because the obstacle geometry is one of the default shapes for which the coordinates are calculated internally. The next 37 cards, item 9, are the trajectory coordinates, indicating time (in minutes from periapsis and the three spacial coordinates normalized by planetary radius). Item 10 indicates that trajectory plots are to be generated. This item also specifies free-stream values of velocity, density, temperature, and magnetic-field strength. The next two cards, item 11, indicates that the fourth, ninth, eleventh, and nineteenth trajectory points are to be marked on the plots for cross-reference. The last input card, item 12 indicates that the given trajectory coordinates are expressed in sun-planet coordinates. The azimuthal and polar angles, Ω and ϕ_p , are also specified by this item as are the free-stream magnetic-field components.

Figure A.5 presents portions of the printed output from this sample case. The full printed output is approximately 6,000 lines. Figure A.6 shows the 19 plots which are produced by the program for this case.

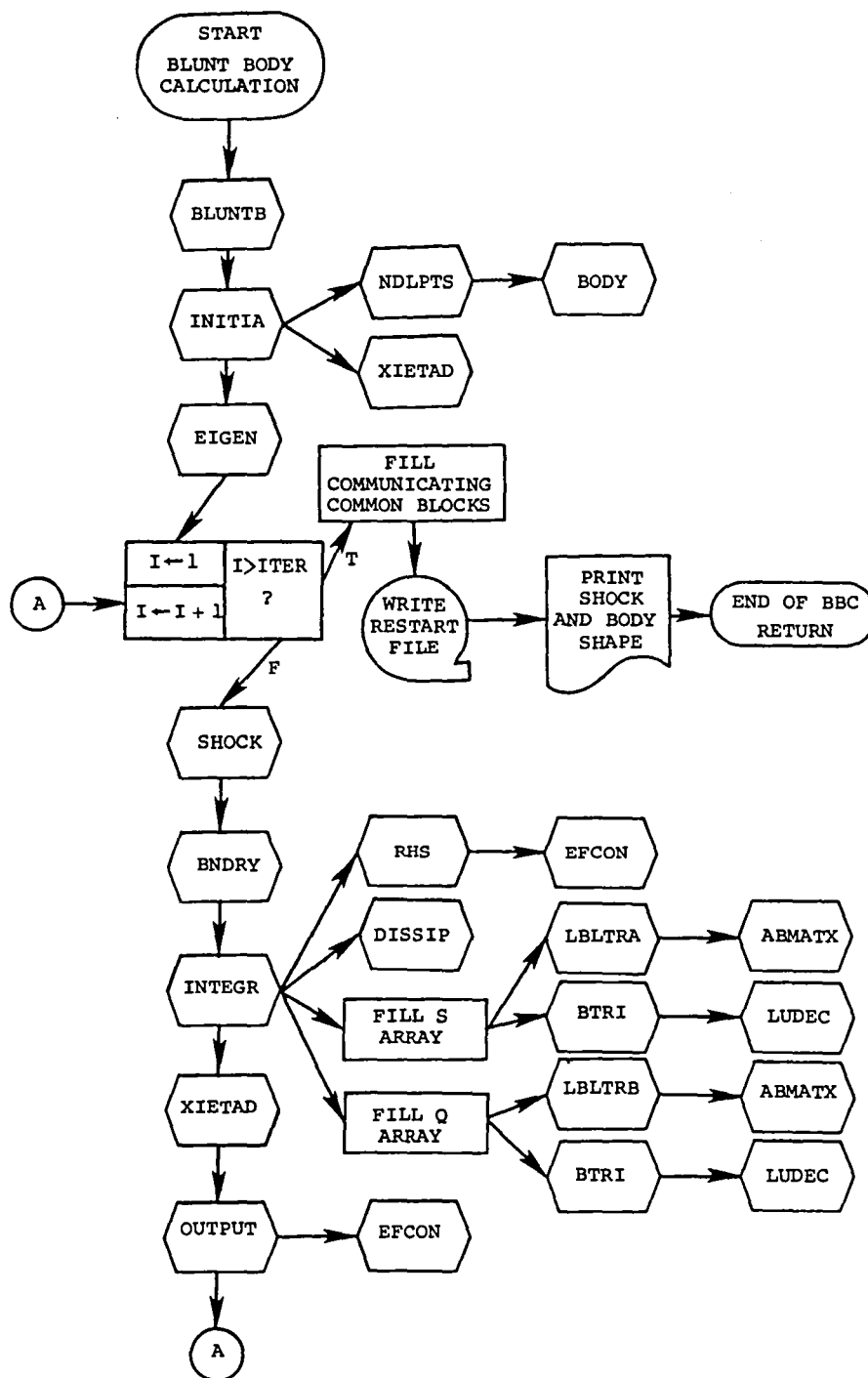


Figure A.1(a).- Flow chart for blunt-body calculation.

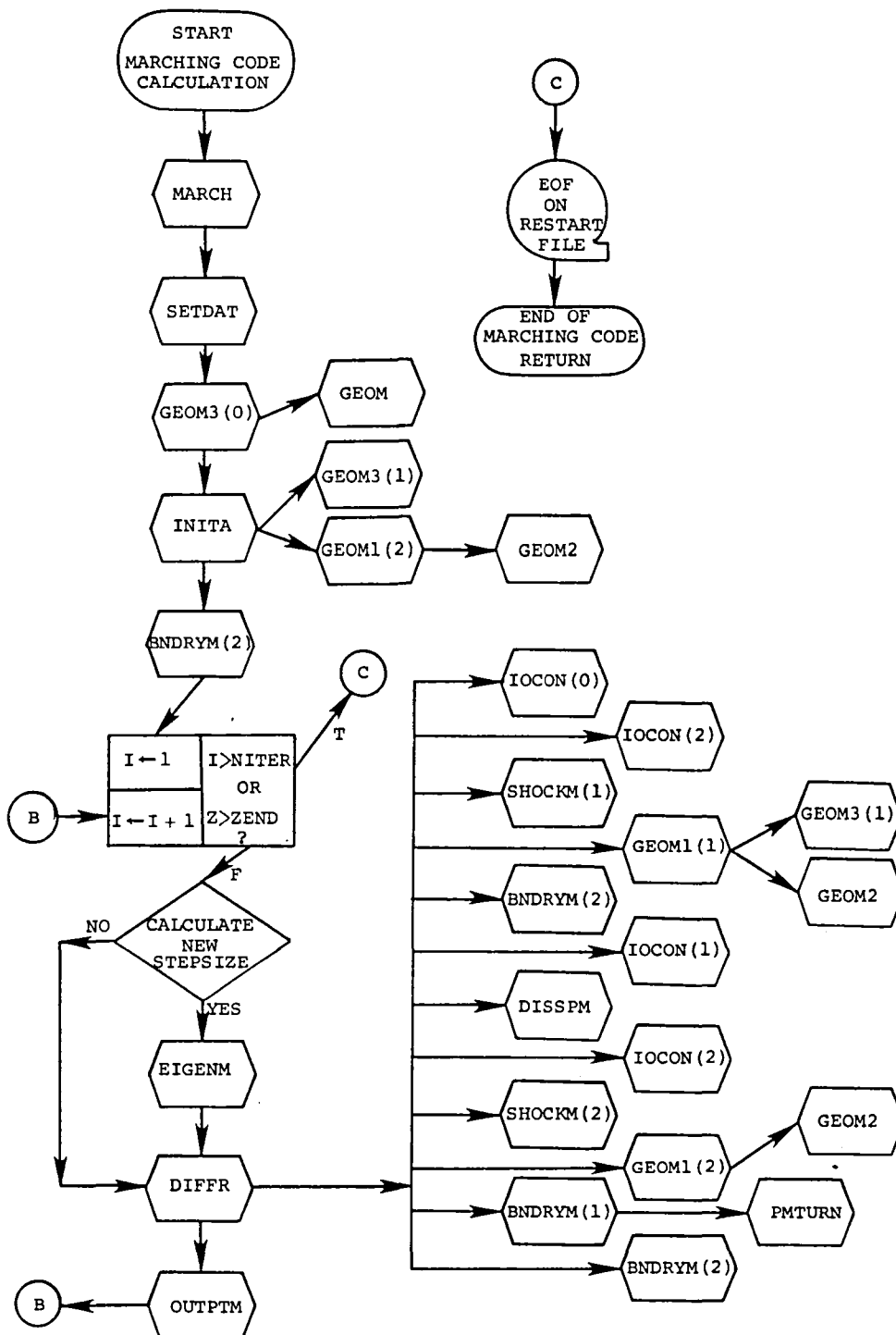


Figure A.1(b).- Flow chart for marching calculation.

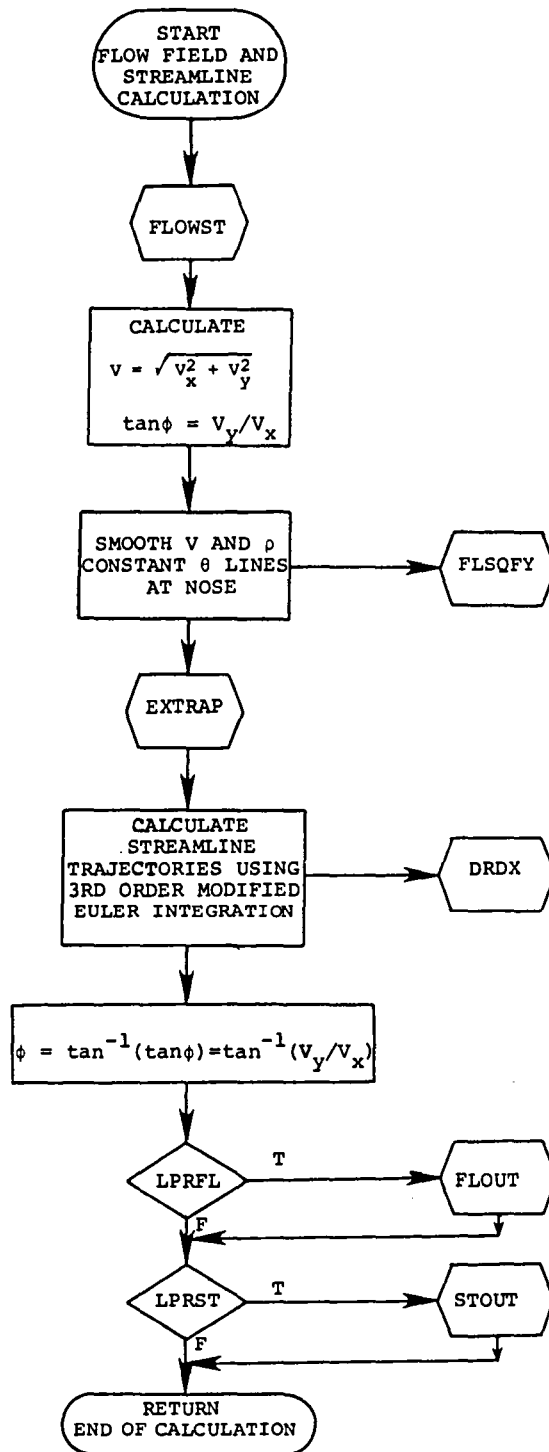


Figure A.1(c).- Flow chart of streamline calculation.

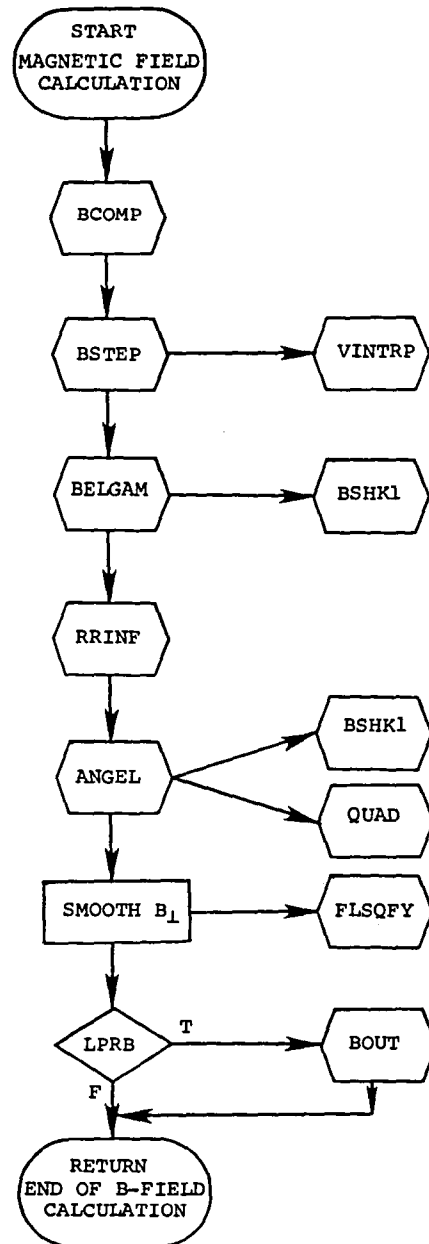


Figure A.1(d).- Flow chart of magnetic-field calculation.

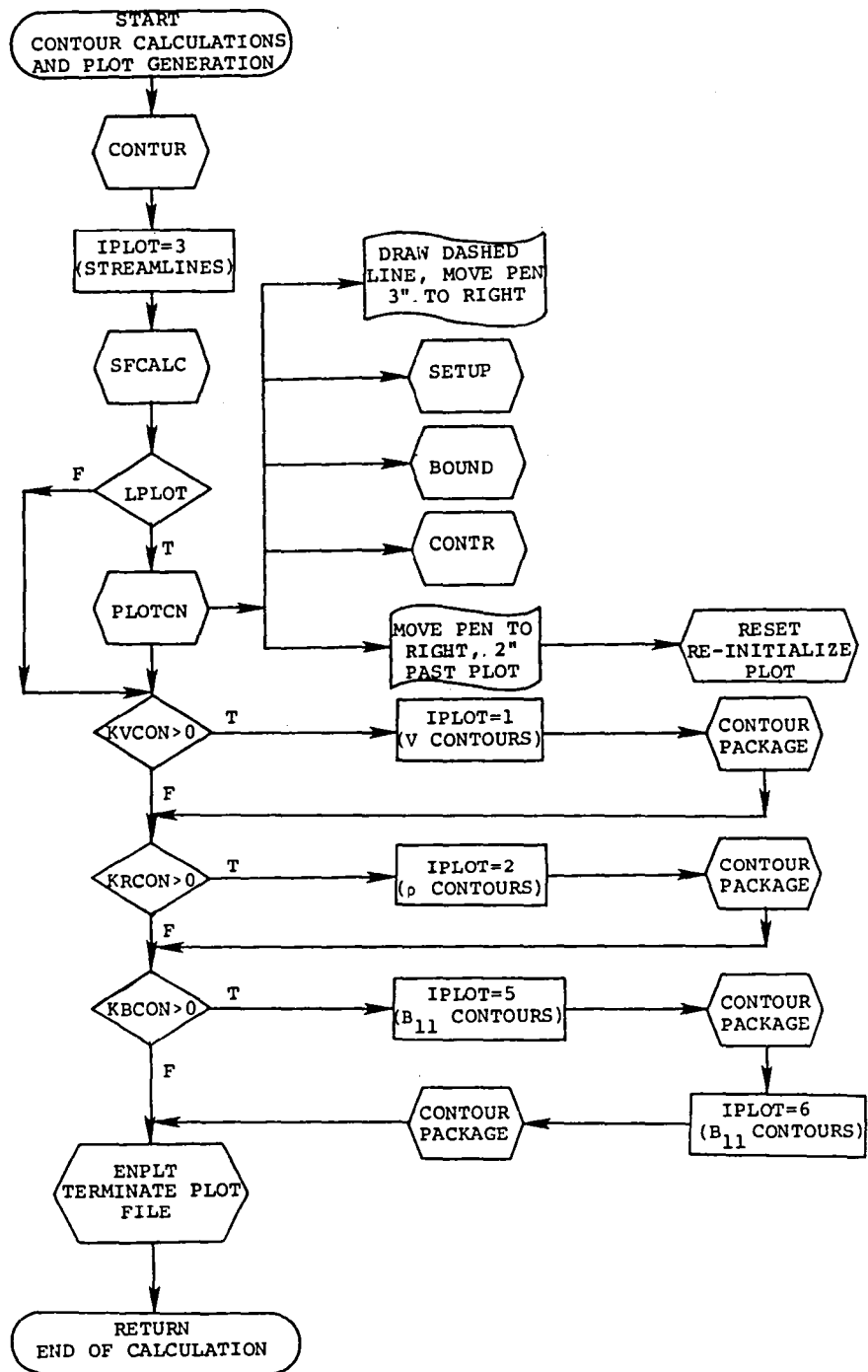


Figure A.1(e).- Flow chart of contour and plot generation calculation.

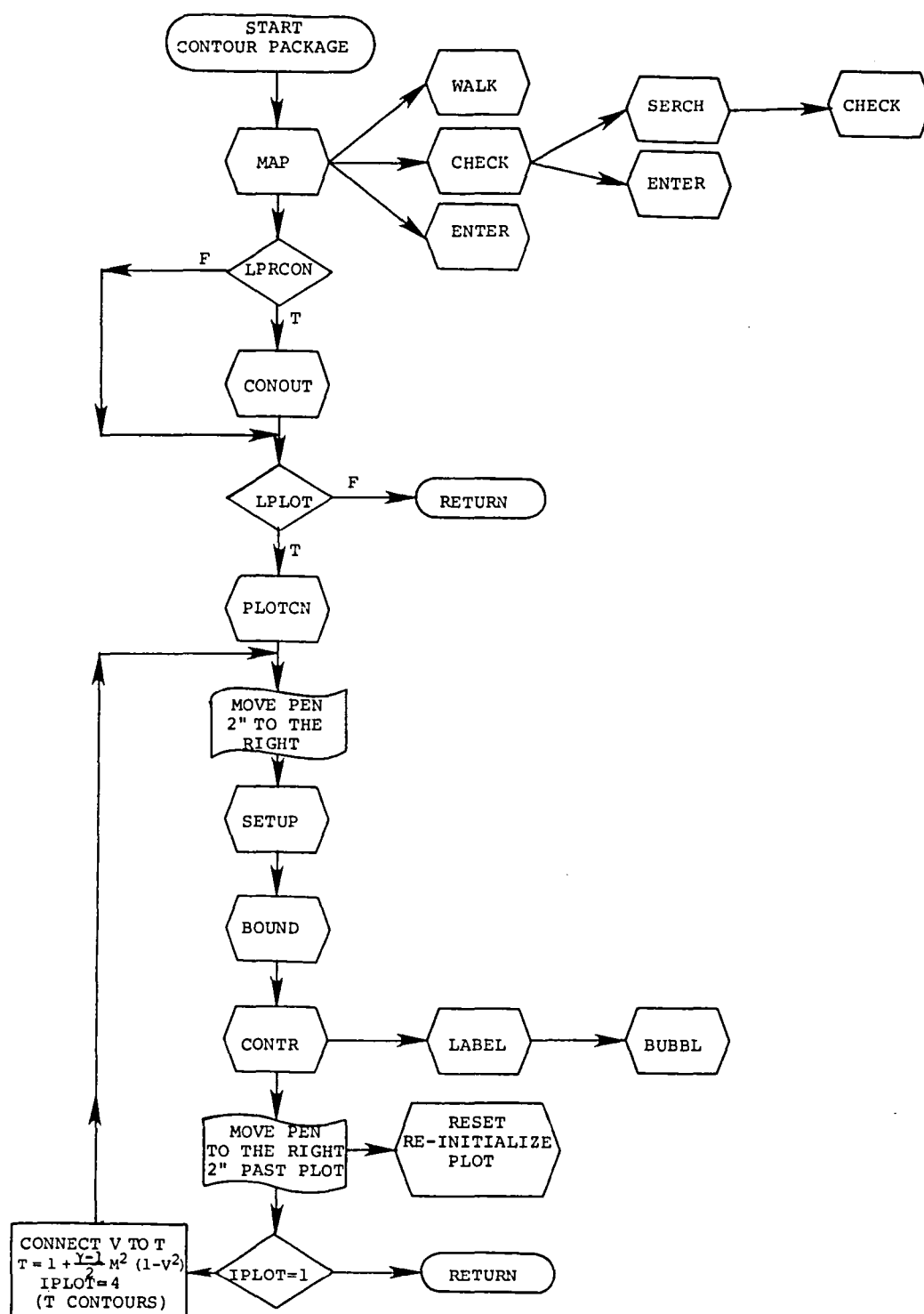


Figure A.1(e).- Concluded

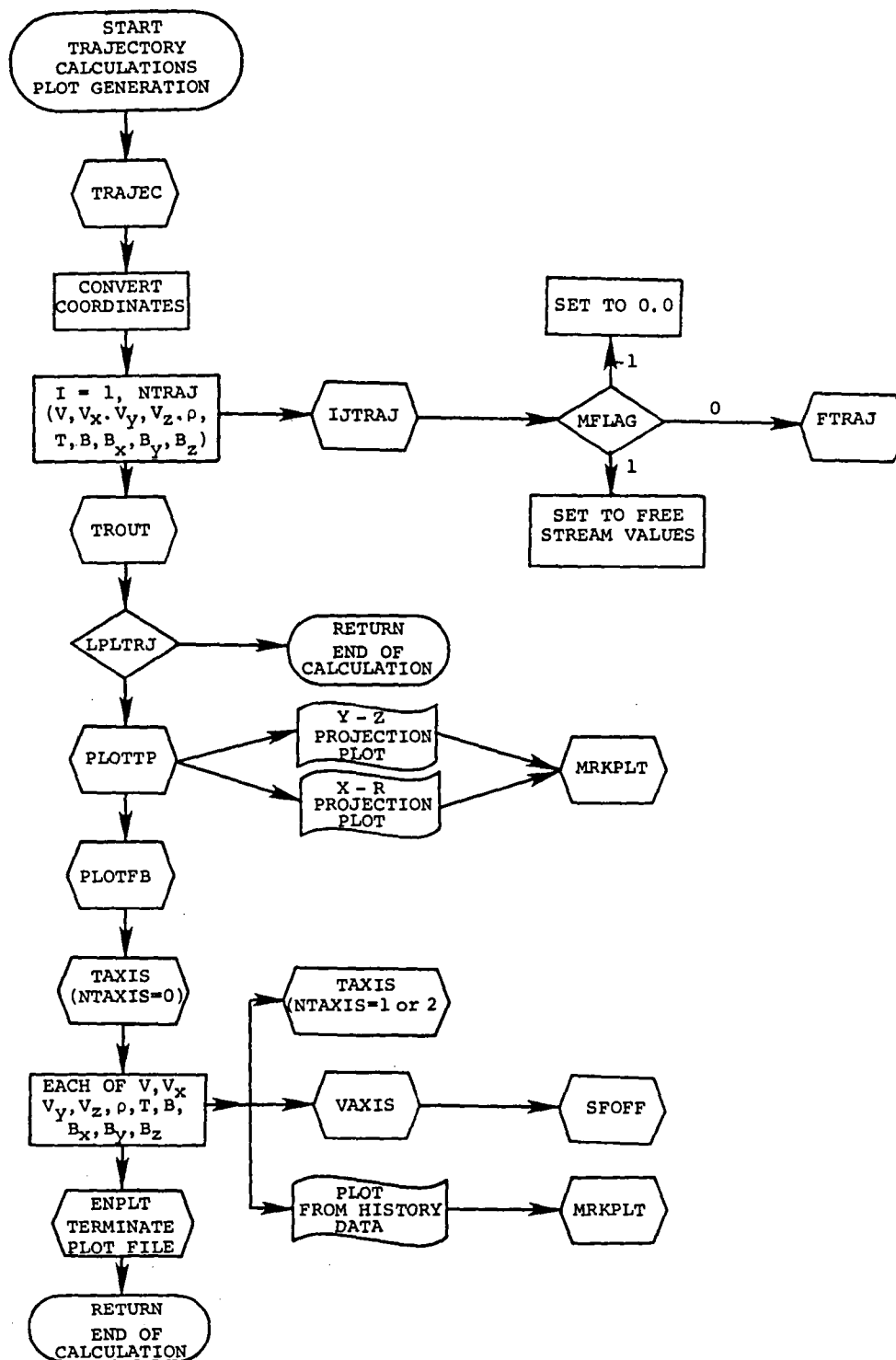


Figure A.1(f).- Flow chart of trajectory calculation.

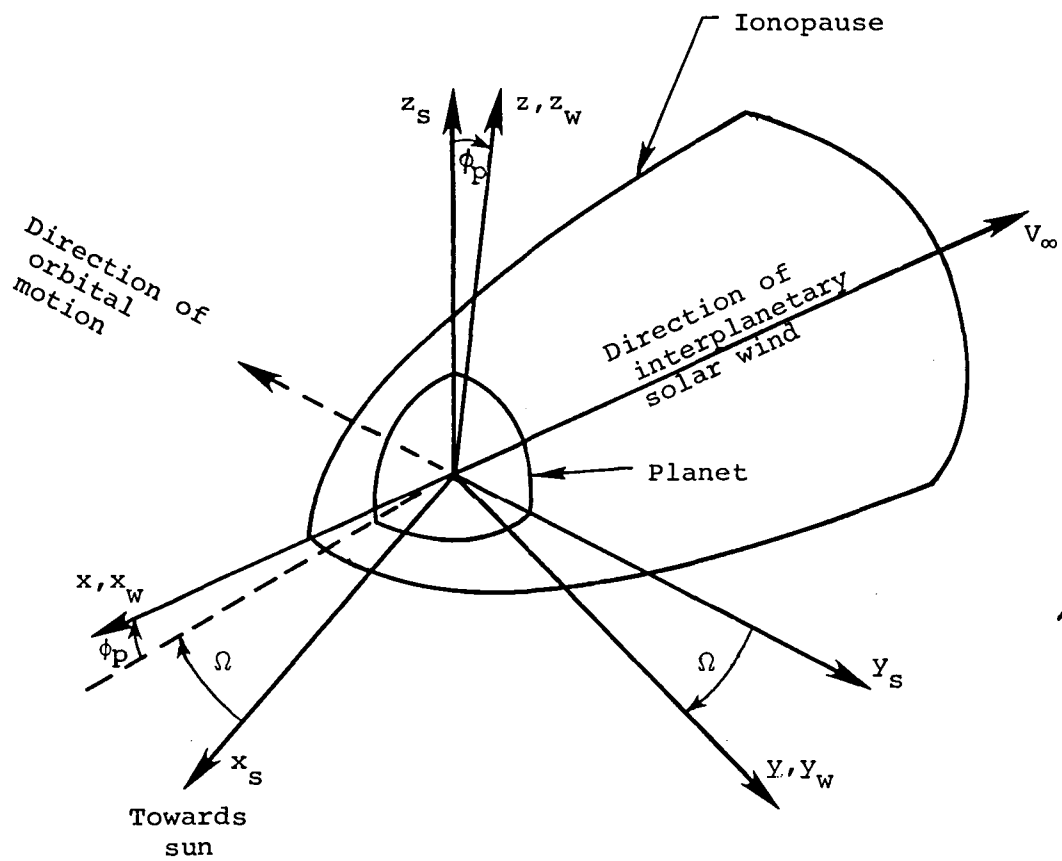


Figure A.2.- Illustration of the azimuthal (Ω) and polar (ϕ_p) solar-wind angles, both shown in a positive sense.

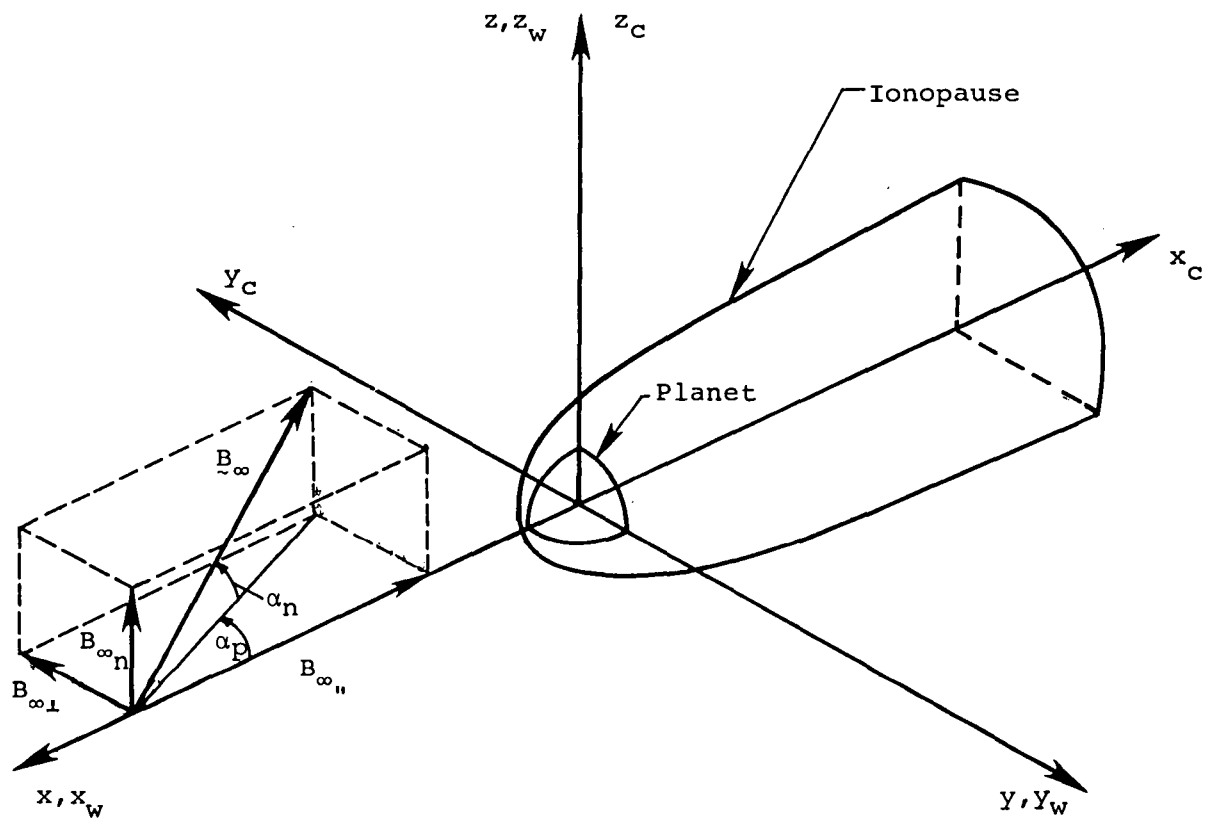


Figure A.3.- Illustration of the interplanetary magnetic field and magnetic-field angles (α_p, α_n) in the solar-wind aligned coordinate systems (x, y, z) , (x_w, y_w, z_w) , and (x_c, y_c, z_c) .

Item No.	Column No.	10	20	30	40	50	60	70	80
0		1							
1		SAMPLE CASE (DEFAULT IONPAUSE SHAPE WITH H/RO = 0.03)							
2		3.0	1.6666667	0.03	-10.0				
3		F	T	T	T	T	T	F	
4		-5.5							
5		14							
		0.1	0.2	0.3	0.4	0.5	0.6	0.7	0.75
		0.8	0.93	0.85	0.9	0.92	0.94		
6		11							
		0.5	0.8	1.2	1.6	2.0	2.5	3.0	3.5
		3.8	4.0	4.2					
7		13							
		0.45	0.6	0.8	1.0	1.25	1.5	2.0	2.5
		3.0	3.5	4.0	5.0	6.0			
9		37							
		-90.870	-0.843	3.787	2.027				
		-85.537	-0.765	3.600	2.045				
		-80.203	-0.684	3.393	2.062				
		-74.870	-0.600	3.177	2.073				
		-70.603	-0.533	2.999	2.078				
		-64.203	-0.430	2.721	2.079				
		-57.802	-0.324	2.427	2.067				
		-51.402	-0.217	2.118	2.043				
		-40.735	-0.034	1.562	1.961				
		-39.668	-0.017	1.509	1.951				
		-38.602	-0.010	1.422	1.932				
		-35.935	0.049	1.281	1.902				
		-34.867	0.67	1.232	1.886				
		-32.735	0.158	1.108	1.852				
		-24.202	0.2456	0.5826	1.6658				
		-21.002	0.2954	0.3749	1.5693				
		-16.735	0.356	0.090	1.409				
		-14.602	0.382	-0.052	1.315				
		-11.402	0.415	-0.205	1.150				
		-8.102	0.437	-0.478	0.945				
		-4.900	0.442	-0.703	0.660				
		6.298	0.309	-1.042	-0.266				
		9.498	0.237	-1.055	-0.546				
		12.593	0.160	-1.038	-0.801				
		17.393	0.034	-0.966	-1.162				
		29.127	-0.275	-0.673	-1.887				
		34.460	-0.407	-0.512	-2.155				
		43.860	-0.561	-0.312	-2.444				
		47.260	-0.705	-0.108	-2.670				
		53.660	-0.844	0.0982	-2.925				
		56.862	-0.91	0.201	-3.031				
		58.993	-0.954	0.269	-3.097				
		60.060	-0.975	0.303	-3.131				
		62.193	-1.018	0.371	-3.195				
		67.528	-1.122	0.541	-3.347				
		73.928	-1.241	0.739	-3.514				
		80.328	-1.357	0.839	-3.671				
10		T	0.968	392.0	20.2	102000.	8.8225		
11		4							
		4	9	11	19				
12		T	3.3	0.15	-1.74	-8.64	0.4		

Figure A.4.- Card input for sample case.

```

*****
PROGRAM SOLAR
*****
DETERMINES
SOLAR WIND FLOW PAST PLANETARY MAGNETO/IONOSPHERES
USING
FULLY CONSERVATIVE FINITE DIFFERENCE ALGORITHMS
*****
WRITTEN BY
STEPHEN S. STAHARA, BARBARA C. TRUONGER,
AND DANIEL J. KLENKE
*****
NIELSEN ENGINEERING AND RESEARCH, INC.
MOUNTAIN VIEW, CALIFORNIA
*****

```

LISTING OF INPUT CARDS FOR THIS RUN

```

1
SAMPLE CASE (DEFAULT TONTPAUSE SHAPE WITH H/R = 0.03)
3.C 1.6666667 0.03 -10.0 T T T T F
F
-3.5
14
0.1 1.2 3.3 0.14 1.5 1.8 0.7 0.75
0.8 0.85 0.88 1.9 2.92 1.94
0.5 1.8 1.2 1.6 2.0 2.5 3.0 3.5
3.8 4.4 4.2
13
3.45 0.6 0.8 1.2 1.25 1.5 2.0 2.5
3.0 3.5 4.0 5.0
37
-90.470 -1.843 3.787 2.027
-89.937 -3.765 3.600 2.045
-80.203 -0.694 3.393 2.062
-74.470 -0.600 3.177 2.073
-70.523 -2.533 2.999 2.078
-64.203 -0.430 2.721 2.079
-57.402 -5.324 2.427 2.067
-51.402 -0.217 2.118 2.045
-40.735 -0.034 1.592 1.961
-39.668 -0.017 1.509 1.951
-38.602 -3.411 1.422 1.932
-35.935 0.649 1.291 1.902
-34.467 0.067 1.232 1.886
-32.745 0.158 1.108 1.852
-24.202 0.2456 0.5826 1.5658
-21.302 1.2094 0.3749 1.5693
-16.735 1.356 0.190 1.449
-14.632 0.382 -0.052 1.315
-11.402 0.415 -0.205 1.150
-3.102 1.437 -1.478 0.945
-4.900 0.442 -0.703 0.660
6.201 1.309 -1.047 -0.266
9.498 1.237 -1.605 -2.545
12.593 0.160 -1.134 -3.801
17.393 1.034 -0.966 -1.162
29.127 -0.275 -0.673 -1.887
34.453 -3.417 -0.512 -2.155
42.854 -1.561 -3.312 -2.444
47.260 -3.705 -0.164 -2.674
53.653 -0.844 0.682 -2.925
56.567 -0.01 0.101 -3.031
59.993 -0.454 0.259 -3.067
60.060 -1.975 0.203 -3.131
67.191 -1.018 0.371 -3.195
67.928 -1.122 0.541 -3.347
73.428 -1.241 0.739 -3.514
83.324 -1.317 0.939 -3.671
T 0.968 392.2 21.2 10230.0 8.0225
4
T 3.3 9 11 13 0.4

```

Figure A.5.- Abbreviated print output for sample case.

SAMPLE CASE: (DEFAULT IONOSPHERE SHAPE WITH $H/R_0 = 0.02$)

INPUT VARIABLES

INTERPLANETARY MACH NO. = 3.00

SPECIFIC HEAT RATIO = 1.667

IONOSPHERE GEOMETRY: DEFAULT IONOSPHERE SHAPE
FOR CONSTANT SCALE HEIGHT WITH $H/R_0 = 0.02$

PARAMETERS FOR BLUNT BODY CALCULATION

NO. OF RADIAL MESH POINTS = 16
NO. OF ANGULAR MESH POINTS = 24
NO. OF ADDITIONAL POINTS IN
BLUNT BODY MESH = 1
COMPACT NUMBER = 3.60
NO. OF ITERATIONS = 300

TERMINAL DOWNSTREAM LOCATION FOR MARCHING CALCULATION, $X/R_0 = 10.00$

TERMINAL DOWNSTREAM LOCATION FOR PLOTTING, $X/R_0 = 5.51$

LPRJN = F

LPPEL = T

LPSTY = T

LPRCIN = T

LPPE = T

LPLOT = T

LTRBJ = T

LRSTRT = F

LPLTRJ = T

Figure A.5.- Continued.

INPUT FOR TRAJ-CORV CALCULATION

UPLANET = 1.3331
INTERPLANETARY VELOCITY = 3.921E+2
INTERPLANETARY DENSITY = 2.2E+1
INTERPLANETARY TEMPERATURE = 1.02E+5
INTERPLANETARY MAGNETIC FIELD
MAGNETIC FIELD COMPONENT = 0.42E+1
VELOCITY COMPONENT = 0.17E+1
VELOCITY COMPONENT = 0.04E+1
VELOCITY COMPONENT = 0.02E+1
AZIMUTHAL ANGLE = 0.33E+1
POLAR ANGLE = 0.15E+1

NTRAJ = 37 NMARKT = 4
I = POINT TO BE MARKED FOR CROSS REFERENCE

N	XTTRAJ	YTTRAJ	ZTTRAJ	WTTRAJ
(SUN-PLANET COORDINATE SYSTEM)				
1	-3.07E+1	-0.543E	3.787E	2.027E
2	-35.537E	-0.705E	3.600E	2.045E
3	-5.02E+1	-0.644E	3.593E	2.052E
4	-74.87E	-0.533E	3.177E	2.072E
5	-73.043E	-0.533E	2.939E	2.079E
6	-66.2E+1	-0.433E	2.722E	2.079E
7	-57.0E+1	-0.324E	2.427E	2.057E
8	-5.04E+1	-0.247E	2.034E	2.043E
9	-40.735E	-0.134E	1.562E	1.951E
10	-34.665E	-0.17E	1.039E	1.951E
11	-34.66E	-0.13E	0.422E	1.932E
12	-31.425E	0.09E	1.245E	1.902E
13	-34.057E	0.07E	1.247E	1.843E
14	-32.715E	0.05E	1.118E	1.832E
15	-24.2E	0.243E	0.526E	1.805E
16	-21.0E+1	0.255E	0.374E	1.509E
17	-15.735E	0.255E	0.09E	1.429E
18	-14.05E	0.312E	-0.057E	1.315E
19	-11.04E	0.435E	-0.2E	0.23E
20	-9.1E+1	0.437E	-0.47E	0.64E
21	-6.0E+1	0.402E	-0.73E	0.29E
22	0.269E	0.39E	-1.047E	-0.26E
23	0.408E	0.237E	-1.045E	-0.24E
24	0.2593E	0.0E	-1.038E	-0.03E
25	17.393E	0.134E	-0.96E	-1.152E
26	23.127E	-0.27E	-0.873E	-1.087E
27	14.440E	-0.47E	-0.513E	-0.555E
28	4.0E+1	-0.4E	-0.112E	-0.444E
29	47.261E	-0.73E	-0.07E	-0.47E
30	33.050E	-0.84E	0.082E	-0.015E
31	54.862E	-0.91E	0.211E	-0.031E
32	34.743E	-0.054E	0.269E	-0.077E
33	51.0E	-0.97E	0.320E	-0.111E
34	62.493E	-0.1E	0.37E	-0.195E
35	67.124E	-1.02E	0.44E	-0.347E
36	73.963E	-1.24E	0.50E	-0.514E
37	80.374E	-1.357E	0.53E	-0.671E

VALUES SPECIFIED FOR CONTOUR CALCULATION

24 CONTOUR LEVELS FOR VELOCITY:

0.100	0.200	0.300	0.400	0.500	0.600
0.700	0.800	0.900	1.000	1.100	1.200
0.050	0.040	0.030	0.020	0.010	0.000

40 CONTOUR LEVELS FOR DENSITY:

0.500	0.600	0.700	0.800	0.900	1.000
1.000	1.100	1.200	1.300	1.400	1.500
1.600	1.700	1.800	1.900	2.000	2.100

40 CONTOUR LEVELS FOR MAGNETIC FIELD STRENGTH:

0.450	0.500	0.550	0.600	0.650	0.700
0.750	0.800	0.850	0.900	0.950	1.000
1.050	1.100	1.150	1.200	1.250	1.300

Figure A.5.- Continued.


```

                                PLUKE BODY CALCULATION
                                *****

ITERATION 1  RMS OF SHOCK SPECTRUM 1.5177E-2  MAXIMUM SHOCK SPECTRUM 5.0866E-2 AT J=25
ITERATION 2  RMS OF SHOCK SPECTRUM 7.5422E-3  MAXIMUM SHOCK SPECTRUM 1.4926E-2 AT J=23
ITERATION 3  RMS OF SHOCK SPECTRUM 1.0212E-2  MAXIMUM SHOCK SPECTRUM 3.6756E-2 AT J=23
ITERATION 4  RMS OF SHOCK SPECTRUM 1.5333E-2  MAXIMUM SHOCK SPECTRUM 6.2555E-2 AT J=23
ITERATION 5  RMS OF SHOCK SPECTRUM 2.1493E-2  MAXIMUM SHOCK SPECTRUM 9.2467E-2 AT J=23

ITERATION 206 RMS OF SHOCK SPECTRUM 1.3365E-4  MAXIMUM SHOCK SPECTRUM 1.2972E-3 AT J=16
ITERATION 207 RMS OF SHOCK SPECTRUM 1.3117E-4  MAXIMUM SHOCK SPECTRUM 1.2751E-3 AT J=16
ITERATION 208 RMS OF SHOCK SPECTRUM 1.2371E-4  MAXIMUM SHOCK SPECTRUM 1.2411E-3 AT J=13
ITERATION 209 RMS OF SHOCK SPECTRUM 7.6775E-5  MAXIMUM SHOCK SPECTRUM 1.2863E-3 AT J=13
ITERATION 306 RMS OF SHOCK SPECTRUM 2.1147E-4  MAXIMUM SHOCK SPECTRUM 1.2772E-3 AT J=13

FINAL SONIC LINE LOCATION

VEL= .5672  PSL= .7745
XSL= .6716  RSL= .8631
XSL= .5497  RSL= .8297
XSL= .5901  RSL= .8523
VEL= .7267  PSL= .8777
VEL= .7211  RSL= .8998
XSL= .7173  RSL= .8237
XSL= .7551  RSL= .9334
VEL= .7763  RSL= .8560
XSL= .7040  RSL= .9639
XSL= .8110  RSL= .8099
XSL= .847  RSL= .8923
VEL= .866  RSL= .9116
XSL= .8492  RSL= 1.0107
XSL= .9153  RSL= 1.0112
XSL= .943  RSL= .9112
VEL= .9718  RSL= .9119
XSL= 1.0074  RSL= .9754
XSL= 1.0121  RSL= .9696

<<<< Y 50000 IN MT = .45492E+01 RMS OF 10000 IN MT = .7440E-1 >>>>

BODY AND FINAL SHOCK SHAPE

J      Y(BOOY)  Y(BOOY)  X(SHOCK)  Y(SHOCK)
2      .9994  .7349  1.3143  .5455
3      .9944  .6746  1.3711  .4336
4      .9556  .4734  1.2504  .2275
5      .9710  .7473  1.2786  .3186
6      .9936  .83.09  1.2589  .4191
7      .6314  .3761  .2374  .4999
8      .9639  .4439  1.2194  .5892
9      .8726  .5039  1.1740  .6517
10     .9372  .5847  1.1419  .7732
11     .7079  .6724  1.0122  .8511
12     .7547  .5795  1.0561  .9212
13     .7173  .7320  1.2107  1.0243
14     .6574  .7134  .9516  1.0129
15     .6036  .8708  .8610  1.0264
16     .5468  .8751  .8241  1.3142
17     .4969  .9158  .7525  1.4152
18     .4244  .9431  .6729  1.5114
19     .3592  .9868  .5476  1.6124
20     .2916  1.0170  .4517  1.7143
21     .2219  .9434  .3677  1.8239
22     .1400  1.0063  .2713  1.9349
23     .0750  1.0057  .1437  2.0555
24     -.0111  1.0117  -.0001  2.1809

```

Figure A.5.- Continued.

MARCHING CALCULATION *****			
STEP NO.	DOWNSTREAM LOCATION	BODY ORIGINATE	SHOCK ORIGINATE
1	-0.468	1.1148	2.2210
2	-0.095	1.1167	2.2655
3	-0.1413	1.1225	2.2903
4	-0.187	1.1273	2.3137
5	-0.2425	1.1319	2.3223
6	-0.2970	1.1354	2.3267
7	-0.3533	1.1380	2.3271
8	-0.4117	1.1400	2.3131
9	-0.4541	1.1414	2.2855
10	-0.5329	1.1425	2.2673
11	-0.5316	1.1432	2.2583
12	-0.5703	1.1436	2.2487
13	-0.7108	1.1438	2.2393
14	-0.8177	1.1440	2.2373
15	-0.9022	1.1441	2.2374
16	-0.9745	1.1441	2.2376
17	-1.0440	1.1441	2.2381
18	-1.1194	1.1441	2.2428
19	-1.1949	1.1441	2.2500
20	-1.2644	1.1441	2.2592
21	-1.3460	1.1441	2.2737
22	-1.4319	1.1441	2.2853
23	-1.5171	1.1441	2.2923
24	-1.6026	1.1441	2.2981
25	-1.6927	1.1441	2.2979
26	-1.7823	1.1441	2.2967
27	-1.8706	1.1441	2.2945
28	-1.9590	1.1441	2.2915
29	-2.0473	1.1441	2.2876
30	-2.1356	1.1441	2.2830
31	-2.2239	1.1441	2.2776
32	-2.3122	1.1441	2.2716
33	-2.4005	1.1441	2.2650
34	-2.4888	1.1441	2.2578
35	-2.5771	1.1441	2.2500
36	-2.6654	1.1441	2.2417
37	-2.7537	1.1441	2.2330
38	-2.8420	1.1441	2.2238
39	-2.9303	1.1441	2.2141
40	-3.0186	1.1441	2.2039
41	-3.1069	1.1441	2.1932
42	-3.1952	1.1441	2.1820
43	-3.2835	1.1441	2.1703
44	-3.3718	1.1441	2.1581
45	-3.4601	1.1441	2.1454
46	-3.5484	1.1441	2.1321
47	-3.6367	1.1441	2.1183
48	-3.7250	1.1441	2.1040
49	-3.8133	1.1441	2.0892
50	-3.9016	1.1441	2.0739
51	-3.9899	1.1441	2.0581
52	-4.0782	1.1441	2.0418
53	-4.1665	1.1441	2.0250
54	-4.2548	1.1441	2.0077
55	-4.3431	1.1441	1.9900
56	-4.4314	1.1441	1.9718
57	-4.5197	1.1441	1.9531
58	-4.6080	1.1441	1.9339
59	-4.6963	1.1441	1.9142
60	-4.7846	1.1441	1.8940
61	-4.8729	1.1441	1.8733
62	-4.9612	1.1441	1.8521
63	-5.0495	1.1441	1.8304
64	-5.1378	1.1441	1.8081
65	-5.2261	1.1441	1.7854
66	-5.3144	1.1441	1.7621
67	-5.4027	1.1441	1.7383
68	-5.4910	1.1441	1.7140
69	-5.5793	1.1441	1.6892
70	-5.6676	1.1441	1.6639
71	-5.7559	1.1441	1.6381
72	-5.8442	1.1441	1.6118
73	-5.9325	1.1441	1.5850
74	-6.0208	1.1441	1.5577
75	-6.1091	1.1441	1.5300
76	-6.1974	1.1441	1.5018
77	-6.2857	1.1441	1.4731
78	-6.3740	1.1441	1.4439
79	-6.4623	1.1441	1.4142
80	-6.5506	1.1441	1.3840
81	-6.6389	1.1441	1.3533
82	-6.7272	1.1441	1.3221
83	-6.8155	1.1441	1.2904
84	-6.9038	1.1441	1.2581
85	-6.9921	1.1441	1.2254
86	-7.0804	1.1441	1.1921
87	-7.1687	1.1441	1.1583
88	-7.2570	1.1441	1.1240
89	-7.3453	1.1441	1.0892
90	-7.4336	1.1441	1.0539
91	-7.5219	1.1441	1.0181
92	-7.6102	1.1441	0.9818
93	-7.6985	1.1441	0.9450
94	-7.7868	1.1441	0.9077
95	-7.8751	1.1441	0.8700
96	-7.9634	1.1441	0.8318
97	-8.0517	1.1441	0.7931
98	-8.1400	1.1441	0.7539
99	-8.2283	1.1441	0.7142
100	-8.3166	1.1441	0.6740

DETAILED FLOW FIELD OUTPUT

FLOW FIELD VALUES EXTRAPOLATED TO SYMMETRY AXIS, THETA = 3.0, DEGREES

Y	P/P ₀	V/V ₀	W/W ₀	T/T ₀	P/P ₀
1	1.0000	0.0000	0.0000	4.0000	13.0730
2	1.0169	0.0740	0.4084	3.9983	13.0279
3	1.0338	0.147	0.4226	3.9946	13.9900
4	1.0507	0.221	0.4341	3.9873	13.9331
5	1.0676	0.295	0.4429	3.9787	13.8578
6	1.0845	0.369	0.4502	3.9687	13.7649
7	1.1014	0.443	0.4551	3.9551	13.6554
8	1.1183	0.517	0.4587	3.9375	13.5303
9	1.1352	0.591	0.4614	3.9169	13.3905
10	1.1521	0.665	0.4631	3.8935	13.2378
11	1.1690	0.739	0.4642	3.8675	13.0711
12	1.1859	0.813	0.4649	3.8390	12.8937
13	1.2028	0.887	0.4654	3.8082	12.7061
14	1.2197	0.961	0.4658	3.7752	12.5094
15	1.2366	1.035	0.4661	3.7403	12.3047
16	1.2535	1.109	0.4663	3.7036	12.0932
17	1.2704	1.183	0.4665	3.6661	11.8760
18	1.2873	1.257	0.4667	3.6278	11.6543
19	1.3042	1.331	0.4669	3.5887	11.4290

Figure A.5.- Continued.

FLTM FIELD VALUES FROM FLIGHT BODY CALCULATION

ANGULAR LOCATION NO. 22, AT THETA = 20.000 DEGREES

I	OP/P	Y/P	Y/P	VR/VINF	VX/VINF	FLTM ANGLE	V/VINF	RM/RH/TNF	T/TINF	P/PINF
1	1.0117	0.340	0.9964	0.150	0.355	14.1063	0.335	3.4261	3.9594	13.6624
2	1.0117	0.355	1.0164	0.231	0.423	14.3068	0.347	3.4113	3.9565	13.6340
3	1.0117	0.370	1.0364	0.247	0.484	14.3113	0.354	3.4144	3.9513	13.5877
4	1.0117	0.385	1.0564	0.262	0.549	14.3208	0.375	3.3940	3.9337	13.5243
5	1.0117	0.400	1.0764	0.277	0.609	13.7745	0.429	3.3433	3.9741	13.4443
6	1.0117	0.415	1.0964	0.292	0.674	13.9714	0.411	3.3589	3.9625	13.3492
7	1.0117	0.430	1.1164	0.307	0.734	14.0799	0.364	3.3525	3.9499	13.2390
8	1.0117	0.445	1.1364	0.322	0.794	14.1874	0.347	3.3339	3.9357	13.1147
9	1.0117	0.460	1.1564	0.337	0.854	14.2949	0.330	3.3132	3.9187	12.9769
10	1.0117	0.475	1.1764	0.352	0.914	14.4024	0.313	3.2904	3.8981	12.8284
11	1.0117	0.490	1.1964	0.367	0.974	14.5099	0.296	3.2657	3.8779	12.6639
12	1.0117	0.505	1.2164	0.382	1.034	14.6174	0.279	3.2400	3.8581	12.4899
13	1.0117	0.520	1.2364	0.397	1.094	14.7249	0.262	3.2102	3.8331	12.3052
14	1.0117	0.535	1.2564	0.412	1.154	14.8324	0.245	3.1797	3.8087	12.1103
15	1.0117	0.550	1.2764	0.427	1.214	14.9399	0.228	3.1473	3.7829	11.9039
16	1.0117	0.565	1.2964	0.442	1.274	15.0474	0.211	3.1133	3.7557	11.6926
17	1.0117	0.580	1.3164	0.457	1.334	15.1549	0.194	3.0779	3.7279	11.4769
18	1.0117	0.595	1.3364	0.472	1.394	15.2624	0.177	3.0401	3.6997	11.2514
19	1.0117	0.610	1.3564	0.487	1.454	15.3699	0.160	3.0011	3.6669	11.0246

ANGULAR LOCATION NO. 23, AT THETA = 20.000 DEGREES

I	OP/P	Y/P	Y/P	VR/VINF	VX/VINF	FLTM ANGLE	V/VINF	RM/RH/TNF	T/TINF	P/PINF
1	1.0117	0.340	0.9964	0.150	0.355	14.3214	0.334	3.4125	3.9514	13.5810
2	1.0117	0.355	1.0164	0.231	0.423	14.4289	0.346	3.3973	3.9362	13.4411
3	1.0117	0.370	1.0364	0.247	0.484	14.5364	0.358	3.3821	3.9210	13.2912
4	1.0117	0.385	1.0564	0.262	0.549	14.6439	0.370	3.3669	3.9058	13.1413
5	1.0117	0.400	1.0764	0.277	0.609	14.7514	0.382	3.3517	3.8906	12.9914
6	1.0117	0.415	1.0964	0.292	0.674	14.8589	0.394	3.3365	3.8754	12.8415
7	1.0117	0.430	1.1164	0.307	0.734	14.9664	0.406	3.3213	3.8602	12.6916
8	1.0117	0.445	1.1364	0.322	0.794	15.0739	0.418	3.3061	3.8450	12.5417
9	1.0117	0.460	1.1564	0.337	0.854	15.1814	0.430	3.2909	3.8298	12.3918
10	1.0117	0.475	1.1764	0.352	0.914	15.2889	0.442	3.2757	3.8146	12.2419
11	1.0117	0.490	1.1964	0.367	0.974	15.3964	0.454	3.2605	3.7994	12.0920
12	1.0117	0.505	1.2164	0.382	1.034	15.5039	0.466	3.2453	3.7842	11.9421
13	1.0117	0.520	1.2364	0.397	1.094	15.6114	0.478	3.2301	3.7690	11.7922
14	1.0117	0.535	1.2564	0.412	1.154	15.7189	0.490	3.2149	3.7538	11.6423
15	1.0117	0.550	1.2764	0.427	1.214	15.8264	0.502	3.1997	3.7386	11.4924
16	1.0117	0.565	1.2964	0.442	1.274	15.9339	0.514	3.1845	3.7234	11.3425
17	1.0117	0.580	1.3164	0.457	1.334	16.0414	0.526	3.1693	3.7082	11.1926
18	1.0117	0.595	1.3364	0.472	1.394	16.1489	0.538	3.1541	3.6930	11.0427
19	1.0117	0.610	1.3564	0.487	1.454	16.2564	0.550	3.1389	3.6778	10.8928

ANGULAR LOCATION NO. 23, AT THETA = 20.000 DEGREES

I	OP/P	Y/P	Y/P	VR/VINF	VX/VINF	FLTM ANGLE	V/VINF	RM/RH/TNF	T/TINF	P/PINF
1	1.0117	0.340	0.9964	0.150	0.355	15.2794	0.464	3.0997	3.7562	1.7381
2	1.0117	0.355	1.0164	0.231	0.423	15.3869	0.476	3.0845	3.7410	2.0213
3	1.0117	0.370	1.0364	0.247	0.484	15.4944	0.488	3.0693	3.7258	2.3045
4	1.0117	0.385	1.0564	0.262	0.549	15.6019	0.500	3.0541	3.7106	2.5877
5	1.0117	0.400	1.0764	0.277	0.609	15.7094	0.512	3.0389	3.6954	2.8709
6	1.0117	0.415	1.0964	0.292	0.674	15.8169	0.524	3.0237	3.6802	3.1541
7	1.0117	0.430	1.1164	0.307	0.734	15.9244	0.536	3.0085	3.6650	3.4373
8	1.0117	0.445	1.1364	0.322	0.794	16.0319	0.548	3.0000	3.6498	3.7205
9	1.0117	0.460	1.1564	0.337	0.854	16.1394	0.560	2.9848	3.6346	4.0037
10	1.0117	0.475	1.1764	0.352	0.914	16.2469	0.572	2.9696	3.6194	4.2869
11	1.0117	0.490	1.1964	0.367	0.974	16.3544	0.584	2.9544	3.6042	4.5701
12	1.0117	0.505	1.2164	0.382	1.034	16.4619	0.596	2.9392	3.5890	4.8533
13	1.0117	0.520	1.2364	0.397	1.094	16.5694	0.608	2.9240	3.5738	5.1365
14	1.0117	0.535	1.2564	0.412	1.154	16.6769	0.620	2.9088	3.5586	5.4197
15	1.0117	0.550	1.2764	0.427	1.214	16.7844	0.632	2.8936	3.5434	5.7029
16	1.0117	0.565	1.2964	0.442	1.274	16.8919	0.644	2.8784	3.5282	5.9861
17	1.0117	0.580	1.3164	0.457	1.334	17.0000	0.656	2.8632	3.5130	6.2693
18	1.0117	0.595	1.3364	0.472	1.394	17.1075	0.668	2.8480	3.4978	6.5525
19	1.0117	0.610	1.3564	0.487	1.454	17.2150	0.680	2.8328	3.4826	6.8357

ANGULAR LOCATION NO. 24, AT THETA = 20.000 DEGREES

I	OP/P	Y/P	Y/P	VR/VINF	VX/VINF	FLTM ANGLE	V/VINF	RM/RH/TNF	T/TINF	P/PINF
1	1.0117	0.340	0.9964	0.150	0.355	16.663	0.680	2.8176	3.4674	7.1189
2	1.0117	0.355	1.0164	0.231	0.423	16.7705	0.692	2.8024	3.4522	7.4021
3	1.0117	0.370	1.0364	0.247	0.484	16.8776	0.704	2.7872	3.4370	7.6853
4	1.0117	0.385	1.0564	0.262	0.549	16.9847	0.716	2.7720	3.4218	7.9685
5	1.0117	0.400	1.0764	0.277	0.609	17.0918	0.728	2.7568	3.4066	8.2517
6	1.0117	0.415	1.0964	0.292	0.674	17.1989	0.740	2.7416	3.3914	8.5349
7	1.0117	0.430	1.1164	0.307	0.734	17.3060	0.752	2.7264	3.3762	8.8181
8	1.0117	0.445	1.1364	0.322	0.794	17.4131	0.764	2.7112	3.3610	9.1013
9	1.0117	0.460	1.1564	0.337	0.854	17.5202	0.776	2.6960	3.3458	9.3845
10	1.0117	0.475	1.1764	0.352	0.914	17.6273	0.788	2.6808	3.3306	9.6677
11	1.0117	0.490	1.1964	0.367	0.974	17.7344	0.800	2.6656	3.3154	9.9509
12	1.0117	0.505	1.2164	0.382	1.034	17.8415	0.812	2.6504	3.3002	10.2341
13	1.0117	0.520	1.2364	0.397	1.094	17.9486	0.824	2.6352	3.2850	10.5173
14	1.0117	0.535	1.2564	0.412	1.154	18.0557	0.836	2.6200	3.2698	10.8005
15	1.0117	0.550	1.2764	0.427	1.214	18.1628	0.848	2.6048	3.2546	11.0837
16	1.0117	0.565	1.2964	0.442	1.274	18.2699	0.860	2.5896	3.2394	11.3669
17	1.0117	0.580	1.3164	0.457	1.334	18.3770	0.872	2.5744	3.2242	11.6501
18	1.0117	0.595	1.3364	0.472	1.394	18.4841	0.884	2.5592	3.2090	11.9333
19	1.0117	0.610	1.3564	0.487	1.454	18.5912	0.896	2.5440	3.1938	12.2165

Figure A.5.- Continued.

FLUX FIELD VALUES FROM MAGNETIC CALCULATION

ADDITIONAL AXIAL LOCATION NO. 10 AT X/P. = -0.465

T	Y/P.	V/VINE	V/VINE	FLOW ANGLE	V/VINE	Y/VINE	P/PINE
1	1.1100	.1421	.1400	0. 4.1	.0. 4	.1421	1.3151
2	1.1175	.1772	.1749	11.1141	.4776	.1772	1.4177
3	1.1233	.2046	.2023	13.1472	.4919	.2046	1.4902
4	1.1291	.2278	.2253	14.1714	.4959	.2278	1.5384
5	1.1347	.2470	.2442	15.1790	.4964	.2470	1.5651
6	1.1411	.2632	.2602	15.1462	.4937	.2632	1.5736
7	1.1461	.2749	.2719	16.1592	.4921	.2749	1.5777
8	1.1510	.2837	.2807	16.1700	.4911	.2837	1.5773
9	1.1557	.2902	.2873	17.1130	.4909	.2902	1.5771
10	1.1604	.2955	.2925	17.1745	.4904	.2955	1.5740
11	1.1627	.2944	.2914	16.162	.4915	.2944	1.5724
12	1.1644	.2978	.2948	15.1452	.4943	.2978	1.5657
13	1.1655	.2958	.2928	14.1453	.4930	.2958	1.5601
14	1.1612	.2934	.2904	13.1400	.4913	.2934	1.5516
15	1.1574	.2857	.2827	12.1311	.4917	.2857	1.5419
16	1.1535	.2777	.2747	11.1211	.4925	.2777	1.5314
17	1.1492	.2682	.2652	10.1159	.4937	.2682	1.5212
18	1.1432	.2576	.2546	9.1111	.4944	.2576	1.5102
19	1.1361	.2472	.2442	8.1040	.4932	.2472	1.4974

ADDITIONAL AXIAL LOCATION NO. 11 AT X/P. = -0.395

T	Y/P.	V/VINE	V/VINE	FLOW ANGLE	V/VINE	Y/VINE	P/PINE
1	1.1100	.1771	.1749	7.1024	.4912	.1771	1.4976
2	1.1175	.2072	.2049	11.1308	.4879	.2072	1.4947
3	1.1243	.2346	.2323	14.1424	.4874	.2346	1.4929
4	1.1303	.2577	.2554	12.1476	.4840	.2577	1.4915
5	1.1370	.2745	.2721	10.1471	.4871	.2745	1.4917
6	1.1436	.2837	.2813	10.1174	.4907	.2837	1.4908
7	1.1497	.2879	.2854	10.1141	.4939	.2879	1.4913
8	1.1551	.2883	.2858	10.1022	.4934	.2883	1.4947
9	1.1611	.2837	.2812	10.1440	.4923	.2837	1.4957
10	1.1664	.2749	.2724	17.1244	.4923	.2749	1.4959
11	1.1721	.2602	.2577	17.1451	.4925	.2602	1.4975
12	1.1757	.2532	.2507	17.1676	.4925	.2532	1.4945
13	1.1792	.2467	.2442	16.1452	.4928	.2467	1.4938
14	1.1827	.2397	.2372	15.1472	.4918	.2397	1.4928
15	1.1863	.2323	.2298	14.1424	.4910	.2323	1.4907
16	1.1898	.2246	.2221	13.1407	.4910	.2246	1.4890
17	1.1934	.2166	.2141	12.1322	.4912	.2166	1.4922
18	1.1969	.2083	.2058	11.1224	.4901	.2083	1.4973
19	1.2001	.2007	.2007	10.1172	.4907	.2007	1.4946

ADDITIONAL AXIAL LOCATION NO. 12 AT X/P. = -0.327

T	Y/P.	V/VINE	V/VINE	FLOW ANGLE	V/VINE	Y/VINE	P/PINE
1	1.1141	.1421	.1400	0. 4.1	.4912	.1421	1.4973
2	1.1191	.1712	.1689	7.1447	.4915	.1712	1.4921
3	1.1241	.2003	.1980	11.1331	.4914	.2003	1.4945
4	1.1291	.2294	.2271	14.1701	.4976	.2294	1.4923
5	1.1341	.2585	.2562	16.1440	.4961	.2585	1.4907
6	1.1391	.2876	.2853	17.1777	.4923	.2876	1.4901
7	1.1441	.3167	.3144	16.1488	.4907	.3167	1.4922
8	1.1491	.3458	.3435	15.1401	.4900	.3458	1.4904
9	1.1541	.3749	.3726	14.1314	.4914	.3749	1.4904
10	1.1591	.4040	.4017	13.1227	.4914	.4040	1.4904
11	1.1641	.4331	.4308	12.1140	.4914	.4331	1.4904
12	1.1691	.4622	.4599	11.1053	.4914	.4622	1.4904
13	1.1741	.4913	.4890	10.1067	.4914	.4913	1.4904
14	1.1791	.5204	.5181	9.1079	.4914	.5204	1.4904
15	1.1841	.5495	.5472	8.1092	.4914	.5495	1.4904
16	1.1891	.5786	.5763	7.1105	.4914	.5786	1.4904
17	1.1941	.6077	.6054	6.1118	.4914	.6077	1.4904
18	1.1991	.6368	.6345	5.1131	.4914	.6368	1.4904
19	1.2041	.6659	.6636	4.1144	.4914	.6659	1.4904

ADDITIONAL AXIAL LOCATION NO. 13 AT X/P. = -0.259

T	Y/P.	V/VINE	V/VINE	FLOW ANGLE	V/VINE	Y/VINE	P/PINE
1	1.1141	.1421	.1400	0. 4.1	.4914	.1421	1.4904
2	1.1191	.1712	.1689	7.1447	.4914	.1712	1.4904
3	1.1241	.2003	.1980	11.1331	.4914	.2003	1.4904
4	1.1291	.2294	.2271	14.1701	.4914	.2294	1.4904
5	1.1341	.2585	.2562	16.1440	.4914	.2585	1.4904
6	1.1391	.2876	.2853	17.1777	.4914	.2876	1.4904
7	1.1441	.3167	.3144	16.1488	.4914	.3167	1.4904
8	1.1491	.3458	.3435	15.1401	.4914	.3458	1.4904
9	1.1541	.3749	.3726	14.1314	.4914	.3749	1.4904
10	1.1591	.4040	.4017	13.1227	.4914	.4040	1.4904
11	1.1641	.4331	.4308	12.1140	.4914	.4331	1.4904
12	1.1691	.4622	.4599	11.1053	.4914	.4622	1.4904
13	1.1741	.4913	.4890	10.1067	.4914	.4913	1.4904
14	1.1791	.5204	.5181	9.1079	.4914	.5204	1.4904
15	1.1841	.5495	.5472	8.1092	.4914	.5495	1.4904
16	1.1891	.5786	.5763	7.1105	.4914	.5786	1.4904
17	1.1941	.6077	.6054	6.1118	.4914	.6077	1.4904
18	1.1991	.6368	.6345	5.1131	.4914	.6368	1.4904
19	1.2041	.6659	.6636	4.1144	.4914	.6659	1.4904

Figure A.5.- Continued.

STRAHLING TRAJECTORY CALCULATION

49 STRAHLINES CALCULATED

NO. 10 STARTING AT YPO. = 1.3143, 0/0 = 1.422
(DEPENDENCE ON YPO. = 1.000000, 0/0. = 1.315)

YPO.	0/0.
1.3143	1.422
1.2742	1.460
1.2321	1.494
1.2226	1.513
1.2099	1.526
1.1736	1.554
1.1477	1.569
1.1117	1.587
1.0756	1.613
1.0399	1.640
1.00434	1.676
0.971	1.710
0.9312	1.749
0.8951	1.793
0.8591	1.843
0.8231	1.899
0.7876	1.963
0.7526	2.035
0.7181	2.117
0.6841	2.209
0.6506	2.313
0.6176	2.429
0.5851	2.557
0.5531	2.697
0.5216	2.849
0.4906	3.013
0.4601	3.189
0.4301	3.377
0.4006	3.577
0.3716	3.789
0.3431	4.013
0.3151	4.249
0.2876	4.497
0.2606	4.757
0.2341	5.029
0.2081	5.313
0.1826	5.609
0.1576	5.917
0.1331	6.237
0.1091	6.569
0.0856	6.913
0.0626	7.269
0.0401	7.637
0.0181	8.017
0.0006	8.409
0.0001	8.813
0.0000	9.229
0.0000	9.657
0.0000	10.097
0.0000	10.549
0.0000	11.013
0.0000	11.489
0.0000	11.977
0.0000	12.477
0.0000	12.989
0.0000	13.513
0.0000	14.049
0.0000	14.597
0.0000	15.157
0.0000	15.729
0.0000	16.313
0.0000	16.909
0.0000	17.517
0.0000	18.137
0.0000	18.769
0.0000	19.413
0.0000	20.069
0.0000	20.737
0.0000	21.417
0.0000	22.109
0.0000	22.813
0.0000	23.529
0.0000	24.257
0.0000	24.997
0.0000	25.749
0.0000	26.513
0.0000	27.289
0.0000	28.077
0.0000	28.877
0.0000	29.689
0.0000	30.513
0.0000	31.349
0.0000	32.197
0.0000	33.057
0.0000	33.929
0.0000	34.813
0.0000	35.709
0.0000	36.617
0.0000	37.537
0.0000	38.469
0.0000	39.413
0.0000	40.369
0.0000	41.337
0.0000	42.317
0.0000	43.309
0.0000	44.313
0.0000	45.329
0.0000	46.357
0.0000	47.397
0.0000	48.449
0.0000	49.513
0.0000	50.589
0.0000	51.677
0.0000	52.777
0.0000	53.889
0.0000	55.013
0.0000	56.149
0.0000	57.297
0.0000	58.457
0.0000	59.629
0.0000	60.813
0.0000	62.009
0.0000	63.217
0.0000	64.437
0.0000	65.669
0.0000	66.913
0.0000	68.169
0.0000	69.437
0.0000	70.717
0.0000	72.009
0.0000	73.313
0.0000	74.629
0.0000	75.957
0.0000	77.297
0.0000	78.649
0.0000	80.013
0.0000	81.389
0.0000	82.777
0.0000	84.177
0.0000	85.589
0.0000	87.013
0.0000	88.449
0.0000	89.889
0.0000	91.343
0.0000	92.809
0.0000	94.287
0.0000	95.777
0.0000	97.279
0.0000	98.793
0.0000	100.317
0.0000	101.853
0.0000	103.397
0.0000	104.953
0.0000	106.517
0.0000	108.089
0.0000	109.669
0.0000	111.257
0.0000	112.853
0.0000	114.457
0.0000	116.069
0.0000	117.689
0.0000	119.317
0.0000	120.953
0.0000	122.597
0.0000	124.249
0.0000	125.909
0.0000	127.577
0.0000	129.253
0.0000	130.937
0.0000	132.629
0.0000	134.329
0.0000	136.037
0.0000	137.753
0.0000	139.477
0.0000	141.209
0.0000	142.949
0.0000	144.697
0.0000	146.453
0.0000	148.217
0.0000	150.000
0.0000	151.789
0.0000	153.589
0.0000	155.397
0.0000	157.213
0.0000	159.037
0.0000	160.869
0.0000	162.709
0.0000	164.557
0.0000	166.413
0.0000	168.277
0.0000	170.149
0.0000	172.029
0.0000	173.913
0.0000	175.803
0.0000	177.697
0.0000	179.597
0.0000	181.503
0.0000	183.413
0.0000	185.329
0.0000	187.253
0.0000	189.183
0.0000	191.117
0.0000	193.057
0.0000	195.003
0.0000	196.953
0.0000	198.909
0.0000	200.869
0.0000	202.833
0.0000	204.803
0.0000	206.777
0.0000	208.753
0.0000	210.737
0.0000	212.729
0.0000	214.729
0.0000	216.737
0.0000	218.753
0.0000	220.769
0.0000	222.789
0.0000	224.813
0.0000	226.843
0.0000	228.877
0.0000	230.913
0.0000	232.953
0.0000	234.997
0.0000	237.043
0.0000	239.093
0.0000	241.143
0.0000	243.197
0.0000	245.253
0.0000	247.309
0.0000	249.369
0.0000	251.429
0.0000	253.489
0.0000	255.549
0.0000	257.609
0.0000	259.669
0.0000	261.729
0.0000	263.789
0.0000	265.849
0.0000	267.909
0.0000	269.969
0.0000	272.029
0.0000	274.089
0.0000	276.149
0.0000	278.209
0.0000	280.269
0.0000	282.329
0.0000	284.389
0.0000	286.449
0.0000	288.509
0.0000	290.569
0.0000	292.629
0.0000	294.689
0.0000	296.749
0.0000	298.809
0.0000	300.869
0.0000	302.929
0.0000	304.989
0.0000	307.049
0.0000	309.109
0.0000	311.169
0.0000	313.229
0.0000	315.289
0.0000	317.349
0.0000	319.409
0.0000	321.469
0.0000	323.529
0.0000	325.589
0.0000	327.649
0.0000	329.709
0.0000	331.769
0.0000	333.829
0.0000	335.889
0.0000	337.949
0.0000	340.009
0.0000	342.069
0.0000	344.129
0.0000	346.189
0.0000	348.249
0.0000	350.309
0.0000	352.369
0.0000	354.429
0.0000	356.489
0.0000	358.549
0.0000	360.609
0.0000	362.669
0.0000	364.729
0.0000	366.789
0.0000	368.849
0.0000	370.909
0.0000	372.969
0.0000	375.029
0.0000	377.089
0.0000	379.149
0.0000	381.209
0.0000	383.269
0.0000	385.329
0.0000	387.389
0.0000	389.449
0.0000	391.509
0.0000	393.569
0.0000	395.629
0.0000	397.689
0.0000	399.749
0.0000	401.809
0.0000	403.869
0.0000	405.929
0.0000	407.989
0.0000	410.049
0.0000	412.109
0.0000	414.169
0.0000	416.229
0.0000	418.289
0.0000	420.349
0.0000	422.409
0.0000	424.469
0.0000	426.529
0.0000	428.589
0.0000	430.649
0.0000	432.709
0.0000	434.769
0.0000	436.829
0.0000	438.889
0.0000	440.949
0.0000	443.009
0.0000	445.069
0.0000	447.129
0.0000	449.189
0.0000	451.249
0.0000	453.309
0.0000	455.369
0.0000	457.429
0.0000	459.489
0.0000	461.549
0.0000	463.609
0.0000	465.669
0.0000	467.729
0.0000	469.789
0.0000	471.849
0.0000	473.909
0.0000	475.969
0.0000	478.029
0.0000	480.089
0.0000	482.149
0.0000	484.209
0.0000	486.269
0.0000	488.329
0.0000	490.389
0.0000	492.449
0.0000	494.509
0.0000	496.569
0.0000	498.629
0.0000	500.689
0.0000	502.749
0.0000	504.809
0.0000	506.869
0.0000	508.929
0.0000	510.989
0.0000	513.049
0.0000	515.109
0.0000	517.169
0.0000	519.229
0.0000	521.289
0.0000	523.349
0.0000	525.409
0.0000	527.469
0.0000	529.529
0.0000	531.589
0.0000	533.649
0.0000	535.709
0.0000	537.769
0.0000	539.829
0.0000	541.889
0.0000	543.949
0.0000	546.009
0.0000	548.069
0.0000	550.129
0.0000	552.189
0.0000	554.249
0.0000	556.309
0.0000	558.369
0.0000	560.429
0.0000	562.489
0.0000	564.549
0.0000	566.609
0.0000	568.669
0.0000	570.729
0.0000	572.789
0.0000	574.849
0.0000	576.909
0.0000	578.969
0.0000	581.029
0.0000	583.089
0.0000	585.149
0.0000	587.209
0.0000	589.269
0.0000	591.329
0.0000	593.389
0.0000	595.449
0.0000	597.509
0.0000	599.569
0.0000	601.629
0.0000	603.689
0.0000	605.749
0.0000	607.809
0.0000	609.869
0.0000	611.929
0.0000	613.989
0.0000	616.049
0.0000	618.109
0.0000	620.169
0.0000	622.229
0.0000	624.289
0.0000	626.349
0.0000	628.409
0.0000	630.469
0.0000	632.529
0.0000	634.589
0.0000	636.649
0.0000	638.709
0.0000	640.769
0.0000	642.829
0.0000	644.889
0.0000	646.949
0.0000	649.009
0.0000	651.069
0.0000	653.129
0.0000	655.189
0.0000	657.249
0.0000	659.309
0.0000	661.369
0.0000	663.429
0.0000	665.489
0.0000	667.549
0.0000	669.609
0.0000	671.669
0.0000	673.729
0.0000	675.789
0.0000	677.849
0.0000	679.909
0.0000	681.969
0.0000	684.029
0.0000	686.089
0.0000	688.149
0.0000	690.209
0.0000	692.269
0.0000	694.329
0.0000	696.389
0.0000	698.449
0.0000	700.509

-7.4315	1.1431
-6.4345	1.1433
-5.4343	1.1407
-4.43577	1.1402
-3.4373	1.1424
-2.4376	1.1403
-1.4352	1.1473
-0.4370	1.1403
0.4345	1.1473
1.4323	1.1473
2.4343	1.1433
3.4315	1.1403
4.4344	1.1433
5.4307	1.1403
6.4321	1.1403
7.4375	1.1403
8.4324	1.1473
9.4343	1.1473
10.4315	1.1403
11.4344	1.1433
12.4307	1.1403
13.4321	1.1403
14.4375	1.1403
15.4324	1.1473
16.4343	1.1473
17.4315	1.1403
18.4344	1.1433
19.4307	1.1403
20.4321	1.1403
21.4375	1.1403
22.4324	1.1473
23.4343	1.1473
24.4315	1.1403
25.4344	1.1433
26.4307	1.1403
27.4321	1.1403
28.4375	1.1403
29.4324	1.1473
30.4343	1.1473
31.4315	1.1403
32.4344	1.1433
33.4307	1.1403
34.4321	1.1403
35.4375	1.1403
36.4324	1.1473
37.4343	1.1473
38.4315	1.1403
39.4344	1.1433
40.4307	1.1403
41.4321	1.1403
42.4375	1.1403
43.4324	1.1473
44.4343	1.1473
45.4315	1.1403
46.4344	1.1433
47.4307	1.1403
48.4321	1.1403
49.4375	1.1403
50.4324	1.1473
51.4343	1.1473
52.4315	1.1403
53.4344	1.1433
54.4307	1.1403
55.4321	1.1403
56.4375	1.1403
57.4324	1.1473
58.4343	1.1473
59.4315	1.1403
60.4344	1.1433
61.4307	1.1403
62.4321	1.1403
63.4375	1.1403
64.4324	1.1473
65.4343	1.1473
66.4315	1.1403
67.4344	1.1433
68.4307	1.1403
69.4321	1.1403
70.4375	1.1403
71.4324	1.1473
72.4343	1.1473
73.4315	1.1403
74.4344	1.1433
75.4307	1.1403
76.4321	1.1403
77.4375	1.1403
78.4324	1.1473
79.4343	1.1473
80.4315	1.1403
81.4344	1.1433
82.4307	1.1403
83.4321	1.1403
84.4375	1.1403
85.4324	1.1473
86.4343	1.1473
87.4315	1.1403
88.4344	1.1433
89.4307	1.1403
90.4321	1.1403
91.4375	1.1403
92.4324	1.1473
93.4343	1.1473
94.4315	1.1403
95.4344	1.1433
96.4307	1.1403
97.4321	1.1403
98.4375	1.1403
99.4324	1.1473
100.4343	1.1473

STRENGTHING NO.42, STARTING AT VPO = -7.4343, RPO = 5.3127

VPO	RPO
-5.4343	5.3127
-4.4307	5.3127
-3.4375	5.3127
-2.4344	5.3127
-1.4315	5.3127
0.4343	5.3127
1.4315	5.3127
2.4344	5.3127
3.4375	5.3127
4.4307	5.3127
5.4343	5.3127

STRENGTHING NO.40, STARTING AT VPO = -7.4313, RPO = 5.4382

VPO	RPO
-5.4313	5.4382
-4.4344	5.4382
-3.4375	5.4382
-2.4344	5.4382
-1.4313	5.4382
0.4313	5.4382
1.4344	5.4382
2.4375	5.4382
3.4344	5.4382
4.4375	5.4382
5.4313	5.4382

Figure A.5.- Continued.

ANGULAR LOCATION NO. 1, AT THETA = 0.0000 DEGREE

T	DOSE	37/31NE (PARALLEL)	37/31NE (100°P)	37/31NE (14°-PLANES)	4-ANGLE (14°-PLANES)	37/31NE (100°P)	37/31NE (RESULTANT)	37/31NE (RESULTANT)	37/31NE (RESULTANT)
1	1.0000	0.0000	0.0000	0.0000	0.0000	0.0000	0.0000	0.0000	0.0000
2	1.0169	0.0000	12.0000	11.8669	89.9445	3.0000	0.1115	11.8724	0.1536
3	1.0338	0.0000	23.7372	23.6703	89.3358	2.0000	0.2113	23.6813	0.2535
4	1.0507	0.0000	35.4745	35.3192	88.7270	1.0000	0.3110	35.3262	0.3531
5	1.0676	0.0000	47.2118	46.9574	88.1181	0.5000	0.4108	47.2311	0.4526
6	1.0845	0.0000	58.9491	58.5900	87.5093	0.2500	0.5106	58.9560	0.5521
7	1.1014	0.0000	70.6864	70.2392	86.9005	0.1250	0.6104	70.6810	0.6516
8	1.1183	0.0000	82.4237	81.8736	86.2917	0.0625	0.7102	82.4160	0.7511
9	1.1352	0.0000	94.1610	93.5077	85.6829	0.0312	0.8100	94.1610	0.8506
10	1.1521	0.0000	105.8983	105.1450	85.0741	0.0156	0.9098	105.8983	0.9501
11	1.1690	0.0000	117.6356	116.7813	84.4653	0.0078	1.0096	117.6356	1.0496
12	1.1859	0.0000	129.3729	128.4186	83.8565	0.0039	1.1094	129.3729	1.1491
13	1.2028	0.0000	141.1102	140.0559	83.2477	0.0019	1.2092	141.1102	1.2486
14	1.2197	0.0000	152.8475	151.6932	82.6389	0.0009	1.3090	152.8475	1.3481
15	1.2366	0.0000	164.5848	163.3305	82.0301	0.0005	1.4088	164.5848	1.4476
16	1.2535	0.0000	176.3221	174.9678	81.4213	0.0002	1.5086	176.3221	1.5471
17	1.2704	0.0000	188.0594	186.6051	80.8125	0.0001	1.6084	188.0594	1.6466
18	1.2873	0.0000	199.7967	198.3424	80.2037	0.0000	1.7082	199.7967	1.7461
19	1.3042	0.0000	211.5340	210.0797	79.5949	0.0000	1.8080	211.5340	1.8456

ANGLE OF LOCATION NO. 3, AT THTA = 2. 11, DEGREES

T	DO/D	R/R/TIME (R/R/L)	R/R/TIME (R/R/P)	R/R/TIME (IN-PLAN)	ANGLE (IN-PLAN)	R/R/TIME (NORMAL)	R/R/TIME (RESULTANT)	R/R/TIME (RESULTANT)	R/R/TIME (RESULTANT)
1	1.0160	3.466							
2	1.0167		11.7904	31.7504	48.1212	5.1935	3.3852	11.7410	2.2372
3	1.0174	1.1978	6.7713	5.6270	16.6154	5.0000	2.2536	5.6133	2.2286
4	1.0180	2.6900	7.1865	7.1018	34.1420	4.7499	2.2209	7.3907	2.1889
5	1.0188	3.7342	6.2139	6.6217	40.1340	4.6008	2.2019	6.1989	2.2167
6	1.0194	3.7666	5.6655	5.6615	44.6064	4.6658	1.8885	5.5925	2.2039
7	1.0197	4.4371	5.0749	5.1341	47.3760	4.3127	2.0811	5.1256	1.9771
8	1.0197	4.4966	4.6036	4.5272	47.3727	4.4792	1.7556	4.4087	1.9100
9	1.0206	4.5791	4.4042	4.5566	47.7519	4.2560	1.7594	4.4085	1.8554
10	1.0222	4.605	4.1268	4.7954	47.6474	3.9327	1.7577	4.2773	1.7977
11	1.0207	4.5567	4.0132	4.6738	47.5317	3.8281	1.7551	4.0658	1.7465
12	1.0204	4.5097	3.6433	3.8505	47.4707	3.7774	1.7527	3.8785	1.6995
13	1.0213	4.7771	3.7939	3.7422	47.2491	3.5965	1.7721	3.7311	1.6444
14	1.0219	4.6000	3.6219	3.6000	47.0000	3.4924	1.7721	3.6786	1.5966
15	1.0227	4.6448	3.4448	3.4440	47.2274	3.4000	1.7721	3.4000	1.5400
16	1.0242	4.6992	3.1605	3.3648	47.1061	3.2473	1.6977	3.3370	1.5162
17	1.0272	4.6774	3.0264	3.2777	47.1714	3.1906	1.5964	3.2206	1.4958
18	1.0283	4.6951	3.0153	3.1764	47.2493	3.1922	1.5011	3.1725	1.4415
19	1.0301	4.6900	3.0000	3.0000	46.4373	3.0000	1.5011	2.9755	1.3772

AMCJLAP LOCATION NO. 3, AT TULSA • 56441, 356025

[illegible]

Figure A.5.- Continued.

7	2.2514	.7747	.72913	.7744	73.6135	1.4441	.2213	.7764	.4777
8	.7744	.7747	.72913	.7744	73.6135	1.4441	.2213	.7764	.4777
9	.7744	.7747	.72913	.7744	73.6135	1.4441	.2213	.7764	.4777
10	.7744	.7747	.72913	.7744	73.6135	1.4441	.2213	.7764	.4777
11	.7744	.7747	.72913	.7744	73.6135	1.4441	.2213	.7764	.4777
12	.7744	.7747	.72913	.7744	73.6135	1.4441	.2213	.7764	.4777
13	.7744	.7747	.72913	.7744	73.6135	1.4441	.2213	.7764	.4777
14	.7744	.7747	.72913	.7744	73.6135	1.4441	.2213	.7764	.4777
15	.7744	.7747	.72913	.7744	73.6135	1.4441	.2213	.7764	.4777
16	.7744	.7747	.72913	.7744	73.6135	1.4441	.2213	.7764	.4777
17	.7744	.7747	.72913	.7744	73.6135	1.4441	.2213	.7764	.4777
18	.7744	.7747	.72913	.7744	73.6135	1.4441	.2213	.7764	.4777
19	.7744	.7747	.72913	.7744	73.6135	1.4441	.2213	.7764	.4777

ADDITIONAL AXIAL LOCATION NO.45, AT Y/P = 0.5367									
T	Y/P	R/RINE (PARALLEL)	R/RINE (PERPEND)	R/RINE (IN-PLANE)	R-ANGLE (IN-PLANE)	R/RINE (NORMAL)	R/RINE (RESULTANT)	R/RINE (RESULTANT)	R/RINE (RESULTANT)
1	1.4441	.7744	.72913	.7744	73.6135	1.4441	.2213	.7764	.4777
2	1.4441	.7744	.72913	.7744	73.6135	1.4441	.2213	.7764	.4777
3	1.4441	.7744	.72913	.7744	73.6135	1.4441	.2213	.7764	.4777
4	1.4441	.7744	.72913	.7744	73.6135	1.4441	.2213	.7764	.4777
5	1.4441	.7744	.72913	.7744	73.6135	1.4441	.2213	.7764	.4777
6	1.4441	.7744	.72913	.7744	73.6135	1.4441	.2213	.7764	.4777
7	1.4441	.7744	.72913	.7744	73.6135	1.4441	.2213	.7764	.4777
8	1.4441	.7744	.72913	.7744	73.6135	1.4441	.2213	.7764	.4777
9	1.4441	.7744	.72913	.7744	73.6135	1.4441	.2213	.7764	.4777
10	1.4441	.7744	.72913	.7744	73.6135	1.4441	.2213	.7764	.4777
11	1.4441	.7744	.72913	.7744	73.6135	1.4441	.2213	.7764	.4777
12	1.4441	.7744	.72913	.7744	73.6135	1.4441	.2213	.7764	.4777
13	1.4441	.7744	.72913	.7744	73.6135	1.4441	.2213	.7764	.4777
14	1.4441	.7744	.72913	.7744	73.6135	1.4441	.2213	.7764	.4777
15	1.4441	.7744	.72913	.7744	73.6135	1.4441	.2213	.7764	.4777
16	1.4441	.7744	.72913	.7744	73.6135	1.4441	.2213	.7764	.4777
17	1.4441	.7744	.72913	.7744	73.6135	1.4441	.2213	.7764	.4777
18	1.4441	.7744	.72913	.7744	73.6135	1.4441	.2213	.7764	.4777
19	1.4441	.7744	.72913	.7744	73.6135	1.4441	.2213	.7764	.4777

VELOCITY AND TEMPERATURE CONTOURS

14 VELOCITY (TEMPERATURE) CONTOUR LINES FOUND

4 PRINTS IN CONTOUR LINE OF V/VINE = .11% T/TINE = 3.47%

Y/P	R/P
1.4441	.7744
1.4441	.7744
1.4441	.7744
1.4441	.7744
1.4441	.7744
1.4441	.7744
1.4441	.7744
1.4441	.7744
1.4441	.7744
1.4441	.7744

14 PRINTS IN CONTOUR LINE OF V/VINE = .20% T/TINE = 3.94%

Y/P	R/P
1.4441	.7744
1.4441	.7744
1.4441	.7744
1.4441	.7744
1.4441	.7744
1.4441	.7744
1.4441	.7744
1.4441	.7744
1.4441	.7744
1.4441	.7744

Figure A.5.- Continued.

21 MAGNETIC FIELD CRYSTAL LINES FOUND
(FOR COMPONENT ALONG FIELD LINES PARALLEL TO FLOW IN FREESTREAM)

Y/P3	R/R2
.9411	.1983
.9999	.1904
1.0112	.1813
1.0212	.1761
1.0313	.1697
1.0452	.1673
1.0792	.1669
1.0812	.1636
1.1101	.0953
1.1144	.1385
1.1198	.0700

YPO	YPO
.9467	.9515
.9553	.9559
.9647	.9634
.9727	.9726
.9824	.9840
.9943	.9937
1.0063	1.0021
1.0164	1.0127
1.0277	1.0264
1.0377	1.0356
1.0477	1.0456
1.0579	1.0556
1.0679	1.0656
1.0782	1.0756
1.0882	1.0856
1.0982	1.0956
1.1082	1.1056
1.1182	1.1156
1.1282	1.1256

[illegible]

W/F	W/F
3741	101242
3721	10076
4427	0733
257	0758
376	0146
3352	0743
5621	0653
0056	020
7736	0754
8523	0770
0052	0721
7748	0056
6430	0751
0350	0439
0643	0725
0065	0321
101244	0417
4074	0343
7712	0207
101220	0173
101207	0120
101202	0757

114

DENSITY CONTOURS

Y DENSITY CONTOUR LINES EQUAL

25 POINTS IN CONTOUR LINE OF RHODORINE = 2.0E7

Y/PJ	P/PJ
.463-	.45.2
.46.55	.47.42
.4701	.4940
.4939	.5111
.49.11	.5200
.4928	.5413
.4941	.5549
.4940	.5672
1.0.11.7	.5775
.49283	.5839
1.0.471	.5925
1.0.469	.5931
1.0.474	.5910
1.0.472	.5945
1.0.472	.5959
1.0.463	.5991
1.0.464	.6030
1.0.47	.6050
1.0.472	.6029
1.0.494	.6027
1.0.480	.6015
1.0.476	.6011
1.0.462	.6061
1.0.487	.6065
1.0.482	.6065

24 POINTS IN CONTOUR LINE OF RHODORINE = 2.0E7

Y/PJ	P/PJ
.6027	.6023
.6060	.6021
.60.5	.6034
.6042	.6070
.6041	.6031
.6071	.6040
.6040	.6043
.60.4	.6047
.6061	.6043
.60.4	.6041
.6099	.6041
.607	1.0.42
.6035	1.0.5.2
.6035	1.0.5.9
.6038	1.0.969
.6040	1.0.13
.6044	1.0.404
.6036	1.0.37
.60.96	1.0.2725
.60.40	1.0.222
.6038	1.0.415
.6041	1.0.412
.60.17	1.0.4027
.6028	1.0.406
.6032	1.0.408
.6037	1.0.423

Figure A.5.- Continued.

14 MAGNETIC FIELD CONTOUR LINES FOUND
 1539 COMPONENT ALONG FIELD LINES NORMAL TO FLOW IN CROSS-STREAM

36 POINTS IN CONTOUR LINE OF R/RINE (NORMAL) = 5.000

X/YD	Q/RD
1.0142	.0087
1.0310	.0075
1.0475	.0076
1.0627	.0115
1.0828	.0117
1.0925	.0117
1.1051	.0155
1.1067	.0154
1.1060	.0154
1.1064	.0201
1.1070	.0311
.0045	.0417
.0043	.0403
.0021	.0364
.0000	.0306
.0022	.0244
.0454	.0115
.7081	.0105
.7450	.0724
.6006	.0219
.6965	.0217
.6726	.0717
.5720	.0114
.5179	.0153
.4416	.0090
.3974	.0072

31 POINTS IN CONTOUR LINE OF R/RINE (NORMAL) = 5.000

X/YD	Q/RD
.2514	1.0744
.2053	1.0645
.3792	1.0391
.4444	.0172
.5155	.0097
.5352	.0109
.5127	.0110
.6441	.0192
.7159	.0112
.7124	.0137
.7647	.0718
.7585	.0737
.8455	.0730
.8610	.0744
.9153	.0574
.9544	.0523
.9651	.0360
.9037	.0645
1.0213	.0442
1.0520	.0414
1.0172	.0273
1.0149	.0228
1.0192	.0121
1.0061	.0113
1.0065	.0157
1.0116	.0111
1.0059	.0101
1.0098	.0140
1.0137	.0161
1.0133	.0161
1.0164	.0117

Figure A.5.- Continued.

TRAJECTORY CALCULATION

(SOLAR WIND COORDINATE SYSTEM)

TRAJECTORY COORDINATES

R /PLANET = 111

N	TIME	V/R	V/O	T/R	R/R	V/PLANET	V/OPLANET	V/RPLANET	R/RPLANET
1	-00.970	1.0000	-0.0000	1.0000	4.01195	1.0000	-0.0000	1.0000	4.01195
2	-00.9370	0.9997	-0.0003	1.0000	4.01195	0.9997	-0.0003	1.0000	4.01195
3	-00.9040	0.9994	-0.0006	1.0000	4.01195	0.9994	-0.0006	1.0000	4.01195
4	-00.8710	0.9991	-0.0009	1.0000	4.01195	0.9991	-0.0009	1.0000	4.01195
5	-00.8380	0.9988	-0.0012	1.0000	4.01195	0.9988	-0.0012	1.0000	4.01195
6	-00.8050	0.9985	-0.0015	1.0000	4.01195	0.9985	-0.0015	1.0000	4.01195
7	-00.7720	0.9982	-0.0018	1.0000	4.01195	0.9982	-0.0018	1.0000	4.01195
8	-00.7390	0.9979	-0.0021	1.0000	4.01195	0.9979	-0.0021	1.0000	4.01195
9	-00.7060	0.9976	-0.0024	1.0000	4.01195	0.9976	-0.0024	1.0000	4.01195
10	-00.6730	0.9973	-0.0027	1.0000	4.01195	0.9973	-0.0027	1.0000	4.01195
11	-00.6400	0.9970	-0.0030	1.0000	4.01195	0.9970	-0.0030	1.0000	4.01195
12	-00.6070	0.9967	-0.0033	1.0000	4.01195	0.9967	-0.0033	1.0000	4.01195
13	-00.5740	0.9964	-0.0036	1.0000	4.01195	0.9964	-0.0036	1.0000	4.01195
14	-00.5410	0.9961	-0.0039	1.0000	4.01195	0.9961	-0.0039	1.0000	4.01195
15	-00.5080	0.9958	-0.0042	1.0000	4.01195	0.9958	-0.0042	1.0000	4.01195
16	-00.4750	0.9955	-0.0045	1.0000	4.01195	0.9955	-0.0045	1.0000	4.01195
17	-00.4420	0.9952	-0.0048	1.0000	4.01195	0.9952	-0.0048	1.0000	4.01195
18	-00.4090	0.9949	-0.0051	1.0000	4.01195	0.9949	-0.0051	1.0000	4.01195
19	-00.3760	0.9946	-0.0054	1.0000	4.01195	0.9946	-0.0054	1.0000	4.01195
20	-00.3430	0.9943	-0.0057	1.0000	4.01195	0.9943	-0.0057	1.0000	4.01195
21	-00.3100	0.9940	-0.0060	1.0000	4.01195	0.9940	-0.0060	1.0000	4.01195
22	-00.2770	0.9937	-0.0063	1.0000	4.01195	0.9937	-0.0063	1.0000	4.01195
23	-00.2440	0.9934	-0.0066	1.0000	4.01195	0.9934	-0.0066	1.0000	4.01195
24	-00.2110	0.9931	-0.0069	1.0000	4.01195	0.9931	-0.0069	1.0000	4.01195
25	-00.1780	0.9928	-0.0072	1.0000	4.01195	0.9928	-0.0072	1.0000	4.01195
26	-00.1450	0.9925	-0.0075	1.0000	4.01195	0.9925	-0.0075	1.0000	4.01195
27	-00.1120	0.9922	-0.0078	1.0000	4.01195	0.9922	-0.0078	1.0000	4.01195
28	-00.0790	0.9919	-0.0081	1.0000	4.01195	0.9919	-0.0081	1.0000	4.01195
29	-00.0460	0.9916	-0.0084	1.0000	4.01195	0.9916	-0.0084	1.0000	4.01195
30	-00.0130	0.9913	-0.0087	1.0000	4.01195	0.9913	-0.0087	1.0000	4.01195
31	0.0200	0.9910	-0.0090	1.0000	4.01195	0.9910	-0.0090	1.0000	4.01195
32	0.0530	0.9907	-0.0093	1.0000	4.01195	0.9907	-0.0093	1.0000	4.01195
33	0.0860	0.9904	-0.0096	1.0000	4.01195	0.9904	-0.0096	1.0000	4.01195
34	0.1190	0.9901	-0.0099	1.0000	4.01195	0.9901	-0.0099	1.0000	4.01195
35	0.1520	0.9898	-0.0102	1.0000	4.01195	0.9898	-0.0102	1.0000	4.01195
36	0.1850	0.9895	-0.0105	1.0000	4.01195	0.9895	-0.0105	1.0000	4.01195
37	0.2180	0.9892	-0.0108	1.0000	4.01195	0.9892	-0.0108	1.0000	4.01195

SCALAR FIELD AND MAGNETIC FIELD COMPONENTS ALONG TRAJECTORY
(SOLAR WIND COORDINATE SYSTEM)

(NOM-ORTHONORMALIZED BY INTERPLANETARY VALUES)

N	TIME	VX/VIN	VY/VIN	VZ/VIN	VX/VIN	VY/VIN	VZ/VIN	TEMP/TEMPIN	R/RIN	VX/RIN	VY/RIN	VZ/RIN
1	-00.970	1.0000	0.0000	0.0000	1.0000	0.0000	0.0000	1.0000	1.0000	1.0000	0.0000	0.0000
2	-00.9370	1.0000	0.0000	0.0000	1.0000	0.0000	0.0000	1.0000	1.0000	1.0000	0.0000	0.0000
3	-00.9040	1.0000	0.0000	0.0000	1.0000	0.0000	0.0000	1.0000	1.0000	1.0000	0.0000	0.0000
4	-00.8710	1.0000	0.0000	0.0000	1.0000	0.0000	0.0000	1.0000	1.0000	1.0000	0.0000	0.0000
5	-00.8380	1.0000	0.0000	0.0000	1.0000	0.0000	0.0000	1.0000	1.0000	1.0000	0.0000	0.0000
6	-00.8050	1.0000	0.0000	0.0000	1.0000	0.0000	0.0000	1.0000	1.0000	1.0000	0.0000	0.0000
7	-00.7720	1.0000	0.0000	0.0000	1.0000	0.0000	0.0000	1.0000	1.0000	1.0000	0.0000	0.0000
8	-00.7390	1.0000	0.0000	0.0000	1.0000	0.0000	0.0000	1.0000	1.0000	1.0000	0.0000	0.0000
9	-00.7060	1.0000	0.0000	0.0000	1.0000	0.0000	0.0000	1.0000	1.0000	1.0000	0.0000	0.0000
10	-00.6730	1.0000	0.0000	0.0000	1.0000	0.0000	0.0000	1.0000	1.0000	1.0000	0.0000	0.0000
11	-00.6400	1.0000	0.0000	0.0000	1.0000	0.0000	0.0000	1.0000	1.0000	1.0000	0.0000	0.0000
12	-00.6070	1.0000	0.0000	0.0000	1.0000	0.0000	0.0000	1.0000	1.0000	1.0000	0.0000	0.0000
13	-00.5740	1.0000	0.0000	0.0000	1.0000	0.0000	0.0000	1.0000	1.0000	1.0000	0.0000	0.0000
14	-00.5410	1.0000	0.0000	0.0000	1.0000	0.0000	0.0000	1.0000	1.0000	1.0000	0.0000	0.0000
15	-00.5080	1.0000	0.0000	0.0000	1.0000	0.0000	0.0000	1.0000	1.0000	1.0000	0.0000	0.0000
16	-00.4750	1.0000	0.0000	0.0000	1.0000	0.0000	0.0000	1.0000	1.0000	1.0000	0.0000	0.0000
17	-00.4420	1.0000	0.0000	0.0000	1.0000	0.0000	0.0000	1.0000	1.0000	1.0000	0.0000	0.0000
18	-00.4090	1.0000	0.0000	0.0000	1.0000	0.0000	0.0000	1.0000	1.0000	1.0000	0.0000	0.0000
19	-00.3760	1.0000	0.0000	0.0000	1.0000	0.0000	0.0000	1.0000	1.0000	1.0000	0.0000	0.0000
20	-00.3430	1.0000	0.0000	0.0000	1.0000	0.0000	0.0000	1.0000	1.0000	1.0000	0.0000	0.0000
21	-00.3100	1.0000	0.0000	0.0000	1.0000	0.0000	0.0000	1.0000	1.0000	1.0000	0.0000	0.0000
22	-00.2770	1.0000	0.0000	0.0000	1.0000	0.0000	0.0000	1.0000	1.0000	1.0000	0.0000	0.0000
23	-00.2440	1.0000	0.0000	0.0000	1.0000	0.0000	0.0000	1.0000	1.0000	1.0000	0.0000	0.0000
24	-00.2110	1.0000	0.0000	0.0000	1.0000	0.0000	0.0000	1.0000	1.0000	1.0000	0.0000	0.0000
25	-00.1780	1.0000	0.0000	0.0000	1.0000	0.0000	0.0000	1.0000	1.0000	1.0000	0.0000	0.0000
26	-00.1450	1.0000	0.0000	0.0000	1.0000	0.0000	0.0000	1.0000	1.0000	1.0000	0.0000	0.0000
27	-00.1120	1.0000	0.0000	0.0000	1.0000	0.0000	0.0000	1.0000	1.0000	1.0000	0.0000	0.0000
28	-00.0790	1.0000	0.0000	0.0000	1.0000	0.0000	0.0000	1.0000	1.0000	1.0000	0.0000	0.0000
29	-00.0460	1.0000	0.0000	0.0000	1.0000	0.0000	0.0000	1.0000	1.0000	1.0000	0.0000	0.0000
30	0.0130	1.0000	0.0000	0.0000	1.0000	0.0000	0.0000	1.0000	1.0000	1.0000	0.0000	0.0000
31	0.0500	1.0000	0.0000	0.0000	1.0000	0.0000	0.0000	1.0000	1.0000	1.0000	0.0000	0.0000
32	0.0870	1.0000	0.0000	0.0000	1.0000	0.0000	0.0000	1.0000	1.0000	1.0000	0.0000	0.0000
33	0.1240	1.0000	0.0000	0.0000	1.0000	0.0000	0.0000	1.0000	1.0000	1.0000	0.0000	0.0000
34	0.1610	1.0000	0.0000	0.0000	1.0000	0.0000	0.0000	1.0000	1.0000	1.0000	0.0000	0.0000
35	0.1980	1.0000	0.0000	0.0000	1.0000	0.0000	0.0000	1.0000	1.0000	1.0000	0.0000	0.0000
36	0.2350	1.0000	0.0000	0.0000	1.0000	0.0000	0.0000	1.0000	1.0000	1.0000	0.0000	0.0000
37	0.2720	1.0000	0.0000	0.0000	1.0000	0.0000	0.0000	1.0000	1.0000	1.0000	0.0000	0.0000

Figure A.5.- Continued.

FLOW FIELD AND MAGNETIC FIELD COMPONENTS ALONG TRAJECTORY
(SOLAR WIND COORDINATE SYSTEM)

(DIMENSIONAL, USING INPUT INTERPLANETARY VALUES)

INTERPLANETARY MACH NUMBER = 3.30 INTERPLANETARY MAGNETIC FIELD
RATIO OF SPECIFIC HEATS = 1.6667 MAGNITUDE = .402E+31
INTERPLANETARY VELOCITY = 3.492E+02 X-COMPONENT = 1.239E+00
INTERPLANETARY DENSITY = 2.020E+01 Y-COMPONENT = 4.726E+00
INTERPLANETARY TEMPERATURE = 1.023E+05 Z-COMPONENT = 4.032E-01

N	TIME	VX	VY	VZ	Q40	TEMP	FB	QV	BY	QZ
1	-90.8700	3.926E+02	3.926E+02	0.	0.	2.020E+01	1.020E+05	8.823E+00	1.239E+00	4.726E+00
2	-89.9370	3.926E+02	3.926E+02	0.	0.	2.020E+01	1.020E+05	8.823E+00	1.239E+00	4.726E+00
3	-89.0030	3.926E+02	3.926E+02	0.	0.	2.020E+01	1.020E+05	8.823E+00	1.239E+00	4.726E+00
4	-74.8700	3.926E+02	3.926E+02	0.	0.	2.020E+01	1.020E+05	8.823E+00	1.239E+00	4.726E+00
5	-70.6630	3.926E+02	3.926E+02	0.	0.	2.020E+01	1.020E+05	8.823E+00	1.239E+00	4.726E+00
6	-64.2430	3.926E+02	3.926E+02	0.	0.	2.020E+01	1.020E+05	8.823E+00	1.239E+00	4.726E+00
7	-57.8620	3.926E+02	3.926E+02	0.	0.	2.020E+01	1.020E+05	8.823E+00	1.239E+00	4.726E+00
8	-51.4020	3.926E+02	3.926E+02	0.	0.	2.020E+01	1.020E+05	8.823E+00	1.239E+00	4.726E+00
9	-40.7330	3.926E+02	3.926E+02	0.	0.	2.020E+01	1.020E+05	8.823E+00	1.239E+00	4.726E+00
10	-39.6680	3.926E+02	3.926E+02	0.	0.	2.020E+01	1.020E+05	8.823E+00	1.239E+00	4.726E+00
11	-38.6620	3.926E+02	3.926E+02	0.	0.	2.020E+01	1.020E+05	8.823E+00	1.239E+00	4.726E+00
12	-35.9350	3.926E+02	3.926E+02	0.	0.	2.020E+01	1.020E+05	8.823E+00	1.239E+00	4.726E+00
13	-34.8670	3.926E+02	3.926E+02	0.	0.	2.020E+01	1.020E+05	8.823E+00	1.239E+00	4.726E+00
14	-32.7350	3.926E+02	3.926E+02	0.	0.	2.020E+01	1.020E+05	8.823E+00	1.239E+00	4.726E+00
15	-24.2120	3.926E+02	3.926E+02	0.	0.	2.020E+01	1.020E+05	8.823E+00	1.239E+00	4.726E+00
16	-21.0420	3.926E+02	3.926E+02	0.	0.	2.020E+01	1.020E+05	8.823E+00	1.239E+00	4.726E+00
17	-16.7350	3.926E+02	3.926E+02	0.	0.	2.020E+01	1.020E+05	8.823E+00	1.239E+00	4.726E+00
18	-14.6420	3.926E+02	3.926E+02	0.	0.	2.020E+01	1.020E+05	8.823E+00	1.239E+00	4.726E+00
19	-11.4620	3.926E+02	3.926E+02	0.	0.	2.020E+01	1.020E+05	8.823E+00	1.239E+00	4.726E+00
20	-8.1620	3.926E+02	3.926E+02	0.	0.	2.020E+01	1.020E+05	8.823E+00	1.239E+00	4.726E+00
21	-4.9600	3.926E+02	3.926E+02	0.	0.	2.020E+01	1.020E+05	8.823E+00	1.239E+00	4.726E+00
22	6.2980	3.926E+02	3.926E+02	0.	0.	2.020E+01	1.020E+05	8.823E+00	1.239E+00	4.726E+00
23	9.4980	3.926E+02	3.926E+02	0.	0.	2.020E+01	1.020E+05	8.823E+00	1.239E+00	4.726E+00
24	12.5930	3.926E+02	3.926E+02	0.	0.	2.020E+01	1.020E+05	8.823E+00	1.239E+00	4.726E+00
25	17.3930	3.926E+02	3.926E+02	0.	0.	2.020E+01	1.020E+05	8.823E+00	1.239E+00	4.726E+00
26	20.1270	3.926E+02	3.926E+02	0.	0.	2.020E+01	1.020E+05	8.823E+00	1.239E+00	4.726E+00
27	34.4600	3.926E+02	3.926E+02	0.	0.	2.020E+01	1.020E+05	8.823E+00	1.239E+00	4.726E+00
28	40.8600	3.926E+02	3.926E+02	0.	0.	2.020E+01	1.020E+05	8.823E+00	1.239E+00	4.726E+00
29	47.2610	3.926E+02	3.926E+02	0.	0.	2.020E+01	1.020E+05	8.823E+00	1.239E+00	4.726E+00
30	55.6660	3.926E+02	3.926E+02	0.	0.	2.020E+01	1.020E+05	8.823E+00	1.239E+00	4.726E+00
31	58.8620	3.926E+02	3.926E+02	0.	0.	2.020E+01	1.020E+05	8.823E+00	1.239E+00	4.726E+00
32	58.8620	3.926E+02	3.926E+02	0.	0.	2.020E+01	1.020E+05	8.823E+00	1.239E+00	4.726E+00
33	60.7660	3.926E+02	3.926E+02	0.	0.	2.020E+01	1.020E+05	8.823E+00	1.239E+00	4.726E+00
34	62.1930	3.926E+02	3.926E+02	0.	0.	2.020E+01	1.020E+05	8.823E+00	1.239E+00	4.726E+00
35	67.5280	3.926E+02	3.926E+02	0.	0.	2.020E+01	1.020E+05	8.823E+00	1.239E+00	4.726E+00
36	73.9280	3.926E+02	3.926E+02	0.	0.	2.020E+01	1.020E+05	8.823E+00	1.239E+00	4.726E+00
37	80.3280	3.926E+02	3.926E+02	0.	0.	2.020E+01	1.020E+05	8.823E+00	1.239E+00	4.726E+00

TRAJECTORY CALCULATION

(SUN-PLANET COORDINATE SYSTEM)

TRAJECTORY COORDINATES

RG/RPLANET = 1.3331

N	TIME	X/RP	Y/RP	Z/RP	R/RP	X/RPLANET	Y/RPLANET	Z/RPLANET	R/RPLANET
1	-90.8700	-0.8160	3.6658	1.9621	4.2579	-0.8430	3.7870	2.0270	4.2954
2	-89.9370	-0.7455	3.4848	1.5796	4.0078	-0.7650	3.6030	2.0450	4.1463
3	-89.0030	-0.6621	3.2844	1.1960	3.8434	-0.6840	3.3930	2.0620	3.9754
4	-74.8700	-0.5808	3.0733	2.6167	3.6721	-0.6000	3.1770	2.0730	3.7935
5	-70.6630	-0.5159	2.9030	2.6125	3.5318	-0.5330	2.9990	2.0780	3.6486
6	-64.2430	-0.4162	2.6339	2.6125	3.3148	-0.4300	2.7210	2.0740	3.4243
7	-57.8620	-0.3136	2.3493	2.6109	3.1459	-0.3243	2.4270	2.0670	3.1979
8	-51.4020	-0.2101	2.0502	1.9776	2.8496	-0.2170	2.1180	2.0430	2.9477
9	-43.7350	-0.0329	1.5121	1.8982	2.4268	-0.0340	1.5620	1.9610	2.5971
10	-39.6680	-0.0165	1.4607	1.8886	2.3875	-0.0170	1.5090	1.9510	2.4655
11	-38.6620	-0.0097	1.3765	1.8712	2.3221	-0.0100	1.4220	1.9320	2.3989
12	-35.9350	-0.0474	1.2400	1.8411	2.2198	-0.0493	1.2810	1.9020	2.2932
13	-34.8670	0.0649	1.1926	1.8256	2.1806	0.0670	1.2320	1.8960	2.2527
14	-32.7350	0.1929	1.0725	1.7927	2.0891	0.1989	1.1080	1.8520	2.1581
15	-24.2620	0.2377	0.9640	1.6125	1.7083	0.2456	0.9826	1.6854	1.7647
16	-21.0420	0.2859	0.8629	1.5191	1.5618	0.2954	0.8749	1.5693	1.6135
17	-16.7350	0.3446	0.8071	1.3639	1.3567	0.3540	0.8000	1.4090	1.4119
18	-14.6420	0.3698	-0.5533	1.2729	1.2739	0.3820	-0.5520	1.3190	1.3160
19	-11.4620	0.4017	-1.0984	1.1132	1.1337	0.4150	-1.0950	1.1500	1.1681
20	-8.1620	0.4230	-0.4627	0.9148	1.0251	0.4370	-0.4780	0.9450	1.0590
21	-4.9600	0.4279	-0.6805	0.6399	0.9314	0.4420	-0.7030	0.6630	0.9643
22	6.2980	0.2991	-1.0087	-0.2575	1.0410	0.3090	-1.0420	-0.2660	1.0754
23	9.4980	0.2294	-0.8212	-0.5285	1.1499	0.2370	-1.0550	-0.5460	1.1479
24	12.5930	0.1549	-1.3048	-0.7794	1.2692	0.1600	-1.0380	-0.8010	1.3111
25	17.3930	0.0329	-0.9351	-1.1248	1.4867	0.0340	-0.9600	-1.1620	1.5111
26	20.1270	-0.2462	-0.6515	-1.0266	1.5935	-0.2470	-0.9830	-1.1870	2.0934
27	34.4600	-0.3940	-0.4956	-2.0860	2.1441	-0.4070	-0.5120	-2.1550	2.2150
28	40.8600	-0.5430	-0.3020	-2.3658	2.3850	-0.5610	-0.3120	-2.4440	2.4638
29	47.2600	-0.6824	-0.1045	-2.5846	2.5867	-0.7050	-0.1080	-2.6700	2.6722
30	55.6600	-0.8170	0.0951	-2.8314	2.8330	-0.8440	0.0982	-2.9250	2.9266
31	58.8620	-0.8809	0.1946	-2.9340	2.9405	-0.9160	0.2010	-3.0310	3.0377
32	58.8620	-0.9235	0.2604	-2.9979	3.0092	-0.9540	0.2600	-3.0970	3.1297
33	60.7660	-0.9438	0.2933	-3.0308	3.0458	-0.9790	0.3030	-3.1310	3.1456
34	62.1930	-0.9854	0.3591	-3.0928	3.1135	-1.0180	0.3710	-3.1950	3.2165
35	67.5280	-1.0861	0.5237	-3.2399	3.2819	-1.1220	0.5410	-3.3470	3.3994
36	73.9280	-1.2013	0.7154	-3.4016	3.4766	-1.2410	0.7390	-3.5140	3.5909
37	80.3280	-1.3136	0.9090	-3.5535	3.6679	-1.3570	0.9390	-3.6710	3.7902

Figure A.5.- Continued.

INFORMALIZATION OF THE PLANTARY VARIATION

[illegible]

(DIMENSIONAL, 16ING INPUT INTERPOLANETARY VALUES)

```

INTERPLANETARY MAGN NUMB2      = 5.000000      INTERPLANETARY MAGNETIC FIELD
DATA OF OBSERVATION DATE      = 19650707      MAGNITUDE      = 19.620000
INTERPLANETARY VELOCITY      = 3.000000E+2      VELOCITY      = 1.900000E+3
INTERPLANETARY DENSITY      = 2.000000E+0      VELOCITY      = 6.600000E+4
INTERPLANETARY TEMPERATURE    = 0.000000E+0      VELOCITY      = 4.000000E+1
OPTIMIZATION ANGLES      = 0.330000
POLAR ANGLE      = 0.000000

```

Y	TIME	VV	VV	VV	V7	340	TEMP	PA	AY	BY	AZ
1	-97.4713	3.9236+02	-3.9133+2	2.2577E+01	-1.1264E+01	2.2577E+01	2.2577E+01	9.8233E+00	-1.7405E+00	-0.6405E+00	4.9000E-01
2	-97.5337	3.9236+02	-3.9133+2	2.2577E+01	-1.1264E+01	2.2577E+01	2.2577E+01	9.8233E+00	-1.7405E+00	-0.6405E+00	4.9000E-01
3	-97.5936	3.9236+02	-3.9133+2	2.2577E+01	-1.1264E+01	2.2577E+01	2.2577E+01	9.8233E+00	-1.7405E+00	-0.6405E+00	4.9000E-01
4	-74.9737	3.9236+02	-3.9133+2	2.2577E+01	-1.1264E+01	2.2577E+01	2.2577E+01	9.8233E+00	-1.7405E+00	-0.6405E+00	4.9000E-01
5	-76.6131	3.9236+02	-3.9133+2	2.2577E+01	-1.1264E+01	2.2577E+01	2.2577E+01	9.8233E+00	-1.7405E+00	-0.6405E+00	4.9000E-01
6	-64.9033	3.9236+02	-3.9133+2	2.2577E+01	-1.1264E+01	2.2577E+01	2.2577E+01	9.8233E+00	-1.7405E+00	-0.6405E+00	4.9000E-01
7	-37.9420	3.9236+02	-3.9133+2	2.2577E+01	-1.1264E+01	2.2577E+01	2.2577E+01	9.8233E+00	-1.7405E+00	-0.6405E+00	4.9000E-01
8	-57.4422	3.9236+02	-3.9133+2	2.2577E+01	-1.1264E+01	2.2577E+01	2.2577E+01	9.8233E+00	-1.7405E+00	-0.6405E+00	4.9000E-01
9	-40.7339	3.9236+02	-3.9133+2	2.2577E+01	-1.1264E+01	2.2577E+01	2.2577E+01	9.8233E+00	-1.7405E+00	-0.6405E+00	4.9000E-01
10	-39.6664	3.9236+02	-3.9133+2	2.2577E+01	-1.1264E+01	2.2577E+01	2.2577E+01	9.8233E+00	-1.7405E+00	-0.6405E+00	4.9000E-01
11	-39.0522	3.9236+02	-3.9133+2	2.2577E+01	-1.1264E+01	2.2577E+01	2.2577E+01	9.8233E+00	-1.7405E+00	-0.6405E+00	4.9000E-01
12	-38.4422	3.9236+02	-3.9133+2	2.2577E+01	-1.1264E+01	2.2577E+01	2.2577E+01	9.8233E+00	-1.7405E+00	-0.6405E+00	4.9000E-01
13	-37.8322	3.9236+02	-3.9133+2	2.2577E+01	-1.1264E+01	2.2577E+01	2.2577E+01	9.8233E+00	-1.7405E+00	-0.6405E+00	4.9000E-01
14	-37.2222	3.9236+02	-3.9133+2	2.2577E+01	-1.1264E+01	2.2577E+01	2.2577E+01	9.8233E+00	-1.7405E+00	-0.6405E+00	4.9000E-01
15	-24.8222	3.9236+02	-3.9133+2	2.2577E+01	-1.1264E+01	2.2577E+01	2.2577E+01	9.8233E+00	-1.7405E+00	-0.6405E+00	4.9000E-01
16	-24.2122	3.9236+02	-3.9133+2	2.2577E+01	-1.1264E+01	2.2577E+01	2.2577E+01	9.8233E+00	-1.7405E+00	-0.6405E+00	4.9000E-01
17	-16.7335	3.9236+02	-3.9133+2	2.2577E+01	-1.1264E+01	2.2577E+01	2.2577E+01	9.8233E+00	-1.7405E+00	-0.6405E+00	4.9000E-01
18	-14.6021	3.9236+02	-3.9133+2	2.2577E+01	-1.1264E+01	2.2577E+01	2.2577E+01	9.8233E+00	-1.7405E+00	-0.6405E+00	4.9000E-01
19	-14.0422	3.9236+02	-3.9133+2	2.2577E+01	-1.1264E+01	2.2577E+01	2.2577E+01	9.8233E+00	-1.7405E+00	-0.6405E+00	4.9000E-01
20	-14.0422	3.9236+02	-3.9133+2	2.2577E+01	-1.1264E+01	2.2577E+01	2.2577E+01	9.8233E+00	-1.7405E+00	-0.6405E+00	4.9000E-01
21	-14.0422	3.9236+02	-3.9133+2	2.2577E+01	-1.1264E+01	2.2577E+01	2.2577E+01	9.8233E+00	-1.7405E+00	-0.6405E+00	4.9000E-01
22	-14.0422	3.9236+02	-3.9133+2	2.2577E+01	-1.1264E+01	2.2577E+01	2.2577E+01	9.8233E+00	-1.7405E+00	-0.6405E+00	4.9000E-01
23	-14.0422	3.9236+02	-3.9133+2	2.2577E+01	-1.1264E+01	2.2577E+01	2.2577E+01	9.8233E+00	-1.7405E+00	-0.6405E+00	4.9000E-01
24	-14.0422	3.9236+02	-3.9133+2	2.2577E+01	-1.1264E+01	2.2577E+01	2.2577E+01	9.8233E+00	-1.7405E+00	-0.6405E+00	4.9000E-01
25	-14.0422	3.9236+02	-3.9133+2	2.2577E+01	-1.1264E+01	2.2577E+01	2.2577E+01	9.8233E+00	-1.7405E+00	-0.6405E+00	4.9000E-01
26	-14.0422	3.9236+02	-3.9133+2	2.2577E+01	-1.1264E+01	2.2577E+01	2.2577E+01	9.8233E+00	-1.7405E+00	-0.6405E+00	4.9000E-01
27	-14.0422	3.9236+02	-3.9133+2	2.2577E+01	-1.1264E+01	2.2577E+01	2.2577E+01	9.8233E+00	-1.7405E+00	-0.6405E+00	4.9000E-01
28	-14.0422	3.9236+02	-3.9133+2	2.2577E+01	-1.1264E+01	2.2577E+01	2.2577E+01	9.8233E+00	-1.7405E+00	-0.6405E+00	4.9000E-01
29	-14.0422	3.9236+02	-3.9133+2	2.2577E+01	-1.1264E+01	2.2577E+01	2.2577E+01	9.8233E+00	-1.7405E+00	-0.6405E+00	4.9000E-01
30	-14.0422	3.9236+02	-3.9133+2	2.2577E+01	-1.1264E+01	2.2577E+01	2.2577E+01	9.8233E+00	-1.7405E+00	-0.6405E+00	4.9000E-01
31	-14.0422	3.9236+02	-3.9133+2	2.2577E+01	-1.1264E+01	2.2577E+01	2.2577E+01	9.8233E+00	-1.7405E+00	-0.6405E+00	4.9000E-01
32	-14.0422	3.9236+02	-3.9133+2	2.2577E+01	-1.1264E+01	2.2577E+01	2.2577E+01	9.8233E+00	-1.7405E+00	-0.6405E+00	4.9000E-01
33	-14.0422	3.9236+02	-3.9133+2	2.2577E+01	-1.1264E+01	2.2577E+01	2.2577E+01	9.8233E+00	-1.7405E+00	-0.6405E+00	4.9000E-01
34	-14.0422	3.9236+02	-3.9133+2	2.2577E+01	-1.1264E+01	2.2577E+01	2.2577E+01	9.8233E+00	-1.7405E+00	-0.6405E+00	4.9000E-01
35	-14.0422	3.9236+02	-3.9133+2	2.2577E+01	-1.1264E+01	2.2577E+01	2.2577E+01	9.8233E+00	-1.7405E+00	-0.6405E+00	4.9000E-01
36	-14.0422	3.9236+02	-3.9133+2	2.2577E+01	-1.1264E+01	2.2577E+01	2.2577E+01	9.8233E+00	-1.7405E+00	-0.6405E+00	4.9000E-01
37	-14.0422	3.9236+02	-3.9133+2	2.2577E+01	-1.1264E+01	2.2577E+01	2.2577E+01	9.8233E+00	-1.7405E+00	-0.6405E+00	4.9000E-01
38	-14.0422	3.9236+02	-3.9133+2	2.2577E+01	-1.1264E+01	2.2577E+01	2.2577E+01	9.8233E+00	-1.7405E+00	-0.6405E+00	4.9000E-01

Figure A.5.- Concluded.

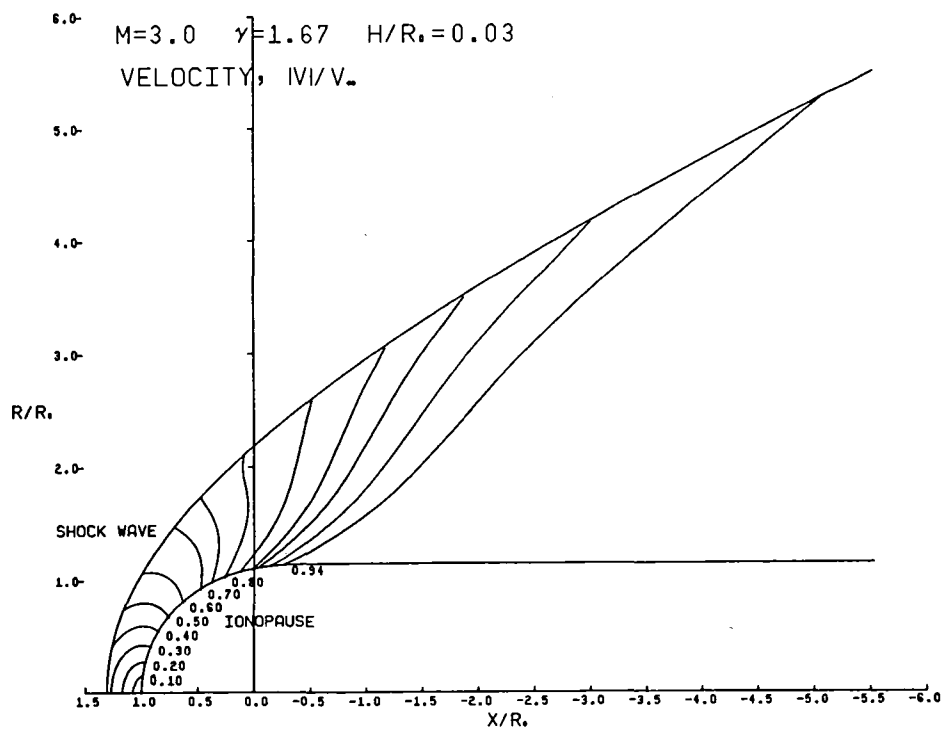
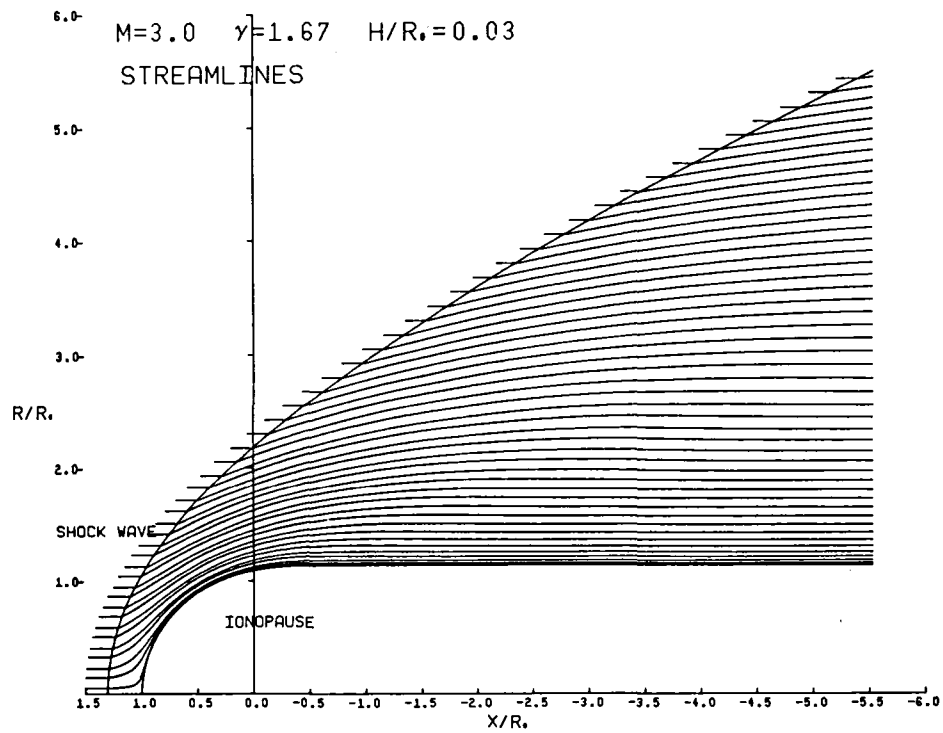


Figure A.6.- Plot output for sample case.

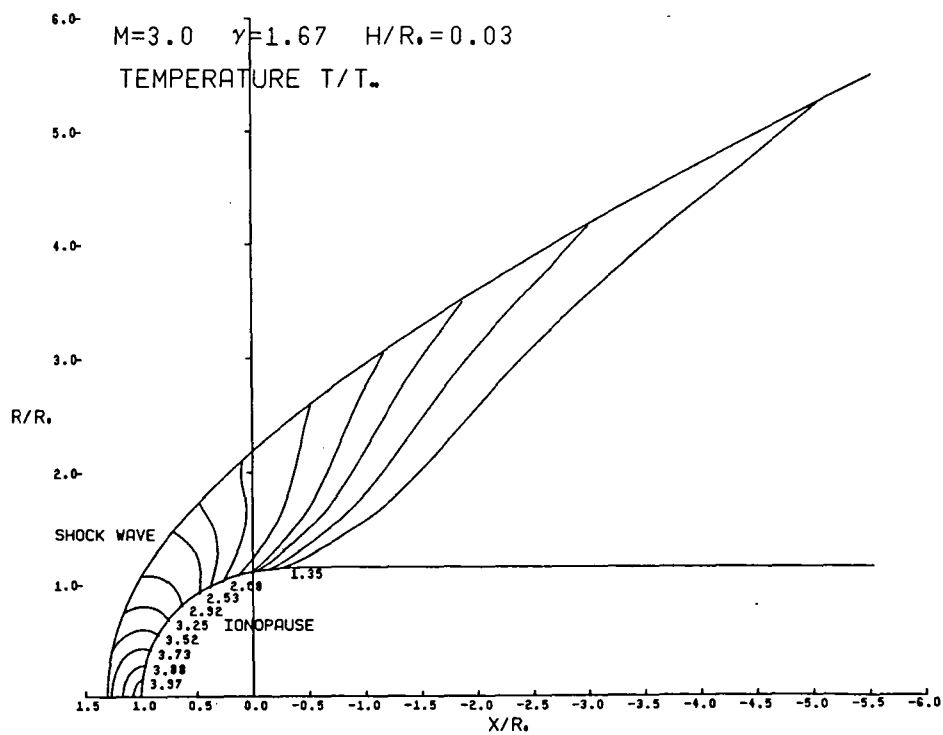
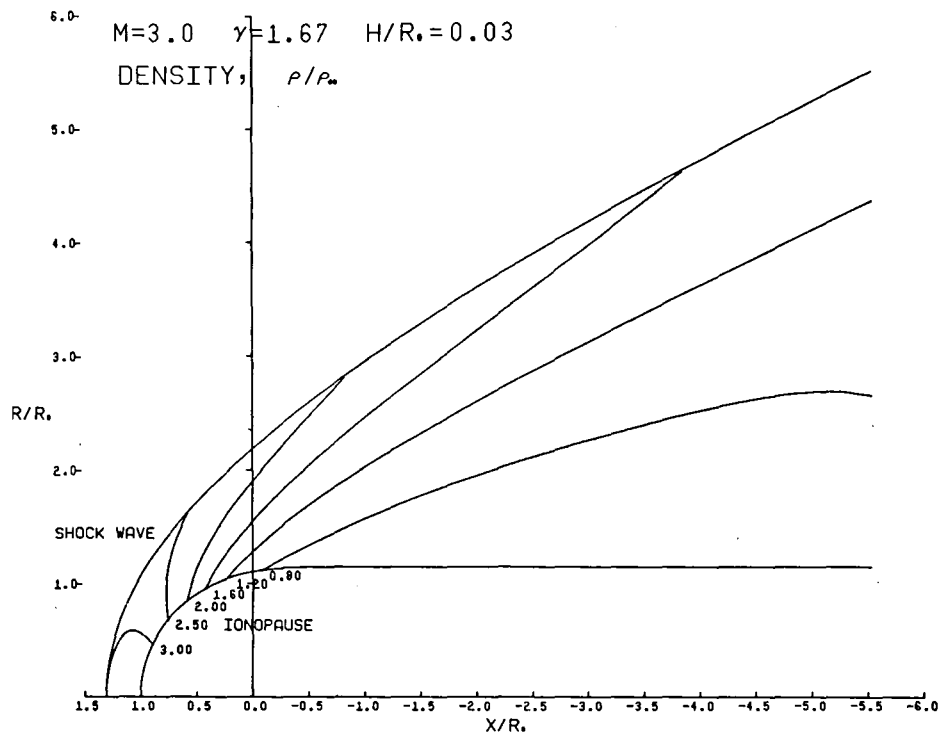


Figure A.6.- Continued

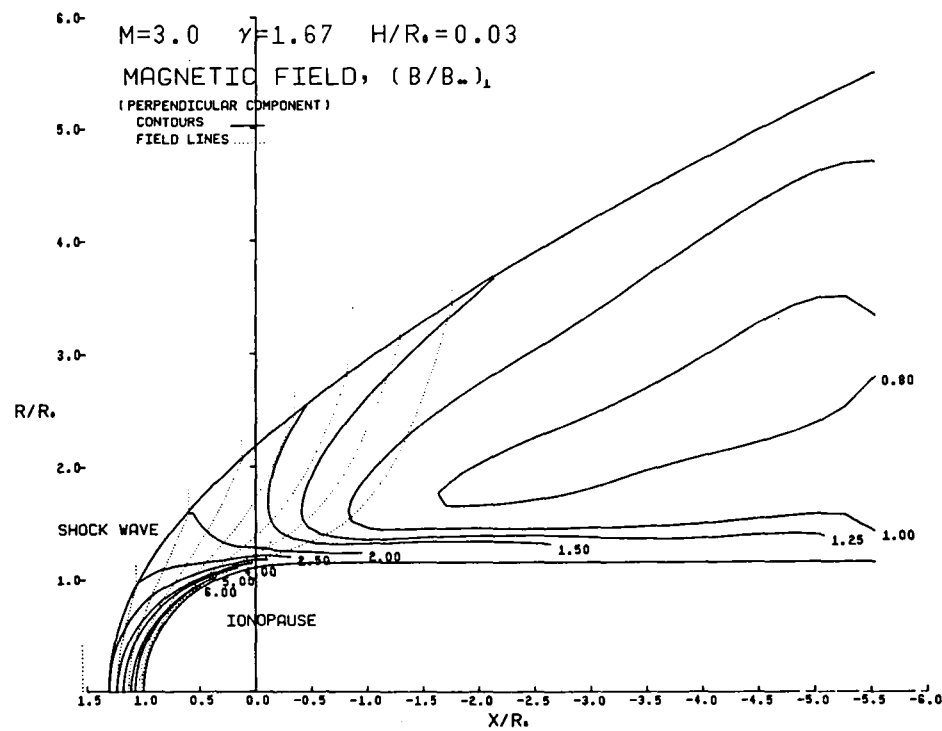
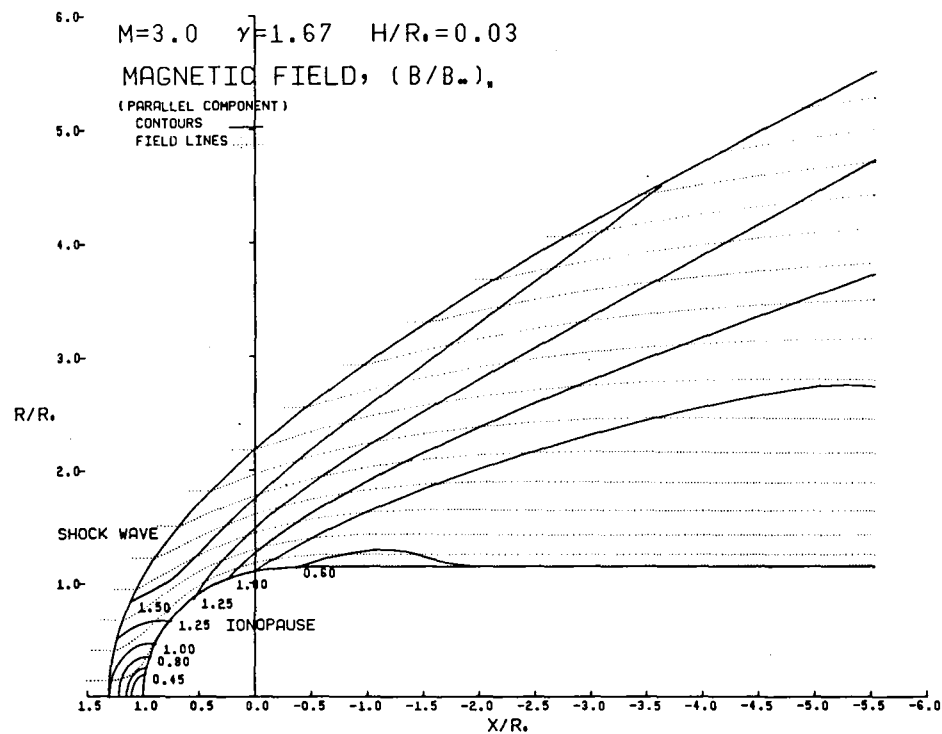


Figure A.6.- Continued

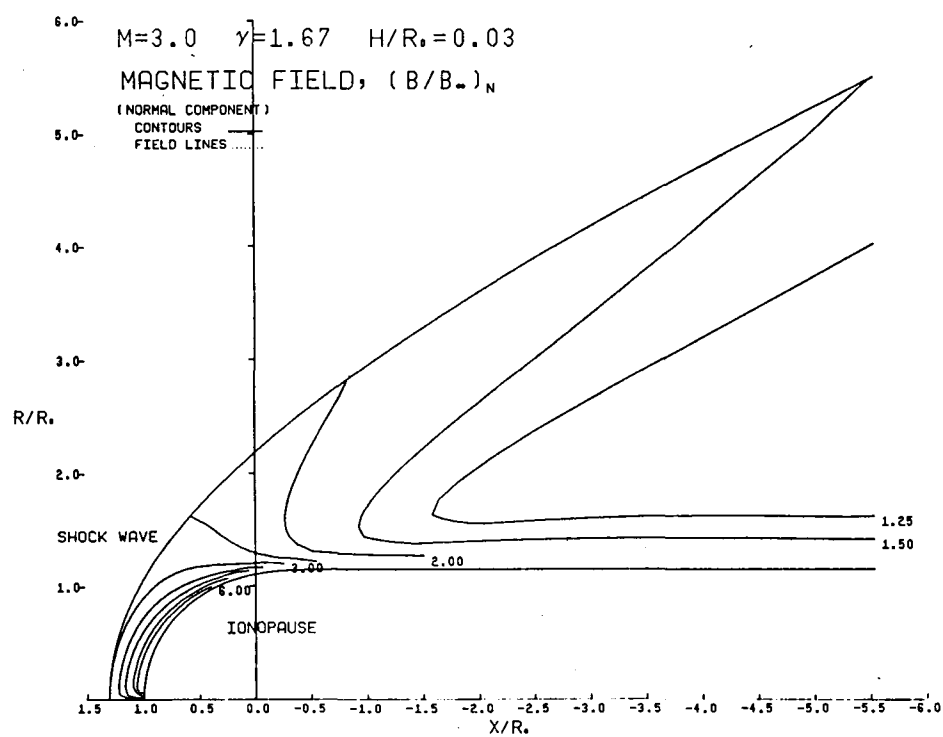


Figure A.6.- Continued

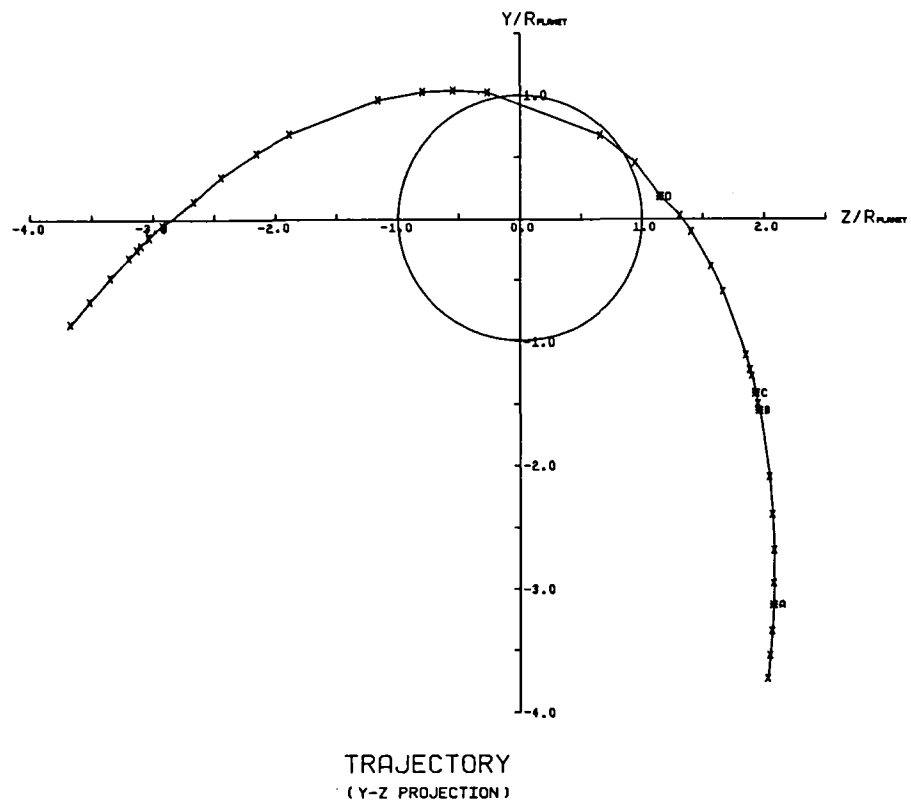
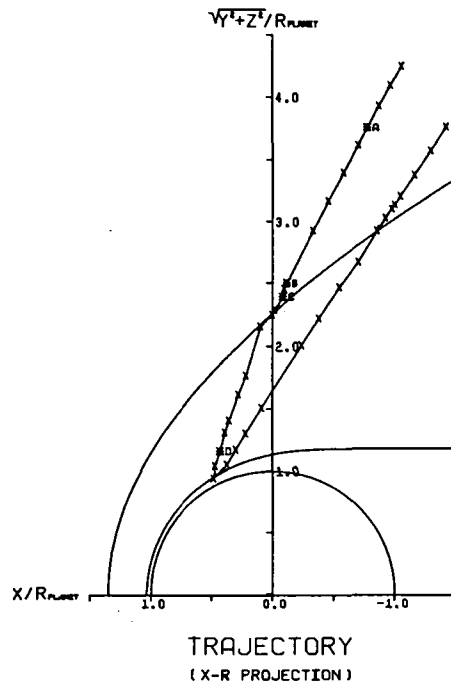
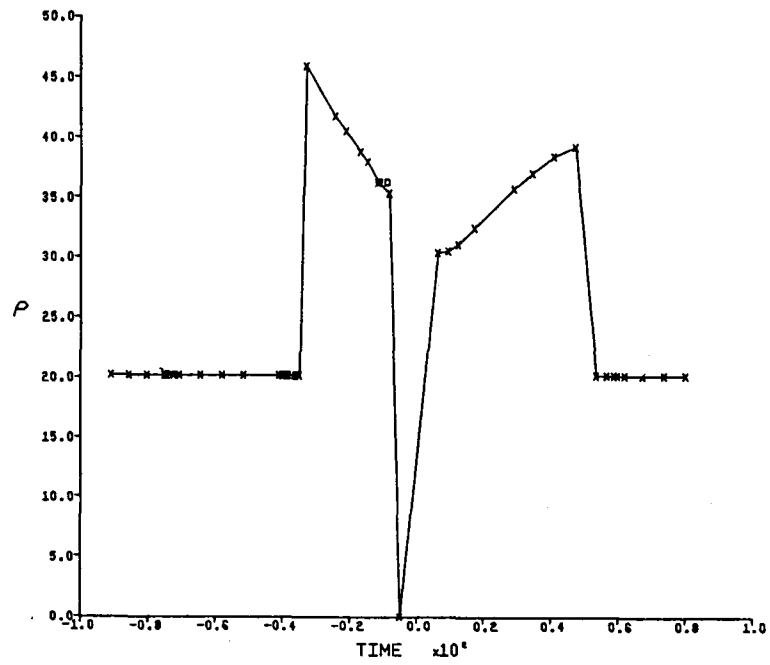


Figure A.6.- Continued

DENSITY vs TIME



TEMPERATURE vs TIME

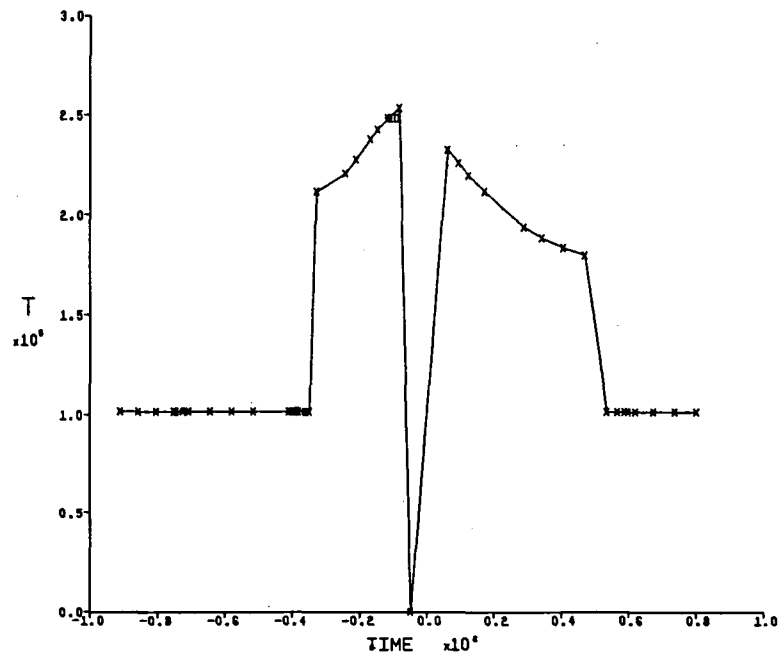


Figure A.6.- Continued.

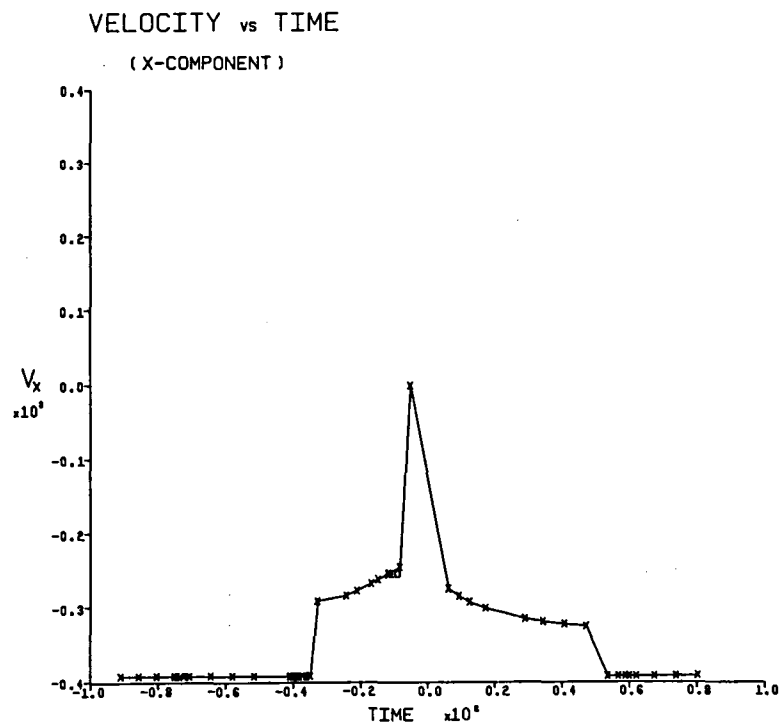
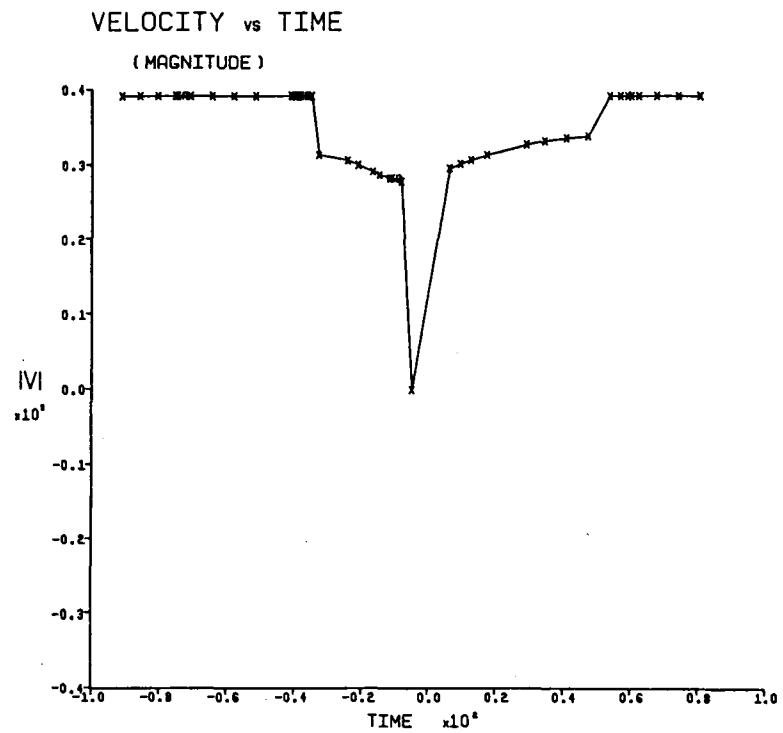


Figure A.6.- Continued

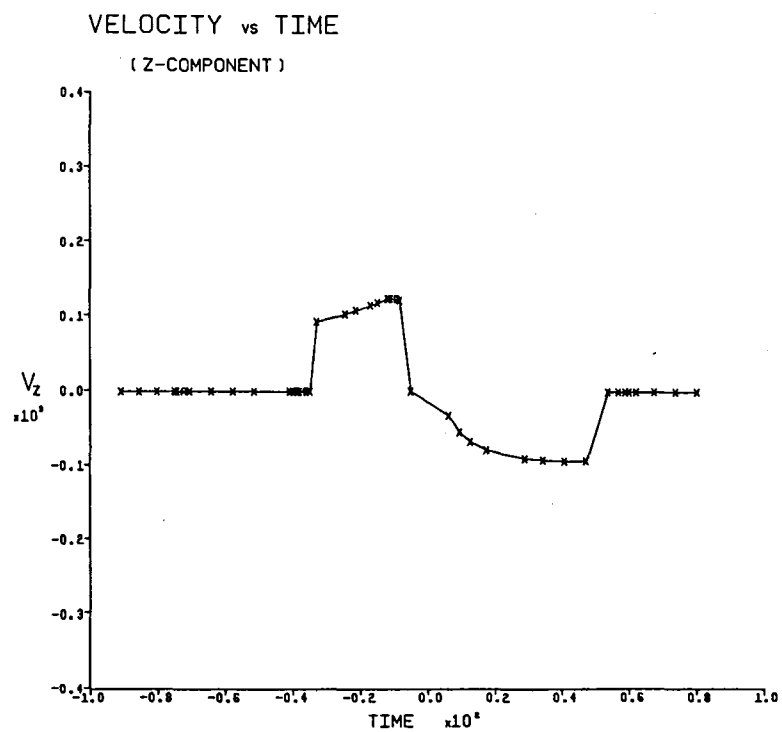
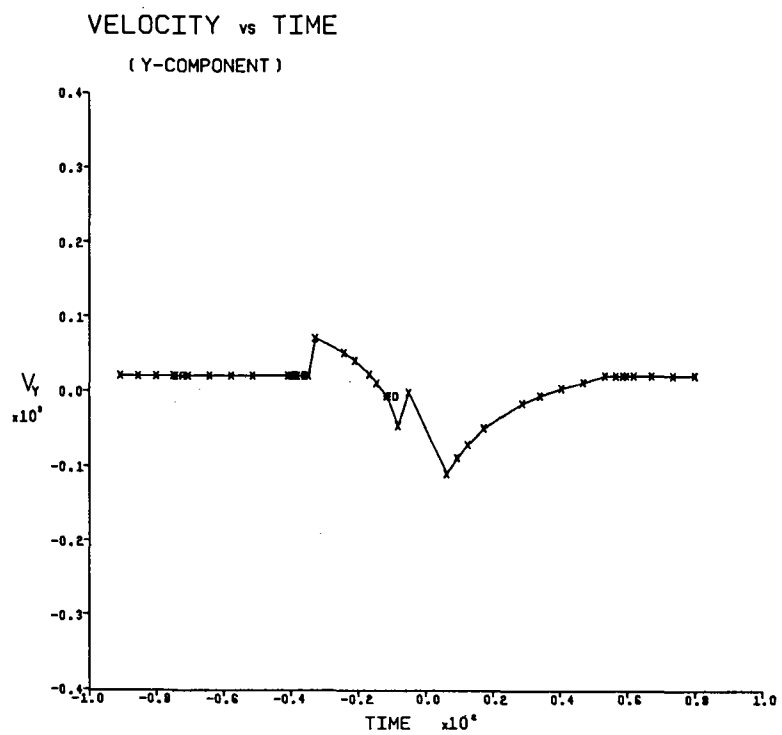


Figure A.6.- Continued.

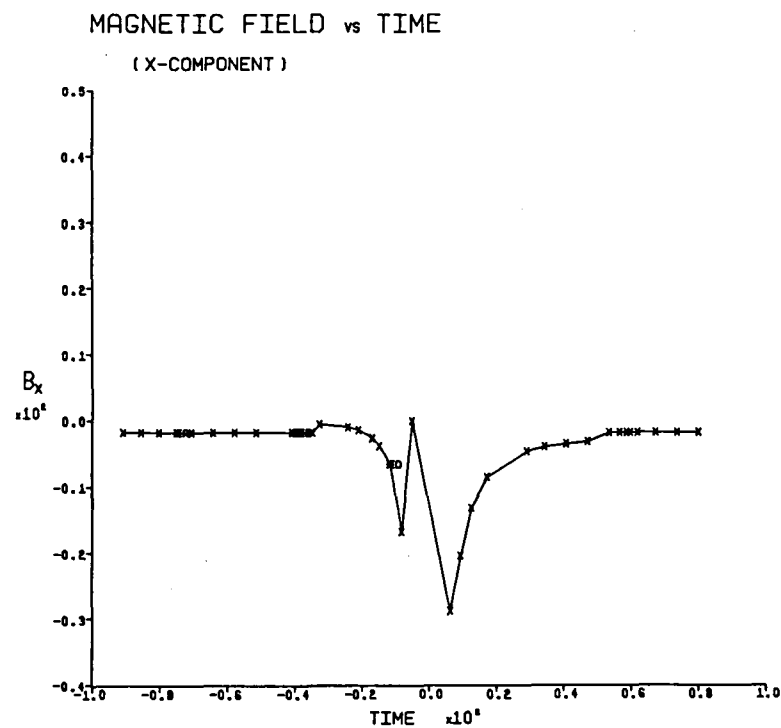
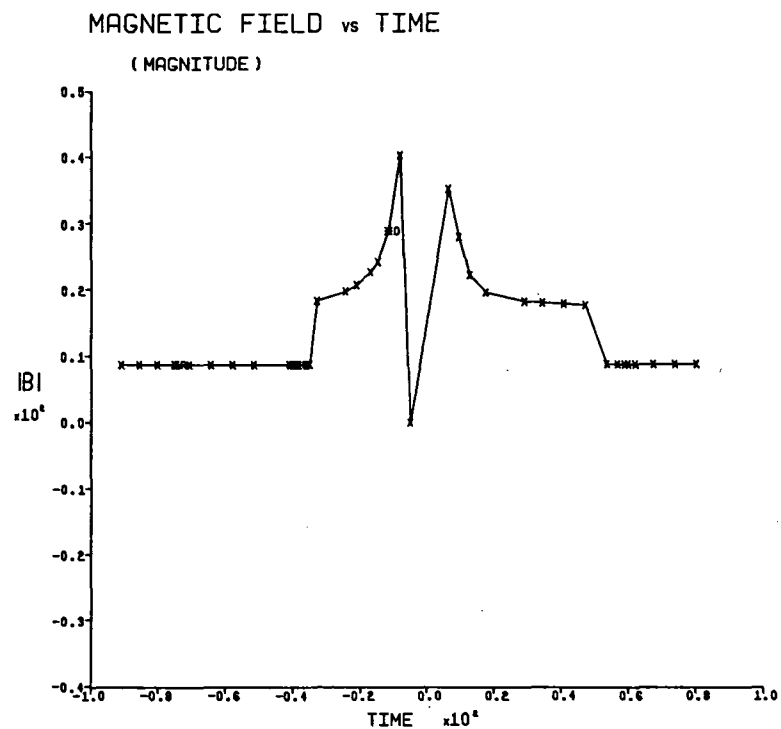


Figure A.6.- Continued.

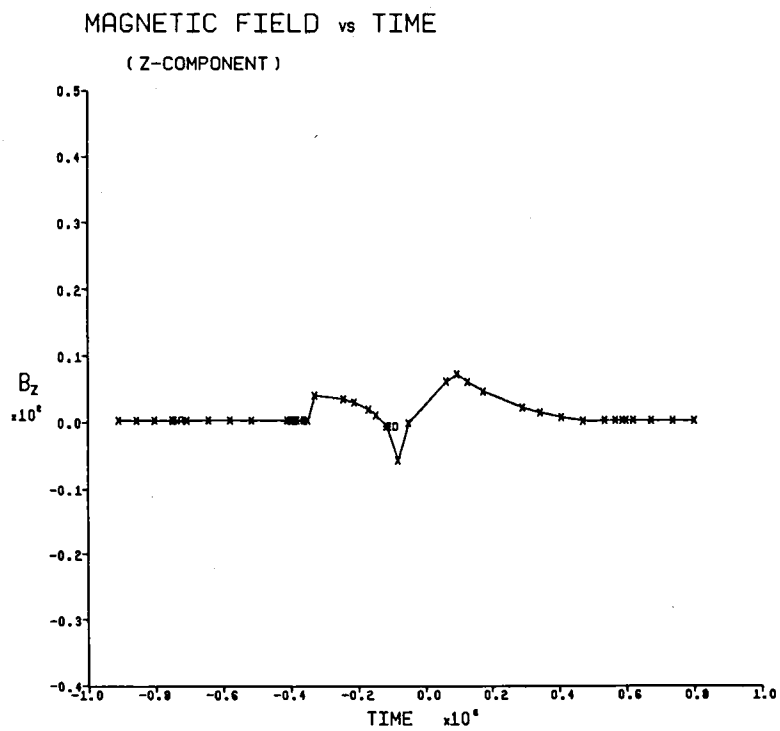
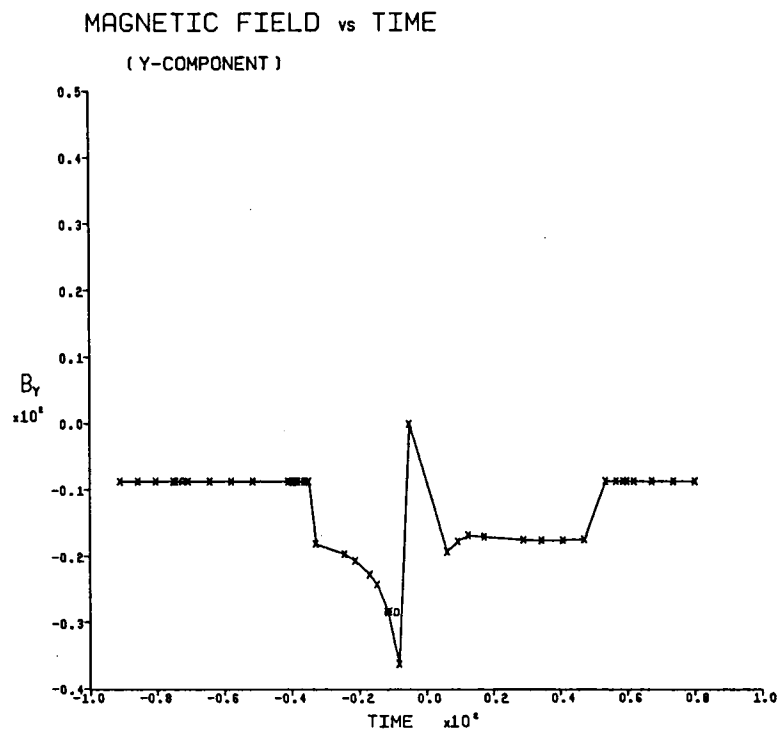


Figure A.6.- Concluded.

APPENDIX B

LISTING OF COMPUTER PROGRAM

	PROGRAM MAIN (INPUT,OUTPUT,TAPE5=INPUT,TAPE6=OUTPUT, TAPE1,TAPE4,TAPE9)	MAIN	1
	LOGICAL LPERUN,LPRFL,LPPST,LPRCON,LPR4,LPLDT,LTRAJ,LRSTRT	MAIN	2
	COMMON /PROPT/ LRERUN,LPPFL,LPRST,LPRCON,LPR4,LPLDT,LTRAJ,LRSTRT	PROPT	3
C		PROPT	3
	WRITE(6,200)	MAIN	5
	CALL ECHIMP	MAIN	6
	OPEN(9,100) NCASE	MAIN	7
	NO 2: (CASE=1,NCASE	MAIN	8
	CALL INPUT	MAIN	9
	IF (LRERUN) GO TO 10	MAIN	10
	CALL ALUNTA	MAIN	11
	CALL NARCH	MAIN	13
	GO TO 15	MAIN	13
13	CALL REPRUN	MAIN	13
13	CONTINUE	MAIN	13
	CALL FLOWST	MAIN	16
	IF (LPRFL) CALL FLOWT	MAIN	17
	IF (LPPST) CALL STOUT	MAIN	18
	CALL SCOMP	MAIN	19
	IF (LPR4) CALL ROUT	MAIN	21
	CALL CONTUR	MAIN	22
	IF (LTRAJ) CALL TRAJEC	MAIN	23
	23 CONTINUE	MAIN	24
	STOP	MAIN	25
C		MAIN	26
	11.3. FORMATT(I,J)	MAIN	27
20.3	FORMAT(I,J) ///////////////33X,62(140)/33X,62(140)/33X,2400,23X,	MAIN	28
	* 13HPROGRAM SFLAR,22X,2400,/,33X,2400,58X,2400,/,33X,2400,24X,	MAIN	29
	* 1CHDERTIMES,24X,2400,/,33X,2400,54X,2400,/,33X,2400,4X,	MAIN	30
	* 50HAPX WIND FLOW PAST PLANETARY MAGNETO/TIONSPHERES,4X,	MAIN	31
	* 2400,/,33X,2400,58X,2400,/,33X,2400,27X,5SHISING,26X,2400,/,	MAIN	32
	* 33X,2400,58X,2400,/,33X,2400,6X,47HFULLY CONSERVATIVE FINITE	MAIN	33
	* DIFFERENCE ALGORITHM,5X,2400,/,33X,2400,54X,2400,/,33X,2400,58X,	MAIN	34
	* 2400,/,33X,2400,58X,2400,/,33X,2400,54X,1CHMPTTIN,5X,24X,	MAIN	35
	* 6400,/,33X,2400,58X,2400,/,33X,2400,3X,41HSTEPHEN % CYMARS, 4ARR	MAIN	36
	* APA C. TRIMMING,8X,2400,/,33X,2400,58X,2400,/,33X,2400,20X,	MAIN	37
	* 20MAD DANGER J. KLENKE,18X,2400,/,33X,2400,54X,2400,/,13X,	MAIN	38
	* 2400,58X,2400,/,33X,2400,58X,2400,/,33X,2400,16X,34MIELTEN	MAIN	39
	* ENGINEERING AND RESEARCH, INC.,10X,2400,/,33X,2400,54X,2400,/,33X,	MAIN	40
	* 2400,17X,25HMOUNTAIN VIEW, CALIFORNIA,16X,2400,/,33X,2400,	MAIN	41
	* 58X,2400,/,33X,2400,58X,2400,/,33X,62(140),/,33X,62(140),	MAIN	42
	END	MAIN	43
		MAIN	44
		MAIN	45
		MAIN	46
		MAIN	47
		MAIN	48
		MAIN	49
		MAIN	50
		MAIN	51
		MAIN	52
		MAIN	53
		MAIN	54
		MAIN	55
		MAIN	56
		MAIN	57
		MAIN	58
		MAIN	59
		MAIN	60
		MAIN	61
		MAIN	62
		MAIN	63
		MAIN	64
		MAIN	65
		MAIN	66
		MAIN	67
		MAIN	68
		MAIN	69
		MAIN	70
		MAIN	71
		MAIN	72
		MAIN	73
		MAIN	74
		MAIN	75
		MAIN	76
		MAIN	77
		MAIN	78
		MAIN	79
		MAIN	80
		MAIN	81
		MAIN	82
		MAIN	83
		MAIN	84
		MAIN	85
		MAIN	86
		MAIN	87
		MAIN	88
		MAIN	89
		MAIN	90
		MAIN	91
		MAIN	92
		MAIN	93
		MAIN	94
		MAIN	95
		MAIN	96
		MAIN	97
		MAIN	98
		MAIN	99
		MAIN	100
		MAIN	101
		MAIN	102
		MAIN	103
		MAIN	104
		MAIN	105
		MAIN	106
		MAIN	107
		MAIN	108
		MAIN	109
		MAIN	110
		MAIN	111
		MAIN	112
		MAIN	113
		MAIN	114
		MAIN	115
		MAIN	116
		MAIN	

43	ELLINF=EL	ANGEL	33
	GAMEL=ANG	ANGEL	34
	RETURN	ANGEL	35
C		ANGEL	36
C	IF POINT IS ON AXIS USE LINEAR INTERPOLATION	ANGEL	37
100	X=XC(I,J)	ANGEL	38
	Y=YC(I,J)	ANGEL	39
	IF (J .GT. 1) GO TO 20J	ANGEL	40
	N=NRF(I)	ANGEL	41
	DO 110 K=1,N	ANGEL	42
	IF (Y .LT. XRF(1,K)) GO TO 125	ANGEL	43
110	CONTINUE	ANGEL	44
120	ELLINF=ELRF(1,K-1)+(X-XRF(1,K-1))*(ELRF(1,K)-ELRF(1,K-1))	ANGEL	45
	/(XRF(1,K)-XRF(2,K-1))	ANGEL	46
	GAMEL=ANG	ANGEL	47
	RETURN	ANGEL	48
C		ANGEL	49
C	IF POINT IS AT X=ZPLOT, USE LINEAR INTERPOLATION	ANGEL	50
C		ANGEL	51
20J	IF (J .LT. NMAX) GO TO 300	ANGEL	52
	N1=NRF(3)+1	ANGEL	53
	DO 210 I=N1,N5T	ANGEL	54
	IN=I+1	ANGEL	55
	N=NRF(IN)+1	ANGEL	56
	IF (Y .LT. RRF(IN,N)) GO TO 220	ANGEL	57
	N1=N	ANGEL	58
210	CONTINUE	ANGEL	59
	ELLINF=ELRF(IN,N)*(Y-RRF(IN,N))*(EL-ELRF(IN,N))	ANGEL	60
	/(YC(NMAX,NMAX)-RRF(IN,N))	ANGEL	61
	GAMEL=GARRF(IN,N)*(Y-RRF(IN,N))*(ANG-GARRF(IN,N))	ANGEL	62
	/(YC(NMAX,NMAX)-RRF(IN,N))	ANGEL	63
	RETURN	ANGEL	64
220	ELLINF=ELRF(IN,N1)*(Y-RRF(IN,N1))*(EL-ELRF(IN,N1)-ELRF(IN,N1))	ANGEL	65
	/(RRF(IN,N)-RRF(IN,N1))	ANGEL	66
	GAMEL=GARRF(IN,N1)*(Y-RRF(IN,N1))*(GARRF(IN,N)-GARRF(IN,N1))	ANGEL	67
	/(RRF(IN,N)-RRF(IN,N1))	ANGEL	68
	RETURN	ANGEL	69
C		ANGEL	70
C	INTERPOL POINT - USE QUADRILATERAL INTERPOLATION	ANGEL	71
C		ANGEL	72
300	N1=NRF(1)	ANGEL	73
	NMAX=NRF(3)+1	ANGEL	74
	DO 310 IST=1,N5T	ANGEL	75
	N2=NRF(IST)+1	ANGEL	76
	IF (N2 .GT. NMAX) N2=NMAX	ANGEL	77
	N=MIN(N1,N2)	ANGEL	78
	DO 311 J=1,N	ANGEL	79
	IF (Y .LT. XRF(IST+1,J)) GO TO 340	ANGEL	80
310	CONTINUE	ANGEL	81
	GO TO 440	ANGEL	82
C		ANGEL	83
C	FIND QUADRILATERAL WHICH CONTAINS POINT	ANGEL	84
C		ANGEL	85
340	IF (Y .GT. RRF(IST+1,J)) GO TO 500	ANGEL	86
	IF (XRF(IST+1,J) .LT. XST(IST,1)) GO TO 520	ANGEL	87
	SLOPE=(RRF(IST+1,J)-Y)/(XRF(IST+1,J)-X)	ANGEL	88
	SLOPE1=(RRF(IST+1,J)-RRF(IST+1,JJ-1))	ANGEL	89
	/(XRF(IST+1,JJ)-XRF(IST+1,JJ-1))	ANGEL	90
	IF (SLOPE1 .GT. SLOPE) GO TO 520	ANGEL	91
	IF (JJ .EQ. N) GO TO 350	ANGEL	92
	SLOPE2=(RRF(IST+1,JJ)-RRF(IST,JJ))/(XRF(IST+1,JJ)-XRF(IST,JJ))	ANGEL	93
	IF (SLOPE2 .LT. SLOPE) GO TO 390	ANGEL	94
350	CONTINUE	ANGEL	95
	XO(1)=XRF(IST+1,J)	ANGEL	96
	XO(2)=RRF(IST+1,J)	ANGEL	97
	ELO(1)=ELRF(IST+1,J)	ANGEL	98
	GAMO(1)=GARRF(IST+1,J)	ANGEL	99
	IF (XRF(IST+1,JJ-1) .LT. XST(IST,1)) GO TO 540	ANGEL	100
	XO(4)=RRF(IST+1,JJ-1)	ANGEL	101
	EO(4)=RRF(IST+1,JJ-1)	ANGEL	102
	ELO(4)=ELRF(IST+1,JJ-1)	ANGEL	103
	GAMO(4)=GARRF(IST+1,JJ-1)	ANGEL	104
	IF (JJ .EQ. N) GO TO 430	ANGEL	105
360	IF (IST .EQ. 1) GO TO 370	ANGEL	106
	IF (XRF(IST,JJ-1) .LT. XST(IST-1,1)) GO TO 560	ANGEL	107
370	XO(3)=XRF(IST,JJ-1)	ANGEL	108
	XO(3)=RRF(IST,JJ-1)	ANGEL	109
	ELO(3)=ELRF(IST,JJ-1)	ANGEL	110
	GAMO(3)=GARRF(IST,JJ-1)	ANGEL	111
380	XO(2)=RRF(IST,JJ)	ANGEL	112
	XO(2)=RRF(IST,JJ)	ANGEL	113
	ELO(2)=ELRF(IST,JJ)	ANGEL	114
	GAMO(2)=GARRF(IST,JJ)	ANGEL	115


```

THIS SUBROUTINE CALCULATES THE MAGNITUDE AND DIRECTION OF
EL/EI FINE AT THE POINTS WHERE THE STREAMLINES INTERSECT THE
MAGNETIC FIELD LINES WHICH ARE PERPENDICULAR TO THE FLOW
IN CROSSSTREAM
      NST(1)=0.5/YST(1,1)
      DO 10 I=2,NST
      NST(I)=1.0/(YST(I,1)-YST(I-1,1))
13 CONTINUE
      SET ARRAYS TO FREE STREAM VALUES
      NST(1)=NST*1
      JREF=JREF(1)
      DO 30 J=1,NST*1
      IF (JREF(I).LT. JREFAX) GO TO 20
      JREF=JREF(I)
33 CONTINUE
      DO 20 J=1,JREFAX
      DO 20 I=1,NST*1
      ELREF(I,1)=0
      CAMRF(I,1)=PI*2
20 CONTINUE
      VALUES ALONG FIELD LINES WHICH CROSS STREAM
      DO 130 J=3,NA
      IF (J.GT. NMF(1)) GO TO 100
      O1=SQRT((YRF(2,J)-YRF(1,J))**2+RPF(2,J)**2)*2.0
      CAM1=PI*2
      XZ2=YRF(3,J)-YRF(2,J)
      NY2=YRF(3,J)-YRF(2,J)
      O2=SQRT(XZ2**2+NY2**2+OR2*OR2)
      CAM2=ATAN(NY2/OX2)
      ELRF(2,J)=O1*O2/(O1*O2)+(NST(21)*NST(11))
      CAMRF(2,J)=(CAM1*O2+CAM2*O1)/(O1*O2)
      GO TO 140
13 CONTINUE
      O1=SQRT((YRF(2,J)-YRF(2,J-1))**2+(RPF(2,J)-RPF(2,J-1))**2)*2.0
      NY2=YRF(3,J)-YRF(2,J)
      O2=SQRT(XZ2**2+NY2**2+OR2*OR2)
      CAM2=ATAN(NY2/OX2)
      O1RF(2,J)=ELRF(2,J-1)+O1*O2/(O1*O2)+O2/(O1*O2)
      CAMRF(2,J)=(O1+CAM2*O2+CAMRF(2,J-1))/(O1*O2)
140 CONTINUE
      DO 110 I=3,NST
      O1=O2
      CAM1=CAM2
      IF (YRF(I+1,J).LT. YST(I+1,1)) GO TO 120
      XZ2=YRF(I+1,J)-YRF(I,J)
      NY2=YRF(I+1,J)-YRF(I,J)
      O2=SQRT(XZ2**2+NY2**2+OR2*OR2)
      ELRF(I,1)=O1*O2/(O1*O2)+(NST(I-1)*NST(I))
      CAM2=ATAN(NY2/OX2)
      CAMRF(I,1)=(CAM1*O2+CAM2*O1)/(O1*O2)
110 CONTINUE
120 YS=YST(I+1,J)
      CALL RS4H(YS,RS4,CAMS4,ELSH)
      XZ2=YS-CAMF(I,J)
      NY2=YS-CAMF(I,J)
      O2=SQRT(XZ2**2+NY2**2+OR2*OR2)*2.0
      ELRF(I,J)=O1*(NST(I-1)+O2*ELSH)/(O1*O2)
      CAMRF(I,J)=(O2+CAM1*O1+CAMSH)/(O1*O2)
12 CONTINUE
      JREF=JREF(3)
      VALUES ALONG FIELD LINES WHICH END AT DOWNSTREAM BOUNDARY
      VJ1=NA*1
      DO 100 J=NA1,JREFAX
      IF (J.GT. NMF(1)) GO TO 150
      O1=SQRT((YRF(2,J)-YRF(1,J))**2+RPF(2,J)**2)*2.0
      ELRF(1,J)=O1*O2/(O1*O2)
      CAM1=PI*2
      XZ2=YRF(3,J)-YRF(2,J)
      NY2=YRF(3,J)-YRF(2,J)
      O2=SQRT(XZ2**2+NY2**2+OR2*OR2)
      CAM2=ATAN(NY2/OX2)
      ELRF(2,J)=O1*O2/(O1*O2)+(NST(21)*NST(11))
      CAMRF(2,J)=(CAM1*O2+CAM2*O1)/(O1*O2)
      GO TO 160
150 O1=SQRT((YRF(2,J)-YRF(2,J-1))**2+(RPF(2,J)-RPF(2,J-1))**2)*2.0

```

RELGAN	9
RELGAN	10
RELGAN	11
RELGAN	12
RELGAN	13
RELGAN	14
RELGAN	15
RELGAN	16
RELGAN	17
RELGAN	18
RELGAN	19
RELGAN	20
RELGAN	21
RELGAN	22
RELGAN	23
RELGAN	24
RELGAN	25
RELGAN	26
RELGAN	27
RELGAN	28
RELGAN	29
RELGAN	30
RELGAN	31
RELGAN	32
RELGAN	33
RELGAN	34
RELGAN	35
RELGAN	36
RELGAN	37
RELGAN	38
RELGAN	39
RELGAN	40
RELGAN	41
RELGAN	42
RELGAN	43
RELGAN	44
RELGAN	45
RELGAN	46
RELGAN	47
RELGAN	48
RELGAN	49
RELGAN	50
RELGAN	51
RELGAN	52
RELGAN	53
RELGAN	54
RELGAN	55
RELGAN	56
RELGAN	57
RELGAN	58
RELGAN	59
RELGAN	60
RELGAN	61
RELGAN	62
RELGAN	63
RELGAN	64
RELGAN	65
RELGAN	66
RELGAN	67
RELGAN	68
RELGAN	69
RELGAN	70
RELGAN	71
RELGAN	72
RELGAN	73
RELGAN	74
RELGAN	75
RELGAN	76
RELGAN	77
RELGAN	78
RELGAN	79
RELGAN	80
RELGAN	81
RELGAN	82
RELGAN	83
RELGAN	84
RELGAN	85
RELGAN	86
RELGAN	87
RELGAN	88
RELGAN	89
RELGAN	90
RELGAN	91
RELGAN	92

```

160  X2=XRF(3,J)-XRF(2,J)
    NR2=XRF(3,J)-XRF(1,J)
    M2=SQRT(NX2*NX2+NR2*NR2)
    GAM2=ATAN(DR2/YR2)
    ELRF(2,J)=(ELRF(2,J-1)+D1*ODST(2))/D1+D2)
    GAMRF(2,J)=(D1+GAM2+D2+GAMRF(2,J-1))/D1+D2)
    CONTINUE
    DO 170 J=3,MST
    IF (MRF(1+J) .LT. J) GO TO 1P3
    D1=D2
    GAM1=GAM2
    X2=XRF(1+J)-XRF(1,J)
    NR2=XRF(1+J)-XRF(1,J)
    D2=SQRT(NX2*NX2+NR2*NR2)
    ELRF(1,J)=(ELRF(1,J-1)+D2*ODST(1))/D1+D2)
    GAMRF(1,J)=(GAM1+D2+GAM2+D1)/D1+D2)
170 CONTINUE
1P3 CONTINUE
    EL1=D1*ODST(1-2)
    D2=D2*ODST(1-1)
    D1=D1+D2
    D2=D2
    ELRF(1,1)=(EL1+D2+EL2*D1)/D1+D2)
    GAMRF(1,1)=(GAM1+D2+GAM2+D1)/D1+D2)
    IF (GAMRF(1,J) .LT. D2) GAMRF(1,1)=D2
190 CONTINUE

EXTROPOLATE ALONG STREAMLINES TO LAST GRID LINE

CALL XRMK1(ZPLOT,Y1,GAM1,EL1)
DO 200 Y=3,MSTP1
    M2=XRF(1)
    M1=M2
    M3=MST(1-1)
    IF (YRF(1,M-1) .LT. YST(1-1,1)) GO TO 221
    FAC=(YPLNT-XRF(1,M-1))/(YRF(1,M)-YRF(1,M-1))
    YRF(1,M+1)=YST(1-1,MUM)
    XRF(1,M+1)=YST(1-1,MUM)
    ELRF(1,M+1)=FAC*ELRF(1,M)+(1.0-FAC)*ELRF(1,M-1)
    GAMRF(1,M+1)=FAC*GAMRF(1,M)+(1.0-FAC)*GAMRF(1,M-1)
    IF (GAMRF(1,M+1) .LT. D2) GAMRF(1,M+1)=D2
    M1=M
    M2=M
    GO TO 200
221 XRF(1,M+1)=YST(1-1,MUM)
    YRF(1,M+1)=YST(1-1,MUM)
    ELRF(1,M+1)=YRF(1,M+1)/(Y1-XRF(1,M+1,1))
    FAC=(YPLNT-XRF(1,M+1))/(YRF(1,M+1)-YRF(1,M+1,1))
    ELRF(1,M+2)=ELRF(1,M+1)+FAC*(EL1-FAC)*EL1
    GAMRF(1,M+2)=GAMRF(1,M+1)+FAC*(GAM1-FAC)*GAM1
    YRF(1,M+2)=YRF(1,M+1)
    GAMRF(1,M+2) .LT. D2) GAMRF(1,M+2)=D2
200 CONTINUE
STOP
END

SUBROUTINE RMIND

THIS ROUTINE DRAWS AND LABELS SHOCK WAVE AND
MAGNETOSPHERE OR IONOSPHERE BOUNDARY.
FOR PLOT SUBROUTINES USED ARE
VECTOR,CHAR,POLAR.

COMMON /BNDHNS/ XND0(100),YND0(100),YSH4(100),YSH4
* NMAY,NMAX,AMACH,GAMMA,MPO,MNINDX
COMMON /SCALE/ XSF,YSF,XMAX,YMAX,XLNGTY,XLNGTY
DIMENSION P(21),A(21)
EXTENSION LABMG(2)
DATA LABMG(1),LABMG(2),LABM/1,CHMAGNETOPAU,2HCF,0
DATA LABS/1,LABSHOCK WAVE/
DATA A/1,.05,15738,.31439,.47124,.62832,.79549,
1 .94241,1.09256,1.25864,1.43372,1.57765,
2 1.71278,1.88496,2.05204,2.21911,2.35519,
3 2.51327,2.67035,2.82743,2.98451,3.14159
4 DATA P/110,1/
DATA M/21/

ARM AND LABEL BODY BOUNDARY.

CALL VECTOR(XRND,YRND,NMAX,1,C,IM 1
XLAB=-1.0,1.0,YFSF
YLAB=.0,6
IF (M4INDX .EQ.1) GO TO 5

```

RELGAH	93
RELGAH	94
RELGAH	95
RELGAH	96
RELGAH	97
RELGAH	98
RELGAH	99
RELGAH	100
RELGAH	101
RELGAH	102
RELGAH	103
RELGAH	104
RELGAH	105
RELGAH	106
RELGAH	107
RELGAH	108
RELGAH	109
RELGAH	110
RELGAH	111
RELGAH	112
RELGAH	113
RELGAH	114
RELGAH	115
RELGAH	116
RELGAH	117
RELGAH	118
RELGAH	119
RELGAH	120
RELGAH	121
RELGAH	122
RELGAH	123
RELGAH	124
RELGAH	125
RELGAH	126
RELGAH	127
RELGAH	128
RELGAH	129
RELGAH	130
RELGAH	131
RELGAH	132
RELGAH	133
RELGAH	134
RELGAH	135
RELGAH	136
RELGAH	137
RELGAH	138
RELGAH	139
RELGAH	140
RELGAH	141
RELGAH	142
RELGAH	143
RELGAH	144
RELGAH	145
RELGAH	146
RELGAH	147
RELGAH	148
RELGAH	149
RELGAH	150
RELGAH	151
RELGAH	152
RELGAH	153
RELGAH	154
RELGAH	155
RELGAH	156
RELGAH	157
RELGAH	158
RELGAH	159
RELGAH	160
RELGAH	161
RELGAH	162
RELGAH	163
RELGAH	164
RELGAH	165
RELGAH	166
RELGAH	167
RELGAH	168
RELGAH	169
RELGAH	170
RELGAH	171
RELGAH	172
RELGAH	173
RELGAH	174
RELGAH	175
RELGAH	176
RELGAH	177
RELGAH	178
RELGAH	179
RELGAH	180
RELGAH	181
RELGAH	182
RELGAH	183
RELGAH	184
RELGAH	185
RELGAH	186
RELGAH	187
RELGAH	188
RELGAH	189
RELGAH	190
RELGAH	191
RELGAH	192
RELGAH	193
RELGAH	194
RELGAH	195
RELGAH	196
RELGAH	197
RELGAH	198
RELGAH	199
RELGAH	200


```

RETURN
END

*****ROUTINE MSTEP

THIS SUBROUTINE CALCULATES THE VERTICAL FIELD LINES,
BY INTEGRATING ALONG EACH STREAMLINE TO LOCATE POSITIONS
AT EQUAL TIME INTERVALS

COMMON /ALUNT/ THETA(25),PP(23,25),N4LUNT
COMMON /R4UND5/ X800(100),YR00(100),XSHK(1:3),YSHK(100),
* NBR4(4),NBR4X(4),N4CH4,G4N4H4,NR0(4),MHTNDX
COMMON /FLOW/ XC(23,100),YC(23,130),VF(20,100),R4OF(20,100)
COMMON /DHSR/ TPLDT,MZEMH,MZADD,MXPLOT
LEVEL 2, M4, M5F, YSF, XSF, ELBF, G4N4F
COMMON /RVAL/ N4,M4F(51),X4F(51,100),R4F(51,100),F4BF(51,100),
* G4N4F(51,100)
LEVEL 2, XST,YST,MUMST,MST
COMMON /STREAM/ XST(50,152),YST(50,152),MUMST(50),MST

SECOND FIELD LINE IS TANGENT TO SHOCK NOSE

J4F4V=99
N4=M4(17PLDT+10.0+14.0,30.0)
YSHK7=YF4N4H4X=11
DSINE=YST(XST,1)-XSHKZ/(FLOTATN4)-1.5)
DELTD=DSINE

CALCULATE WHERE VERTICAL FIELD LINES CROSS SYMMETRY AXIS

DO 600 J=1,J4F4V
  DMC(1,1)=0.0
61) CONTINUE
  YF(1,1)=XSHK7-DSINE
  YF(1,2)=XSHKZ

ASSUME CONSTANT DECELERATION BETWEEN POINTS

J=2
TOLD=0.0
Y0=N4H4V
VZ=YF(1,1)
62) V1=VZ
  TP=TP0=1
  IF (TP .LT. 0) GO TO 640
  W=VF(1,1)
  TP=TP0+(TP-1)-XC(100,11)/(VZ+V1)
  V1=(VZ-V1)/TP
  TNEW=TOLD+TP
  IF (TNLW .GE. DELT) GO TO 620
  TOLD=TNEW
  GO TO 610
63) RT=DELTD-TOLD
  DELS=V1+RT+0.5*RT*RT
  J=J+1
  YF(1,1)=XC(100,11)+DELS
  TOLD=TNEW+DELTD
  IF (1 .GE. J4F4V) GO TO 640
  IF (TOLD .LT. DELT) GO TO 610
  V1=V1+RT
  DELS=V1+DELTD+0.5*RT*RT+0.2
  TOLD=TOLD+DELTD
  RT=DELTD
  J=J+1
  YF(1,1)=YF(1,1)+DELS
  GO TO 630
64) CONTINUE
  N4F(1)=J
  T=1

CALCULATE WHERE VERTICAL FIELD LINES CROSS STREAMLINE

DO 700 IP=1,MST
  T=TP=1
  YF(1,1)=XSHKZ-DSINE
  R4F(1,1)=YST(IP,1)
  YF(1,2)=XSHKZ
  R4F(1,2)=YST(IP,1)
  LOCATE POINTS BEFORE SHOCK WAVE

```

95 HK1	35
95 HK1	36

```

NN 710 I=1,N8
TF (YAF(I,J-1)+DSINF .GT. XST(IM,1)) GO TO 72C
XRF(I,J)=XRF(I,J-1)+DSINF
XRF(I,J)=YST(IM,1)
713 CONTINUE

LOCATE POINTS WITHIN THE MAGNETOSPHERE

720 TOLN=XST(IM,1)-XRF(I,J-1)
J=J-1
KST=1
TF (IM .GE. NMLUNT) GO TO P11
V2=VF(NMAX,I)
GO TO 730

P11 ON P2= JJ=NMLUNT,NMAX
TF (XST(IM,1) .GT. XC(NRMAX,JJ)) GO TO P21
V2=VF(NMAX,JJ-1)+(VF(NRMAX,JJ)-VF(NRMAX,JJ-1))
* (XST(IM,1)-XC(NRMAX,JJ-1))/(XC(NRMAX,JJ)-XC(NRMAX,JJ-1))
GO TO 730

P20 CONTINUE
731 V1=V2
V1=XST(IM,KST+1)
V1=YST(IM,KST+1)
V2=V1+V2*P(X1,V1)
NST=NST+(XST(IM,KST+1)-XST(IM,KST))**2
* (YST(IM,KST+1)-YST(IM,KST))**2
NT=2./NST/(V1+V2)
A=(V2-V1)/NT
TNEW=TOLD+DT
TF (TNEW .GE. DELT) GO TO 74C
KST=KST+1
TOLD=TNEW
TF (KST .GE. NMLST(IM)) GO TO 76C
GO TO 73C

74C J=J+1
NT=DEL-TOLD
NELS=V1+NT+0.5*A*NT*NT
XRF(I,J)=XRF(I,M,KST+1)+DEL*(XST(IM,KST+1)-XST(IM,KST))/NST
PXF(I,J)=YST(IM,KST+1)+DEL*(YST(IM,KST+1)-YST(IM,KST))/NST
TOLD=TNEW-DELT
KST=KST+1
TF (KST .GE. NMLST(IM)) GO TO 76C
75C J=J+1
V1=V2+0*NT
NELS=V1+DEL+0.5*A*DEL*DEL
XRF(I,J)=XRF(I,J-1)+DEL*(XST(IM,KST)-XST(IM,KST-1))/NST
PXF(I,J)=XRF(I,J-1)+DEL*(YST(IM,KST)-YST(IM,KST-1))/NST
NT=DEL
TOLD=TOLD-DELT
GO TO 75C

76C CONTINUE
NRC(I)=J
TF (J .GT. NAF(I-1)) NAF(I)=NAF(I-1)
76C CONTINUE
RETURN
END

```

85 T5E	76
85 T5E	77
85 T5E	78
85 T5E	79
85 T5E	81
85 T5E	81
85 T5E	82
85 T5E	83
85 T5E	84
85 T5E	85
85 T5E	86
85 T5E	87
85 T5E	88
85 T5E	89
85 T5E	90
85 T5E	91
85 T5E	92
85 T5E	93
85 T5E	94
85 T5E	95
85 T5E	96
85 T5E	97
85 T5E	98
85 T5E	99
85 T5E	100
85 T5E	101
85 T5E	102
85 T5E	103
85 T5E	104
85 T5E	105
85 T5E	106
85 T5E	107
85 T5E	108
85 T5E	109
85 T5E	110
85 T5E	111
85 T5E	112
85 T5E	113
85 T5E	114
85 T5E	115
85 T5E	116
85 T5E	117
85 T5E	118
85 T5E	119
85 T5E	120
85 T5E	121
85 T5E	122
85 T5E	123
85 T5E	124
85 T5E	125
85 T5E	126
85 T5E	127
85 T5E	128
85 T5E	129
85 T5E	130
85 T5E	131
85 T5E	132
85 T5E	133

USING A BUBBLE TECHNIQUE, THIS ROUTINE SORTS THE REAL
ARRAYS IN AN ASCENDING ORDER AND CHANGES
THE ORDER OF ABRAYS A AND B IN A CORRESPONDING
MANNER. K IS THE NUMBER OF DATA POINTS TO
BE SORTED.

q1j1q1	2
q1j1q1	3
q1j1q1	4
q1j1q1	5
q1j1q1	6
q1j1q1	7
q1j1q1	8
q1j1q1	9
q1j1q1	10
q1j1q1	11
q1j1q1	12
q1j1q1	13
q1j1q1	14
q1j1q1	15
q1j1q1	16
q1j1q1	17
q1j1q1	18
q1j1q1	19
q1j1q1	20
q1j1q1	21
q1j1q1	22

```

DIMENSION A(11),S(1),Q(1),TLN(1)

```

```

IF(K.EQ.1) RETURN
K1=K-1
DO 100 I=1,K1
L=I+1
DO 110 J=L,K
IF(S(J).GT.S(I)) GO TO 100

```

INTERCHANGE ARRAYS

```
TEMP=S(I)
S(I)=S(J)
```

```

S(I)=TEMP
TEMP=A(I)
A(I)=A(J)
A(J)=TEMP
TEMP=A(I)
A(I)=A(J)
A(J)=TEMP
103 CONTINUE
C
RETURN
END

SUBROUTINE CHECK(ICM,NV,KOD2,J,K,NVAL,KOD9)
C
C   CONTOUR PROGRAMS MAP, VALY, SEARCH, ENTER, AND CHECK
C   WRITTEN BY REESE SORFENSON, NASA-AMES RES. CTR., AUG., 1974.
C   (MODIFIED VERSION)
C
C   GIVEN THAT A LINE PASSES THROUGH AN INTERVAL UNDER
C   INVESTIGATION, QUESTION: IS IT A NEW LINE, OR IS IT
C   PART OF A LINE ALREADY RECORDED?
C
C   KOD9 =1   OK, NEW POINT.
C   KOD9 =2   OLD POINT.
C
C   DIMENSION ICM(4,1)
C
C   DO 1 L=1,NV
C   IF(KOD2.NE.ICM(L,1)) GO TO 1
C   IF(J.NE.ICM(L,1)) GO TO 1
C   IF(K.NE.ICM(L,1)) GO TO 1
C   IF(NVAL.EQ.ICM(L,1)) GO TO 2
C   CONTINUE
C   KOD9=1
C   GO TO 3
C   KOD9=2
C   RETURN
C   END

SUBROUTINE CONOUT (ACONT,FACT,NHINDX)
C
C   THIS ROUTINE WRITES OUT THE CONTOUR LINES FOUND BY
C   SUBROUTINE MAP
C
C   COMMON /TCHECK/ ICM(4,120)
C   COMMON /PLOT/ CONTX(100),CONTY(100),CVAL(30),NAD(30),IPLT
C   DIMENSION ACONT(1)
C
C   WRITE 4FACING FOR THIS SET OF CONTOURS
C
C   NMAX=NAD(1)
C   IF(IPLT.EQ.2) GO TO 13
C   IF (IPLT .GT. 4) GO TO 15
C   WRITE(6,400) NMAX
C   GO TO 20
C 1. WRITE(6,500) NMAX
C   GO TO 21
C 15 IF (IPLT .EQ. 5) WRITE(6,600) NMAX
C   IF (IPLT .EQ. 6) WRITE(6,610) NMAX
C   IF (IPLT.EQ.7) WRITE (6,640) NMAX
C 20 CONTINUE
C
C   REVERSE SIGN OF X FOR OUTPUT
C
C   JMAX=NAD(NMAX+1)-1
C   DO 2 J=1,JMAX
C   2 CONTX(J)=CONTX(J)
C
C   PRINT CONTOUR LINE FOR EACH VALUE
C
C   NAD(1)=1
C   DO 1 M=1,NMAX
C   NP=NAD(N+1)-NAD(N)
C   MCOUNT=NAD(N)
C   I=ICM(4,MCOUNT)
C   CVAL(N)=ACONT(I)

```

```

MURRL 23
MURRL 24
MURRL 25
MURRL 26
MURRL 27
MURRL 28
MURRL 29
MURRL 30
MURRL 31
MURRL 32
MURRL 33
CHECK 2
CHECK 3
CHECK 4
CHECK 5
CHECK 6
CHECK 7
CHECK 8
CHECK 9
CHECK 10
CHECK 11
CHECK 12
CHECK 13
CHECK 14
CHECK 15
CHECK 16
CHECK 17
CHECK 18
CHECK 19
CHECK 20
CHECK 21
CHECK 22
CHECK 23
CHECK 24
CHECK 25
CHECK 26
CONOUT 2
CONOUT 3
CONOUT 4
CONOUT 5
CONOUT 6
CONOUT 7
CONOUT 8
CONOUT 9
CONOUT 10
CONOUT 11
CONOUT 12
CONOUT 13
CONOUT 14
CONOUT 15
CONOUT 16
CONOUT 17
CONOUT 18
CONOUT 19
CONOUT 20
CONOUT 21
CONOUT 22
CONOUT 23
CONOUT 24
CONOUT 25
CONOUT 26
CONOUT 27
CONOUT 28
CONOUT 29
CONOUT 30
CONOUT 31
CONOUT 32
CONOUT 33
CONOUT 34
CONOUT 35
CONOUT 36
CONOUT 37
CONOUT 38

```

```

M1=NAD(N)
M2=NAD(N+1)-1
IF(IPLT.EQ.2) GO TO 30
IF (IPLT .GT. 4) GO TO 35
TVAL=1.0+FACT*(1.0-CVAL(N)+*2)
WRITE(6,410) NP,CVAL(N),TVAL
GO TO 43
30 WRITE(6,510) NP,CVAL(N)
GO TO 42
35 IF (IPLT .EQ. 5) WRITE(6,620) NP,CVAL(N)
IF (IPLT .EQ. 6) WRITE(6,630) NP,CVAL(N)
IF (IPLT.EQ.7) WRITE (6,650) NP,CVAL(N)
40 IF(NHINDX.EQ.1) GO TO 45
WRITE(6,420)
GO TO 46
45 WRITE(6,425)
50 CONTINUE
WRITE(6,430) (CONTX(I),CONTY(I),I=M1,M2)
1 CONTINUE
NAD(1)=NMAX
C
C   RESTORE SIGN OF X
C
C   DO 3 J=1,JMAX
C   3 CONTX(J)=-CONTX(J)
C   RETURN
C
400 FORMAT(1H//49X,33HVELOCITY AND TEMPERATURE CONTOURS/49X,33(1H//)
* 10X,13,43H VELOCITY (TEMPERATURE) CONTOUR LINES FOUND)
410 FORMAT(//5X,13,35H POINTS IN CONTOUR LINE OF V/INF =,F7.3,
* 11H, T/TINF =,F7.3//)
420 FORMAT(14X,34X/0,17X,34H//)
425 FORMAT(14X,44X/0,10X,44H//)
430 FORMAT(0F10,4,13X,13,41
* 10X,13,28H DENSITY CONTOUR LINES FOUND)
* 10X,13,394 POINTS IN CONTOUR LINE OF RHO/RHINF =,F7.3//)
510 FORMAT(//5X,13,394 POINTS IN CONTOUR LINE OF RHO/RHINF =,F7.3//)
670 FORMAT(14/153X,23H MAGNETIC FIELD CONTOURS/53X,23(1H//)
* 10X,13,354 MAGNETIC FIELD CONTOUR LINES FOUND)
* 14X,33HFOR COMPONENT ALONG FIELD LINES ,
* 33HPARALLEL TO FLOW IN FREESTREAM)
610 FORMAT(14/153X,13,354 MAGNETIC FIELD CONTOUR LINES FOUND)
* 14X,33HFOR COMPONENT ALONG FIELD LINES ,
* 36HPERPENDICULAR TO FLOW IN FREESTREAM)
620 FORMAT(//5X,13,344 POINTS IN CONTOUR LINE OF R/INF ,
* 12H(PARALLEL) =,F7.3//)
630 FORMAT(//5X,13,344 POINTS IN CONTOUR LINE OF R/INF ,
* 17H(PERPENDICULAR) =,F7.3//)
640 FORMAT(14/153X,13,354 MAGNETIC FIELD CONTOUR LINES FOUND)
* 14X,33HFOR COMPONENT ALONG FIELD LINES ,
* 29HNORMAL TO FLOW IN FREESTREAM)
650 FORMAT(//5X,13,344 POINTS IN CONTOUR LINE OF R/INF ,
* 16H(NORMAL) =,F7.3//)
END

SUBROUTINE CONTR
C
C   THIS SUBROUTINE PLOTS AND LABELS CONTOUR LINES.
C   ALSO DRAWS FIELD LINES FOR MAGNETIC FIELD STRENGTH PLOTS.
C   MCC PLIST SUBROUTINES USED ARE
C   DOTLN,MUMPL,VECTOR.
C
C   DIMENSION YSI(53),YSI(53)
C   COMMON /LARS/ YLAR(50),YLAR(30),CV(30),NCL(10),NLAR
C   COMMON /SCALE/ XSF,YSF,XMAX,YMAX,XLMFT4,YLMFT4
C   LEVEL 3,NM,NVF,YVF,PVF,ELRF,GARF
C   COMMON /VAL/ NVL,NVF(52),YVF(52,10),PVF(52,100),ELRF(2,100),
* GARF(52,10)
C   COMMON /CONTR/ IPLT,NZEND,NZAND,NXPLOT
C   COMMON /RUNDNS/ XND(13),YND(13),PSH(1,1),VSH(1,1),
* NMAX,NMAXX,AMAX,GARF,MPO,NHINDX
C   LEVEL 2, YST,YST,NHST,NST
C   COMMON /STREAM/ XST(50,152),YST(50,152),NMST(50),NST
C   COMMON /PLOT/ CONTX(100),CONTY(100),CVAL(30),NAD(30),IPLT
C
C   IF(IPLT.EQ.3) GO TO 70
C
C   DRAW CONTOUR LINES.
C
C   TA=1

```

```

CONOUT 39
CONOUT 40
CONOUT 41
CONOUT 42
CONOUT 43
CONOUT 44
CONOUT 45
CONOUT 46
CONOUT 47
CONOUT 48
CONOUT 49
CONOUT 50
CONOUT 51
CONOUT 52
CONOUT 53
CONOUT 54
CONOUT 55
CONOUT 56
CONOUT 57
CONOUT 58
CONOUT 59
CONOUT 60
CONOUT 61
CONOUT 62
CONOUT 63
CONOUT 64
CONOUT 65
CONOUT 66
CONOUT 67
CONOUT 68
CONOUT 69
CONOUT 70
CONOUT 71
CONOUT 72
CONOUT 73
CONOUT 74
CONOUT 75
CONOUT 76
CONOUT 77
CONOUT 78
CONOUT 79
CONOUT 80
CONOUT 81
CONOUT 82
CONOUT 83
CONOUT 84
CONOUT 85
CONOUT 86
CONOUT 87
CONOUT 88
CONOUT 89
CONOUT 90
CONOUT 91
CONOUT 92
CONTR 2
CONTR 3
CONTR 4
CONTR 5
CONTR 6
CONTR 7
CONTR 8
CONTR 9
CONTR 10
CONTR 11
CONTR 12
CONTR 13
CONTR 14
CONTR 15
CONTR 16
CONTR 17
CONTR 18
CONTR 19
CONTR 20
CONTR 21
CONTR 22
CONTR 23
CONTR 24
CONTR 25
CONTR 26
CONTR 27
CONTR 28
CONTR 29
CONTR 30
CONTR 31
CONTR 32
CONTR 33
CONTR 34
CONTR 35
CONTR 36
CONTR 37
CONTR 38
CONTR 39
CONTR 40
CONTR 41
CONTR 42
CONTR 43
CONTR 44
CONTR 45
CONTR 46
CONTR 47
CONTR 48
CONTR 49
CONTR 50
CONTR 51
CONTR 52
CONTR 53
CONTR 54
CONTR 55
CONTR 56
CONTR 57
CONTR 58
CONTR 59
CONTR 60
CONTR 61
CONTR 62
CONTR 63
CONTR 64
CONTR 65
CONTR 66
CONTR 67
CONTR 68
CONTR 69
CONTR 70
CONTR 71
CONTR 72
CONTR 73
CONTR 74
CONTR 75
CONTR 76
CONTR 77
CONTR 78
CONTR 79
CONTR 80
CONTR 81
CONTR 82
CONTR 83
CONTR 84
CONTR 85
CONTR 86
CONTR 87
CONTR 88
CONTR 89
CONTR 90
CONTR 91
CONTR 92

```



```

103 DO 110 J=2,NST,3
104   M=MOD(J,4)
105   IF (M.EQ.1) THEN
106     YS(1)=Y(1),XS(1)=X(1)
107   ELSE IF (M.EQ.2) THEN
108     YS(2)=Y(2),XS(2)=X(2)
109   ELSE IF (M.EQ.3) THEN
110     YS(3)=Y(3),XS(3)=X(3)
111   ELSE IF (M.EQ.4) THEN
112     YS(4)=Y(4),XS(4)=X(4)
113   END IF
114   CALL DOTLMERS(M),YS(M),XS(M),YS(M+1),XS(M+1),25.0)
115   CONTINUE
116   RETURN
117 C
118 C DRAW PERPENDICULAR FIELD LINES FOR MAGNETIC FIELD PLOT
119 C
120 C
121 C
122 C
123 CONTINUE
124   YS(1)=Y(1),XS(1)=X(1)
125   YS(2)=Y(2),XS(2)=X(2)
126   YS(3)=Y(3),XS(3)=X(3)
127   YS(4)=Y(4),XS(4)=X(4)
128   CALL DOTLMERS(M),YS(M),XS(M),YS(M+1),XS(M+1),25.0)
129   CONTINUE
130   RETURN
131 C
132 CONTINUE
133   DO 130 J=1,NM
134     CALL DOTLMERS(M),YS(M),XS(M),YS(M+1),XS(M+1),25.0)
135     CONTINUE
136     RETURN
137 C
138 C DRAW PERPENDICULAR FIELD LINES FOR MAGNETIC FIELD PLOT
139 C
140 C
141 C
142 C
143 CONTINUE
144   YS(1)=Y(1),XS(1)=X(1)
145   YS(2)=Y(2),XS(2)=X(2)
146   YS(3)=Y(3),XS(3)=X(3)
147   YS(4)=Y(4),XS(4)=X(4)
148   CALL DOTLMERS(M),YS(M),XS(M),YS(M+1),XS(M+1),25.0)
149   CONTINUE
150   RETURN
151 C
152 CONTINUE
153   DO 150 J=1,NM
154     CALL DOTLMERS(M),YS(M),XS(M),YS(M+1),XS(M+1),25.0)
155     CONTINUE
156     RETURN
157 C
158 C DRAW PERPENDICULAR FIELD LINES FOR MAGNETIC FIELD PLOT
159 C
160 C
161 C
162 C
163 CONTINUE
164   YS(1)=Y(1),XS(1)=X(1)
165   YS(2)=Y(2),XS(2)=X(2)
166   YS(3)=Y(3),XS(3)=X(3)
167   YS(4)=Y(4),XS(4)=X(4)
168   CALL DOTLMERS(M),YS(M),XS(M),YS(M+1),XS(M+1),25.0)
169   CONTINUE
170   RETURN
171 C
172 CONTINUE
173   DO 170 J=1,NM
174     CALL DOTLMERS(M),YS(M),XS(M),YS(M+1),XS(M+1),25.0)
175     CONTINUE
176     RETURN
177 C
178 C DRAW PERPENDICULAR FIELD LINES FOR MAGNETIC FIELD PLOT
179 C
180 C
181 C
182 C
183 CONTINUE
184   YS(1)=Y(1),XS(1)=X(1)
185   YS(2)=Y(2),XS(2)=X(2)
186   YS(3)=Y(3),XS(3)=X(3)
187   YS(4)=Y(4),XS(4)=X(4)
188   CALL DOTLMERS(M),YS(M),XS(M),YS(M+1),XS(M+1),25.0)
189   CONTINUE
190   RETURN
191 C
192 CONTINUE
193   DO 190 J=1,NM
194     CALL DOTLMERS(M),YS(M),XS(M),YS(M+1),XS(M+1),25.0)
195     CONTINUE
196     RETURN
197 C
198 C DRAW PERPENDICULAR FIELD LINES FOR MAGNETIC FIELD PLOT
199 C
200 C
201 C
202 C
203 CONTINUE
204   YS(1)=Y(1),XS(1)=X(1)
205   YS(2)=Y(2),XS(2)=X(2)
206   YS(3)=Y(3),XS(3)=X(3)
207   YS(4)=Y(4),XS(4)=X(4)
208   CALL DOTLMERS(M),YS(M),XS(M),YS(M+1),XS(M+1),25.0)
209   CONTINUE
210   RETURN
211 C
212 CONTINUE
213   DO 210 J=1,NM
214     CALL DOTLMERS(M),YS(M),XS(M),YS(M+1),XS(M+1),25.0)
215     CONTINUE
216     RETURN
217 C
218 C DRAW PERPENDICULAR FIELD LINES FOR MAGNETIC FIELD PLOT
219 C
220 C
221 C
222 C
223 CONTINUE
224   YS(1)=Y(1),XS(1)=X(1)
225   YS(2)=Y(2),XS(2)=X(2)
226   YS(3)=Y(3),XS(3)=X(3)
227   YS(4)=Y(4),XS(4)=X(4)
228   CALL DOTLMERS(M),YS(M),XS(M),YS(M+1),XS(M+1),25.0)
229   CONTINUE
230   RETURN
231 C
232 CONTINUE
233   DO 230 J=1,NM
234     CALL DOTLMERS(M),YS(M),XS(M),YS(M+1),XS(M+1),25.0)
235     CONTINUE
236     RETURN
237 C
238 C DRAW PERPENDICULAR FIELD LINES FOR MAGNETIC FIELD PLOT
239 C
240 C
241 C
242 C
243 CONTINUE
244   YS(1)=Y(1),XS(1)=X(1)
245   YS(2)=Y(2),XS(2)=X(2)
246   YS(3)=Y(3),XS(3)=X(3)
247   YS(4)=Y(4),XS(4)=X(4)
248   CALL DOTLMERS(M),YS(M),XS(M),YS(M+1),XS(M+1),25.0)
249   CONTINUE
250   RETURN
251 C
252 CONTINUE
253   DO 250 J=1,NM
254     CALL DOTLMERS(M),YS(M),XS(M),YS(M+1),XS(M+1),25.0)
255     CONTINUE
256     RETURN
257 C
258 C DRAW PERPENDICULAR FIELD LINES FOR MAGNETIC FIELD PLOT
259 C
260 C
261 C
262 C
263 CONTINUE
264   YS(1)=Y(1),XS(1)=X(1)
265   YS(2)=Y(2),XS(2)=X(2)
266   YS(3)=Y(3),XS(3)=X(3)
267   YS(4)=Y(4),XS(4)=X(4)
268   CALL DOTLMERS(M),YS(M),XS(M),YS(M+1),XS(M+1),25.0)
269   CONTINUE
270   RETURN
271 C
272 CONTINUE
273   DO 270 J=1,NM
274     CALL DOTLMERS(M),YS(M),XS(M),YS(M+1),XS(M+1),25.0)
275     CONTINUE
276     RETURN
277 C
278 C DRAW PERPENDICULAR FIELD LINES FOR MAGNETIC FIELD PLOT
279 C
280 C
281 C
282 C
283 CONTINUE
284   YS(1)=Y(1),XS(1)=X(1)
285   YS(2)=Y(2),XS(2)=X(2)
286   YS(3)=Y(3),XS(3)=X(3)
287   YS(4)=Y(4),XS(4)=X(4)
288   CALL DOTLMERS(M),YS(M),XS(M),YS(M+1),XS(M+1),25.0)
289   CONTINUE
290   RETURN
291 C
292 CONTINUE
293   DO 290 J=1,NM
294     CALL DOTLMERS(M),YS(M),XS(M),YS(M+1),XS(M+1),25.0)
295     CONTINUE
296     RETURN
297 C
298 C DRAW PERPENDICULAR FIELD LINES FOR MAGNETIC FIELD PLOT
299 C
300 C
301 C
302 C
303 CONTINUE
304   YS(1)=Y(1),XS(1)=X(1)
305   YS(2)=Y(2),XS(2)=X(2)
306   YS(3)=Y(3),XS(3)=X(3)
307   YS(4)=Y(4),XS(4)=X(4)
308   CALL DOTLMERS(M),YS(M),XS(M),YS(M+1),XS(M+1),25.0)
309   CONTINUE
310   RETURN
311 C
312 CONTINUE
313   DO 310 J=1,NM
314     CALL DOTLMERS(M),YS(M),XS(M),YS(M+1),XS(M+1),25.0)
315     CONTINUE
316     RETURN
317 C
318 C DRAW PERPENDICULAR FIELD LINES FOR MAGNETIC FIELD PLOT
319 C
320 C
321 C
322 C
323 CONTINUE
324   YS(1)=Y(1),XS(1)=X(1)
325   YS(2)=Y(2),XS(2)=X(2)
326   YS(3)=Y(3),XS(3)=X(3)
327   YS(4)=Y(4),XS(4)=X(4)
328   CALL DOTLMERS(M),YS(M),XS(M),YS(M+1),XS(M+1),25.0)
329   CONTINUE
330   RETURN
331 C
332 CONTINUE
333   DO 330 J=1,NM
334     CALL DOTLMERS(M),YS(M),XS(M),YS(M+1),XS(M+1),25.0)
335     CONTINUE
336     RETURN
337 C
338 C DRAW PERPENDICULAR FIELD LINES FOR MAGNETIC FIELD PLOT
339 C
340 C
341 C
342 C
343 CONTINUE
344   YS(1)=Y(1),XS(1)=X(1)
345   YS(2)=Y(2),XS(2)=X(2)
346   YS(3)=Y(3),XS(3)=X(3)
347   YS(4)=Y(4),XS(4)=X(4)
348   CALL DOTLMERS(M),YS(M),XS(M),YS(M+1),XS(M+1),25.0)
349   CONTINUE
350   RETURN
351 C
352 CONTINUE
353   DO 350 J=1,NM
354     CALL DOTLMERS(M),YS(M),XS(M),YS(M+1),XS(M+1),25.0)
355     CONTINUE
356     RETURN
357 C
358 C DRAW PERPENDICULAR FIELD LINES FOR MAGNETIC FIELD PLOT
359 C
360 C
361 C
362 C
363 CONTINUE
364   YS(1)=Y(1),XS(1)=X(1)
365   YS(2)=Y(2),XS(2)=X(2)
366   YS(3)=Y(3),XS(3)=X(3)
367   YS(4)=Y(4),XS(4)=X(4)
368   CALL DOTLMERS(M),YS(M),XS(M),YS(M+1),XS(M+1),25.0)
369   CONTINUE
370   RETURN
371 C
372 CONTINUE
373   DO 370 J=1,NM
374     CALL DOTLMERS(M),YS(M),XS(M),YS(M+1),XS(M+1),25.0)
375     CONTINUE
376     RETURN
377 C
378 C DRAW PERPENDICULAR FIELD LINES FOR MAGNETIC FIELD PLOT
379 C
380 C
381 C
382 C
383 CONTINUE
384   YS(1)=Y(1),XS(1)=X(1)
385   YS(2)=Y(2),XS(2)=X(2)
386   YS(3)=Y(3),XS(3)=X(3)
387   YS(4)=Y(4),XS(4)=X(4)
388   CALL DOTLMERS(M),YS(M),XS(M),YS(M+1),XS(M+1),25.0)
389   CONTINUE
390   RETURN
391 C
392 CONTINUE
393   DO 390 J=1,NM
394     CALL DOTLMERS(M),YS(M),XS(M),YS(M+1),XS(M+1),25.0)
395     CONTINUE
396     RETURN
397 C
398 C DRAW PERPENDICULAR FIELD LINES FOR MAGNETIC FIELD PLOT
399 C
400 C
401 C
402 C
403 CONTINUE
404   YS(1)=Y(1),XS(1)=X(1)
405   YS(2)=Y(2),XS(2)=X(2)
406   YS(3)=Y(3),XS(3)=X(3)
407   YS(4)=Y(4),XS(4)=X(4)
408   CALL DOTLMERS(M),YS(M),XS(M),YS(M+1),XS(M+1),25.0)
409   CONTINUE
410   RETURN
411 C
412 CONTINUE
413   DO 410 J=1,NM
414     CALL DOTLMERS(M),YS(M),XS(M),YS(M+1),XS(M+1),25.0)
415     CONTINUE
416     RETURN
417 C
418 C DRAW PERPENDICULAR FIELD LINES FOR MAGNETIC FIELD PLOT
419 C
420 C
421 C
4
```

```

244 YSXND=YS(N-1)+(YS(N)-YS(N-1))/(XND(J)-XS(N-1))
IF (YSXND .LT. Y900(J)) N1=N
245 CONTINUE
DO 250 N=1,N1
CALL DNTLN(XS(N),YS(N),YSIN+1,YSIN+1,20,3)
250 CONTINUE
252 CONTINUE
RETURN
END

```

```

CONTUR 101
CONTUR 102
CONTUR 103
CONTUR 104
CONTUR 105
CONTUR 106
CONTUR 107
CONTUR 108
CONTUR 109
CONTUR 200

```

```

C SUBROUTINE CONTUR
C SUBROUTINE CONTUR CONTROL CALCULATING AND PRINTING THE CONTOURS
C AND CREATING THE PLOTS

```

```

C COMMON /INT/ ANG,ANGH,VRCON,RCON(23)
C LEVEL 2, NPARA,PERP,RHND,AMAG,ANAG
C COMMON /CONDS/ NPARA(20,100),PERP(20,100),RHND(20,100),
C AMAG(20,100),ANAG(20,100)
C COMMON /RNDMS/ Y900(100),Y900(100),Y900(100),Y900(100),
C NRMAY,NRMAY,AMACH,GAMMA,HRO,NHINDX
C COMMON /CONV/ KVCN,VCON(20),KRCN,RCN(20)
C COMMON /FLOW/ XC(20,100),YC(20,100),VF(20,100),RHO(20,100)
C COMMON /DNTN/ TPLDT,NZEM,NZAD,NMPLDT
C COMMON /PLOT/ CONTC(100),CONTY(100),CVAL(100),NAN(100),TPLDT
C LOGICAL LRSUM,LPRFL,LPRST,LPRCN,LPRP,LPLDT,LTRAJ,LPRST
C COMMON /PROPT/ LRSUM,LPRFL,LPRST,LPRCN,LPRP,LPLDT,LTRAJ,LPRST
C LEVEL 2, XST,YST,NHST,NST
C COMMON /STREAM/ XST(20,152),YST(20,152),NHST(20,152)
C COMMON /TCHK/ TCHK(4,100)
C DIMENSION ASCH(20,100)

```

```

C PLOT STREAMLINES
C IF (LPLDT) CALL SPALC(XCHK,YCHK,NHMAX)
C TPLDT=1
C IF (LPLDT) CALL PLOTCH

```

```

C CALCULATE VELOCITY CONTOUR LINES
C (GRID IS NRMAY BY NRMAY)

```

```

C IF (KVCN .LE. 5) GO TO 11
C CALL MAP(VCN,20,CONTC,CONTY,KVCN,2,VCON,NAD,100,30,TCHK,
C 1,1,NRMAY,NHMAX)

```

```

C PLOT VELOCITY AND TEMPERATURE CONTOURS
C TPLDT=1
C FACT=1.5*(GAMMA-1.0)*AMACH*AMACH
C IF (LPRCN) CALL CONOUT(VCN,FACT,NHINDX)
C IF (LPLDT) CALL PLOTCH

```

```

C CALCULATE DENSITY CONTOUR LINES
C IF (KRCN .LE. 5) GO TO 21
C CALL MAP(RCN,20,CONTC,CONTY,KRCN,2,RCN,NAD,100,30,TCHK,
C 1,1,NRMAY,NHMAX)

```

```

C PLOT DENSITY CONTOURS
C TPLDT=2
C IF (LPRCN) CALL CONOUT(RCN,FACT,NHINDX)
C IF (LPLDT) CALL PLOTCH

```

```

C CALCULATE, PRINT, AND PLOT CONTOUR LINES AND PARALLEL
C AND PERPENDICULAR MAGNETIC FIELD COMPONENTS

```

```

C 2) IF (KRCN .LE. 5) GO TO 20
C DO 100 J=1,NHMAX
C DO 100 I=1,NHMAX
C ASCH(I,J)=NPARA(I,J)

```

```

C 10) CONTINUE
C CALL MAP(ASCH,20,CONTC,CONTY,KRCN,2,RCN,NAD,100,30,TCHK,
C 1,1,NRMAY,NHMAX)
C TPLDT=3
C IF (LPRCN) CALL CONOUT(RCN,FACT,NHINDX)
C IF (LPLDT) CALL PLOTCH
C DO 110 J=1,NHMAX

```

```

C 11) CONTINUE
C CALL MAP(ASCH,20,CONTC,CONTY,KRCN,2,RCN,NAD,100,30,TCHK,
C 1,1,NRMAY,NHMAX)
C TPLDT=4
C IF (LPRCN) CALL CONOUT(RCN,FACT,NHINDX)
C IF (LPLDT) CALL PLOTCH
C DO 120 J=1,NHMAX

```

```

C 12) CONTINUE
C CALL MAP(ASCH,20,CONTC,CONTY,KRCN,2,RCN,NAD,100,30,TCHK,
C 1,1,NRMAY,NHMAX)
C TPLDT=5
C IF (LPRCN) CALL CONOUT(RCN,FACT,NHINDX)
C IF (LPLDT) CALL PLOTCH
C DO 130 J=1,NHMAX

```

```

C 13) CONTINUE
C CALL MAP(ASCH,20,CONTC,CONTY,KRCN,2,RCN,NAD,100,30,TCHK,
C 1,1,NRMAY,NHMAX)
C TPLDT=6
C IF (LPRCN) CALL CONOUT(RCN,FACT,NHINDX)
C IF (LPLDT) CALL PLOTCH
C DO 140 J=1,NHMAX

```

```

C 14) CONTINUE
C CALL MAP(ASCH,20,CONTC,CONTY,KRCN,2,RCN,NAD,100,30,TCHK,
C 1,1,NRMAY,NHMAX)
C TPLDT=7
C IF (LPRCN) CALL CONOUT(RCN,FACT,NHINDX)
C IF (LPLDT) CALL PLOTCH
C DO 150 J=1,NHMAX

```

```

C 15) CONTINUE
C CALL MAP(ASCH,20,CONTC,CONTY,KRCN,2,RCN,NAD,100,30,TCHK,
C 1,1,NRMAY,NHMAX)
C TPLDT=8
C IF (LPRCN) CALL CONOUT(RCN,FACT,NHINDX)
C IF (LPLDT) CALL PLOTCH
C DO 160 J=1,NHMAX

```

```

C 16) CONTINUE
C CALL MAP(ASCH,20,CONTC,CONTY,KRCN,2,RCN,NAD,100,30,TCHK,
C 1,1,NRMAY,NHMAX)
C TPLDT=9
C IF (LPRCN) CALL CONOUT(RCN,FACT,NHINDX)
C IF (LPLDT) CALL PLOTCH
C DO 170 J=1,NHMAX

```

```

C 17) CONTINUE
C CALL MAP(ASCH,20,CONTC,CONTY,KRCN,2,RCN,NAD,100,30,TCHK,
C 1,1,NRMAY,NHMAX)
C TPLDT=10
C IF (LPRCN) CALL CONOUT(RCN,FACT,NHINDX)
C IF (LPLDT) CALL PLOTCH
C DO 180 J=1,NHMAX

```

```

C 18) CONTINUE
C CALL MAP(ASCH,20,CONTC,CONTY,KRCN,2,RCN,NAD,100,30,TCHK,
C 1,1,NRMAY,NHMAX)
C TPLDT=11
C IF (LPRCN) CALL CONOUT(RCN,FACT,NHINDX)
C IF (LPLDT) CALL PLOTCH
C DO 190 J=1,NHMAX

```

```

C 19) CONTINUE
C CALL MAP(ASCH,20,CONTC,CONTY,KRCN,2,RCN,NAD,100,30,TCHK,
C 1,1,NRMAY,NHMAX)
C TPLDT=12
C IF (LPRCN) CALL CONOUT(RCN,FACT,NHINDX)
C IF (LPLDT) CALL PLOTCH
C DO 200 J=1,NHMAX

```

```

C 20) CONTINUE
C CALL MAP(ASCH,20,CONTC,CONTY,KRCN,2,RCN,NAD,100,30,TCHK,
C 1,1,NRMAY,NHMAX)
C TPLDT=13
C IF (LPRCN) CALL CONOUT(RCN,FACT,NHINDX)
C IF (LPLDT) CALL PLOTCH
C DO 210 J=1,NHMAX

```

```

DO 110 T=2,NRMAY
ASCH(I,J)=PERP(I,J)
110 CONTINUE
CALL MAP(ASCH,20,CONTC,CONTY,KRCN,2,RCN,NAD,100,30,TCHK,
C 2,1,NRMAY,NHMAX)
C TPLDT=6
C IF (LPRCN) CALL CONOUT(RCN,FACT,NHINDX)
C IF (LPLDT) CALL PLOTCH
C DO 120 J=1,NHMAX
C DO 120 T=2,NRMAY
C ASCH(I,J)=NHND(I,J)

```

```

12) CONTINUE
CALL MAP(ASCH,20,CONTC,CONTY,KRCN,2,RCN,NAD,100,30,TCHK,
C 2,1,NRMAY,NHMAX)
C TPLDT=7
C IF (LPRCN) CALL CONOUT(RCN,FACT,NHINDX)
C IF (LPLDT) CALL PLOTCH
C 20) CONTINUE
C IF (LPLDT) CALL ENPLT(3,0,0,0)
C RETURN
C END

```

```

C 20) CONTINUE
C IF (LPLDT) CALL ENPLT(3,0,0,0)
C RETURN
C END

```

```

C FUNCTION DROTX(Y)
C THIS FUNCTION DETERMINES THE SLOPE OF THE STREAMLINE
C AT THE POINT (X,Y)

```

```

C COMMON /RNDMS/ X900(100),Y900(100),Y900(100),Y900(100),
C NRMAY,NRMAY,AMACH,GAMMA,HRO,NHINDX
C LEVEL 2, ANG,DXTH,DEG
C COMMON /DNTN/ TPLDT,NZEM,NZAD,NMPLDT
C COMMON /FLOW/ XC(20,100),YC(20,100),VF(20,100),RHO(20,100)

```

```

C LOCATING POINT IN GRID
C IF (Y .GE. 0.5) GO TO 10
C THETA=ATAN2(Y,-Y)*DEG
C X=X900(Y*2+0.5)
C DO 3 J=1,NHMAX
C IF (THETA(I)-GT.THETA) GO TO 5

```

```

C 3) CONTINUE
C J=NHMAX
C 5) J=J-1
C IF (J.LT.1) JP=1
C SLOPE=(THETA-THETA(JR))/DXTH(JR)
C P2=PP(1,JR)+PP(1,JR+1)-PP(1,JR)*SLOPE
C R1=R2
C R2=PP(1,JR)+PP(1,JR+1)-PP(1,JR)*SLOPE
C IF (R2 .GT. R1) GO TO 8

```

```

C 7) CONTINUE
C I=NHMAX
C 1) GO TO 21

```

```

C 1) CONTINUE
C DOY
C DO 13 J=NHMAX,NHMAX
C IF (XC(I,J).GT.X) GO TO 15

```

```

C 13) CONTINUE
C J=NHMAX
C 15) J=J-1
C IF (J.LT.1) JP=NHMAX
C SLOPE=(X-XC(1,JR))/DXTH(JR)
C R2=YC(1,JR)+YC(1,JR+1)-YC(1,JR)*SLOPE
C DO 17 T=2,NHMAX
C R1=R2
C R2=YC(1,JR)+YC(1,JR+1)-YC(1,JR)*SLOPE
C IF (R2 .GT. R1) GO TO 18

```

```

C 17) CONTINUE
C I=NHMAX
C 1) CONTINUE

```

```

C 1) CONTINUE
C 1) CONTINUE

```

```

C 1) CONTINUE
C 1) CONTINUE

```

```

C 1) CONTINUE
C 1) CONTINUE

```

```

C 1) CONTINUE
C 1) CONTINUE

```

```

C 1) CONTINUE
C 1) CONTINUE

```

```

C 1) CONTINUE
C 1) CONTINUE

```

```

C 1) CONTINUE
C 1) CONTINUE

```

```

C 1) CONTINUE
C 1) CONTINUE

```

```

C 1) CONTINUE
C 1) CONTINUE

```

```

C 1) CONTINUE
C 1) CONTINUE

```

```

C 1) CONTINUE
C 1) CONTINUE

```

```

C 1) CONTINUE
C 1) CONTINUE

```

```

C 1) CONTINUE
C 1) CONTINUE

```

```

C 1) CONTINUE
C 1) CONTINUE

```

```

CONTUR 66
CONTUR 67
CONTUR 68
CONTUR 69
CONTUR 70
CONTUR 71
CONTUR 72
CONTUR 73
CONTUR 74
CONTUR 75
CONTUR 76
CONTUR 77
CONTUR 78
CONTUR 79
CONTUR 80
CONTUR 81
CONTUR 82
CONTUR 83
CONTUR 84
CONTUR 85
CONTUR 86
CONTUR 87

```

```

DROTX 2
DROTX 3
DROTX 4
DROTX 5
DROTX 6
DROTX 7
DROTX 8
DROTX 9
DROTX 10
DROTX 11
DROTX 12
DROTX 13
DROTX 14
DROTX 15
DROTX 16
DROTX 17
DROTX 18
DROTX 19
DROTX 20
DROTX 21
DROTX 22
DROTX 23
DROTX 24
DROTX 25
DROTX 26
DROTX 27
DROTX 28
DROTX 29
DROTX 30
DROTX 31
DROTX 32
DROTX 33
DROTX 34
DROTX 35
DROTX 36
DROTX 37
DROTX 38
DROTX 39
DROTX 40
DROTX 41
DROTX 42
DROTX 43
DROTX 44
DROTX 45
DROTX 46
DROTX 47
DROTX 48
DROTX 49
DROTX 50
DROTX 51
DROTX 52
DROTX 53
DROTX 54
DROTX 55
DROTX 56

```

```

RETURN
END

SUBROUTINE ECHIMP
PRINTS INPUT CARDS USED FOR RIM
DIMENSION CRO(4)
WRITE (6,116)
12 CONTINUE
READ (5,116) CRO
IF (CRO(1) .EQ. 30.20)
20 CONTINUE
WRITE (6,101) CRO
FOR TO 10
30 CONTINUE
RETURN
END
100 FORMAT(10A10)
101 FORMAT(1X,6A10)
11) FORMAT(1M,40X,35M) LISTING OF INPUT CARDS FOR THIS RUN/40X,35(1M)
1 ///
END

SUBROUTINE ENTER(KOD2,J,K,NVAL,A1,A2,JMIN,KMIN,ICM,KOD4,X,Y,NXY,
* ACNT,ISIZ1)
CONTAIN PROGRAMS PAP, WALK, SEARCH, ENTER, AND CHECK
WRITTEN BY PEESE SORENSON, NASA-AMES RES. CTR., AUG., 1974.
(MODIFIED VERSION)
ASSUMING THAT A POINT ON A CONTOUR LINE HAS BEEN FOUND,
THIS SUBROUTINE RECORDS THAT POINT IN THE BOOKKEEPING ARRAYS.
COMMON /FLOW/ XC(20,100),YC(20,100),VF(20,100),RHOF(20,100)
DIMENSION ICM(4,1),V(1),ACNT(1)
NXY=NXY+1
IF (NXY.GT.ISIZ1) GO TO 1
(ICM(1,NXY)=KOD2
ICM(2,NXY)=J
ICM(3,NXY)=K
ICM(4,NXY)=NVAL
IF ENDPOINTS ARE EQUAL, ENTER MIDPOINT
IF ((A2-A1).EQ.0.0) GO TO 6
DIF=ACNT(NVAL)-A1/(A2-A1)
GO TO (2,3),KOD2
DIF=0.5
GO TO (2,3),KOD2
INTERPOLATE FOR CONTOUR POSITION
2 V2=YC(J,K+1)
Y2=YC(J,K+1)
GO TO 4
3 V2=XC(1+J,K)
Y2=YC(J+1,K)
4 V1=XC(J,K)
V1=YC(J,K)
X(NXY)=X1+DIF*(X2-V1)
Y(NXY)=Y1+DIF*(Y2-V1)
KOD4=1
GO TO 5
WRITE(6,121)
101 FORMAT(9M) CONTOUR SEARCH SORTED - TABLE OVERFLOW IN (X,Y)
KOD4=2
CONTINUE
RETURN
END

```

DRX 97
DRX 98

DRX 99
DRX 60
DRX 61
DRX 62
DRX 63
DRX 64
DRX 65
DRX 66
DRX 67
DRX 68
DRX 69
DRX 70
DRX 71
DRX 72
DRX 73
DRX 74
DRX 75
DRX 76
DRX 77
DRX 78
DRX 79

ENTER 2
ENTER 3
ENTER 4
ENTER 5
ENTER 6
ENTER 7
ENTER 8
ENTER 9
ENTER 10
ENTER 11
FLOW 12
ENTER 13
ENTER 14
ENTER 15
ENTER 16
ENTER 17
ENTER 18
ENTER 19
ENTER 20
ENTER 21
ENTER 22
ENTER 23
ENTER 24
ENTER 25
ENTER 26
ENTER 27
ENTER 28
ENTER 29
ENTER 30
ENTER 31
ENTER 32
ENTER 33
ENTER 34
ENTER 35
ENTER 36
ENTER 37
ENTER 38
ENTER 39
ENTER 40
ENTER 41
ENTER 42
ENTER 43
ENTER 44
ENTER 45
ENTER 46
ENTER 47
ENTER 48
ENTER 49
ENTER 50
ENTER 51

SUBROUTINE EXTRAP
THIS ROUTINE CALCULATES EXTRAPOLATED VALUES OF
RHO AND VF AT POINTS ALONG THE BOUNDARY THETA=9 USING
A LAGRANGIAN INTERPOLATING POLYNOMIAL OVER
THREE UNEQUALLY SPACED POINTS ON EACH RADIAL CURVE.

COMMON /BLUNT/ THETA(25),RP(20,25),NRBLUNT
COMMON /BOUNDS/ X500(100),Y500(100),X5MK(100),Y5MK(100),
* NRMAX,NRMAX,AMAX,GAMMA,NRN,NHINDX
COMMON /FLOW/ XC(20,100),YC(20,100),VF(20,100),RHOF(20,100)
COMMON /SHOCKS/ DRSDX(100),DST(50)

CALCULATE LAGRANGIAN COEFFICIENTS

TH23=THETA(2)-THETA(3)
TH24=THETA(2)-THETA(4)
TH34=THETA(3)-THETA(4)
E2=THETA(3)*THETA(4)/(TH23*TH24)
F3=THETA(2)*THETA(4)/(TH23*TH34)
F4=THETA(2)*THETA(3)/(TH24*TH34)

CALCULATE XC, RHO, AND V AT THETA=0.

AM2=AMAX*AMAX
GO 1) 1=2,NRMAX
YC(1,1)=0.0
XC(1,1)=(E2*RP(1,2)+E3*RP(1,3)+E4*RP(1,4))
RP(1,1)=XC(1,1)
IF (1.FO.NRMAX) GO TO 10
RHOF(1,1)=E2*RHOF(1,2)+E3*RHOF(1,3)+E4*RHOF(1,4)
VF(1,1)=E2*VF(1,2)+E3*VF(1,3)+E4*VF(1,4)
IF (VF(1,1) .LT. 0.) VF(1,1)=0.

1) CONTINUE

CALCULATE EXACT VALUES AT SHOCK WAVE

RHOF(NRMAX,1)=(GAMMA+1.)*AM2/(GAMMA-1.)*AM2+2.)
VF(NRMAX,1)=1.0/RHOF(NRMAX,1)

EXACT VALUES AT BODY

YC(1,1)=0.0
YC(1,1)=-1.0
RP(1,1)=1.0
VF(1,1)=0.0
RHOF(1,1)=RHOF(NRMAX,1)*(GAMMA+1.0)*2*AM2+2.0/(2.0+GAMMA+AM2-
* (GAMMA-1.0))*1.0/(GAMMA-1.0)
NRSDX(1)=9999.0

DEFINE BOUNDARY ARRAYS FOR IONPAUSE/MAGNETOPAUSE AND SHOCK
DO 2) J=1,NRMAX
VRDD(J)=YC(1,J)
VRDD(J)=VF(1,J)
VCMK(J)=XC(NRMAX,J)
VSHK(J)=YC(NRMAX,J)

2) CONTINUE

RETURN

END

SUBROUTINE FLOUT

THIS ROUTINE PRINTS THE FLOW FIELD VALUES WHICH WILL BE USED
TO CALCULATE THE STREAMLINES AND CONTOURS

COMMON /BLUNT/ THETA(25),RP(20,25),NRBLUNT
COMMON /BOUNDS/ X500(100),Y500(100),X5MK(100),Y5MK(100),
* NRMAX,NRMAX,AMAX,GAMMA,NRN,NHINDX
LEVEL 2, ANG.DTH,DEG
COMMON /DRD/ ANG(20,100),DTH(100),DEG
COMMON /FLOW/ XC(20,100),YC(20,100),VF(20,100),RHOF(20,100)
LEVEL 7, VX,VY
COMMON /VCOMP/ VX(20,100),VY(20,100)
COMMON /DISTRN/ ZPLOT,NZEND,NZADD,NXPLOT

REVERSE SIGN OF XC FOR OUTPUT

EXTRAP 2
EXTRAP 3
EXTRAP 4
EXTRAP 5
EXTRAP 6
EXTRAP 7
EXTRAP 8
ALUNT 2
BOUNDS 2
BOUNDS 3
FLOW 2
SHOCKS 2
EXTRAP 13
EXTRAP 14
EXTRAP 15
EXTRAP 16
EXTRAP 17
EXTRAP 18
EXTRAP 19
EXTRAP 20
EXTRAP 21
EXTRAP 22
EXTRAP 23
EXTRAP 24
EXTRAP 25
EXTRAP 26
EXTRAP 27
EXTRAP 28
EXTRAP 29
EXTRAP 30
EXTRAP 31
EXTRAP 32
EXTRAP 33
EXTRAP 34
EXTRAP 35
EXTRAP 36
EXTRAP 37
EXTRAP 38
EXTRAP 39
EXTRAP 40
EXTRAP 41
EXTRAP 42
EXTRAP 43
EXTRAP 44
EXTRAP 45
EXTRAP 46
EXTRAP 47
EXTRAP 48
EXTRAP 49
EXTRAP 50
EXTRAP 51
EXTRAP 52
EXTRAP 53
EXTRAP 54
EXTRAP 55
EXTRAP 56
EXTRAP 57
EXTRAP 58
EXTRAP 59
EXTRAP 60
EXTRAP 61

FLOUT 2
FLOUT 3
FLOUT 4
FLOUT 5
FLOUT 6
ALUNT 2
BOUNDS 2
BOUNDS 3
DRD 2
DRD 3
FLOW 2
VCOMP 2
VCOMP 3
DISTRN 2
FLOUT 13
FLOUT 14
FLOUT 15

```

JMAX=47*ND+NZADD      FLOWT 16
ND 2 J=1,JMAX         FLOWT 17
ND 2 I=1,NRMAX        FLOWT 18
2 XC(I,J)=XC(I,J)     FLOWT 19
C PRINT VALUES ALONG SYMMETRY AXIS FLOWT 20
C WRITE(6,213)         FLOWT 21
FACT=2.0*(SAXMA-1.0)*AMACH*AMACH FLOWT 22
IF(MIN(X,EQ.1) GO TO 10 FLOWT 23
WRITE(6,223)          FLOWT 24
GO TO 2              FLOWT 25
15 WRITE(6,230)        FLOWT 26
20 CONTINUE          FLOWT 27
ND 33 I=1,NRMAX      FLOWT 28
T=1.0+FACT*(1.0-VF(I,J)**2) FLOWT 29
P=RHOF(I,J)*T        FLOWT 30
WRITE(6,200) I,XC(I,1),VF(I,1),RHOF(I,1),T,P FLOWT 31
70 CONTINUE          FLOWT 32
C PRINT VALUES OVER PLUNT BODY FLOWT 33
C WRITE(6,242)         FLOWT 34
ND 40 J=2,NRLUNT     FLOWT 35
WRITE(6,251) J,THETA(J) FLOWT 36
IF(MIN(X,EQ.1) GO TO 50 FLOWT 37
WRITE(6,262)         FLOWT 38
GO TO 62             FLOWT 39
50 WRITE(6,273)       FLOWT 40
60 CONTINUE          FLOWT 41
ND 40 I=1,NRMAX      FLOWT 42
T=1.0+FACT*(1.0-VF(I,J)**2) FLOWT 43
P=RHOF(I,J)*T        FLOWT 44
ALPHA=DEG*ANG(I,J)  FLOWT 45
WRITE(6,275) T,P,VF(I,J),YC(I,J),XC(I,J),VY(I,J),VX(I,J),ALPHA FLOWT 46
VF(I,J),RHOF(I,J),T,P FLOWT 47
40 CONTINUE          FLOWT 48
C PRINT VALUES FOR MARCHING CODE REGION FLOWT 49
C WRITE(6,282)         FLOWT 50
NVI=NRLUNT+1         FLOWT 51
ND 70 J=1,NRMAX      FLOWT 52
JZ=J-NRLUNT          FLOWT 53
IF(MIN(X,EQ.1) GO TO 80 FLOWT 54
WRITE(6,293) JZ,XC(1,J) FLOWT 55
WRITE(6,311)         FLOWT 56
GO TO 90             FLOWT 57
80 WRITE(6,310) JZ,XC(1,J) FLOWT 58
WRITE(6,323)         FLOWT 59
90 CONTINUE          FLOWT 60
ND 70 I=1,NRMAX      FLOWT 61
T=1.0+FACT*(1.0-VF(I,J)**2) FLOWT 62
P=RHOF(I,J)*T        FLOWT 63
ALPHA=DEG*ANG(I,J)  FLOWT 64
WRITE(6,290) I,YC(I,J),VY(I,J),VX(I,J),ALPHA,VF(I,J),RHOF(I,J),T,P FLOWT 65
70 CONTINUE          FLOWT 66
C RESTORE SIGN OF XC FLOWT 67
ND 3 J=1,JMAX        FLOWT 68
ND 3 I=1,NRMAX        FLOWT 69
3 XC(I,J)=-VF(I,J)   FLOWT 70
RTURN                FLOWT 71
C 203 FORMAT(2X,I3,10(2X,F10.4)) FLOWT 72
213 FORMAT(14I,7X,14F10.4,2X,24(10H)//// FLOWT 73
C 5CM FLOW FIELD VALUES EXTRAPOLATED TO SYMMETRY AXES, FLOWT 74
C 7CM THETA = 3.00 DEGREES FLOWT 75
22 FORMAT(4X,14I,7X,14F10.4,2X,10(4H)RHOINF,5X,6HT/TTINF, FLOWT 76
C 6X,6HP/PIINF) FLOWT 77
233 FORMAT(4X,14I,7X,14F10.4,2X,10(4H)RHOINF,5X,6HT/TTINF, FLOWT 78
C 6X,6HP/PIINF) FLOWT 79
24 FORMAT(14I,41X,43F10.4) FLOWT 80
253 FORMAT(14I,41X,43F10.4) FLOWT 81
C 8H DEGREES FLOWT 82
260 FORMAT(6X,14I,7X,14F10.4,2X,10(4H)RHOINF,5X, FLOWT 83
C 7HVV/VINF,3X,10HFLOW ANGLE,5X,6HV/VINF,3X,10(4H)RHOINF,5X, FLOWT 84
C 6HT/TTINF,6X,6HP/PIINF) FLOWT 85
273 FORMAT(6X,14I,6X,5HP/RC,6X,4HP/RO,6X,4HV/RO,6X,7HVV/VINF,5X, FLOWT 86
C 7HVV/VINF,3X,10HFLOW ANGLE,5X,6HV/VINF,3X,10(4H)RHOINF,5X, FLOWT 87
C 6HT/TTINF,6X,6HP/PIINF) FLOWT 88
283 FORMAT(14I,41X,43F10.4) FLOWT 89
293 FORMAT(14I,41X,43F10.4) FLOWT 90

```

```

303 FORMAT(4X,14I,7X,14F10.4,2X,10(4H)RHOINF,5X,7HVV/VINF,3X, FLOWT 136
C 10HFLOW ANGLE,5X,6HV/VINF,3X,10(4H)RHOINF,5X,6HT/TTINF,6X, FLOWT 137
C 6HP/PIINF) FLOWT 138
313 FORMAT(14I,7X,14F10.4,2X,10(4H)RHOINF,5X,6HT/TTINF,6X, FLOWT 139
C 6HP/PIINF) FLOWT 140
323 FORMAT(4X,14I,7X,14F10.4,2X,10(4H)RHOINF,5X,7HVV/VINF,3X, FLOWT 141
C 10HFLOW ANGLE,5X,6HV/VINF,3X,10(4H)RHOINF,5X,6HT/TTINF,6X, FLOWT 142
C 6HP/PIINF) FLOWT 143
END FLOWT 144

```

SUBROUTINE FLOWST

THIS ROUTINE CALCULATES THE MAGNITUDE AND DIRECTION OF THE VELOCITY. THEN CALCULATES THE TRAJECTORY STREAMLINES

```

COMMON /RLUNT/ THETA(25),PP(2,25),NRLUNT FLOWST 2
COMMON /RHOINF/ XHND(100),YHND(100),VSHK(100),VSHK(100), FLOWST 3
C NRMAX,NRMAX,AMACH,GAMMA,MR,NMINDX FLOWST 4
COMMON /DNSTRM/ ZPLOT,NZADD,NRMAX,NRMAX FLOWST 5
LEVEL 2, ANG,DXTM,DEG FLOWST 6
COMMON /DRD/ ANG(25,100),DXTM(100),DEG FLOWST 7
COMMON /FLOW/ XC(25,100),YC(25,100),VF(25,100),RHOF(25,100) FLOWST 8
LEVEL 2, XST,YST,NUMST,NST FLOWST 9
COMMON /STREAM/ XST(100,100),YST(100,100),NUMST(100),NST FLOWST 10
LEVEL 2, VV,VV FLOWST 11
COMMON /VCOMP/ VV(25,100),VV(25,100) FLOWST 12
DIMENSION W(25),S(25,6),A(5),A(5) FLOWST 13
DATA W(25),S(25,6),A(5),A(5) FLOWST 14

```

CALCULATE VELOCITY AND FLOW ANGLE FROM VELOCITY COMPONENTS

POLAR COORDINATE REGION

```

DEG=57.29577951 FLOWST 15
THETA(1)=0.0 FLOWST 16
NRMAX=NRMAX+NZADD FLOWST 17
ND 10 J=2,NRLUNT FLOWST 18
THETA(J)=THETA(J-1)+DEG FLOWST 19
DXTM(J)=THETA(J)-THETA(J-1) FLOWST 20
ND 1, NRMAX FLOWST 21
VF(1,J)=50+VF(I,J)**2 FLOWST 22
IF (ANG(VX(I,J)) .LT. 1.0E-4) GO TO 5 FLOWST 23
ANG(I,J)=VF(I,J)/VX(I,J) FLOWST 24
GO TO 10 FLOWST 25
5 ANG(I,J)=1.0E-4 FLOWST 26
10 CONTINUE FLOWST 27

```

CYLINDRICAL COORDINATE REGION

```

NVI=NRLUNT+1 FLOWST 28
ND 20 I=1,NRMAX FLOWST 29
VYTH(J)=XC(2,J)-XC(1,J-1) FLOWST 30
ND 20 I=1,NRMAX FLOWST 31
VF(I,J)=50+VF(I,J)**2 FLOWST 32
IF (ANG(VX(I,J)) .LT. 1.0E-4) GO TO 10 FLOWST 33
ANG(I,J)=VF(I,J)/VX(I,J) FLOWST 34
GO TO 20 FLOWST 35
10 ANG(I,J)=1.0E-4 FLOWST 36
20 CONTINUE FLOWST 37

```

SMOOTH RHOINF AND VF ALONG CONSTANT-THETA LINES AT NOSE, USING THIRD DEGREE LEAST SQUARES FIT

```

ND 25 J=2,NRLUNT FLOWST 38
CALL FLSQFV(NRMAX,3,PP(1,J),RHOF(1,J),W,25,5,AR,TER) FLOWST 39
CALL FLSQFV(NRMAX,3,PP(2,J),VF(1,J),W,25,5,AV,TER) FLOWST 40
ND 25 I=1,NRMAX FLOWST 41
VPP=PP(1,J) FLOWST 42
VF(I,J)=((AV(I)*XPP+AV(2))*VPP+AV(3))*VPP+AV(4) FLOWST 43
RHOF(I,J)=((AR(I)*XPP+AR(2))*VPP+AR(3))*VPP+AR(4) FLOWST 44
25 CONTINUE FLOWST 45

```

EXTRAPOLATE FOR VALUES ALONG AXES OF SYMMETRY

```

CALL EXTRAP FLOWST 46
ND 30 I=1,NRMAX FLOWST 47
ANG(I,1)=0.0 FLOWST 48
30 CONTINUE FLOWST 49

```

CCC

11

CC

```

      TF (NR,NE,2) NR = DSQ/RR
      SI(T,6) = RR
      C      THRU 240 - CALCULATIONS FOR NEXT T, SKIP WHEN I=N+1
      C      ALPHA(I+1)=(XP(I),XP(I))/W(I,I)
      TF (I,25,N2) GO TO 240
      SI(T,3)=XKPP/UPP
      UPPD=UPP
      UPP=AL
      RT=SI(T,4)
      AL=SI(T,3)
      C      P(T+1)=(X-ALPHA(I+1))P(I)-BETA(I)P(I-1)
      C      W(T+1,1)=W(P(I+1),P(I+1)), B(I+1)=W(I+1,T+1)/W(I,I)
      C      TEMP=(X(I)-AL)SI(J,2)-RT*SI(J,1)
      UPP=UPP+(J)*TEMP*2
      SI(J,1)=SI(J,2)
      230 SI(J,2)=TEMP
      SI(T+1,4)=UPP/UPPD
      240 CONTINUE
      C      *** COMPUTE COEFFICIENTS OF LEAST SQUARES POLYNOMIAL
      C      A = S(1)P(1),...S(N)P(N)
      C      B(1)=1, P(1)=0, A(1)=S(1), B(2)=S(2)
      C      DO 300 I=1,N-1
      C      A(I)=0
      C      SI(I+1)=P(I)
      C      300 SI(I+2)=0
      C      SI(I+2)=0
      C      A(I)=SI(I,1)
      C      SUM 1000 THRU 310, I = ORDER OF POLYNOMIAL FORMED
      C      DO 310 I=1,N
      C      AL=SI(I,3)
      C      RT=SI(I,4)
      C      T2=0
      C      T1 = T+1
      C      FORM P(I+1)=XP(I)-ALPHA(I+1)P(I)-BETA(I)P(I-1)
      C      AND ADD TO POLYNOMIAL SUM IN A
      C      DO 310 I=1,N
      C      T2=AL*SI(I,2)-RT*SI(I,1)
      C      T2=SI(I,2)
      C      SI(I+1)=SI(I,2)
      C      SI(I+2)=T1
      C      310 A(I+1)=A(I+1)+SI(I+1,1)
      C      T2 = 0
      C      900 RETURN
      C      END

```

```

      FLSPY 96
      FLSPY 97
      FLSPY 98
      FLSPY 99
      FLSPY 91
      FLSPY 92
      FLSPY 93
      FLSPY 94
      FLSPY 95
      FLSPY 96
      FLSPY 97
      FLSPY 98
      FLSPY 99
      FLSPY 100
      FLSPY 101
      FLSPY 102
      FLSPY 103
      FLSPY 104
      FLSPY 105
      FLSPY 106
      FLSPY 107
      FLSPY 108
      FLSPY 109
      FLSPY 110
      FLSPY 111
      FLSPY 112
      FLSPY 113
      FLSPY 114
      FLSPY 115
      FLSPY 116
      FLSPY 117
      FLSPY 118
      FLSPY 119
      FLSPY 120
      FLSPY 121
      FLSPY 122
      FLSPY 123
      FLSPY 124
      FLSPY 125
      FLSPY 126
      FLSPY 127
      FLSPY 128
      FLSPY 129
      FLSPY 130
      FLSPY 131

```

```

      40 IT=I-1
      OI=(P2-R)/(R2-R1)
      WFLAC=O
      RETURN
      C      POINT IS IN RECTANGULAR COORDINATE REGION
      C
      50 CONTINUE
      NXI=NRLUNT+1
      DO 60 J=NXI,NXMAX
      TF (YC(I,J),GT,XP) GO TO 70
      60 CONTINUE
      J=NXTAT
      70 JT=J-1
      OJ=(YC(I,JT+1)-YP)/DXT4(JT)
      YZ=YC(I,JT)+OJ*YC(I,JT+1)*(1,J-OJ)
      TF (YP,LT, YZ) GO TO 100
      DO 80 I=2,NXMAX
      Y1=YZ
      Y2=YC(I,JT)+OJ*YC(I,JT+1)*(1,J-OJ)
      TF (Y2,GT, Y1) GO TO 90
      90 CONTINUE
      GO TO 100
      90 IT=I-1
      OI=(Y2-Y1)/(Y2-Y1)
      WFLAC=1
      RETURN
      C      POINT IS INSIDE IONPAUSE
      C
      100 CONTINUE
      WFLAC=1
      RETURN
      C      POINT IS BEYOND BOW SHOCK
      C
      150 CONTINUE
      WFLAC=1
      RETURN
      C      END

```

```

      IJTRAJ 33
      IJTRAJ 34
      IJTRAJ 35
      IJTRAJ 36
      IJTRAJ 37
      IJTRAJ 38
      IJTRAJ 39
      IJTRAJ 40
      IJTRAJ 41
      IJTRAJ 42
      IJTRAJ 43
      IJTRAJ 44
      IJTRAJ 45
      IJTRAJ 46
      IJTRAJ 47
      IJTRAJ 48
      IJTRAJ 49
      IJTRAJ 50
      IJTRAJ 51
      IJTRAJ 52
      IJTRAJ 53
      IJTRAJ 54
      IJTRAJ 55
      IJTRAJ 56
      IJTRAJ 57
      IJTRAJ 58
      IJTRAJ 59
      IJTRAJ 60
      IJTRAJ 61
      IJTRAJ 62
      IJTRAJ 63
      IJTRAJ 64
      IJTRAJ 65
      IJTRAJ 66
      IJTRAJ 67
      IJTRAJ 68
      IJTRAJ 69
      IJTRAJ 70
      IJTRAJ 71
      IJTRAJ 72
      IJTRAJ 73

```

```

      SUBROUTINE IJTRAJ(XP,YP,IT,JT,OT,OJ,WFLAC)
      C      THIS SUBROUTINE LOCATES A TRAJECTORY POINT IN
      C      THE COMPUTATIONAL GRID
      C      IT,JT IS LOWER LEFT CORNER OF GRID SECTION CONTAINING (XP,YP)
      C
      COMMON /ALUNT/ THETA(25),PP(2,25),NRLUNT
      COMMON /RUMUND/ XADD(100),YADD(100),YCHK(100),YSHK(100),
      C      NMAX,NMAX,ANACH,GAMMA,MRO,MHINDEX
      C      LEVEL,2,ANG,DXT4,DEG
      COMMON /ORD/ ANG(2,100),DXT4(100),PER
      COMMON /FLTM/ XC(2,100),YC(2,100),VF(2,100),RMHF(20,100)
      C
      C      POINT IS IN POLAR COORDINATE REGION
      C
      TF (YP,GE,0.0) GO TO 50
      THA=ATAN2(YP,-Y1)*DEG
      W=SQRT(YP**2+XPP**2)
      DO 10 I=2,NRLUNT
      TF (THETA(I),GT,THA) GO TO 20
      10 CONTINUE
      J=NRLUNT
      20 JT=J-1
      OJ=(THETA(I)-THA)/DXT4(JT)
      YZ=PP(I,JT)+OJ*PP(I,JT+1)*(1,J-OJ)
      TF (P,LT,P2) GO TO 100
      DO 30 I=2,NRMAX
      Y1=YZ
      Y2=PP(I,JT)+OJ*PP(I,JT+1)*(1,J-OJ)
      TF (P2,GT, P1) GO TO 40
      30 CONTINUE
      GO TO 100

```

```

      IJTRAJ 2
      IJTRAJ 3
      IJTRAJ 4
      IJTRAJ 5
      IJTRAJ 6
      IJTRAJ 7
      IJTRAJ 8
      IJTRAJ 9
      IJTRAJ 10
      IJTRAJ 11
      IJTRAJ 12
      IJTRAJ 13
      IJTRAJ 14
      IJTRAJ 15
      IJTRAJ 16
      IJTRAJ 17
      IJTRAJ 18
      IJTRAJ 19
      IJTRAJ 20
      IJTRAJ 21
      IJTRAJ 22
      IJTRAJ 23
      IJTRAJ 24
      IJTRAJ 25
      IJTRAJ 26
      IJTRAJ 27
      IJTRAJ 28
      IJTRAJ 29
      IJTRAJ 30
      IJTRAJ 31
      IJTRAJ 32

```

```

      SUBROUTINE INPUT
      C      THIS ROUTINE READS ALL DATA REQUIRED FOR ONE CASE,
      C      EXCEPT FLOW FIELD DATA FOR REMUM
      C
      COMMON /RTM/ ANGP,ANGM,KKCON,RCON(20)
      COMMON /CMI/ JMAX,KMAX,JH,KH,XHAC,ALPHA,GAM,GMHI,CH,DT,SMI,IPRT,
      C      PHOPI,NCI,NCI,NCI,AA,M,OMEGA,MU,ML,IT,TAU,ITEP,ENT,PTORT,PIHF,
      C      PHF,OTAF,PIHF,JCI,TH,CLUS,PT,MORN,PHNSE,NCASE,NPUNCH
      COMMON /CDNT/ KVCOM,VCON(20),KPCOM,RCOM(2)
      COMMON /ALUNT/ THETA(25),PP(2,25),NRLUNT
      COMMON /ONSTRM/ ZPLDT,MZEND,MZADD,NXPLDT
      COMMON /JOE/ZL1,CF1,CF2,ZLF,ZTRAN,DZTRAN
      C      LOGICAL LGRAV
      COMMON /MURAD/ XX(100),YY(100),NEOD,LGRAV
      COMMON /RUMUND/ XADD(100),YADD(100),YCHK(100),YSHK(100),
      C      NMAX,NMAX,ANACH,GAMMA,MRO,MHINDEX
      C      LOGICAL LREUM,LPRFL,LPRST,LPRON,LPRP,LPLNT,LTRAJ,LRSTRT
      COMMON /PROPT/ LREUM,LPRFL,LPRST,LPRON,LPRP,LPLNT,LTRAJ,LRSTRT
      C      COMMON /TRJDAT/ NTRAJ,ITRAJ(100),YTRAJ(100),YTRAJ(100),ZTRAJ(100),
      C      YTRAJ(100),YTRAJ(100),YTRAJ(100),YTRAJ(100),YTRAJ(100),
      C      YTRAJ(100)
      COMMON /MKPLOT/ MKAPKT,MARKT(12)
      C      LOGICAL LPLTRJ
      COMMON /JTRPT/ LPLTRJ,LPLMT,VINF,RMFINF,THPINF,OTINF
      C      LOGICAL LSUM
      COMMON /SUMDAT/ LSUM,XTRAJS(100),YTRAJS(100),ZTRAJS(100),
      C      YTRAJS(100),AZANG,POLANG,RV1,RV1,RZ1
      C      DIMENSION TITLE(8)
      C      DIMENSION NK(100)
      C      DIMENSION RR(100)
      C      EQUIVALENCE (RR(1),YY(1))
      C      DATA WFLAC/14 /,MSTAR/140/
      C
      C      READ CARD INPUT FOR ONE COMPLETE CALCULATION
      C
      READ(5,100) TITLE

```

```

      INPUT 2
      INPUT 3
      INPUT 4
      INPUT 5
      INPUT 6
      RTM 7
      CMI 8
      PHOPI 9
      PHF 10
      PHF 11
      CDNT 12
      ALUNT 13
      ONSTRM 14
      JOE 15
      MURAD 16
      RUMUND 17
      RUMUND 18
      LOGICAL 19
      PROPT 20
      TRJDAT 21
      TRJDAT 22
      TRJDAT 23
      TRJDAT 24
      TRJDAT 25
      TRJDAT 26
      TRJDAT 27
      TRJDAT 28
      TRJDAT 29
      TRJDAT 30
      TRJDAT 31
      TRJDAT 32
      TRJDAT 33
      TRJDAT 34
      TRJDAT 35
      TRJDAT 36
      TRJDAT 37
      TRJDAT 38
      TRJDAT 39
      TRJDAT 40
      TRJDAT 41
      TRJDAT 42
      TRJDAT 43
      TRJDAT 44
      TRJDAT 45
      TRJDAT 46
      TRJDAT 47
      TRJDAT 48
      TRJDAT 49
      TRJDAT 50
      TRJDAT 51
      TRJDAT 52
      TRJDAT 53
      TRJDAT 54
      TRJDAT 55
      TRJDAT 56
      TRJDAT 57
      TRJDAT 58
      TRJDAT 59
      TRJDAT 60
      TRJDAT 61
      TRJDAT 62
      TRJDAT 63
      TRJDAT 64
      TRJDAT 65
      TRJDAT 66
      TRJDAT 67
      TRJDAT 68
      TRJDAT 69
      TRJDAT 70
      TRJDAT 71
      TRJDAT 72
      TRJDAT 73

```

```

READ(5,110) ANACH,GAPMA,HRO,XCALC,NR,NRLUNT,CN,ITER
NMPN=NRN
READ(5,120) LRERUN,LPRFL,LPRST,LPRCON,LPRP,LPLNT,LTRAJ,LPRSTRT
READ(5,130) XPLNT,ANGP,ANGM,NKADD,LGRAV
IF (LPLNT) LPRCON=.TRUE.
IF (LPLNT) GE. G.0) XPLNT=-1.)
XPLNT=XPLNT
READ(5,140) KVCOM
IF (KVCOM.GT. 0) READ(5,160) (VCON(I),I=1,KVCOM)
READ(5,141) KRCON
IF (KRCON.GT. 0) READ(5,160) (RCON(I),I=1,KRCON)
READ(5,143) KRCON
IF (KRCON.GT. 0) READ(5,160) (RCON(I),I=1,KRCON)
IF (LMPN) LTRAJ GO TO 5
READ(5,170) NTRAJ,ITRAJ(I),XTRAJ(I),YTRAJ(I),ZTRAJ(I),T=1,NTRAJ)
READ(5,190) NTRAJ,NPLNT,VINF,RHINF,TINF,ATNF
READ(5,143) NMARKT
IF (NMARKT.GT. 0) READ(5,190) (MARKT(I),I=1,NMARKT)
READ(5,190) LSIN,ASANG,POLANG,RYL,RYI,RYJ
IF (LSIN) CALL ROTAT(1)
5 CONTINUE
NMPN=NMPN
IF (NMPN.GT. 0.0) NINDEX=1
IF (NINDEX) GO TO 10
IF (NMPN.LT. 0.0) READ(5,130) NADD,(XX(I),YY(I),I=1,NADD)
INITIALIZE DEFAULT PARAMETERS
IF (XCALC.GE. C.0) XCALC=-1.0
XCALC=XCALC
IF (NMPN.LE. 0) NR=10
IF (NRLUNT.LE. 0) NRLUNT=24
IF (CN.LE. 0) CN=3.0
IF (ITER.LE. 0) ITER=300
IF (NKADD.LE. 0) NKADD=0
JMAX=NRLUNT+NKADD+1
NMARKT=JMAX-1
NMPN=NR
NMPN=JMAX-1
NTRAJ=N
NMPN=ANACH
CAN=GAPMA
WRITE OUT INPUT AND DEFAULT VALUES TO BE USED
10 CONTINUE
WRITE(6,200) TITLE
IF (LGRAV) RETURN
WRITE(6,210) ANACH,GAPMA
WRITE(6,220) NRLUNT,NR,ANACH,GAPMA,ANGP
IF (NMPN) 14,16,18
14 WRITE(6,214) NADD,(XX(I),YY(I),I=1,NADD)
WRITE(6,214) NADD,(XX(I),YY(I),I=1,NADD)
GO TO 2
16 WRITE(6,216)
GO TO 20
18 IF (LGRAV) GO TO 10
WRITE(6,218) HCRN
GO TO 20
20 WRITE(6,219) NMPN
21 CONTINUE
WRITE(6,223) NR,NRLUNT,NKADD,CN,ITER,XCALC
WRITE(6,230) XPLNT
IF (LSIN) GO TO 17
WRITE(6,231) ANGP,ANGM
17 CONTINUE
WRITE(6,235) LRERUN,LPRFL,LPRST,LPRCON,LPRP,LPLNT,LTRAJ,LPRSTRT
IF (LMPN) LTRAJ GO TO 23
NCRP=1,NRPLNT
WRITE(6,260) LPLNT,NCRP,VINF,RHINF,TINF
IF (LSIN) WRITE(6,260) RINF,RYI,RYJ,ASANG,POLANG
WRITE(6,263) NTRAJ,NMARKT
GO TO 21 N=1,NTRAJ
21 N=N+1,NMARKT
IF (NMARKT.LE. 0) GO TO 24
GO TO 21 N=1,NMARKT
22 N=N+1,NMARKT
23 CONTINUE
WRITE(6,268)
WRITE(6,267) (N,NK(N),XTRAJ(N),YTRAJ(N),ZTRAJ(N),T=1,NTRAJ)
25 CONTINUE

```

```

WRITE(6,240)
WRITE(6,242) KVCOM
IF (KVCOM.GT. 0) WRITE(6,250) (VCON(I),I=1,KVCOM)
WRITE(6,244) KRCON
IF (KRCON.GT. 0) WRITE(6,250) (RCON(I),I=1,KRCON)
WRITE(6,246) KRCON
IF (KRCON.GT. 0) WRITE(6,250) (RCON(I),I=1,KRCON)
NCON=.01745329232
ANGP=ANGP+DTR
ANGM=ANGM+DTR
RETURN
C
100 FORMAT(A10)
110 FORMAT(F10.0,2E11.7,F10.0,11C)
120 FORMAT(41C)
130 FORMAT(3F10.0,11C,11C)
140 FORMAT(11C)
150 FORMAT(11,12F10.0)
160 FORMAT(F10.0)
170 FORMAT(11,12F10.0)
180 FORMAT(11C)
190 FORMAT(11,12F10.0)
200 FORMAT(11,12F10.0)
210 FORMAT(11,12F10.0)
220 FORMAT(11,12F10.0)
230 FORMAT(11,12F10.0)
240 FORMAT(11,12F10.0)
250 FORMAT(11,12F10.0)
260 FORMAT(11,12F10.0)
270 FORMAT(11,12F10.0)
280 FORMAT(11,12F10.0)
290 FORMAT(11,12F10.0)
300 FORMAT(11,12F10.0)
310 FORMAT(11,12F10.0)
320 FORMAT(11,12F10.0)
330 FORMAT(11,12F10.0)
340 FORMAT(11,12F10.0)
350 FORMAT(11,12F10.0)
360 FORMAT(11,12F10.0)
370 FORMAT(11,12F10.0)
380 FORMAT(11,12F10.0)
390 FORMAT(11,12F10.0)
400 FORMAT(11,12F10.0)
410 FORMAT(11,12F10.0)
420 FORMAT(11,12F10.0)
430 FORMAT(11,12F10.0)
440 FORMAT(11,12F10.0)
450 FORMAT(11,12F10.0)
460 FORMAT(11,12F10.0)
470 FORMAT(11,12F10.0)
480 FORMAT(11,12F10.0)
490 FORMAT(11,12F10.0)
500 FORMAT(11,12F10.0)
510 FORMAT(11,12F10.0)
520 FORMAT(11,12F10.0)
530 FORMAT(11,12F10.0)
540 FORMAT(11,12F10.0)
550 FORMAT(11,12F10.0)
560 FORMAT(11,12F10.0)
570 FORMAT(11,12F10.0)
580 FORMAT(11,12F10.0)
590 FORMAT(11,12F10.0)
600 FORMAT(11,12F10.0)
610 FORMAT(11,12F10.0)
620 FORMAT(11,12F10.0)
630 FORMAT(11,12F10.0)
640 FORMAT(11,12F10.0)
650 FORMAT(11,12F10.0)
660 FORMAT(11,12F10.0)
670 FORMAT(11,12F10.0)
680 FORMAT(11,12F10.0)
690 FORMAT(11,12F10.0)
700 FORMAT(11,12F10.0)
710 FORMAT(11,12F10.0)
720 FORMAT(11,12F10.0)
730 FORMAT(11,12F10.0)
740 FORMAT(11,12F10.0)
750 FORMAT(11,12F10.0)
760 FORMAT(11,12F10.0)
770 FORMAT(11,12F10.0)
780 FORMAT(11,12F10.0)
790 FORMAT(11,12F10.0)
800 FORMAT(11,12F10.0)
810 FORMAT(11,12F10.0)
820 FORMAT(11,12F10.0)
830 FORMAT(11,12F10.0)
840 FORMAT(11,12F10.0)
850 FORMAT(11,12F10.0)
860 FORMAT(11,12F10.0)
870 FORMAT(11,12F10.0)
880 FORMAT(11,12F10.0)
890 FORMAT(11,12F10.0)
900 FORMAT(11,12F10.0)
910 FORMAT(11,12F10.0)
920 FORMAT(11,12F10.0)
930 FORMAT(11,12F10.0)
940 FORMAT(11,12F10.0)
950 FORMAT(11,12F10.0)
960 FORMAT(11,12F10.0)
970 FORMAT(11,12F10.0)
980 FORMAT(11,12F10.0)
990 FORMAT(11,12F10.0)
1000 FORMAT(11,12F10.0)
1010 FORMAT(11,12F10.0)
1020 FORMAT(11,12F10.0)
1030 FORMAT(11,12F10.0)
1040 FORMAT(11,12F10.0)
1050 FORMAT(11,12F10.0)
1060 FORMAT(11,12F10.0)
1070 FORMAT(11,12F10.0)
1080 FORMAT(11,12F10.0)
1090 FORMAT(11,12F10.0)
1100 FORMAT(11,12F10.0)
1110 FORMAT(11,12F10.0)
1120 FORMAT(11,12F10.0)
1130 FORMAT(11,12F10.0)
1140 FORMAT(11,12F10.0)
1150 FORMAT(11,12F10.0)
1160 FORMAT(11,12F10.0)
1170 FORMAT(11,12F10.0)
1180 FORMAT(11,12F10.0)
1190 FORMAT(11,12F10.0)
1200 FORMAT(11,12F10.0)
1210 FORMAT(11,12F10.0)
1220 FORMAT(11,12F10.0)
1230 FORMAT(11,12F10.0)
1240 FORMAT(11,12F10.0)
1250 FORMAT(11,12F10.0)
1260 FORMAT(11,12F10.0)
1270 FORMAT(11,12F10.0)
1280 FORMAT(11,12F10.0)
1290 FORMAT(11,12F10.0)
1300 FORMAT(11,12F10.0)
1310 FORMAT(11,12F10.0)
1320 FORMAT(11,12F10.0)
1330 FORMAT(11,12F10.0)
1340 FORMAT(11,12F10.0)
1350 FORMAT(11,12F10.0)
1360 FORMAT(11,12F10.0)
1370 FORMAT(11,12F10.0)
1380 FORMAT(11,12F10.0)
1390 FORMAT(11,12F10.0)
1400 FORMAT(11,12F10.0)
1410 FORMAT(11,12F10.0)
1420 FORMAT(11,12F10.0)
1430 FORMAT(11,12F10.0)
1440 FORMAT(11,12F10.0)
1450 FORMAT(11,12F10.0)
1460 FORMAT(11,12F10.0)
1470 FORMAT(11,12F10.0)
1480 FORMAT(11,12F10.0)
1490 FORMAT(11,12F10.0)
1500 FORMAT(11,12F10.0)
1510 FORMAT(11,12F10.0)
1520 FORMAT(11,12F10.0)
1530 FORMAT(11,12F10.0)
1540 FORMAT(11,12F10.0)
1550 FORMAT(11,12F10.0)
1560 FORMAT(11,12F10.0)
1570 FORMAT(11,12F10.0)
1580 FORMAT(11,12F10.0)
1590 FORMAT(11,12F10.0)
1600 FORMAT(11,12F10.0)
1610 FORMAT(11,12F10.0)
1620 FORMAT(11,12F10.0)
1630 FORMAT(11,12F10.0)
1640 FORMAT(11,12F10.0)
1650 FORMAT(11,12F10.0)
1660 FORMAT(11,12F10.0)
1670 FORMAT(11,12F10.0)
1680 FORMAT(11,12F10.0)
1690 FORMAT(11,12F10.0)
1700 FORMAT(11,12F10.0)
1710 FORMAT(11,12F10.0)
1720 FORMAT(11,12F10.0)
1730 FORMAT(11,12F10.0)
1740 FORMAT(11,12F10.0)
1750 FORMAT(11,12F10.0)
1760 FORMAT(11,12F10.0)
1770 FORMAT(11,12F10.0)
1780 FORMAT(11,12F10.0)
1790 FORMAT(11,12F10.0)
1800 FORMAT(11,12F10.0)
1810 FORMAT(11,12F10.0)
1820 FORMAT(11,12F10.0)
1830 FORMAT(11,12F10.0)
1840 FORMAT(11,12F10.0)
1850 FORMAT(11,12F10.0)
1860 FORMAT(11,12F10.0)
1870 FORMAT(11,12F10.0)
1880 FORMAT(11,12F10.0)
1890 FORMAT(11,12F10.0)
1900 FORMAT(11,12F10.0)
1910 FORMAT(11,12F10.0)
1920 FORMAT(11,12F10.0)
1930 FORMAT(11,12F10.0)
1940 FORMAT(11,12F10.0)
1950 FORMAT(11,12F10.0)
1960 FORMAT(11,12F10.0)
1970 FORMAT(11,12F10.0)
1980 FORMAT(11,12F10.0)
1990 FORMAT(11,12F10.0)
2000 FORMAT(11,12F10.0)

```

```

SUBROUTINE LABEL
THIS ROUTINE ELIMINATES OVERLAP IN PLOTTING A
SET OF CONTOUR LABELS.
COMMON /LABLE/ YL4(30),YL4(30),CV(30),NCL,TL4(30),ML4
COMMON /SCALE/ XSF,YSF,XMAX,YMAX,XLENGTH,YLENGTH
SORT THE ARRAY YL4 INTO ASCENDING ORDER. CHANGE
THE ORDER OF XL4 AND CV TO CORRESPOND.
CALL MURK(XL4,YL4,CV,NCL,TL4,ML4)
FIND FIRST LABEL FROM SORTED ARRAY THAT IS ABOVE X-AXIS.
DO 5 K=1,NCL
  IF(YL4(K).LT.0.) GO TO 5
  KMIN=K
  GO TO 10
5 CONTINUE
NO LABELS FOUND ABOVE X-AXIS. NO SET OF CONTOUR VALUES
SPECIFIED. STOP PROGRAM.
WRITE(6,Z10)
2) J. FORMATE (141,10)*****1)X,48)MURKLE TO LABEL CONTOUR LINES REC
10)IF OF OVERLAP,10)1C*****
STOP
1) TL4(1)=KMIN
NCL=1
IF(NCL.EQ.1) RETURN
EXAMINE ALL LABELS BEYOND LABEL KMIN FOR OVERLAP.
K=2
KMINP=KMIN+1
DO 15 I=KMINP,NCL
  IF(YL4(I).LT.YL4(KMIN)+.1/YSF.AND.XL4(I).LT.XL4(KMIN))
    1 0.4/YSF) GO TO 15
SAVE ARRAY INDEK FOR LABEL TO BE PLOTTED.
KMINP=I
JL4(K)=I
NCL=NCL-1
K=K+1
15 CONTINUE
INSURE THAT THE LAST LABEL IS PLOTTED.
JL4(NCL)=NCL
RETURN
END

```

```

LABEL 2
LABEL 3
LABEL 4
LABEL 5
LABEL 6
LABEL 7
LABEL 8
LABEL 9
LABEL 10
LABEL 11
LABEL 12
LABEL 13
LABEL 14
LABEL 15
LABEL 16
LABEL 17
LABEL 18
LABEL 19
LABEL 20
LABEL 21
LABEL 22
LABEL 23
LABEL 24
LABEL 25
LABEL 26
LABEL 27
LABEL 28
LABEL 29
LABEL 30
LABEL 31
LABEL 32
LABEL 33
LABEL 34
LABEL 35
LABEL 36
LABEL 37
LABEL 38
LABEL 39
LABEL 40
LABEL 41
LABEL 42
LABEL 43
LABEL 44
LABEL 45
LABEL 46
LABEL 47
LABEL 48
LABEL 49
LABEL 50
LABEL 51
LABEL 52
LABEL 53
LABEL 54
LABEL 55
LABEL 56
LABEL 57
LABEL 58

```

```

ACONT ARRAY OF CONTOUR LEVELS. SCRATCH IF KOD=1.
IF KOD=2, ACONT MUST BE FILLED WITH MONOTONICALLY
INCREASING CONTOUR LEVELS. SHOULD BE DIMENSIONED
AT LEAST MLIN.
NAD IT SHOULD BE RECOGNIZED THAT MANY CONTOUR LINES
MIGHT RESULT FROM EACH CONTOUR LEVEL.
UPON RETURN, NAD(1) IS THE TOTAL NUMBER OF CONTOUR
LINES. ALL THE LINES ARE RUN-TOGETHER, HEAD TO TAIL
IN ARRAYS X AND Y. THE FIRST LINE STARTS AT X(1)
AND Y(1) AND ENDS AT X(1) AND Y(1) FOR I=NAD(2)-1.
THE N-TH CONTOUR LINE STARTS AT X(1) AND Y(1) FOR
I=NAD(1) AND ENDS AT X(1) AND Y(1) FOR I=NAD(1)+1.
NAD(1) FOR N=2 IS THE STARTING ADDRESS IN X AND Y
OF THE N-TH CONTOUR LINE.
ISIZ1 DIMENSION SIZE OF X AND Y.
ISIZ2 DIMENSION SIZE OF NAD. IT IS DIFFICULT TO SAY
HOW LARGE X, Y, AND NAD SHOULD BE DIMENSIONED.
THIS DEPENDS ON THE DIMENSION SIZE OF ARRAY A,
THE VALUE OF MLIN, AND THE DEGREE OF ECCENTRICITY
OF THE SURFACE REPRESENTED BY ARRAY A. ERROR MESSAGES
WILL RESULT IF THESE ARRAYS ARE TOO SMALL.
ICM AN ARRAY TO BE USED AS SCRATCH BY THE CONTOUR PROGRAMS.
IT SHOULD HAVE AT LEAST 4*ISIZ1 CELLS.
JMIN,KMIN,JMAX,KMAX IT IS RECOGNIZED THAT ONE MIGHT
WISH TO CONTOUR PLOT AN ARRAY A FOR SUBSCRIPTS
STARTING AT SOME VALUE LARGER THAN 1. THIS SUBROUTINE
WILL PROCESS ARRAY A(J,K) FOR JMIN,LE,J,LE,JMAX,
AND KMIN,LE,K,LE,KMAX. JMIN, KMIN, JMAX, AND KMAX
ARE THE LIMITS ON THE SUBSCRIPTS. JMIN AND KMIN MAY
BE 1.
DIMENSION A(1),X(1),Y(1),ACONT(1),NAD(1),ICM(4,1)
INDEX(J,K)=J+(K-1)*JMIN
FIND JMAX AND JMIN
I=INDEX(JMIN,KMIN)
AMAX=AT(I)
AMIN=AMAX
DO 1 K=KMIN,KMAX
  DO 1 J=JMIN,JMAX
    I=INDEX(J,K)
    YL=AT(I)
    IF(YL-AMAX)2,1,3
    AMAX=YL
    GO TO 2
    IF(YL-AMIN)4,1,1
    AMIN=YL
    CONTINUE
FIND ACONT BY LINEARLY INTERPOLATING
GO TO (5,6),KOD
IF(AMAX-AMIN)/FLOAT(MLIN+1)
DO 7 M=1,MLIN
  ACONT(M)=AMIN+FLOAT(M)*DIF
  NAD(M)=1
  NMAX=NCLM
  GO TO 8
CHECK ACONT IF GIVEN BY USER
NAD=NAD+1
IF(NAD(1).GT.MLIN) GO TO 9
IF(AMIN.GT.ACONT(NAD)) GO TO 10
NMAX=MLIN+1
NAD=NMAX-1
IF(NMAX.LT.1) GO TO 9
IF(AMAX.LT.ACONT(NMAX)) GO TO 11
IF(NAD(1).GT.NMAX) GO TO 9
IF (NMIN.EQ.NMAX) GO TO 12
NAD=NAD+1
DO 13 N=NAD,NMAX
  IF(ACONT(N).LE.ACONT(N-1)) GO TO 9
CONTINUE
12 CONTINUE
PART 11 GO AROUND THE BOUNDARY LOOKING FOR LINES WHICH
INTERSECT THE BOUNDARY.
NAD(1)=0
J=JMIN
K=KMIN

```

```

NAD 24
NAD 25
NAD 26
NAD 27
NAD 28
NAD 29
NAD 30
NAD 31
NAD 32
NAD 33
NAD 34
NAD 35
NAD 36
NAD 37
NAD 38
NAD 39
NAD 40
NAD 41
NAD 42
NAD 43
NAD 44
NAD 45
NAD 46
NAD 47
NAD 48
NAD 49
NAD 50
NAD 51
NAD 52
NAD 53
NAD 54
NAD 55
NAD 56
NAD 57
NAD 58
NAD 59
NAD 60
NAD 61
NAD 62
NAD 63
NAD 64
NAD 65
NAD 66
NAD 67
NAD 68
NAD 69
NAD 70
NAD 71
NAD 72
NAD 73
NAD 74
NAD 75
NAD 76
NAD 77
NAD 78
NAD 79
NAD 80
NAD 81
NAD 82
NAD 83
NAD 84
NAD 85
NAD 86
NAD 87
NAD 88
NAD 89
NAD 90
NAD 91
NAD 92
NAD 93
NAD 94
NAD 95
NAD 96
NAD 97
NAD 98
NAD 99
NAD 100
NAD 101
NAD 102
NAD 103
NAD 104
NAD 105
NAD 106
NAD 107

```

```

SUBROUTINE MAP (A,JMIN,X,Y,MLIN,KOD,ACONT,NAD,ISIZ1,ISIZ2,ICM,
JMIN,KMIN,JMAX,KMAX)
CONTOUR PROGRAMS MAP, WALK, SEARCH, ENTER, AND CHECK
WRITTEN BY PEESE SOFPMSON, NASA-GMES PPS, CTR., AUG., 1974.
(MODIFIED VERSION)
THIS SUBROUTINE AND THOSE WHICH IT CALLS PREPARE DATA
FOR CONTOUR PLOTTING.
CALLING PARAMETERS:
A TWO-DIMENSIONAL ARRAY TO BE CONTOUR PLOTTED.
JMIN FIRST-POSITION DIMENSION-SIZE OF A.
X,Y ARRAYS TO CONTAIN CONTOUR LINE DATA UPON RETURN.
EACH PAIR OF X(I) AND Y(I) REPRESENTS A POINT ON A
CONTOUR LINE.
MLIN IS THE NUMBER OF CONSTANT-A CONTOUR LEVELS.
KOD =1 IF CONTOUR LEVELS ARE TO BE COMPUTED INTERNALLY
BY LINEARLY INTERPOLATING BETWEEN THE MAXIMUM AND
MINIMUM VALUES OF A.
=2 IF CONTOUR LEVELS ARE TO BE GIVEN BY THE USER.

```

```

MAP 2
MAP 3
MAP 4
MAP 5
MAP 6
MAP 7
MAP 8
MAP 9
MAP 10
MAP 11
MAP 12
MAP 13
MAP 14
MAP 15
MAP 16
MAP 17
MAP 18
MAP 19
MAP 20
MAP 21
MAP 22
MAP 23

```

```

C 6
C 7
C 8
C 9
C 10
C 11
C 12
C 13
C 14
C 15
C 16
C 17
C 18
C 19
C 20
C 21
C 22
C 23
C 24
C 25
C 26
C 27
C 28
C 29
C 30
C 31
C 32
C 33
C 34
C 35
C 36
C 37
C 38
C 39
C 40
C 41
C 42
C 43
C 44
C 45
C 46
C 47
C 48
C 49
C 50
C 51
C 52
C 53
C 54
C 55
C 56
C 57
C 58
C 59
C 60
C 61
C 62
C 63
C 64
C 65
C 66
C 67
C 68
C 69
C 70
C 71
C 72
C 73
C 74
C 75
C 76
C 77
C 78
C 79
C 80
C 81
C 82
C 83
C 84
C 85
C 86
C 87
C 88
C 89
C 90
C 91
C 92
C 93
C 94
C 95
C 96
C 97
C 98
C 99
C 100
C 101
C 102
C 103
C 104
C 105
C 106
C 107
C 108
C 109
C 110
C 111
C 112
C 113
C 114
C 115
C 116
C 117
C 118
C 119
C 120

```


	NINT=2*(JMAX-JMIN)+2*(KMAX-KMIN)	MAP	100	YFINDJH.GT.TSIZ2) GO TO 35	MAP	192
	KOD7=2	MAP	101	NAD(1)=NDUM	MAP	193
	KOD2=1	MAP	110	CALL ENTERKOD2,J,K,NVAL,A1,A2,JMIN,KMIN,ICM,KOD4,X,Y,NXY,ACONT,	MAP	194
	I=IDEX(JMIN,KMIN)	MAP	111	TSIZ1)	MAP	195
	AI=A(I)	MAP	112	IF(KOD4.EQ.2) GO TO 70	MAP	196
	NXY=C	MAP	113	NAD(MJMIN)=NXY	MAP	197
C	DO 25 N=1,NINT	MAP	114		MAP	198
	GO TO (71,22,23,24),KOD7	MAP	115		MAP	199
C		MAP	116		MAP	200
	ORIENTATION 1: UPWARDS	MAP	117		MAP	201
21	J=J-1	MAP	118		MAP	202
	I=IDEX(J,K)	MAP	119		MAP	203
	IF(J.GT.JMIN) GO TO 25	MAP	120		MAP	204
	J=JMIN	MAP	121		MAP	205
	I=IDEX(J,K+1)	MAP	122		MAP	206
	KOD7=2	MAP	123		MAP	207
	KOD2=1	MAP	124		MAP	208
	GO TO 25	MAP	125		MAP	209
C		MAP	126		MAP	210
	ORIENTATION 2: TO THE RIGHT	MAP	127		MAP	211
22	K=K+1	MAP	128		MAP	212
	I=IDEX(J,K+1)	MAP	129		MAP	213
	IF(K.LT.KMAX) GO TO 25	MAP	130		MAP	214
	I=IDEX(J+1,K)	MAP	131		MAP	215
	KOD7=1	MAP	132		MAP	216
	KOD2=2	MAP	133		MAP	217
	GO TO 25	MAP	134		MAP	218
C		MAP	135		MAP	219
	ORIENTATION 3: DOWNWARD	MAP	136		MAP	220
23	J=J+1	MAP	137		MAP	221
	I=IDEX(J+1,K)	MAP	138		MAP	222
	IF(J.LT.JMAX) GO TO 25	MAP	139		MAP	223
	K=KMAX-1	MAP	140		MAP	224
	I=IDEX(J,K)	MAP	141		MAP	225
	KOD7=4	MAP	142		MAP	226
	KOD2=1	MAP	143		MAP	227
	GO TO 25	MAP	144		MAP	228
C		MAP	145		MAP	229
	ORIENTATION 4: TO THE LEFT	MAP	146		MAP	230
24	K=K-1	MAP	147		MAP	231
	I=IDEX(J,K)	MAP	148		MAP	232
	IF(K.GT.KMIN) GO TO 25	MAP	149		MAP	233
	K=KMIN	MAP	150		MAP	234
	J=JMAX-1	MAP	151		MAP	235
	I=IDEX(J,K)	MAP	152		MAP	236
	KOD7=1	MAP	153		MAP	237
	KOD2=2	MAP	154		MAP	238
C		MAP	155		MAP	239
	FIND A4 AND A1	MAP	156		MAP	240
25	A4=A4	MAP	157		MAP	241
	AI=A(I)	MAP	158		MAP	242
	IF(A4-A1).GE.26.77	MAP	159		MAP	243
26	A4=A4	MAP	160		MAP	244
	AI=AI	MAP	161		MAP	245
	GO TO 24	MAP	162		MAP	246
27	AI=AI	MAP	163		MAP	247
	AI=AI	MAP	164		MAP	248
C		MAP	165		MAP	249
	CHECK TO SEE IF A CONTOUR LINE PASSES THROUGH THE INTERVAL	MAP	166		MAP	250
C	UNDER CONSIDERATION.	MAP	167		MAP	251
28	KOD8=1	MAP	168		MAP	252
	DO 29 NVAL=MIN,MNAX	MAP	169		MAP	253
	VAL=ACONT(NVAL)	MAP	170		MAP	254
	GO TO (37,30),KOD8	MAP	171		MAP	255
37	IF(VAL.LT.AI) GO TO 29	MAP	172		MAP	256
	KOD8=2	MAP	173		MAP	257
30	IF(VAL.GT.A4) GO TO 23	MAP	174		MAP	258
C		MAP	175		MAP	259
	CHECK TO SEE IF THE CONTOUR LINE POINT JUST FOUND IS A	MAP	176		MAP	260
C	NEW ONE, OR THE TAIL END OF ONE ALREADY FOUND.	MAP	177		MAP	261
	CALL CHECK(ICM,NXY,KOD2,J,K,NVAL,KOD9)	MAP	178		MAP	262
	IF(KOD9.EQ.2) GO TO 29	MAP	179		MAP	263
C		MAP	180		MAP	264
	DETERMINE A1 AND A2	MAP	181		MAP	265
32	IF(KOD7.EQ.1.OR.KOD7.EQ.4) GO TO 32	MAP	182		MAP	266
	A2=AI	MAP	183		MAP	267
	A1=AI	MAP	184		MAP	268
	GO TO 33	MAP	185		MAP	269
33	A2=AI	MAP	186		MAP	270
	A1=AI	MAP	187		MAP	271
C		MAP	188		MAP	272
	ENTER IN THE TABLE THE POINT JUST FOUND.	MAP	189		MAP	273
33	NDUM=NAD(1)+1	MAP	190		MAP	274
		MAP	191		MAP	275
		MAP	192		MAP	276
		MAP	193		MAP	277
		MAP	194		MAP	278
		MAP	195		MAP	279
		MAP	196		MAP	280
		MAP	197		MAP	281
		MAP	198		MAP	282
		MAP	199		MAP	283
		MAP	200		MAP	284
		MAP	201		MAP	285
		MAP	202		MAP	286
		MAP	203		MAP	287
		MAP	204		MAP	288
		MAP	205		MAP	289
		MAP	206		MAP	290
		MAP	207		MAP	291
		MAP	208		MAP	292
		MAP	209		MAP	293
		MAP	210		MAP	294
		MAP	211		MAP	295
		MAP	212		MAP	296
		MAP	213		MAP	297
		MAP	214		MAP	298
		MAP	215		MAP	299
		MAP	216		MAP	300
		MAP	217		MAP	301
		MAP	218		MAP	302
		MAP	219		MAP	303
		MAP	220		MAP	304
		MAP	221		MAP	305
		MAP	222		MAP	306
		MAP	223		MAP	307
		MAP	224		MAP	308
		MAP	225		MAP	309
		MAP	226		MAP	310
		MAP	227		MAP	311
		MAP	228		MAP	312
		MAP	229		MAP	313
		MAP	230		MAP	314
		MAP	231		MAP	315
		MAP	232		MAP	316
		MAP	233		MAP	317
		MAP	234		MAP	318
		MAP	235		MAP	319
		MAP	236		MAP	320
		MAP	237		MAP	321
		MAP	238		MAP	322
		MAP	239		MAP	323
		MAP	240		MAP	324
		MAP	241		MAP	325
		MAP	242		MAP	326
		MAP	243		MAP	327
		MAP	244		MAP	328
		MAP	245		MAP	329
		MAP	246		MAP	330
		MAP	247		MAP	331
		MAP	248		MAP	332
		MAP	249		MAP	333
		MAP	250		MAP	334
		MAP	251		MAP	335
		MAP	252		MAP	336
		MAP	253		MAP	337
		MAP	254		MAP	338
		MAP	255		MAP	339
		MAP	256		MAP	340
		MAP	257		MAP	341
		MAP	258		MAP	342
		MAP	259		MAP	343
		MAP	260		MAP	344
		MAP	261		MAP	345
		MAP	262		MAP	346
		MAP	263		MAP	347
		MAP	264		MAP	348
		MAP	265		MAP	349
		MAP	266		MAP	350
		MAP	267		MAP	351
		MAP	268		MAP	352
		MAP	269		MAP	353
		MAP	270		MAP	354
		MAP	271		MAP	355
		MAP	272		MAP	356
		MAP	273		MAP	357
		MAP	274		MAP	358
		MAP	275		MAP	359

MRKP LT	2
MRKP LT	3
MRKP LT	4
MRKP LT	6
MRKP LT	8
MRKP LT	7
MRKP LT	2
MRKP LT	0
MRKP LT	11
MRKP LT	10
MRKP LT	12
MRKP LT	13
MRKP LT	14
MRKP LT	15
MRKP LT	16
MRKP LT	17
MRKP LT	18
MRKP LT	19
MRKP LT	20
MRKP LT	21
MRKP LT	22
MRKP LT	23
MRKP LT	24
MRKP LT	25

PLOTCH	2
PLOTCH	3
PLOTCH	4
PLOTCH	5
PLOTCH	6
PLOTCH	7
PLOTCH	8
PLOTCH	9
PLOTCH	10

1

```
C
C      SUBROUTINE PLOT8B
C
C      THIS SUBROUTINE CONTROLS THE DRAWING OF THE TIME HISTOY PLOTS
C      OF VELOCITY, TEMPERATURE, DENSITY, AND MAGNETIC FIELD
C
C      COMMON /TPJDAT/ MTRAJ,TPTAJ(100),XTPAJ(100),VTPAJ(100),ZTPAJ(100),
C      * VTPAJ(100),VYTRAJ(100),VYTRAJ(100),VYTRAJ(100),THMTRAJ(100),
C      * XTPAJ(100),XTPAJ(100),XYTRAJ(100),XYTRAJ(100),POTRAJ(100),
C      * POTRAJ(100)
C      LOCAL LPLTRJ
C      COMMON /TOPRT/ LPLTRJ,RPLNT,VINF,PHOINF,THMINF,BINF
C      DATA PLTSZE/7.0/, TINGTH/P.O/
C      DATA MSYN/4H     , ISYMI/
```

C
C CALCULATE SETUP PARAMETERS FOR TIME AXIS

```
C      NTAXIS=0
      CALL TAXIS(TIMESE,TOFFST,TLNGTH,NTAXIS)
```

```

C      PLOT V VS TIME
C
C      CALL TAXIS(TIMESF,TOFFST,TLNGTH,MTAXIS,
C      CALL VAXIS(VSF,VOFFST,VINP,PLTSIZE,2))
C      CALL SCALE(TIMESF,VSF,1)

```

PLAYER	2
PLAYER	3
PLAYER	4
PLAYER	5
TRJAT	2
TRJAT	3
TRJAT	4
TRJAT	5
TRJPT	2
TRJPT	3
PLAYER	9
PLAYER	10
PLAYER	11
PLAYER	12
PLAYER	13
PLAYER	14
PLAYER	17
PLAYER	16
PLAYER	17
PLAYER	18
PLAYER	19
PLAYER	20
PLAYER	21

C	CALL OFFST(TOFFST,VOFFST,1)	PLTFB	22	C	CALL TAXIS(TIMESF,TOFFST,TLNGTH,NTAXIS)	PLTFB	106
C	CALL VECTOP(UTTRAJ,VUTRAJ,UTRAJ,1,ISYN,MSYN)	PLTFB	23	C	CALL VAXIS(VSF,VOFFST,VINF,PLTSE,42)	PLTFB	107
C	CALL MXPPLT(UTTRAJ,VUTRAJ,TIMESF,VSF)	PLTFB	24	C	CALL SCALF(TIMESF,VSF,1)	PLTFB	108
C	CALL RESET	PLTFB	25	C	CALL OFFST(TOFFST,VOFFST,1)	PLTFB	109
C	CALL PLOT(PLTSE,0,0,-3)	PLTFB	26	C	CALL VECTOP(UTTRAJ,VUTRAJ,UTRAJ,1,ISYN,MSYN)	PLTFB	110
C	PLT VZ VS TIME	PLTFB	27	C	CALL MXPPLT(UTTRAJ,VUTRAJ,TIMESF,VSF)	PLTFB	111
C	CALL TAXIS(TIMESF,TOFFST,TLNGTH,NTAXIS)	PLTFB	28	C	CALL RESET	PLTFB	112
C	CALL VAXIS(VSF,VOFFST,VINF,PLTSE,11)	PLTFB	29	C	CALL PLOT(PLTSE,0,0,-3)	PLTFB	113
C	CALL SCALF(TIMESF,VSF,1)	PLTFB	30	C	PLT AZ VS TIME	PLTFB	114
C	CALL OFFST(TOFFST,VOFFST,1)	PLTFB	31	C	CALL TAXIS(TIMESF,TOFFST,TLNGTH,NTAXIS)	PLTFB	115
C	CALL VECTOP(UTTRAJ,VUTRAJ,UTRAJ,1,ISYN,MSYN)	PLTFB	32	C	CALL VAXIS(VSF,VOFFST,VINF,PLTSE,43)	PLTFB	116
C	CALL MXPPLT(UTTRAJ,VUTRAJ,TIMESF,VSF)	PLTFB	33	C	CALL SCALF(TIMESF,VSF,1)	PLTFB	117
C	CALL RESET	PLTFB	34	C	CALL OFFST(TOFFST,VOFFST,1)	PLTFB	118
C	CALL PLOT(PLTSE,0,0,-3)	PLTFB	35	C	CALL VECTOP(UTTRAJ,VUTRAJ,UTRAJ,1,ISYN,MSYN)	PLTFB	119
C	PLT VY VS TIME	PLTFB	36	C	CALL MXPPLT(UTTRAJ,VUTRAJ,TIMESF,VSF)	PLTFB	120
C	CALL TAXIS(TIMESF,TOFFST,TLNGTH,NTAXIS)	PLTFB	37	C	CALL RESET	PLTFB	121
C	CALL VAXIS(VSF,VOFFST,VINF,PLTSE,12)	PLTFB	38	C	CALL PLOT(PLTSE,0,0,-3)	PLTFB	122
C	CALL SCALF(TIMESF,VSF,1)	PLTFB	39	C	CALL EMPLOT(3,0,0)	PLTFB	123
C	CALL OFFST(TOFFST,VOFFST,1)	PLTFB	40	C	RETURN	PLTFB	124
C	CALL VECTOP(UTTRAJ,VUTRAJ,UTRAJ,1,ISYN,MSYN)	PLTFB	41	C	END	PLTFB	125
C	CALL MXPPLT(UTTRAJ,VUTRAJ,TIMESF,VSF)	PLTFB	42				
C	CALL RESET	PLTFB	43				
C	CALL PLOT(PLTSE,0,0,-3)	PLTFB	44				
C	PLT VZ VS TIME	PLTFB	45				
C	CALL TAXIS(TIMESF,TOFFST,TLNGTH,NTAXIS)	PLTFB	46				
C	CALL VAXIS(VSF,VOFFST,VINF,PLTSE,13)	PLTFB	47				
C	CALL SCALF(TIMESF,VSF,1)	PLTFB	48				
C	CALL OFFST(TOFFST,VOFFST,1)	PLTFB	49				
C	CALL VECTOP(UTTRAJ,VUTRAJ,UTRAJ,1,ISYN,MSYN)	PLTFB	50				
C	CALL MXPPLT(UTTRAJ,VUTRAJ,TIMESF,VSF)	PLTFB	51				
C	CALL RESET	PLTFB	52				
C	CALL PLOT(PLTSE,0,0,-3)	PLTFB	53				
C	PLT VY VS TIME	PLTFB	54				
C	CALL TAXIS(TIMESF,TOFFST,TLNGTH,NTAXIS)	PLTFB	55				
C	CALL VAXIS(VSF,VOFFST,VINF,PLTSE,14)	PLTFB	56				
C	CALL SCALF(TIMESF,VSF,1)	PLTFB	57				
C	CALL OFFST(TOFFST,VOFFST,1)	PLTFB	58				
C	CALL VECTOP(UTTRAJ,VUTRAJ,UTRAJ,1,ISYN,MSYN)	PLTFB	59				
C	CALL MXPPLT(UTTRAJ,VUTRAJ,TIMESF,VSF)	PLTFB	60				
C	CALL RESET	PLTFB	61				
C	CALL PLOT(PLTSE,0,0,-3)	PLTFB	62				
C	PLT VZ VS TIME	PLTFB	63				
C	CALL TAXIS(TIMESF,TOFFST,TLNGTH,NTAXIS)	PLTFB	64				
C	CALL VAXIS(VSF,VOFFST,VINF,PLTSE,15)	PLTFB	65				
C	CALL SCALF(TIMESF,VSF,1)	PLTFB	66				
C	CALL OFFST(TOFFST,VOFFST,1)	PLTFB	67				
C	CALL VECTOP(UTTRAJ,VUTRAJ,UTRAJ,1,ISYN,MSYN)	PLTFB	68				
C	CALL MXPPLT(UTTRAJ,VUTRAJ,TIMESF,VSF)	PLTFB	69				
C	CALL RESET	PLTFB	70				
C	CALL PLOT(PLTSE,0,0,-3)	PLTFB	71				
C	PLT VY VS TIME	PLTFB	72				
C	CALL TAXIS(TIMESF,TOFFST,TLNGTH,NTAXIS)	PLTFB	73				
C	CALL VAXIS(VSF,VOFFST,VINF,PLTSE,16)	PLTFB	74				
C	CALL SCALF(TIMESF,VSF,1)	PLTFB	75				
C	CALL OFFST(TOFFST,VOFFST,1)	PLTFB	76				
C	CALL VECTOP(UTTRAJ,VUTRAJ,UTRAJ,1,ISYN,MSYN)	PLTFB	77				
C	CALL MXPPLT(UTTRAJ,VUTRAJ,TIMESF,VSF)	PLTFB	78				
C	CALL RESET	PLTFB	79				
C	CALL P						

```

      YTHAX=0.5*INT(2.0*ZTHAX+.000)
      YTHIN=0.5*INT(2.0*ZTHIN+.000)
      ZTHAX=0.5*INT(2.0*ZTHAX+.000)

C
C      COMPUTE SCALE FACTOR
C
      YTSIZE=YTHAX-YTHIN
      TSF=PLTTSF/ANAL1(YTSIZE,RTMAX)
      TSFRO=TSF*RH0SE
      CALL PLNT(4,0,-12,0,-3)

C
C      (Y,Z) PROJECTION
C
C      DRAW AXIS USING SUBROUTINE AXIS
C
      CALL PLNT(0,0,1.5-YTHIN*TSF,-3)
      NTC=INT(2.0*(ZTHAX-ZTHIN)+1.0)
      CALL AXIS(0,0,0.0,14,1,ZTHAX-ZTHIN)*TSF,-NTC,1,0,0)
      CALL PLNT(1-ZTHIN*TSF,YTHIN*TSF,-3)
      NTC=INT(2.0*YTSIZE+1.0)
      CALL AXIS(0,0,0.0,14,0,YTSIZE*TSF,-NTC,2,PI*72)
      CALL PLNT(0,0,1-YTHIN*TSF,-3)

C
C      LABEL AND ANNOTATE Z-AXIS (HORIZONTAL)
C
      CALL SCALF(TSF,TSF,1)
      YCH=-.15/TSF
      YCH=INT(YTHIN)
      DYC42=1.0
100 CONTINUE
      CALL WXPPLT(ZCH,YCH,0.0,-0.1,ZCH*1)
      ZCH=ZCH+DYC42
      IF (ZCH.LE.ZTHAX) GO TO 100
      ZCH=ZTHAX+.2/TSF
      YCH=-.05/TSF
      CALL CHAR(ZCH,YCH,0.0,14,34/R,3)
      ZCH=ZCH+.42/TSF
      CALL CHAR(ZCH,YCH,0.0,14,66,6HPLANET,6)

C
C      LABEL AND ANNOTATE Y-AXIS (VERTICAL)
C
      YCH=INT(YTHIN)
      DYC42=1.0
      YCH=-.15/TSF
110 CONTINUE
      IF (YCH.NE.0.0) CALL WXPPLT(ZCH,YCH-.05/TSF,0.0,0.1,YCH*1)
      YCH=YCH+DYC42
      IF (YCH.LE.YTHAX) GO TO 110
      YCH=YTHAX+.2/TSF
      IF (PLNT .LE. 6.0) GO TO 120
      YCH=YCH+.42/TSF
      CALL CHAR(ZCH,YCH,0.0,14,66,6HPLANET,6)

C
C      DRAW PLANET AND LABEL PLOT
C
120 CONTINUE
      CALL ELIPS(1.0,0.0,1.0,1.0,0.0,0.0,0.0,0.0,3)
      YCH=0.5*(ZTHAX-ZTHIN)-1.0/TSF
      YCH=YTHIN-1.0/TSF
      CALL CHAR(ZCH,YCH,0.0,2,TITLE1,10)
      YCH=YCH+.04/TSF
      YCH=YCH+.03/TSF
      CALL CHAR(ZCH,YCH,0.0,12,TITLE7,16)

C
C      DRAW (Y,Z) PROJECTION
C
      YTHAX=YTHAX*PLNT
      YTHIN=YTHIN*PLNT
      CALL PLNT(0,0,0.0,3)
      CALL SCALF(TSF,TSF,1)
      CALL VECTOR(ZTRAJ,YTRAJ,NTRAJ,1,1,14)
      CALL WXPPLT(ZTRAJ,YTRAJ,TSF,TSF)
      CALL PLNT(ZTHAX,YTHIN,-3)
      CALL RESET

C
C      (X,R) PROJECTION
C
C      DRAW, LABEL, AND ANNOTATE X-AXIS (HORIZONTAL)
      NTC=INT(2.0*(XTHAX-XTHIN)+1.0)
      YCH=0.0
      PLOTT 93
      PLOTT 94
      PLOTT 95
      PLOTT 96
      PLOTT 97
      PLOTT 98
      PLOTT 99
      PLOTT 100
      PLOTT 101
      PLOTT 102
      PLOTT 103
      PLOTT 104
      PLOTT 105
      PLOTT 106
      PLOTT 107
      PLOTT 108
      PLOTT 109
      PLOTT 110
      PLOTT 111
      PLOTT 112
      PLOTT 113
      PLOTT 114
      PLOTT 115
      PLOTT 116
      PLOTT 117
      PLOTT 118
      PLOTT 119
      PLOTT 120
      PLOTT 121
      PLOTT 122
      PLOTT 123
      PLOTT 124
      PLOTT 125
      PLOTT 126
      PLOTT 127
      PLOTT 128
      PLOTT 129
      PLOTT 130
      PLOTT 131
      PLOTT 132
      PLOTT 133
      PLOTT 134
      PLOTT 135
      PLOTT 136

      IF (YTSIZE=RTMAX,GE,1.0) YCH=0.5
      CALL PLNT(4,0,YCH,-3)
      CALL AXIS(0,0,0.0,14,-1,(XTHAX-XTHIN)*TSF,-NTC,1,0,0)
      CALL PLNT(1-XTHIN*TSF,0.0,-3)
      CALL SCALF(TSF,TSF,1)
      YCH=-.15/TSF
      YCH=INT(XTHIN)
      DYC42=1.0
200 CONTINUE
      CALL WXPPLT(XCH,YCH,0.0,-0.1,-XCH*1)
      XCH=XCH+DYC42
      IF (XCH.LE.XTHAX) GO TO 200
      XCH=XTHAX+.2/TSF
      YCH=-.05/TSF
      CALL CHAR(XCH,YCH,0.0,14,34/R,3)
      YCH=YCH+.42/TSF
      CALL CHAR(XCH,YCH,0.0,14,66,6HPLANET,6)

C
C      DRAW, LABEL, AND ANNOTATE R-AXIS (VERTICAL)
C
      NTC=INT(2.0*(RTHAX+1.0))
      CALL AXIS(0,0,0.0,14,0,RTHAX*TSF,-NTC,2,PI*72)
      YCH=1.0
      RCH=1.0
      YCH=-.05/TSF
210 CONTINUE
      CALL WXPPLT(XCH,YCH-.05/TSF,0.0,0.1,RCH*1)
      RCH=RCH+DYC42
      IF (RCH.LE.RTHAX) GO TO 210
      RCH=RTHAX+.1/TSF
      CALL HATH(XCH,RCH,.24/TSF,6.0,21)
      XCH=XCH+.16/TSF
      CALL PLNT(XCH,.55/TSF,RCH+.20/TSF,2)
      CALL CHAR(XCH,RCH,0.0,14,14/R,1)
      CALL CHAR(XCH,.14/TSF,RCH+.11/TSF,6.0,06,142,1)
      YCH=YCH+.2/TSF
      CALL CHAR(XCH,RCH,0.0,14,24/R,2)
      CALL CHAR(XCH,.28/TSF,RCH+.11/TSF,0.0,06,142,1)
      YCH=YCH+.35/TSF
      CALL CHAR(XCH,RCH,0.0,14,24/R,2)
      IF (PLNT .LE. 6.0) GO TO 210
      YCH=YCH+.28/TSF
      CALL CHAR(XCH,RCH,0.0,14,66,6HPLANET,6)

C
C      DRAW PLANET AND IDHOPAUSE, AND LABEL PLOT
C
      CALL ELIPS(1.0,0.0,1.0,1.0,0.0,0.0,100,0,3)
215 CONTINUE
      XTHAX=XTHAX*PLNT
      YTHAX=YTHAX*PLNT
      RTHAX=RTHAX*PLNT
      CALL PLNT(0,0,0.0,3)
      CALL SCALF(TSF,TSF,1)
      DO 220 I=1,NTHAX
      IF (XTHAX(I).GT.YTHAX) GO TO 230
      IF (YTHAX(I).GT.RTHAX) GO TO 230
      NTHAX=I
220 CONTINUE
230 CONTINUE
      IF (YTHAX(I).GT.XTHAX) GO TO 250
      IF (YTHAX(I).GT.RTHAX) GO TO 250
      NTHAX=I
240 CONTINUE
250 CONTINUE
      CALL VECTOR(XBOD,YBOD,NBOD,1,1,14)
      CALL VECTOR(XSHR,YSHR,NSHR,1,1,14)
      YCH=0.5*(XTHAX-XTHIN)-1.0/TSFRO
      RCH=-0.7/TSFRO
      CALL CHAR(XCH,RCH,0.0,0.2,TITLE1,10)
      YCH=XCH+.04/TSFRO
      RCH=RCH+.03/TSFRO
      CALL CHAR(XCH,RCH,0.0,0.12,TITLEX,16)

C
C      DRAW (X,R) PROJECTION
C
      CALL VECTOR(XTRAJ,RTRAJ,NTRAJ,1,1,14)
      CALL WXPPLT(XTRAJ,RTRAJ,TSF,TSF)
      CALL PLNT(XTHAX,0.0,-3)
      CALL RESET
      RETURN
      END
      PLOTT 137
      PLOTT 138
      PLOTT 139
      PLOTT 140
      PLOTT 141
      PLOTT 142
      PLOTT 143
      PLOTT 144
      PLOTT 145
      PLOTT 146
      PLOTT 147
      PLOTT 148
      PLOTT 149
      PLOTT 150
      PLOTT 151
      PLOTT 152
      PLOTT 153
      PLOTT 154
      PLOTT 155
      PLOTT 156
      PLOTT 157
      PLOTT 158
      PLOTT 159
      PLOTT 160
      PLOTT 161
      PLOTT 162
      PLOTT 163
      PLOTT 164
      PLOTT 165
      PLOTT 166
      PLOTT 167
      PLOTT 168
      PLOTT 169
      PLOTT 170
      PLOTT 171
      PLOTT 172
      PLOTT 173
      PLOTT 174
      PLOTT 175
      PLOTT 176
      PLOTT 177
      PLOTT 178
      PLOTT 179
      PLOTT 180
      PLOTT 181
      PLOTT 182
      PLOTT 183
      PLOTT 184
      PLOTT 185
      PLOTT 186
      PLOTT 187
      PLOTT 188
      PLOTT 189
      PLOTT 190
      PLOTT 191
      PLOTT 192
      PLOTT 193
      PLOTT 194
      PLOTT 195
      PLOTT 196
      PLOTT 197
      PLOTT 198
      PLOTT 199
      PLOTT 200
      PLOTT 201
      PLOTT 202
      PLOTT 203
      PLOTT 204
      PLOTT 205
      PLOTT 206
      PLOTT 207
      PLOTT 208
      PLOTT 209
      PLOTT 210
      PLOTT 211
      PLOTT 212
      PLOTT 213
      PLOTT 214
      PLOTT 215
      PLOTT 216
      PLOTT 217
      PLOTT 218
      PLOTT 219

```


151

[illegible]

```

SUBROUTINE SERCH(J,K,KOD2,A,JDTH,ICM,KRY,KOD3,NVAL,A1,A2,ACONT)
CONTOUT PROGRAMS PAP, VALK, SERCH, ENTER, AND CHECK
WRITTEN BY REESE SORENSON, NASA-AMES RES. CTR., AUG., 1974.
(MODIFIED VERSION)

THIS SUBROUTINE CHECKS WHETHER A CONTOUR LINE AT LEVEL NVAL
PASSES THROUGH AN INTERVAL HAVING INDICES J,K AT ITS
LEFT(KOD2=2) OR RIGHT(KOD2=1) POINT.

DIMENSION A(1),ACONT(1),ICM(4,1)
IFEV(J,K)=J*(K-1)+JMIN
GO TO (1,2),KOD2
1 T=IDEX(J,K+1)
GO TO 3
2 T=IDEX(J,K)
A2=AT(T)
T=IDEX(J,K)
A1=AT(T)
VF(A1-A2)/5,5
A4=A2
A1=A1
GO TO 4
A4=A1
A1=A2
VAL=ACONT(NVAL)
TF(VAL,LT,A1) GO TO 12
TF(VAL,GT,A4) GO TO 12
CALL CHECK(ICM,KRY,KOD2,J,K,NVAL,KOD3)
TF(KOD3,EO,2) GO TO 12
KOD3=1
GO TO 20
KOD3=3
RETURN
END

```

SUBROUTINE SETUP(PLT,THACH,SAM,INDRY)

THIS ROUTINE ESTABLISHES PLOT ORIGIN, DRAWS
AND LABELS AXES, AND WRITES TITLE.
HCC PLOT SUBROUTINES USED ARE
PLT,AXIS,HUMPLT,CHAR,SCALE,
GREEK,MATH,PLTLN,OTTLN.

DIMENSION TITLE(12),TITLE(4,2)
DIMENSION TITLES(12),TITLES(3),TITLES(7,2),TITLES(4,2)
DIMENSION TITLEF(2)
COMMON /SCALE/ XSF,YSF,XMAX,YMAX,XLNSTH,YLNSTH
DATA PTZ/1.57079633/
DATA TITLE1,TITLE2/04VELOCITY,04DENSITY,/
DATA TITLES(1),TITLES(2)/10MSTREAMLINE,14S/
DATA TITLE4(1),TITLE4(2)/10TEMPERATURE,14S/
DATA TITLES(3),TITLES(4)/10HORIZONTAL,10HORIZONTAL,/
DATA TITLES(5),TITLES(6)/10DEPENDENT,10SIMILAR COEFF,/
1 5MENT,/
DATA TITLE7(1),TITLE7(2)/10NORMAL CO,10DEPENDENT,/
DATA TITLES(1),TITLES(2)/10MAGNETIC F,5MTFLD,/
DATA TITLEF/04CONTOURS/,TITLE(1),TITLE(2)/10FIELD LINE,14S/
SET ORIGIN AT LEFT END OF X-AXIS
XS=VSC
YS=VSF
CALL SCALF(XS,YS,1)
DRAW AND LABEL X-AXIS. NOTE THAT SUBROUTINE AXIS
REQUIRES PARAMETERS IN INCHES, NOT USER UNITS.
NTC=INT(2.0*(XMAX+1.5)+1.0)
CALL AXSTD(0.0,0.0,1H,0,XLNSTH,-NTC,2,PIZ)
SET PERMANENT ORIGIN AT X=0

```

SERCH 2
SERCH 3
SERCH 4
SERCH 5
SERCH 6
SERCH 7
SERCH 8
SERCH 9
SERCH 10
SERCH 11
SERCH 12
SERCH 13
SERCH 14
SERCH 15
SERCH 16
SERCH 17
SERCH 18
SERCH 19
SERCH 20
SERCH 21
SERCH 22
SERCH 23
SERCH 24
SERCH 25
SERCH 26
SERCH 27
SERCH 28
SERCH 29
SERCH 30
SERCH 31
SERCH 32
SERCH 33
SERCH 34
SERCH 35
SERCH 36
SERCH 37
SERCH 38
SERCH 39
SERCH 40
SERCH 41
SERCH 42

```

```

CALL PLT(1.5,0.0,-3)
XS=XSF
YS=VSF
CALL SCALF(XS,YS,1)
DRAW Y-AXIS
NTC=INT(YMAX)+1
CALL AXSTD(0.0,0.0,1H,0,YLNSTH,-NTC,2,PIZ)
LABEL Y-AXIS
YCH=-.4/YSF
YCM=0.5*XMAX-.75-.21/XSF
TF (INDRY,EO,1) GO TO 2
CALL CHAR(YCH,YCM,0.0,0.14,3HV/D,3)
GO TO 3
2 CALL CHAR(YCH,YCM,0.0,0.14,3HV/D,3)
YCM=YCM+.42/XSF
CALL CHAR(YCH,YCM,0.0,0.05,1H,1)
3 CONTINUE
ANNOTATE Y-AXIS - NOTE ANNOTATION IS POSITIVE LEFT.
YV=-.15/YSF
YV=C
YV=-1.5
5 DELY=PLAT(Y)*C.5
YDX=XMAX*DEL
CALL HUMPLT(YDX,YV,0.0,0.1,-YDX,1)
TF(YV,LT,XMAX) GO TO 5
ANNOTATE Y-AXIS AT SIDE EDGE OF PLOT
YV=0.0
10 YV=YV+.1C
YCM=-1.5+.25/XSF
CALL HUMPLT(YCH,YV-.05/YSF,0.0,0.1,YY,1)
YVTC=YCM+.16/XSF
CALL CHAR(YTC,YV-.05/YSF,0.0,0.09,1H,1)
TF(YV,LT,YMAX) GO TO 10
LABEL Y-AXIS.
YCH=-1.5-C.05/XSF
YCM=INT(YMAX-1.0)*C.5+0.5-.37/YSF
TF (INDRY,EO,1) GO TO 12
CALL CHAR(YCH,YCM,0.0,0.14,3HV/D,3)
GO TO 13
12 CALL CHAR(YCH,YCM,0.0,0.14,3HV/D,3)
YCM=YCM+.42/XSF
CALL CHAR(YCH,YCM,0.0,0.05,1H,1)
13 CONTINUE
DRAW TITLE. I PLOT DETERMINES WHICH TITLE
SHOULD BE DRAWN.
YCH=YMAX-C.05/YSF
YCM=-1.5-C.05/XSF
TF(PLT,EO,2) GO TO 15
TF(PLT,FO,3) GO TO 20
TF (PLT,EO,4) GO TO 14
TF (PLT,GT,4) GO TO 21
VELOCITY PLOT
CALL CHAR(YCH,YCM,0.0,0.20,TITLE1,9)
YCM=YCM+.2/XSF
CALL PLTLN(YCH,YCM,YCM,YCM+.2/YSF)
CALL CHAR(YCH,YCM,0.05/XSF,YCM,0.0,2,1HV/D,3)
YCM=YCM+.25/XSF
CALL PLTLN(YCH,YCM,YCM,YCM+.2/YSF)
CALL CHAR(YCH,YCM,0.05/XSF,YCM,0.0,2,2HV/D,3)
CALL MATH(XCM+.4/XSF,YCM-.05/YSF,.15/XSF,0.0,3,15)
GO TO 25
TEMPERATURE PLOT
14 CONTINUE
CALL CHAR(YCH,YCM,0.0,0.20,TITLE4,11)
YCM=YCM+.2/XSF
CALL CHAR(YCH,YCM,0.0,0.2,3MT/7,3)
CALL MATH(XCM+.25/XSF,YCM-.05/YSF,.15/XSF,0.0,3,15)

```

```

SETUP 40
SETUP 41
SETUP 42
SETUP 43
SETUP 44
SETUP 45
SETUP 46
SETUP 47
SETUP 48
SETUP 49
SETUP 50
SETUP 51
SETUP 52
SETUP 53
SETUP 54
SETUP 55
SETUP 56
SETUP 57
SETUP 58
SETUP 59
SETUP 60
SETUP 61
SETUP 62
SETUP 63
SETUP 64
SETUP 65
SETUP 66
SETUP 67
SETUP 68
SETUP 69
SETUP 70
SETUP 71
SETUP 72
SETUP 73
SETUP 74
SETUP 75
SETUP 76
SETUP 77
SETUP 78
SETUP 79
SETUP 80
SETUP 81
SETUP 82
SETUP 83
SETUP 84
SETUP 85
SETUP 86
SETUP 87
SETUP 88
SETUP 89
SETUP 90
SETUP 91
SETUP 92
SETUP 93
SETUP 94
SETUP 95
SETUP 96
SETUP 97
SETUP 98
SETUP 99
SETUP 100
SETUP 101
SETUP 102
SETUP 103
SETUP 104
SETUP 105
SETUP 106
SETUP 107
SETUP 108
SETUP 109
SETUP 110
SETUP 111
SETUP 112
SETUP 113
SETUP 114
SETUP 115
SETUP 116
SETUP 117
SETUP 118
SETUP 119
SETUP 120
SETUP 121
SETUP 122
SETUP 123

```

```

C      GO TO 25
C      DENSITY PLOT
C      19 CONTINUE
C      CALL CHAR(XCH,YCH,0.0,2,TITLE2,9)
C      YCH=YCH+2/XSF
C      CALL GREEK(XCH,YCH,2,0,0,17)
C      CALL CHAR(XCH+2/XSF,YCH,0,0,2,1H,1)
C      CALL GREEK(XCH+2/XSF,YCH,2,0,0,17)
C      CALL MATHE(XCH+2/XSF,YCH,0,0,2,1H,1)
C      GO TO 25
C      STREAMLINES PLOT
C      2. CONTINUE
C      CALL CHAR(XCH,YCH,0.0,2,TITLE3,11)
C      GO TO 25
C      MAGNETIC FIELD PLOTS
C      2. CONTINUE
C      CALL CHAR(XCH,YCH,0.0,2,TITLE5,15)
C      YCH=YCH+2/XSF
C      CALL CHAR(XCH,YCH,2,0,2,4H,9,8,4)
C      CALL MATHE(XCH+2/XSF,YCH,0,0,2,1H,1)
C      CALL CHAR(XCH+2/XSF,YCH,0,0,2,1H,1)
C      IF (PLMT.EQ.0) GO TO 22
C      IF (PLMT.EQ.1) GO TO 24
C      CALL CHAR(XCH+2/XSF,YCH,0,0,2,1H,1)
C      YCH=YCH+2/XSF
C      CALL CHAR(XCH,YCH,0,0,2,TITLE5,23)
C      GO TO 25
C      22 CALL CHAR(XCH+1,15/XSF,YCH,0,0,5/YSF,3,14,6,3,1,1H,1)
C      YCH=YCH+1,1/XSF
C      CALL CHAR(XCH,YCH,0,0,2,TITLE5,25)
C      GO TO 25
C      24 CALL CHAR(XCH+1,15/XSF,YCH,0,0,5/YSF,3,14,6,3,1,1H,1)
C      YCH=YCH+1,1/XSF
C      CALL CHAR(XCH,YCH,0,0,2,TITLE7,23)
C      YCH=YCH+1,1/XSF
C      CALL CHAR(XCH,YCH,0,0,2,TITLEC,8)
C      CALL PLTLINE(XCH+1,1/XSF,YCH,XCH+1,5/XSF,YCH)
C      YCH=YCH+1,1/XSF
C      CALL CHAR(XCH,YCH,0,0,2,TITLEF,11)
C      CALL PLTLINE(XCH+1,15/XSF,YCH,XCH+1,5/XSF,YCH,2,0,0)
C      DRAW EACH NUMBER (N) AND RATIO OF SPECIFIC
C      HEATS (GAMMA).
C      25 CONTINUE
C      YCH=YCH+1,1/XSF
C      YCH=YCH+1,1/XSF
C      CALL CHAR(XCH,YCH,0,0,2,2H,0,2)
C      CALL MIMPLET(XCH+4/XSF,YCH,0,0,2,TNCH,2)
C      YCH=YCH+1,1/XSF
C      CALL GREEK(XCH,YCH,2,0,0,3)
C      CALL CHAR(XCH+2/XSF,YCH,0,0,2,1H,1)
C      CALL MIMPLET(XCH+4/XSF,YCH,0,0,2,6H,2)
C      RETURN
C      END
C      SUBROUTINE SFCALC(XSHK,YSHK,NTMAX)
C      THIS ROUTINE DETERMINES SCALE FACTORS AND TYPE OF PLOT.
C      COMMON /SCALE/ XSF,YSF,YMAX,YMAX,YLENGTH,YLENGTH
C      DIMENSION XSHK(1),YSHK(1)
C      DATA YSIZE/8.0/
C      CALCULATE XMAX AND YMAX BASED ON LAST POINT OF SHOCK WAVE.
C      XMAX=AMT(XSHK(NTMAX))+0.5
C      IF(YMAX.LT.XSHK(NTMAX)) YMAX=XMAX+0.5
C      YMAX=AMT(YSHK(NTMAX))+1.0

```

```

SETUP 124
SETUP 125
SETUP 126
SETUP 127
SETUP 128
SETUP 129
SETUP 130
SETUP 131
SETUP 132
SETUP 133
SETUP 134
SETUP 135
SETUP 136
SETUP 137
SETUP 138
SETUP 139
SETUP 140
SETUP 141
SETUP 142
SETUP 143
SETUP 144
SETUP 145
SETUP 146
SETUP 147
SETUP 148
SETUP 149
SETUP 150
SETUP 151
SETUP 152
SETUP 153
SETUP 154
SETUP 155
SETUP 156
SETUP 157
SETUP 158
SETUP 159
SETUP 160
SETUP 161
SETUP 162
SETUP 163
SETUP 164
SETUP 165
SETUP 166
SETUP 167
SETUP 168
SETUP 169
SETUP 170
SETUP 171
SETUP 172
SETUP 173
SETUP 174
SETUP 175
SETUP 176
SETUP 177
SETUP 178
SETUP 179
SETUP 180
SETUP 181
SETUP 182
SETUP 183
SETUP 184
SETUP 185
SETUP 186
SETUP 187
SETUP 188
SETUP 189

```

```

IF(YMAX.LT.3.0)YMAX=3.0
IF(XMAX.LT.3.0) XMAX=3.0
RTY PLOT SIZE IN Y-DIRECTION
ADJUST SCALE FACTORS FOR EQUAL X AND Y SCALE FACTORS
VLNGTH=YSTVE
YSF=VLNGTH/YMAX
YSF=YSF
VLNGTH=YSF*(XMAX+1.5)
RETURN
END
SUBROUTINE SFOFF(LF,FINF,PLTSE,PSF,PFFST,NA,NTICK,AMTN,ANEL,
* FPEL)
THIS SUBROUTINE CALCULATES THE PARAMETERS REQUIRED TO DRAW THE
VERTICAL AXIS OF THE TRAJECTORY DATA PLOTS
LF = 1 VELOCITY
    = 2 TEMPERATURE
    = 3 DENSITY
    = 4 MAGNETIC FIELD
COMMON /TRJDAT/ NTRAJ,TTTRAJ(100),XTRAJ(100),YTRAJ(100),
* VTRAJ(100),VYTRAJ(100),VYTRAJ(100),VYTRAJ(100),
* VYTRAJ(100),VYTRAJ(100),VYTRAJ(100),VYTRAJ(100),
* RTOT(100)
GO TO (100,200,300,400),LF
VELOCITY
100 FMIN=0.0
DO 110 I=1,NTRAJ
IF (VYTRAJ(I).LT. FMIN) FMIN=VYTRAJ(I)
110 CONTINUE
DO 120 I=1,NTRAJ
IF (VYTRAJ(I).LT. FMIN) FMIN=VYTRAJ(I)
120 CONTINUE
DO 130 I=1,NTRAJ
IF (VYTRAJ(I).LT. FMIN) FMIN=VYTRAJ(I)
130 CONTINUE
FMIN=FMIN*FINF
FMAX=FINF
GO TO 700
TEMPERATURE
200 FMIN=0.0
FMAX=0.0
DO 210 I=1,NTRAJ
IF (TTRAJ(I).GT. FMAX) FMAX=TTRAJ(I)
210 CONTINUE
FMAX=FMAX*FINF
GO TO 700
DENSITY
300 FMIN=0.0
FMAX=0.0
DO 310 I=1,NTRAJ
IF (RTTRAJ(I).GT. FMAX) FMAX=RTTRAJ(I)
310 CONTINUE
FMAX=FMAX*FINF
GO TO 700
MAGNETIC FIELD STRENGTH
400 FMIN=0.0
FMAX=0.0
DO 410 I=1,NTRAJ
IF (RTTRAJ(I).LT. FMIN) FMIN=RTTRAJ(I)
410 CONTINUE
DO 420 I=1,NTRAJ
IF (RTTRAJ(I).LT. FMIN) FMIN=RTTRAJ(I)
420 CONTINUE
DO 430 I=1,NTRAJ
IF (RTTRAJ(I).LT. FMIN) FMIN=RTTRAJ(I)
430 CONTINUE
DO 440 I=1,NTRAJ

```

```

SFCALC 15
SFCALC 16
SFCALC 17
SFCALC 18
SFCALC 19
SFCALC 20
SFCALC 21
SFCALC 22
SFCALC 23
SFCALC 24
SFCALC 25
SFCALC 26
SFOFF 2
SFOFF 3
SFOFF 4
SFOFF 5
SFOFF 6
SFOFF 7
SFOFF 8
SFOFF 9
SFOFF 10
SFOFF 11
SFOFF 12
TRJDAT 2
TRJDAT 3
TRJDAT 4
TRJDAT 5
SFOFF 14
SFOFF 15
SFOFF 16
SFOFF 17
SFOFF 18
SFOFF 19
SFOFF 20
SFOFF 21
SFOFF 22
SFOFF 23
SFOFF 24
SFOFF 25
SFOFF 26
SFOFF 27
SFOFF 28
SFOFF 29
SFOFF 30
SFOFF 31
SFOFF 32
SFOFF 33
SFOFF 34
SFOFF 35
SFOFF 36
SFOFF 37
SFOFF 38
SFOFF 39
SFOFF 40
SFOFF 41
SFOFF 42
SFOFF 43
SFOFF 44
SFOFF 45
SFOFF 46
SFOFF 47
SFOFF 48
SFOFF 49
SFOFF 50
SFOFF 51
SFOFF 52
SFOFF 53
SFOFF 54
SFOFF 55
SFOFF 56
SFOFF 57
SFOFF 58
SFOFF 59
SFOFF 60
SFOFF 61
SFOFF 62
SFOFF 63
SFOFF 64
SFOFF 65
SFOFF 66

```



```

      IF (NTRAJ(I) .GT. NMAX) NMAX=NTRAJ(I)
440 CONTINUE
      NMAX=NMAX+1
      NTRAJ=NTRAJ+1
      FIND ORDER OF MAGNITUDE
C
C
700 CONTINUE
      NTRF=NMAX-NMIN
      FLAG=ALOG10(NTRF)
      NLOG=INT(FLAG)
      IF (FLAG .LT. 0.0) NLOG=NLOG-1
C
C FIND INCREMENT AS POWER OF 10 TIMES .1, .2, OR .5
C
      ANTRF=NTRF*10.**(NLOG)
      IF (ANTRF .GT. 2.0) GO TO 720
      NDEL=.2
      NA=NLOG
      GO TO 740
720 CONTINUE
      IF (ANTRF .GT. 5.0) GO TO 730
      NDEL=.5
      NA=NLOG
      GO TO 740
730 CONTINUE
      NDEL=.1
      NA=NLOG+1
740 AION=10.00NA
      IF (NA .NE. 1) GO TO 750
      NDEL=NDEL*10.
      NA=0
      AION=1.0
750 CONTINUE
C
C CALCULATE SCALE AND OFFSET
C
      NMIN=0.0
      IF (NMIN .LT. 0.0) NMIN=1.0-1.0E-6
      NMIN=INT((NMIN/DEL+AION)-NMIN)
      NMAX=1.0E-6
      NMAX=INT((NMAX/(DEL+AION)+NMAX)
      NTRF=NMAX-NMIN+1
      NTRN=FLOAT(NMIN)/DEL
      NMAX=FLOAT(NMAX)/DEL
      NTRF=FLOAT(NMIN)/NTRF
      NMAX=FLOAT(NMAX)/NTRF
      NDEL=DEL*(NMAX-NMIN)/AION
      NDEL=NDEL/NTRF
      RETURN
      END
C
C SUBROUTINE STOUT
C
C THIS SUBROUTINE PRINTS THE STREAMLINES CALCULATED
C IN SUBROUTINE FLOWST
C
      COMMON /PLUNT/ THETA(25), RP(25), NPLUNT
      COMMON /RINDOS/ X(100), Y(100), XSHK(100), YSHK(100),
      * NMAX, NMAX, NMAX, NMAX, NMAX, NMAX, NMAX, NMAX,
      LEVEL 2, XST, YST, NUNST, NUNST
      COMMON /STREAM/ XST(50,152), YST(50,152), NUNST(50,152)
C
C REVERSE SIGN OF XST FOR OUTPUT
C
      DO 2 K=1, NUNST
      NN=NUNST(K)
      DO 2 J=1, NN
      XST(K,J)=-XST(K,J)
C
C STREAMLINES FOR MAGNETOSPHERE
C
      WRITE(6,600) NUNST
      IF (NMIN .EQ. 1) GO TO 1
      DO 10 K=1, NUNST
      WRITE(6,610) K, XST(K,1), YST(K,1)
      IF (XST(K,1) .GE. 0.0) WRITE(6,620) THETA(K+1), RP(NMAX, K+1)
      NN=NUNST(K)
      WRITE(6,630) (XST(K,J), YST(K,J), J=1, NN)
10 CONTINUE

```

```

      SPOFF 67
      SPOFF 68
      SPOFF 69
      SPOFF 70
      SPOFF 71
      SPOFF 72
      SPOFF 73
      SPOFF 74
      SPOFF 75
      SPOFF 76
      SPOFF 77
      SPOFF 78
      SPOFF 79
      SPOFF 80
      SPOFF 81
      SPOFF 82
      SPOFF 83
      SPOFF 84
      SPOFF 85
      SPOFF 86
      SPOFF 87
      SPOFF 88
      SPOFF 89
      SPOFF 90
      SPOFF 91
      SPOFF 92
      SPOFF 93
      SPOFF 94
      SPOFF 95
      SPOFF 96
      SPOFF 97
      SPOFF 98
      SPOFF 99
      SPOFF 100
      SPOFF 101
      SPOFF 102
      SPOFF 103
      SPOFF 104
      SPOFF 105
      SPOFF 106
      SPOFF 107
      SPOFF 108
      SPOFF 109
      SPOFF 110
      SPOFF 111

```

```

      GO TO 4
C
C STREAMLINES FOR IONOSPHERE SHAPE
C
      DO 11 K=1, NUNST
      WRITE(6,611) K, XST(K,1), YST(K,1)
      IF (XST(K,1) .GE. 0.0) WRITE(6,621) THETA(K+1), RP(NMAX, K+1)
      NN=NUNST(K)
      WRITE(6,631) (XST(K,J), YST(K,J), J=1, NN)
11 CONTINUE
C
C RESTORE SIGN OF XST
C
      DO 3 K=1, NUNST
      NN=NUNST(K)
      DO 3 J=1, NN
      XST(K,J)=-XST(K,J)
      RETURN
C
      COMMON /PLUNT/ THETA(25), RP(25), NPLUNT
      COMMON /RINDOS/ X(100), Y(100), XSHK(100), YSHK(100),
      * NMAX, NMAX, NMAX, NMAX, NMAX, NMAX, NMAX, NMAX,
      LEVEL 2, XST, YST, NUNST, NUNST
      COMMON /STREAM/ XST(50,152), YST(50,152), NUNST(50,152)
C
C SUBROUTINE TAXIS(TIMESE, TPOFFST, PLTST, NMAXIS)
C
C THIS SUBROUTINE TAXIS CALCULATES THE SCALE FACTOR AND OFFSET FOR
C THE TIME AXIS, AND PARAMETERS REQUIRED TO DRAW THE AXIS.
C WHEN NMAXIS=1,2 THE TIME AXIS IS PLOTTED
C
      COMMON /TRJDAT/ NTRAJ, TTRAJ(100), XTRAJ(100), YTRAJ(100), ZTRAJ(100),
      * VTRAJ(100), VTRAJ(100), VTRAJ(100), VTRAJ(100), TPTTRAJ(100),
      * RTRAJ(100), RTRAJ(100), RTRAJ(100), RTRAJ(100), RTRAJ(100),
      * RTRAJ(100)
C
C FIND THE RANGE AND INCREMENT REQUIRED
C INCREMENT IS POWER OF 10 TIMES .1, .2, OR .5
C
      IF (NMAXIS .GT. 0) GO TO 100
      NAXIS=1
      TMIN=TTRAJ(1)
      TMAX=TTRAJ(NTRAJ)
      TDIFF=TMAX-TMIN
      TLOG=ALOG10(TDIFF)
      NTRN=INT(TLOG)
      IF (NTRN .LT. 0) NTRN=NTRN-1
      ANTRF=TDIFF*10.**(NTRN)
      IF (ANTRF .GT. 2.0) GO TO 20
      NDEL=.2
      NA=NLOG
      GO TO 40
20 CONTINUE
      IF (ANTRF .GT. 5.0) GO TO 40
      NDEL=.5
      NA=NLOG-1
      GO TO 60
40 CONTINUE
      NDEL=.1
      NA=NLOG+1
60 CONTINUE
      NMIN=0.0
      AION=10.00NA
      IF (NA .LT. 0.0) NA=NA+1
      GO TO 100
      NDEL=NDEL*10.
      NA=0
      AION=1.0
      NAXIS=2
C
C CALCULATE SCALE AND OFFSET
C
      TAXIS 2
      TAXIS 3
      TAXIS 4
      TAXIS 5
      TAXIS 6
      TAXIS 7
      TAXIS 8
      TAXIS 9
      TAXIS 10
      TAXIS 11
      TAXIS 12
      TAXIS 13
      TAXIS 14
      TAXIS 15
      TAXIS 16
      TAXIS 17
      TAXIS 18
      TAXIS 19
      TAXIS 20
      TAXIS 21
      TAXIS 22
      TAXIS 23
      TAXIS 24
      TAXIS 25
      TAXIS 26
      TAXIS 27
      TAXIS 28
      TAXIS 29
      TAXIS 30
      TAXIS 31
      TAXIS 32
      TAXIS 33
      TAXIS 34
      TAXIS 35
      TAXIS 36
      TAXIS 37
      TAXIS 38
      TAXIS 39
      TAXIS 40
      TAXIS 41
      TAXIS 42
      TAXIS 43
      TAXIS 44

```


[illegible]

WRITE(6,1700) ANACH,GAMMA,RINF,VINF,XD,PHOINF,YD,THPINF,ZD	TRQUT	1
WRITE(6,1800)	TRQUT	62
DO 66 N=1,NTRAJ	TRQUT	63
VDI=M-VTRAJ(N)*VINF	TRQUT	64
VXI=M-VTPAJ(N)*VINF	TRQUT	65
VYI=M-VVTRAJ(N)*VINF	TRQUT	66
VZI=M-VVTRAJ(N)*VINF	TRQUT	67
RMODI=MODTRAJ(N)*PHOINF	TRQUT	68
TPMODI=THPTRAJ(N)*THPINF	TRQUT	69
QDI=M-VTRAJ(N)*QINF	TRQUT	70
AYDI=M-VTRAJ(N)*QINF	TRQUT	71
AYDI=M-VVTRAJ(N)*QINF	TRQUT	72
AYDI=M-VVTRAJ(N)*QINF	TRQUT	73
WRITE(6,ZZJ) N,TTRAJ(N),VDI,XDI,VYDI,YDI,ZDI,RMODI,TPMODI,	TRQUT	74
QDI,AYDI,AYDI,AYDI,RZDI	TRQUT	75
63 CONTINUE	TRQUT	76
IF (LCHI) GO TO 70	TRQUT	77
RETURN	TRQUT	78
TRANSFORM OUTPUT QUANTITIES TO SUN-PLANET COORDINATE SYSTEM		
	TRQUT	79
	TRQUT	80
73. CONTINUE	TRQUT	81
DO 75 N=1,NTRAJ	TRQUT	82
VTRAJ(N)=VTRAJ(N)*PLMT	TRQUT	83
VTRAJ(N)=VTRAJ(N)*PLMT	TRQUT	84
VTRAJ(N)=VTRAJ(N)*PLMT	TRQUT	85
75 CONTINUE	TRQUT	86
TEMP7=AZANG*.01745329	TRQUT	87
TEMP8=POLANG*.01745329	TRQUT	88
CA7=5*(ITE=PAZ)	TRQUT	89
CA7=COF(ITS=PAZ)	TRQUT	90
SPOL=TIME*POL	TRQUT	91
CPOL=COS(ITE*POL)	TRQUT	92
DO 80 N=1,NTRAJ	TRQUT	93
RTPAJ(N)=SQRT(VTRAJ(N)*VTRAJ(N)+VTRAJ(N)*VTRAJ(N))	TRQUT	94
VTRAJ(N)=CAZ*CPOL*VTRAJ(N)-SAZ*VTRAJ(N)-CAZ*SPOL*VTRAJ(N)	TRQUT	95
VTRAJ(N)=SAZ*CPOL*VTRAJ(N)-CA7*VTRAJ(N)+CA7*SPOL*VTRAJ(N)	TRQUT	96
VTRAJ(N)=SPOL*VTRAJ(N)+CPOL*VTRAJ(N)	TRQUT	97
VTRAJ(N)=CA7*CPOL*VTRAJ(N)-SAZ*VTRAJ(N)-CA7*SPOL*VTRAJ(N)	TRQUT	98
VTRAJ(N)=SAZ*CPOL*VTRAJ(N)+CA7*VTRAJ(N)+CA7*SPOL*VTRAJ(N)	TRQUT	99
VTRAJ(N)=SPOL*VTRAJ(N)+CPOL*VTRAJ(N)	TRQUT	100
80 CONTINUE	TRQUT	101
XCS=-CA7*SPOL*XD-SA7*XD-CA7*SPOL*YD	TRQUT	102
YCS=SA7*CPOL*XD-CA7*YD-SA7*SPOL*YD	TRQUT	103
ZCS=-SPOL*XD+CPOL*YD	TRQUT	104
	TRQUT	105
WRITE COORDINATES (X,Y,Z) AS A FUNCTION OF TIME	TRQUT	106
IN UNITS OF BOTH RD AND PLANET	TRQUT	107
	TRQUT	108
WRITE (6,1300)	TRQUT	109
WRITE (6,1302)	TRQUT	110
WRITE (6,1303) PHOSE	TRQUT	111
WRITE (6,1300)	TRQUT	112
DO 90 N=1,NTRAJ	TRQUT	113
VRPLTS=VTRAJ(N)*RNOSE	TRQUT	114
VRPLTS=VTRAJ(N)*RNOSE	TRQUT	115
VRPLTS=VTRAJ(N)*RNOSE	TRQUT	116
VRPLTS=VTRAJ(N)*RNOSE	TRQUT	117
VRPLTS=VTRAJ(N)*RNOSE	TRQUT	118
VRPLTS=VTRAJ(N)*RNOSE	TRQUT	119
WRITE (6,ZLW) N,TTRAJ(N),XCS,VTRAJ(N),ZPAJ(N),RTPAJ(N),VRPLTS	TRQUT	120
VRPLTS,ZRPLTS,VRPLTS	TRQUT	121
90 CONTINUE	TRQUT	122
	TRQUT	123
WRITE FLOW FIELD AND MAGNETIC FIELD COMPONENTS	TRQUT	124
NON-DIMENSIONALIZED WITH RESPECT TO FREESTREAM	TRQUT	125
	TRQUT	126
WRITE (6,1300)	TRQUT	127
WRITE (6,1002)	TRQUT	128
WRITE (6,1403)	TRQUT	129
WRITE (6,1500)	TRQUT	130
DO 95 N=1,NTRAJ	TRQUT	131
WRITE (6,2100) N,TTRAJ(N),VTRAJ(N),VTRAJ(N),VTRAJ(N),	TRQUT	132
VTRAJ(N),VTRAJ(N),VTRAJ(N),VTRAJ(N),VTRAJ(N),	TRQUT	133
VTRAJ(N),VTRAJ(N),VTRAJ(N)	TRQUT	134
95 CONTINUE	TRQUT	135
	TRQUT	136
WRITE FLOW FIELD AND MAGNETIC FIELD COMPONENTS	TRQUT	137
DIMENSIONALIZED BY INPUT FREESTREAM VALUES	TRQUT	138
	TRQUT	139
WRITE (6,1300)	TRQUT	140
WRITE (6,1002)	TRQUT	141
WRITE (6,1600)	TRQUT	142
WRITE (6,1700) ANACH,GAMMA,RINF,VINF,XOS,PHOINF,YOS,THPINF,ZOS	TRQUT	143
WRITE (6,1701) AZANG,POLANG	TRQUT	144


```

C      FUNCTION VINTPP(X,Y)
C      THIS FUNCTION INTERPOLATES FOR V AT (X,Y) FROM THE GRID VALUES
C
COMMON /ALUNT/ THETA(25),PP(25,25),NRLUNT
COMMON /SPUNDS/ XSD(100),YSD(100),VSHK(1,1),VSHK(1,10),
  6  NRMAY,NRMAY,AMACH,GAMMA,HRO,NMINDX
COMMON /FLOW/ XC(2,100),YC(2,100),VF(2,1,1),VHNF(2,1,1)
DATA /DE/57.29578/
TFLX,CT,CC,1) GO TO 100
TMT=ATANH(-YX)/DEG
DO 10 NT=1,NRLUNT
  TETH=LT,THETA(NT) GO TO 20
10 CONTINUE
20 P=SQRT(X+Y+Y)
  THT=THETA(NT)-THT/(THETA(NT)-THETA(NT-1))
  PP2=PP*PP(1,NT-1)+(1,0-DTHT)*PP(1,NT)
  DO 30 NR=1,NRMAY
    PP2=DTHT*PP(NT,NT-1)+(1,0-DTHT)*PP(NT,NT)
    TFLX,LT,PP2) GO TO 40
  PP2=PP
30 CONTINUE
40 NR=(PP2-1)/(PP2-PP1)
  VINTPP=(DTHT*VF(NT-1,NT-1)+(1,0-DTHT)*VF(NT,NT))+(1,0-
    6  DTHT)*VF(NT,NT-1)+(1,0-DTHT)*VF(NT,NT)+(1,0-PP)
    PP2)
100 DO 110 NT=NRLUNT,NRMAY
  TFLX,LT,VF(1,NT) GO TO 120
110 CONTINUE
  NT=NRMAY
120 THT=VF(1,NT)-X/(XC(1,NT)-XC(1,NT-1))
  PP1=DTHT*YC(1,NT-1)+(1,0-DTHT)*YC(1,NT)
  DO 140 NR=1,NRMAY
    PP2=DTHT*YC(NR,NT-1)+(1,0-DTHT)*YC(NR,NT)
    TFLX,LT,PP2) GO TO 40
  PP2=PP
130 CONTINUE
  RETURN
END

C      SUBROUTINE WALK(KONS,J,K,A,JOIN,TCMK,JMIN,JMAX,KMIN,KMAX,KON4,
  6  NXY,ACONT,KONS,X,Y,NVAL,TST1)
C      CONTOUR PROGRAMS MAP, WALK, SEARCH, ENTER, AND CHECK
C      WRITTEN BY REESE Sorenson, NASA-AMES RES. CTG., AUG. 1974.
C      (REVISED VERSION)
C      GIVEN ONE POINT ON A LINE, THIS SUBROUTINE WALKS AROUND
C      THE REST OF THE LINE, RECORDING THE REST OF THE LINE.
C      DIMENSION A(1),TCMK(4,1),ACONT(1)
C      DIMENSION K3(3),A2(3),A2(3),JJ(3),KK(3),K2(3)
C      DO 70 (10,11,12,13),KONS
C      ORIENTATION 1: UPWARD
C      JJ(1)=1
C      JJ(2)=J
C      JJ(3)=J+1
C      KK(1)=K
C      KK(2)=K+1
C      KK(3)=K
C      GO TO 15
C      ORIENTATION 2: TO THE RIGHT
C      JJ(1)=J
C      JJ(2)=J+1
C      JJ(3)=J+1
C      KK(1)=K
C      KK(2)=K
C      KK(3)=K+1
C      GO TO 15
C      ORIENTATION 3: DOWNWARD
C      JJ(1)=J+1
C      JJ(2)=J
C      JJ(3)=J
C      KK(1)=K+1
C      KK(2)=K
C      KK(3)=K
C      GO TO 15
C      ORIENTATION 4: TO THE LEFT
C      JJ(1)=J-1
C      JJ(2)=J-1
C      JJ(3)=J-1
C      KK(1)=K
C      KK(2)=K
C      KK(3)=K+1
C      K2(2)=1
C      K2(3)=2
C      SEARCH THE 3 POSSIBLE DIRECTIONS.
C      DO 17 N=1,3
C      CALL SEARCH(JJ(N),KK(N),K2(N),A,JOIN,TCMK,NXY,K3(N),NVAL,A1(N),
  6  A2(N),ACONT)
C      K35=K3(1)+K3(2)+K3(3)
C      TFLX35=11,2,19
C      BRANCH POINT
C      TFLX(KONS),N=1) GO TO 9
C      K6=K35
C      GO TO 4
C      ONE IN, ONE OUT. FIND WHERE OUT.
C      DO 3 N=1,3
C      TFLX(K6),EQ=1) GO TO 4
C      CONTINUE
C      RECORD THE POINT
C      CALL ENTER(K3(K6),JJ(K6),KK(K6),NVAL,A1(K6),A2(K6),JMIN,KMIN,TCMK,
  6  KONS,X,Y,NXY,ACONT,TST1)
C      RESET J AND K
C      J=JJ(K6)
C      K=KK(K6)
C      REF TO WE08 AT A BOUNDARY. IF SO, QUIT.
C      TFLX,CT,JMIN) GO TO 23
C      GO TO (70,19,24,23),KONS
C      TFLX,LT,JMAX) GO TO 19
C      GO TO (24,25,26,19),KONS
C      TFLX,EQ=1) GO TO 1
C      GO TO 10
C      TFLX,EQ=2) GO TO 1
C      GO TO 19
C      TFLX,EN=1) GO TO 1
C      IF K6,CT,KMIN) GO TO 27
C      GO TO (2,3,29,28),KONS
C      IF K6,LT,KMAX) GO TO 8
C      GO TO (29,28,9,20),KONS
C      TFLX,EQ=1) GO TO 1
C      GO TO 4
C      IF K6,EO=2) GO TO 1
C      GO TO 4
C      TFLX,EO=3) GO TO 1
C      PREPARE FOR NEXT STEP
C      KONS=KONS+K6-2
C      KONS=KONS+K6-2
C      TFLX(KONS,CT,4) KONS=KONS+4
C      TFLX(KONS,LT,1) KONS=KONS+4
C      GO TO 31
C      CONTINUE
C      KONS=0
C      RETURN
C      END

C      SUBROUTINE ARWATX(J,K,I)
C      COMMON/CON1/JMAX,KMAX,JN,KN,VMACH,ALPHA,GAM,GAM1,CM,DT,SMU,SPRT,
  6  CHOD,NFA,NCR,NCC,AA,M,OREGA,MU,ML,IT,TAU,ITPR,ENT,PTORT,PTMF,
  6  ARWATX
C      CON1
  6  3

```



```

      12 W=1.0/4.0
      13 W=1.0/4.0
      14 W=1.0/4.0
      15 W=1.0/4.0
      16 W=1.0/4.0
      17 W=1.0/4.0
      18 W=1.0/4.0
      19 W=1.0/4.0
      20 W=1.0/4.0
      21 W=1.0/4.0
      22 W=1.0/4.0
      23 W=1.0/4.0
      24 W=1.0/4.0
      25 W=1.0/4.0
      26 W=1.0/4.0
      27 W=1.0/4.0
      28 W=1.0/4.0
      29 W=1.0/4.0
      30 W=1.0/4.0
      31 W=1.0/4.0
      32 W=1.0/4.0
      33 W=1.0/4.0
      34 W=1.0/4.0
      35 W=1.0/4.0
      36 W=1.0/4.0
      37 W=1.0/4.0
      38 W=1.0/4.0
      39 W=1.0/4.0
      40 W=1.0/4.0
      41 W=1.0/4.0
      42 W=1.0/4.0
      43 W=1.0/4.0
      44 W=1.0/4.0
      45 W=1.0/4.0
      46 W=1.0/4.0
      47 W=1.0/4.0
      48 W=1.0/4.0
      49 W=1.0/4.0
      50 W=1.0/4.0
      51 W=1.0/4.0
      52 W=1.0/4.0
      53 W=1.0/4.0
      54 W=1.0/4.0
      55 W=1.0/4.0
      56 W=1.0/4.0
      57 W=1.0/4.0
      58 W=1.0/4.0
      59 W=1.0/4.0
      60 W=1.0/4.0
      61 W=1.0/4.0
      62 W=1.0/4.0
      63 W=1.0/4.0
      64 W=1.0/4.0
      65 W=1.0/4.0
      66 W=1.0/4.0
      67 W=1.0/4.0
      68 W=1.0/4.0
      69 W=1.0/4.0
      70 W=1.0/4.0
      71 W=1.0/4.0
      72 W=1.0/4.0
      73 W=1.0/4.0
      74 W=1.0/4.0
      75 W=1.0/4.0
      76 W=1.0/4.0
      77 W=1.0/4.0
      78 W=1.0/4.0
      79 W=1.0/4.0
      80 W=1.0/4.0
      81 W=1.0/4.0
      82 W=1.0/4.0
      83 W=1.0/4.0
      84 W=1.0/4.0
      85 W=1.0/4.0
      86 W=1.0/4.0
      87 W=1.0/4.0
      88 W=1.0/4.0
      89 W=1.0/4.0
      90 W=1.0/4.0
      91 W=1.0/4.0
      92 W=1.0/4.0
      93 W=1.0/4.0
      94 W=1.0/4.0
      95 W=1.0/4.0
      96 W=1.0/4.0
      97 W=1.0/4.0
      98 W=1.0/4.0
      99 W=1.0/4.0
      100 W=1.0/4.0

```

84000Y	8
84000Z	9
84000Y	10
84000Y	11
84000Y	12
84000Y	13
84000Y	14
84000Y	15
84000Y	16
84000Y	17
84000Y	18
84000Y	19
84000Y	20
84000Y	21
84000Y	22
84000Y	23
84000Y	24
84000Y	25
84000Y	26
84000Y	27
84000Y	28
84000Y	29
84000Y	30
84000Y	31
84000Y	32
84000Y	33
84000Y	34
84000Y	35
84000Y	36
84000Y	37
84000Y	38
84000Y	39
84000Y	40
84000Y	41
84000Y	42
84000Y	43
84000Y	44
84000Y	45
84000Y	46
84000Y	47
84000Y	48
84000Y	49
84000Y	50
84000Y	51
84000Y	52
84000Y	53
84000Y	54
84000Y	55
84000Y	56
84000Y	57
84000Y	58
84000Y	59
84000Y	60
84000Y	61
84000Y	62
84000Y	63
84000Y	64
84000Y	65
84000Y	66
84000Y	67
84000Y	68
84000Y	69
84000Y	70
84000Y	71
84000Y	72
84000Y	73
84000Y	74
84000Y	75
84000Y	76
84000Y	77
84000Y	78
84000Y	79
84000Y	80
84000Y	81
84000Y	82
84000Y	83
84000Y	84
84000Y	85
84000Y	86
84000Y	87
84000Y	88
84000Y	89
84000Y	90

[illegible]

```

C.....PERFORM INTEGRATION FROM / TO ANG DEGREES
C
  DO 15 I=1,IMAXM1
    PREDICTOR
      THETA1=THETA
      P=0.1*DELTA*(G(R1,THETA1)+G(R,THETA1))
      THETA=THETA+DELTA
      CORRECTOR
        P1=P+.5*DELTA*(G(R1,THETA1)+G(R,THETA1))
        P1=P
      CONTINUE
      Y1=Y-R*CMS(ANG)
      Y=Y+DELTA*ANG
      RETURN
C.....INTERPOLATE FROM USER-SUPPLIED BODY SHAPE
C
  35 CONTINUE
  DO 39 I=2,NR0D
    IF (ATAN2(Y(I),X(I)).GT. ANG) GO TO 4
  39 CONTINUE
  40 R1=SQRT(Y(I)**2+X(I)**2)
  R2=SQRT(Y(I-1)**2+X(I-1)**2)
  ANG1=ATAN2(Y(I),X(I))
  ANG2=ATAN2(Y(I-1),X(I-1))
  P=0.1*(ANG-ANG1)/(ANG2-ANG1)*(R2-R1)
  Y=1.0-P*CMS(ANG)
  Y=STN(ANG)*P
  RETURN
C.....DETERMINES BODY SHAPE WITH GRAVITATIONAL VARIATION IN 4
C
  45 CONTINUE
  IF (M.LT.1) GO TO 20
C.....PERFORM INTEGRATION FROM 3 TO ANG DEGREES
C
  DO 55 I=1,ISTART,IMAXM1
    AS=INT(THETA)
    AC=COS(THETA)
    THETA1=THETA
    CORRECTOR
      A1=F3(R,M)
      K=1
      DRX=F2(R1,AS,AC,A1)
      IF (DRX.LT.0) DRX=2.0*AS*AC
      P=1.0*DELTA*DELTA
      THETA=THETA+DELTA
      AS1=INT(THETA)
      AC1=COS(THETA)
    CORRECTOR
      51 CONTINUE
      A11=F3(R,M)
      DRX=F2(R,AS1,AC1,A11)
      IF (DRX.LT.0) DRX=2.0*AS1*AC1
      CLOPE=.5*(DRX+DRX1)
      P=1.0*DELTA*DELTA
      K=K+1
      IF (M.LT.3) GO TO 51
      Y=1.0-P*AC
      Y=P*AS1
      K=K
    CONTINUE
    RETURN
    ENH
  SURROUTINE BTRI(IL,IU)
    LFEEL 2,0,EF,5,6,AA
    COMMON /COM1/ Q(40,20,4),EF(40,4),*(40,20,4),G(4),AR(4,4)
    LEVEL 2, A,B,C,M0
    COMMON /COM4/ A(40,4,4),B(40,4,4),C(40,4,4),M0(40,4,4)
    REAL L11,L21,L22,L31,L32,L33,L41,L42,L43,L44
    COMMON /LUD/ L11,L21,L22,L31,L32,L33,L41,L42,L43,L44,V1,V2,V3,V4,
    * U12,U13,U14,U23,U24,U34
    DIMENSION H(4,4)
  INVERSION OF BLOCK TRIANGONAL... A,B,C ARE 4*4 BLOCKS
  EF IS FINISHING FUNCTION AND SOLUTION IS OUTPUT IN EF, 4 IS OVERLOADED
  BLOCK INVERSIONS USE NONPIVOTED LU DECOMPOSITION
  IL AND IU ARE STARTING AND FINISHING INDICES
  RTOT 2
  COM3 3
  COM4 3
  COM1 3
  LUD 2
  LUD 3
  RTOT 4
  RTOT 7
  RTOT 9
  RTOT 10
  IS = IL + 1
  I = IL
  DO 11 M=1,4
    DO 11 N=1,4
      11 H(M,N)=R(I,M,N)
      CALL LUDEC(M)
      R1 = V1*EF(I,1)
      R2 = V2*EF(I,2) - L21*R1
      R3 = V3*EF(I,3) - L31*R1 - L32*R2
      R4 = V4*EF(I,4) - L41*R1 - L42*R2 - L43*R3
      EF(I,4) = R4
      EF(I,3) = R3 - U34*R4
      EF(I,2) = R2 - U24*R4 - U23*EF(I,3)
      EF(I,1) = R1 - U14*R4 - U13*EF(I,3) - U12*EF(I,2)
      DO 12 M=1,4
        R1 = V1*EF(I,1,M)
        R2 = V2*EF(I,2,M) - L21*R1
        R3 = V3*EF(I,3,M) - L31*R1 - L32*R2
        R4 = V4*EF(I,4,M) - L41*R1 - L42*R2 - L43*R3
        H(I,4,M) = R4
        H(I,3,M) = R3 - U34*R4
        H(I,2,M) = R2 - U24*R4 - U23*EF(I,3,M)
        H(I,1,M) = R1 - U14*R4 - U13*EF(I,3,M) - U12*EF(I,2,M)
      C...FORWARD SVEEP
      12 CONTINUE
      DO 13 I=IS,IU
        I = I - 1
        DO 14 M=1,4
          EF(I,M) = EF(I,M) - A(I,M,1)*EF(I,1) - A(I,M,2)*EF(I,2)
          * -A(I,M,3)*EF(I,3) - A(I,M,4)*EF(I,4)
          DO 14 N=1,4
            H(I,M,N) = A(I,M,1)*EF(I,1,N) - A(I,M,2)*EF(I,2,N)
            * -A(I,M,3)*EF(I,3,N) - A(I,M,4)*EF(I,4,N)
          14 CONTINUE
          CALL LUDEC(M)
          R1 = V1*EF(I,1)
          R2 = V2*EF(I,2) - L21*R1
          R3 = V3*EF(I,3) - L31*R1 - L32*R2
          R4 = V4*EF(I,4) - L41*R1 - L42*R2 - L43*R3
          EF(I,4) = R4
          EF(I,3) = R3 - U34*R4
          EF(I,2) = R2 - U24*R4 - U23*EF(I,3)
          EF(I,1) = R1 - U14*R4 - U13*EF(I,3) - U12*EF(I,2)
          IF (I = IU) 16,13,13
        15 CONTINUE
        DO 15 M=1,4
          R1 = V1*EF(I,1,M)
          R2 = V2*EF(I,2,M) - L21*R1
          R3 = V3*EF(I,3,M) - L31*R1 - L32*R2
          R4 = V4*EF(I,4,M) - L41*R1 - L42*R2 - L43*R3
          H(I,4,M) = R4
          H(I,3,M) = R3 - U34*R4
          H(I,2,M) = R2 - U24*R4 - U23*EF(I,3,M)
          H(I,1,M) = R1 - U14*R4 - U13*EF(I,3,M) - U12*EF(I,2,M)
        15 CONTINUE
        13 CONTINUE
      C...BACK SUBSTITUTION
      IT = IL + IU
      DO 21 T = IS,IU
        T = IT - IT
        T = T + 1
        DO 22 M=1,4
          EF(T,M) = EF(T,M) - A(I,M,1)*EF(I,1) - A(I,M,2)*EF(I,2)
          * -A(I,M,3)*EF(I,3) - A(I,M,4)*EF(I,4)
        22 CONTINUE
        21 CONTINUE
      RETURN
      ENH
  SURROUTINE DISSIP
    COMMON /COM1/ JMAX,KMAX,JM,KM,XHACH,ALPHA,GAM,GAMH1,CM,DT,SMU,TPRT,
    * CMOR0,MCA,MCA,MCC,AA,M,MEGA,MU,ML,IT,TAU,ITER,EXT,PTOT,*INF,
    * RINF,DIRF,CINF,JCS,TM,CLUS,PT,MORN,RMSE,MCA5F,MPUNCH
    LEVEL 2,X,Y,XET,XEX,XEY,D
    COMMON /COM2/ X(40,20),Y(40,20),XET(40,20,2),XEX(40,20,2),
    * XEY(40,20,2),D(40,20)
    LEVEL 2,0,EF,5,6,AA
    COMMON /COM3/ Q(40,20,4),EF(40,4),*(40,20,4),G(4),AR(4,4)
  C...SMOOTH IN THE X AND Y DIRECTIONS AND ADD SMOOTHING TERM TO S ARRAY
    KRM=KRM-1
    DISSIP 2
    COM1 2
    COM1 3
    COM1 4
    COM2 2
    COM2 3
    COM2 4
    COM3 2
    COM3 3
    DISSIP 6
    DISSIP 7

```


[illegible][illegible]

SUBROUTINE FICEN	FICEN	2
COMMON /C0M1/ JMAX,KMAX,JM,KM,XMACH,ALF4,GAM,GAMH1,CN,DT,CSM1,TTOT,	C0M1	3
CM,CMH2,CMC,KMCC,CM,CMGEM,MM1,M1,DT,TAIL,XTF,ENT,TOTRT,PINF,	C0M1	4
C0TNE,CNFC,CINF,JCS,TM,CLUS,DT,KMGR,QNCS,MCAS1,MDINFC	C0M1	5
LEVEL,CM,XE1,XE2,XE3,VEY0,	C0M2	2
COMMON /C0M2/ I(40,20),Y(40,20),X(40,20),Y(40,20),	C0M2	3
CM,VEY(40,20),Z(40,20)	C0M2	4
LEVEL,CM,DT,VEY0,GA0	C0M3	2
COMMON /C0M3/ Q(40,20,4),F(40,4),S(40,20,4),C(4),AP(4,4)	C0M3	3
C...COMPUTE STEPSIZE GIVEN CURRENT NUMBER	FICEN	6
IF(TTOT,DT,CS) WRITE(6,103)	FICEN	7
FICEN=0.0	FICEN	8
DO 1 J=JMAX	FICEN	9
DO 1 J=JMAX	FICEN	10

[illegible]

CH0001TIME INITIA	INITIA	9
COMMON/CPM1/JMAX,KMAX,JM,KM,KMAX,ALPHA,GAM,GAMM1,CM,PT,SMI,IPRT,	CM1	2
>CHP001/CM1/NFC,NFC,AA,OMFGL,NII,NL,VT,TAI,ITZO,INT,PTORT,PINF,	CM1	3
<CHIE,CINFC,CINFC,JCS,TC,CIIIS,PT,MMRM,QMPC,NFC,FE,MDUNC	CM1	4
LEVFL=,V,V,XET,XEY,XEY,0	CM1	5
COMMON /CM2/ 1,4,3,2,1,YE4,2,3, XET(4,2,3),XEY(4,2,3),2,1,	CM2	6
* XEY(4,2,3),2,1,DIF4,-2C1	CM2	7
LEVFL=,0,0,5,C,F,AB	CM2	8
COMMON /CM3/ 0(4),2,4,1,EF(4,4),S(4,2,4),C(4),AP(4,4)	CM3	9
LEVFL=,2,4,2,4,4N	CM4	2
COMMON /CM4/ 4(4C,4,4),P(4C,4,4),C(4),4,4,4,4(4C,4,4,4)	CM4	3
PTA,14579256	INITIA	7
DANTA=,2057795]	INITIA	8
CTNF=]C	INITIA	9
CTNF=.C	INITIA	10
TPD Ta.	INITIA	11
ALPHA=.C	INITIA	12
JPM=]	INITIA	13
OMPC=,1,1	INITIA	14
CM1=.4	INITIA	15
CTNF=SDPT(PTNF+GAM/PINF)	INITIA	16
ALPHA=ALPHA/PAI	INITIA	17
CTNF=YMPC+CTNF	INITIA	18
CTNF=QTNF/OS(ALPH4)	INITIA	19
YMPC=QTNF+S(ALPH4)	INITIA	20
JM=JMAX=1	INITIA	21
KM=KMAX=1	INITIA	22
GAMM=CM=1.:	INITIA	23
CM=]T=1./GAMM1	INITIA	24
TAU=0.7	INITIA	25

[illegible]

```

P5=(2.0*GAN*XY-GAMH1)/GAMP1*PINF
P6=GAMP1*XX/(GAMH1*XX+2.0)*PINF
P5=(1.0-2.0*P5-1.0)*GAMH1*FXMACH**21*QINF
V5=2.0*P5*(1.0)*COS(SANG)/(GA*P1*XMACH**2)*SIN(SANG))*QINF
IF(JLGT,2) GO TO 3
Y1=(2.0*GAN*XMACH**2-GAMH1)/(GAN+1.0)
Y2=(GAN+1.0)*XMACH**2/(GAMH1*XMACH**2+2.0)
P1=X1*PINF
P2=X2*PINF
ENTP1/P1**GAN
P1=(1.0*FX1)**(1.0/GAMH1)*(0.5*(GAN+1.0)*YHAC**2)**(GAN/GAMH1)*PINF
Y1=L.0*0.5*GAMH1*XMACH**2
PTORT=X2*PINF/RINF
3 CONTINUE
PB=PINF*(1*P/PINF-1.0)*(1.0-1.02*SIN(THET))*2*0.12*SIN(THET)**4+
  1.0)
RR=(PR/ENT)**(1.0/GAM)
OR=SQRT(2.0*GAN/GAMH1*AS(PTORT-PB/RR))
YY=PI*0.5*THET
VU=OR*OS(VV)
VR=OR*OS(VV)
ZKM=KMAX-1
DO 2 K=1,KMAX
  VV=FLOAT(K-1)/ZKM
  PPESS=PV*VV*(PS-PB)
  RMD=OR*VV*(RS-RB)
  VVEL=UR*VV*(US-UR)
  VVEL=VR*VV*(VS-VB)
  OI=L.0/FF(K)
  OI(J,K,1)=RMD*DI
  OI(J,K,2)=RMD*VVEL*DI
  OI(J,K,3)=RMD*VVEL*DI
  2 OI(J,K,4)=(PPESS*GAMH1+RMD*(VVEL**2+VVEL**2)*0.5)*DI
C...SELECT METRICS AND DEPENDENT VARIABLES ABOUT PLANE OF SYMMETRY
DO 4 K=1,KMAX
  ND=(L.0)*JCS
  ND=(L.0)*JCS
  OI(K,1)=PI, K1=OD
  YEX(1,K,1)=YEX(2,K,1)
  YEX(1,K,1)=YEX(2,K,1)
  YEX(1,K,2)=YEX(2,K,2)
  YEX(1,K,2)=YEX(2,K,2)
  DO 3 N=1,4
  3 OI(K,N)=OI(2,K,N)*DD
  4 OI(K,3)=OI(2,K,3)*DD
  RETURN
END

```

```

INITIA 53
INITIA 54
INITIA 55
INITIA 56
INITIA 57
INITIA 58
INITIA 59
INITIA 60
INITIA 61
INITIA 62
INITIA 63
INITIA 64
INITIA 65
INITIA 66
INITIA 67
INITIA 68
INITIA 69
INITIA 70
INITIA 71
INITIA 72
INITIA 73
INITIA 74
INITIA 75
INITIA 76
INITIA 77
INITIA 78
INITIA 79
INITIA 80
INITIA 81
INITIA 82
INITIA 83
INITIA 84
INITIA 85
INITIA 86
INITIA 87
INITIA 88
INITIA 89
INITIA 90
INITIA 91
INITIA 92
INITIA 93
INITIA 94
INITIA 95
INITIA 96
INITIA 97
INITIA 98
INITIA 99

```

```

TAU=TAU+DT
RETURN
END

```

```

INTEGR 31
INTEGR 32
INTEGR 33

```

```

SUBROUTINE LBLTRAK1
COMMON/COM1/JMAX,KMAX,JM,KH,KNACH,ALPHA,GAM,GAMH1,CH,DT,SHU,TPRT,
  > CHORD,NCA,NCC,NCC,AA,4,OMEGA,MU,ML,IT,TAU,ITER,ENT,PTORT,PINF,
  <PINF,OTNF,CINF,JCS,TH,CLUS,PT,HORN,RNOSE,NCASE,NPUNCH
LEVEL 2,0,EF,S,G,AB
COMMON /COM3/ Q(40,20,4),EF(40,4),S(40,20,4),G(4),AR(4,4)
LEVEL 2, 4, R,C,MD
COMMON /COM4/ A(40,4,4),A(40,4,4),C(40,4,4),MD(40,4,4)
DO 1 J=1,JMAX
  CALL AMATX(J,K,1)
  DO 1 M=1,4
  DO 1 L=1,4
    1 MD(J,L,M)=A(J,L,M)
  C...FILL OFF-DIAGONAL AND DIAGONAL ELEMENTS BASED ON A 2-ND ORDER
  C...CENTRAL DIFFERENCE
  DO 2 J=2,JM
  DO 2 M=1,4
  DO 3 L=1,4
    A(J,L,M)=MD(J-1,L,M)*M
    A(J,L,M)=MD(J-1,L,M)*M
    3 C(J,L,M)=MD(J+1,L,M)*M
  C...FILL FORCING FUNCTION FROM S ARRAY
  FF(J,M)=S(J,K,M)
  C...SET R ON THE DIAGONAL REPRESENTING THE IDENTITY MATRIX TO ONE
  2 R(J,M,M)=1.0
  RETURN
END

```

```

LBLTRA 2
COM1 2
COM1 3
COM1 4
COM1 4
COM3 2
COM3 3
COM4 2
COM4 3
LBLTRA 6
LBLTRA 7
LBLTRA 9
LBLTRA 10
LBLTRA 11
LBLTRA 12
LBLTRA 13
LBLTRA 14
LBLTRA 15
LBLTRA 16
LBLTRA 17
LBLTRA 18
LBLTRA 19
LBLTRA 20
LBLTRA 21
LBLTRA 22
LBLTRA 23
LBLTRA 24
LBLTRA 25

```

```

SUBROUTINE LBLTR(J)
COMMON/COM1/JMAX,KMAX,JM,KH,KNACH,ALPHA,GAM,GAMH1,CH,DT,SHU,TPRT,
  > CHORD,NCA,NCC,NCC,AA,4,OMEGA,MU,ML,IT,TAU,ITER,ENT,PTORT,PINF,
  <PINF,OTNF,CINF,JCS,TH,CLUS,PT,HORN,RNOSE,NCASE,NPUNCH
LEVEL 2,0,EF,S,G,AB
COMMON /COM3/ Q(40,20,4),EF(40,4),S(40,20,4),G(4),AR(4,4)
LEVEL 2, 4, R,C,MD
COMMON /COM4/ A(40,4,4),A(40,4,4),C(40,4,4),MD(40,4,4)
DO 1 K=1,KMAX
  CALL LBLTR(K,2)
  DO 1 M=1,4
  DO 1 L=1,4
    1 MD(K,L,M)=A(K,L,M)
  C...FILL OFF-DIAGONAL AND DIAGONAL ELEMENTS BASED ON A 2-ND ORDER
  C...CENTRAL DIFFERENCE
  DO 2 J=2,KH
  DO 2 M=1,4
  DO 3 L=1,4
    A(K,L,M)=MD(K-1,L,M)*M
    A(K,L,M)=MD(K-1,L,M)*M
    3 C(K,L,M)=MD(K+1,L,M)*M
  C...FILL FORCING FUNCTION FROM S ARRAY
  FF(M,M)=S(J,K,M)
  C...SET R ON THE DIAGONAL REPRESENTING THE IDENTITY MATRIX TO ONE
  2 R(K,M,M)=1.0
  RETURN
END

```

```

LBLTRA 2
COM1 2
COM1 3
COM1 4
COM1 4
COM3 2
COM3 3
COM4 2
COM4 3
LBLTRA 6
LBLTRA 7
LBLTRA 9
LBLTRA 10
LBLTRA 11
LBLTRA 12
LBLTRA 13
LBLTRA 14
LBLTRA 15
LBLTRA 16
LBLTRA 17
LBLTRA 18
LBLTRA 19
LBLTRA 20
LBLTRA 21
LBLTRA 22
LBLTRA 23
LBLTRA 24
LBLTRA 25

```

```

SUBROUTINE LUDEC(A)
DIMENSION A(4,4)
REAL L11,L22,L22,L31,L32,L33,L41,L42,L43,L44
COMMON /LUD/ L11,L21,L22,L31,L32,L33,L41,L42,L43,L44,V1,V2,V3,V4,
  * U12,U13,U14,U23,U24,U34
C SUBROUTINE COMPUTES L-U DECOMPOSITION ELEMENTS
L11 = A(1,1)
V1 = 1./L11

```

```

LUDEC 2
LUDEC 3
LUD 3
LUD 4
LUD 4
LUDEC 5
LUDEC 6
LUDEC 7

```

```

U12 = V10*(1,2)
U13 = V10*(1,3)
U14 = V10*(1,4)
L21 = A(2,1)
L22 = A(2,2) - L21*U12
V2 = 1./L22
H2 = ( A(2,3) -L21*U13)+ V2
H24 = ( A(2,4) - L21*U14)+ V2
L31 = A(3,1)
L32 = A(3,2) - L31*U12
L33 = A(3,3) - L31*U13 -L32*U23
V3 = 1./L33
H34 = ( A(3,4) - L31*U14 - L32*U24)+ V3
L41 = A(4,1)
L42 = A(4,2) - L41*U12
L43 = A(4,3) - L41*U13 - L42*U23
L44 = A(4,4) - L41*U14 -L42*U24 -L43*U34
V4 = 1./L44
RETURN
END

SUBROUTINE NOLPTS
COMMON/CON1/JMAX,KMAX,JH,KH,XHACH,ALPHA,GAM,GAMH1,CN,DT,SMU,IPRT,
+ CMOD,NCI,NCB,HCC,AA,MO,MEGA,MU,NL,IT,TAU,ITER,ENT,PTORT,PINF,
+ CMNF,OMF,CINF,JCS,TR,CLUS,PT,MORN,RNDS,NCASE,NPUNCH
LEVEL 2,K,X,Y,XET,XEY,XEYD
COMMON /CM2/ X(40,2),Y(40,2),XET(40,2),XEY(40,2),
+ XEY(40,2),D(40,2)
LOGICAL LPRUN,LPRFL,LPRST,LPRCON,LPRH,LPLT,LTRAJ,LRSTRT
COMMON /PPORT/ LPRUN,LPRFL,LPRST,LPRCON,LPRH,LPLT,LTRAJ,LRSTRT
COMMON /NLUNT/ THETA(25),RPI(25,25),NBLUNT
C.....THIS SUBROUTINE DETERMINES THE X AND Y LOCATIONS OF THE NODE POINTS
C.....FOR CYLINDER, 3-D FOR SPHERE.
DELTA=(GAMH1*XHACH**2+2.*C)/(GAMH1.0+XHACH**2)*DT*78.3,C**PI-(JCS-
+ 1.25)*0.44)/AA**JCS
IF (MORN.LT. 0.0) GO TO 13
IF MORN.LT. 0.1 .AND. MORN.GT. C.JION TO 14
ANG=93./57.2957795
DELTA=DELTA**1.2710+0.0090*XHACH*(0.904+0.659*MORN)
DELTA=DELTA**13.95+0.394*MORN+0.854*MORN**2)*VQD
DELTA=1.3*(GAMH1*XHACH**2+2.)/(GAMH1.0+XHACH**2)*DT*0.9+0.5*MORN)
C.....CONTINUE
DO 40 J=2,JMAX
C.....BODY SHAPE
THETA=(PI*AT(13)-1.5)*DT*MET
IF (LRSTRT) THETA=ATAN2(Y(1,1),X(J,1))
CALL MODV(YA,XH,RNDS,THET,MORN)
YA=YA
C.....SMALL SHAPE
IF (LRSTRT) GO TO 20
IF (MORN.LT. 0.0) GO TO 15
IF (MORN.LT.0.1 .AND. MORN.GT.C.3) GO TO 15
IF (J.GT. NBLUNT) GO TO 12
ANG=DELTA**2*(1.-SIN(THET)**2)/SIN(THET)**2/(1.+DELTA)
FOURACC=0.498*(1.+DELTA)
YA=1.4*(MORN-SORT(RNDS**2+FOURACC))*0.5
THET=90.-5.70796326679
IF (THET-THET90) .GT. C.5)XA=1.+(BRN*SORT(499**2+FOURACC))*0.5
YA=DELTA*SORT((1.+DELTA)-(1.-YA))/SORT(1.+DELTA)
GO TO 30
C.....CONTINUE
IF (J.GT. NBLUNT) THET=ATAN2(YA,1.-YA)
DELTA=1.4*(0.6+0.4*THET**2+0.16*THET**4)*DELTA
IF (J.GT. NBLUNT) GO TO 17
YA=1.0-(1.-DELTA)*COS(THET)
17 YA=(1.-DELTA)*SIN(THET)
GO TO 30
2. CONTINUE
YA=X(J,KHAX)
YA=Y(J,KHAX)
C.....CALCULATE MODAL POINTS
3C CONTINUE
XK=XHAX-1
OX=(XA-XH)/ZKH
OY=(YA-YH)/ZKH
NO 40 K=1,KHAX
ZK=K-1
NOLPTS 2
NOLPTS 3
NOLPTS 4
NOLPTS 5
NOLPTS 6
NOLPTS 7
NOLPTS 8
NOLPTS 9
NOLPTS 10
NOLPTS 11
NOLPTS 12
NOLPTS 13
NOLPTS 14
NOLPTS 15
NOLPTS 16
NOLPTS 17
NOLPTS 18
NOLPTS 19
NOLPTS 20
NOLPTS 21
NOLPTS 22
NOLPTS 23
NOLPTS 24
NOLPTS 25
NOLPTS 26
NOLPTS 27
NOLPTS 28
NOLPTS 29
NOLPTS 30
NOLPTS 31
NOLPTS 32
NOLPTS 33
NOLPTS 34
NOLPTS 35
NOLPTS 36
NOLPTS 37
NOLPTS 38
NOLPTS 39
NOLPTS 40
NOLPTS 41
NOLPTS 42
NOLPTS 43
NOLPTS 44
NOLPTS 45
NOLPTS 46
NOLPTS 47
NOLPTS 48
NOLPTS 49
NOLPTS 50
NOLPTS 51
NOLPTS 52
NOLPTS 53
NOLPTS 54
NOLPTS 55
NOLPTS 56
NOLPTS 57
NOLPTS 58
NOLPTS 59
NOLPTS 60
NOLPTS 61
NOLPTS 62
NOLPTS 63
NOLPTS 64
NOLPTS 65
NOLPTS 66
NOLPTS 67
NOLPTS 68
NOLPTS 69
NOLPTS 70
NOLPTS 71
NOLPTS 72
NOLPTS 73
NOLPTS 74
NOLPTS 75
NOLPTS 76
NOLPTS 77
NOLPTS 78
NOLPTS 79
NOLPTS 80
NOLPTS 81
NOLPTS 82
NOLPTS 83
NOLPTS 84
NOLPTS 85
NOLPTS 86
NOLPTS 87
NOLPTS 88
NOLPTS 89
NOLPTS 90
NOLPTS 91
NOLPTS 92
NOLPTS 93
NOLPTS 94
NOLPTS 95
NOLPTS 96
NOLPTS 97
NOLPTS 98
NOLPTS 99
NOLPTS 100
NOLPTS 101
NOLPTS 102
NOLPTS 103
NOLPTS 104
NOLPTS 105
NOLPTS 106
NOLPTS 107
NOLPTS 108
NOLPTS 109
NOLPTS 110
NOLPTS 111
NOLPTS 112
NOLPTS 113
NOLPTS 114
NOLPTS 115
NOLPTS 116
NOLPTS 117
NOLPTS 118
NOLPTS 119
NOLPTS 120
NOLPTS 121
NOLPTS 122
NOLPTS 123
NOLPTS 124
NOLPTS 125
NOLPTS 126
NOLPTS 127
NOLPTS 128
NOLPTS 129
NOLPTS 130
NOLPTS 131
NOLPTS 132
NOLPTS 133
NOLPTS 134
NOLPTS 135
NOLPTS 136
NOLPTS 137
NOLPTS 138
NOLPTS 139
NOLPTS 140
NOLPTS 141
NOLPTS 142
NOLPTS 143
NOLPTS 144
NOLPTS 145
NOLPTS 146
NOLPTS 147
NOLPTS 148
NOLPTS 149
NOLPTS 150
NOLPTS 151
NOLPTS 152
NOLPTS 153
NOLPTS 154
NOLPTS 155
NOLPTS 156
NOLPTS 157
NOLPTS 158
NOLPTS 159
NOLPTS 160
NOLPTS 161
NOLPTS 162
NOLPTS 163
NOLPTS 164
NOLPTS 165
NOLPTS 166
NOLPTS 167
NOLPTS 168
NOLPTS 169
NOLPTS 170
NOLPTS 171
NOLPTS 172
NOLPTS 173
NOLPTS 174
NOLPTS 175
NOLPTS 176
NOLPTS 177
NOLPTS 178
NOLPTS 179
NOLPTS 180
NOLPTS 181
NOLPTS 182
NOLPTS 183
NOLPTS 184
NOLPTS 185
NOLPTS 186
NOLPTS 187
NOLPTS 188
NOLPTS 189
NOLPTS 190
NOLPTS 191
NOLPTS 192
NOLPTS 193
NOLPTS 194
NOLPTS 195
NOLPTS 196
NOLPTS 197
NOLPTS 198
NOLPTS 199
NOLPTS 200
NOLPTS 201
NOLPTS 202
NOLPTS 203
NOLPTS 204
NOLPTS 205
NOLPTS 206
NOLPTS 207
NOLPTS 208
NOLPTS 209
NOLPTS 210
NOLPTS 211
NOLPTS 212
NOLPTS 213
NOLPTS 214
NOLPTS 215
NOLPTS 216
NOLPTS 217
NOLPTS 218
NOLPTS 219
NOLPTS 220
NOLPTS 221
NOLPTS 222
NOLPTS 223
NOLPTS 224
NOLPTS 225
NOLPTS 226
NOLPTS 227
NOLPTS 228
NOLPTS 229
NOLPTS 230
NOLPTS 231
NOLPTS 232
NOLPTS 233
NOLPTS 234
NOLPTS 235
NOLPTS 236
NOLPTS 237
NOLPTS 238
NOLPTS 239
NOLPTS 240
NOLPTS 241
NOLPTS 242
NOLPTS 243
NOLPTS 244
NOLPTS 245
NOLPTS 246
NOLPTS 247
NOLPTS 248
NOLPTS 249
NOLPTS 250
NOLPTS 251
NOLPTS 252
NOLPTS 253
NOLPTS 254
NOLPTS 255
NOLPTS 256
NOLPTS 257
NOLPTS 258
NOLPTS 259
NOLPTS 260
NOLPTS 261
NOLPTS 262
NOLPTS 263
NOLPTS 264
NOLPTS 265
NOLPTS 266
NOLPTS 267
NOLPTS 268
NOLPTS 269
NOLPTS 270
NOLPTS 271
NOLPTS 272
NOLPTS 273
NOLPTS 274
NOLPTS 275
NOLPTS 276
NOLPTS 277
NOLPTS 278
NOLPTS 279
NOLPTS 280
NOLPTS 281
NOLPTS 282
NOLPTS 283
NOLPTS 284
NOLPTS 285
NOLPTS 286
NOLPTS 287
NOLPTS 288
NOLPTS 289
NOLPTS 290
NOLPTS 291
NOLPTS 292
NOLPTS 293
NOLPTS 294
NOLPTS 295
NOLPTS 296
NOLPTS 297
NOLPTS 298
NOLPTS 299
NOLPTS 300
NOLPTS 301
NOLPTS 302
NOLPTS 303
NOLPTS 304
NOLPTS 305
NOLPTS 306
NOLPTS 307
NOLPTS 308
NOLPTS 309
NOLPTS 310
NOLPTS 311
NOLPTS 312
NOLPTS 313
NOLPTS 314
NOLPTS 315
NOLPTS 316
NOLPTS 317
NOLPTS 318
NOLPTS 319
NOLPTS 320
NOLPTS 321
NOLPTS 322
NOLPTS 323
NOLPTS 324
NOLPTS 325
NOLPTS 326
NOLPTS 327
NOLPTS 328
NOLPTS 329
NOLPTS 330
NOLPTS 331
NOLPTS 332
NOLPTS 333
NOLPTS 334
NOLPTS 335
NOLPTS 336
NOLPTS 337
NOLPTS 338
NOLPTS 339
NOLPTS 340
NOLPTS 341
NOLPTS 342
NOLPTS 343
NOLPTS 344
NOLPTS 345
NOLPTS 346
NOLPTS 347
NOLPTS 348
NOLPTS 349
NOLPTS 350
NOLPTS 351
NOLPTS 352
NOLPTS 35
```

```

RETURN
103 FORMATE(140,37X,32M<<< CONSERVATIVE VARIABLES >>>>)
104 FORMATE(3MOK=I2/F4X,1M3,6X,2HE1,10X,2HE2,10X,2HE3,10X,2HE4,10X,
> 2HF1,10X,2HF2,10X,2HF3,10X,2HF4/)
105 FORMATE(115,2E12,4)
107 FORMATE(140,32M<<< X ERROR IN HT =>E12,4,3X,22HRMS OF T ERROR IN HT
> =>E12,4,3X >>>)
108 FORMATE(1M3,3X,1M3,4X,1M3,8X,1M3,11X,1M3,10X,4M1-T,8X,4M1-X,8X,
> 4M1-Y,7X,5M1A-T,7X,5M1A-X,7X,5M1A-Y,8X,1M3/)
109 FORMATE(215,0E12,6)
110 FORMATE(5M,7SL=>F7,4,3X,4M1SL=>F7,4)
111 FORMATE(726H FINAL SONIC LINE LOCATION/)
END

```

```

OUTPUT 67
OUTPUT 68
OUTPUT 69
OUTPUT 70
OUTPUT 71
OUTPUT 72
OUTPUT 73
OUTPUT 74
OUTPUT 75
OUTPUT 76
OUTPUT 77
OUTPUT 78
OUTPUT 79

```

```

SUBROUTINE RMS
COMMON/COM1/JMAX,KMAX,JH,KH,XHAC4,ALPHA,GAM,GAMH1,CN,DT,SHU,IPRT,
> CND0D,NCA,NCB,NCC,AA,4,MDEGA,MU,NL,IT,TAU,ITER,ENT,PTORT,PINF,
> CINF,OTMF,CINF,JCS,TH,CLUS,PT,MORH,MNOCSE,NFASF,NPUNCH
LEVEL 2,X,Y,XET,XEX,XEY,D
COMMON /COM2/ X(4),Z(4),Y(4),Z(4),XET(4),Z(4),Y(4),Z(4),
> XEY(4),Z(4),Y(4),Z(4)
LEVEL 2,0,EF,5,6,4H
COMMON /COM3/ O(40,20,4),EF(4),4),S(40,20,4),G(4),A(4,4)
C...THIS SUBROUTINE COMPUTES THE RIGHT HAND SIDE OF THE DELTA FORM
C...EQUATION
C...FORM E CONSERVATIVE VARIABLES AND DIFFERENCE. STORE IN THE S ARRAY
DO 1 K=2,KH
DO 2 J=1,JMAX
CALL ECOM(J,K,1)
DO 2 M=1,4
2 EF(J,M)=G(M)
C...CENTRAL DIFFERENCE E CONSERVATIVE VARIABLE
DO 1 M=1,4
DO 1 J=2,JH
1 EF(J,M)=(EF(J+1,M)-EF(J-1,M))*M
C...FORM F CONSERVATIVE VARIABLES AND DIFFERENCE. AND TO PREVIOUS S
C...ARRAY
DO 3 K=2,KH
DO 4 M=1,4
CALL ECOM(J,K,2)
DO 4 N=1,4
4 EF(K,M)=G(M)
C...CENTRAL DIFFERENCE F CONSERVATIVE VARIABLE
DO 3 M=1,4
DO 3 K=2,KH
3 EF(K,M)=(EF(K+1,M)-EF(K-1,M))*M
RETURN
END

```

```

RMS 2
COM1 2
COM1 3
COM1 4
COM2 2
COM3 3
RMS 5
RMS 6
RMS 7
RMS 8
RMS 9
RMS 10
RMS 11
RMS 12
RMS 13
RMS 14
RMS 15
RMS 16
RMS 17
RMS 18
RMS 19
RMS 20
RMS 21
RMS 22
RMS 23
RMS 24
RMS 25
RMS 26
RMS 27
RMS 28
RMS 29
RMS 30

```

```

SUBROUTINE SHOCK
COMMON/COM1/JMAX,KMAX,JH,KH,XHAC4,ALPHA,GAM,GAMH1,CN,DT,SHU,IPRT,
> CND0D,NCA,NCB,NCC,AA,4,MDEGA,MU,NL,IT,TAU,ITER,ENT,PTORT,PINF,
> CINF,OTMF,CINF,JCS,TH,CLUS,PT,MORH,MNOCSE,NFASF,NPUNCH
LEVEL 2,X,Y,XET,XEX,XEY,D
COMMON /COM2/ X(4),Z(4),Y(4),Z(4),XET(4),Z(4),Y(4),Z(4),
> XEY(4),Z(4),Y(4),Z(4)
LEVEL 2,0,EF,5,6,4H
COMMON /COM3/ O(40,20,4),EF(4),4),S(40,20,4),G(4),A(4,4)
COMMON /COM4/ P(40,3),PX(140),ETA(140),U(40,3),V(140),UETA(40),
> V(40,3),VXI(40),VETA(40),R(40,3)
C...COMPUTE THE FLOW VARIABLES ONE MESH INTERVAL BEFORE SHOCK
RMS=0.0
OSEM=3.0
JHM=JMAX-2
JKN=KMAX-1
DO 3 K=1,3
DO 3 J=1,JMAX
KK=KMAX-3+K
J=J-1+J*(J,K,1)
R(J,K)=O(J,KK,1)*O(J,KK)
U(J,K)=O(J,KK,2)*O
V(J,K)=O(J,KK,3)*O
E2=O(J,KK,4)*O(J,KK)
3 R(J,K)=(E2-0.5*R(J,K))*O(J,K,1)*O2+V(J,K,1)*O2+GAMH1
C...COMPUTE P=1, U=XI, P=ETA, U=ETA, AND V=ETA DERIVATIVES
DO 4 J=2,JH
PVI(J)=(P(J+1,3)-P(J-1,3))*O.5
UXI(J)=(U(J+1,3)-U(J-1,3))*O.5

```

```

SHOCK 2
COM1 2
COM1 3
COM1 4
COM2 2
COM2 3
COM2 4
COM2 5
COM2 6
COM2 7
COM2 8
COM2 9
COM2 10
COM2 11
COM2 12
COM2 13
COM2 14
COM2 15
COM2 16
COM2 17
COM2 18
COM2 19
COM2 20
COM2 21
COM2 22
COM2 23
COM2 24
COM2 25
COM2 26
COM2 27
COM2 28
COM2 29
COM2 30

```

```

4 VXI(J)=(V(J+1,3)-V(J-1,3))*O.5
PXI(J)=(P(J+1,3)-P(J-1,3))*O.5
UXI(J)=(U(J+1,3)-U(J-1,3))*O.5
VXI(J)=(V(J+1,3)-V(J-1,3))*O.5
UXI(J)=(U(J+1,3)-U(J-1,3))*O.5
VXI(J)=(V(J+1,3)-V(J-1,3))*O.5
DO 5 J=1,JMAX
PETA(J)=(P(J+1,3)-P(J-1,3))*O.5
UETA(J)=(U(J+1,3)-U(J-1,3))*O.5
VETA(J)=(V(J+1,3)-V(J-1,3))*O.5
TF(J,E0,1,CR,J,E0,JMAX) GO TO 5
P(J,7)=P(J+1,3)+P(J-1,3)-2.0*P(J,3)
5 CONTINUE
P(1,2)=P(2,2)
P(JMAX,2)=3.0
DO 1 J=1,JMAX
K=KMAX
C...DETERMINE SHOCK ANGLE DELTA=ARCTAN(-ETAY/ETAX) J,KMAX
DELTA=ATAN(-XEY(J,K,2)/XEX(J,K,2))
SN=SIN(DELTA)
CN=COS(DELTA)
U1=U1*CN+O1
HNA=VEY(J,K,1)+U(J,3)*VEY(J,K,1)+V(J,3)*VEY(J,K,1)
VNA=VEY(J,K,2)+U(J,3)*VEY(J,K,2)+V(J,3)*VEY(J,K,2)
RCS=CND0D/J,3)
PTAU=HNA*PVI(J,1)-VNA*PVI(J,1)-RCS*O1*UXI(J,K,1)+
> VXI(J)*VEY(J,K,1)+VETA(J)*VEY(J,K,2)+VETA(J)*VEY(J,K,2)+
> IV(J,3)/V(J,K,1)*FLOAT(JCS)
P2=P(J,3)+PTAU*DT*O.2*O.1*P(J,2)
TF(J,E0,JMAX)P2=2.0*P(JH,3)-P(JH-1,3)
IF(P2,LE,3.0) GO TO 6
7 GAM=1.0
KNA=O1*P2/5/GAM*P2/PINF*2+GAMH1)
OS=CTH*P2*PINF-UIT
PA=P(J,3)
PB=P(J,3)
VA=U(J,3)
VB=V(J,3)
SA=PA/GAMH1*O.5*P2*(UO2+V2*O2)
U2=2.0*(1.0-XH*O2)*CINF/(GAM+1.0)*XHX*UIT
R2=THF*(P2/PINF+GAMH1/2)/(1.0+GAMH1*7*P2/PINF)
U2=OTMF*O2*O2*U2*O2
V2=OTMF*O2*O2*V2*O2
E2=P2/GAMH1*O.5*P2*(U2+V2*O2)
C...COMPUTE CONSERVATIVE VARIABLES AT SHOCK
K=KMAX
RT=1.0/P(J,K)
O(J,K,1)=R2*O1
O(J,K,2)=R2*O2*O1
O(J,K,3)=R2*O2*O1
O(J,K,4)=R2*O1
C...DETERMINE ANGLE OF XI=CONST LINE WITH X-AXIS
K=KMAX
TF(ARS(XEY(J,K,1))-0.037001) 7,7,0
7 THETA=1.5779633
GO TO 9
9 CONTINUE
THETA=ATAN(XEY(J,K,1)/XEX(J,K,1))
10 CONTINUE
C...COMPUTE SHOCK SPEED IN X AND Y DIRECTIONS
ETA=THETA-DELTA
OSE=OS/COS(ETA)
TF(ARS(OSE) ,GE, ARS(OSEM))JOS=J
TF(ARS(OSE) ,GE, ARS(OSEM))OSEM=OSE
RMS=OSE*OSE*2
XST=OSE*OS/SIN(THETA)
YST=OSE*OS/SIN(THETA)
THETA=THETA+ST.29578
DELTA=DELTA+ST.29578
ETA=ETA+ST.29578
C...PROPAGATE SHOCK
V(J,K)=V(J,K)+XST*DT
V(J,K)=V(J,K)+YST*DT
C...JUST OTHER GRID POINTS
DO 2 K=2,KH
ZFAC=FLOAT(K-1)/ZKN
X(J,V)=X(J,KMAX)-X(J,1)*ZKFAC+X(J,1)
V(J,K)=V(J,KMAX)-V(J,1)*ZKFAC+V(J,1)
2 CONTINUE
1 CONTINUE
RMS=5*DT*(RMS/FLOAT(JMAX))
WRITE(6,172) IT,RMS,OSEM,JOS
RETURN

```

```

SHOCK 25
SHOCK 26
SHOCK 27
SHOCK 28
SHOCK 29
SHOCK 30
SHOCK 31
SHOCK 32
SHOCK 33
SHOCK 34
SHOCK 35
SHOCK 36
SHOCK 37
SHOCK 38
SHOCK 39
SHOCK 40
SHOCK 41
SHOCK 42
SHOCK 43
SHOCK 44
SHOCK 45
SHOCK 46
SHOCK 47
SHOCK 48
SHOCK 49
SHOCK 50
SHOCK 51
SHOCK 52
SHOCK 53
SHOCK 54
SHOCK 55
SHOCK 56
SHOCK 57
SHOCK 58
SHOCK 59
SHOCK 60
SHOCK 61
SHOCK 62
SHOCK 63
SHOCK 64
SHOCK 65
SHOCK 66
SHOCK 67
SHOCK 68
SHOCK 69
SHOCK 70
SHOCK 71
SHOCK 72
SHOCK 73
SHOCK 74
SHOCK 75
SHOCK 76
SHOCK 77
SHOCK 78
SHOCK 79
SHOCK 80
SHOCK 81
SHOCK 82
SHOCK 83
SHOCK 84
SHOCK 85
SHOCK 86
SHOCK 87
SHOCK 88
SHOCK 89
SHOCK 90
SHOCK 91
SHOCK 92
SHOCK 93
SHOCK 94
SHOCK 95
SHOCK 96
SHOCK 97
SHOCK 98
SHOCK 99
SHOCK 100
SHOCK 101
SHOCK 102
SHOCK 103
SHOCK 104
SHOCK 105
SHOCK 106
SHOCK 107
SHOCK 108

```

```

5 CONTINUE
WRITE(6,103) J,P2,P(J,3),PTAU
STOP
102 FORMAT(10H ITERATION,10,4X,10HRMS OF SHOCK SPEED=,1PE11,4,X,
* ZCMATHMUR SHOCK SPEED=,E11,4,6H AT J=,I2)
103 F0RMAT(10H,41MNEGATIVE PRESSURE DETECTED BY SHOCK AT J=,I2/
* 3T,3HPH=,1PE10,3,3T,3HPD=,3T,E10,3,3X,5H*TAU=,E10,3)
END

```

```

SHOCK 109
SWCK 110
SHOCK 111
SHOCK 112
SHOCK 113
SHOCK 114
SHOCK 115
SHOCK 116

```

```

SURROUNTIME XIEAD (IFLAG)
COMMON/CON1/JMAX,KMAX,3M,KH,KHACH,ALPHA,GAM,GAMH1,CM,DT,SMU,EPOT,
* C4ORD,MCA,MCD,MCC,AA,M,OMEGA,MU,NL,TT,YAU,ITER,ENT,PTORT,PTNF,
* QINF,QINF,CINF,JCS,TH,CUS,PT,MORN,RNDS,MCASE,NPUNCH
LEVEL 2,X,Y,XET,YEX,XY,D
COMMON /COM2/ X(40,20),Y(40,20),XET(40,20,2),YEX(40,20,2),
* XEY(40,20,2),D(40,20)
LEVEL 2,O,EF,S,G,AB
COMMON /COM3/ O(40,20,4),EF(4,4),S(4,20,4),C(4),AB(4,4)
DO 11 K=1,KMAX
DO 11 J=1,JMAX
YET(J,K,2)=O,G
XET(J,K,2)=O,G
11 CONTINUE
JMN=J-1
KMN=K-1
C...COMPUTE Y-YI AND Y-XI; DXY AND DETA = 1
DO 1 K=1,KMAX
DO 2 J=2,JH
YET(J,K,2)=X(J,1,K)-X(J-1,K)100.5
XET(J,K,2)=Y(J,1,K)-Y(J-1,K)100.5
2 YET(J,K,2)=(-3.0*Y(J,K)-Y(J-1,K)+Y(J-2,K))100.5
XET(J,K,2)=(-3.0*Y(J,K)+Y(J-2,K))100.5
YET(J,K,2)=(-3.0*Y(J,K)+Y(J-2,K))100.5
XET(J,K,2)=(-3.0*Y(J,K)+Y(J-2,K))100.5
1 XET(J,K,2)=(-3.0*Y(J,K)+Y(J-2,K))100.5
C...COMPUTE Y-ETA AND Y-ETA
DO 3 J=1,JMAX
DO 4 K=2,KH
YET(J,K,1)=X(J,K,1)-X(J,K-1)100.5
XET(J,K,1)=Y(J,K,1)-Y(J,K-1)100.5
4 YET(J,K,1)=(-3.0*Y(J,K)+Y(J-2,K))100.5
XET(J,K,1)=(-3.0*Y(J,K)+Y(J-2,K))100.5
YET(J,K,1)=(-3.0*Y(J,K)+Y(J-2,K))100.5
XET(J,K,1)=(-3.0*Y(J,K)+Y(J-2,K))100.5
3 YET(J,K,1)=(-3.0*Y(J,K)+Y(J-2,K))100.5
C...COMPUTE YI-Y, YI-Y, ETA-Y, AND ETA-Y
DO 5 K=1,KMAX
DO 5 J=1,JMAX
DT=1.0/((X(J,K,1)+X(J,K,2))-X(J,K,1)+X(J,K,2))
DT=DT
IF(ETAG,FO,0) GO TO 7
C...ADJUST CONSERVATIVE VARIABLES BASED ON NEW MESH
DO 6 M=1,4
O(J,K,M)=O(J,K,M)*DT
7 CONTINUE
C...THE GEOMETRIC JACOBIAN IS DEFINED HERE AND STORED IN THE D ARRAY
Y(J,K)=DTI
Y(J,K,1)=X(J,K,1)*DTI
Y(J,K,2)=X(J,K,2)*DTI
Y(J,K,3)=X(J,K,3)*DTI
Y(J,K,4)=X(J,K,4)*DTI
5 YET(J,K,2)=YET(J,K,2)*DTI
C...REFLECT METRICS AND DEPENDENT VARIABLES ABOUT PLANE OF SYMMETRY
IF(ETAG,EO,0) GO TO 8
DO 9 K=1,KMAX
DO 10 J=1,JH
Y(J,K)=O(J,K)
Y(J,K,1)=O(J,K,1)
Y(J,K,2)=O(J,K,2)
Y(J,K,3)=O(J,K,3)
Y(J,K,4)=O(J,K,4)
DO 10 K=1,4
O(J,K,M)=O(J,K,M)*DTI
9 O(J,K,3)=O(J,K,3)*DD
6 CONTINUE
RETURN
END

```

SURROUNTIME MARCH

```

XIEAD 2
COM1 3
COM2 3
COM3 4
COM2 2
COM2 4
COM2 2
COM3 3
XIEAD 6
XIEAD 7
XIEAD 8
XIEAD 9
XIEAD 10
XIEAD 11
XIEAD 12
XIEAD 13
XIEAD 14
XIEAD 15
XIEAD 16
XIEAD 17
XIEAD 18
XIEAD 19
XIEAD 20
XIEAD 21
XIEAD 22
XIEAD 23
XIEAD 24
XIEAD 25
XIEAD 26
XIEAD 27
XIEAD 28
XIEAD 29
XIEAD 30
XIEAD 31
XIEAD 32
XIEAD 33
XIEAD 34
XIEAD 35
XIEAD 36
XIEAD 37
XIEAD 38
XIEAD 39
XIEAD 40
XIEAD 41
XIEAD 42
XIEAD 43
XIEAD 44
XIEAD 45
XIEAD 46
XIEAD 47
XIEAD 48
XIEAD 49
XIEAD 50
XIEAD 51
XIEAD 52
XIEAD 53
XIEAD 54
XIEAD 55
XIEAD 56
XIEAD 57
XIEAD 58
XIEAD 59
XIEAD 60
XIEAD 61

```

MARCH 2

```

COMMON /INVARB/RK,ETA(41),PHI(41),DTIL(41),DTILE(41),META,TP(24)
COMMON/JOE/ZL1,CF1,CF2,ZLFL,ZTRAM,DZTRAM
LEVEL 2, RHO,P,PH,PHR,ROBZ,VINF,VINF,ROBPH,RB,PHZ,PHPH,DTOPH,
* ACT,DTOT,DTOR,ACT,ICONST,GAM,CONST,NREGON,RS,RST,PSPHI,RST,PSZT,
* PSPT
COMMON /PVARS/ PHO(24,41), P(24,41), U(24,41), V(24,41), W(24,41),
* POR(41), ROBZ(41), VINF(41), VINF(41),
* ROBPH(41), PH(41), PHZ(41), RAPH(41),
* DTOPH(24,41), BCT(41), DTOT(24,41),DTOP(41), ACT(41),
* ICONST(50), GAM(20), CONST(50),NREGON, RS(41),
* PSZ(41), PSMI(41), RST(41), PSZT(41), PSMIT(41)
COMMON/SVARS/PT, PH1, DT, DT, DPMT, PTNY,
* TEND, PT, ALPHA, GAMMA, SIGMA, XHACH, TAPE1,
* TAPE2, DISK1, ALPH, DISK2, SIGM, NPHNT, DTOT,
* DTOPH, ZH, TEND, TMLD, TMM, TML, NPHI,
* TTM, PT, AZ, NPHI, NIT, KPHI, NITER,
* NPHI, NPHI1, NPHI2, NPHI3, NPHM1, NPHM2, NPHM3,
* NT, NT1, NT2, NT3, PHIFO, NCON, RAD1,
* PHIF, METHOD, LAG, MSC, PINF, RHOIN, UINF,
* QINF,GASCON,NREAL,NPUNCH
COMMON /DNSTRM/ ZPLOT,NZEND,NZADD,NXPLOT

```

```

CALL SETDAT
CALL CENDM(0,PHI,PHI,7,RA,R7,PSPHI,TPNT)
SIGMA=ATAN(CF2)*ST.29578
ICONST(40)=0
CALL INITA
IF (7,ACT, TEND) GO TO 19
MTEP=100-MTEND
WRITE(6,61)
STOP=MTEP-1
CALL ANNYM(2)
DO 4 PH1=1,MITER
TCONST(5)=JUDI
C...COMPUTE AUTOMATIC STEPSIZE
IF (MTEP,EO, 1) GO TO 3
IF (MTEP,JUDI,ICONST(49)),NE,C) GO TO 5
3 CALL STEPM
IF (MTEP,LT, 1.3) GO TO 5
MTEP=MTPE
MTEP=MTPE
MTEP=MTPE
MTEP=MTPE
5 CONTINUE
CALL DTFR
C...WRITE DATA FOR REFIN ON TAPE9
CALL DTFR
IF (7,ACT, TEND) GO TO 19
CONTINUE
19 CONTINUE
C...ALL DATA REQUIRED FOR REFIN OF THIS CASE IS NOW ON TAPE9
END FILE 9
RETURN
610 FORMAT(10H//54X,20HARCHING CALCULATION//54X,2C(10H)///
* 2X,MSTEP NO.,4X,10HDOWNSTREAM LOCATION,4X,10HDOY OPTIMATE,
* 5X,14HSHOCK ORIGINATE/)
END

```

```

SURROUNTIME MARCH 2
COMMON/ENTRO/5(41),PHS,ZFLD,ITORT,ITORT,MCASE,NTDSNS
LEVEL 2, RHO,P,PH,PHR,ROBZ,VINF,VINF,ROBPH,RB,PHZ,PHPH,DTOPH,
* ACT,DTOT,DTOR,ACT,ICONST,GAM,CONST,NREGON,RS,RST,PSPHI,RST,PSZT,
* PSPT
COMMON /PVARS/ PHO(24,41), P(24,41), U(24,41), V(24,41), W(24,41),
* POR(41), ROBZ(41), VINF(41), VINF(41),
* ROBPH(41), PH(41), PHZ(41), RAPH(41),
* DTOPH(24,41), ACT(41), DTOT(24,41),DTOP(41), ACT(41),
* ICONST(50), GAM(20), CONST(50),NREGON, RS(41),
* PSZ(41), PSMI(41), RST(41), PSZT(41), PSMIT(41)
COMMON/SVARS/PT, PH1, DT, DT, DPMT, PTNY,
* TEND, PT, ALPHA, GAMMA, SIGMA, XHACH, TAPE1,
* TAPE2, DISK1, ALPH, DISK2, SIGM, NPHNT, DTOT,
* DTOPH, ZH, TEND, TMLD, TMM, TML, NPHI,
* TTM, PT, AZ, NPHI, NIT, KPHI, NITER,
* NPHI, NPHI1, NPHI2, NPHI3, NPHM1, NPHM2, NPHM3,
* NT, NT1, NT2, NT3, PHIFO, NCON, RAD1,
* PHIF, METHOD, LAG, MSC, PINF, RHOIN, UINF,
* QINF,GASCON,NREAL,NPUNCH
SURROUNTIME MARCH 10

```

```

DTMNSTON PK13(41),PK14(41),PK21(41),PK22(41),PK23(41)
LOGICAL IT2ND
ARSTN(41)=ASIN(41)
GN TO (10,10,11),K1
CONTINUE
C..WEAK OR SMALL ANGLE CORRECTIONS (USES WRANDTL-MEYER RELATIONS)
DO 9 K=3,NPHI
PK4=1.0/SORT(RBT(K)**2+1.0*(RAPH(K)/R4(K))**2)
PK1=-RBT(K)*PK4
PK2=PK4
PK3=-RAPH(K)/R4(K)*PK4
IT2ND=.FALSE.
QSO=U(3,K)*Q2*V(3,K)**2+W(3,K)**2
IF(P(3,K).GE.P(6)) GO TO 4
C..NEGATIVE SURFACE PRESSURE
ICHECK=1
Y=1,C=-7
IF (K .EQ. 3) WRITE(6,100) X,P(3,K),RHO(3,K),U(3,K),V(3,K)
P(3,K)=INF(1.0-0.5*GAMMA)
RHO(3,K)=(P(3,K)/S(K))**1.0/GAMMA
Q3K=SQRT(1.0-P(3,K)/RHO(3,K))
U(3,K)=U(3,K)*Q3K/QSO**0.5
V(3,K)=V(3,K)*Q3K/QSO**0.5
W(3,K)=W(3,K)*Q3K/QSO**0.5
QSO=Q3K**2
CONTINUE
IF(RHUS(K) .GE. 0.0160 TO 5
ICHECK=2
Y=1,C=-7
IF (K .EQ. 3) WRITE(6,100) X,P(3,K),RHO(3,K),U(3,K),V(3,K)
RHO(3,K)=(P(3,K)/S(K))**1.0/GAMMA
Q3K=SQRT(1.0-P(3,K)/RHO(3,K))
U(3,K)=U(3,K)*Q3K/QSO**0.5
V(3,K)=V(3,K)*Q3K/QSO**0.5
W(3,K)=W(3,K)*Q3K/QSO**0.5
CONTINUE
PK5=SQRT(QSO)
PK6=(PK1**2+PK2**2+PK3**2+PK5**2)/PK5
PK7=60SIN(PK6)
PK8=GAMMA(1+P(3,K)/RHO(3,K))
PK9=PK5**2/PK8
PK10=PK9-1.0
IF(PK10 .GT. 0.0160 TO 6
ICHECK=4
Y=1,C=-7
IF (K .EQ. 3) WRITE(6,100) X,P(3,K),RHO(3,K),U(3,K),V(3,K)
PK10=0.5
PK9=1.5
PK8=PK5**2/PK9
RHO(3,K)=GAMMA(1+P(3,K)/PK8)
Q3K=SQRT(1.0-P(3,K)/RHO(3,K))
U(3,K)=U(3,K)*Q3K/QSO**0.5
V(3,K)=V(3,K)*Q3K/QSO**0.5
W(3,K)=W(3,K)*Q3K/QSO**0.5
CONTINUE
PK11=GAMMA*PK9/SORT(PK10)
PK12=GAMMA*PK9/((GAMMA+1.0)*PK9**2-4.0*PK10/(4.0*PK10**2))
PK13(K)=P(3,K)*(1.0-PK11*PK7+PK12*PK7**2)
EACTN=3.5*GAMMA*PK9/(PK10**3.5)
TERM1=(GAMMA+1.0)*PK9**4/6.0
TERM2=-19.0*GAMMA**2.0*GAMMA**2*PK9**3/6.0
TERM3=-5.0*GAMMA**1.0*PK9**2/3.0
TERM4=4.0/3.0-2.0*PK9
CDEF3=FACTOR*(TERM1+TERM2+TERM3+TERM4)
PTEST=PK13(K)-P(3,K)*CDEF3*PK7**3
IF (ABS(PTEST).LT.A95(6.01) GO TO 123
Y=1 .C= SORT(PK9)
CALL PHTURN(X,K1,PK7,P21,MTTS,GAMMA)
P2NUE = P13(K)*P21
PTEST = P2NUE
123 CONTINUE
PK13(K)=PTEST
PK14(K)=(PK13(K)/S(K))**1.0/GAMMA
PK15=SQRT(1.0-PK13(K)/RHO(3,K))
PK16=PK6*PK5*PK4
PK17=U(3,K)*PK16*PK7(K)
PK18=W(3,K)*PK16
PK19=U(3,K)*PK16*RAPH(K)/R4(K)
PK20=SQRT(PK17**2+PK18**2+PK19**2)
PK24=PK15/PK20
PK21(K)=PK24*PK17
PK22(K)=PK24*PK18
PK23(K)=PK24*PK19
CONTINUE
CONTINUE

```

```

ENDRYM 6
ENDRYM 7
ENDRYM 8
ENDRYM 9
ENDRYM 10
ENDRYM 11
ENDRYM 12
ENDRYM 13
ENDRYM 14
ENDRYM 15
ENDRYM 16
ENDRYM 17
ENDRYM 18
ENDRYM 19
ENDRYM 20
ENDRYM 21
ENDRYM 22
ENDRYM 23
ENDRYM 24
ENDRYM 25
ENDRYM 26
ENDRYM 27
ENDRYM 28
ENDRYM 29
ENDRYM 30
ENDRYM 31
ENDRYM 32
ENDRYM 33
ENDRYM 34
ENDRYM 35
ENDRYM 36
ENDRYM 37
ENDRYM 38
ENDRYM 39
ENDRYM 40
ENDRYM 41
ENDRYM 42
ENDRYM 43
ENDRYM 44
ENDRYM 45
ENDRYM 46
ENDRYM 47
ENDRYM 48
ENDRYM 49
ENDRYM 50
ENDRYM 51
ENDRYM 52
ENDRYM 53
ENDRYM 54
ENDRYM 55
ENDRYM 56
ENDRYM 57
ENDRYM 58
ENDRYM 59
ENDRYM 60
ENDRYM 61
ENDRYM 62
ENDRYM 63
ENDRYM 64
ENDRYM 65
ENDRYM 66
ENDRYM 67
ENDRYM 68
ENDRYM 69
ENDRYM 70
ENDRYM 71
ENDRYM 72
ENDRYM 73
ENDRYM 74
ENDRYM 75
ENDRYM 76
ENDRYM 77
ENDRYM 78
ENDRYM 79
ENDRYM 80
ENDRYM 81
ENDRYM 82
ENDRYM 83
ENDRYM 84
ENDRYM 85
ENDRYM 86
ENDRYM 87
ENDRYM 88
ENDRYM 89
ENDRYM 90

```

```

C..RESFT BODY VARIABLES TO THOSE CALCULATED BY A9NETTS SCHEME
DO 12 N=3,NPHI
P(3,K)=PK13(K)
RHO(3,K)=PK14(K)
U(3,K)=PK21(K)
V(3,K)=PK22(K)
W(3,K)=PK23(K)
CONTINUE
GN TO 21
18 CONTINUE
C..APPLY REFLECTION PRINCIPLE AT PLANES OF SYMMETRY
C
DO 1 K=1,2
M=6-K
L=NPHI-K
M=NPHI-K
DO 1 J=3,MT2
P(J,K)=P(J,M)
RHO(J,K)=RHO(J,M)
P(J,K)=P(J,M)
P(J,L)=P(J,M)
U(J,K)=U(J,M)
U(J,L)=U(J,M)
V(J,K)=V(J,M)
V(J,L)=V(J,M)
W(J,K)=W(J,M)
W(J,L)=W(J,M)
U(J,3)=U(J,4)
V(J,3)=V(J,4)
CONTINUE
21 CONTINUE
1. FORMAT(24,49,NEGATIVE PRESSURE OR DENSITY ON BODY DETECTED BY
* 1144NDRY AT X=F7.3/3X,3444,PE11.3,3X,54440,PE10.3,3X,
* 44444,PE10.3,3X,44444,PE10.3)
RETURN
END
DIFFR 2
CDEF 2
CDEF 3
CDEF 4
CDEF 5
CDEF 6
CDEF 7
CDEF 8
CDEF 9
CDEF 10
CDEF 11
CDEF 12
CDEF 13
CDEF 14
CDEF 15
CDEF 16
CDEF 17
CDEF 18
CDEF 19
CDEF 20
CDEF 21
CDEF 22
CDEF 23
CDEF 24
CDEF 25
CDEF 26
CDEF 27
CDEF 28
CDEF 29
CDEF 30
CDEF 31
CDEF 32
CDEF 33
CDEF 34
CDEF 35
CDEF 36
CDEF 37
CDEF 38
CDEF 39
CDEF 40
CDEF 41
CDEF 42
CDEF 43
CDEF 44
CDEF 45
CDEF 46
CDEF 47
CDEF 48
CDEF 49
CDEF 50
CDEF 51
CDEF 52
CDEF 53
CDEF 54
CDEF 55
CDEF 56
CDEF 57
CDEF 58
CDEF 59
CDEF 60
CDEF 61
CDEF 62
CDEF 63
CDEF 64
CDEF 65
CDEF 66
CDEF 67
CDEF 68
CDEF 69
CDEF 70
CDEF 71
CDEF 72
CDEF 73
CDEF 74
CDEF 75
CDEF 76
CDEF 77
CDEF 78
CDEF 79
CDEF 80
CDEF 81
CDEF 82
CDEF 83
CDEF 84
CDEF 85
CDEF 86
CDEF 87
CDEF 88
CDEF 89
CDEF 90

```

```

C00.CALCULATES GEOMETRIC FACTORS BASED ON NEW BODY AND SHOCK GEOMETRY
    CALL GEOM(1)
C00.APPLIES PLANE OF SYMMETRY BOUNDARY CONDITIONS
    CALL BNDRYM(2)
C00.FORM INTERMEDIATE CONSERVATIVE VARIABLES AT ALL POINTS
    CALL ITCOM(1)
    DO 3 KPHI=3,NPHI
    DO 3 J=3,NTZ
    DO 3 I=1,4
    K=KPHI
C00.DIFFUSION FUNCTION
    DISS=0.0
    IF (CONST(4).NE.C0.3 .OR. CONST(5).NE.C0.1) CALL DISSPHIN(J,K,DISS)
    IF (J=3) GO TO 5
    IF (J=5) NTZ1 GO TO 5
C00.CORRECTOR IN FIELD
    FTEPH=(N,J,K)*C0.5*(EO(N,J,K)+ETEPH(N,J,K)-(N77)*FO(N,J,K)
    +FO(N,J,K)-O2DPM*(GO(N,J,K)-GO(N,J,K-1)+O2*HO(N,J,K))+DISS)
    GO TO 4
4    CONTINUE
C00.CORRECTOR AT SHOCK
    FTEPH=(N,J,K)*C0.5*(ETEPH(N,J,K)+EO(N,J,K)-(N77)*FO(N,J,K)
    +FO(N,J,K-1)+O2DPM*(GO(N,J,K)-GO(N,J,K-1)+O2*HO(N,J,K))+DISS)
    GO TO 3
3    CONTINUE
C00.CORRECTOR AT BODY
    FTEPH=(N,J,K)*C0.5*(ETEPH(N,J,K)+EO(N,J,K)-(N77)*FO(N,J,K)-FO(N,J,
    3)
    +O2DPM*(GO(N,J,K)-GO(N,J,K-1)+O2*HO(N,J,K))+DISS)
3    CONTINUE
C00.DECODE CONSERVATIVE VARIABLES
    CALL ITCOM(2)
C00.CALCULATE CORRECTED SHOCK VALUES
    CALL SHOCKM(2)
C00.CALCULATES GEOMETRIC FACTORS BASED ON OLD BODY AND NEW SHOCK GEOMETRY
    CALL GEOM(2)
C00.RESETS BODY VARIABLES
    CALL BNDRYM(1)
C00.APPLIES PLANE OF SYMMETRY BOUNDARY CONDITIONS
    CALL BNDRYM(2)
    RETURN
END

```

```

      SUBROUTINE DISSPH4(J,K,DISS)
      DIMENSION ETEMP(4,24,41),GE(4,24,41),
      *          FC(4,24,41),GC(4,24,41),
      *          F0(4,24,41),G0(4,24,41),
      *          F1(4,24,41),G1(4,24,41),
      *          F2(4,24,41),G2(4,24,41),
      *          F3(4,24,41),G3(4,24,41),
      *          F4(4,24,41),G4(4,24,41),
      *          F5(4,24,41),G5(4,24,41),
      *          F6(4,24,41),G6(4,24,41),
      *          F7(4,24,41),G7(4,24,41),
      *          F8(4,24,41),G8(4,24,41),
      *          F9(4,24,41),G9(4,24,41),
      *          F10(4,24,41),G10(4,24,41),
      *          F11(4,24,41),G11(4,24,41),
      *          F12(4,24,41),G12(4,24,41),
      *          F13(4,24,41),G13(4,24,41),
      *          F14(4,24,41),G14(4,24,41),
      *          F15(4,24,41),G15(4,24,41),
      *          F16(4,24,41),G16(4,24,41),
      *          F17(4,24,41),G17(4,24,41),
      *          F18(4,24,41),G18(4,24,41),
      *          F19(4,24,41),G19(4,24,41),
      *          F20(4,24,41),G20(4,24,41),
      *          F21(4,24,41),G21(4,24,41),
      *          F22(4,24,41),G22(4,24,41),
      *          F23(4,24,41),G23(4,24,41),
      *          F24(4,24,41),G24(4,24,41),
      *          F25(4,24,41),G25(4,24,41),
      *          F26(4,24,41),G26(4,24,41),
      *          F27(4,24,41),G27(4,24,41),
      *          F28(4,24,41),G28(4,24,41),
      *          F29(4,24,41),G29(4,24,41),
      *          F30(4,24,41),G30(4,24,41),
      *          F31(4,24,41),G31(4,24,41),
      *          F32(4,24,41),G32(4,24,41),
      *          F33(4,24,41),G33(4,24,41),
      *          F34(4,24,41),G34(4,24,41),
      *          F35(4,24,41),G35(4,24,41),
      *          F36(4,24,41),G36(4,24,41),
      *          F37(4,24,41),G37(4,24,41),
      *          F38(4,24,41),G38(4,24,41),
      *          F39(4,24,41),G39(4,24,41),
      *          F40(4,24,41),G40(4,24,41),
      *          F41(4,24,41),G41(4,24,41),
      *          F42(4,24,41),G42(4,24,41),
      *          F43(4,24,41),G43(4,24,41),
      *          F44(4,24,41),G44(4,24,41),
      *          F45(4,24,41),G45(4,24,41),
      *          F46(4,24,41),G46(4,24,41),
      *          F47(4,24,41),G47(4,24,41),
      *          F48(4,24,41),G48(4,24,41),
      *          F49(4,24,41),G49(4,24,41),
      *          F50(4,24,41),G50(4,24,41),
      *          F51(4,24,41),G51(4,24,41),
      *          F52(4,24,41),G52(4,24,41),
      *          F53(4,24,41),G53(4,24,41),
      *          F54(4,24,41),G54(4,24,41),
      *          F55(4,24,41),G55(4,24,41),
      *          F56(4,24,41),G56(4,24,41),
      *          F57(4,24,41),G57(4,24,41),
      *          F58(4,24,41),G58(4,24,41),
      *          F59(4,24,41),G59(4,24,41),
      *          F60(4,24,41),G60(4,24,41),
      *          F61(4,24,41),G61(4,24,41),
      *          F62(4,24,41),G62(4,24,41),
      *          F63(4,24,41),G63(4,24,41),
      *          F64(4,24,41),G64(4,24,41),
      *          F65(4,24,41),G65(4,24,41),
      *          F66(4,24,41),G66(4,24,41),
      *          F67(4,24,41),G67(4,24,41),
      *          F68(4,24,41),G68(4,24,41),
      *          F69(4,24,41),G69(4,24,41),
      *          F70(4,24,41),G70(4,24,41),
      *          F71(4,24,41),G71(4,24,41),
      *          F72(4,24,41),G72(4,24,41),
      *          F73(4,24,41),G73(4,24,41),
      *          F74(4,24,41),G74(4,24,41),
      *          F75(4,24,41),G75(4,24,41),
      *          F76(4,24,41),G76(4,24,41),
      *          F77(4,24,41),G77(4,24,41),
      *          F78(4,24,41),G78(4,24,41),
      *          F79(4,24,41),G79(4,24,41),
      *          F80(4,24,41),G80(4,24,41),
      *          F81(4,24,41),G81(4,24,41),
      *          F82(4,24,41),G82(4,24,41),
      *          F83(4,24,41),G83(4,24,41),
      *          F84(4,24,41),G84(4,24,41),
      *          F85(4,24,41),G85(4,24,41),
      *          F86(4,24,41),G86(4,24,41),
      *          F87(4,24,41),G87(4,24,41),
      *          F88(4,24,41),G88(4,24,41),
      *          F89(4,24,41),G89(4,24,41),
      *          F90(4,24,41),G90(4,24,41),
      *          F91(4,24,41),G91(4,24,41),
      *          F92(4,24,41),G92(4,24,41),
      *          F93(4,24,41),G93(4,24,41),
      *          F94(4,24,41),G94(4,24,41),
      *          F95(4,24,41),G95(4,24,41),
      *          F96(4,24,41),G96(4,24,41),
      *          F97(4,24,41),G97(4,24,41),
      *          F98(4,24,41),G98(4,24,41),
      *          F99(4,24,41),G99(4,24,41),
      *          F100(4,24,41),G100(4,24,41),
      *          F101(4,24,41),G101(4,24,41),
      *          F102(4,24,41),G102(4,24,41),
      *          F103(4,24,41),G103(4,24,41),
      *          F104(4,24,41),G104(4,24,41),
      *          F105(4,24,41),G105(4,24,41),
      *          F106(4,24,41),G106(4,24,41),
      *          F107(4,24,41),G107(4,24,41),
      *          F108(4,24,41),G108(4,24,41),
      *          F109(4,24,41),G109(4,24,41),
      *          F110(4,24,41),G110(4,24,41),
      *          F111(4,24,41),G111(4,24,41),
      *          F112(4,24,41),G112(4,24,41),
      *          F113(4,24,41),G113(4,24,41),
      *          F114(4,24,41),G114(4,24,41),
      *          F115(4,24,41),G115(4,24,41),
      *          F116(4,24,41),G116(4,24,41),
      *          F117(4,24,41),G117(4,24,41),
      *          F118(4,24,41),G118(4,24,41),
      *          F119(4,24,41),G119(4,24,41),
      *          F120(4,24,41),G120(4,24,41),
      *          F121(4,24,41),G121(4,24,41),
      *          F122(4,24,41),G122(4,24,41),
      *          F123(4,24,41),G123(4,24,41),
      *          F124(4,24,41),G124(4,24,41),
      *          F125(4,24,41),G125(4,24,41),
      *          F126(4,24,41),G126(4,24,41),
      *          F127(4,24,41),G127(4,24,41),
      *          F128(4,24,41),G128(4,24,41),
      *          F129(4,24,41),G129(4,24,41),
      *          F130(4,24,41),G130(4,24,41),
      *          F131(4,24,41),G131(4,24,41),
      *          F132(4,24,41),G132(4,24,41),
      *          F133(4,24,41),G133(4,24,41),
      *          F134(4,24,41),G134(4,24,41),
      *          F135(4,24,41),G135(4,24,41),
      *          F136(4,24,41),G136(4,24,41),
      *          F137(4,24,41),G137(4,24,41),
      *          F138(4,24,41),G138(4,24,41),
      *          F139(4,24,41),G139(4,24,41),
      *          F140(4,24,41),G140(4,24,41),
      *          F141(4,24,41),G14
```

01FFFF	27
01FFFF	29
01FFFF	30
01FFFF	31
01FFFF	32
01FFFF	33
01FFFF	34
01FFFF	35
01FFFF	36
01FFFF	37
01FFFF	38
01FFFF	39
01FFFF	40
01FFFF	41
01FFFF	42
01FFFF	43
01FFFF	44
01FFFF	45
01FFFF	46
01FFFF	47
01FFFF	48
01FFFF	49
01FFFF	50
01FFFF	51
01FFFF	52
01FFFF	53
01FFFF	54
01FFFF	55
01FFFF	56
01FFFF	57
01FFFF	58
01FFFF	59
01FFFF	60
01FFFF	61
01FFFF	62
01FFFF	63
01FFFF	64
01FFFF	65
01FFFF	66
01FFFF	67
01FFFF	68
01FFFF	69
01FFFF	70
01FFFF	71
01FFFF	72
01FFFF	73
01FFFF	74
01FFFF	75
01FFFF	76
01FFFF	77
01FFFF	78
01FFFF	79
01FFFF	80
01FFFF	81
01FFFF	82
01FFFF	83
01FFFF	84
01FFFF	85
01FFFF	86
01FFFF	87
01FFFF	88
01FFFF	89
01FFFF	90
01FFFF	91
01FFFF	92
01FFFF	93
01FFFF	94
01FFFF	95
01FFFF	96
01FFFF	97
01FFFF	98
01FFFF	99
01FFFF	100

```

5  JN=J
5  DISSP=-CONST(4)*Q*J1*(E0(N,JD+2,K)+E0(N,JN-2,K)-4*Q*(F(N,JD+1,K)
  *E0(N,JD-1,K))+6*Q*E0(N,JD,K))
  GO TO 2
21 CONTINUE
  IF(J.GE.4.AND.J.LE.NT1)GO TO 33
  IF(J.LT.4)GO TO 70
  JN=NT
  GO TO 60
70 JN=4
  GO TO 60
50 JN=J
60 DISSP=-CONST(4)*Q*1.25*(E0(N,JD+1,K)+F0(N,JN-1,K))-Q*25*E0(N,JD,K)
  GO TO 2
1  *ISSP=3.0
C
C
C..... CONST(5)<0 , LAX DAMPING
C..... CONST(5)=0 , NO DAMPING
C..... CONST(5)>0 , 4TH ORDER DAMPING
C

```

```

2   IF(CONST(5))J1:=0.1
C=DISPERATION TERM IN THE DIAGONAL DIRECTION
3   CONTINUE
    IF(K-GE. 4 .AND. K.LE. NPMH1GO TO 80
    IFK.LT. 4IGOTO 100
    K=NPMH1
    GO TO 9.
16.  C=M4
    GO TO 90
    K=M4
91.  H(C)=CONST(5)*(.125*(E(N,J,KD+1)+EO(N,J,K7-1))-0.75*EC(N,J,KD)
    GO TO 4.
11 CONTINUE
    T(E,N,3) P(J,1)=P(J,5)
    IF(K.EQ.NM41) P(J,NPMH2)=P(J,NPMH2)
    PF=AR((J,K+2)-2.0*(J,K+1)+(J,K))/((J,K+2)+2.0*(J,K+1)+P(J,K)
    * )
    *F2=AR((J,K+1)-2.0*(J,K)+P(J,K-1))/(J,K+1)+2.0*(J,K)+P(J,K
    * )
    *F3=AR(F(J,K)-2.0*(J,K-1)+P(J,K-2))/(P(J,K)+2.0*(J,K-1)+P(J,K
    * )
    HTSS=.75*DETAA*(PF1+PF2)+EO(N,J,K+1)-EO(N,J,K1)-
    * (PF2+PF3)*(E(N,J,K)-EO(N,J,K-1))*CONST("
    GO TO 4
3   HTSS=.0
4   HTS=HTSS+DISSP
    RETURN
END

```

[illegible]

```

C.....K=1 IMPLIES EIGENVALUES AND STEPSIZE
      IPNT=ICONS(4)
      STG1?M=0.6
      STG34M=0.0
      DO 1 K=3,NPNT
      11 J=3,NT2
      T=XI(J)
      R=T*(R7R(K)-R8(K))+R9(K)

```

01SSPP	22
01SSPP	23
01SSPP	24
01SSPP	25
01SSPP	26
01SSPP	27
01SSPP	28
01SSPP	29
01SSPP	30
01SSPP	31
01SSPP	32
01SSPP	33
01SSPP	34
01SSPP	35
01SSPP	36
01SSPP	37
01SSPP	38
01SSPP	39
01SSPP	40
01SSPP	41
01SSPP	42
01SSPP	43
01SSPP	44
01SSPP	45
01SSPP	46
01SSPP	47
01SSPP	48
01SSPP	49
01SSPP	50
01SSPP	51
01SSPP	52
01SSPP	53
01SSPP	54
01SSPP	55
01SSPP	56
01SSPP	57
01SSPP	58
01SSPP	59
01SSPP	60
01SSPP	61
01SSPP	62
01SSPP	63
01SSPP	64
01SSPP	65
01SSPP	66
01SSPP	67
01SSPP	68
01SSPP	69
01SSPP	70
01SSPP	71

[illegible]

ETEGNN	19
ETEGNN	16
ETEGNN	17
ETEGNN	18
ETEGNN	19
ETEGNN	20
ETEGNN	21
ETEGNN	22
ETEGNN	23
ETEGNN	24
ETEGNN	25
ETEGNN	26
ETEGNN	27
ETEGNN	28
ETEGNN	29
ETEGNN	30
ETEGNN	31
ETEGNN	32
ETEGNN	33
ETEGNN	34
ETEGNN	35
ETEGNN	36
ETEGNN	37
ETEGNN	38
ETEGNN	39
ETEGNN	40
ETEGNN	41
ETEGNN	42
ETEGNN	43
ETEGNN	44
ETEGNN	45
ETEGNN	46
ETEGNN	47
ETEGNN	48
ETEGNN	49
ETEGNN	50
ETEGNN	51
ETEGNN	52
ETEGNN	53
ETEGNN	54
ETEGNN	55
ETEGNN	56
ETEGNN	57
ETEGNN	58
ETEGNN	59
ETEGNN	60
ETEGNN	61
ETEGNN	62
ETEGNN	63
ETEGNN	64
ETEGNN	65
ETEGNN	66
ETEGNN	67
ETEGNN	68
ETEGNN	69
ETEGNN	70
ETEGNN	71
ETEGNN	72
ETEGNN	73
ETEGNN	74
ETEGNN	75
ETEGNN	76
ETEGNN	77
ETEGNN	78
ETEGNN	79
ETEGNN	80
ETEGNN	81
ETEGNN	82
ETEGNN	83
ETEGNN	84
ETEGNN	85
ETEGNN	86
ETEGNN	87
ETEGNN	88
ETEGNN	89
ETEGNN	90
ETEGNN	91

[illegible]

GEOM	2
GEOM	3


```

      THETA=THETA
      *R1=DELTA*G(R1,THETA1)
      THETA=THETA+DELTA
C.....CORRECTOR
      *R1=0.5*DELTA*(G(P1,THETA1)+G(R1,THETA))
      DRDT=G(R1,THETA)
      R1=R
      IF (THETA .LT. PI) GO TO 15
      YTA(J)=R*SIN(THETA)
      P7(J)=R*COS(THETA)
      DRDZ(J)=(-DRDT*COS(THETA)+R*SIN(THETA))/
      * (-DRDT*SIN(THETA)-R*COS(THETA))
      J=J+1
15 CONTINUE
      MAX=J-1
      RETURN
C
C.....BODY SHAPE TABLE SUPPLIED BY USER
C
      2. CONTINUE
      J=1
      NXZ=C*H
      NRZ=Z*Z
      MRDZ=MRDZ-1
      N1 25 I=1,MRDZM
      RX1=NXZ
      RY1=NRZ
      NXZ=XX(I+1)-XX(I)
      RYZ=YY(I+1)-YY(I)
      IF (XX(I) .GT.9.0) GO TO 25
      YTA(J)=XX(I)
      P7(J)=YY(I)
      P1=SQRT(RY1*DR1+DX1*DX1)
      P2=SQRT(RY2*DR2+DX2*DX2)
      DRDZ(J)=(-DR1*P2/RX1+DR2*P1/DX2)/(P1+P2)
      I=I+1
25 CONTINUE
      YTA(J)=XX(MRDZ)
      P7(J)=YY(MRDZ)
      DRDZ(J)=(-DR2*(Z+C*DZ+D1)/DX2+R1*D2/DV1)/(D1+D2)
      MAX=J
      RETURN
      3. CONTINUE
      YTA(1)=0.0
      P7(1)=RQ
      THETA1=THETA
      A1=3*(P1,M)
      DRDZ(1)=P2*(R1,1,C*J,L,A1)/RQ
      I=2
      IMAX=1-IMAX-1
      N1 50 I=1,IMAX=1
      AS=C*IN(THETA)
      AC=COS(THETA)
C.....PREDICTOR
      A1=C*(P1,M)
      K=0
      RY=F2(R1,AS,AC,A1)
      IF (RXY.LT.0.0) DRX=2.*H*AS*AC
      *R1=DRX*DELTA
      THETA=THETA+DELTA
      AS1=C*IN(THETA)
      AC1=COS(THETA)
C.....CORRECTOR
      45 CONTINUE
      A11=C*(R1,M)
      RPY=F2(R1,AS1,AC1,A1)
      IF (RPY.LT.0.0) DRX=2.*H*AS1*AC1
      *LPOPE=.5*(DRX+DRXY)
      *R1=LPOPE*DELTA
      IF (R1.LT.5) GO TO 45
      YTA(J)=R*AC1
      P7(J)=R*AS1
      DRDZ(J)=(R*AC1+AS1*SLOPE)/(R+AS1-AC1*SLOPE)
      R1=R
      J=J+1
      CONTINUE
      MAX=J-1
      RETURN
      END

```

GEOM	87
GEOM	88
GEOM	89
GEOM	90
GEOM	91
GEOM	92
GEOM	93
GEOM	94
GEOM	95
GEOM	96
GEOM	97
GEOM	98
GEOM	99
GEOM	100
GEOM	101
GEOM	102
GEOM	103
GEOM	104
GEOM	105
GEOM	106
GEOM	107
GEOM	108
GEOM	109
GEOM	110
GEOM	111
GEOM	112
GEOM	113
GEOM	114
GEOM	115
GEOM	116
GEOM	117
GEOM	118
GEOM	119
GEOM	120
GEOM	121
GEOM	122
GEOM	123
GEOM	124
GEOM	125
GEOM	126
GEOM	127
GEOM	128
GEOM	129
GEOM	130
GEOM	131
GEOM	132
GEOM	133
GEOM	134
GEOM	135
GEOM	136
GEOM	137
GEOM	138
GEOM	139
GEOM	140
GEOM	141
GEOM	142
GEOM	143
GEOM	144
GEOM	145
GEOM	146
GEOM	147
GEOM	148
GEOM	149
GEOM	150
GEOM	151
GEOM	152
GEOM	153
GEOM	154
GEOM	155
GEOM	156
GEOM	157
GEOM	158
GEOM	159
GEOM	160
GEOM	161
GEOM	162
GEOM	163
GEOM	164
GEOM	165
GEOM	166

ROUTINE GEOM2(K3)	GEOM2	2
COMMON /CLUSTB/RK, XI(24), TXI(24), TXIT(24)	CLUSTB	2
COMMON /IDVAR/RK, ETA(41), PHIP(41), DTIL(41), DTILE(41), DEYA, TP(24)	IDVAR	2
LEVEL 2, RND, P, U, V, W, ROR, ROBZ, VINP, WINF, RORP, R, R, RZ, RRP, OTDP, P	PVAR	2
ACT, OTDZ, OTDR, ACT, ICONST, GAM, CONST, NREGON, RS, RSZ, RSPH, RST, RSTZ,	PVAR	3
RSPIIT	PVAR	4
COMMON /PVAR/ RMO(24,41), P(24,41), U(24,41), V(24,41), W(24,41),	PVAR	5
ROR(41), RORZ(41), WINF(41), WINF(41), WINF(41),	PVAR	6
RORPH(41), RZ(41), RZ(41), RZ(41), RRP(41),	PVAR	7
OTDPH(24,41), RCT(41), OTDZ(24,41), OTDR(41), ACT(41),	PVAR	8
ICONST(50), GAM(20), CONST(50), NREGON, RS(41),	PVAR	9
RSZ(41), RSPH(41), RST(41), RSTZ(41), RSPHIT(41)	PVAR	10
COMMON /SVAR/ T, Z, PHI, DT, DZ, DPHI, ZINT,	SVAR	2
TEND, PI, ALPHA, GAMMA, SIGMA, XNACH, TAPE1,	SVAR	3
TAPE2, DISK1, ALPH, DISK2, SIGM, NPRT, DZOT,	SVAR	4
OTDPH, ZH, TEND, TMLD, TWH, TML, TTHW,	SVAR	5
TYML, RZ, RZ, NIPIH, MIT, NPHI, NITER,	SVAR	6
NPHI, NPHI1, NPHI2, NPHI3, NPHM1, NPHM2, NPHM3,	SVAR	7
NT, NT1, NT2, NT3, PMTFD, NCONE, RADT,	SVAR	8
PHF, METHOD, LAG, NSC, PINF, RMDTN, UINF,	SVAR	9
OTINF, GASCON, NREAL, NPUNCH	SVAR	10
TPRNT=ICONST(4)	GEOM1	7
TP(KS,FO,2) GO TO 12	GEOM1	8
CALL GEOM3(1, PHIP, NPHI, Z, PB, RZ, RORP, TPRT)	GEOM1	9
CONTINUE	GEOM1	9
CALL GEOM2(K5)	GEOM1	10
DO 1 J=3, NTZ	GEOM1	11
T=V(I,J)	GEOM1	12
DO 2 K=2, NPHI1	GEOM1	13
PHI=PHI(P(K))	GEOM1	14
A=PHI(K)-T*(RORZ(K)-ROR(K))	GEOM1	15
B=ORPH(K)-T*(RORPH(K)-RORPH(K))	GEOM1	16
C=OROP(K)-ROR(K)	GEOM1	17
D=(RORZ(K)-ROR(K))	GEOM1	18
E=(OROPH(K)-RORPH(K))	GEOM1	19
OTDZ(K,X)=A/C	GEOM1	20
OTDPH(J,K)=B/C	GEOM1	21
OTDR(K)=1.0/C	GEOM1	22
ACT(K)=D/C	GEOM1	23
RCT(K)=E/C	GEOM1	24
RCTOT=ACT(K)	GEOM1	25
T=OTSTH(PHI)	GEOM1	26
T=OTCOS(PHI)	GEOM1	27
CONTINUE	GEOM1	28
CONTINUE	GEOM1	29
RETURN	GEOM1	30
END	GEOM1	31
	GEOM1	32
ROUTINE GEOM2(K3)	GEOM2	2
COMMON /IDVAR/RK, ETA(41), PHIP(41), DTIL(41), DTILE(41), DEYA, TP(24)	IDVAR	2
LEVEL 2, RND, P, U, V, W, ROR, ROBZ, VINP, WINF, RORP, R, R, RZ, RRP, OTDP, P	PVAR	2
ACT, OTDZ, OTDR, ACT, ICONST, GAM, CONST, NREGON, RS, RSZ, RSPH, RST, RSTZ,	PVAR	3
RSPIIT	PVAR	4
COMMON /PVAR/ RMO(24,41), P(24,41), U(24,41), V(24,41), W(24,41),	PVAR	5
ROR(41), RORZ(41), WINF(41), WINF(41), WINF(41),	PVAR	6
RORPH(41), RZ(41), RZ(41), RZ(41), RRP(41),	PVAR	7
OTDPH(24,41), RCT(41), OTDZ(24,41), OTDR(41), ACT(41),	PVAR	8
ICONST(50), GAM(20), CONST(50), NREGON, RS(41),	PVAR	9
RSZ(41), RSPH(41), RST(41), RSTZ(41), RSPHIT(41)	PVAR	10
COMMON /SVAR/ T, Z, PHI, DT, DZ, DPHI, ZINT,	SVAR	2
TEND, PI, ALPHA, GAMMA, SIGMA, XNACH, TAPE1,	SVAR	3
TAPE2, DISK1, ALPH, DISK2, SIGM, NPRT, DZOT,	SVAR	4
OTDPH, ZH, TEND, TMLD, TWH, TML, TTHW,	SVAR	5
TYML, RZ, RZ, NIPIH, MIT, NPHI, NITER,	SVAR	6
NPHI, NPHI1, NPHI2, NPHI3, NPHM1, NPHM2, NPHM3,	SVAR	7
NT, NT1, NT2, NT3, PMTFD, NCONE, RADT,	SVAR	8
PHF, METHOD, LAG, NSC, PINF, RMDTN, UINF,	SVAR	9
OTINF, GASCON, NREAL, NPUNCH	SVAR	10
DO 1 K=1, NPHI2	GEOM2	6
PHI=PHI(P(K))	GEOM2	7
GO TO (3,2), K3	GEOM2	8
CONTINUE	GEOM2	9
ROR(K)=RS(K)	GEOM2	10
RORZ(K)=RZ(K)	GEOM2	11
RORPH(K)=RSPH(K)	GEOM2	12
GO TO 4	GEOM2	13
CONTINUE	GEOM2	14
ROR(K)=RST(K)	GEOM2	15
RORZ(K)=RSTZ(K)	GEOM2	16
RORPH(K)=RSPHIT(K)	GEOM2	17

```

4  CONTINUE
1  CONTINUE
   RETURN
   END

SUBROUTINE GEOM3(K7,PHT,PHTI,Z,RB,RBT,RPH,IPOINT)
COMMON /JOE/ ZL1,CF1,CF2,ZLF,ZTRAN,DZTRAN
COMMON /TRANSF/ AMACH,GAMF,KM2,PLINF,PLINF,V1INF,PQL(20,3),
* RHQ90(20,3),U90(20,3),V90(20,3),W90(20,3),R590(3),
* P5Z90(3),RSPH90(3),HRO,R90,XINIT
LEVEL 2, P9,R90,R9Z
DTMENSTON P9(41),R9PH(41),PRZ(41),PHT(41)
DTMENSTON ZSTA(200),DRDZ(200),PZ(200)
C
C.....CONSTANTS
C
TF(K7,NEAL) GO TO 1
CF2=1.5
AMG=9.5
NST=1
N=NRD
RNOSE=1.
CALL GEOM3(RNOSE,AMG,RZ,DRDZ,ZSTA,H,R90,NMAY)
NMAY=NMAY-1
RETURN
C
C.....FIND CORRECT Z INTERVAL
C
1 CONTINUE
N=NST
TF (7,LT,ZSTA(NST)) GO TO 22
DO 18 N=NST,NMAY1
TF (7,LT,ZSTA(N+1)) GO TO 20
20 CONTINUE
N=NMAV1
22 CONTINUE
P90DY=PZ(N)+(PZ(N+1)-RZ(N))/(ZSTA(N+1)-ZSTA(N))*(7-ZSTA(N))
R90DY7=DRDZ(N)+(DRDZ(N+1)-DRDZ(N))/(ZSTA(N+1)-ZSTA(N))*(7-ZSTA(N))
R90DPH=0.0
DO 30 K=3,NPHI
R9(K)=P90DY
R9PH(K)=R90DPH
R9PH(K)=P90DY
30 CONTINUE
DO 36 K=1,2
M=K
T=NPHI+K
N=NPHI+K
R9(K)=R9(N)
R9PH(K)=R9PH(N)
R9Z(K)=R9Z(N)
R9PH(K)=R9PH(N)
R9PH(K)=R9PH(N)
R9PH(K)=R9PH(N)
36 CONTINUE
RETURN
END

SUBROUTINE INITA
COMMON /CLUSTER/ J,XI(24),YXI(24),YXIT(24)
COMMON /ENTRO/ S(41),Z0S,ZFLO,ITPRTS,ITPRTF,MCASE,NTOSOS
COMMON /ZDVARB/RK,ETA(41),PHI(41),DTIL(41),DTILE(41),DETA,TP(24)
COMMON /JOE/ ZL1,CF1,CF2,ZLF,ZTRAN,DZTRAN
LEVEL 2, P9,P9U,P9V,P9W,P9R,P9Z,VINF,VINF,R9PH4,R9R,P9T,R9PH,DTDPH,
* ACT,NTDZ,DTDR,ACT,ICONST,GAM,CONST,MREGON,R5,RST,PSPHI,RST,PS7T,
* RSPHT
COMMON /PVARR/ P90(24,41), P9Z(41), U(24,41), V(24,41), W(24,41),
* R9P(41), R9B7(41), VINF(41), WINF(41),
* R9PH(41), R9T(41), R9Z(41), R9R(41), R9PH(41),
* DTDPH(24,41), DCT(41), DT0Z(24,41), DTOR(41), ACT(41),
* ICONST(50), GAM(20), CONST(50), MREGON, R5(41),
* RST(41), RSPHT(41), RST(41), RSTT(41), RSPHTT(41)
COMMON /SVARR/ T,Z, PHI, DT, DZ, DPHI, ZTMT,
* ZEND, PI, ALPHA, GAMMA, SIGMA, XNACH, TAPE1,

```

```

GEOM2 18
GEOM2 19
GEOM2 20
GEOM2 21

GEOM3 2
JTE 2
TRANSF 2
TRANSF 3
TRANSF 4
GEOM3 5
GEOM3 6
GEOM3 7
GEOM3 8
GEOM3 9
GEOM3 10
GEOM3 11
GEOM3 12
GEOM3 13
GEOM3 14
GEOM3 15
GEOM3 16
GEOM3 17
GEOM3 18
GEOM3 19
GEOM3 20
GEOM3 21
GEOM3 22
GEOM3 23
GEOM3 24
GEOM3 25
GEOM3 26
GEOM3 27
GEOM3 28
GEOM3 29
GEOM3 30
GEOM3 31
GEOM3 32
GEOM3 33
GEOM3 34
GEOM3 35
GEOM3 36
GEOM3 37
GEOM3 38
GEOM3 39
GEOM3 40
GEOM3 41
GEOM3 42
GEOM3 43
GEOM3 44
GEOM3 45
GEOM3 46
GEOM3 47
GEOM3 48
GEOM3 49
GEOM3 50
GEOM3 51
GEOM3 52
GEOM3 53

```

```

* TAPE2, DISK1, ALPH, DISK2, SIGN, NPHI, DZOT,
* DZOPH, ZN, THWD, THLD, TRW, TML, TTRW,
* TTHL, RZ, BZ, NPHI, NIT, KPHI, NITER,
* NPHI, NPHI1, NPHI2, NPHI3, NPHI4, NPHI5, NPHI6, NPHI7,
* NT, NT1, NT2, NT3, PHTF, NCON, RANT,
* PHTF, METHOD, LAG, MOC, PTNC, P90IN, UINF,
* GINF,GASCON,MREAL,NPUNCH
COMMON /TRANSF/ AMACH,GAMF,KM2,PLINF,PLINF,V1INF,PQL(20,3),
* RHQ90(20,3),U90(20,3),V90(20,3),W90(20,3),R590(3),
* P5Z90(3),RSPH90(3),HRO,R90,XINIT
RADI=57.29578
PT=3.14159265
TINT=XINIT
T=7TMT
ZEND=ZLF
ALPHA=0.0
NPHI=0
NIT=KM2
XNACH=AMACH
GAMMA=GAMF
ALPH=ALPHA/RADI
SIGMA=SIGMA/RADI
PHTF=1/PLINF*1/RADI
NPHI1=NPHI+3
NPHI2=NPHI+1
NPHI3=NPHI+2
NPHI4=NPHI-1
NPHI5=NPHI-2
NT=NT+2
NT1=NT+1
NT2=NT+2
ICNST(1)=1
ICNST(101)=1
TPNT=ICNST(4)
IF (ICNST(40).NE.1) ICNST(5)=0
LAG=1
DETA=PHTF/PLINF*ATN(PHT)
RPHI=DETA
DT=1./FLOAT(NT-1)
RZ=DT*NT+DT
DTDPH=DT/DETA
GAM(1)=(GAMMA-1.0)*0.5
GAM(2)=GAM(1)/GAMMA
C..MERIDIONAL CLUSTERING
PHI(0)=0
PK=0.7
PJ=0.3
TF(RK,EO,0.0) GO TO 15
V9=0.5/RK*ALOG(1.3+(EXP(RK)-1.0)*PHTF/1*0.01/
* (1.0-(1.0-EXP(-RK))*PHTF/100.0))
V91=STNH(RK*V9)
V92=V91/(RK*PHI/RADI)
15 CONTINUE
DO 35 IT=2,NPHI1
ZI=IT-3
CTA(ZI)=ZT*DETA
TF(RK,GT,0.0) GO TO 40
PHI(ZI)=CTA(ZI)
DTIL(ZI)=1.0
DTILE(ZI)=0.0
GO TO 35
CONTINUE
Y3=PK*(DETA(ZI)/PI-YC)
SHETA=STNH(Y3)
CHETA=COSH(Y3)
PHI(ZI)=PHI(ZI)/RADI*(1.0+SHETA/Y3)
DTILE(ZI)=V3*PK/CHETA
DTILE(ZI)=V3*PK*SHETA/CHETA**2
CONTINUE
PHI(ZI)=PHI(ZI)
PHI(NPHI1)=PHI(NPHI1)
DTIL(2)=DTIL(4)
DTIL(NPHI1)=DTIL(NPHI1)
DTILE(2)=DTILE(4)
DTILE(NPHI1)=DTILE(NPHI1)
DTILE(3)=0.0
DTIL(NPHI1)=0.0
C..RADIAL CLUSTERING
XNACH=STNH(RJ)
DO 36 IT=1,NT2
ZT=IT-5
TP(IT)=7TMT
IF(RJ,EO,0.0) GO TO 41
DT=RJ*TP(IT)

```

```

SVARR 4
SVARR 5
SVARR 6
SVARR 7
SVARR 8
SVARR 9
SVARR 10
TRANSF 2
TRANSF 3
TRANSF 4
TNITA 10
TNITA 11
TNITA 12
TNITA 13
TNITA 14
TNITA 15
TNITA 16
TNITA 17
TNITA 18
TNITA 19
TNITA 20
TNITA 21
TNITA 22
TNITA 23
TNITA 24
TNITA 25
TNITA 26
TNITA 27
TNITA 28
TNITA 29
TNITA 30
TNITA 31
TNITA 32
TNITA 33
TNITA 34
TNITA 35
TNITA 36
TNITA 37
TNITA 38
TNITA 39
TNITA 40
TNITA 41
TNITA 42
TNITA 43
TNITA 44
TNITA 45
TNITA 46
TNITA 47
TNITA 48
TNITA 49
TNITA 50
TNITA 51
TNITA 52
TNITA 53
TNITA 54
TNITA 55
TNITA 56
TNITA 57
TNITA 58
TNITA 59
TNITA 60
TNITA 61
TNITA 62
TNITA 63
TNITA 64
TNITA 65
TNITA 66
TNITA 67
TNITA 68
TNITA 69
TNITA 70
TNITA 71
TNITA 72
TNITA 73
TNITA 74
TNITA 75
TNITA 76
TNITA 77
TNITA 78
TNITA 79
TNITA 80
TNITA 81
TNITA 82
TNITA 83

```


	QJ 16 N=1,4	TOCCN	73
	H(N)=H(N)	TOCCN	74
	F(N)=F(N)+X(I,J)	TOCCN	75
	G(N)=G(N)+Y(I,K)	TOCCN	76
16	CONTINUE	TOCCN	77
	GO TO (17,18),IT	TOCCN	78
17	CONTINUE	TOCCN	79
	C...SET CONSERVATIVE VARIABLES AT 4	TOCCN	80
	QJ 20 N=1,4	TOCCN	81
	D(N,J,K)=F(N)	TOCCN	82
	F2(N,J,K)=F(N)	TOCCN	83
	G(N,J,K)=G(N)	TOCCN	84
	H(N,J,K)=H(N)	TOCCN	85
2.	CONTINUE	TOCCN	86
	GO TO 3	TOCCN	87
18	CONTINUE	TOCCN	88
	C...SET CONSERVATIVE VARIABLES AT N+1 TILDE	TOCCN	89
	QJ 0 N=1,4	TOCCN	90
	F(I,J,K)=G(N+1) GO TO 3A	TOCCN	91
	GO TO 3B	TOCCN	92
	C...SET STATE AT BODY AND SHOCK	TOCCN	93
3A	STATE(N,J,K)=E(N)	TOCCN	94
3B	CONTINUE	TOCCN	95
	F(N,J,K)=F(N)	TOCCN	96
	G(N,J,K)=G(N)	TOCCN	97
	H(N,J,K)=H(N)	TOCCN	98
0	CONTINUE	TOCCN	99
3	CONTINUE	TOCCN	100
	RETURN	TOCCN	101
2	CONTINUE	TOCCN	102
	C...D-CODE CONSERVATIVE VARIABLES--PERFECT GAS.	TOCCN	103
	AA=1-CO=CAL(2)	TOCCN	104
	QJ 1 N=1,NP(K)	TOCCN	105
	QJ 1 J=3,NTL	TOCCN	106
	A=STATEP(1,J,K)	TOCCN	107
	B=ETC=0(2,J,K)	TOCCN	108
	C=ETC=0(3,J,K)	TOCCN	109
	D=ETC=0(4,J,K)	TOCCN	110
	BB=AA*1	TOCCN	111
	W(J,K)=1/A	TOCCN	112
	W(J,K)=1/A	TOCCN	113
	CC=CAL(2)(AA,-W(J,K)**2-W(J,K)**2)	TOCCN	114
	DD=AA*2=AA**AA*CC	TOCCN	115
	YF(N,J) 7,8,9	TOCCN	116
7	CONTINUE	TOCCN	117
	DD=C	TOCCN	118
4	CONTINUE	TOCCN	119
	U(J,K)=(-AA*SQRT(DD))/12.0*AA	TOCCN	120
	B=U(J,K)=1/U(J,K)	TOCCN	121
	D(J,K)=0.4*U(J,K)*AA,-U(J,K)**2-W(J,K)**2)	TOCCN	122
	CONTINUE	TOCCN	123
	OTURN	TOCCN	124
	END	TOCCN	125

FACT=0,5*YFAC+0.5*MAC*(GAMMA-1.0)	OUTPTM	12
FACD=(FACT+1.0)*0.1/((GAMMA-1.0))	OUTPTM	13
FACV=SQRT((FACT+1.0)/FACT)	OUTPTM	14
NZADN=N*ZADN+1	OUTPTM	15
K7=N*EMN+N*ADD	OUTPTM	16
ZC=7	OUTPTM	17
WRITE(6,6J3) NZADN,ZC,R(3),R7(3)	OUTPTM	18
ORSDX(K7)=RDM7(3)	OUTPTM	19
WRITE(9) NZADN,Z,ORSDX(KZ)	OUTPTM	20
DO 20 J=3,N7Z	OUTPTM	21
V=X(I,J)	OUTPTM	22
V=Y+Z*ORJ(3)-R(3)+R(3)	OUTPTM	23
JZ=J-2	OUTPTM	24
ZC(JZ,KZ)=Z	OUTPTM	25
V(I,JZ,K7)=V	OUTPTM	26
V(I,J,KZ)=U(J,3)+FACV	OUTPTM	27
V(I,J,K7)=U(J,3)+FACV	OUTPTM	28
ORH(I,J,KZ)=RDM7(3)+FACD	OUTPTM	29
WRITE(9) J,V,VX(JZ,KZ),V(I,JZ,KZ),RDM7(3,K7)	OUTPTM	30
2) CONTINUE	OUTPTM	31
ETION	OUTPTM	32
6.7. FORMAT(5X,I3,3(10X,F10.4))	OUTPTM	33
END	OUTPTM	34
	OUTPTM	35

SUBPRTIME	PTIME(M1,DMU,P21,MITS,G4M4)	PTIME	2
QFAL M1,M2,M		PTIME	3
YMU(M) = ATAN(SORT(C*(MOM-1))) / SORT(C-ATAN(SORT(MOM-1)))		PTIME	4
YMU(M) = SORT(MOM-1) / ((1+(GM-1) / 2 * 4 * M) / M		PTIME	5
GM=GM4M4		PTIME	6
C = (CM-1) / (GM+1)		PTIME	7
SORT = SORT(C)		PTIME	8
CM = 2.15-0		PTIME	9
YMU1 = YMU(M)		PTIME	10
YMU2 = YMU1 + DM1		PTIME	11
VM = M		PTIME	12
TM 10 T=1,20		PTIME	13
MITS = T		PTIME	14
M2 = M - (YMU1(M1-YMU2) / YMU(P(M))		PTIME	15
TE (M2,GT,10,0) GO TO 20		PTIME	16
TE (145*(M1-CM) / VM) .LT. (P21) GO TO 30		PTIME	17
CM = M2		PTIME	18
2 CONTINUE		PTIME	19
M2 = 1.0-0		PTIME	20
VP1(T(M+1)		PTIME	21
30 CONTINUE		PTIME	22
P21 = ((1+(GM-1) / 2 * 4 * M1) / ((1+(GM-1) / 2 * 4 * M2))) * (GM / (GM-1))		PTIME	23
DETUM		PTIME	24
1 FORMATTED,47M- - - - RNDY TUM STOD=9 AT M2 = 100.0 - - -		PTIME	25
END		PTIME	26

[illegible][illegible]

```

DRSDZ(A,B,C,D)=UINF+C+A*SORT(D*(1+B*9)+C*C)/D
RHOS(A)=(A+GRATIO)/1+GRATIO+1
ANAP(A,B,C,D,E,F)=(-1)*ASS(-UINF+D+A*ROE)/(1+D*B+1+E*E)+F
US(A,B,C)=A-C*B
WS(A,B,C)=A-B*C
GAMMA1=GAMMA+1
GAMMA1=GAMMA-1
GRATIO=GAMMA/GAMPA
GAMPA1=GAMMA/GAMMA
C1=0.5*GAMMA*PINF/RHOIN
C2=0.5*GAMPA*GOC1
DO TO (1,2),K4
1
CONTINUE
C..CHECK CORRECTOR
DO 3 K=3,NPHI
  PST(K)=PST(K)+DZ*RSZ(K)
3
DO 4 K=1,2
  M=6-K
  I=NPHI+K
  N=NPHI-K
  PST(K)=PST(K)
  PST(I)=PST(I)
4
CONTINUE
DO 5 K=3,NPHI
  RSPHIT(I)=(RST(K+1)-RST(K-1))/(2.0*DETA)*DTIL(K)
  PS=PINT2,K
  PSRAT=PS/PINF
  ULT=ULT+D(PSRAT)
  RHRAT=RHOS(PSRAT)
  PSI=PST(K)
  RSPH=RSPTH(K)
  RSPH=RSPTH/RS1
  FACT1=VINP(K)-VINP(K)*RSPH
  FACT2=UINF+UINF-ULT*ULT
  IF(FACT2.LT.0.)ULT=-ULT
  RST1=RSRSTZ(ULT,RSPH,FACT1,FACT2)
  RST(K)=RST1
  ANART=ANAP(VINP(K),VINP(K),PST1,RSPH,RHRAT)
  UST=US(VINP(K),ANART,RSZ1)
  VST=VS(VINP(K),ANART)
  WST=WS(VINP(K),ANART,RSPH)
  IF (NREAL.EQ.0) ROST=RHRAT/RHOIN
  RHOINT2,K)=ROST
  VINT2,K)=UST
  WINT2,K)=WST
5
CONTINUE
DO 6 K=1,2
  M=6-K
  I=NPHI+K
  N=NPHI-K
  RST(K)=RST(K)
  RST(I)=RST(I)
  RSPHIT(I)=RSPHIT(I)
  RSPHIT(I)=RSPHIT(I)
6
CONTINUE
RETURN
CONTINUE
C..S40CK CORRECTOR
DO 8 K=3,NPHI
  RST(K)=RST(K)+.5*(RST(K)+RST(K)+DZ
8
DO 9 K=1,2
  M=6-K
  I=NPHI+K
  N=NPHI-K
  RST(K)=RST(K)
  RST(I)=RST(I)
9
CONTINUE
DO 10 K=3,NPHI
  RSPHIT(K)=(RST(K+1)-RST(K-1))/(2.0*DETA)*DTIL(K)
  PS=PINT2,K
  PSRAT=PS/PINF
  ULT=ULT+D(PSRAT)
  RHRAT=RHOS(PSRAT)
  PSI=PST(K)
  RSPH=RSPTH(K)
  RSPH=RSPTH/RS1
  FACT1=VINP(K)-VINP(K)*RSPH
  FACT2=UINF+UINF-ULT*ULT
  IF(FACT2.LT.0.)ULT=-ULT
  RST1=DRSDZ(ULT,RSPH,FACT1,FACT2)
  RST(K)=RST1
  ANART=ANAP(VINP(K),VINP(K),PST1,RSPH,RHRAT)

```

```

USF=US(VINP(K),ANART,RSZ1)
VSF=VS(VINP(K),ANART)
USF=US(VINP(K),ANART,RSPH)
IF (NREAL.EQ.0) ROSF=RHRAT/RHOIN
RHOINT2,K)=ROSF
UIN2,K)=USF
VINT2,K)=VSF
WINT2,K)=WSF
10
CONTINUE
DO 11 K=1,2
  M=6-K
  I=NPHI+K
  N=NPHI-K
  RST(K)=RST(K)
  RST(I)=RST(I)
  RSPHIT(K)=RSPHIT(K)
  RSPHIT(I)=RSPHIT(I)
11
CONTINUE
RETURN
END

```

```

SUBROUTINE SETDAT
COMMON/CLUSTR/RJ,VI(24),TXI(24),TXIT(24)
LEVEL 2,EYE=0,E0,F3,60,MD
COMMON /CVARS/ ETENP(4,24,41), E0(4,24,41),
  * E01(4,24,41) , GD(4,24,41) , H0(4,24,41)
COMMON/ETENP/S(41),ZBS,ZFLD,ITPRT8,ITPRTF,NCASE,MTDSOS
COMMON /IDVARS/RK,ETA(41),PHI(41),DTIL(41),DTILE(41),DETA,TP(24)
* JDE
LEVEL 3, *H0,P,U,V,W,ROH,ROST,VINF,WINF,ROAPH,RB,RSZ,BRPH,DTDPH,
* BFT,DTOT,DTDR,ACT,ICONST,GAM,CONST,NREGON,RS,RST,RSPHIT,PS,PSZT,
* RSPHIT
COMMON /PVARS/ RMO(24,41), P(24,41), U(24,41), V(24,41), W(24,41),
  * ROR(41) , RORZ(41) , VINP(41) , WINF(41) ,
  * RORPHI(41) , ROR(41) , RRT(41) , RRPPI(41) ,
  * DTDPH(24,41) , BCT(41) , DTOT(24,41),DTDR(41) , ACT(41) ,
  * ICONST(50) , GAM(20) , CONST(50) , NREGON , RS(41) ,
  * PSZ(41) , RSPHIT(41) , RST(41) , RSTT(41) , RSPHIT(41)
COMMON/SVARS/DT,PHI,DT,DZ,DPHI,ZINT,
  * TEND , PI , ALPHA , GAMMA , SIGMA , XNACH , TAPE1 ,
  * TAPE2 , DISK1 , ALPH , DISF2 , SIGM , NPNY , DZOT ,
  * ZNPH , ZH , THUD , TMLD , TML , TTMW ,
  * TPL , RZ , RZ , RHPH , RHT , RPHI , RHTER ,
  * RPHI , RPHI1 , RPHI2 , RPHI3 , RPHI4 , RPHI5 , RPHI6 ,
  * NT , NTL , NYZ , NTS , PHIFN , NCONC , RADIE ,
  * PHIF , RETHOD , LAG , NDC , PINF , RHOIN , UINF ,
  * RINF,GASCON,NREAL,NPUNCH
SETDAT 2
CLUSTR 2
CVARS 2
CVARS 3
CVARS 4
ENTRO 2
IDVARS 2
JDE 2
PVAR 2
PVAR 3
PVAR 4
PVAR 5
PVAR 6
PVAR 7
PVAR 8
PVAR 9
PVAR 10
SVARS 2
SVARS 3
SVARS 4
SVARS 5
SVARS 6
SVARS 7
SVARS 8
SVARS 9
SVARS 10
SETDAT 10
SETDAT 10
SETDAT 11
SETDAT 12
SETDAT 13
SETDAT 14
SETDAT 15
SETDAT 16
SETDAT 17
SETDAT 18
SETDAT 19
SETDAT 20
SETDAT 21
SETDAT 22
SETDAT 23
SETDAT 24
SETDAT 25
SETDAT 26
SETDAT 27
SETDAT 28
SETDAT 29
SETDAT 30
SETDAT 31
SETDAT 32
SETDAT 33
SETDAT 34
SETDAT 35
SETDAT 36
SETDAT 37
SETDAT 38
SETDAT 39
SETDAT 40
SETDAT 41
SETDAT 42

```

```

ACT(I)=0.0
DTR(I)=0.0
ACT(I)=0.0
RS(I)=0.0
RSZ(I)=0.0
RSPHT(I)=0.0
RST(I)=0.0
RST(I)=0.0
RSPHT(I)=0.0
ETA(I)=0.0
PHT(I)=0.0
DTIL(I)=0.0
DTILE(I)=0.0
DO 11 J=1,24
RMD(J,I)=0.0
PIJ,I)=0.0
UIJ,I)=0.0
VIJ,I)=0.0
WIJ,I)=0.0
DTOPH(J,I)=0.0
DTDZ(J,I)=0.0
11 CONTINUE
RETURN
END

```

```

SETDAT 43
SETDAT 44
SETDAT 45
SETDAT 46
SETDAT 47
SETDAT 48
SETDAT 49
SETDAT 50
SETDAT 51
SETDAT 52
SETDAT 53
SETDAT 54
SETDAT 55
SETDAT 56
SETDAT 57
SETDAT 58
SETDAT 59
SETDAT 60
SETDAT 61
SETDAT 62
SETDAT 63
SETDAT 64
SETDAT 65
SETDAT 66

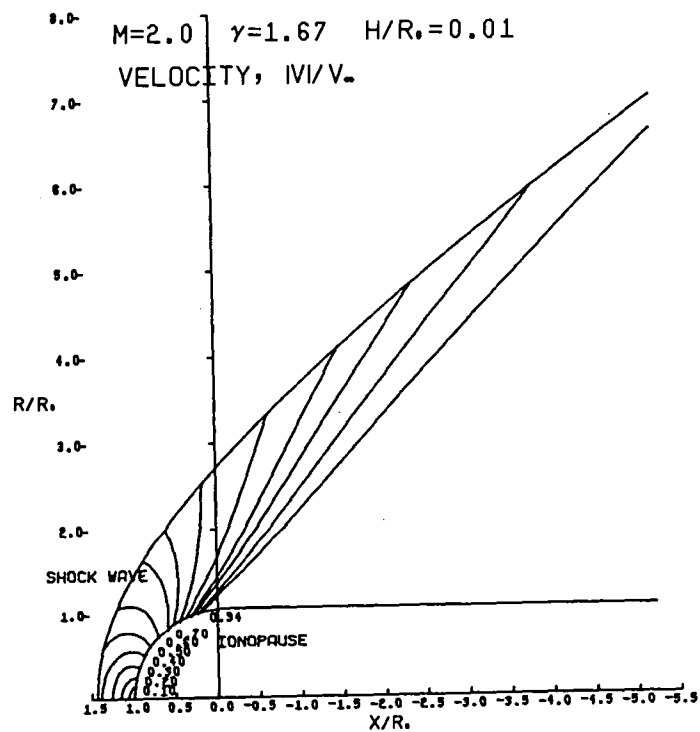
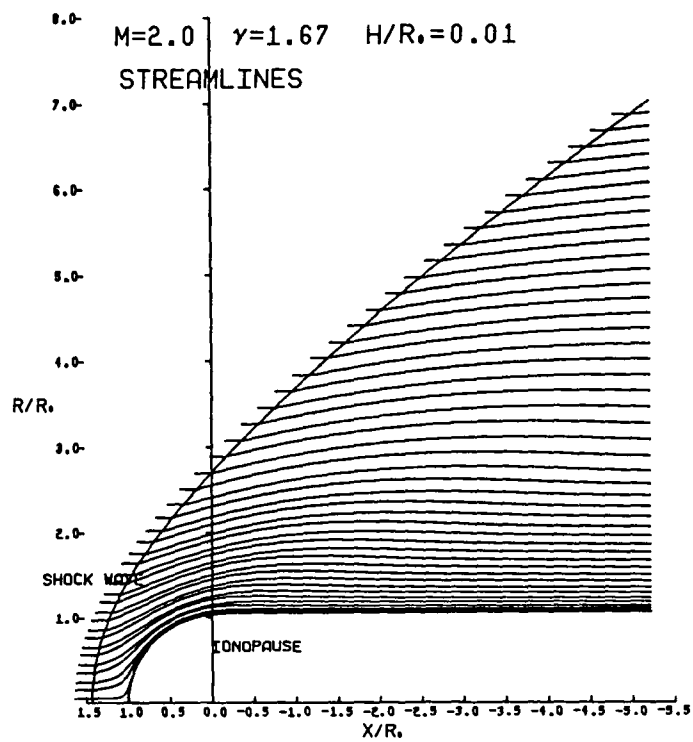
```

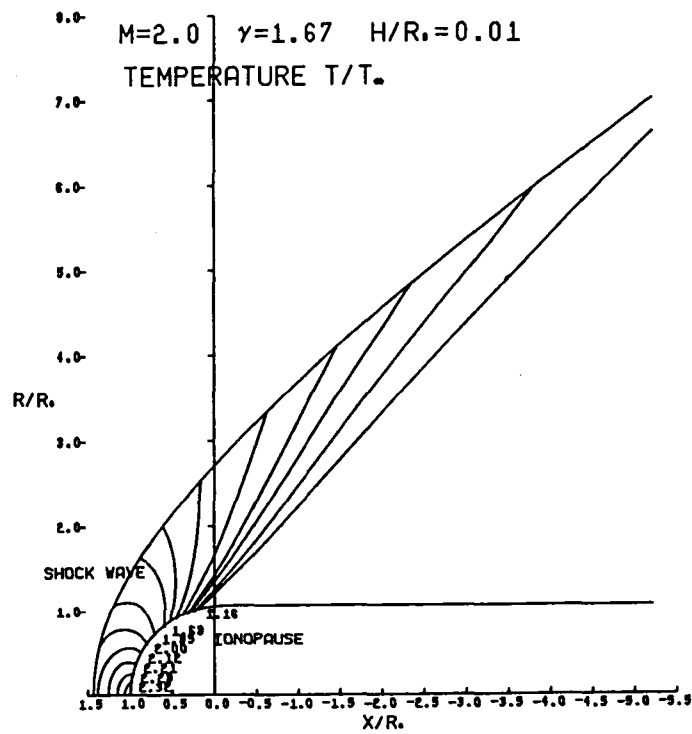
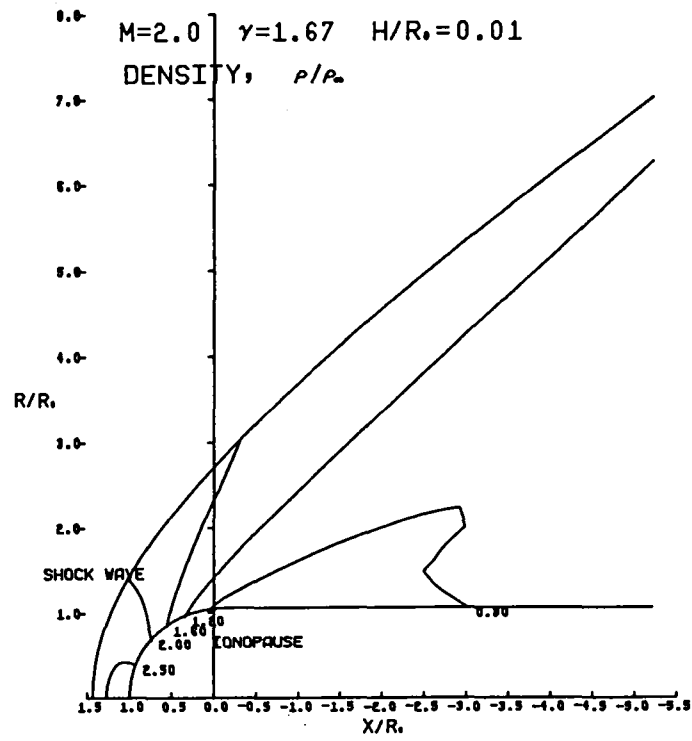
This Page Intentionally Left Blank

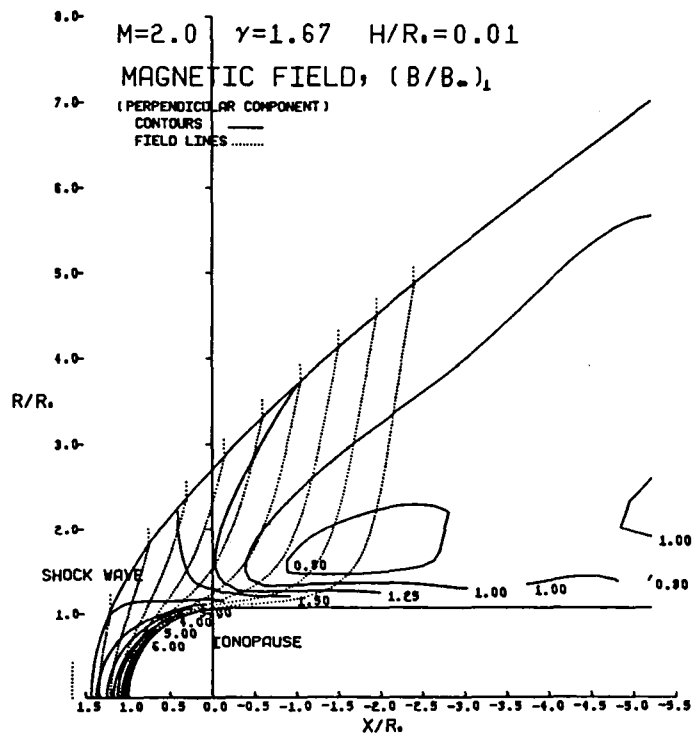
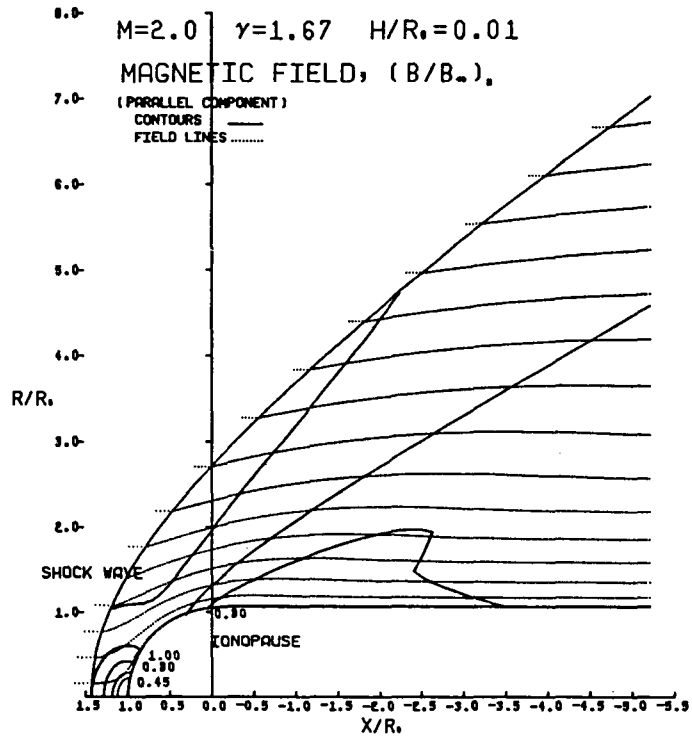
APPENDIX C
CATALOG OF TEST CASES

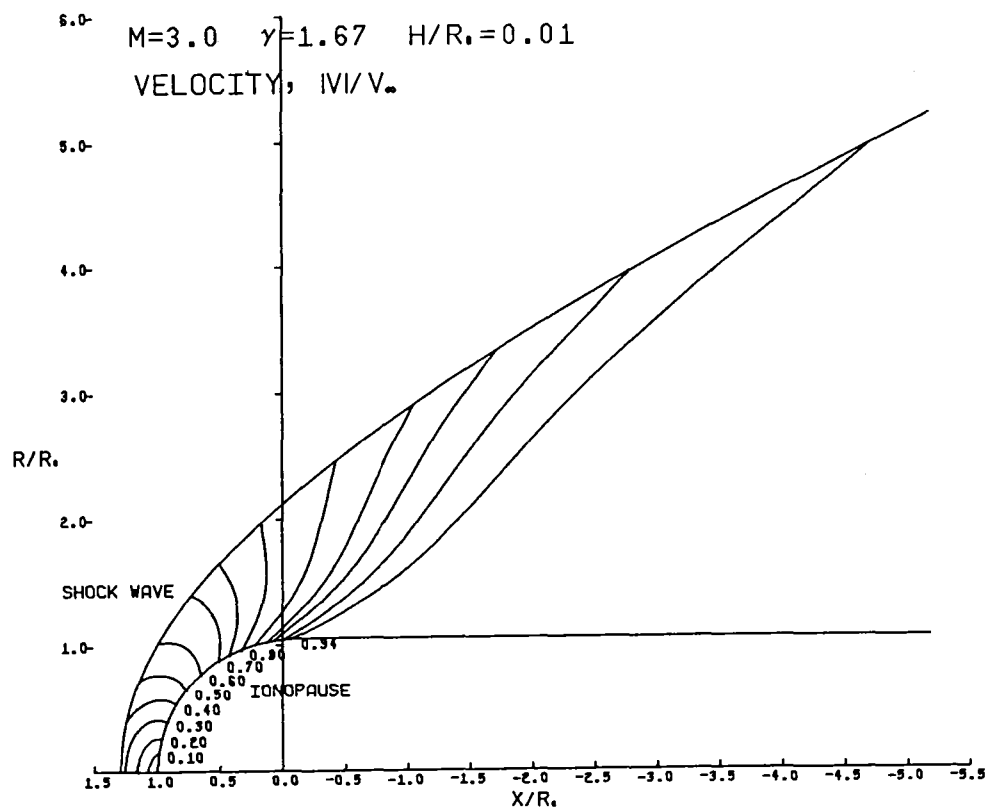
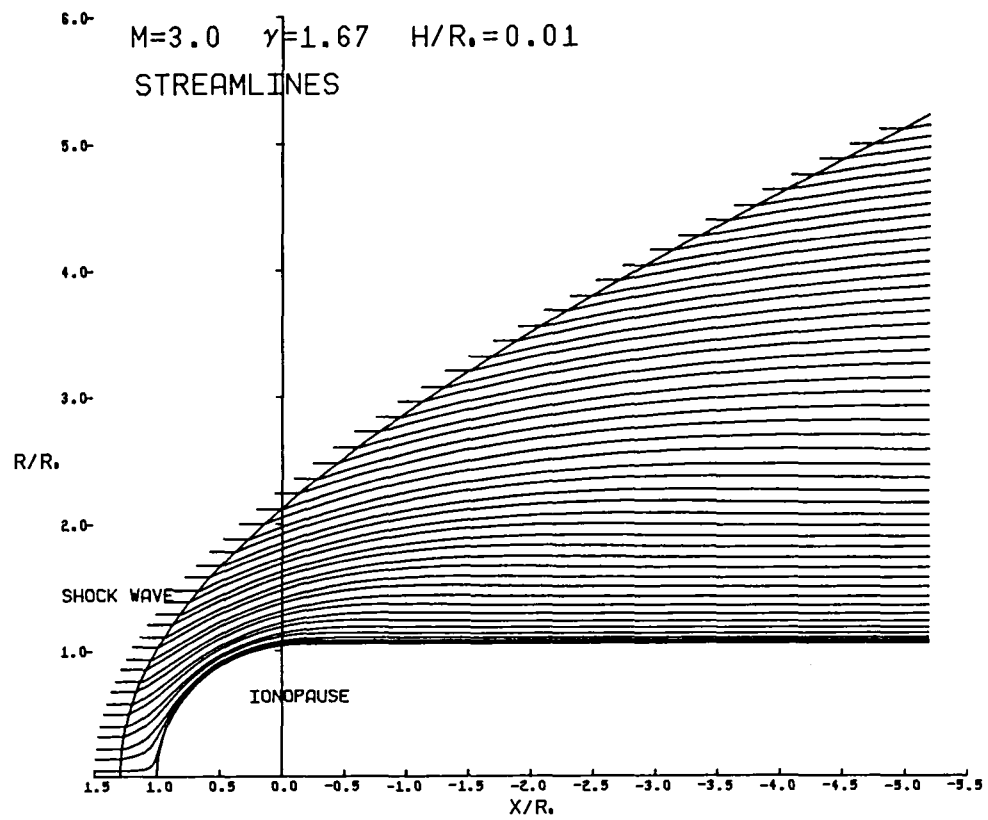
Catalog page number index for plasma streamline, velocity magnitude, density, temperature, and unit magnetic-field maps for various solar-wind flows past planetary ionopauses

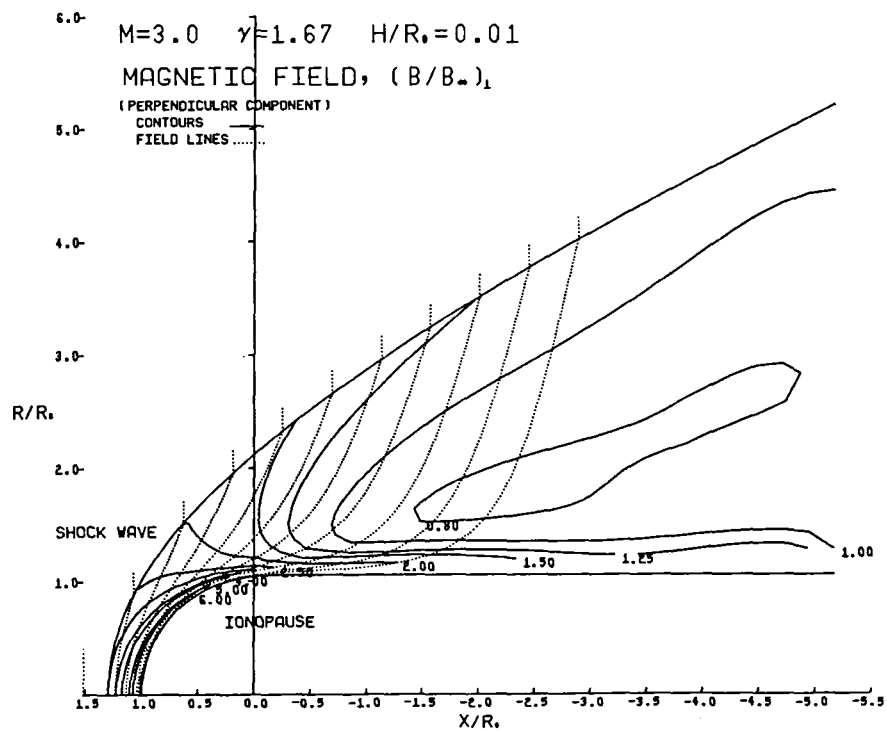
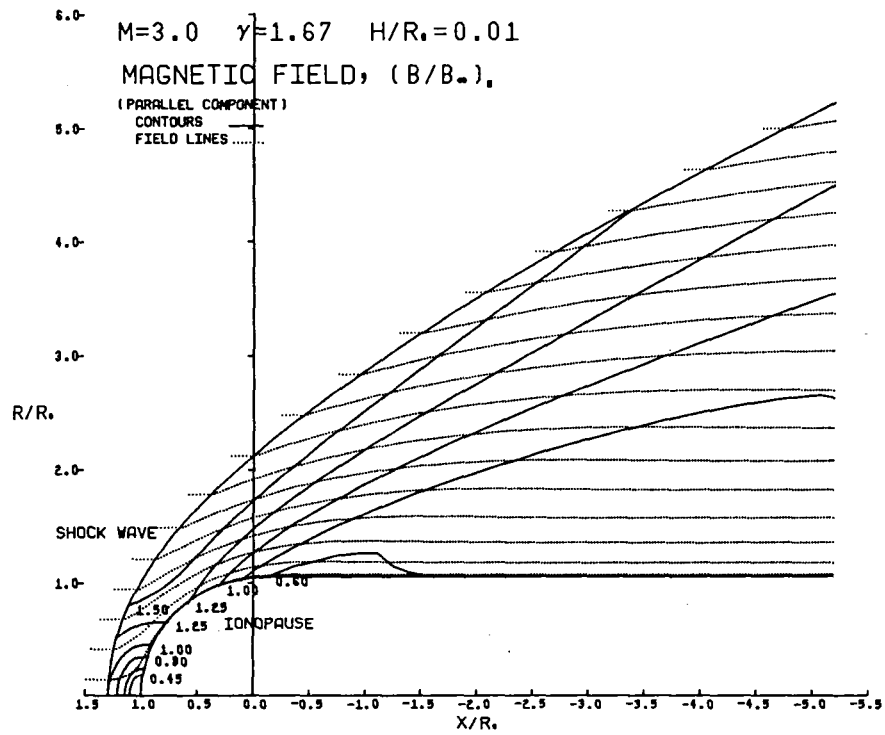
H/R_0	M_∞	γ	(Page No.) Streamlines	(Page No.) Velocity magnitude $ v /v_\infty$	(Page No.) Density ρ/ρ_∞	(Page No.) Temperature T/T_∞	(Page No.) Parallel magnetic field $(B /B_\infty)_\parallel$	(Page No.) Perpendicular magnetic field $(B /B_\infty)_\perp$
.01 ↓ .10 ↓ .25 ↓	2.0 3.0 5.0 8.0 12.0 25.0 2.0 3.0 5.0 8.0 12.0 25.0 2.0 3.0 5.0 8.0 12.0 25.0	5/3 ↓	179 182 185 188 191 194 197 200 203 206 209 212 215 218 221 224 227 230	179 182 185 188 191 194 197 200 203 206 209 212 215 218 221 224 227 230	180 183 186 189 192 195 198 201 204 207 210 213 216 219 222 225 228 231	180 183 186 189 192 195 198 201 204 207 210 213 216 219 222 225 228 231	181 184 187 190 193 196 199 202 205 208 211 214 217 220 223 226 229 232	181 184 187 190 193 196 199 202 205 208 211 214 217 220 223 226 229 232
\bar{H}/R_0	M_∞	γ	Streamlines	$ v /v_\infty$	ρ/ρ_∞	T/T_∞	$(B /B_\infty)_\parallel$	$(B /B_\infty)_\perp$
.10 ↓ .20 ↓ .25 ↓	2.0 3.0 5.0 8.0 12.0 25.0 2.0 3.0 5.0 8.0 12.0 25.0 2.0 3.0 5.0 8.0 12.0 25.0	5/3 ↓	233 236 239 242 245 248 251 254 257 260 263 266 269 272 275 278 281 284	233 236 239 242 245 248 251 254 257 260 263 266 269 272 275 278 281 284	234 237 240 243 246 249 252 255 258 261 264 267 270 273 276 279 282 285	234 237 240 243 246 249 252 255 258 261 264 267 270 273 276 279 282 285	235 238 241 244 247 250 253 256 259 262 265 268 271 274 277 280 283 286	235 238 241 244 247 250 253 256 259 262 265 268 271 274 277 280 283 286

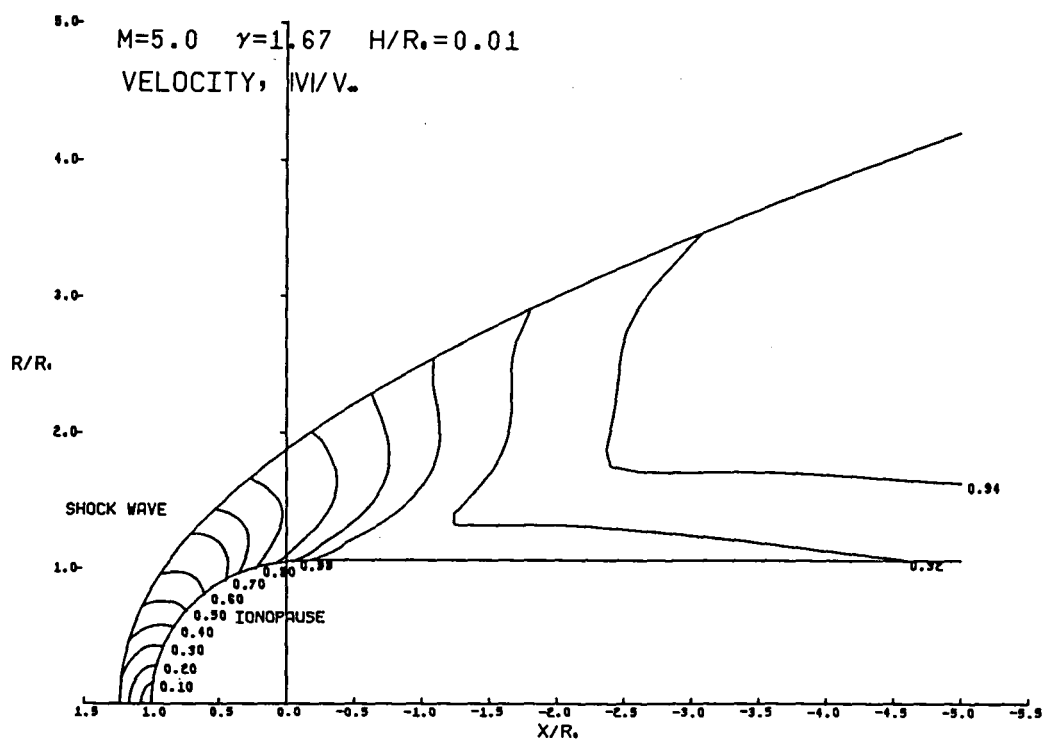
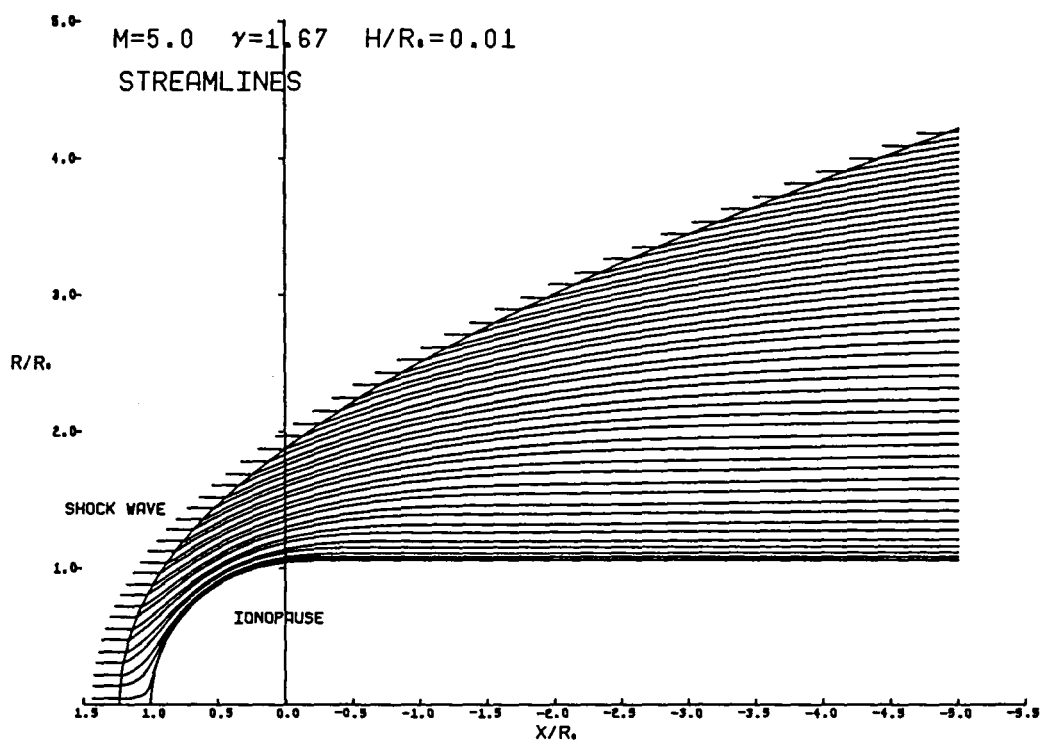


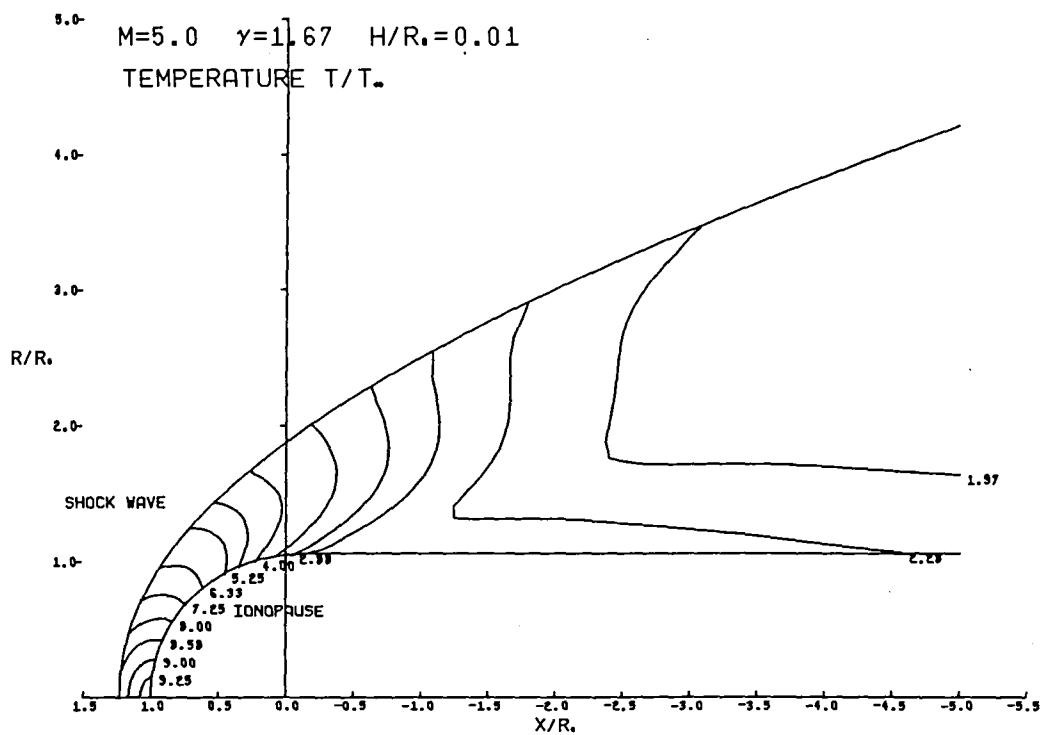
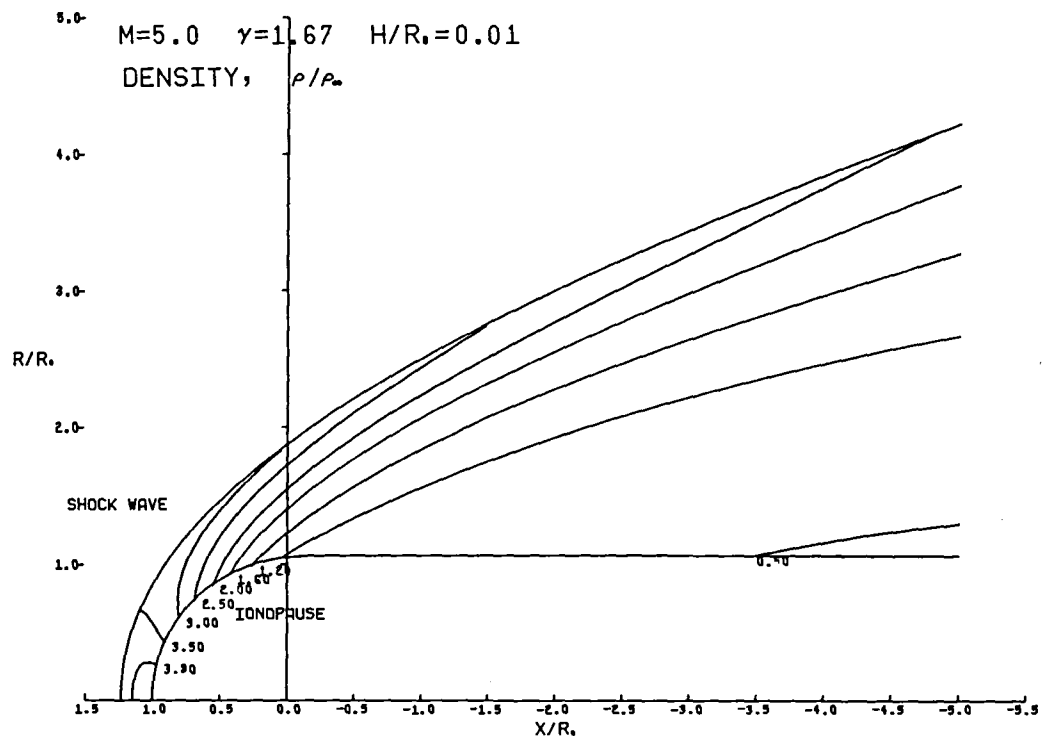


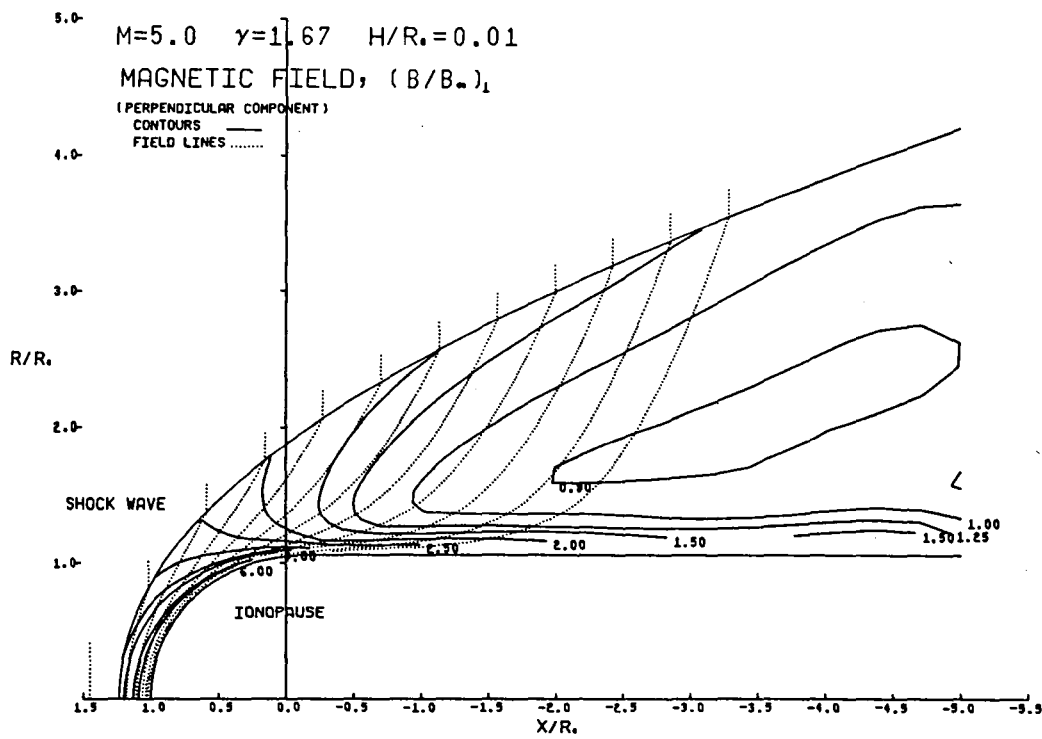
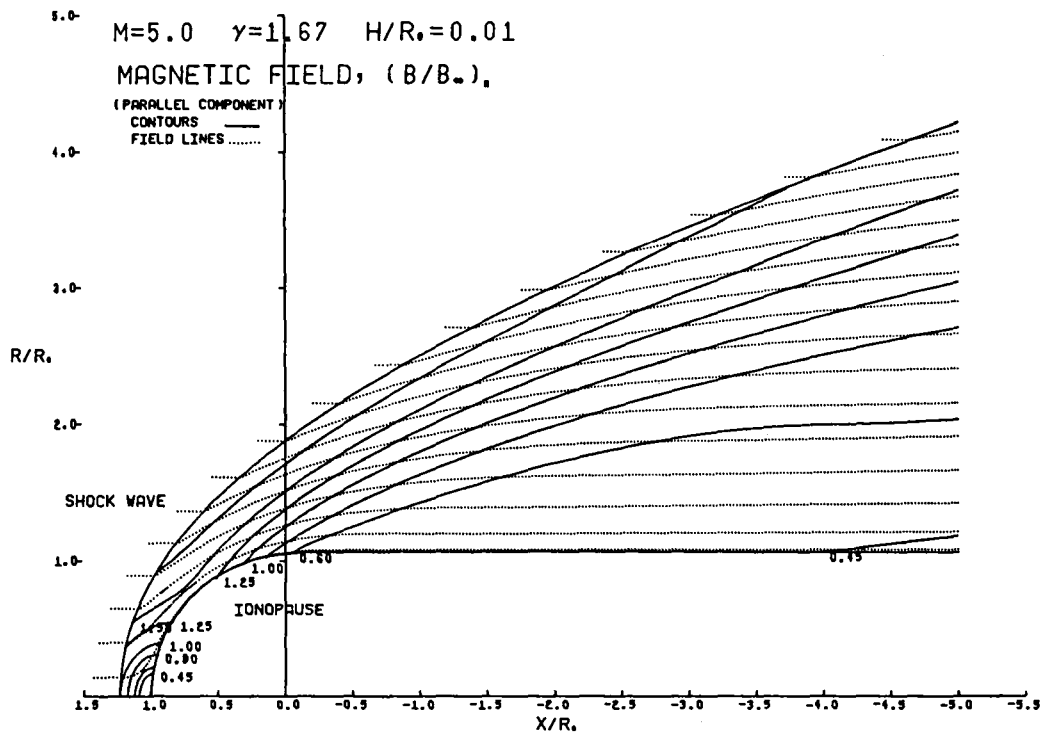


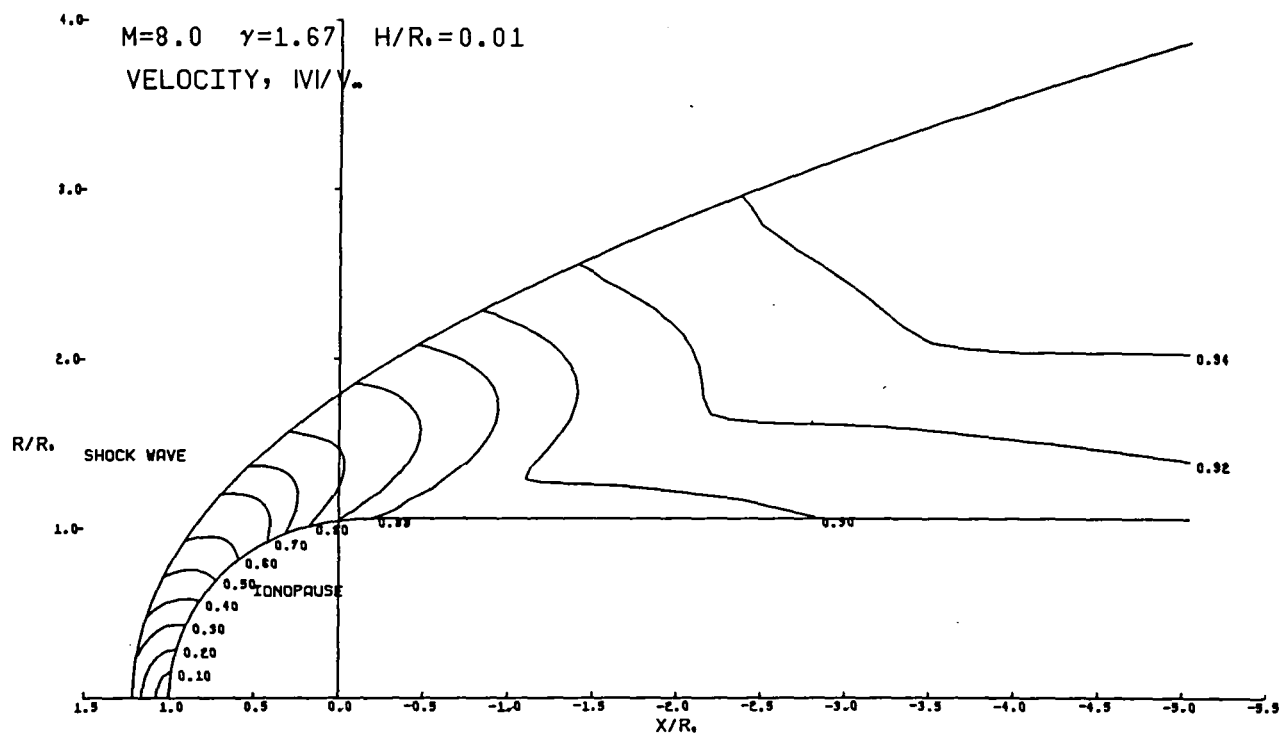
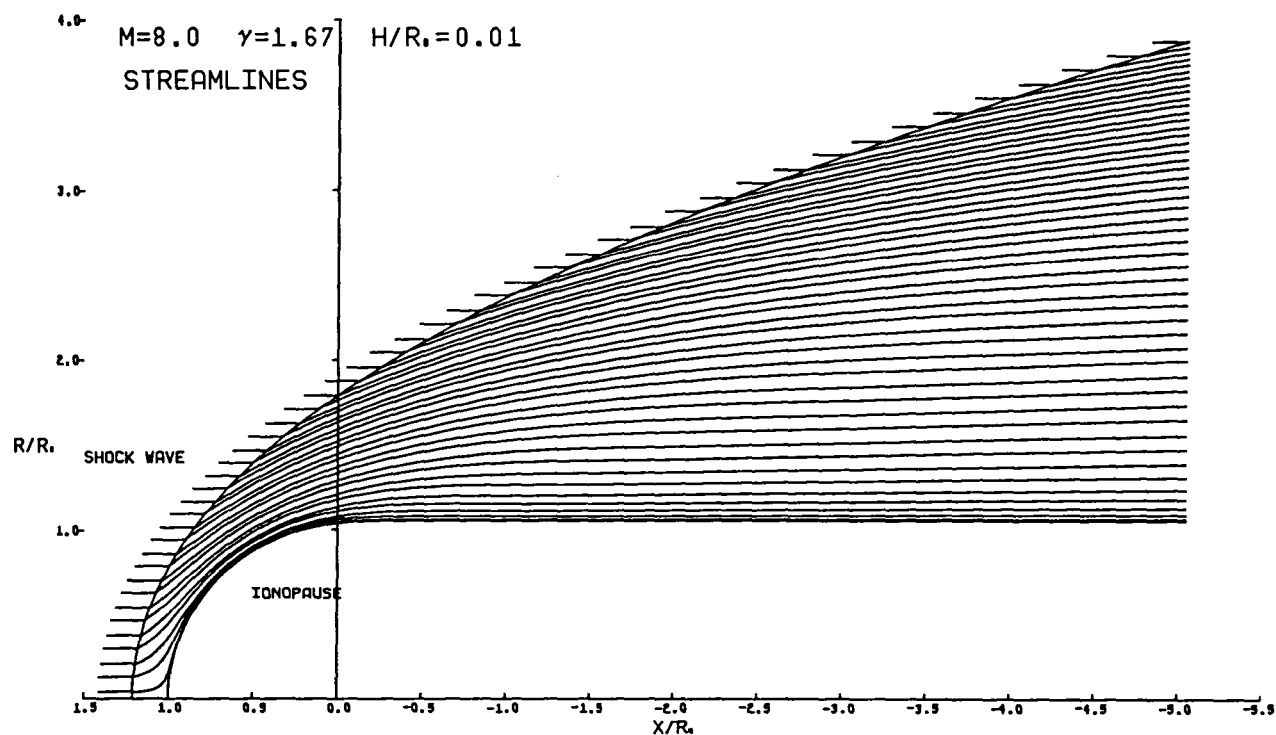


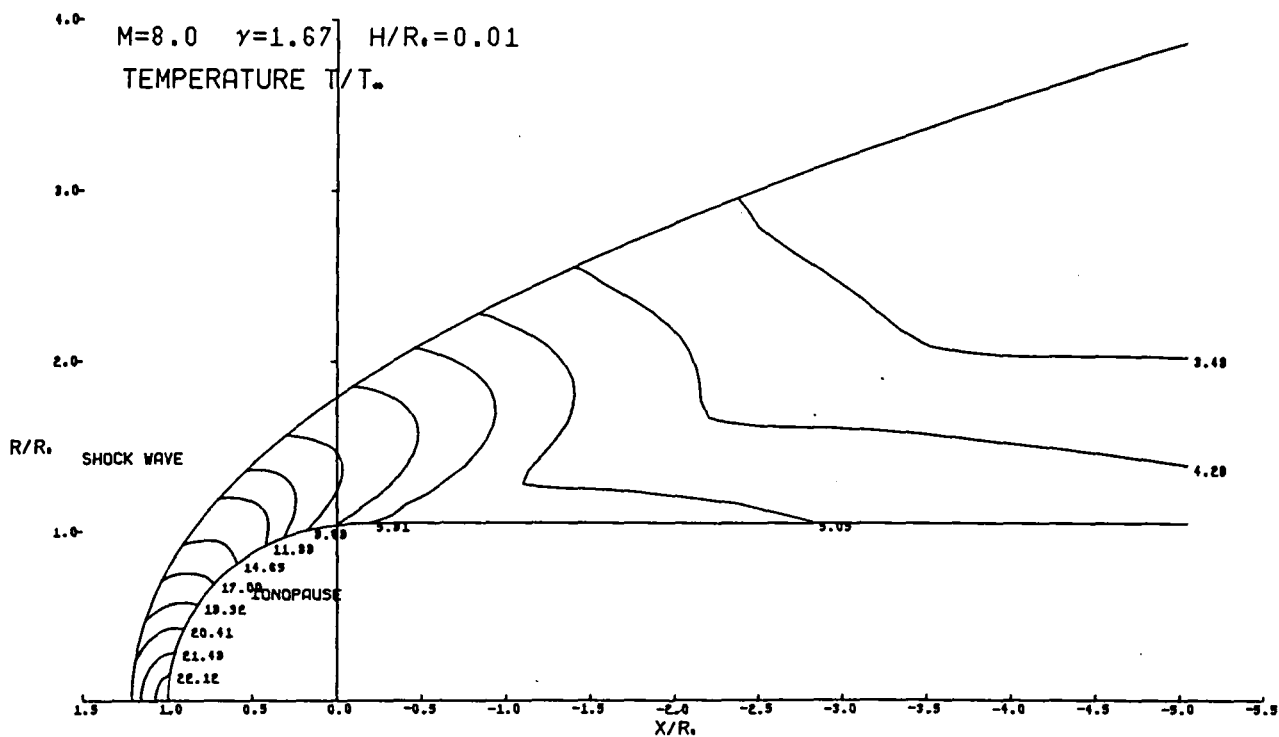
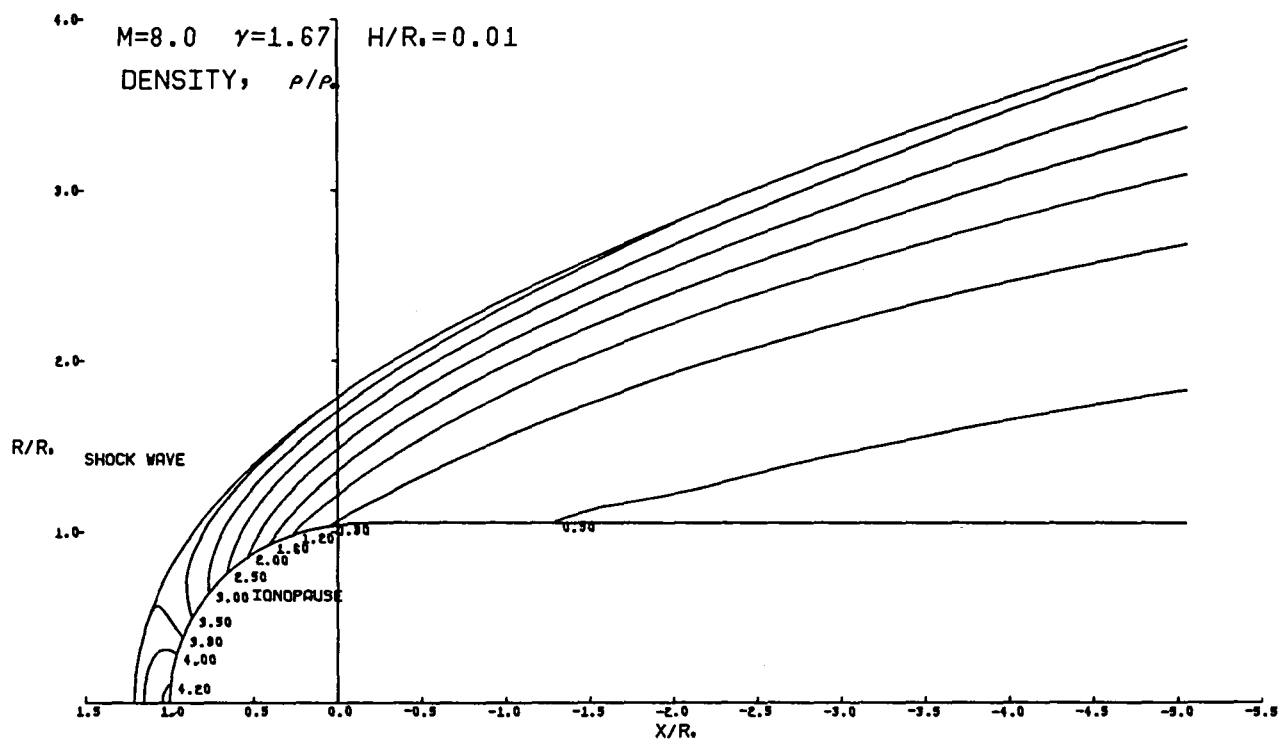


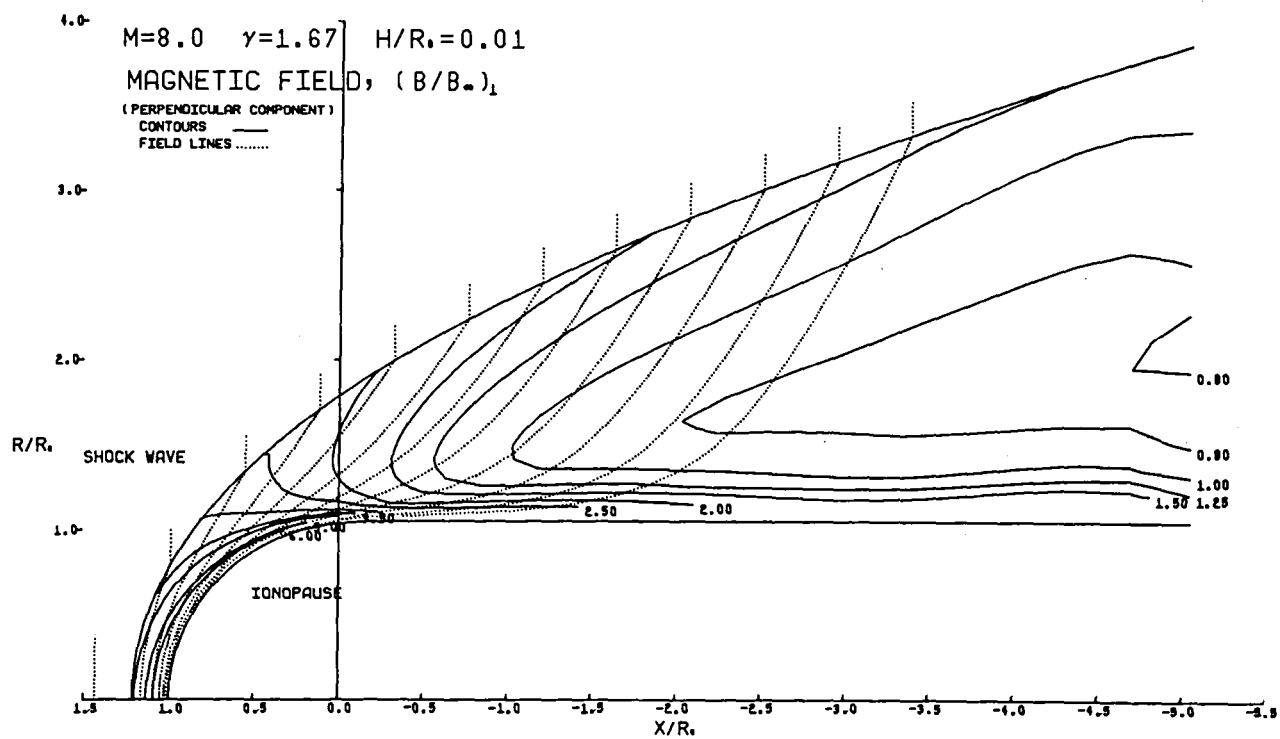
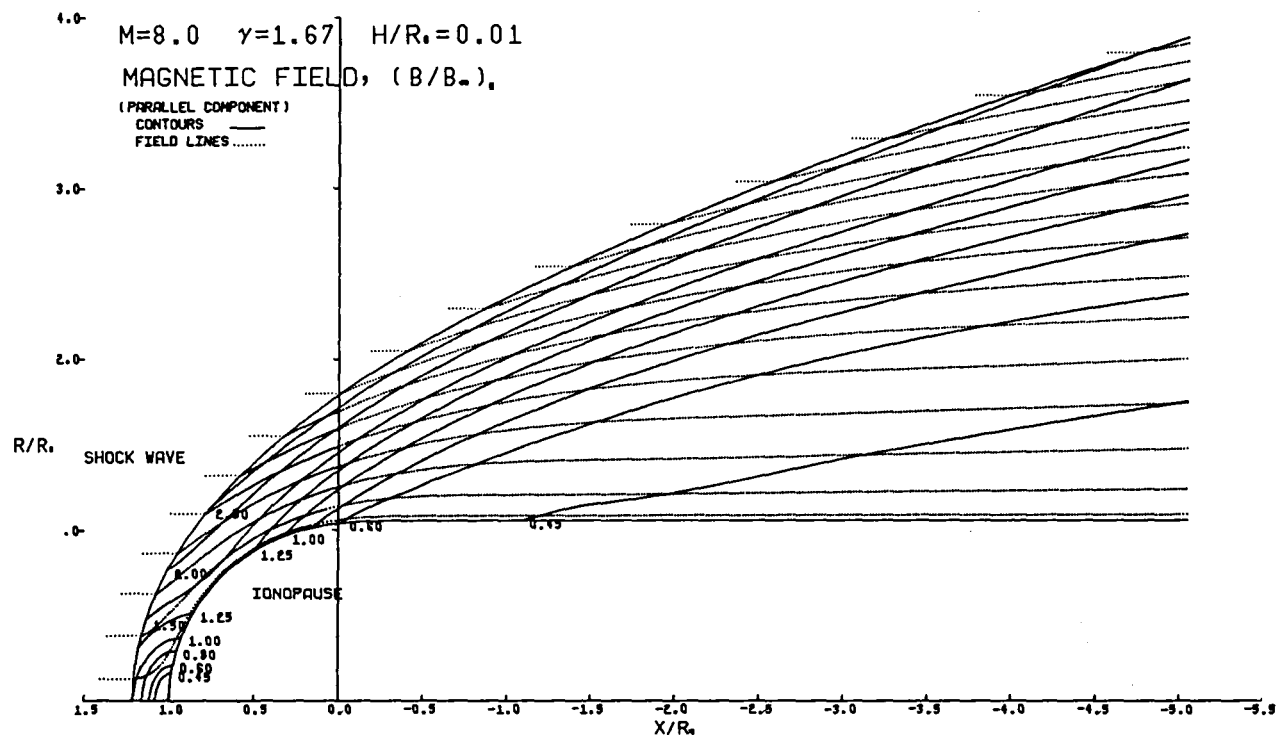


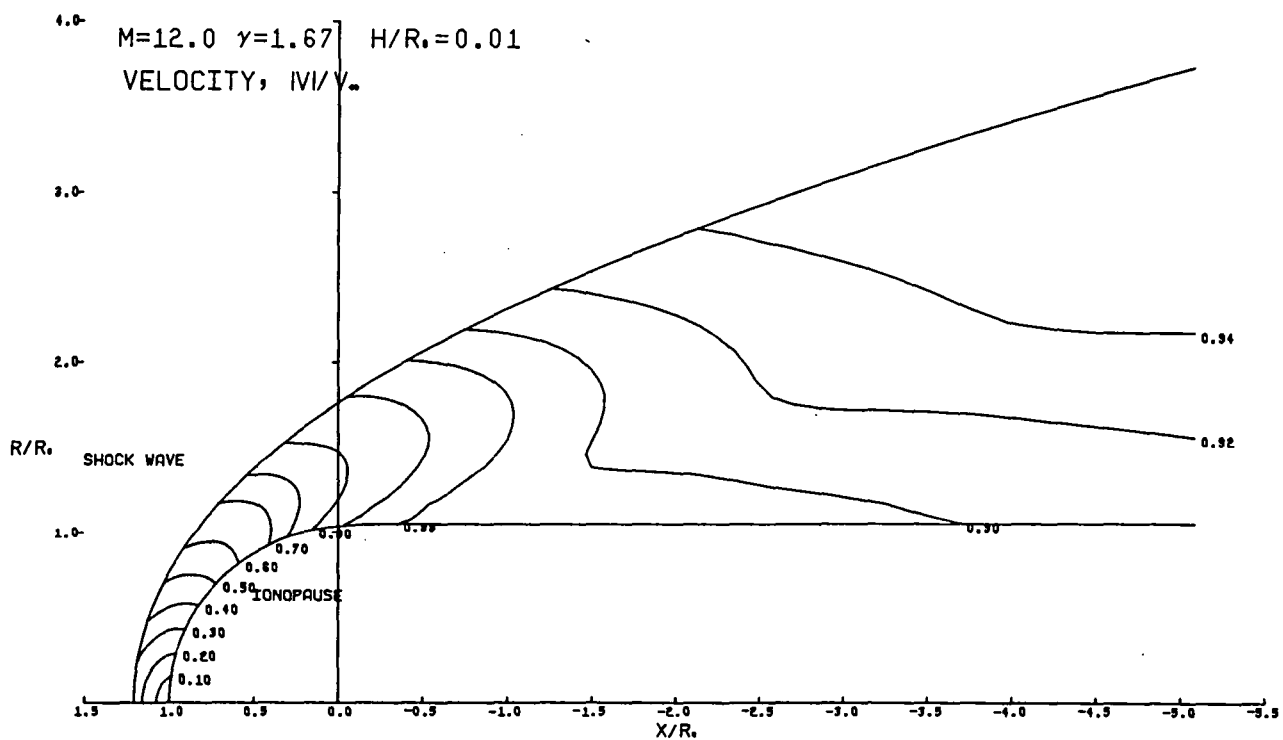
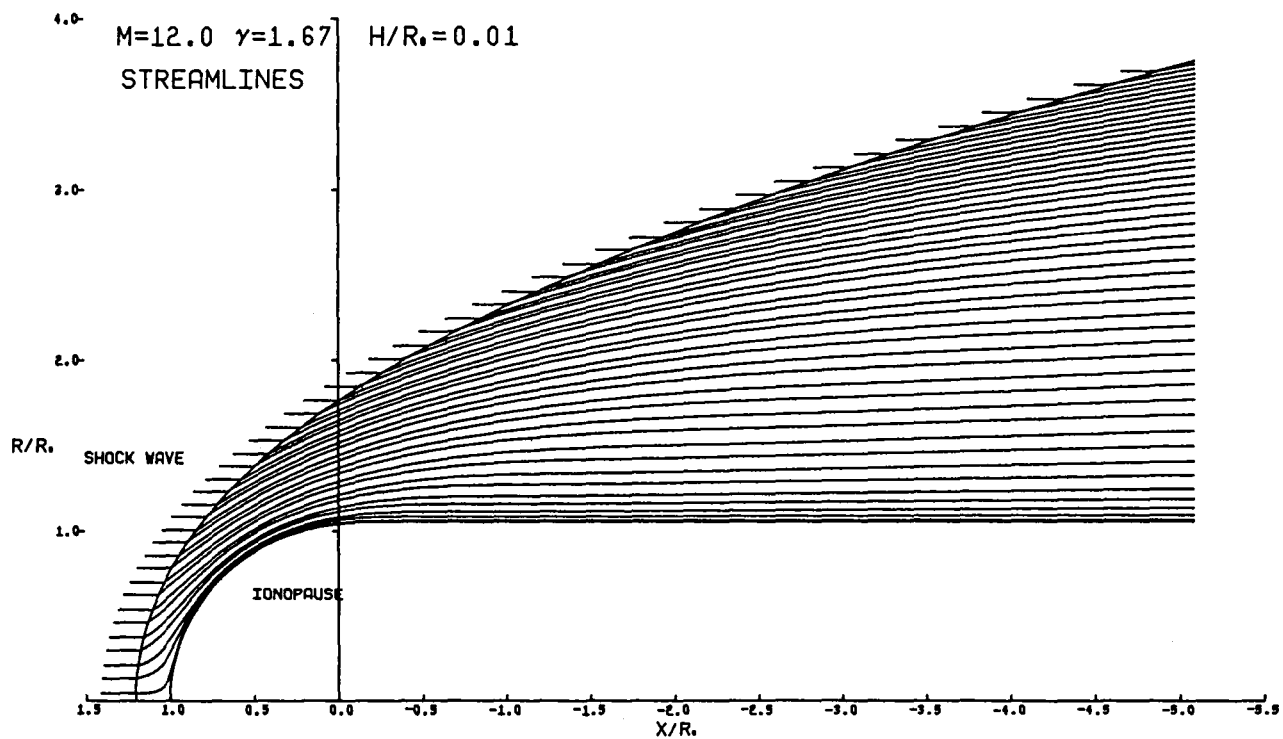


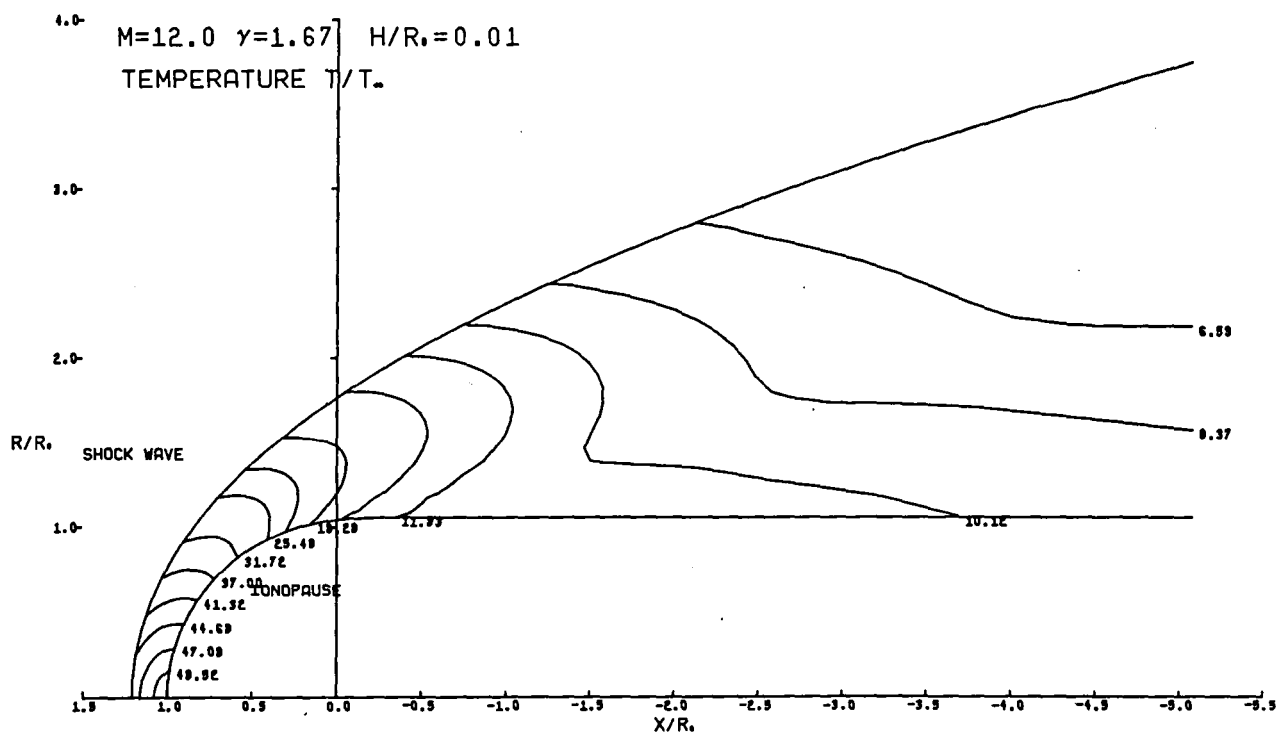
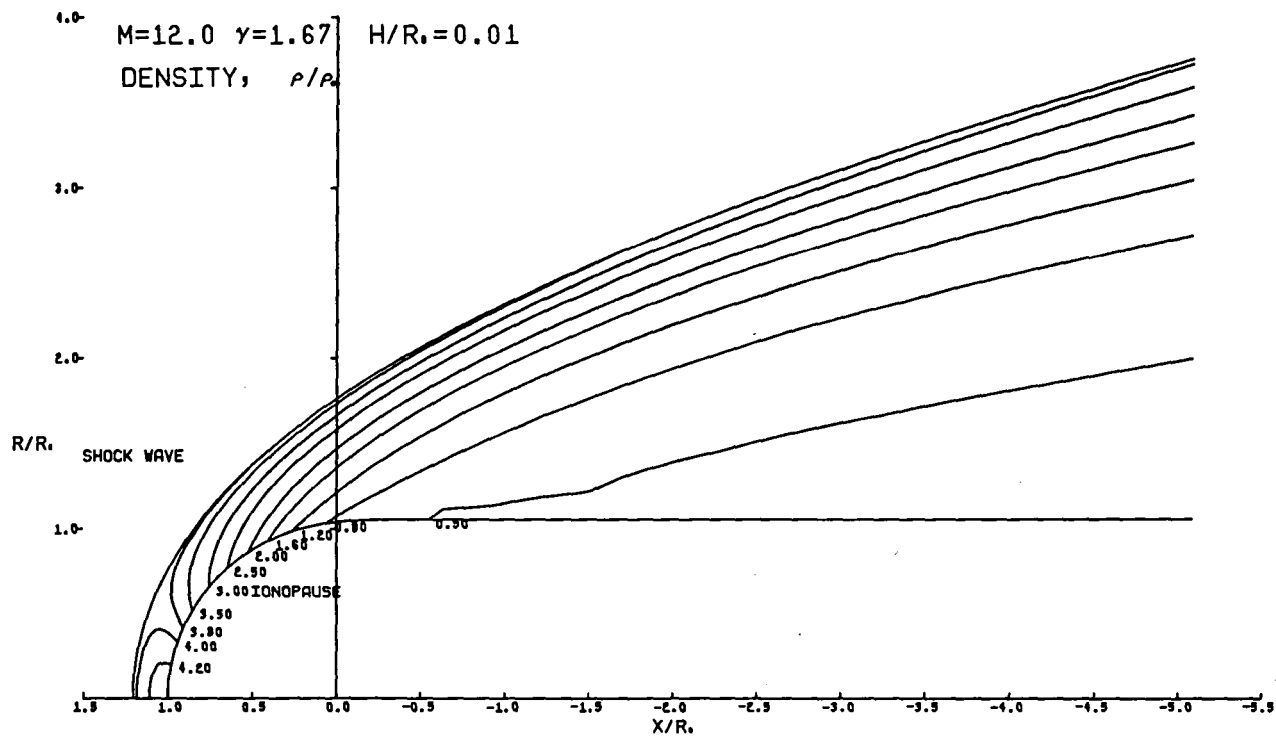


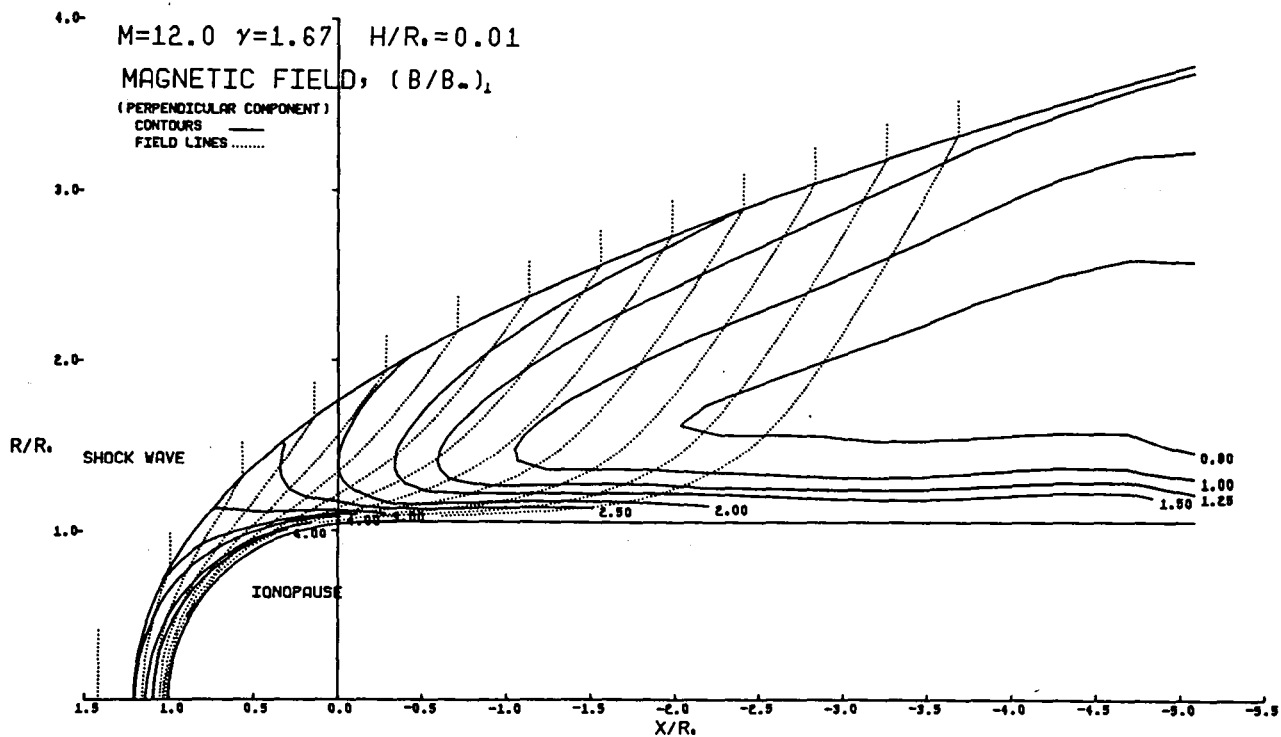
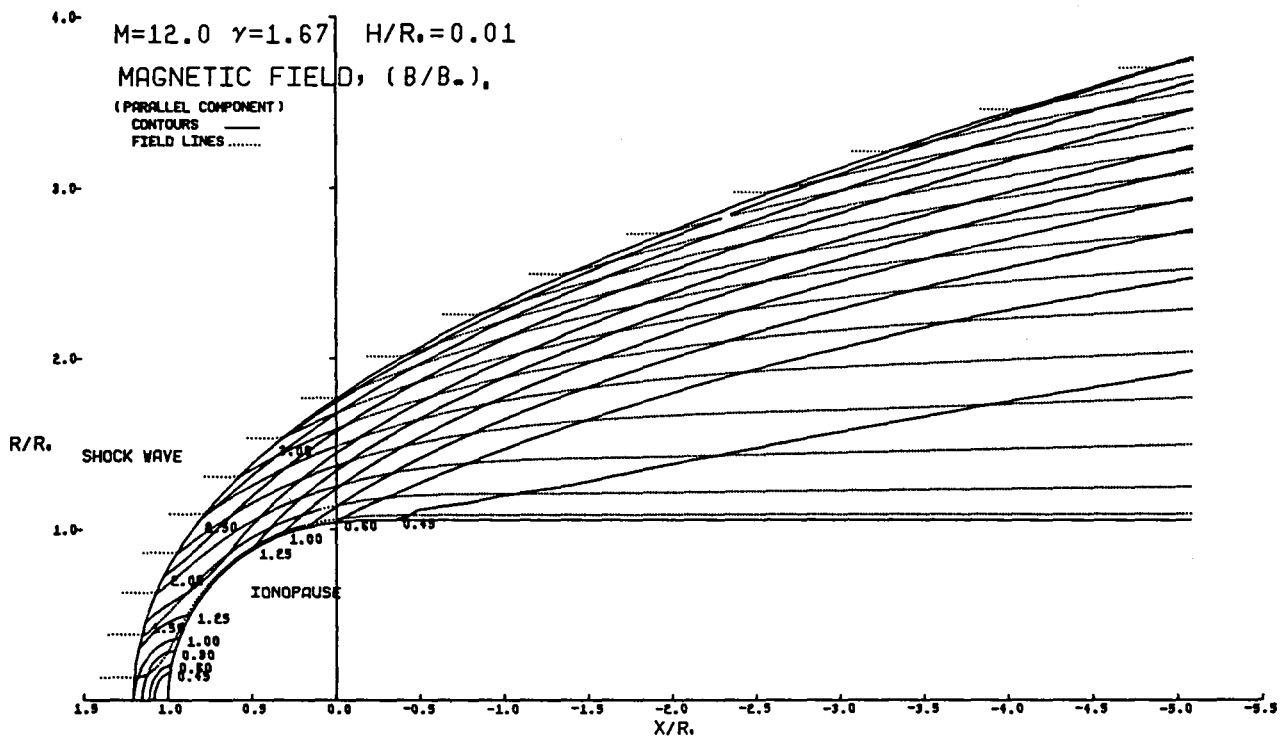


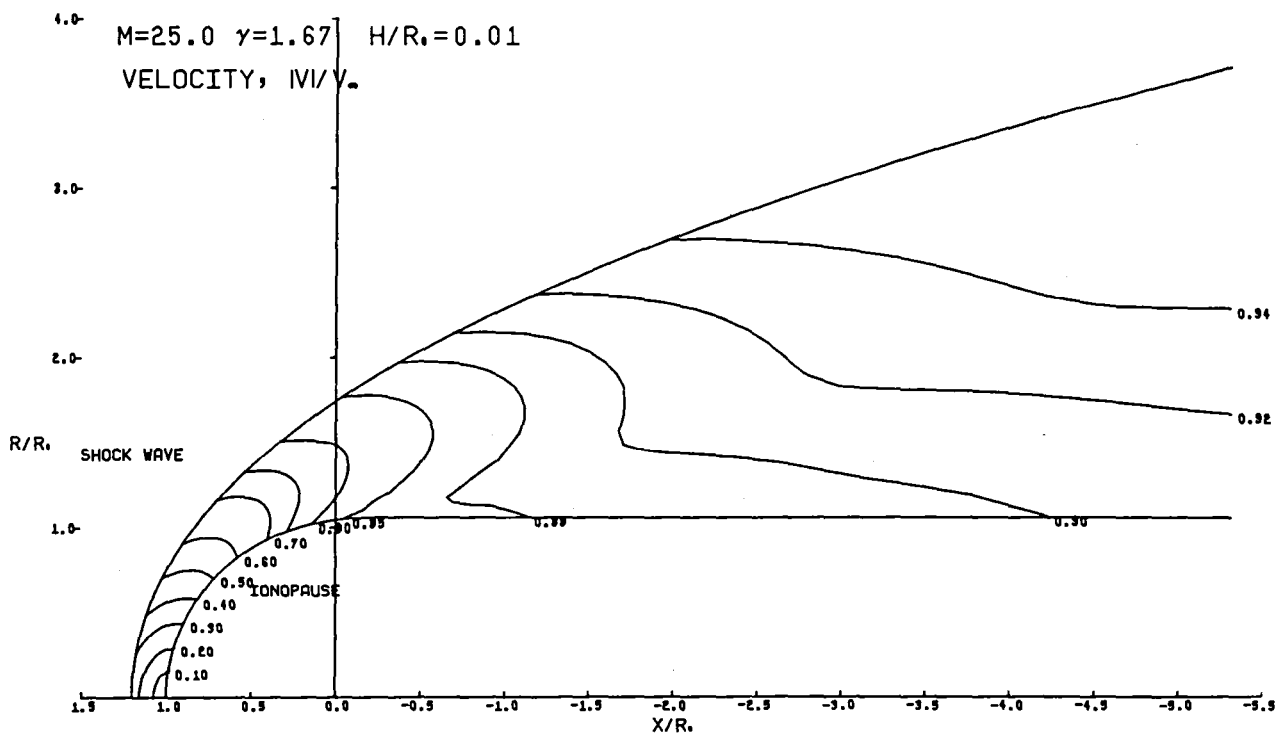
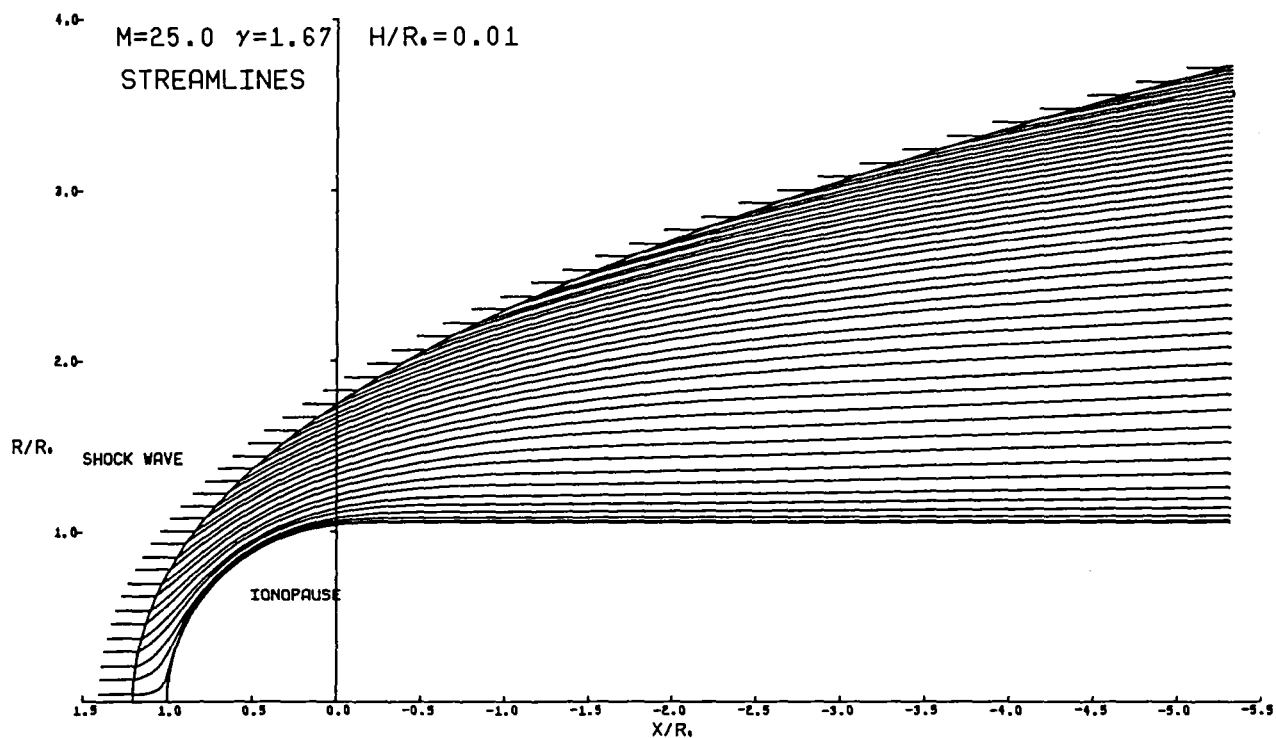


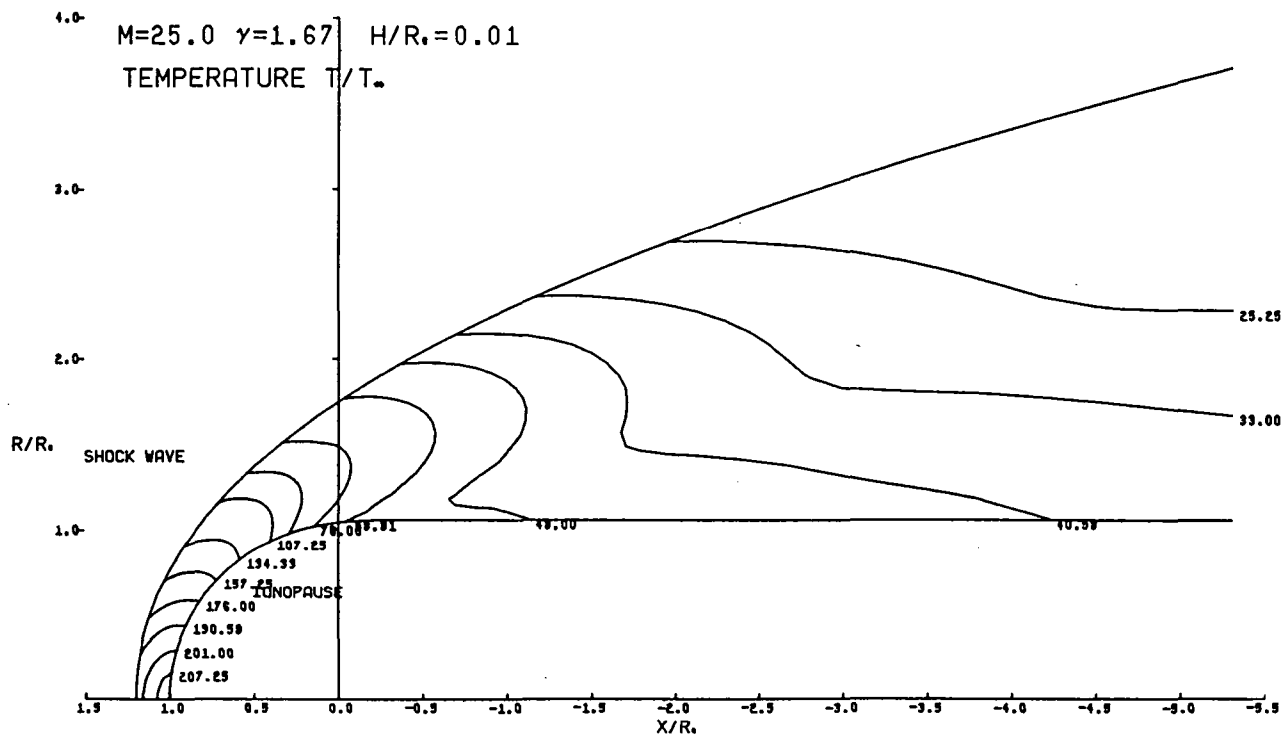
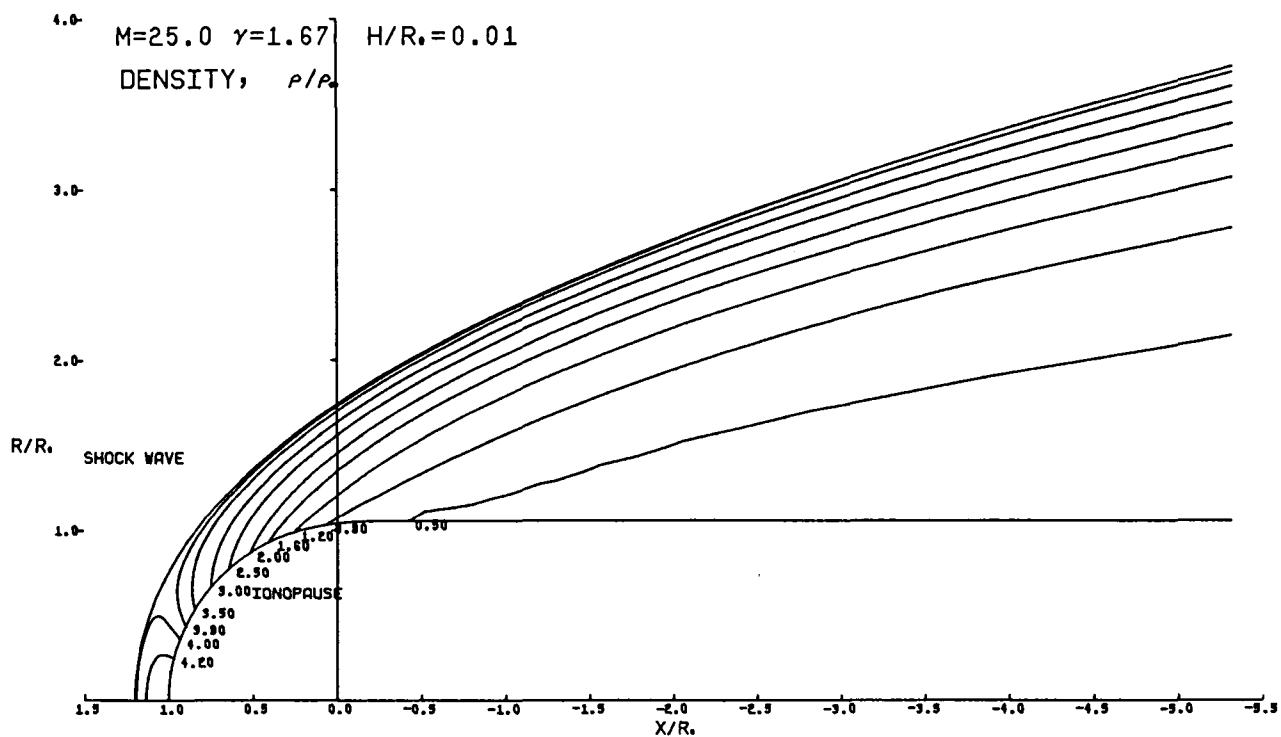


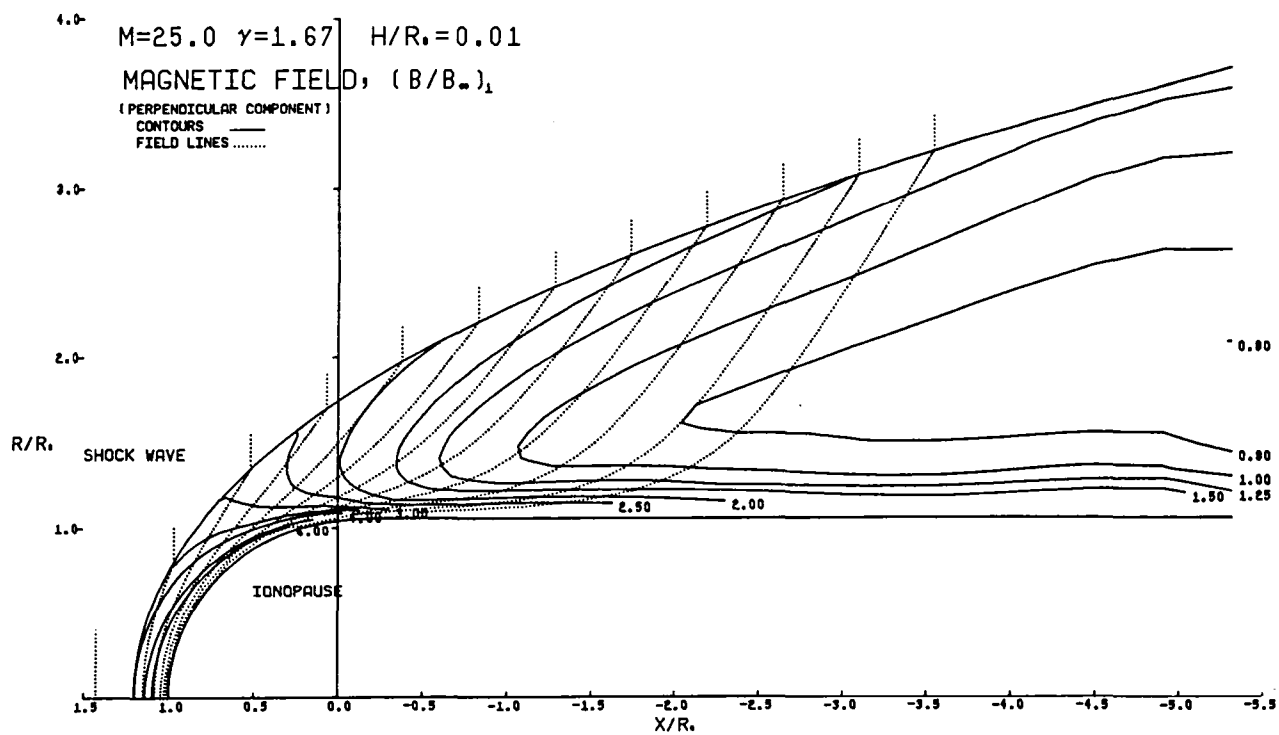
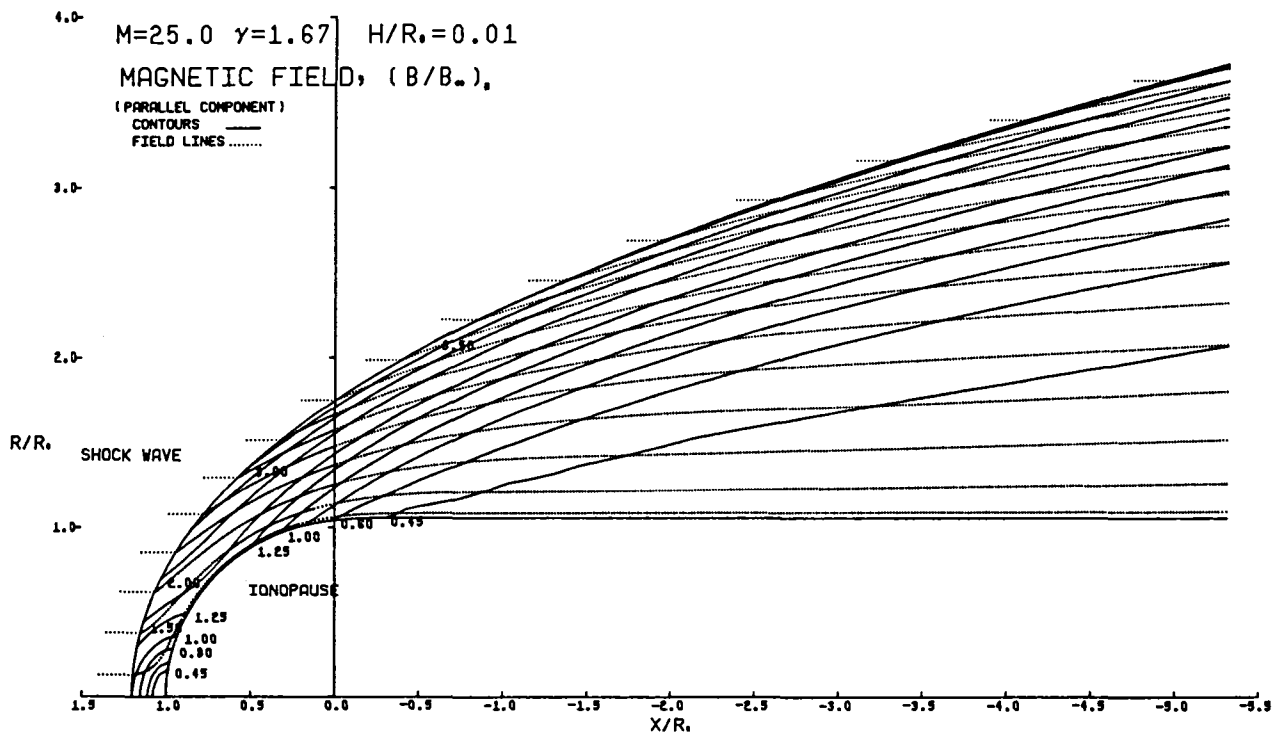


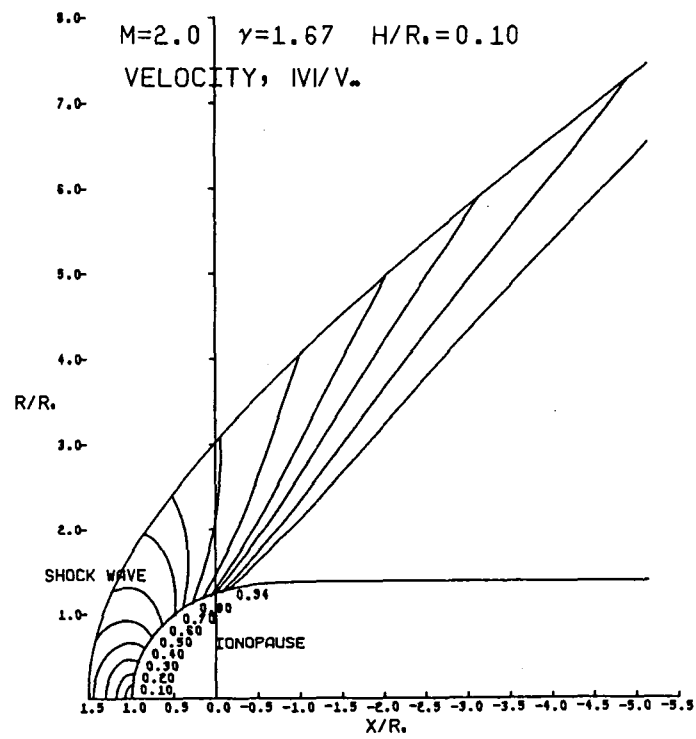
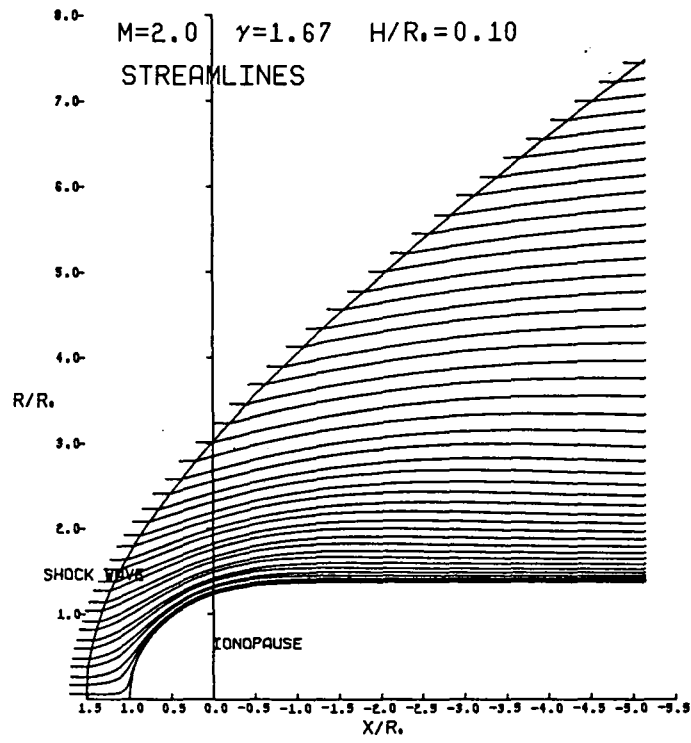


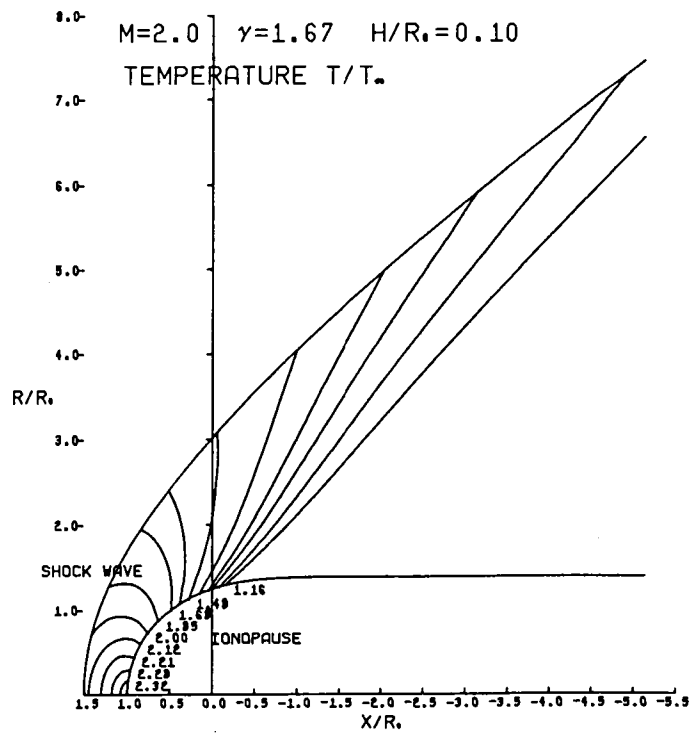
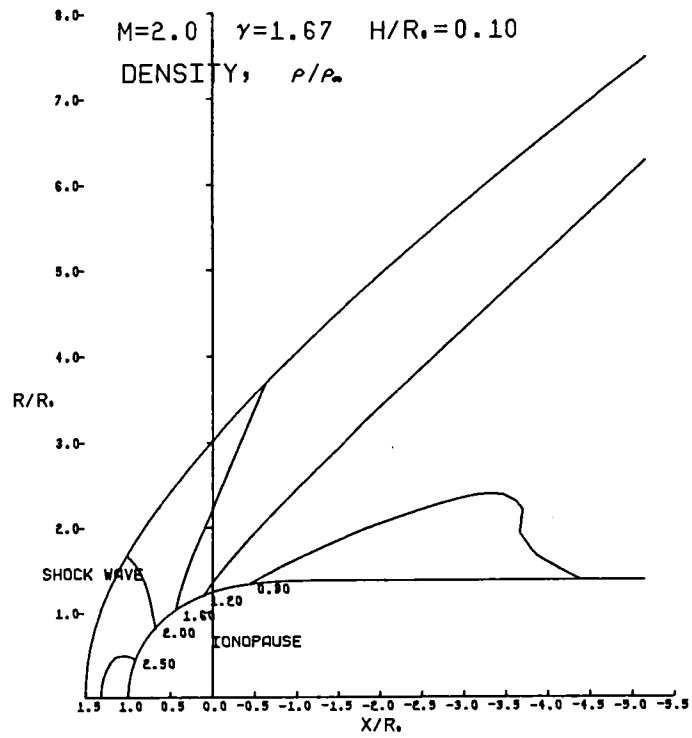


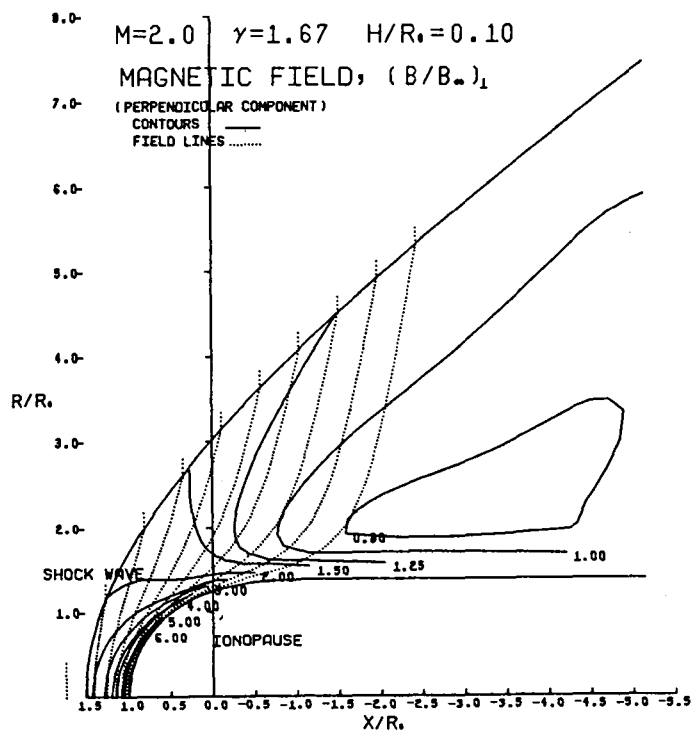
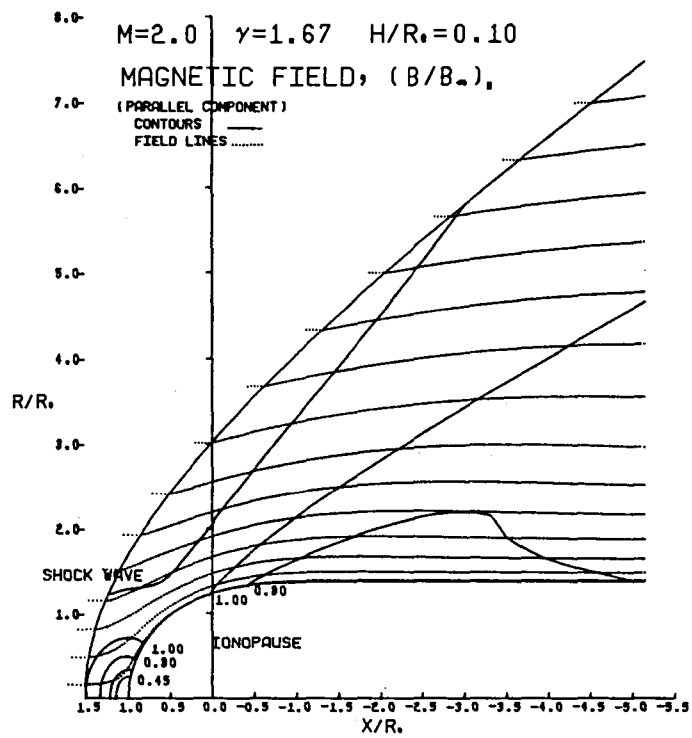


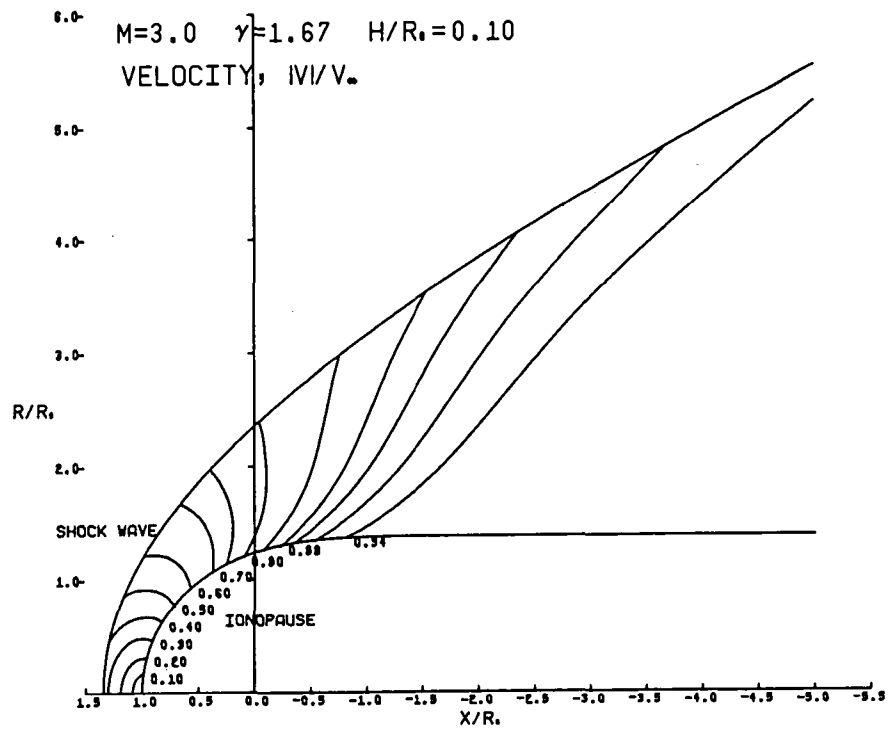
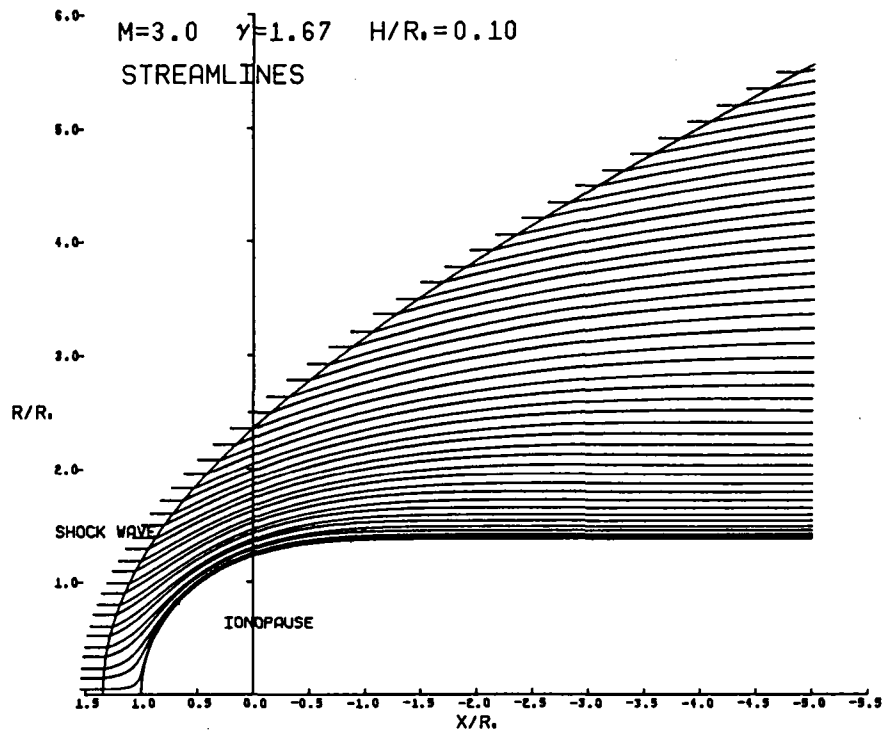


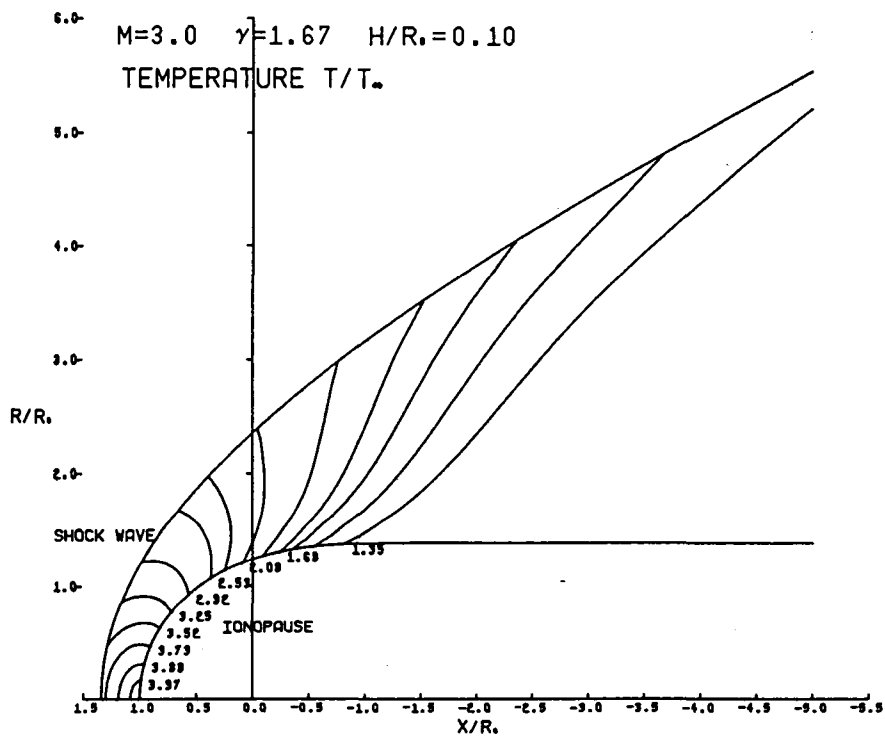
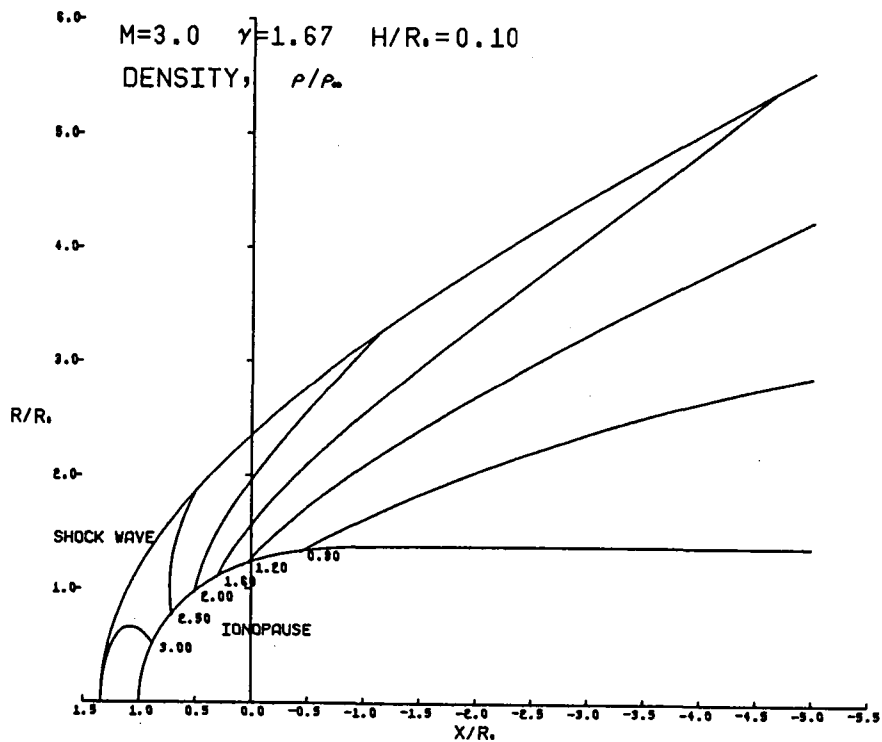


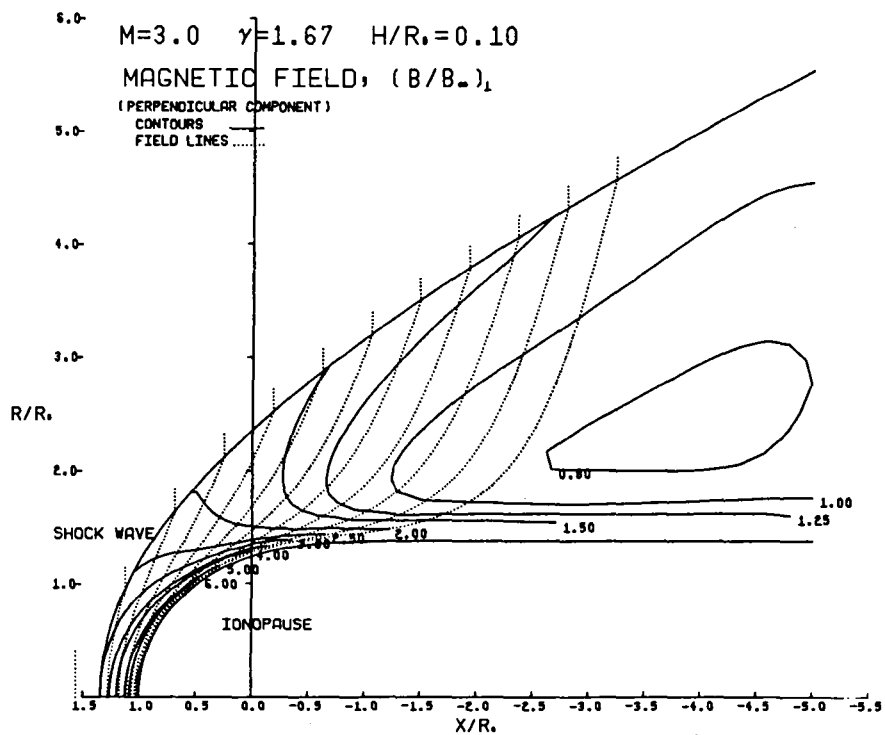
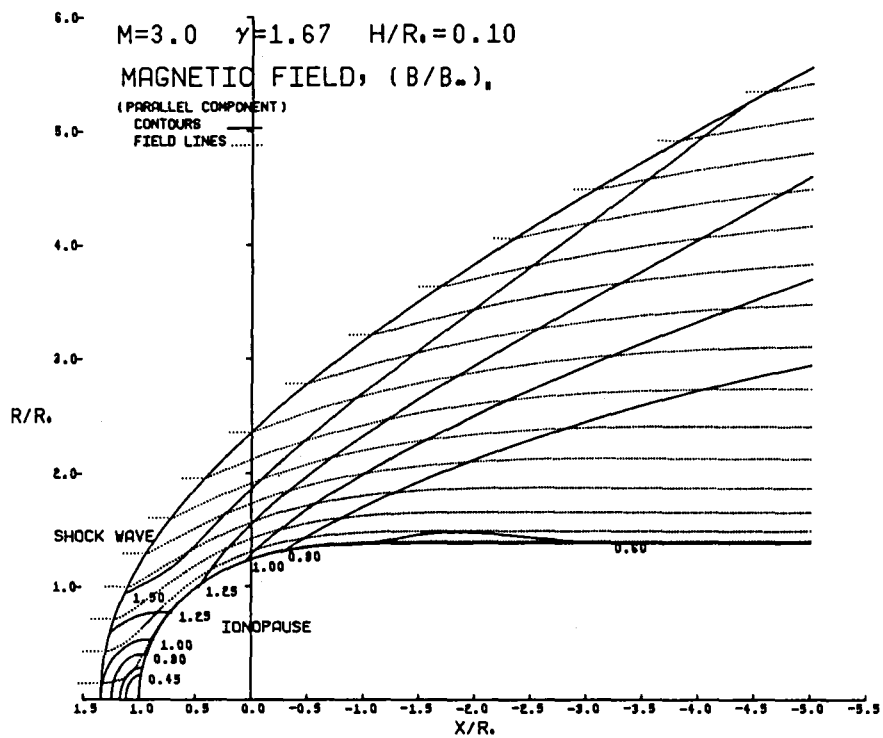


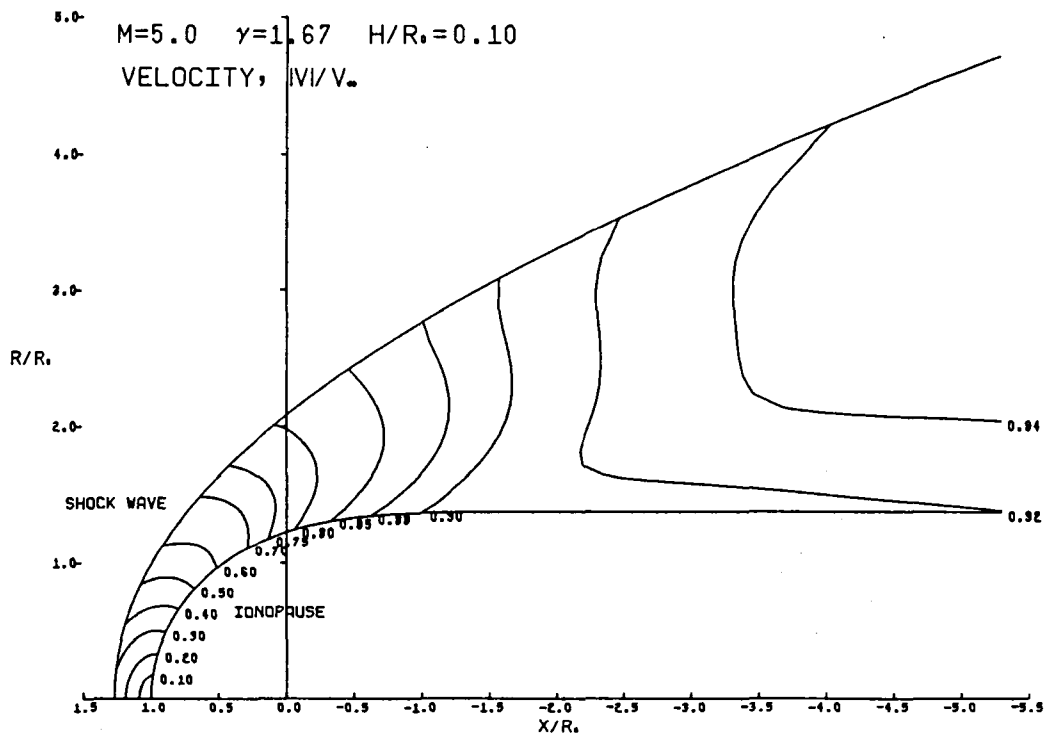
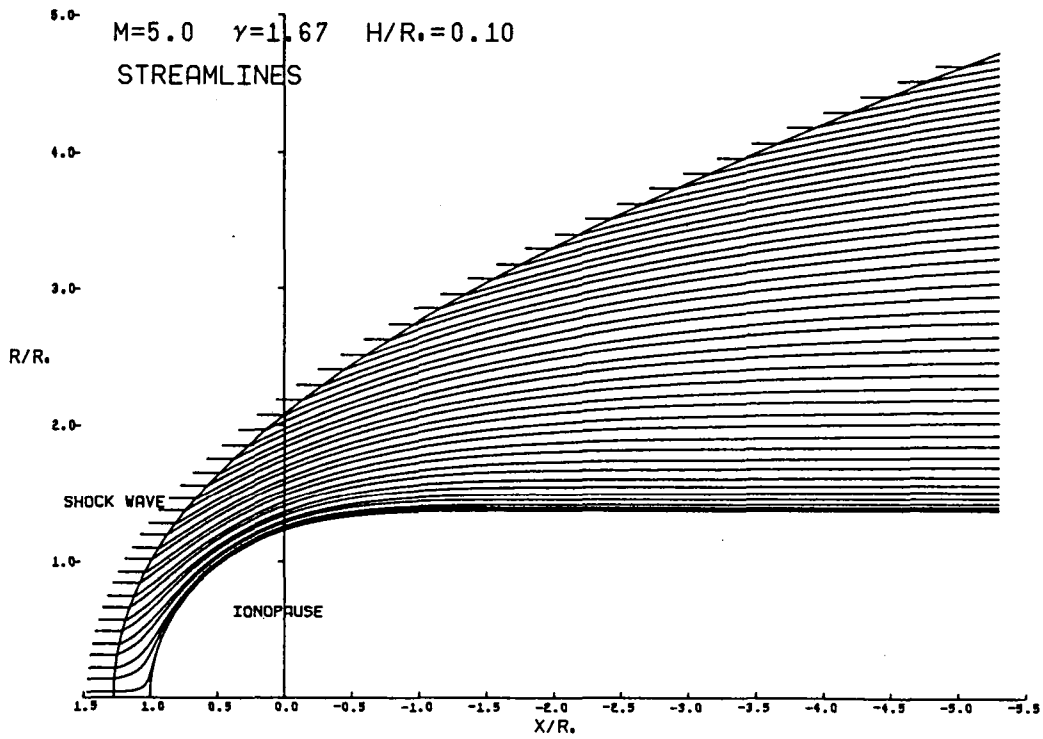


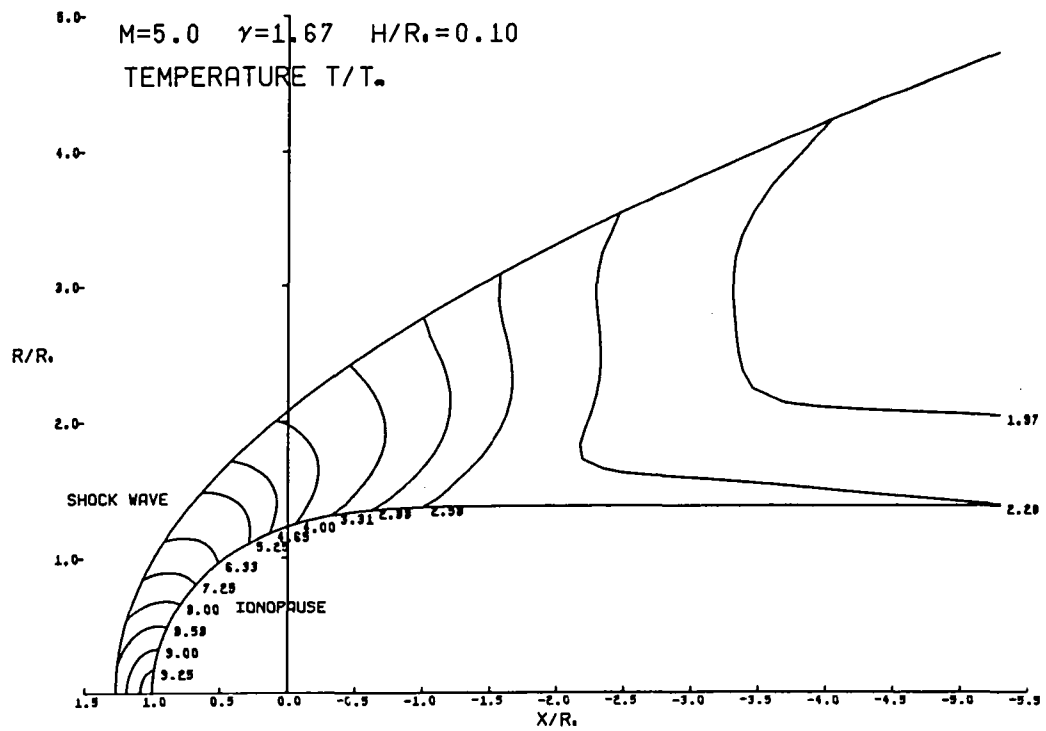
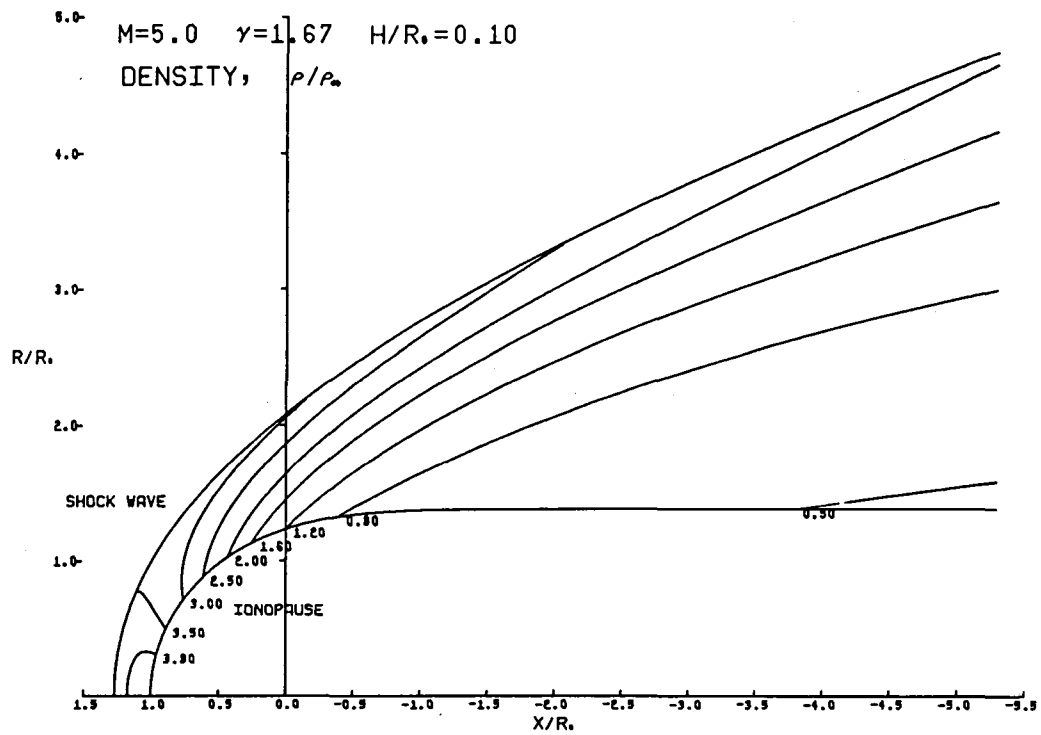


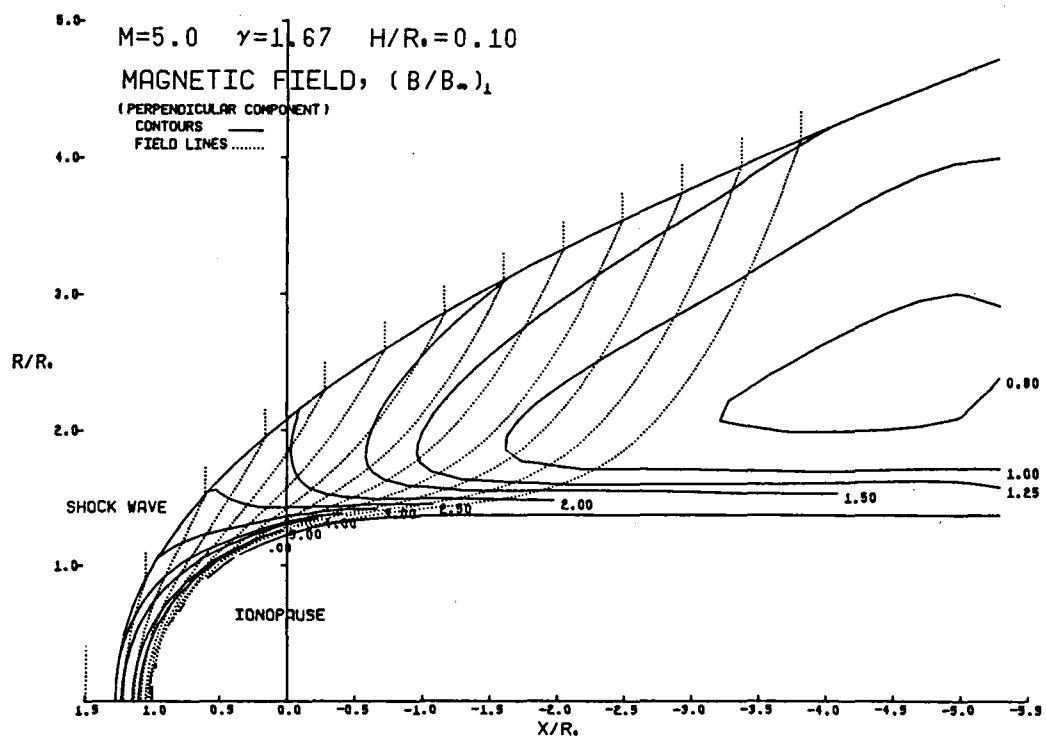
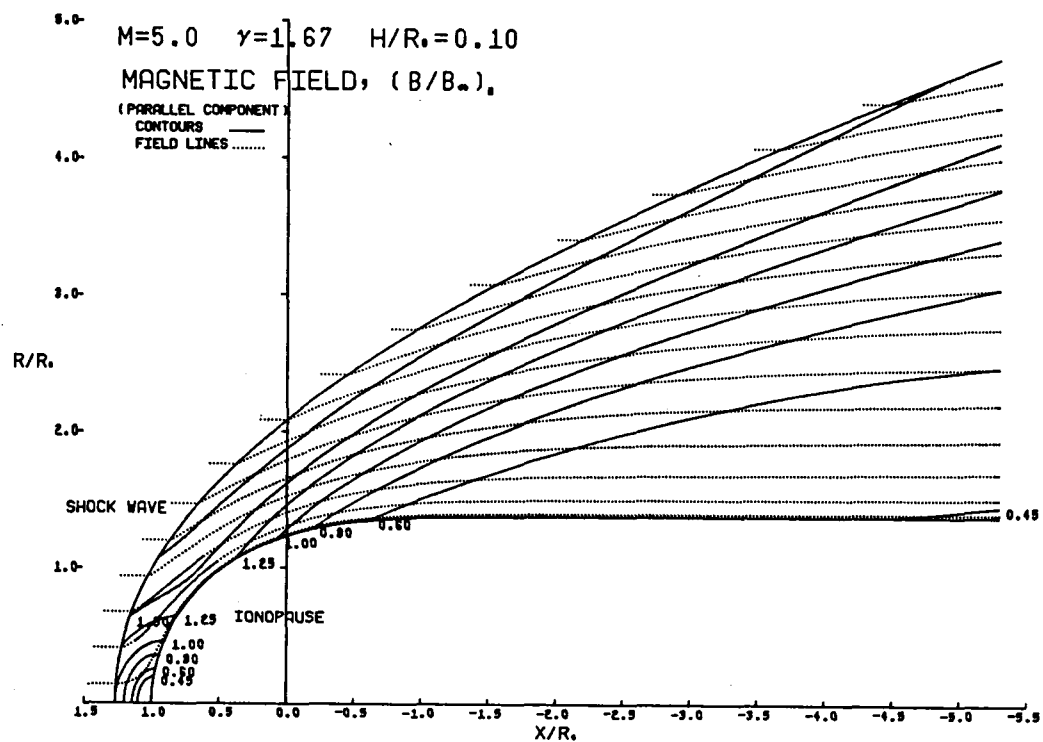


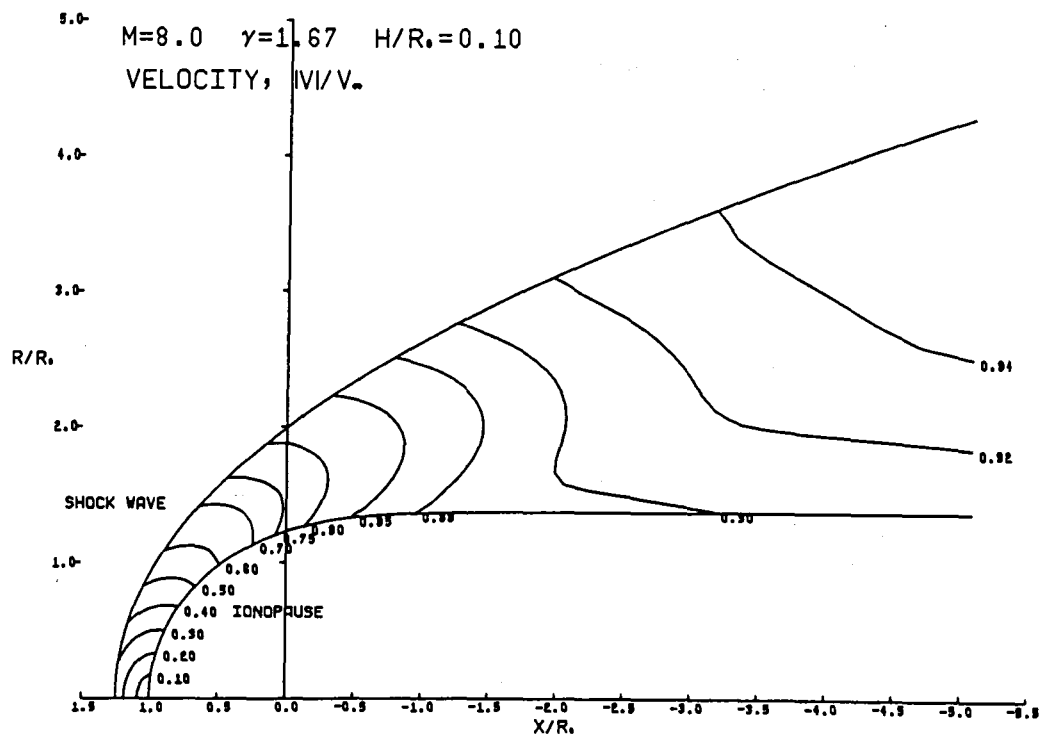
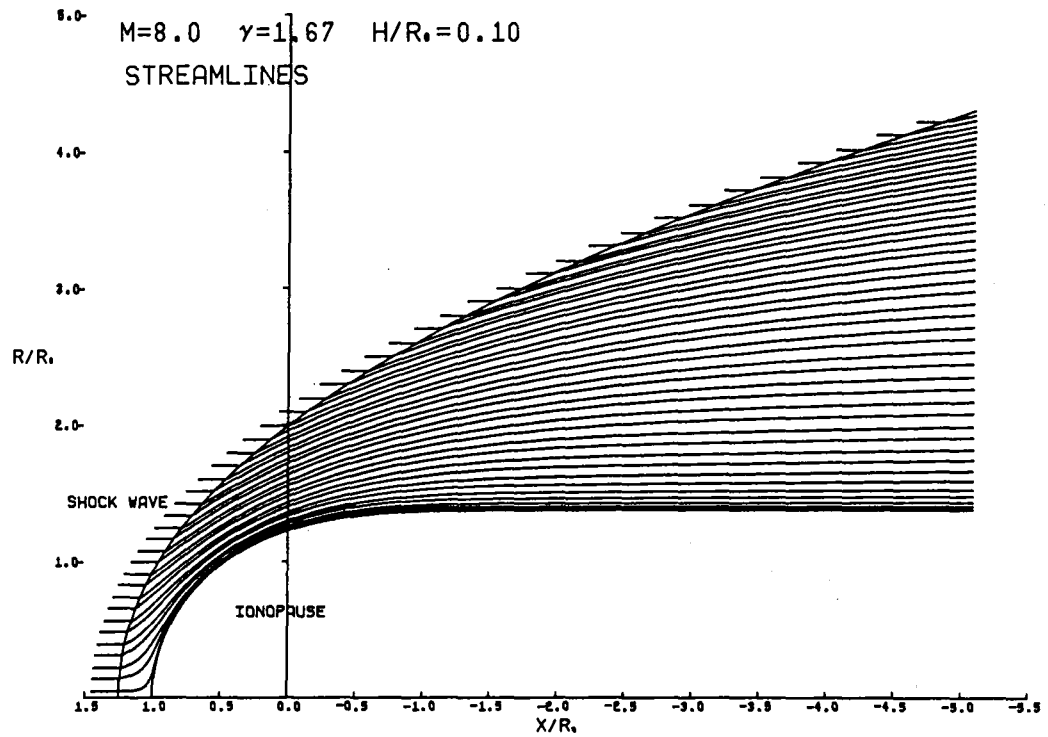


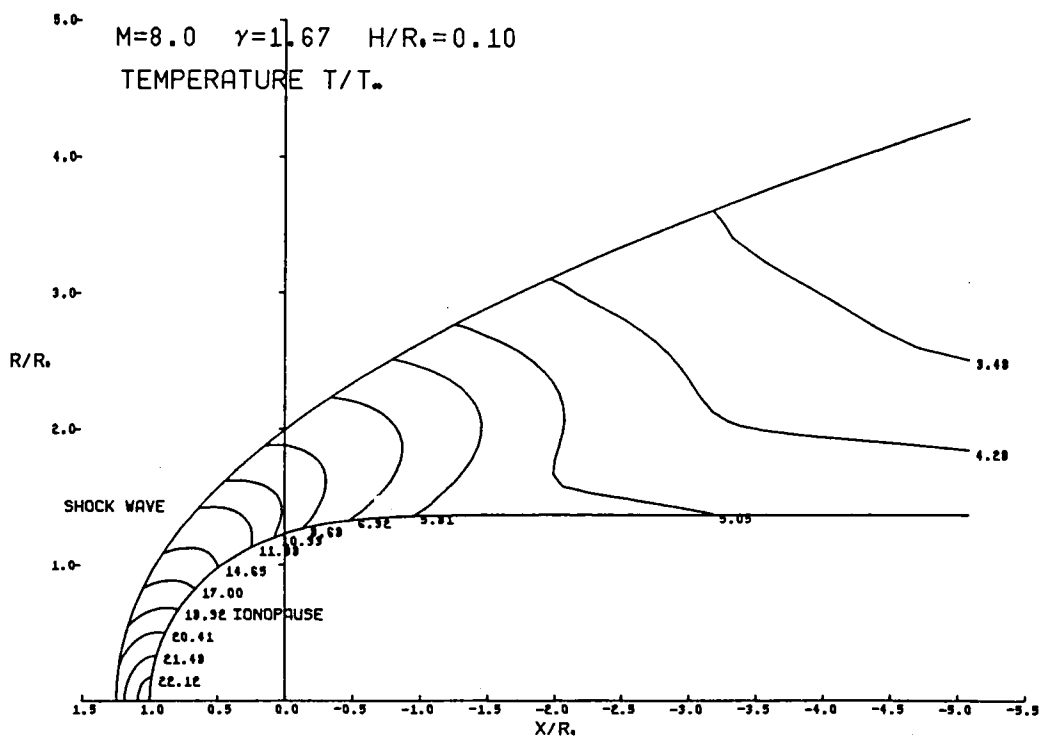
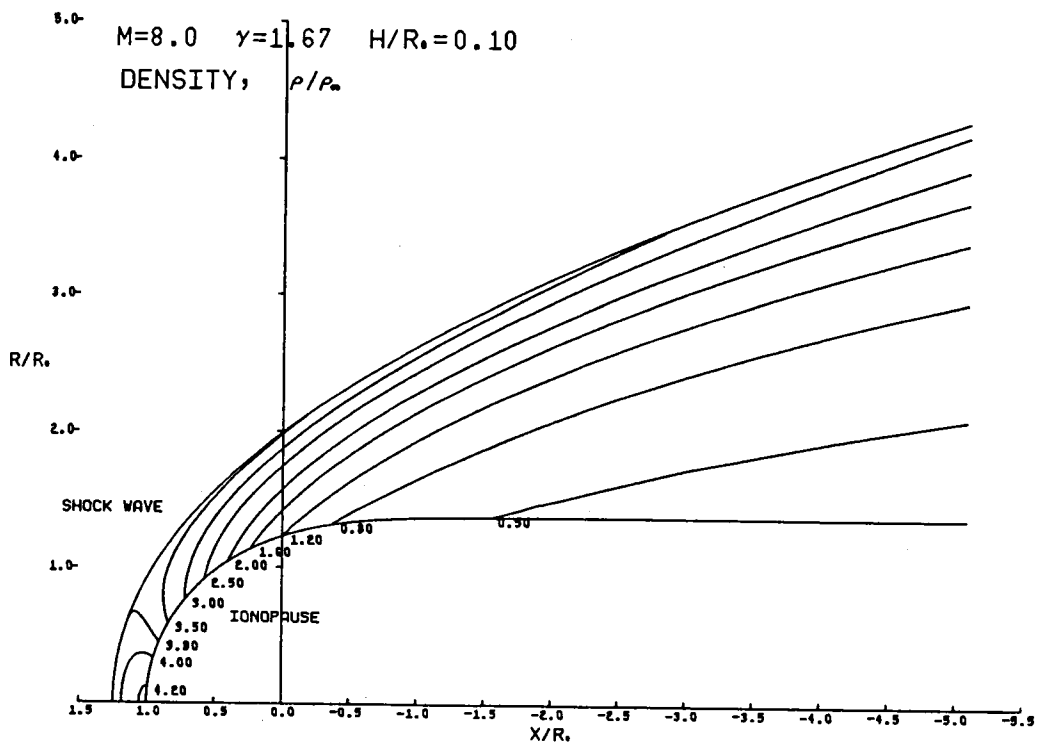


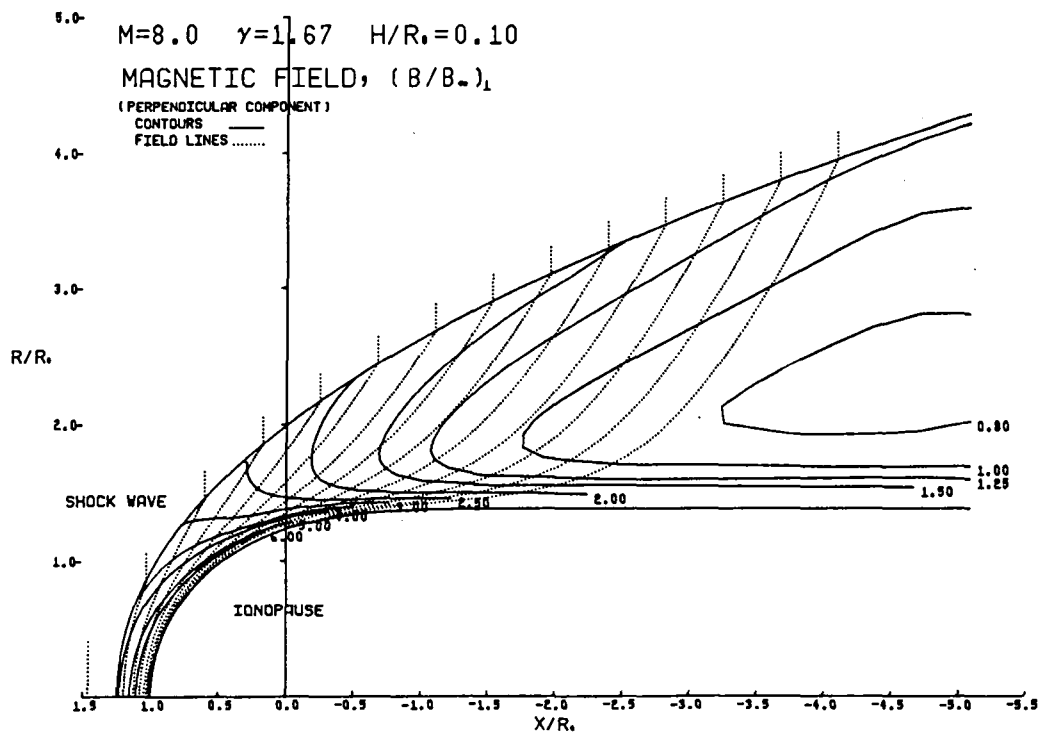
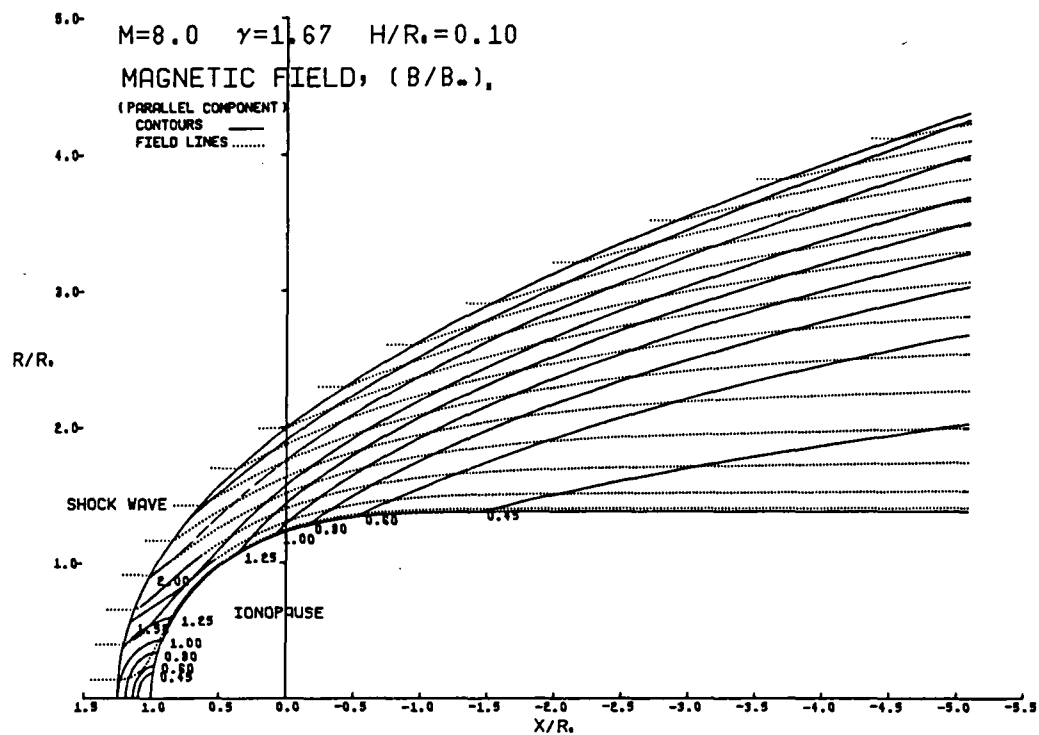


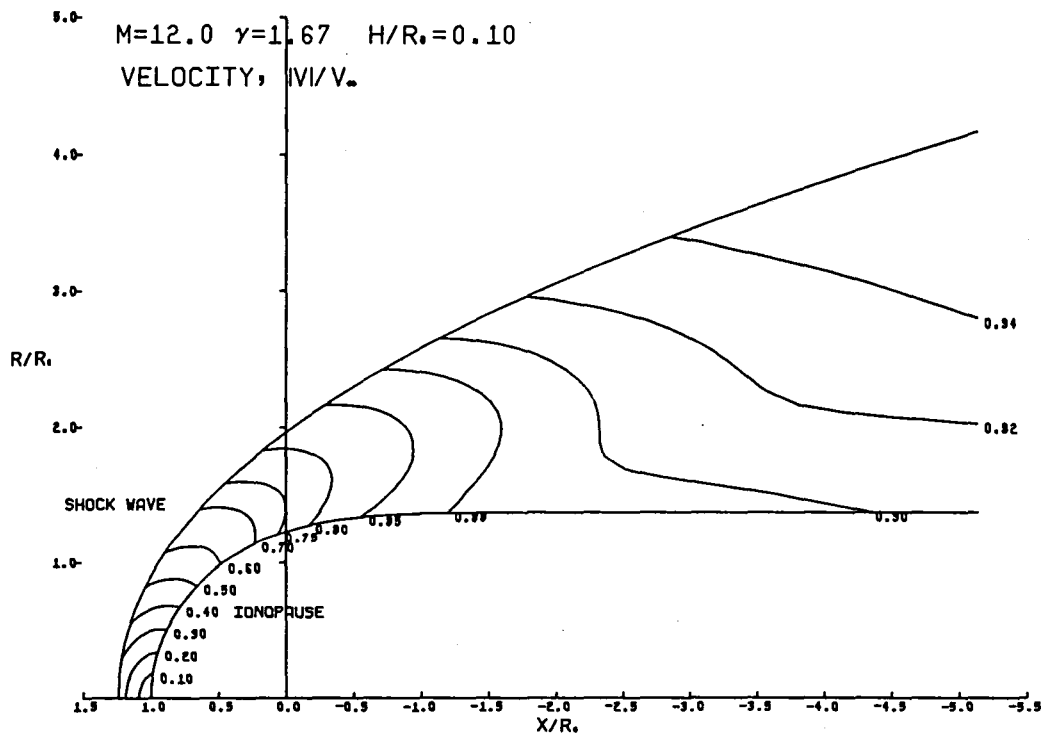
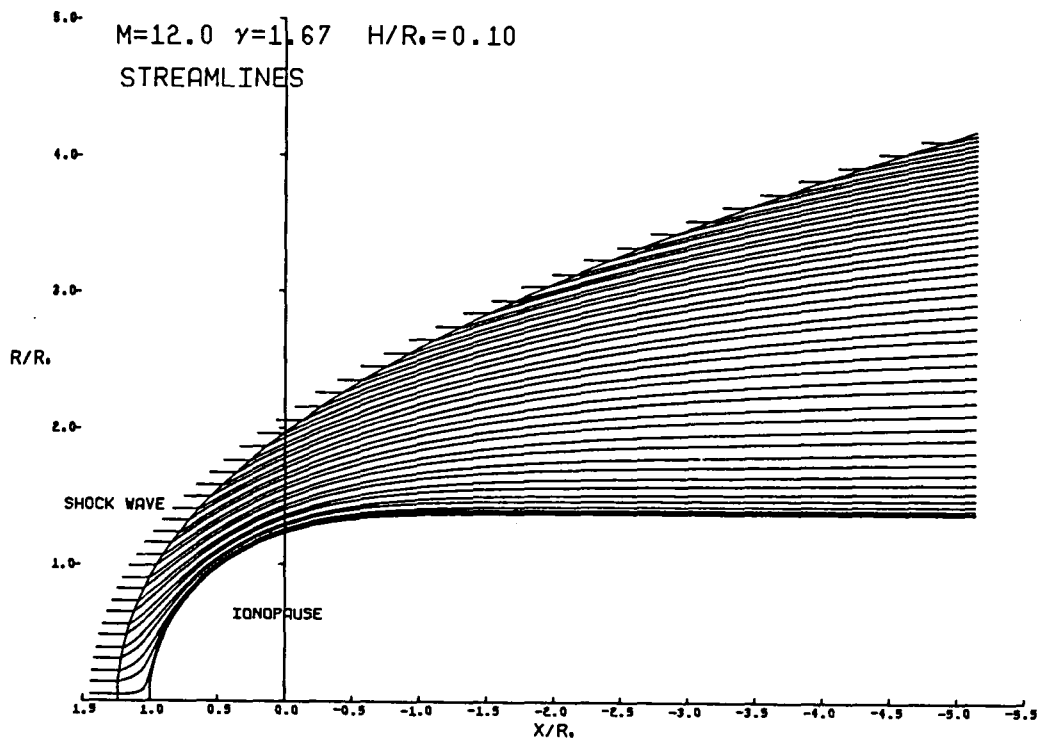


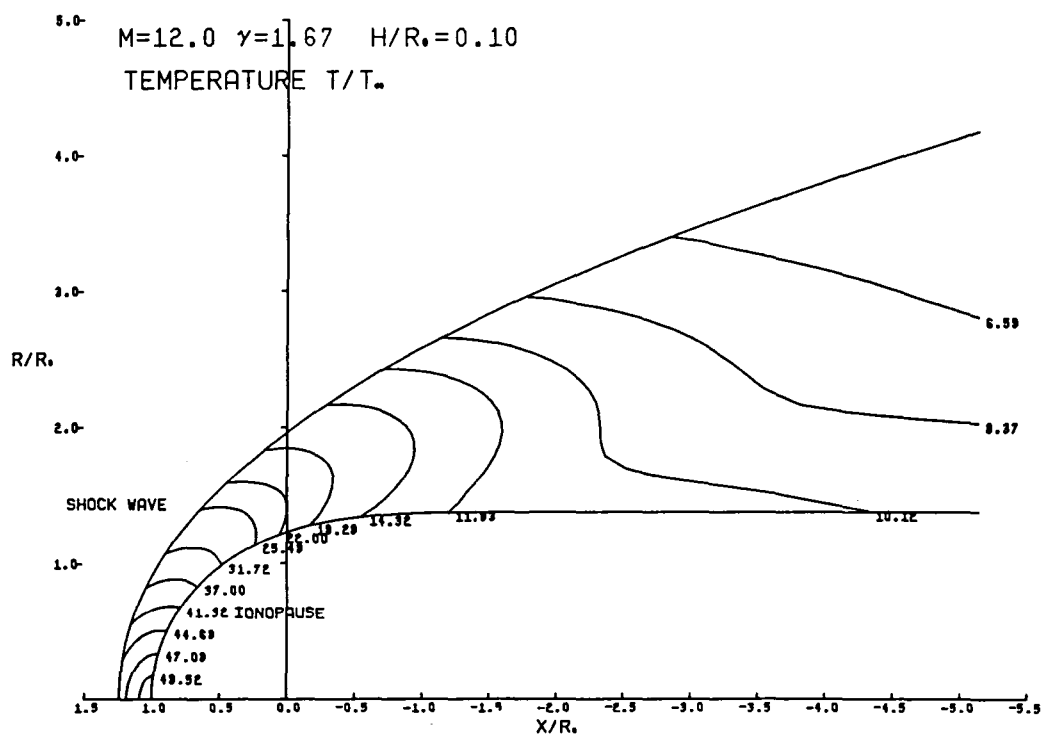
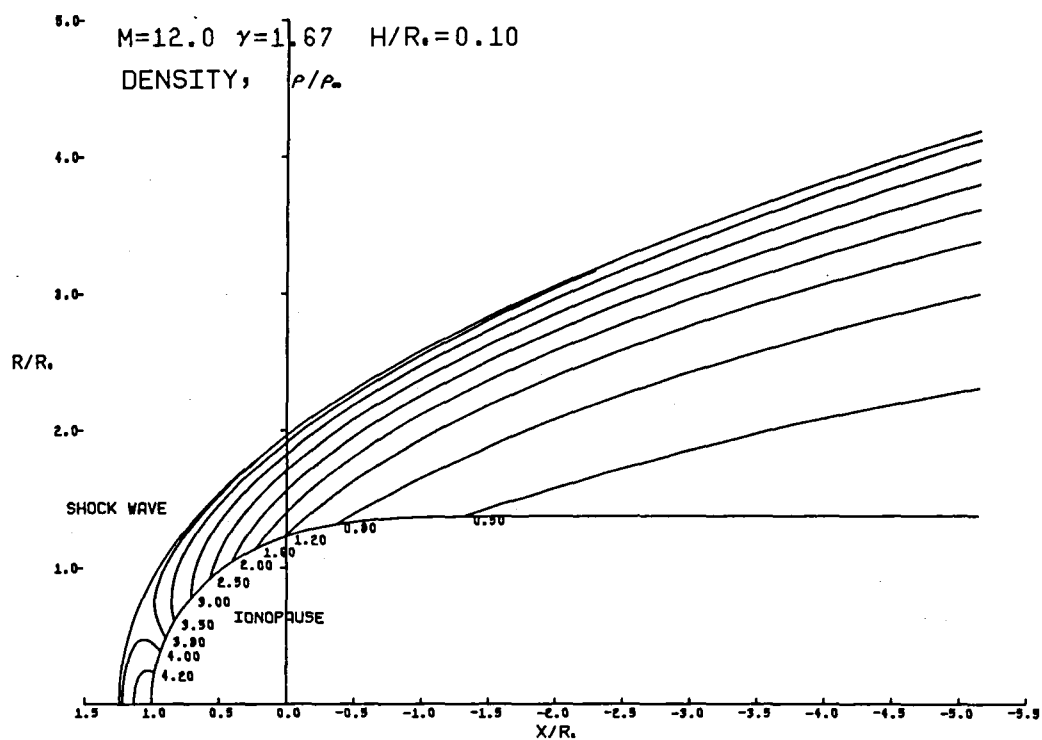


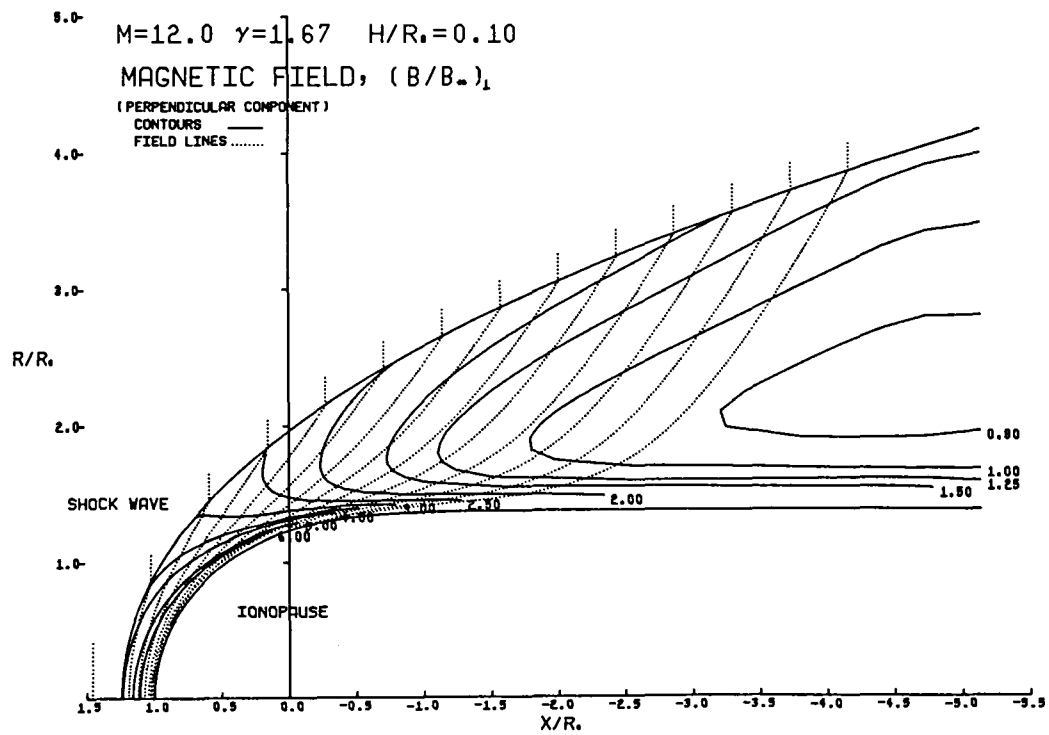
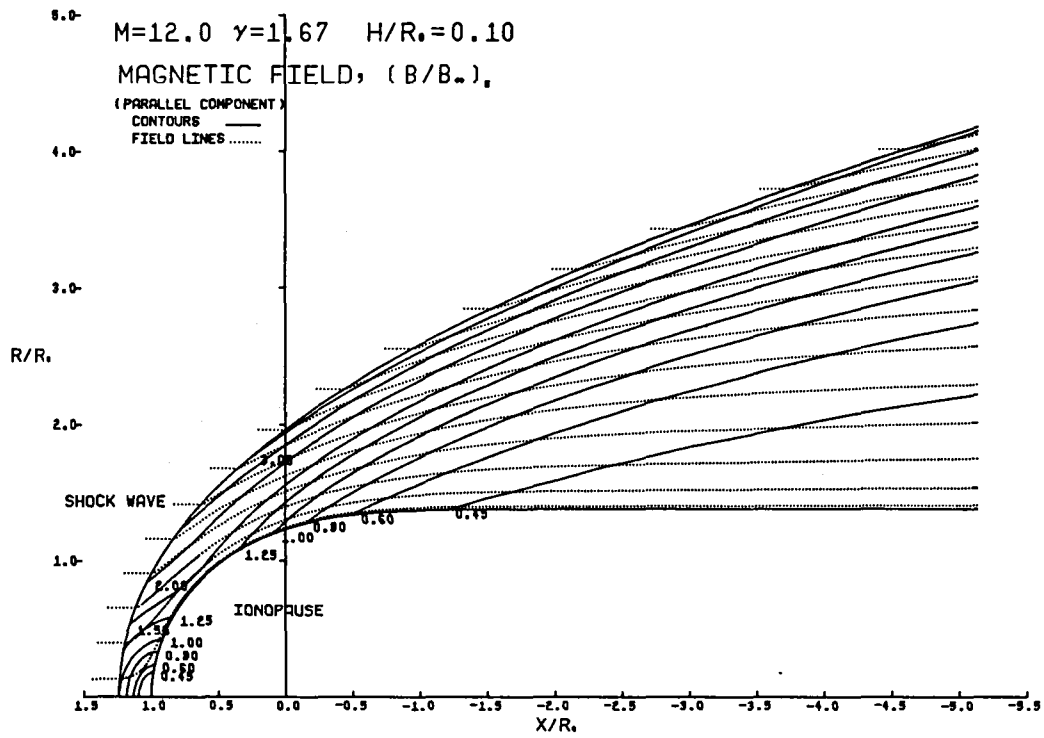


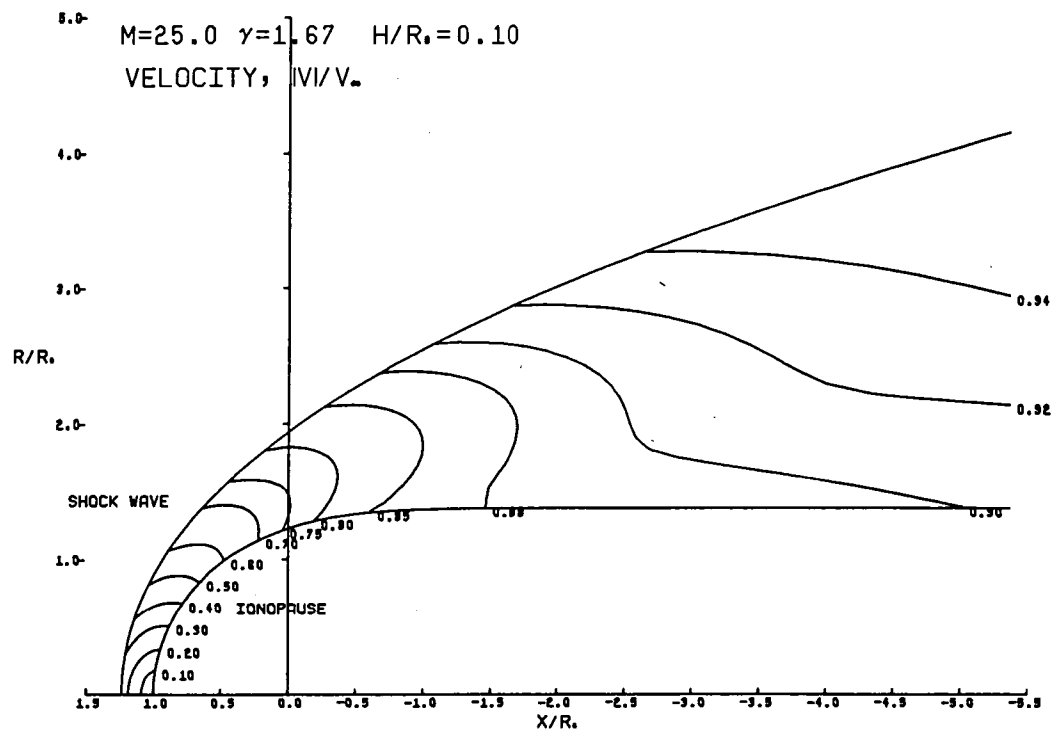
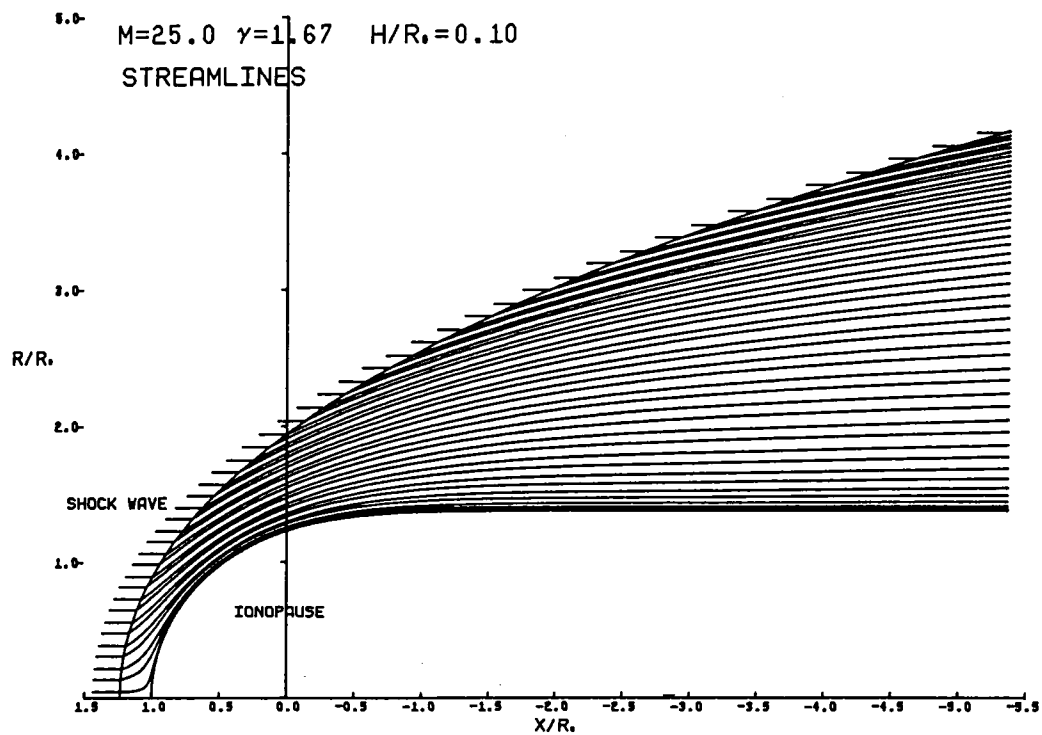


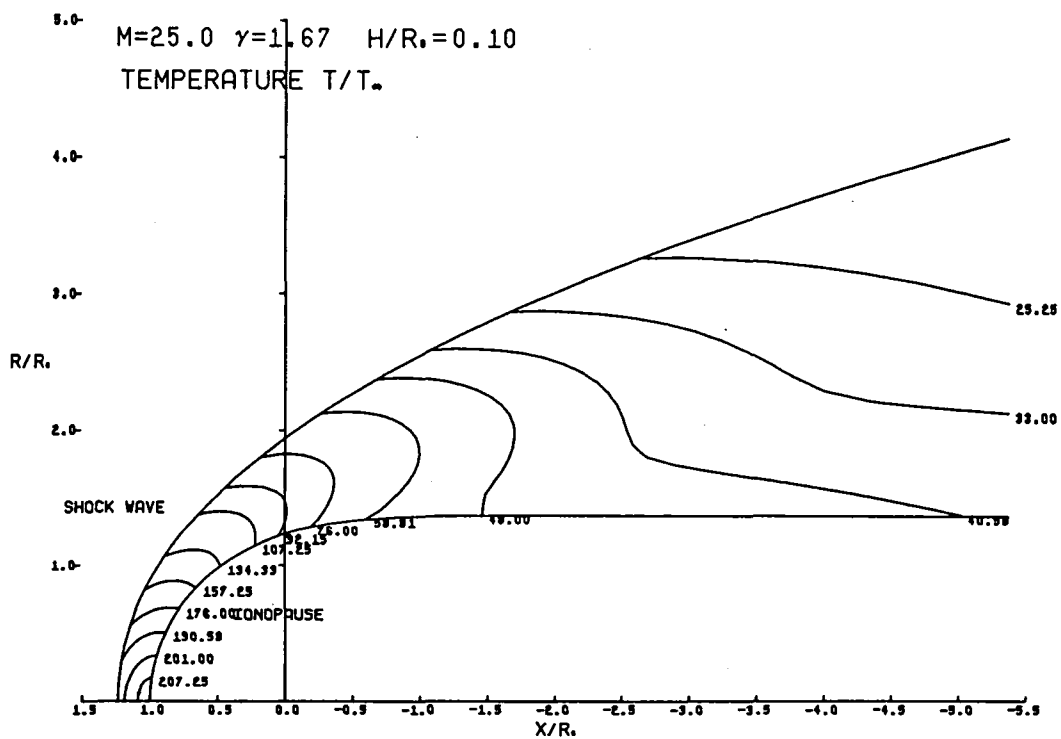
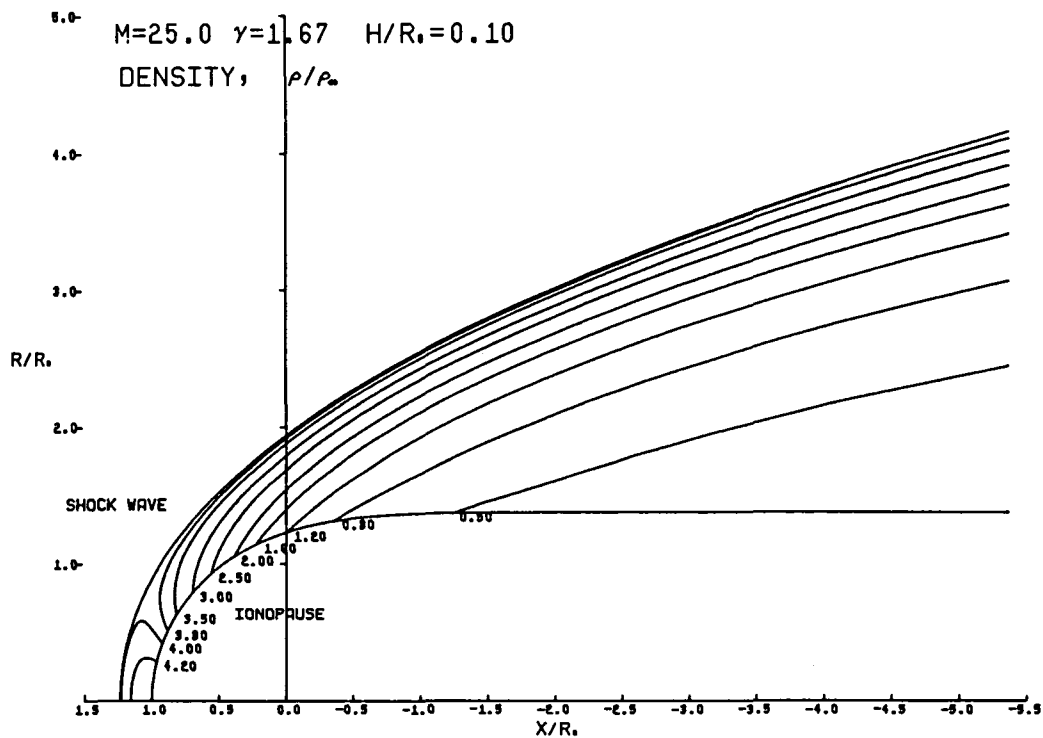


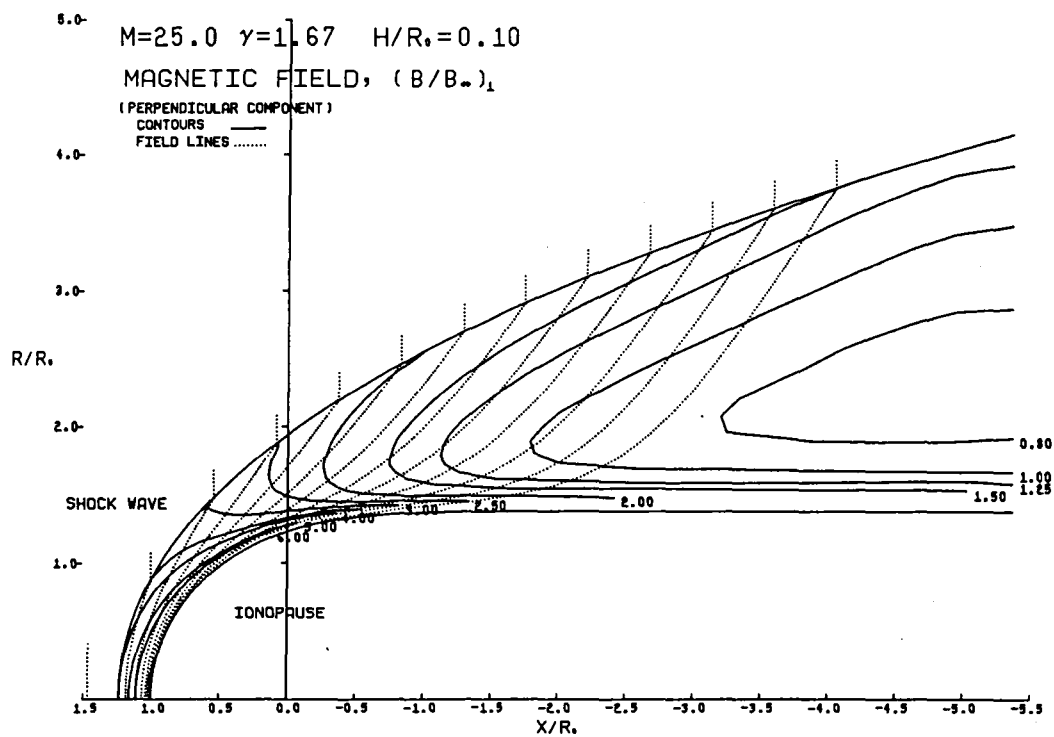
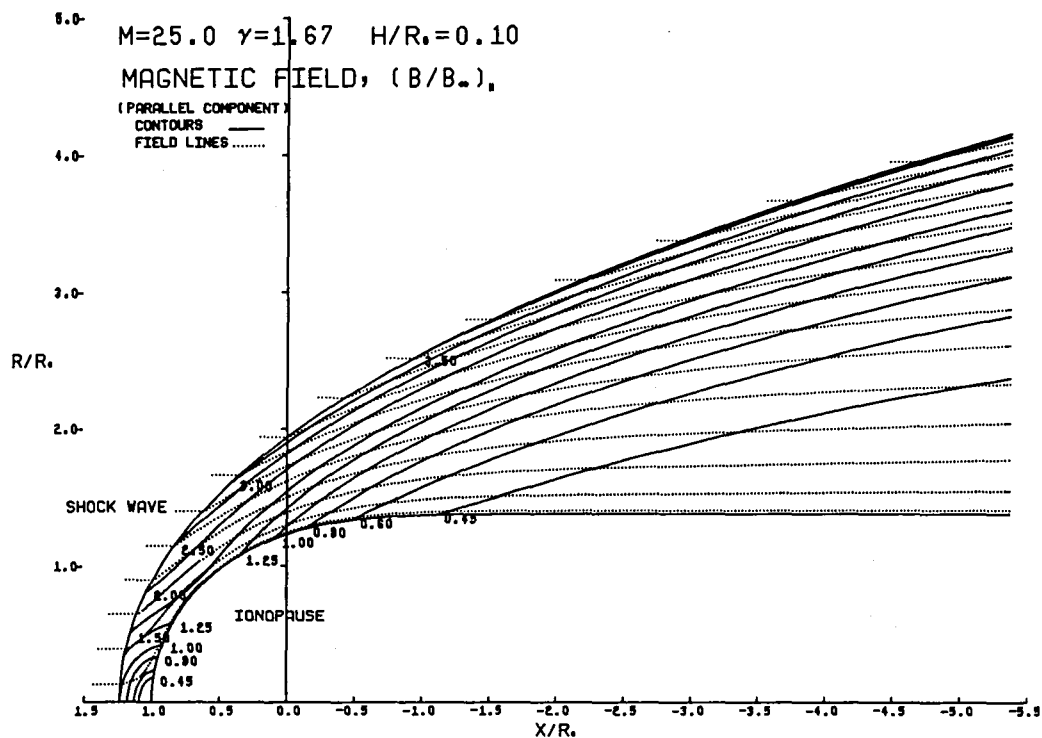


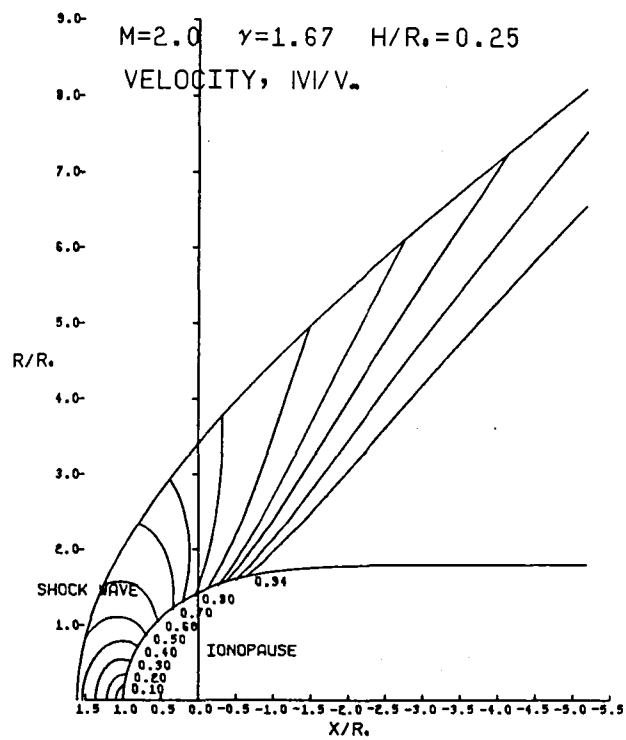
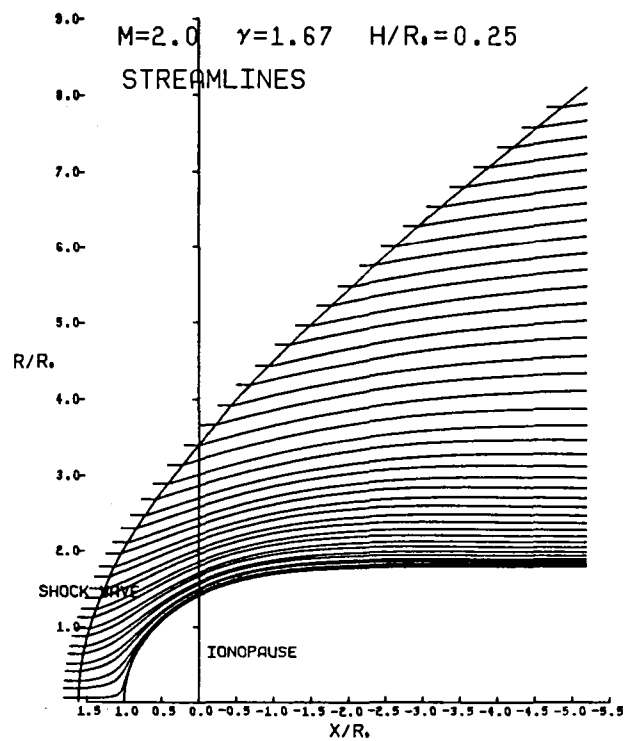


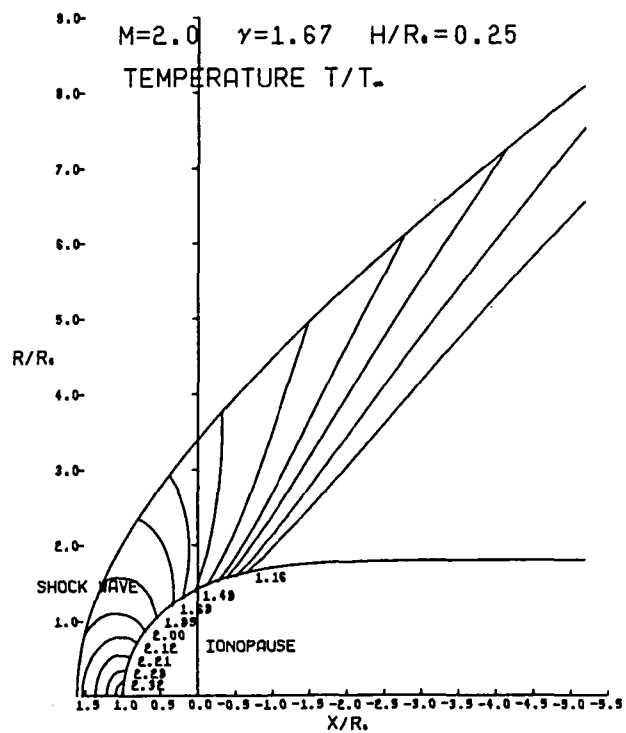
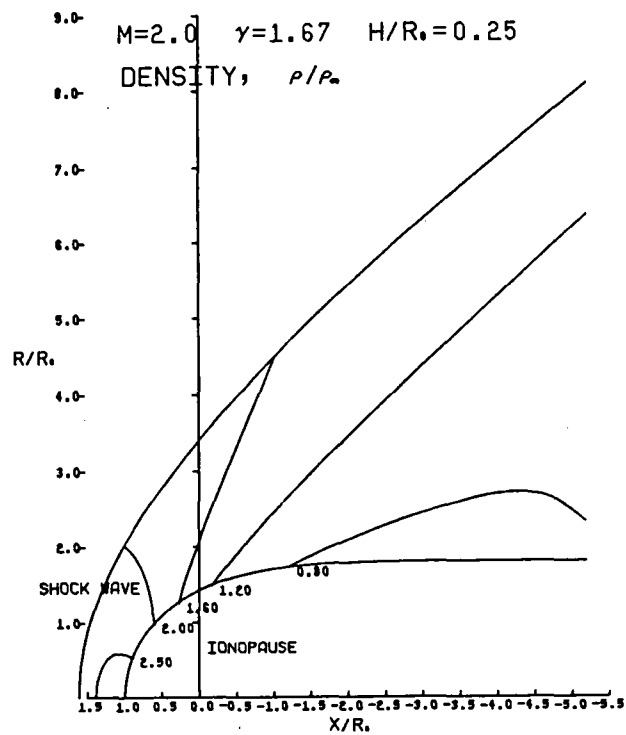


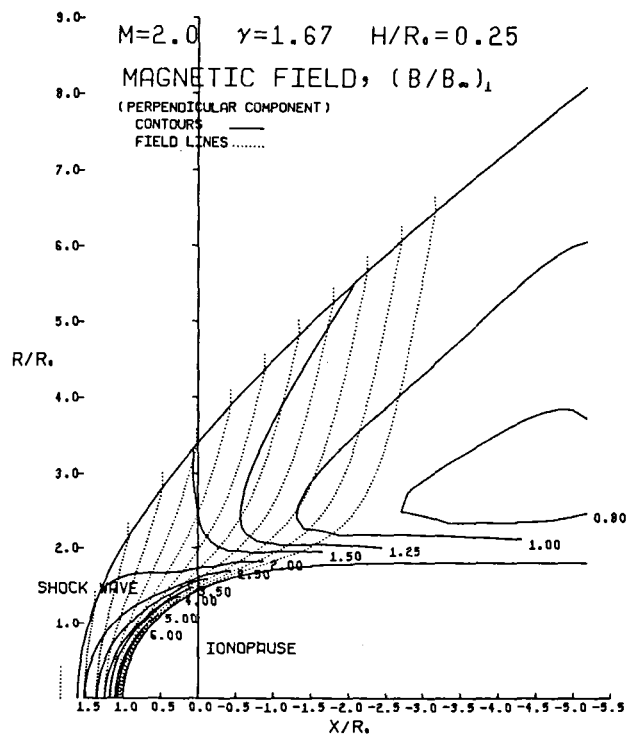
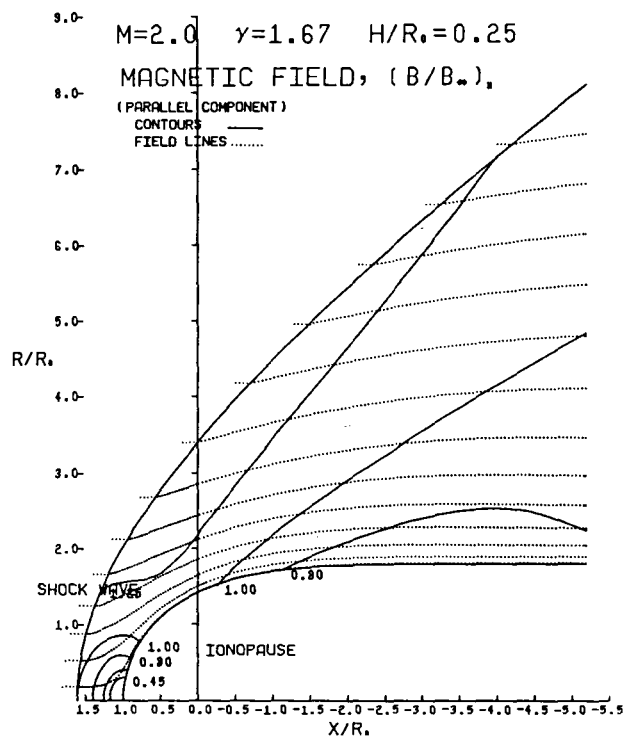


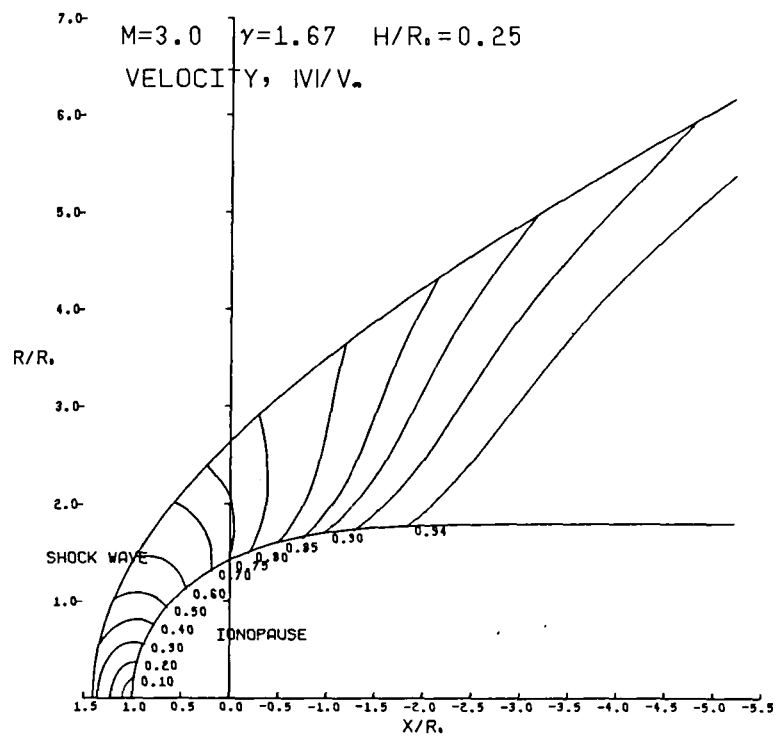
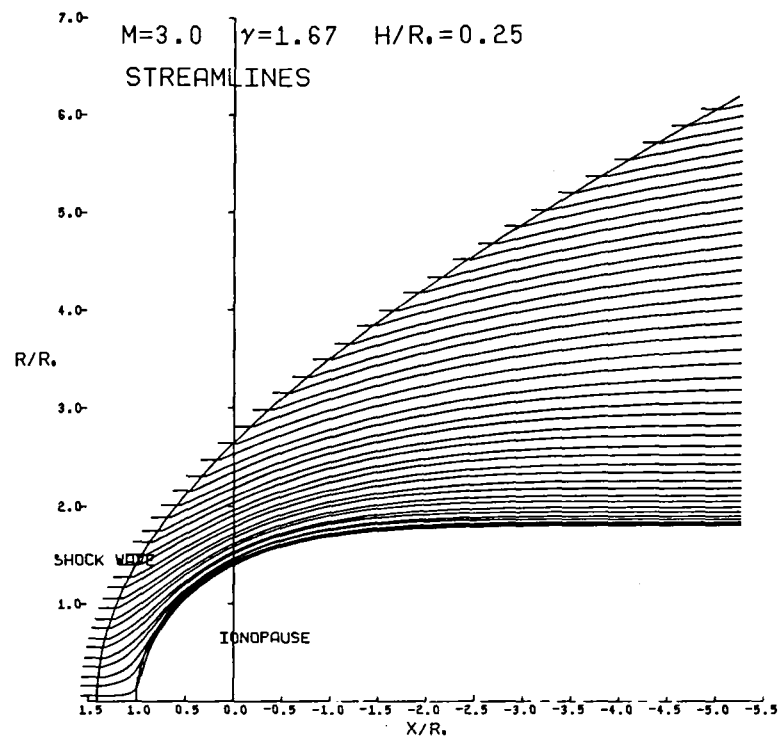


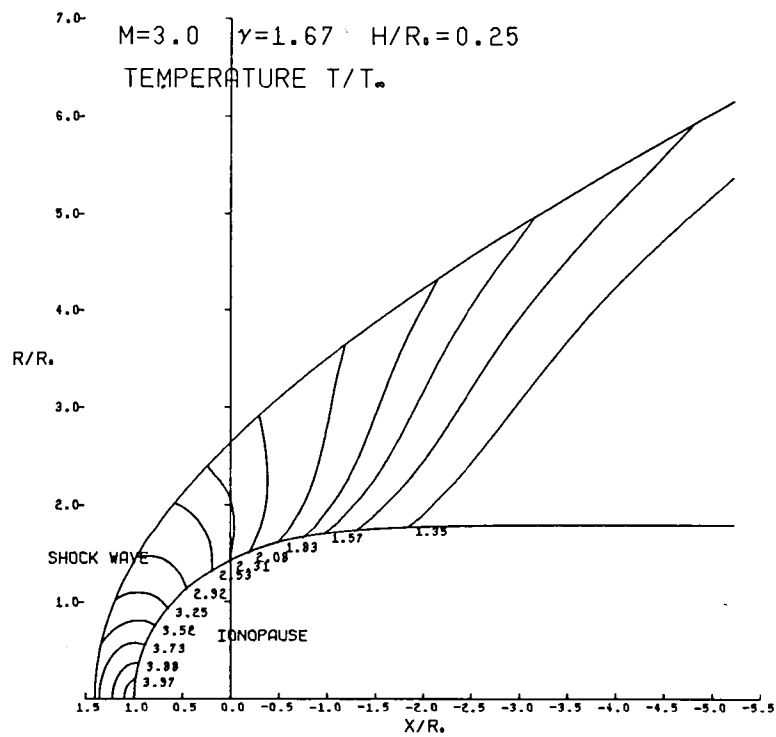
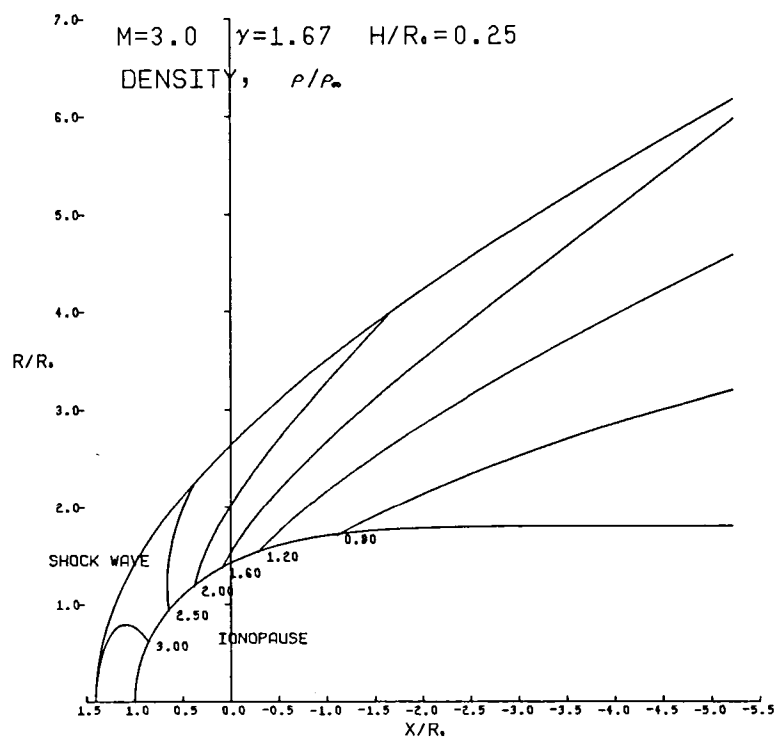


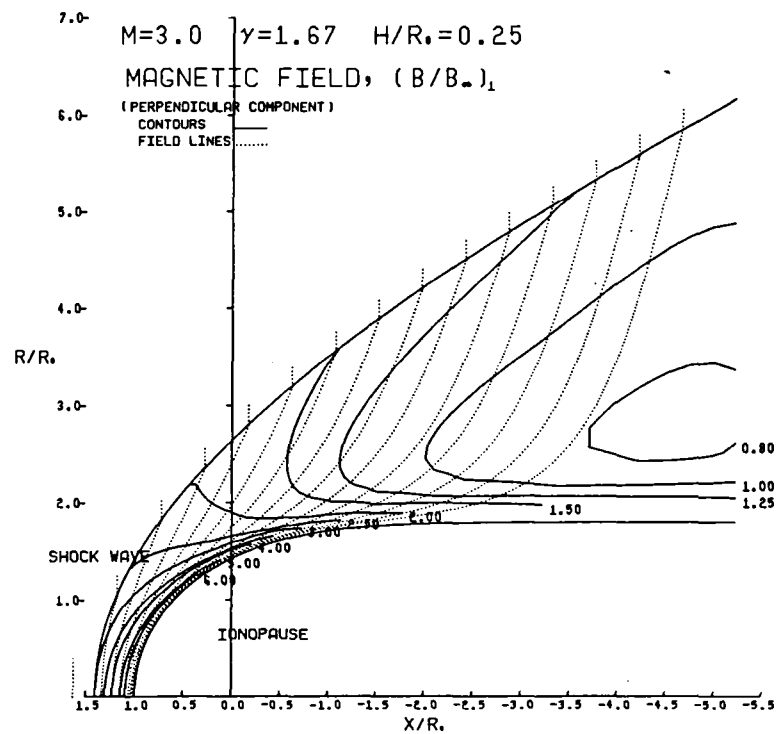
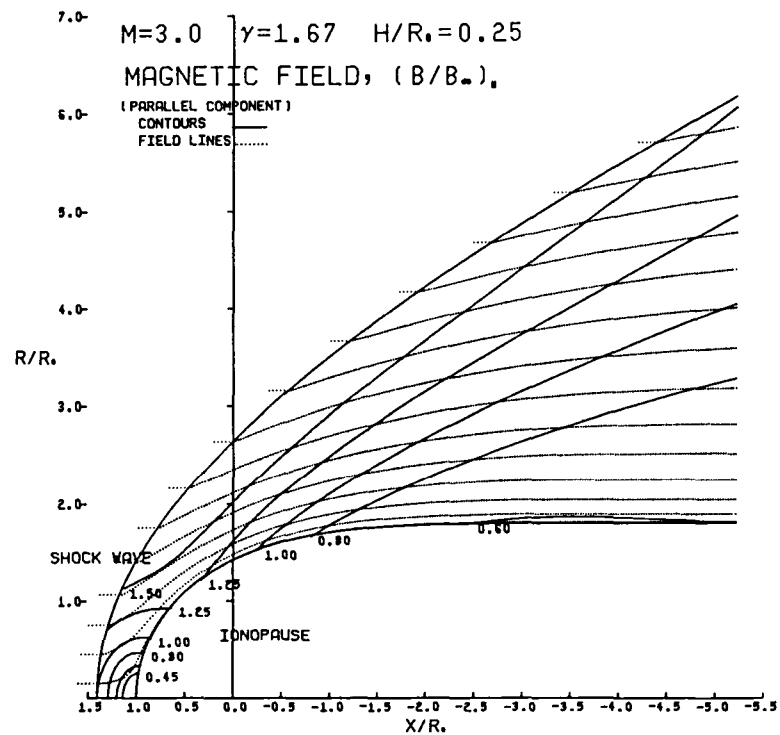


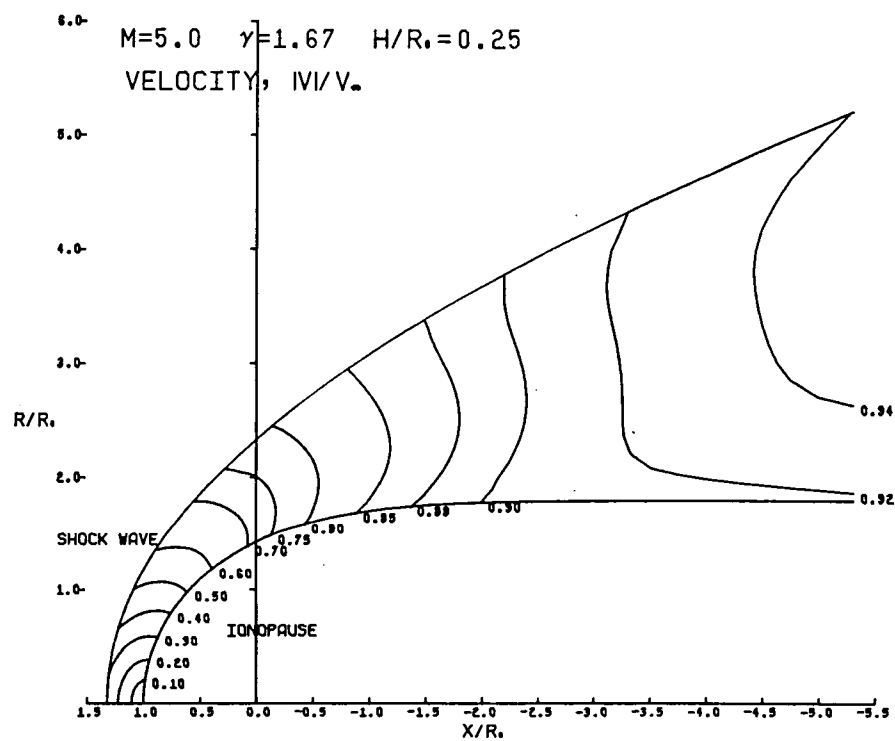
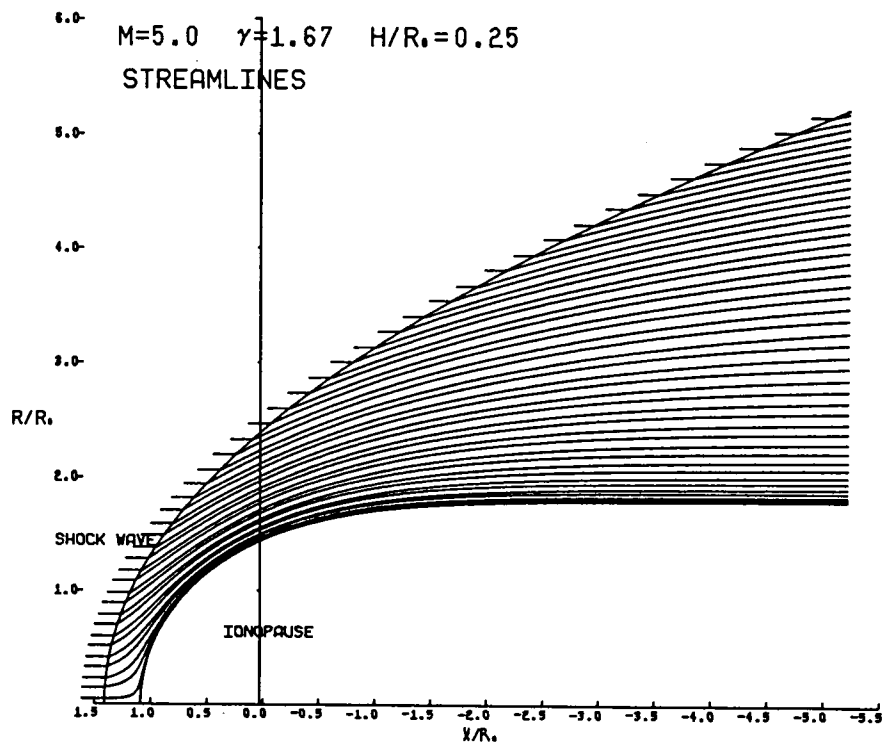


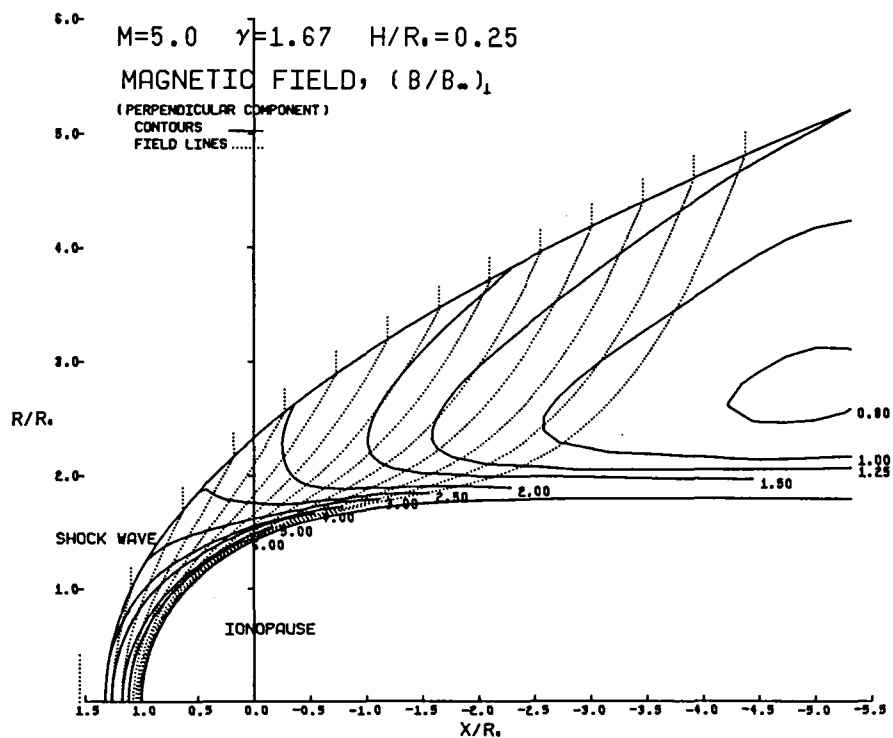
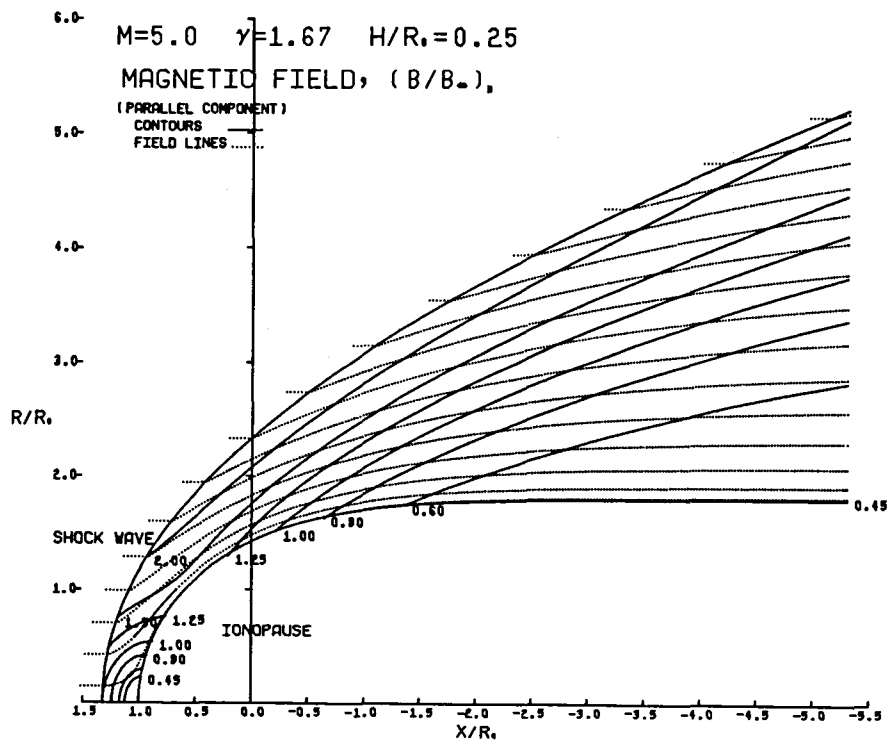


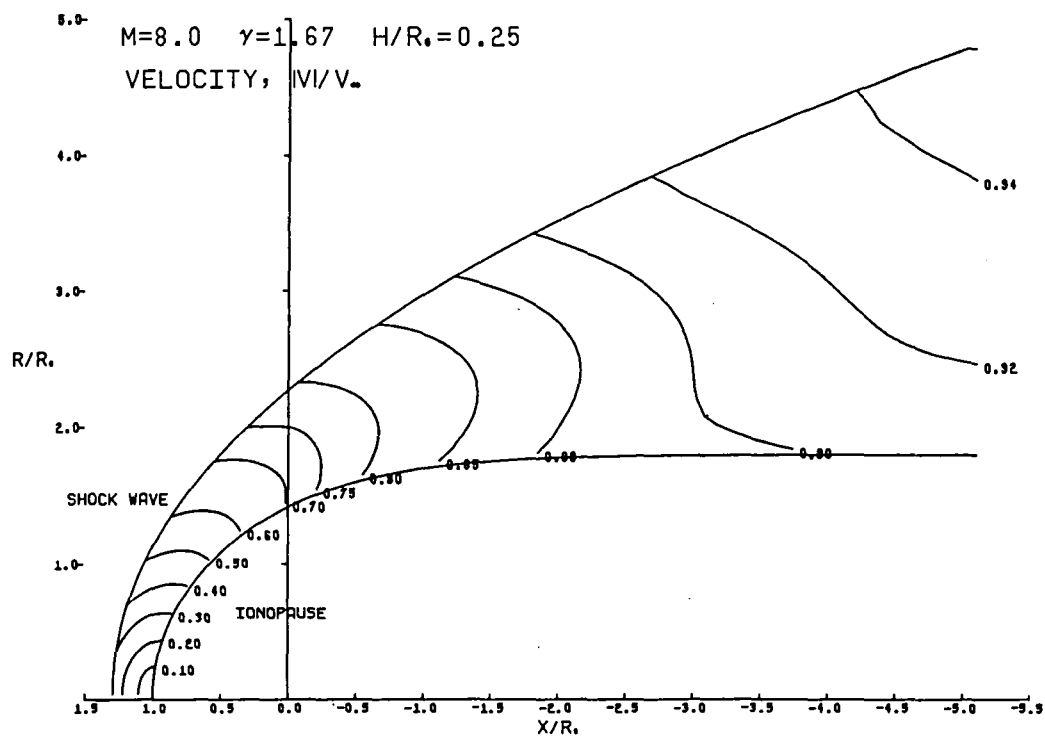
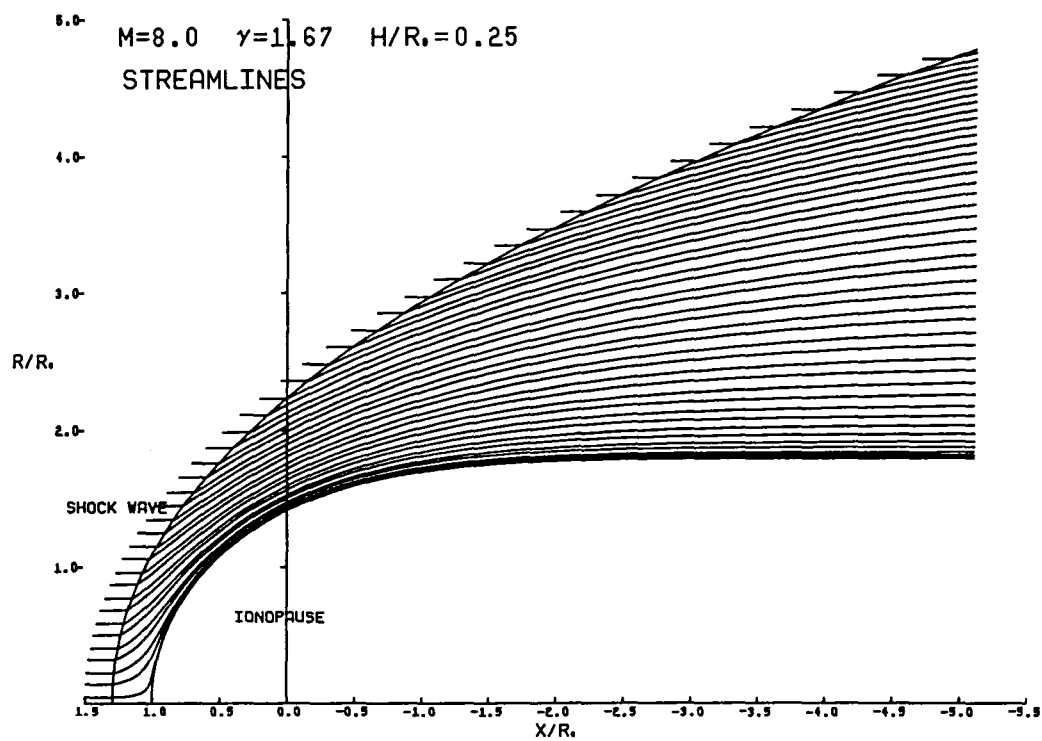


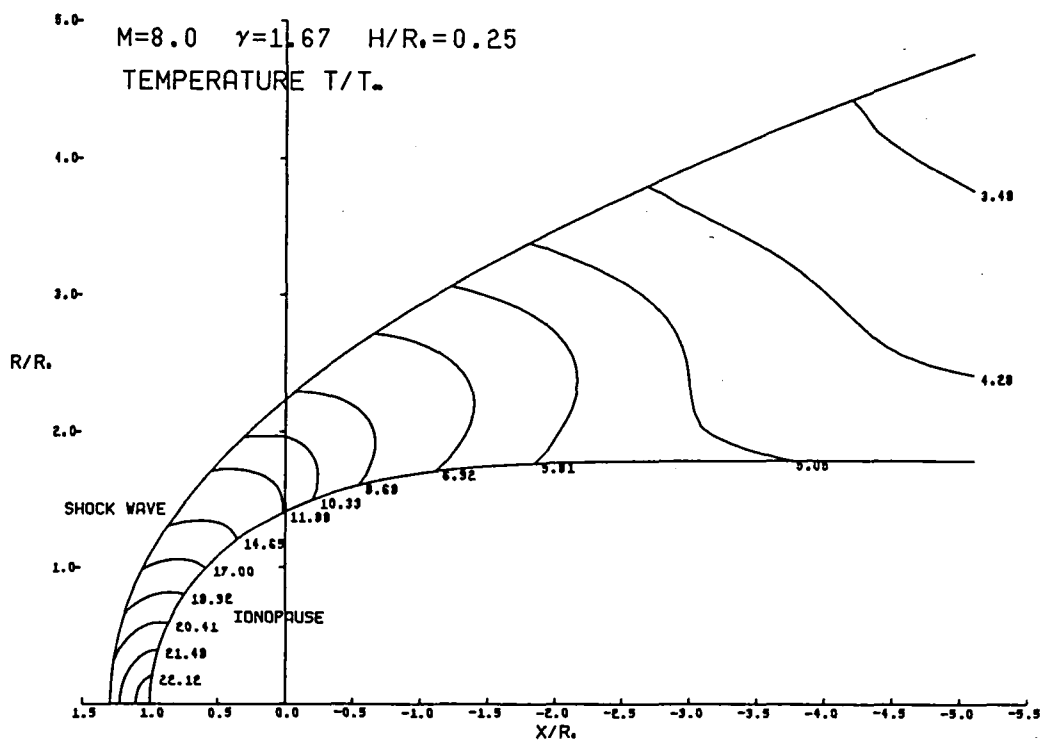
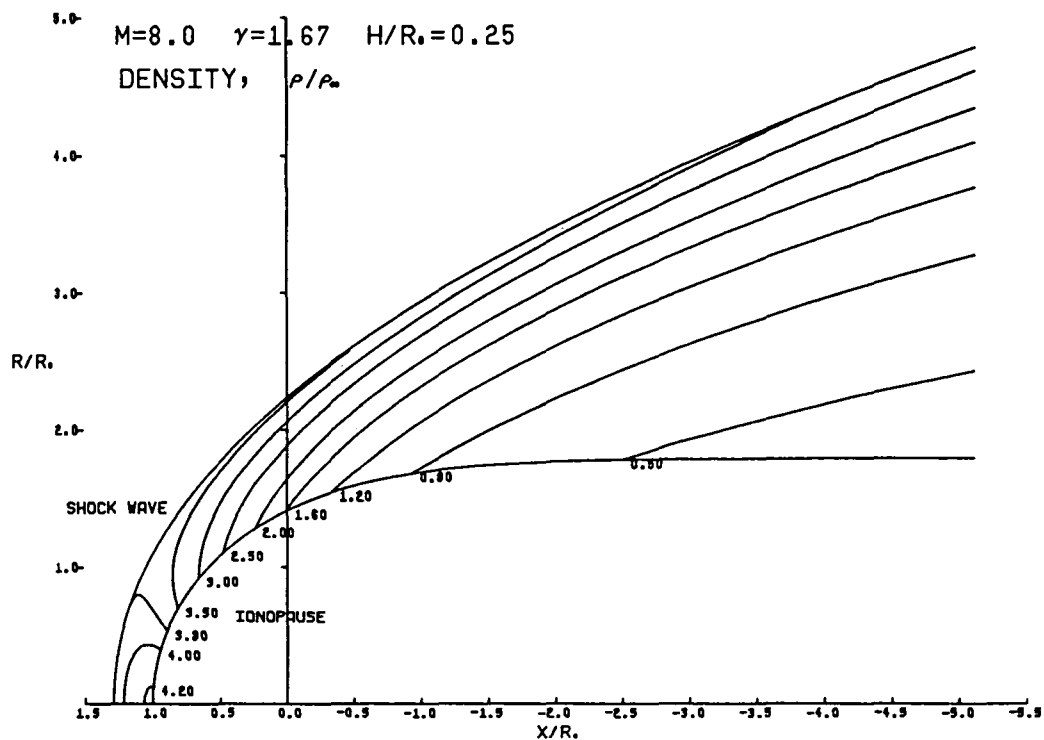


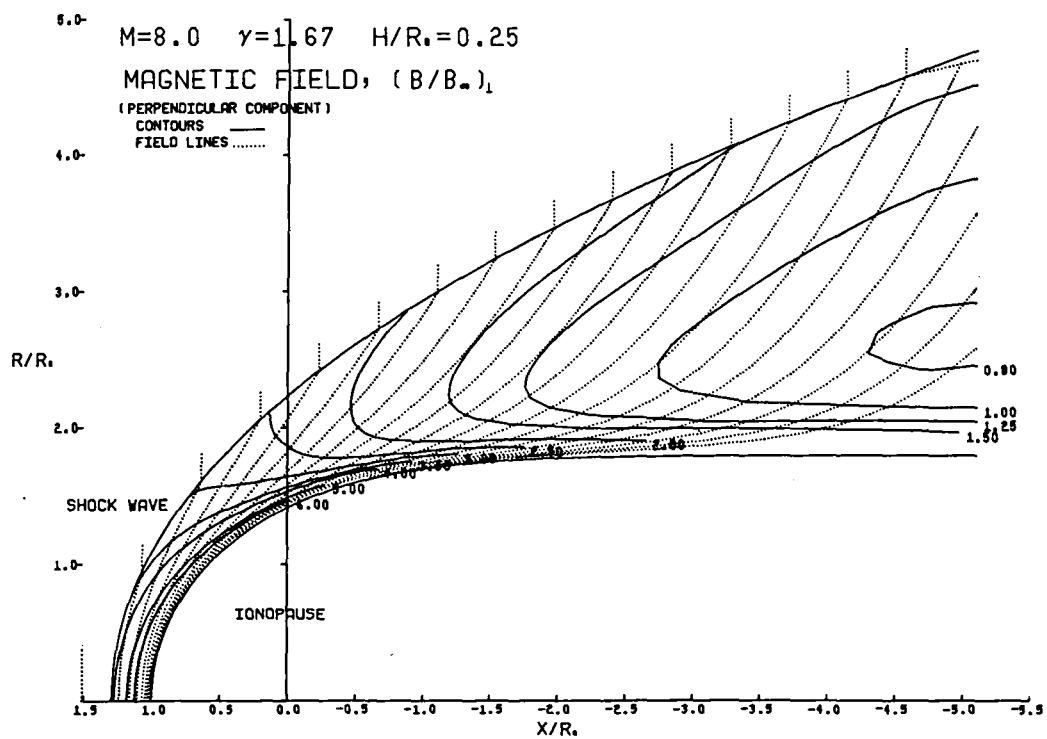
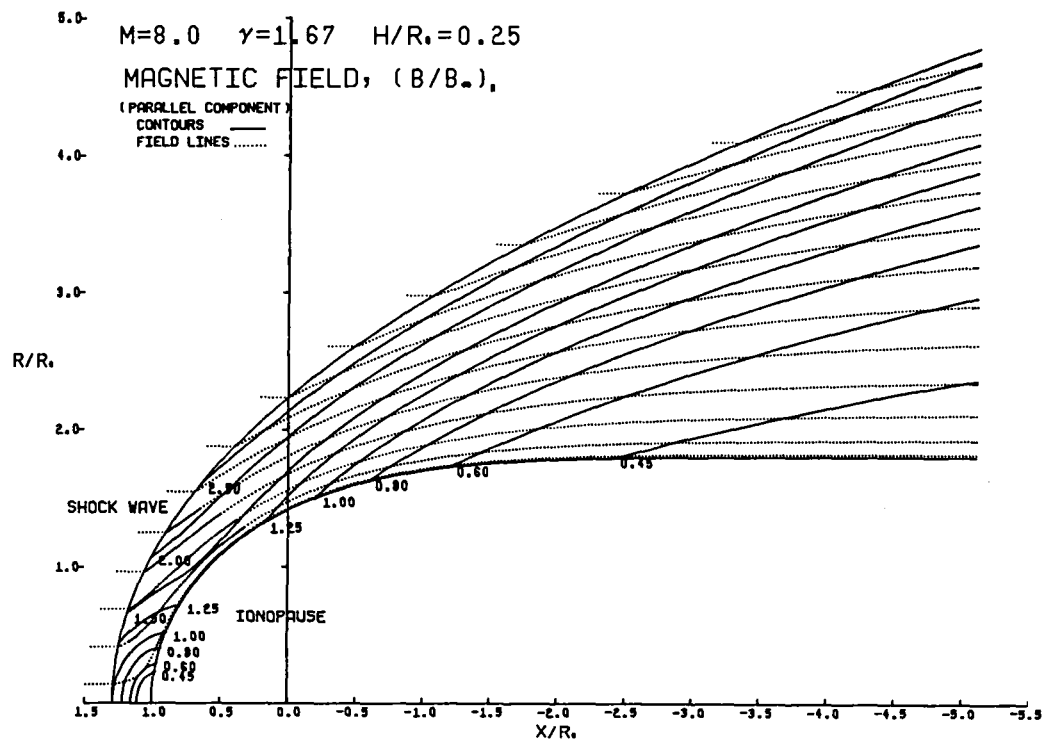


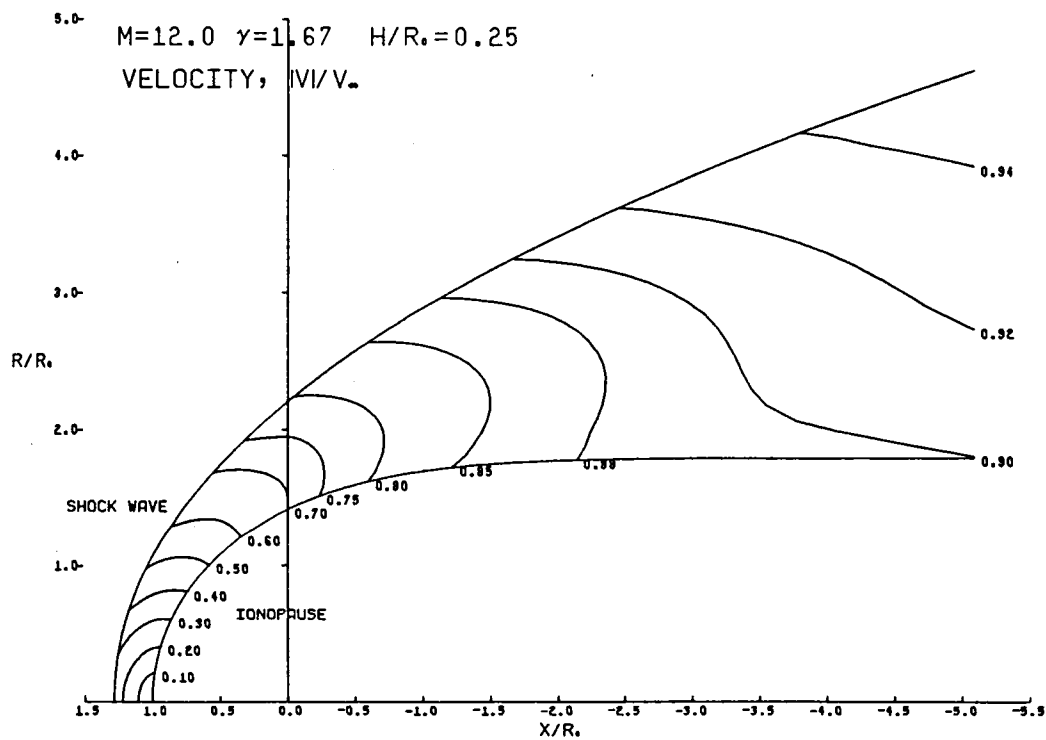
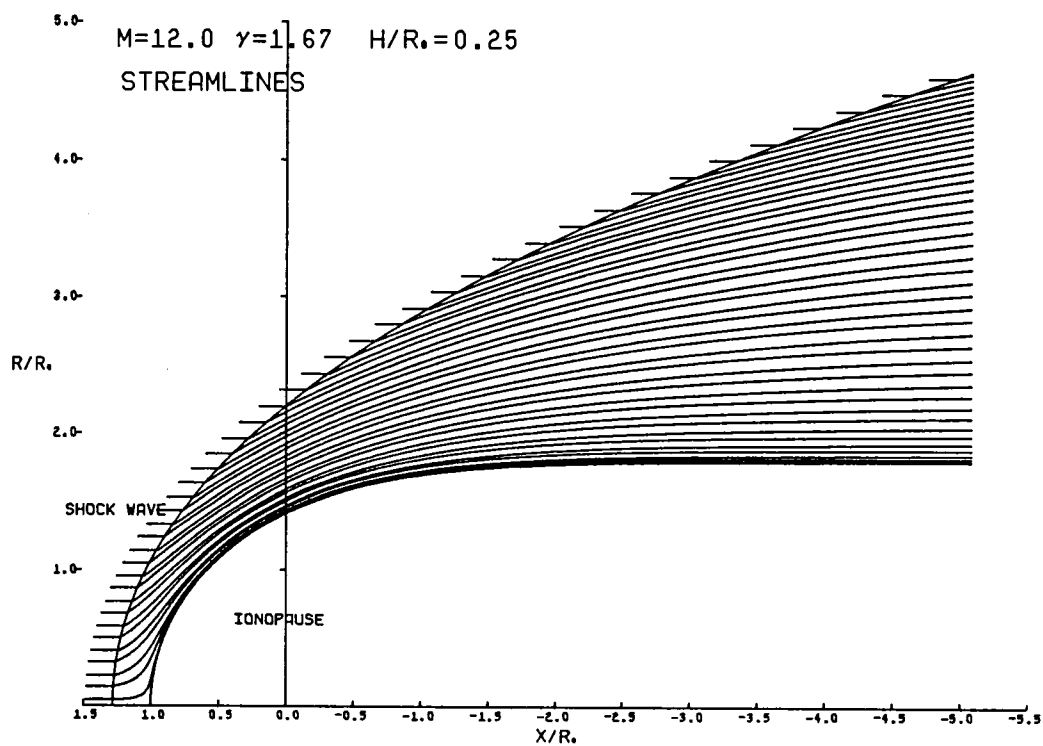


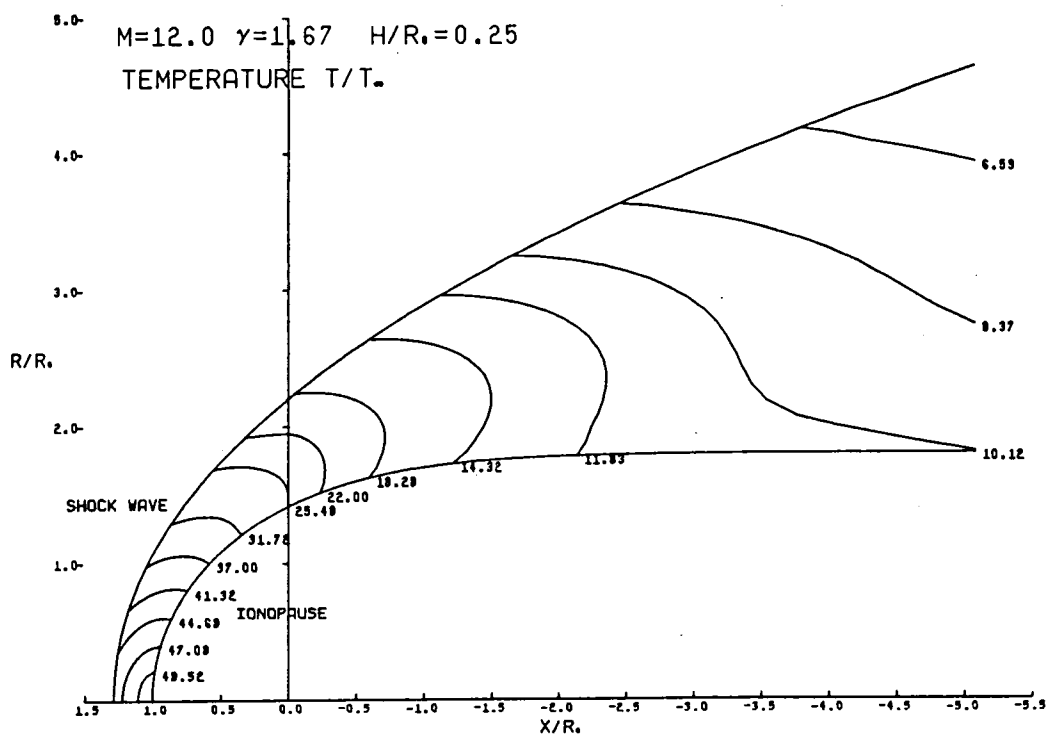
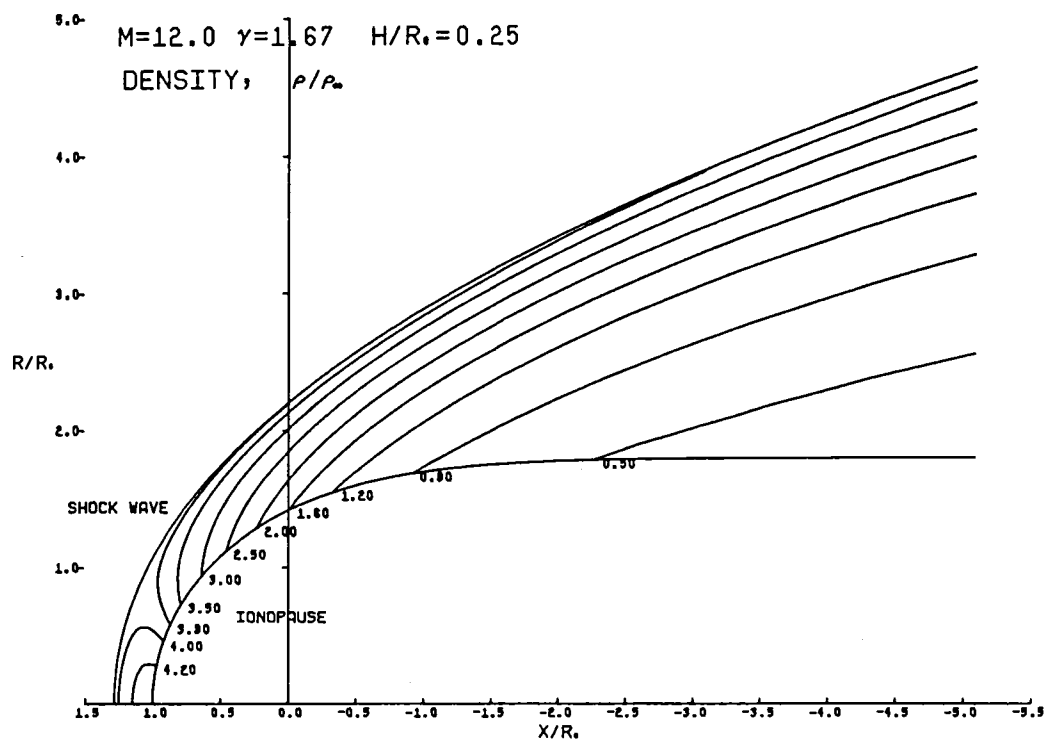


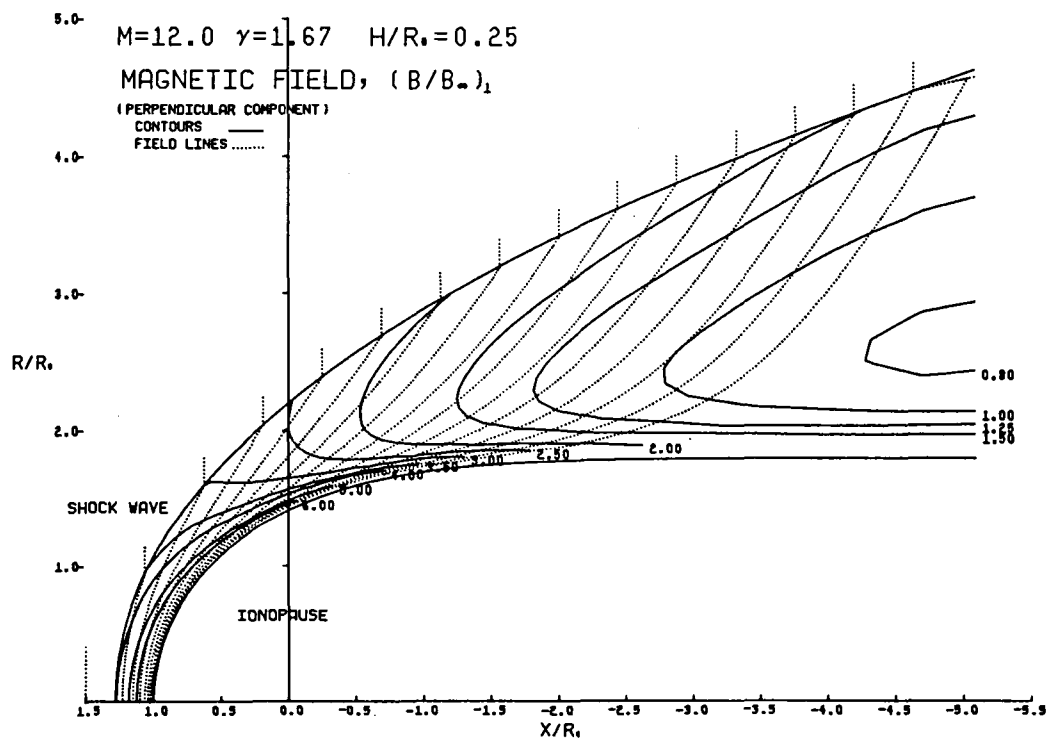
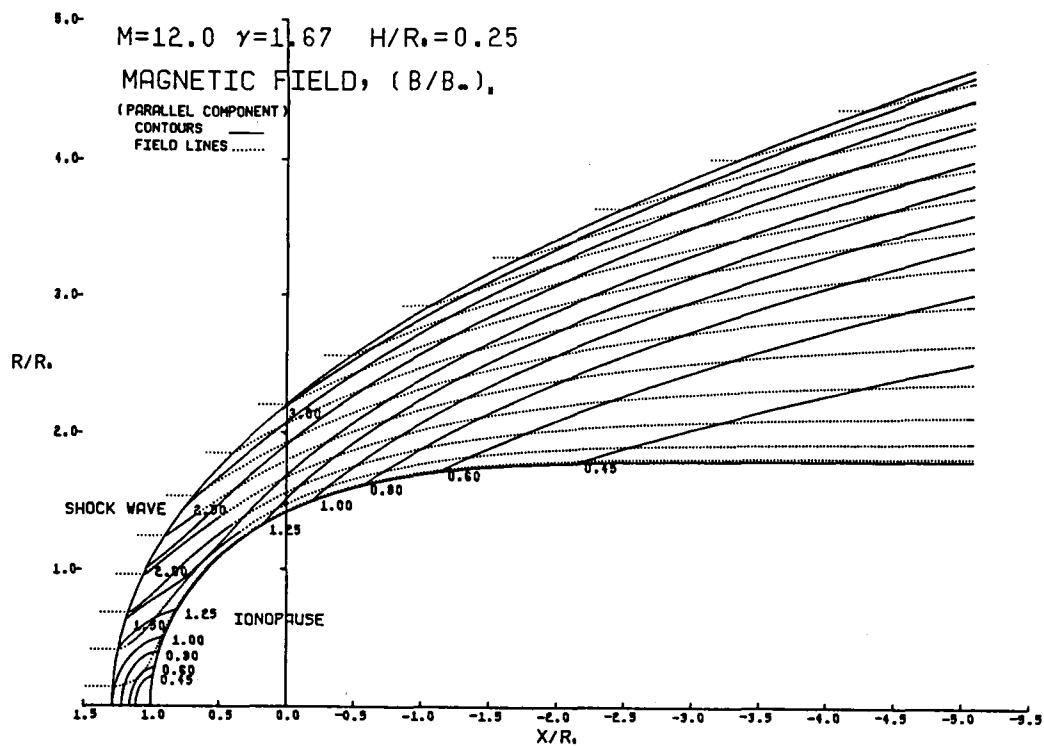


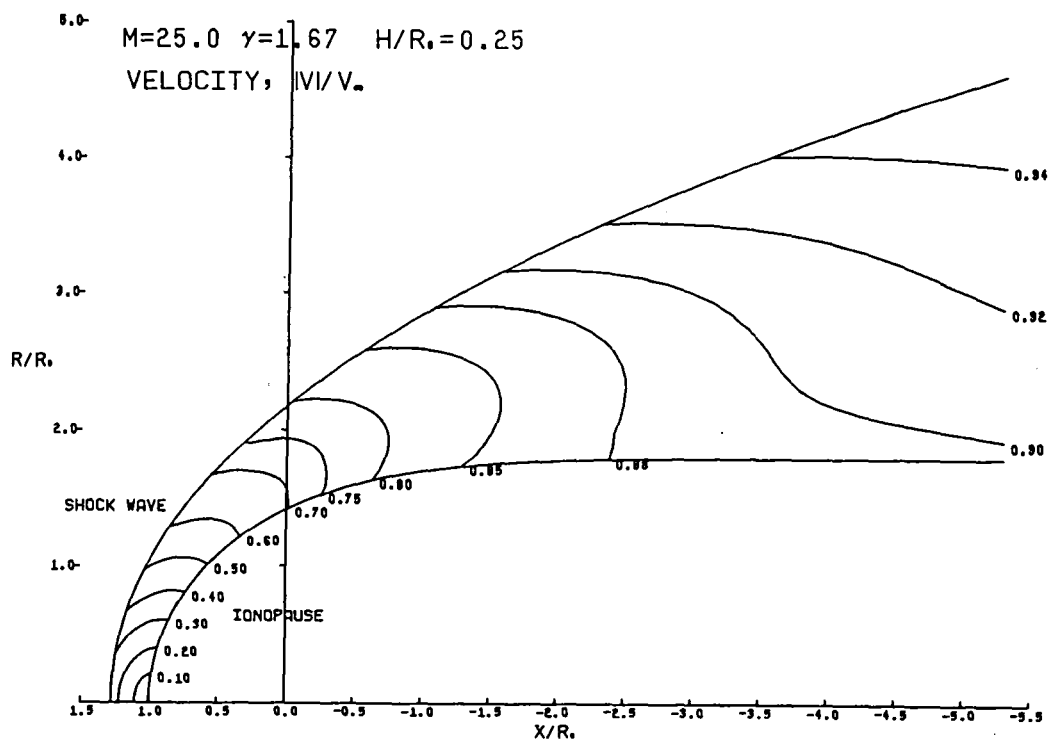
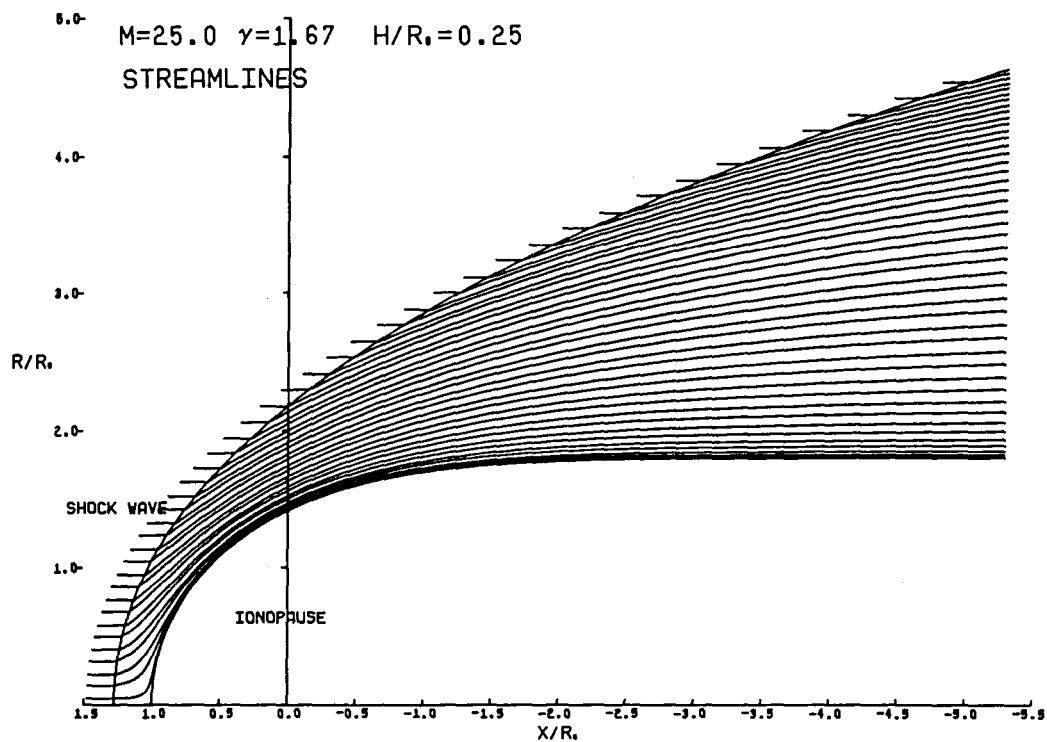


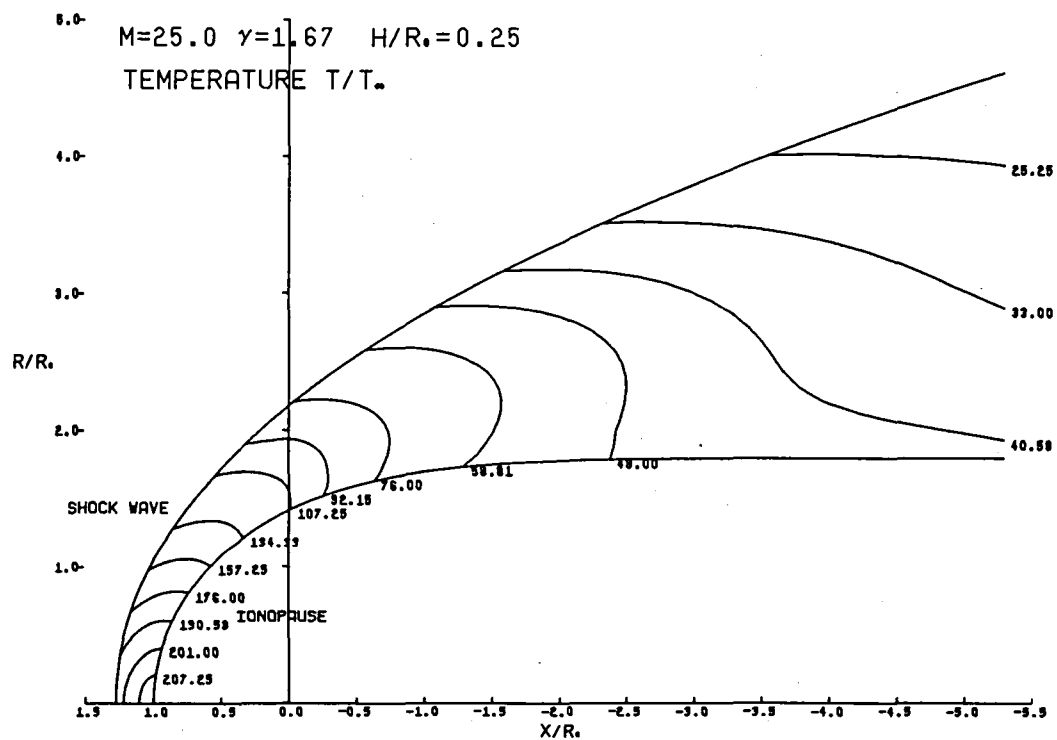
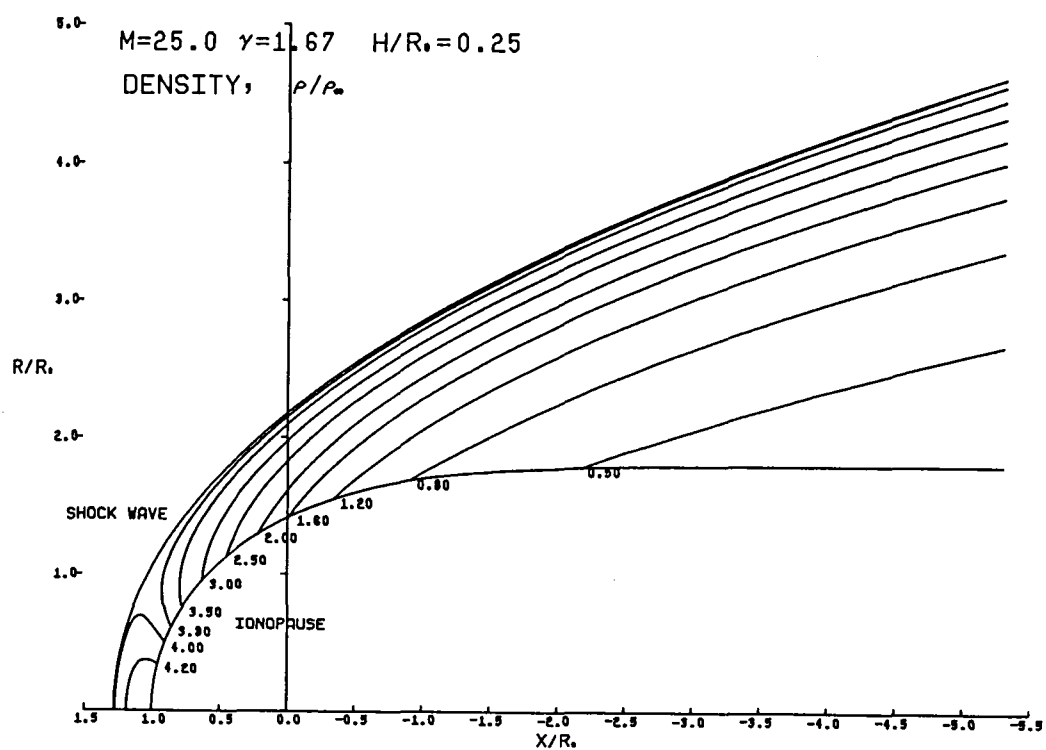


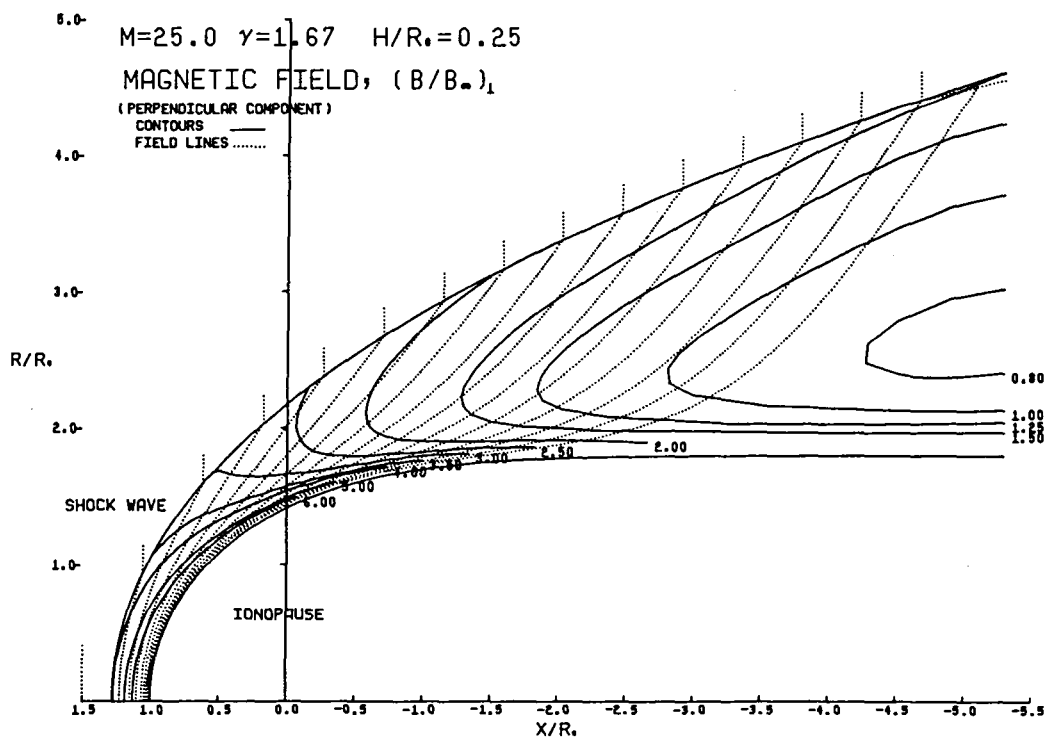
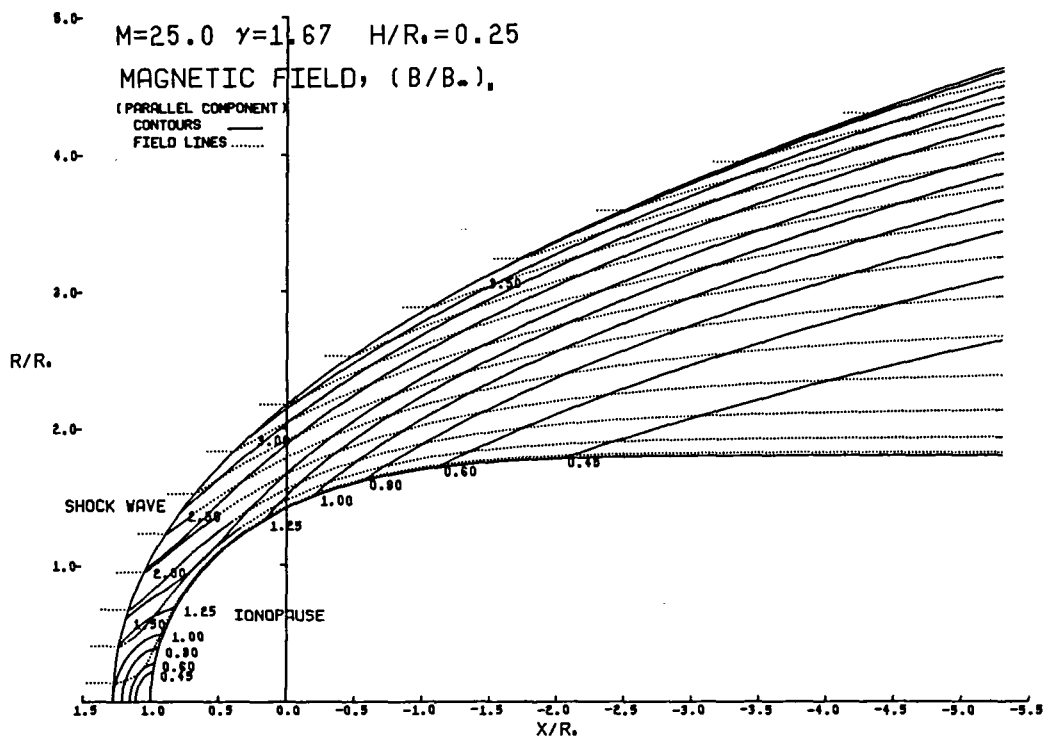


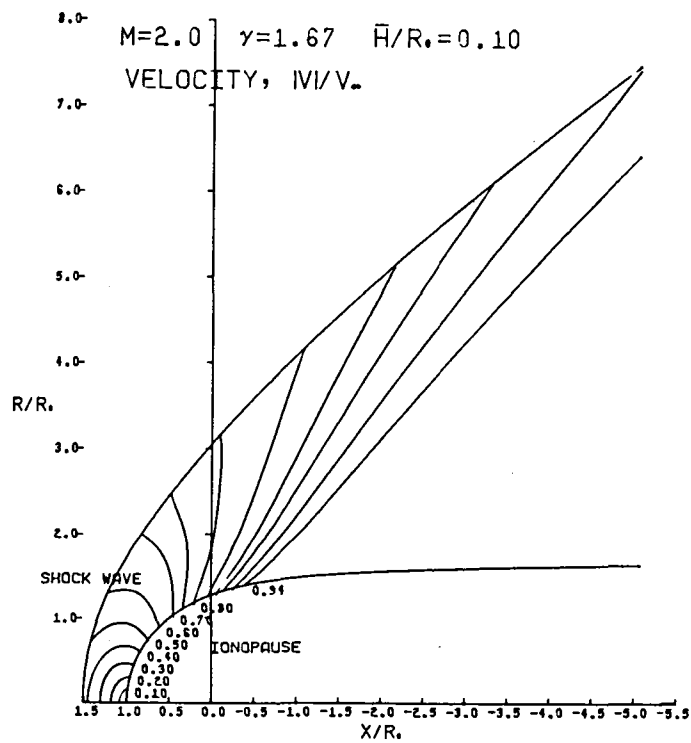
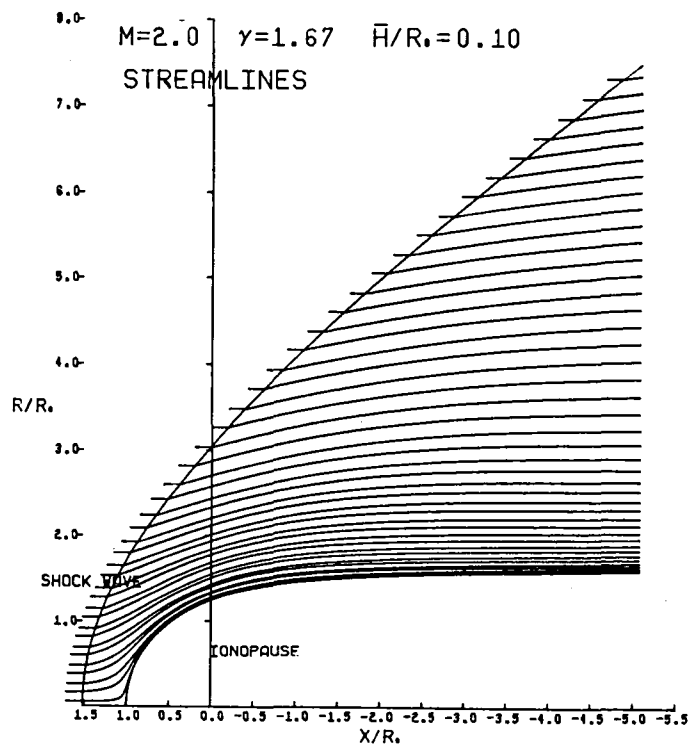


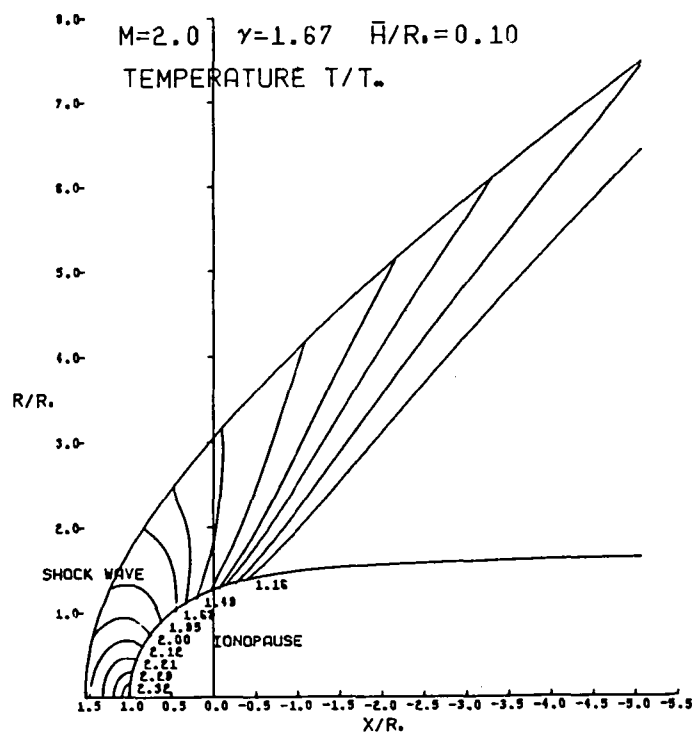
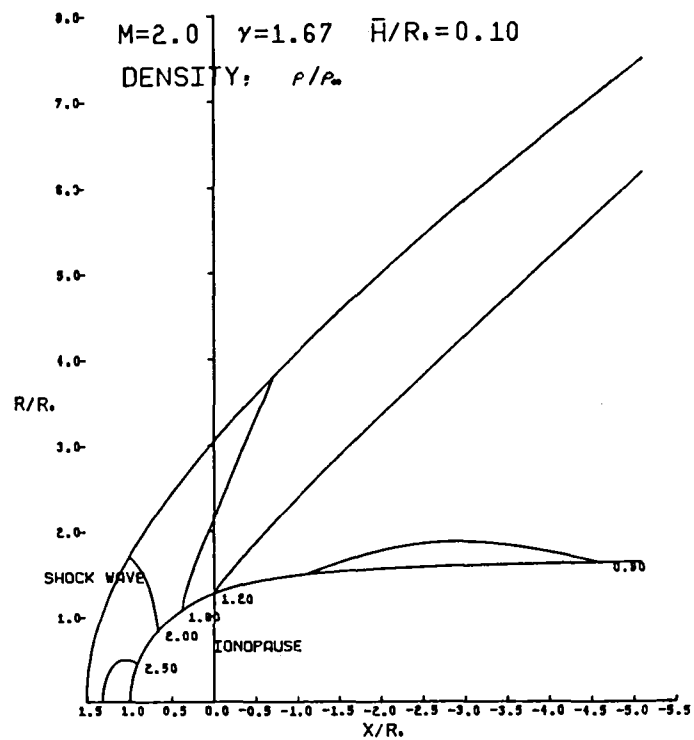


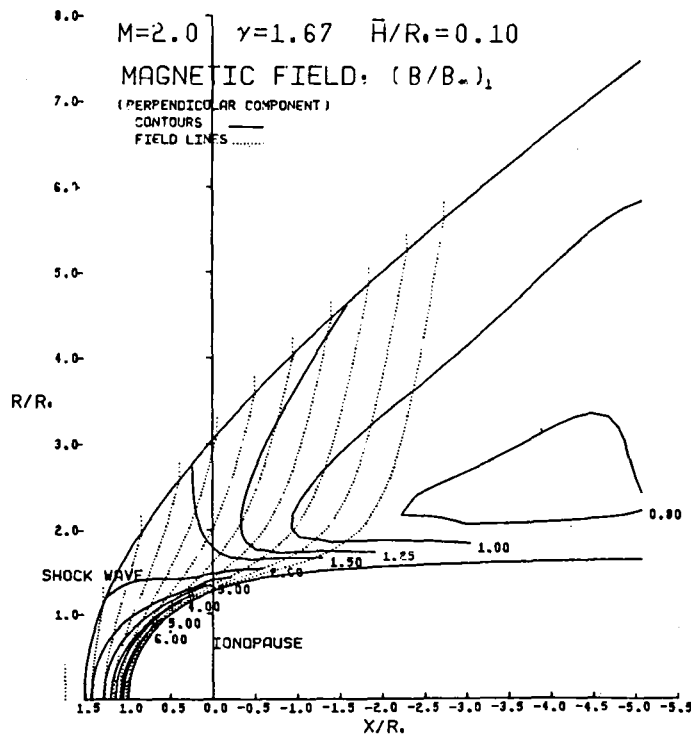
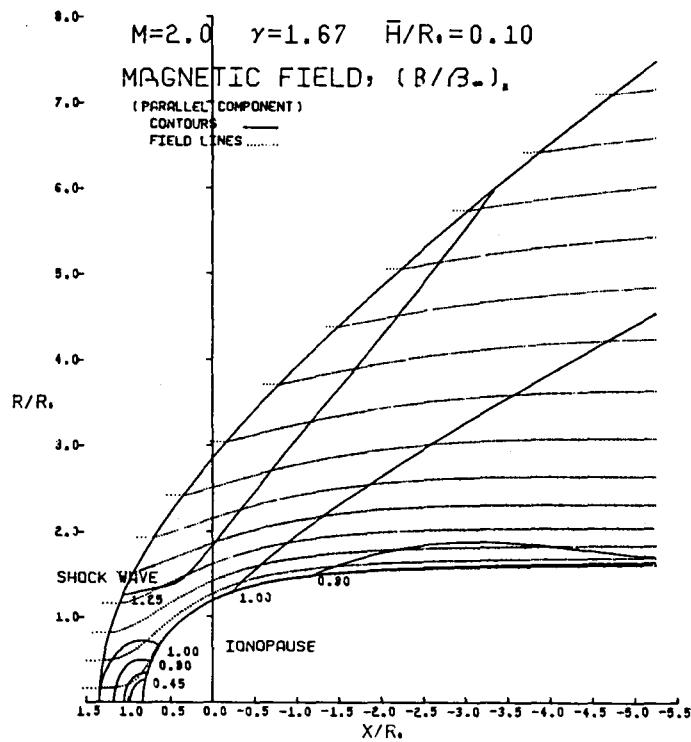


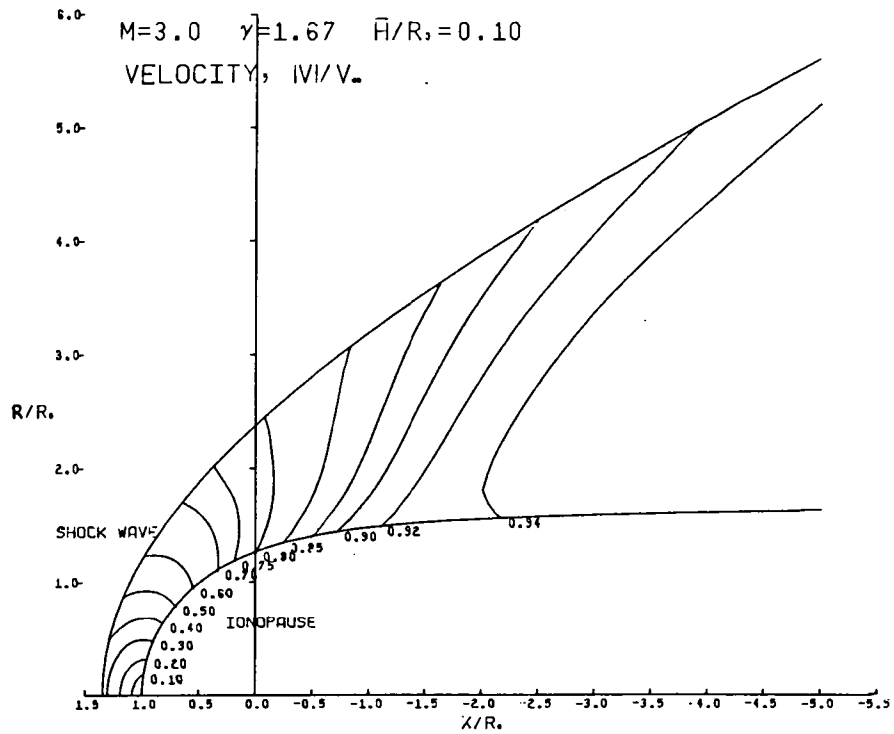
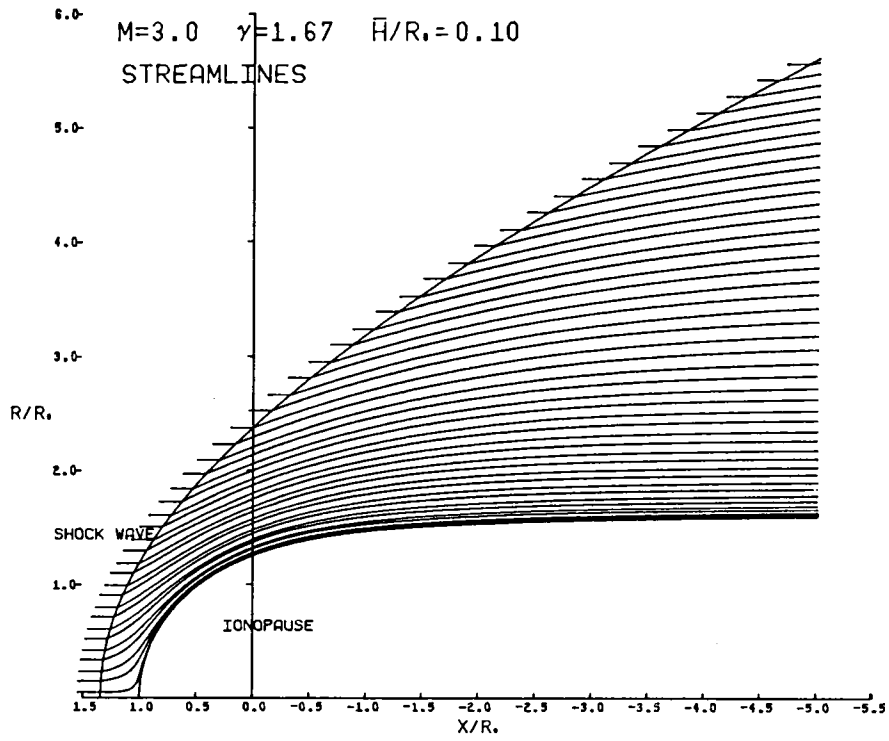


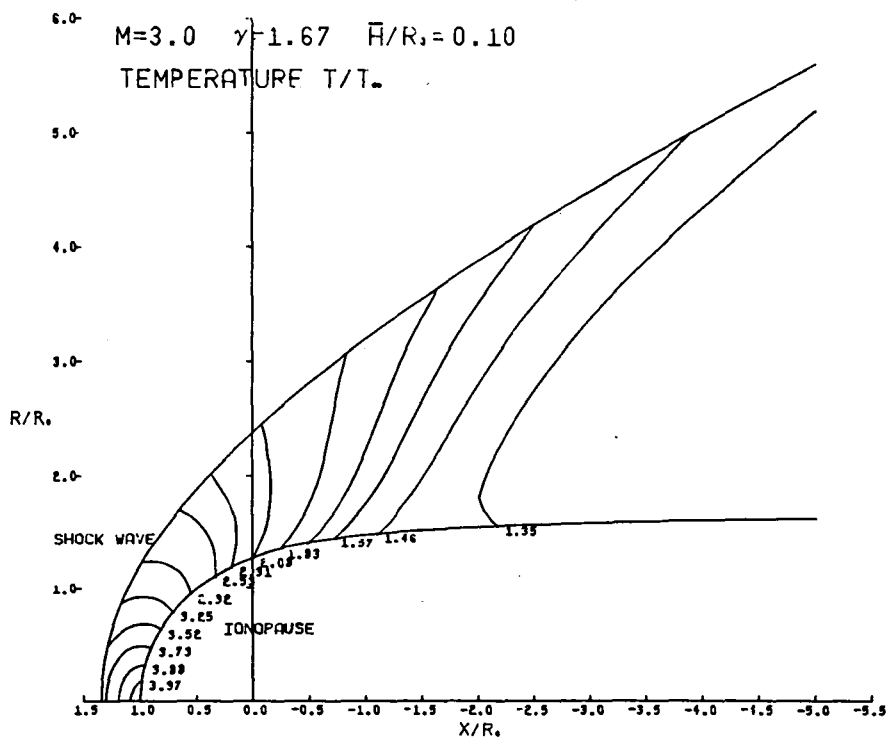
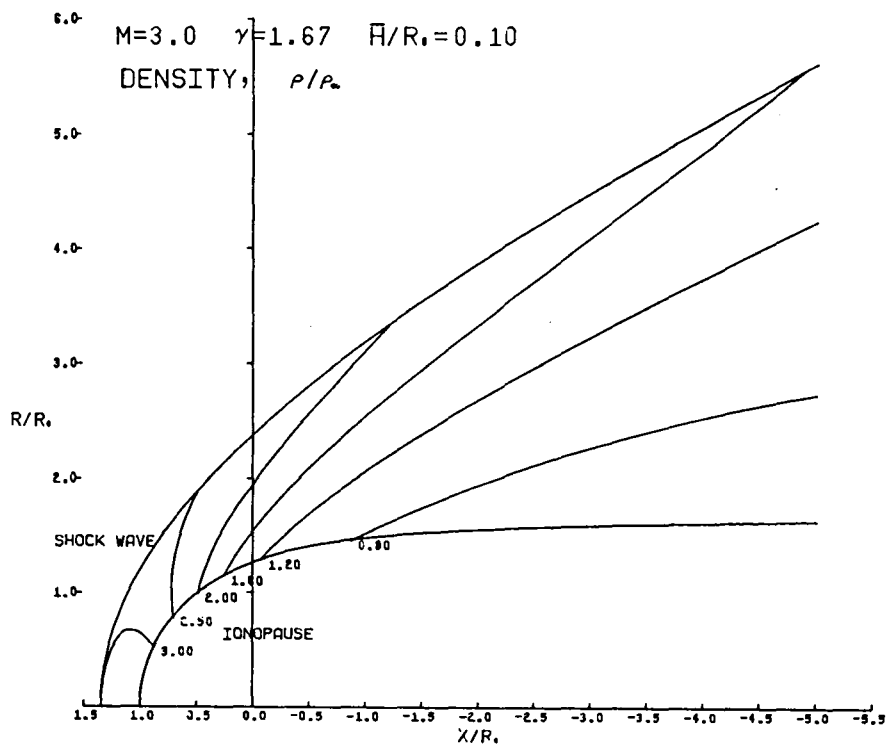


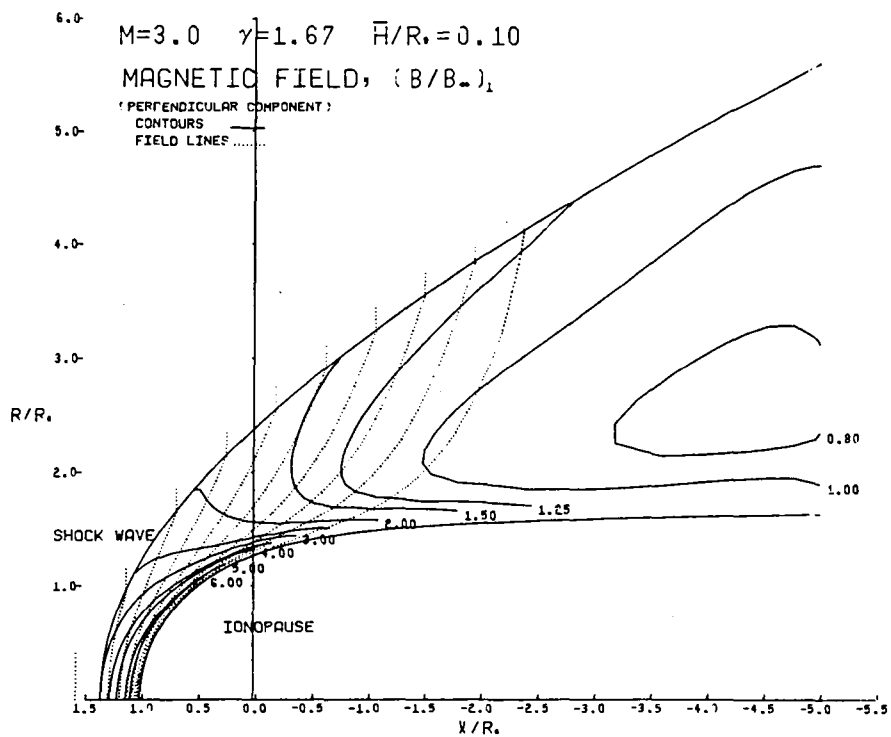
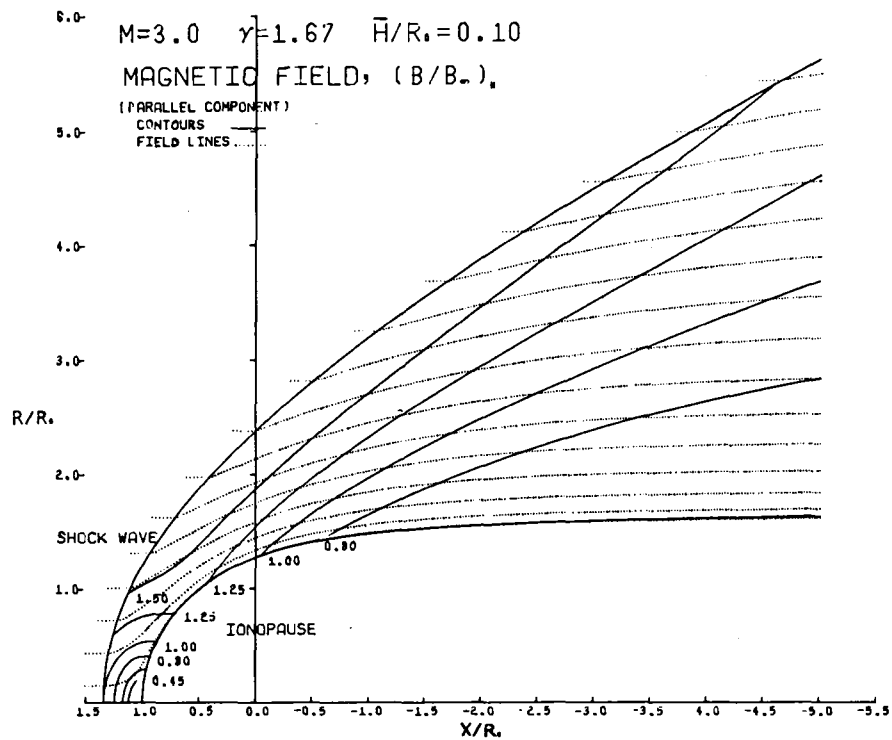


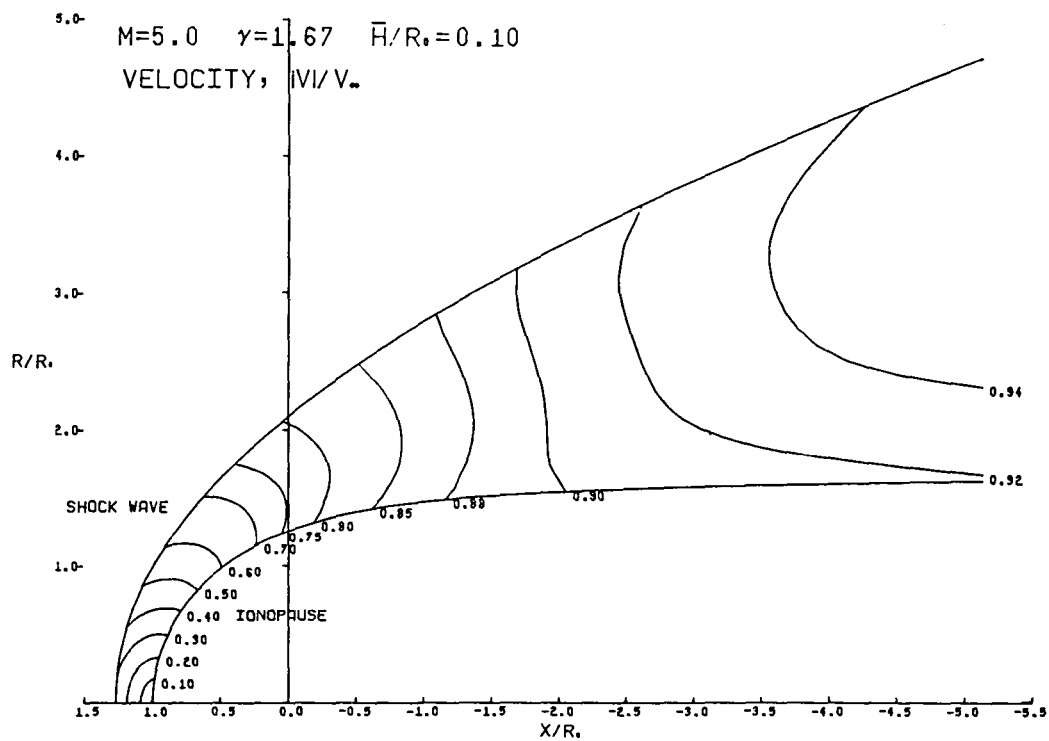
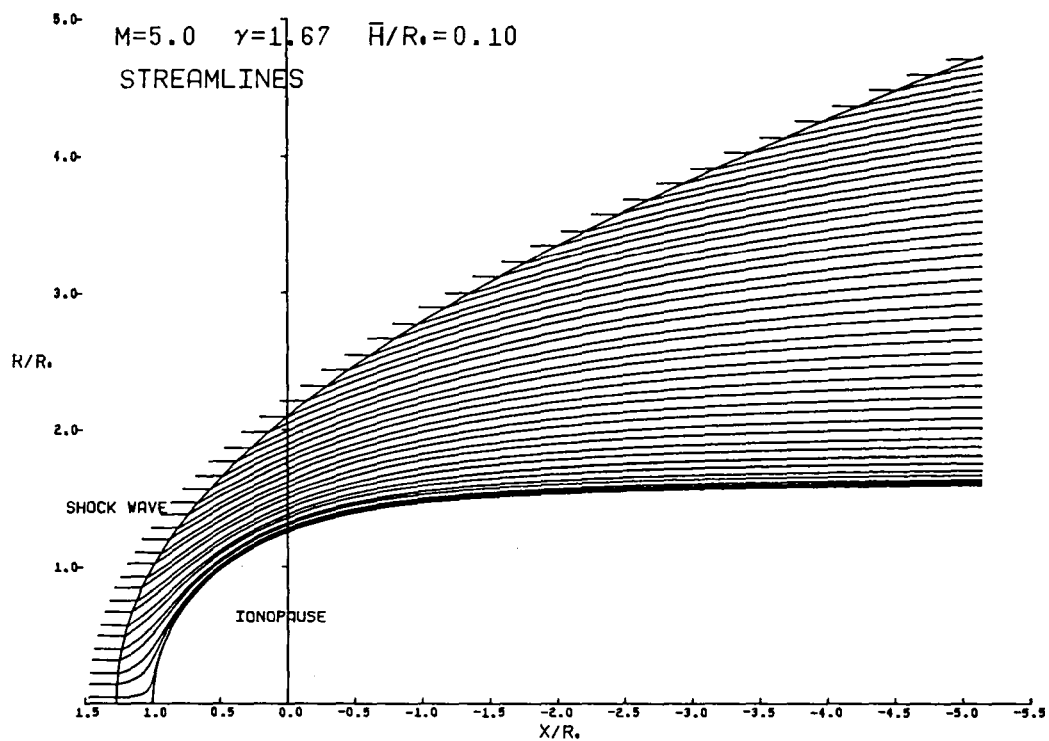


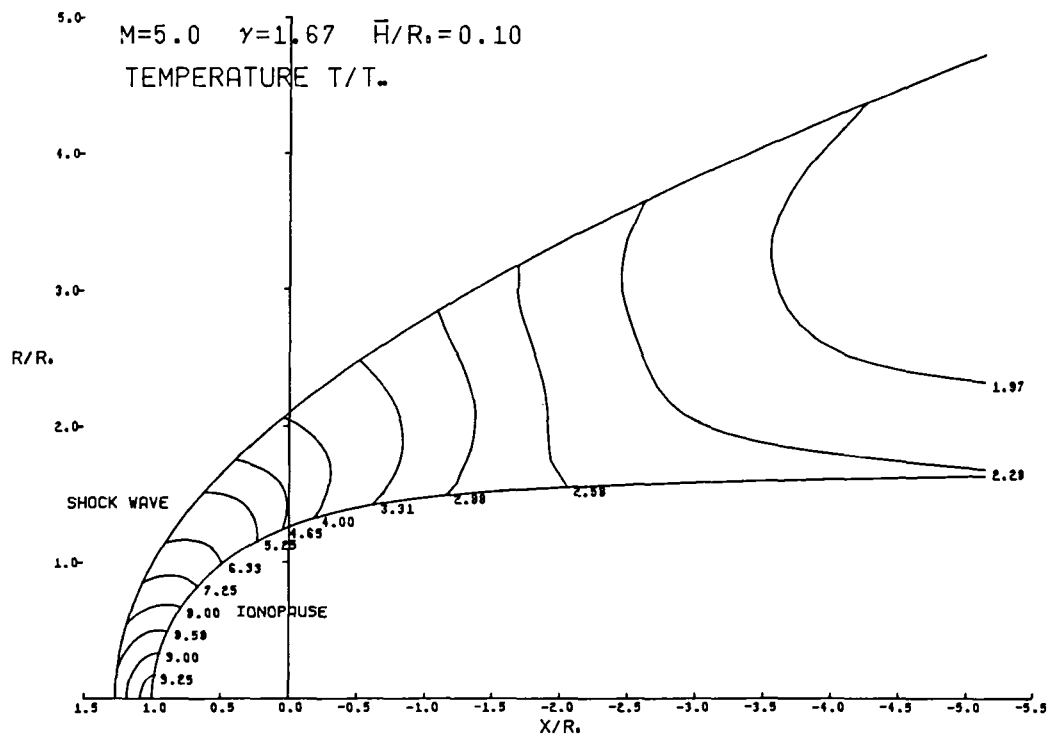
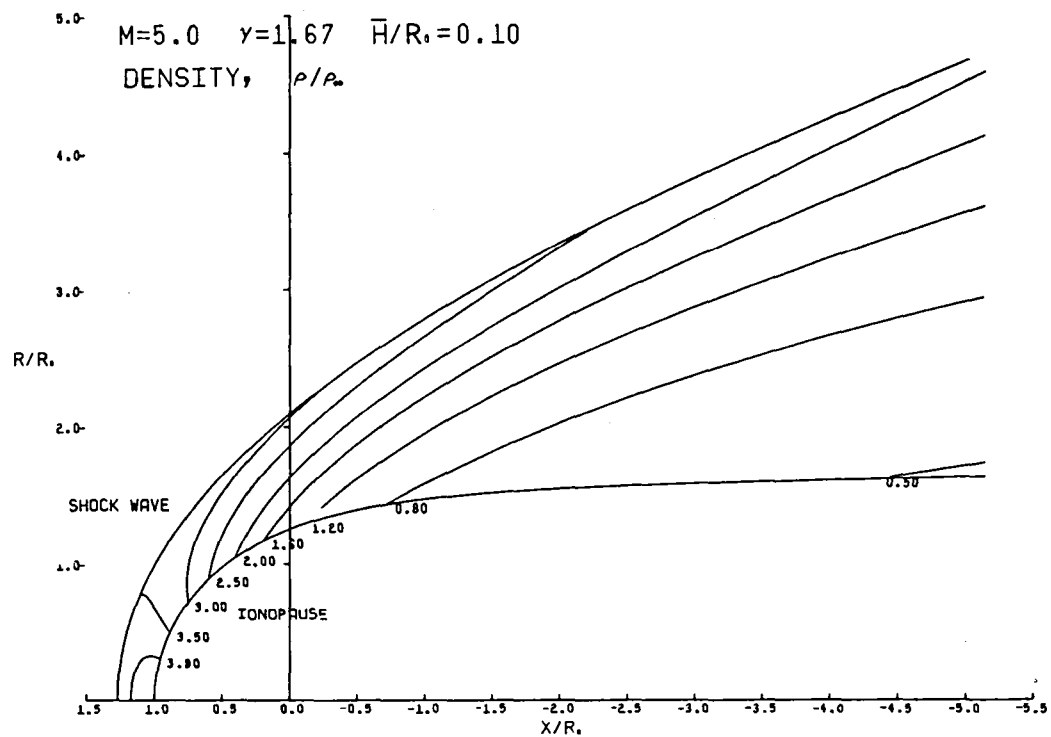


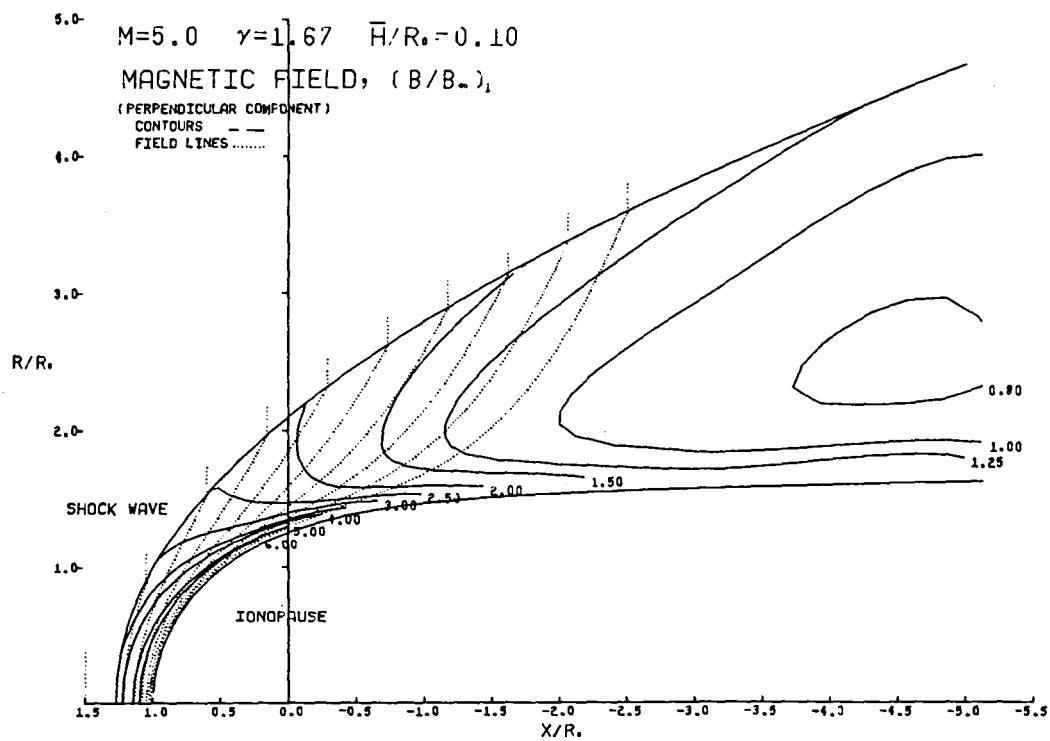
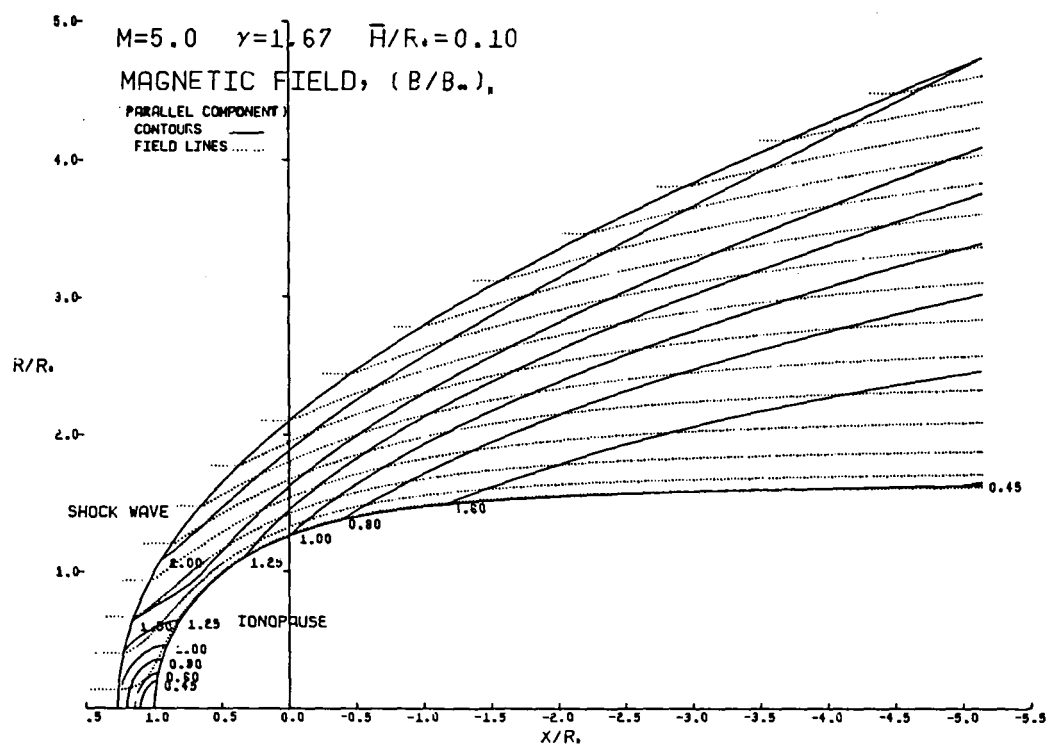


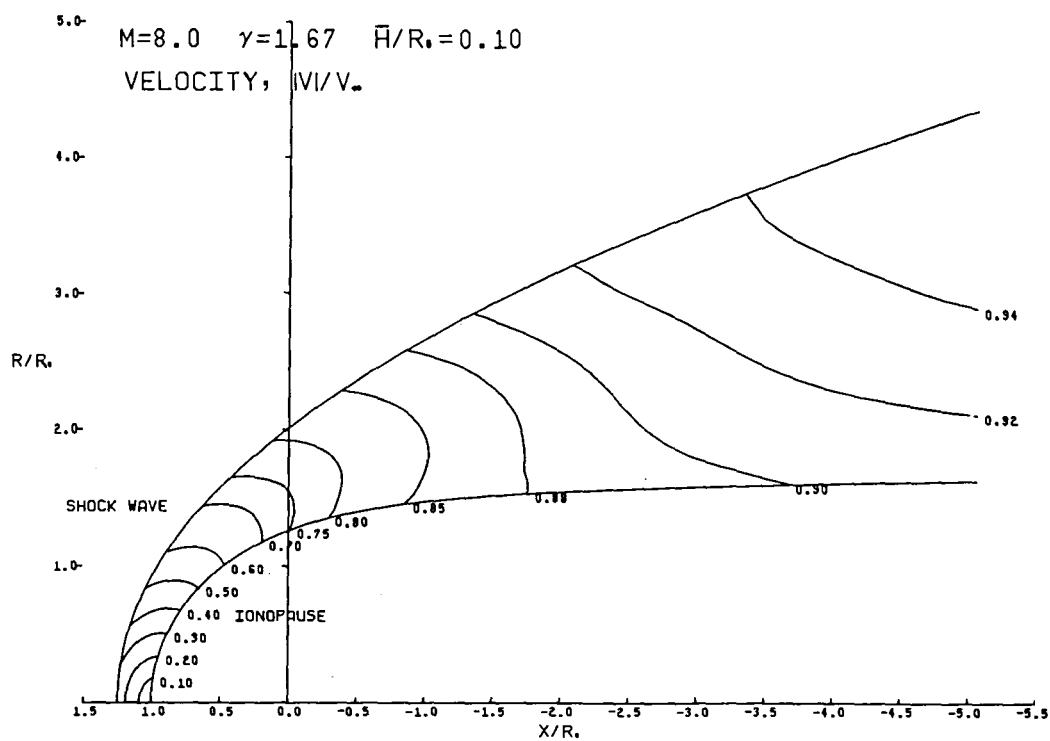
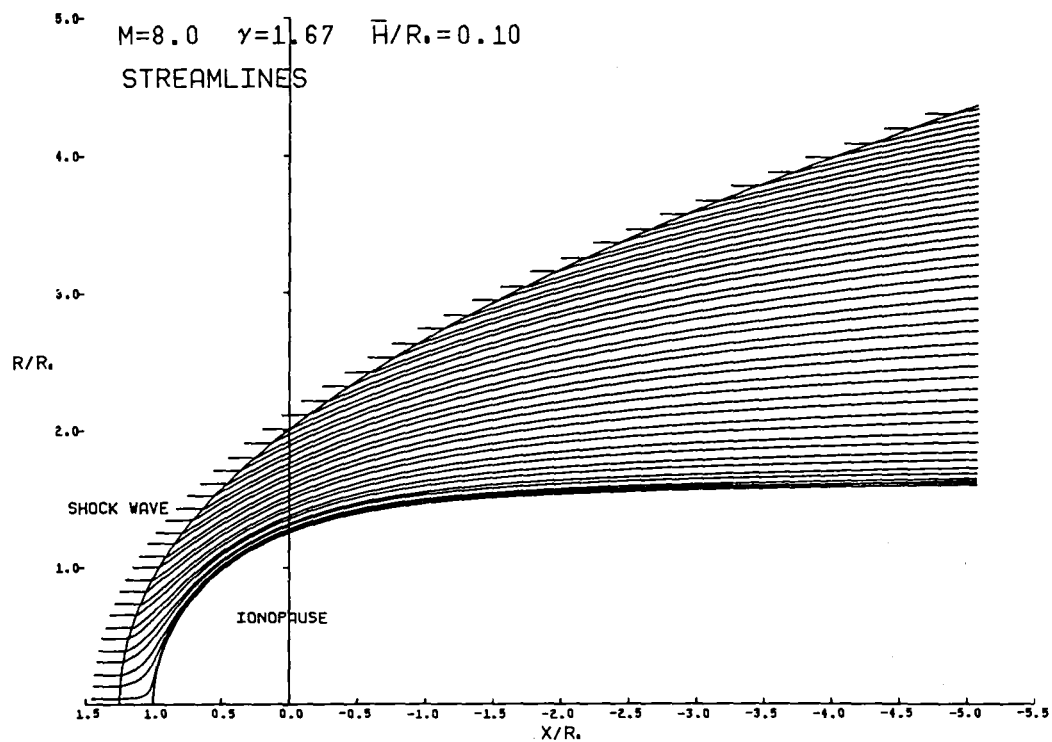


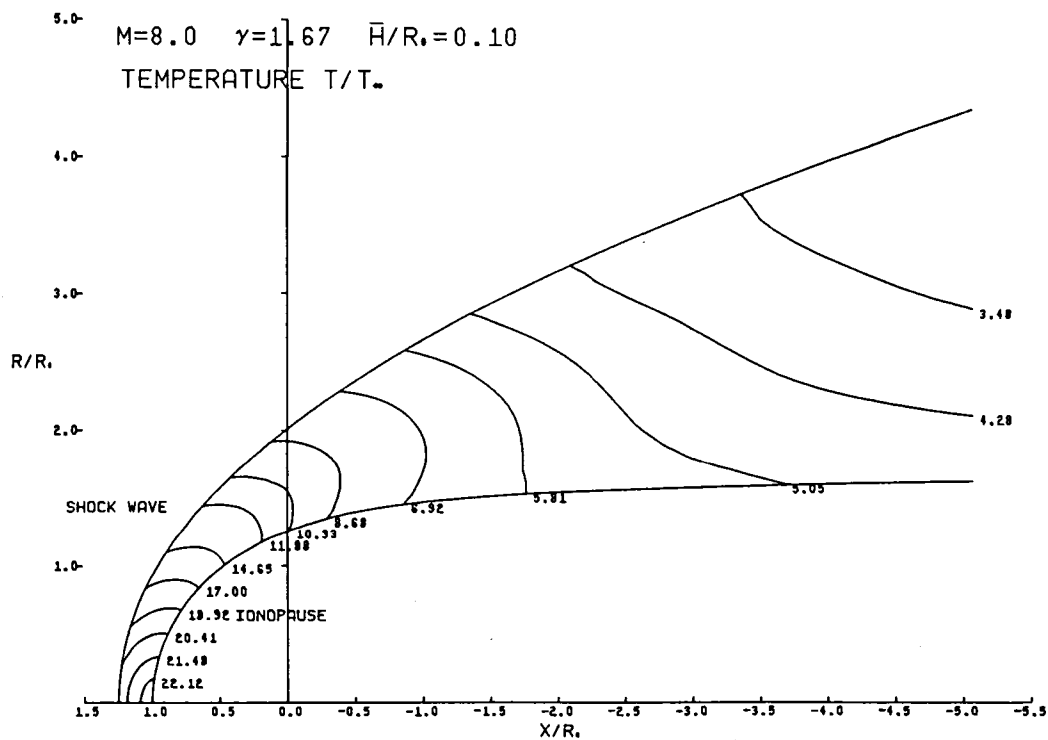
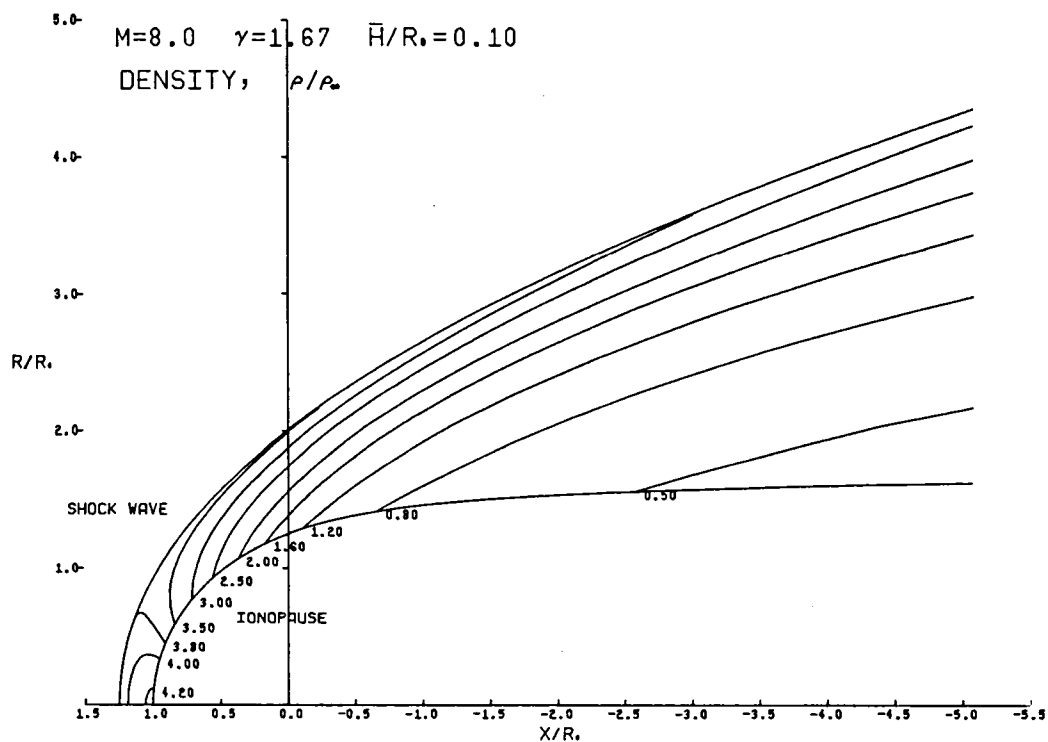


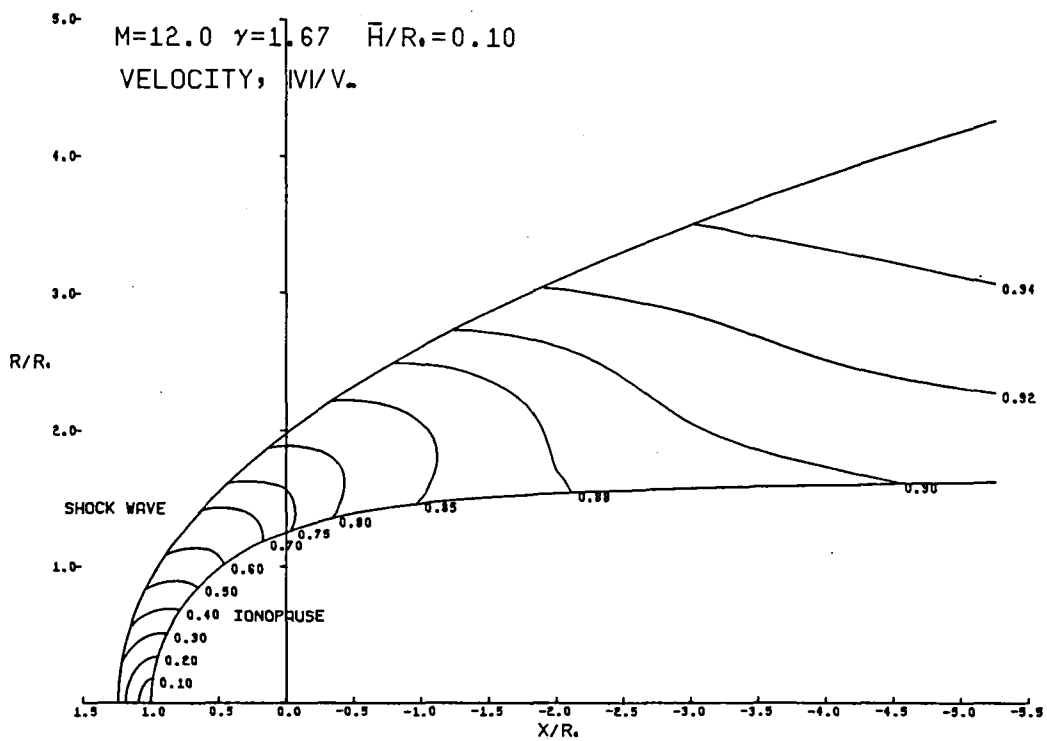
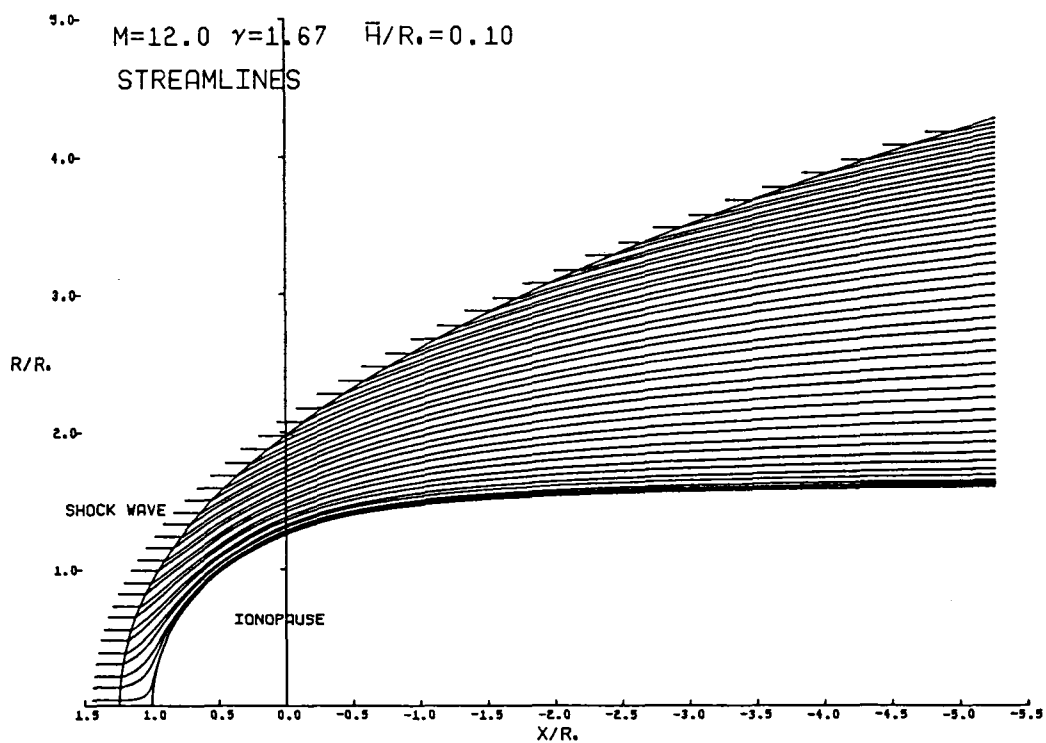


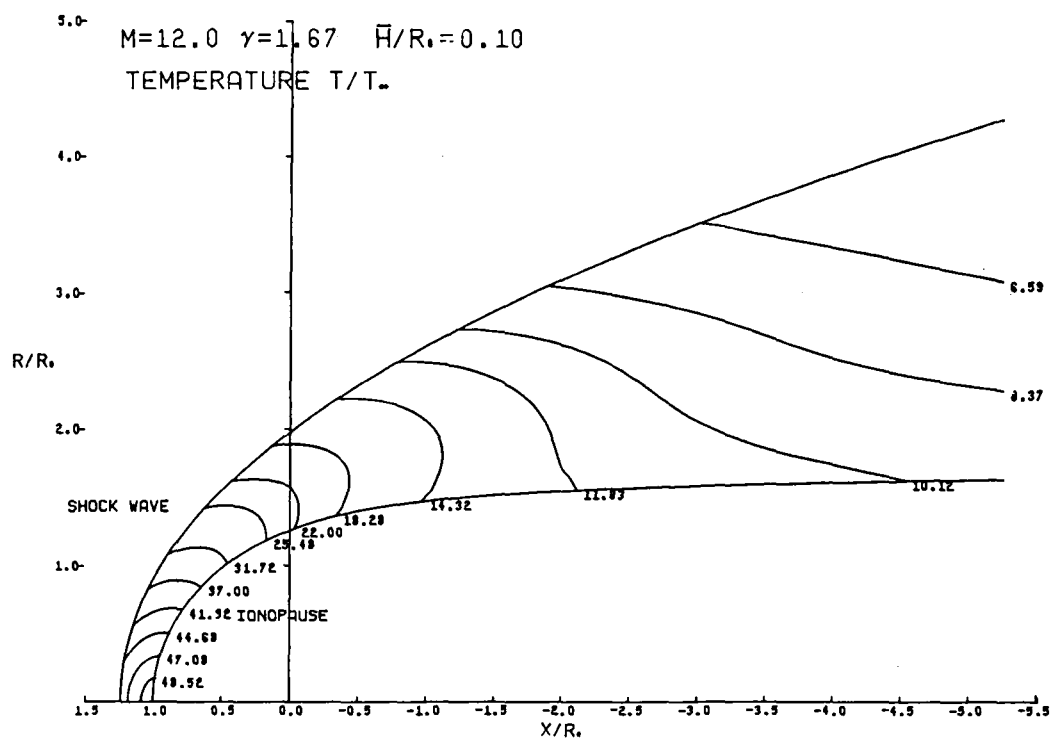
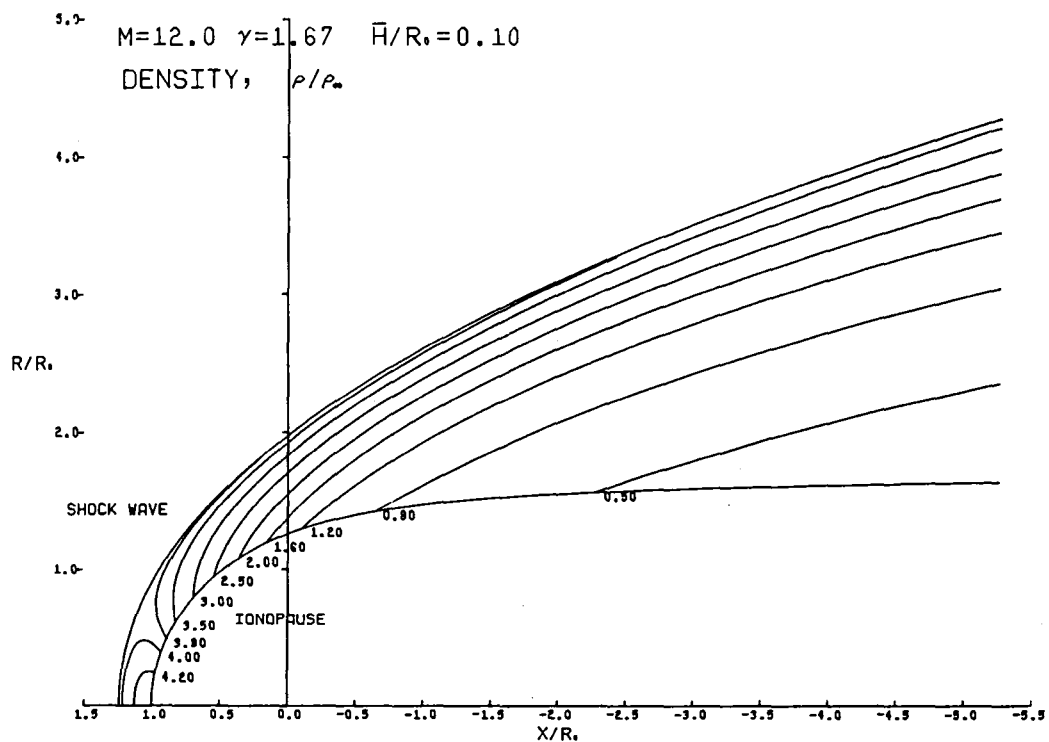


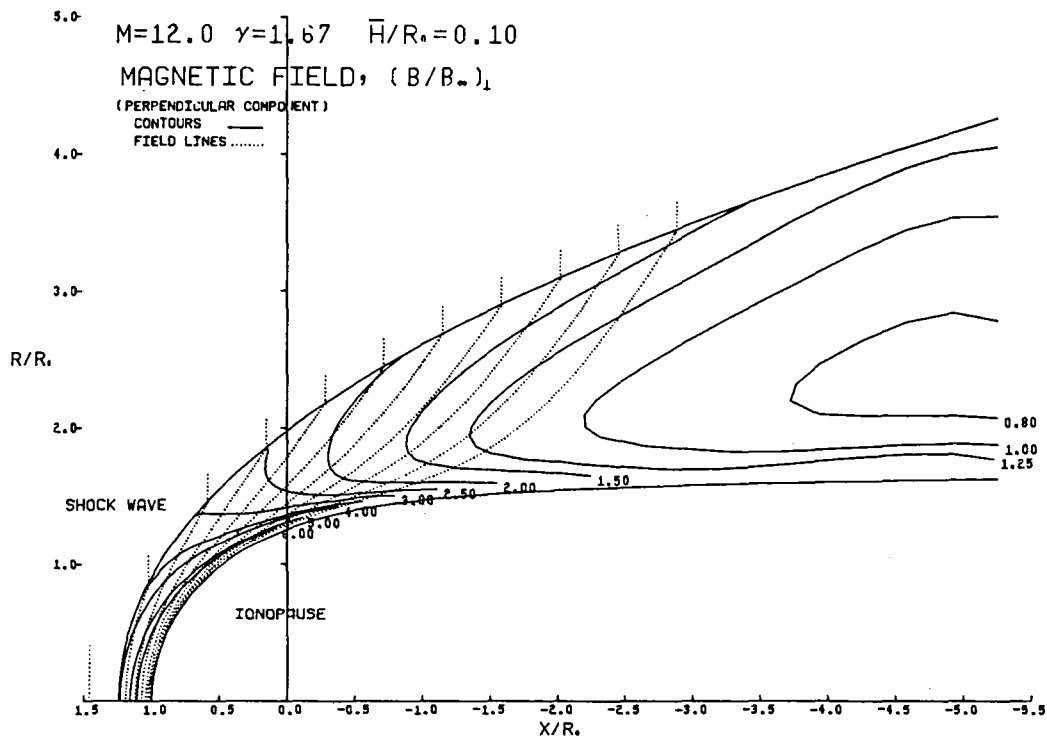
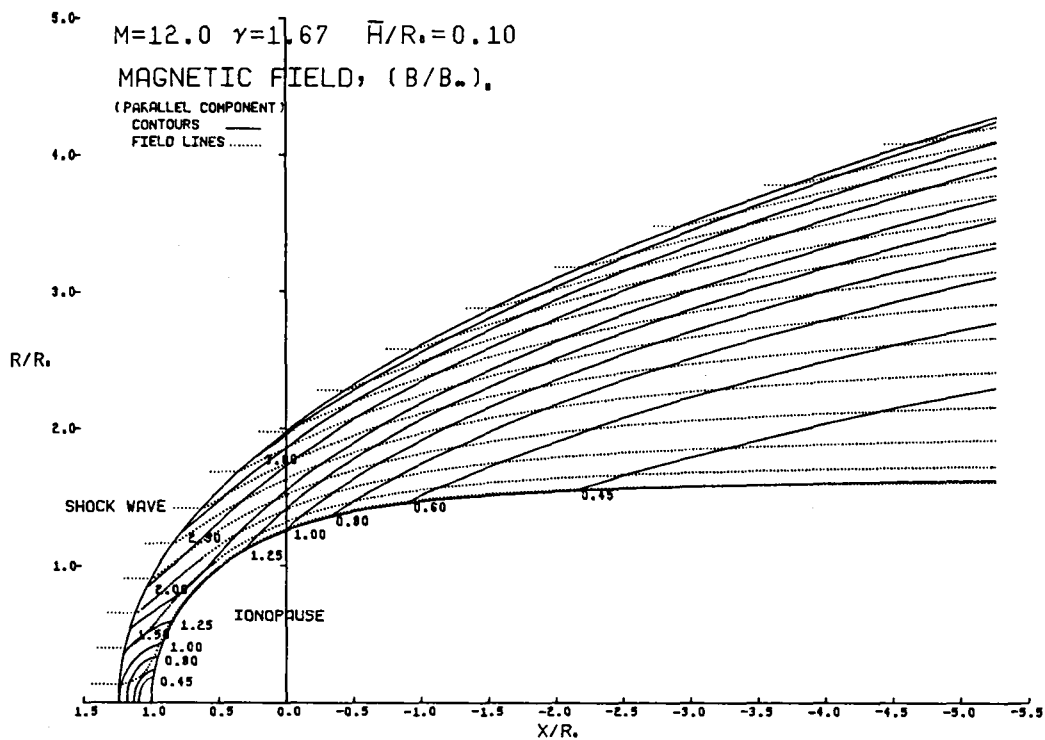


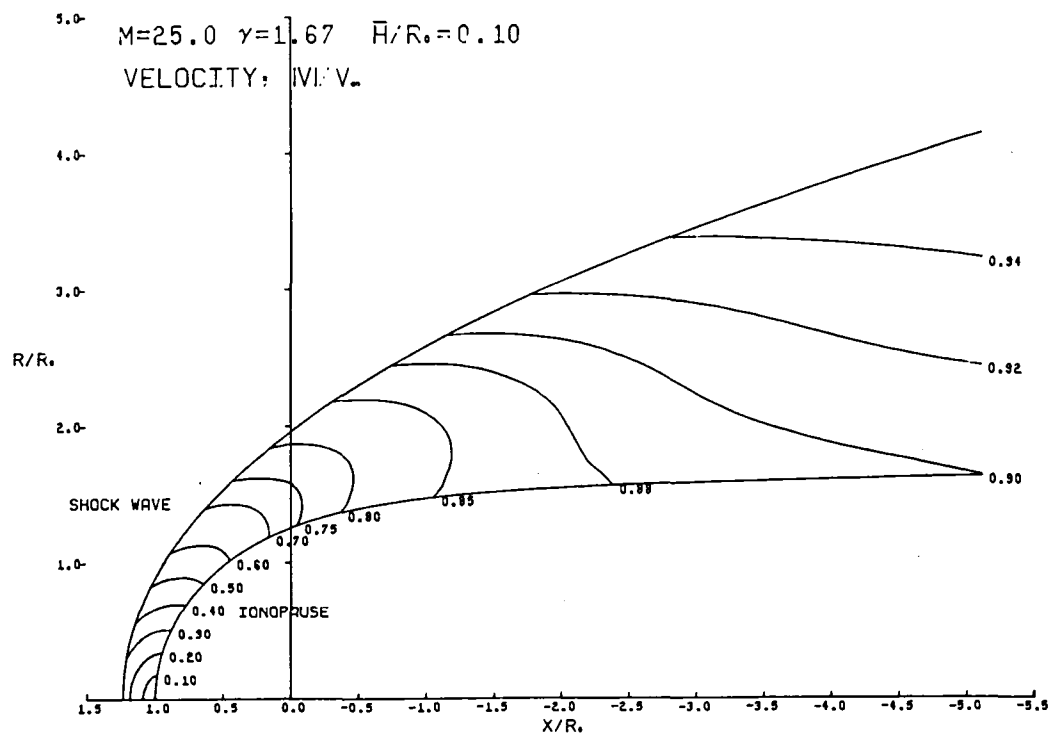
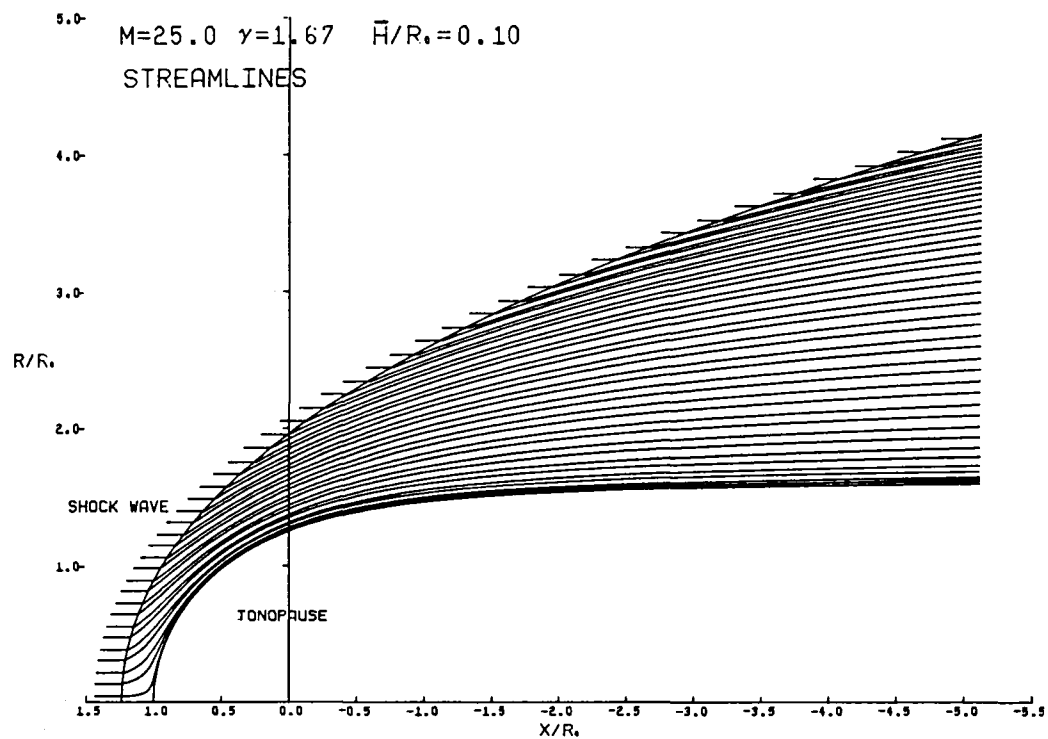


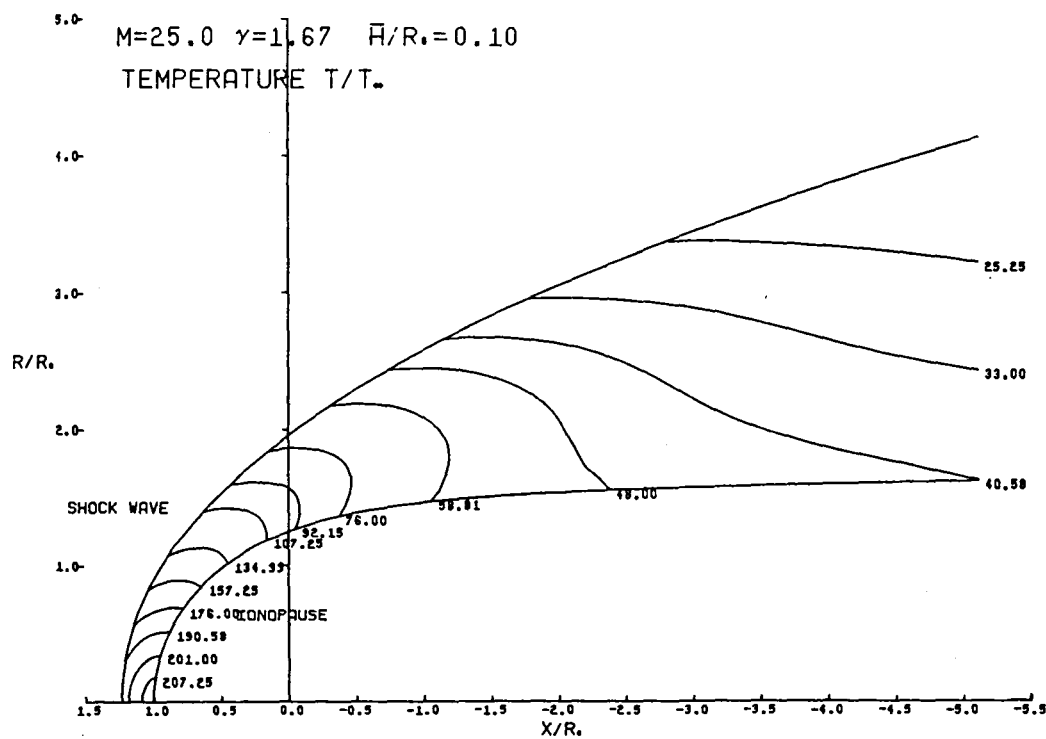
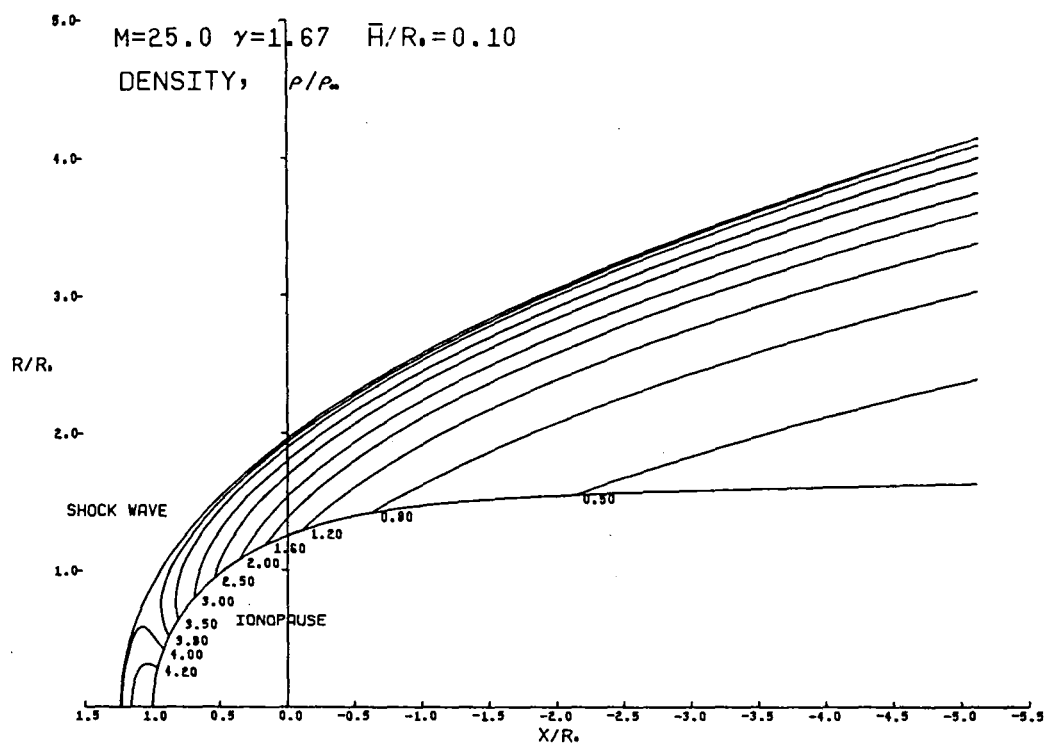


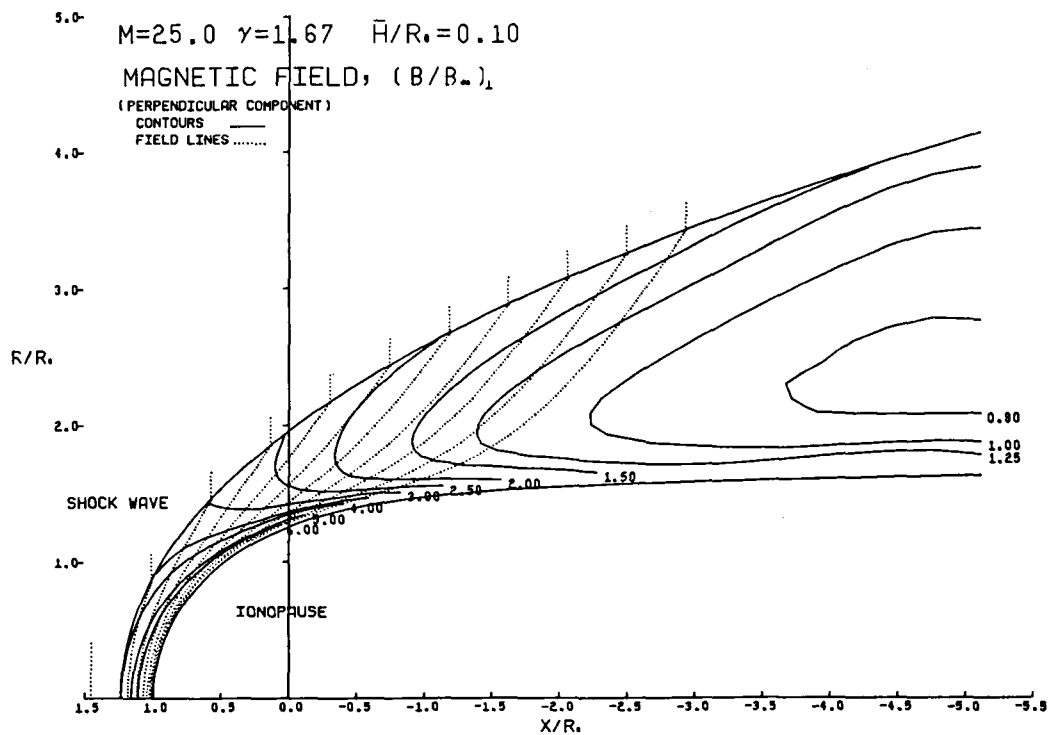
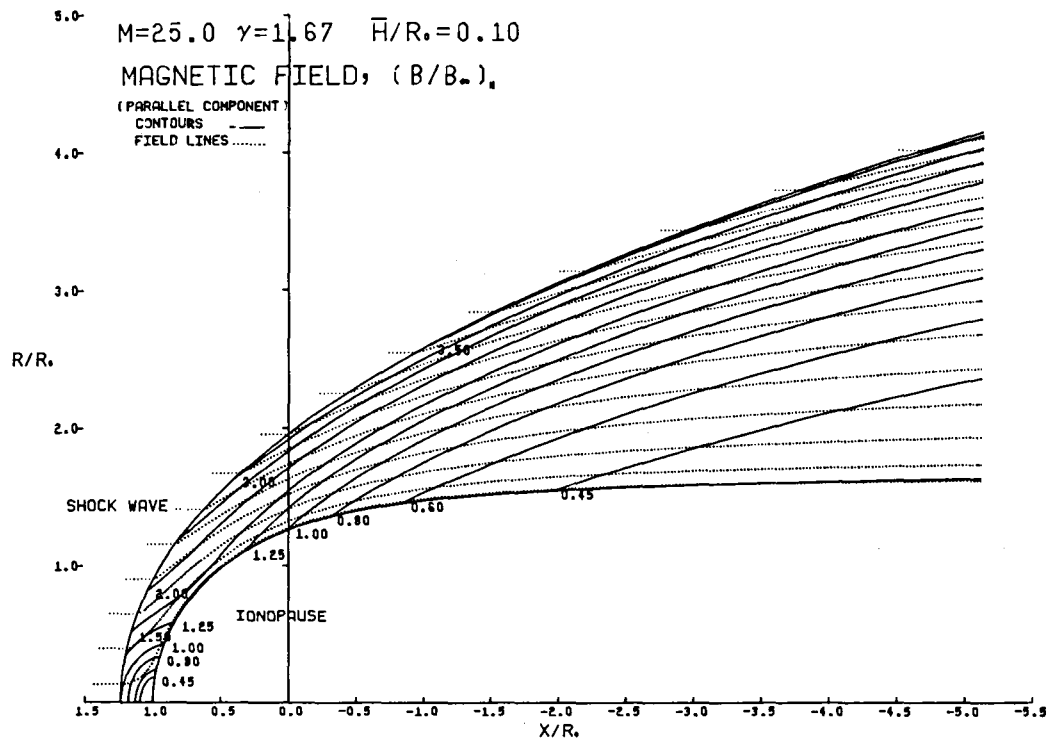


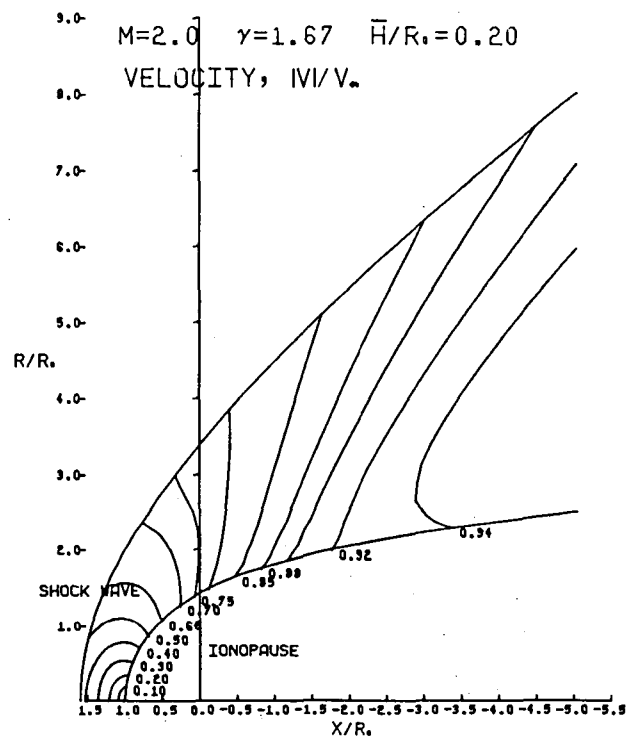
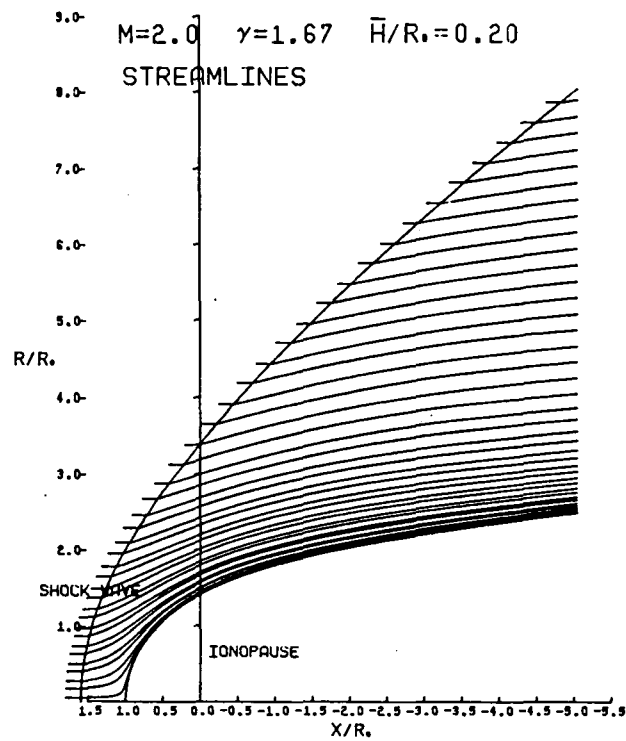


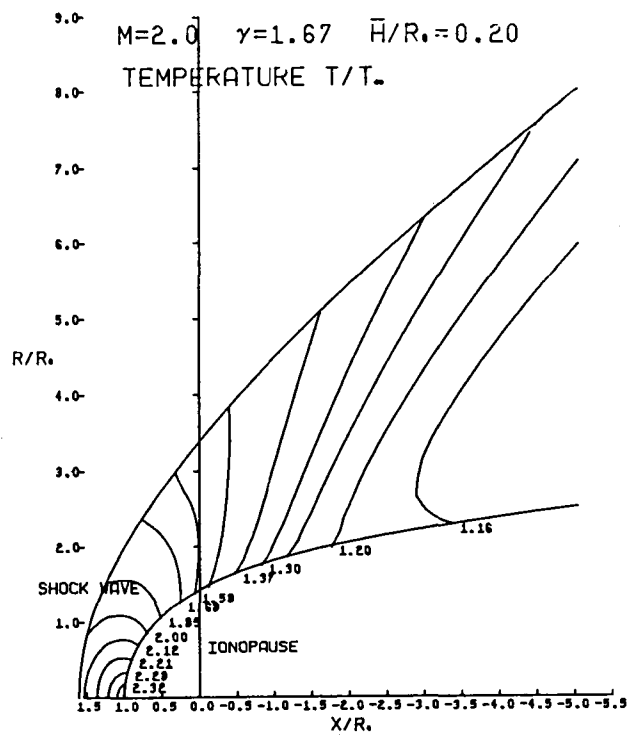
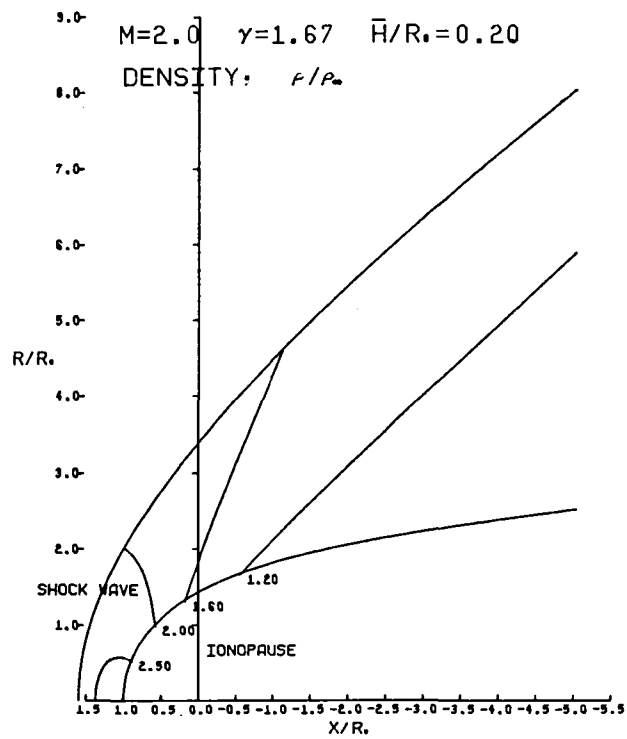


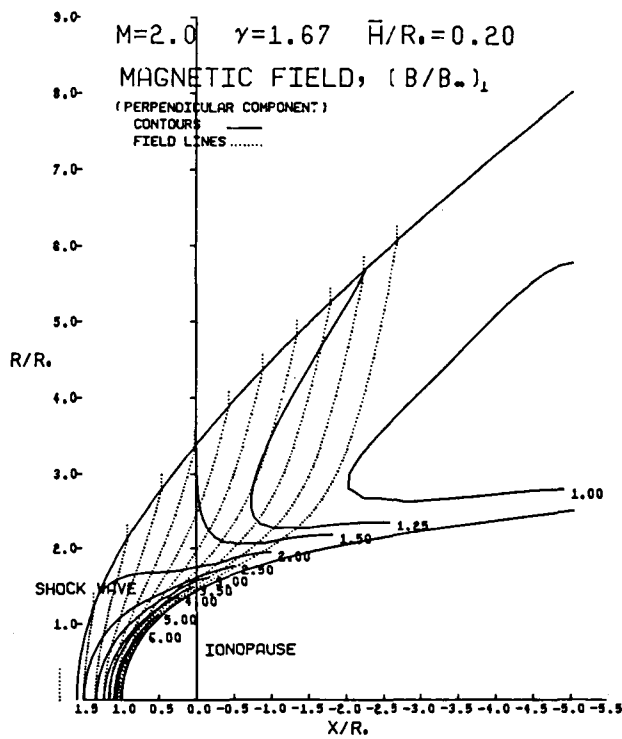
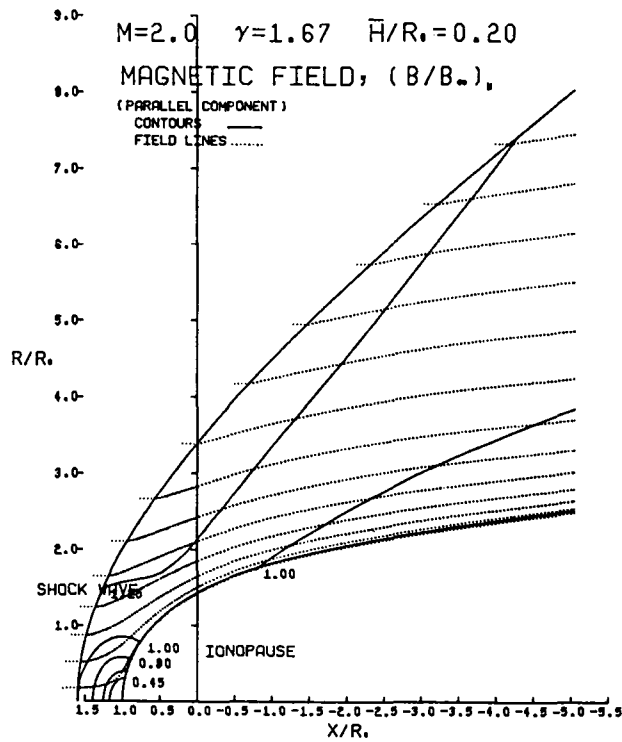


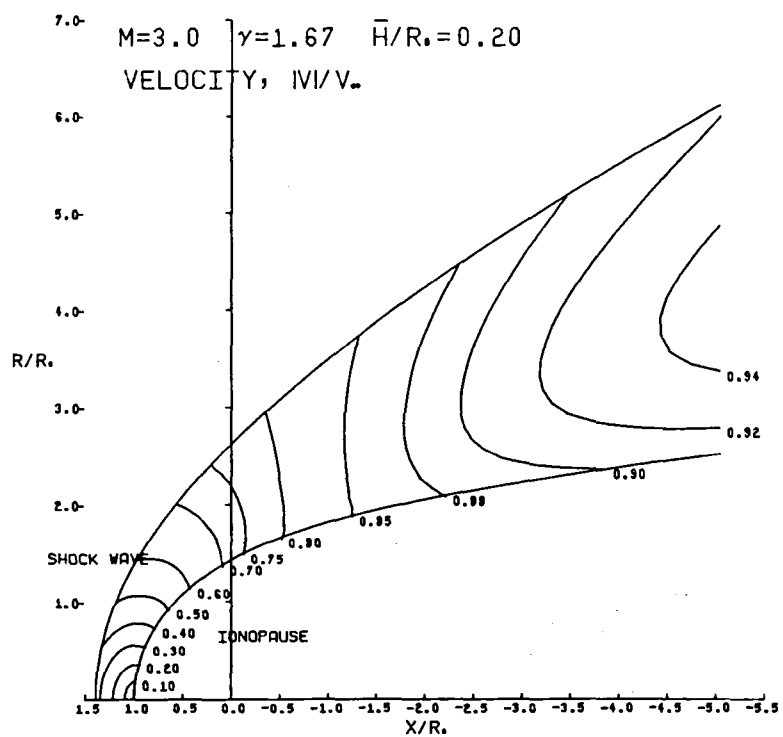
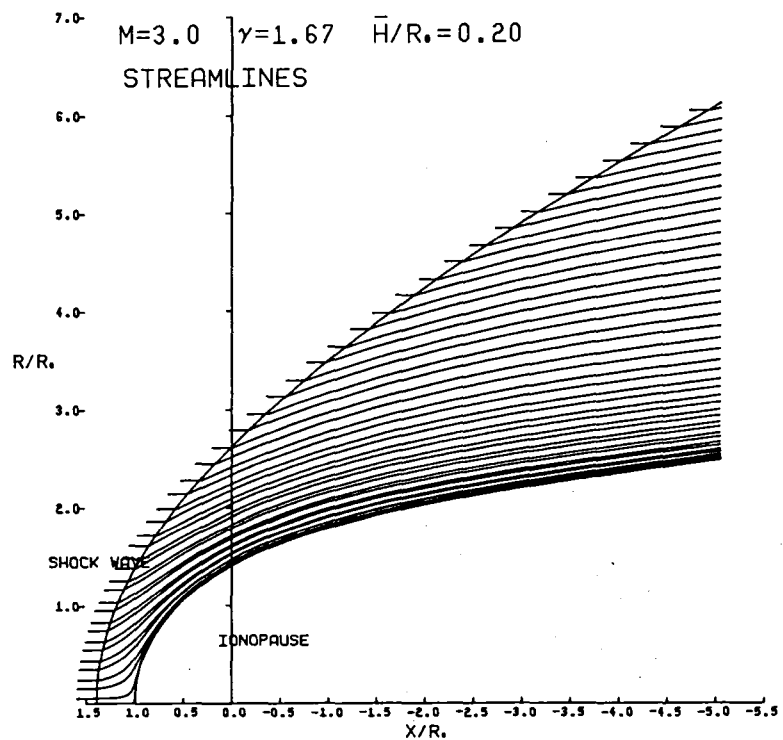


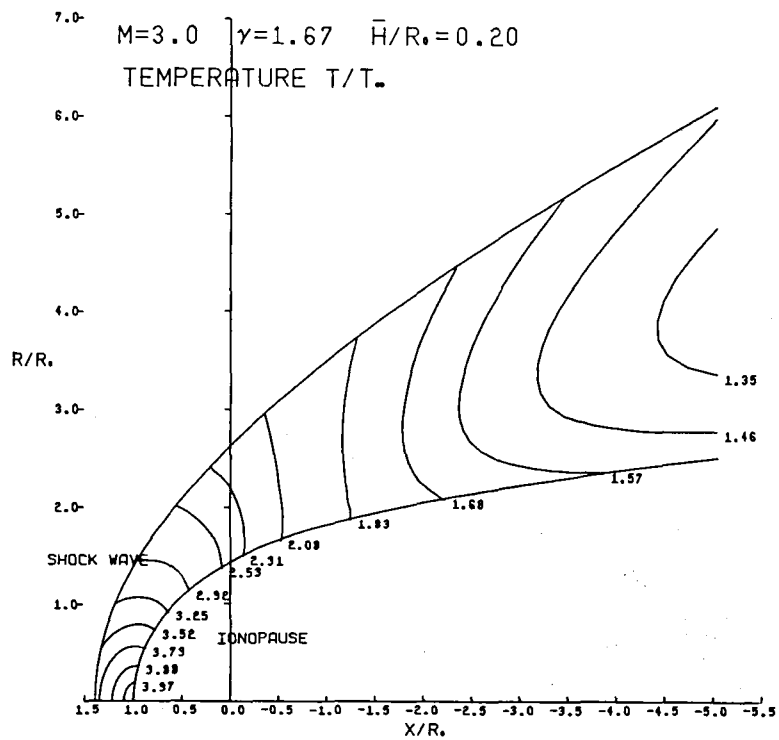
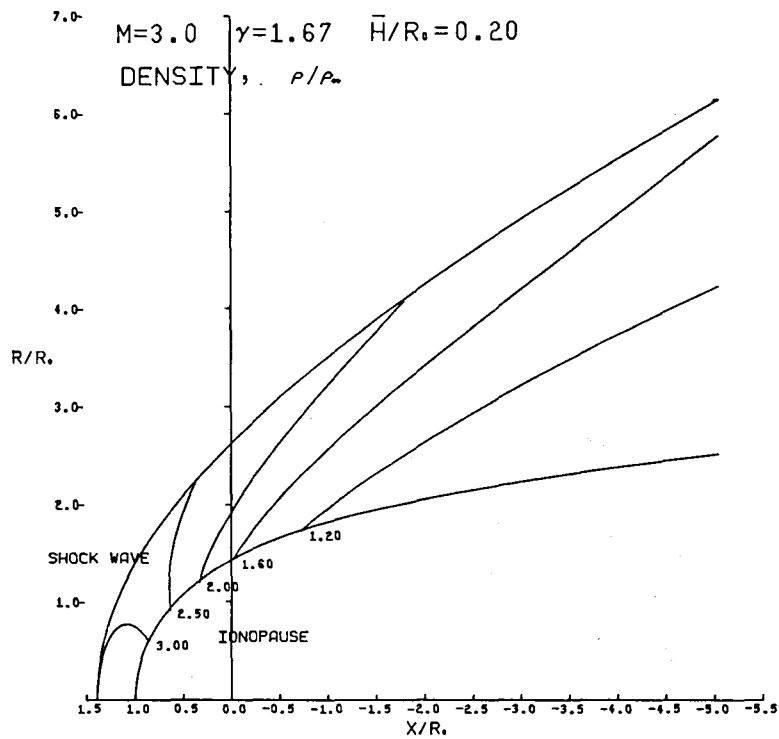


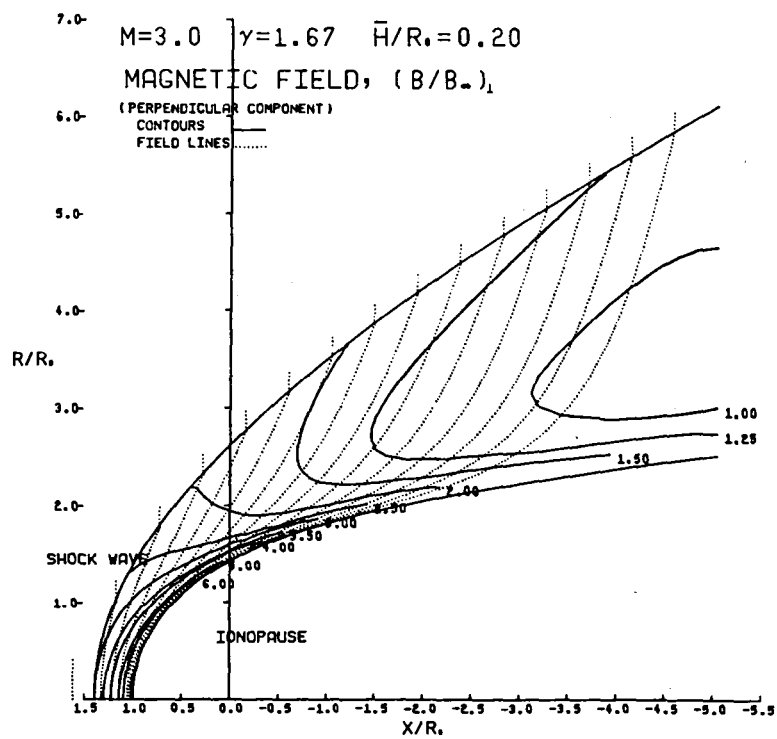
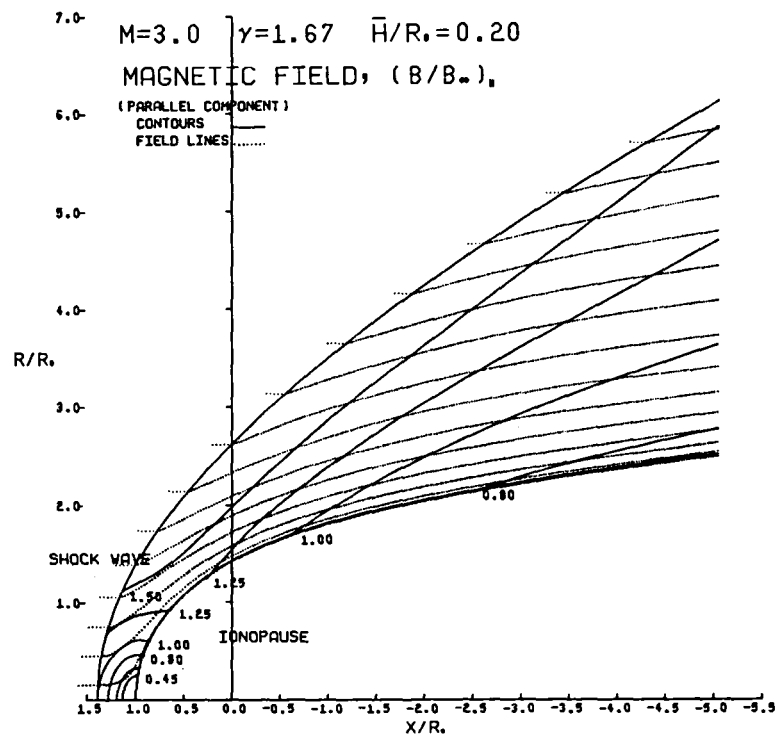


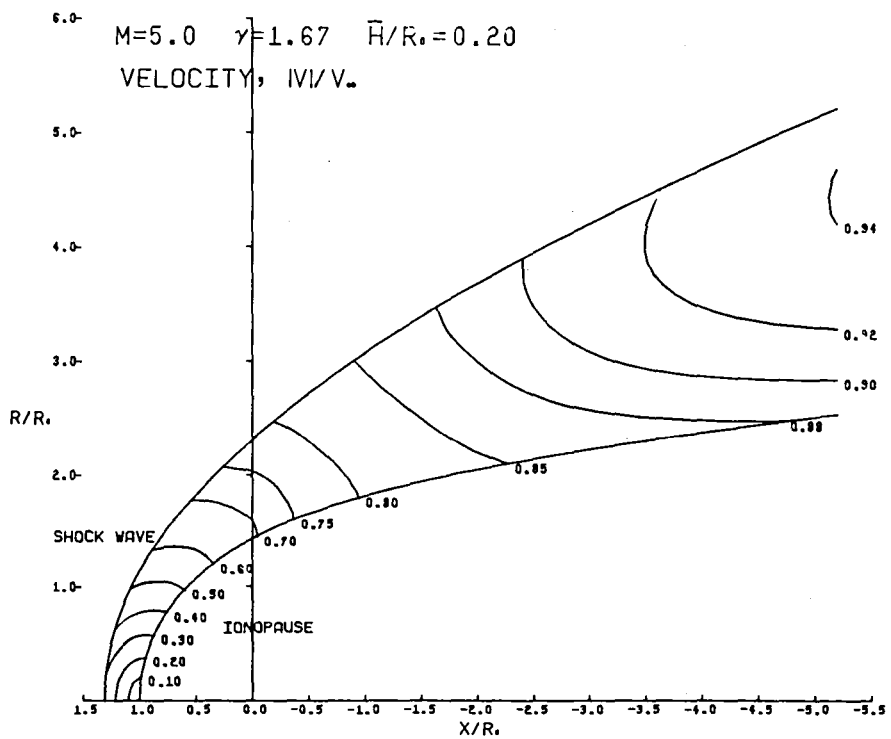
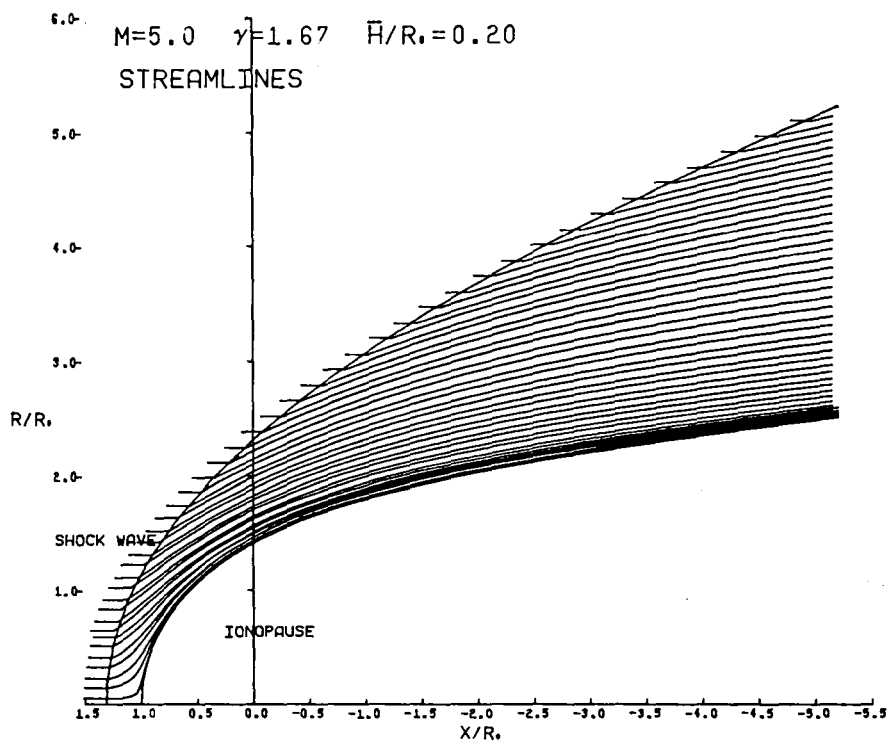


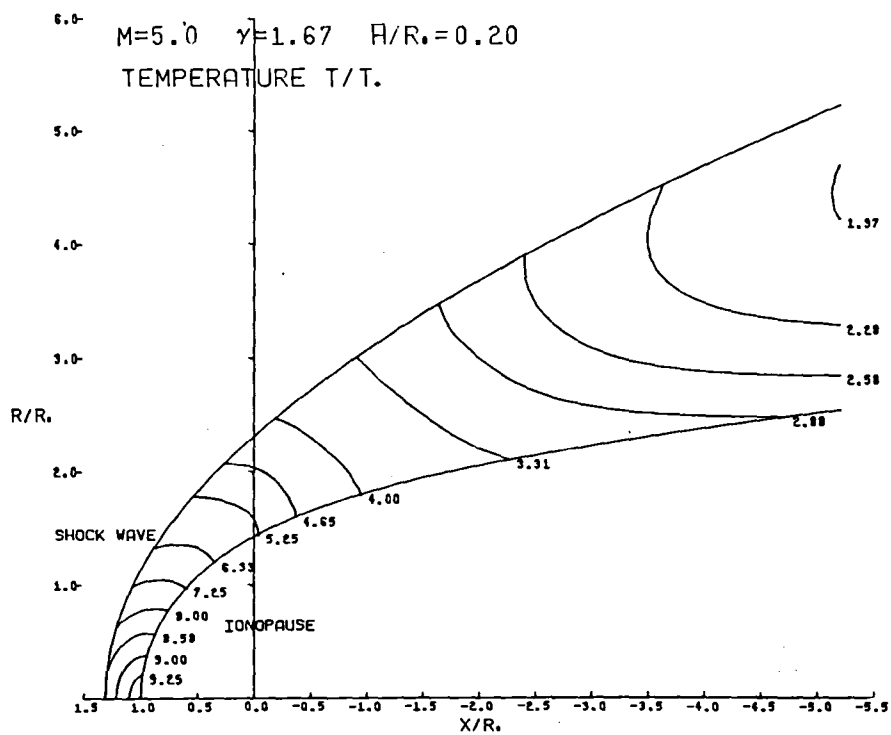
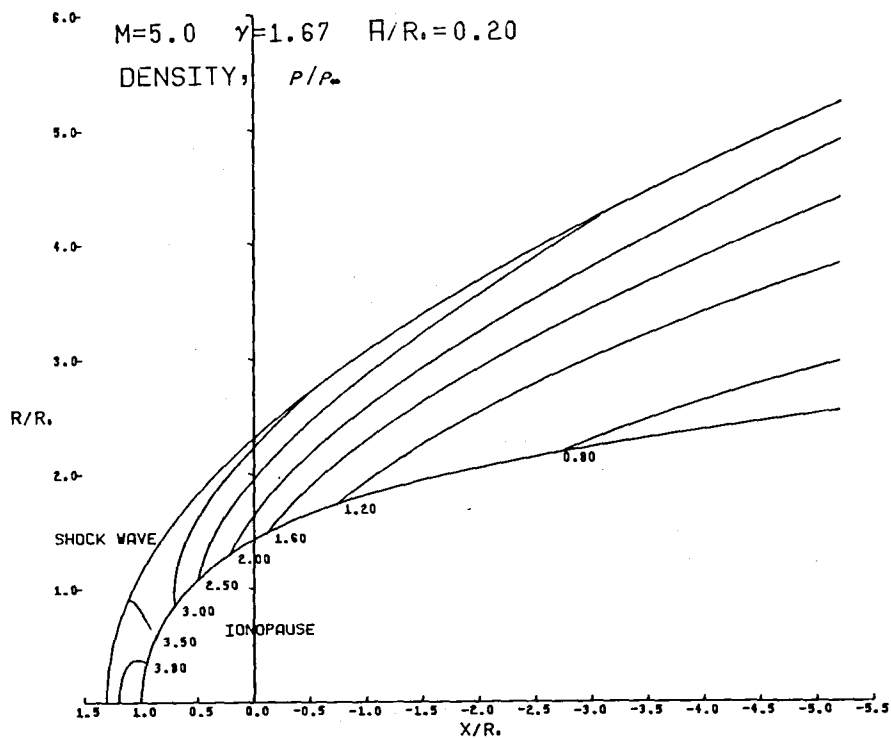


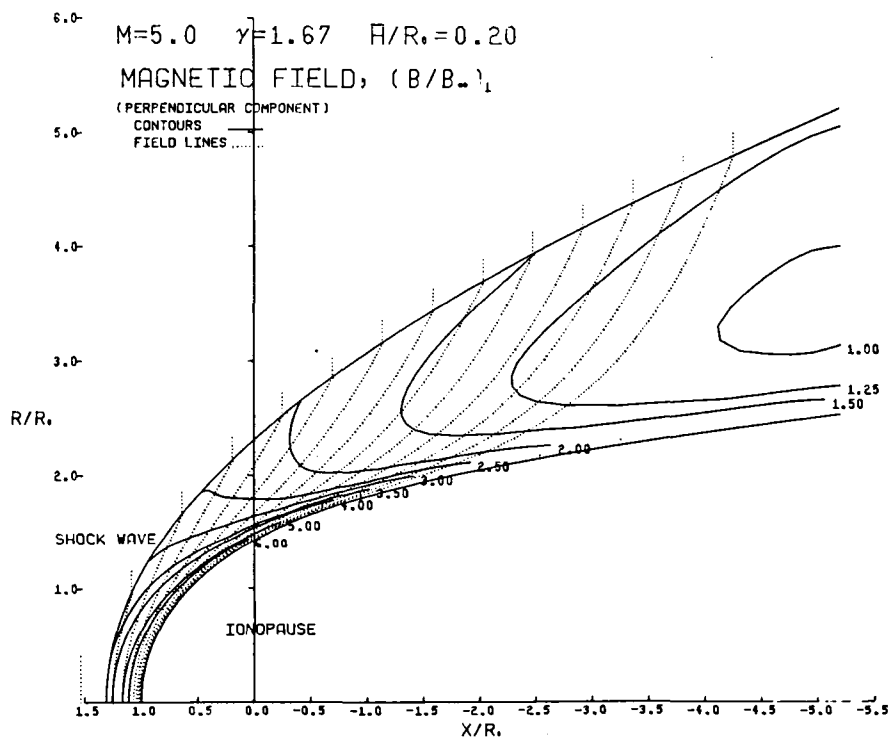
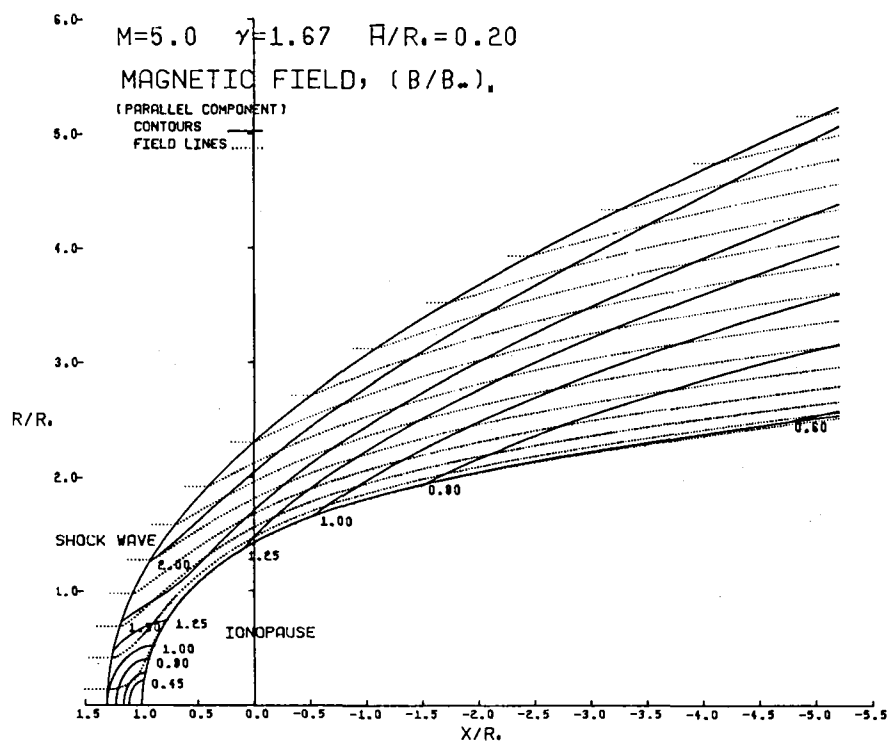


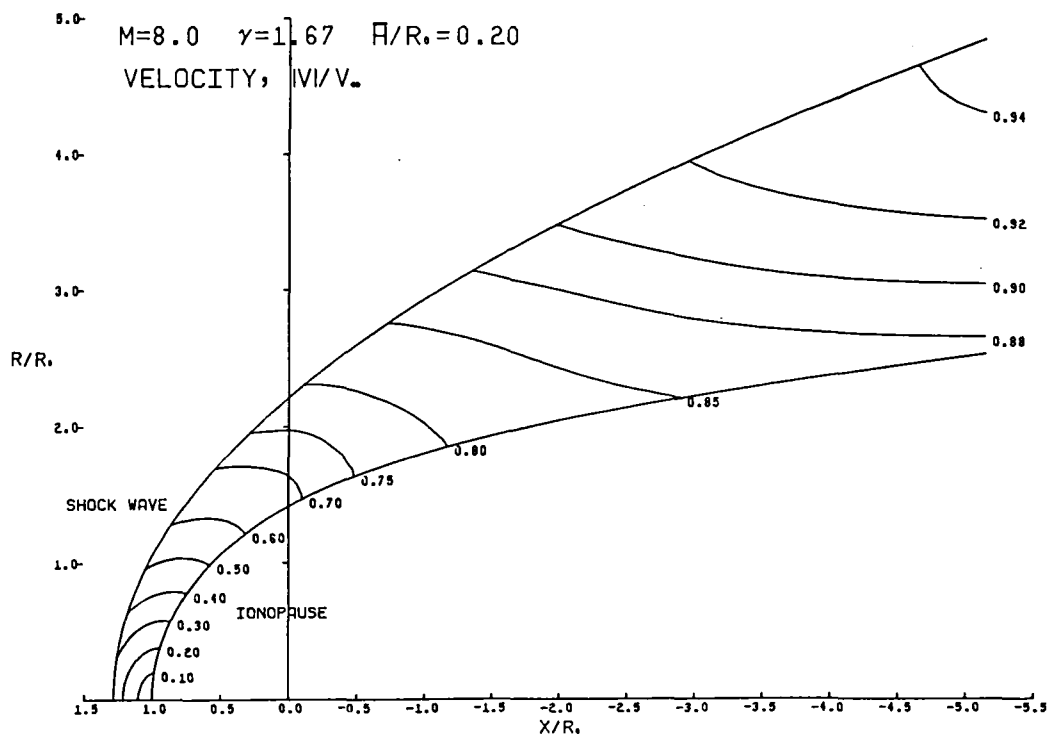
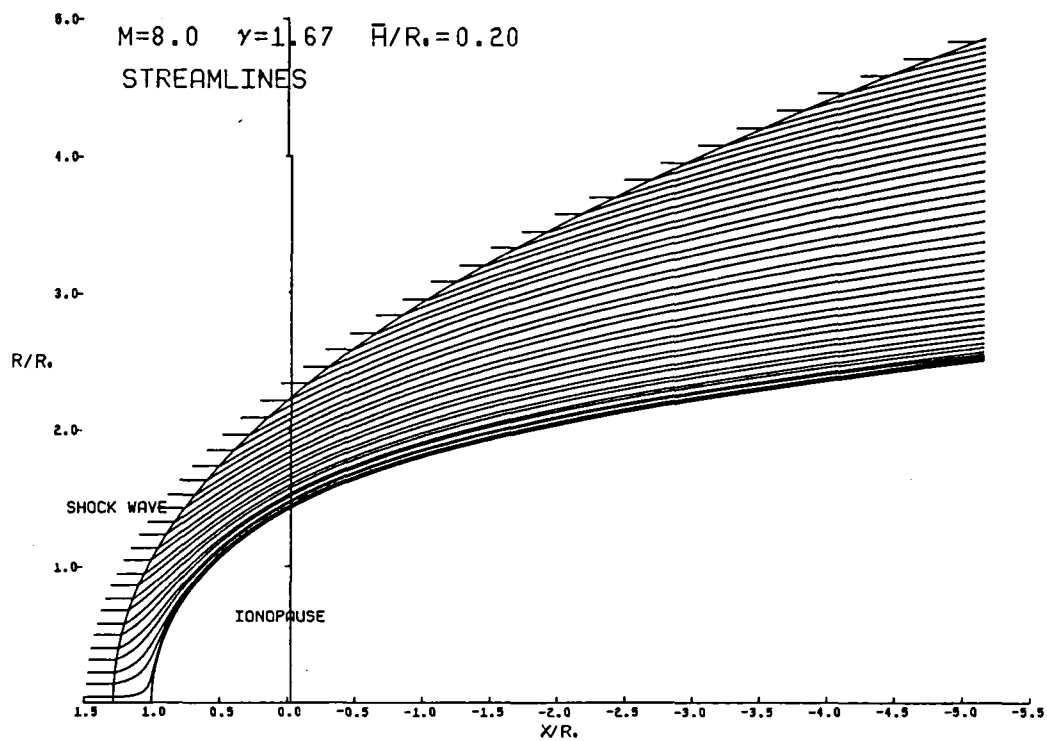


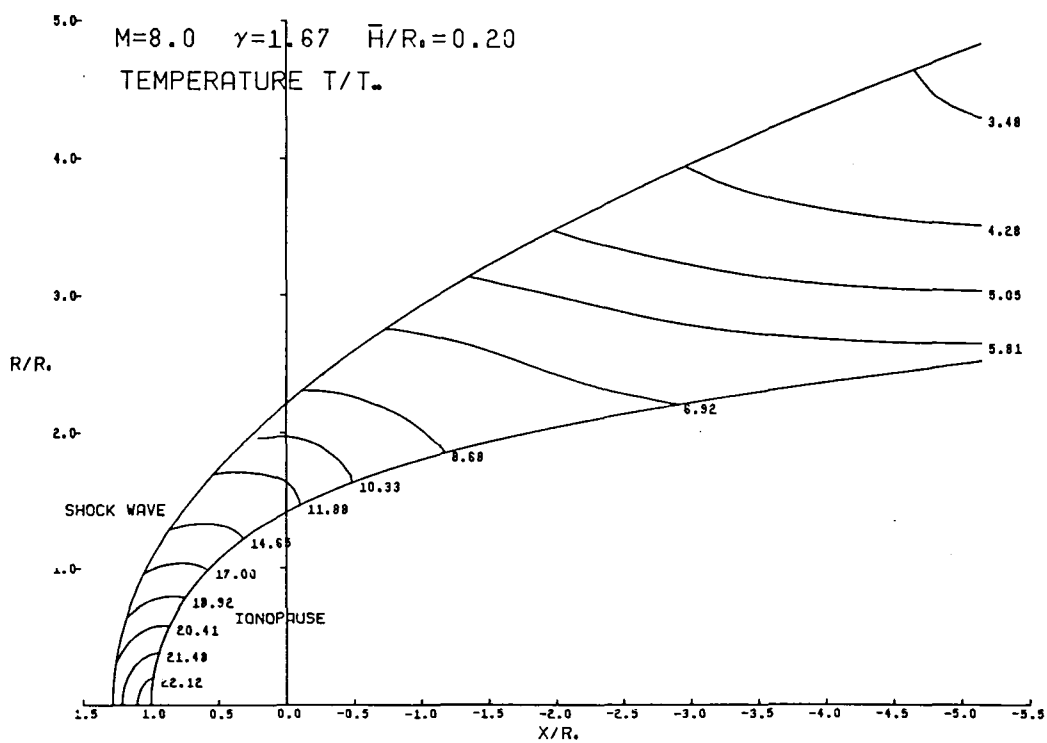
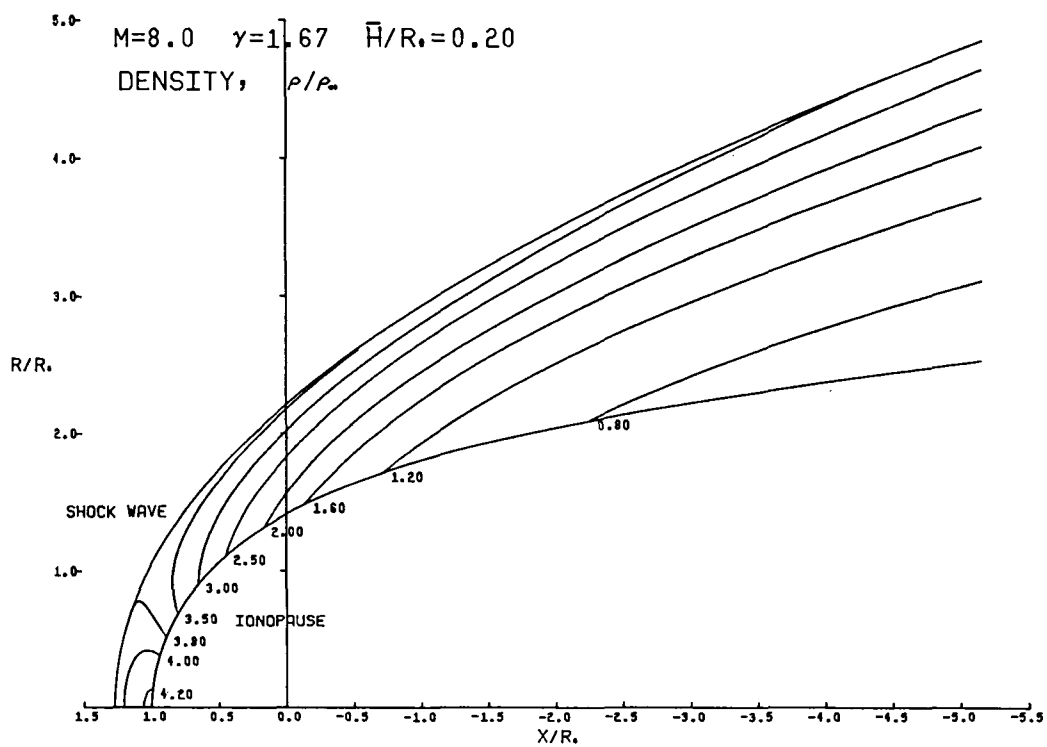


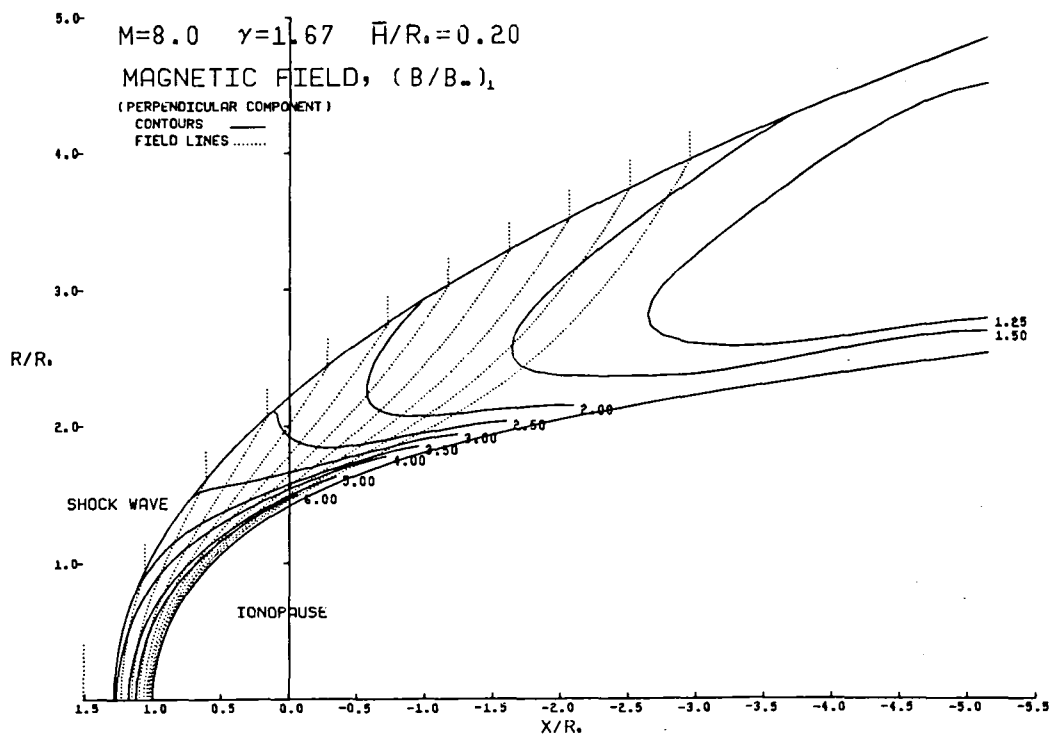
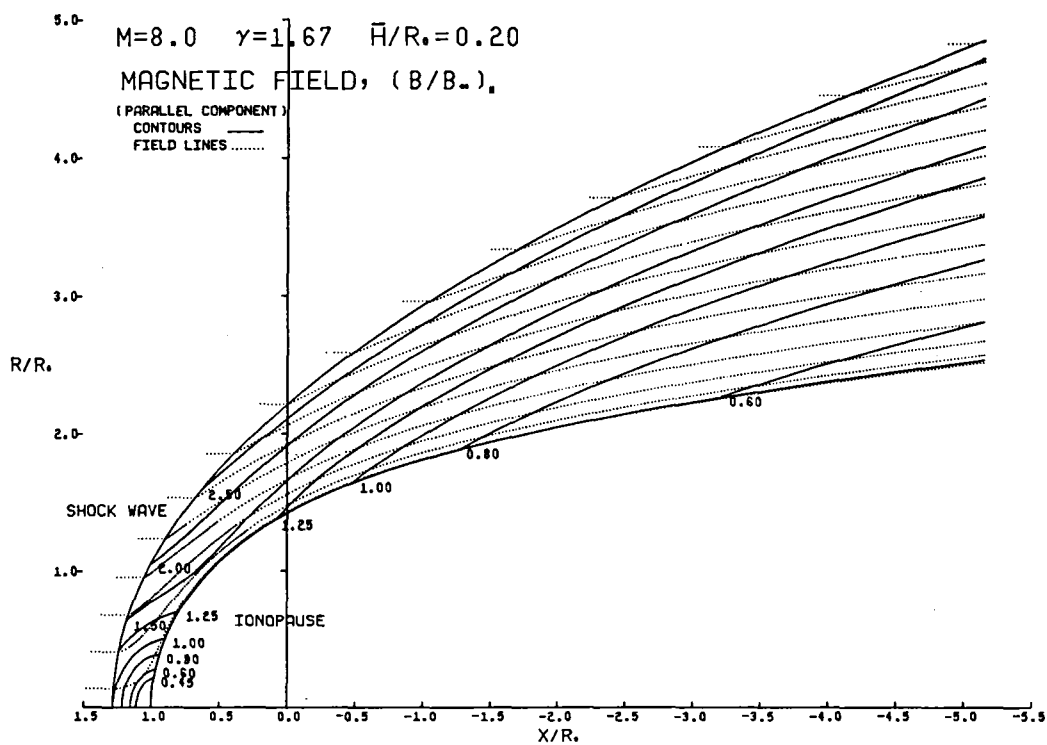


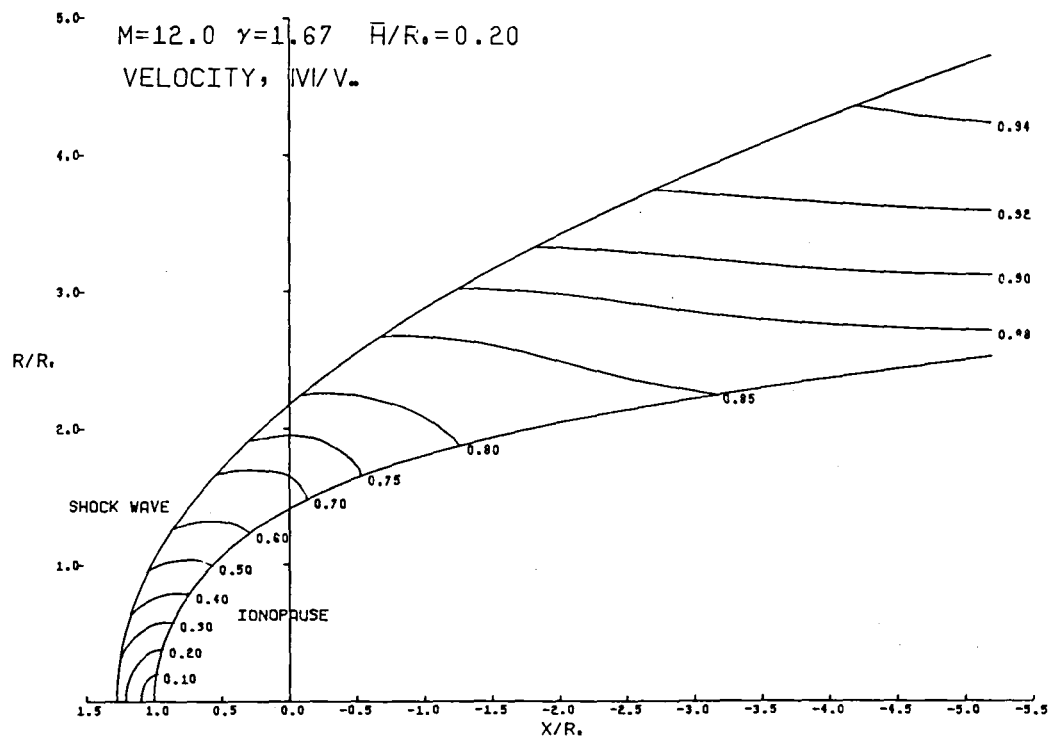
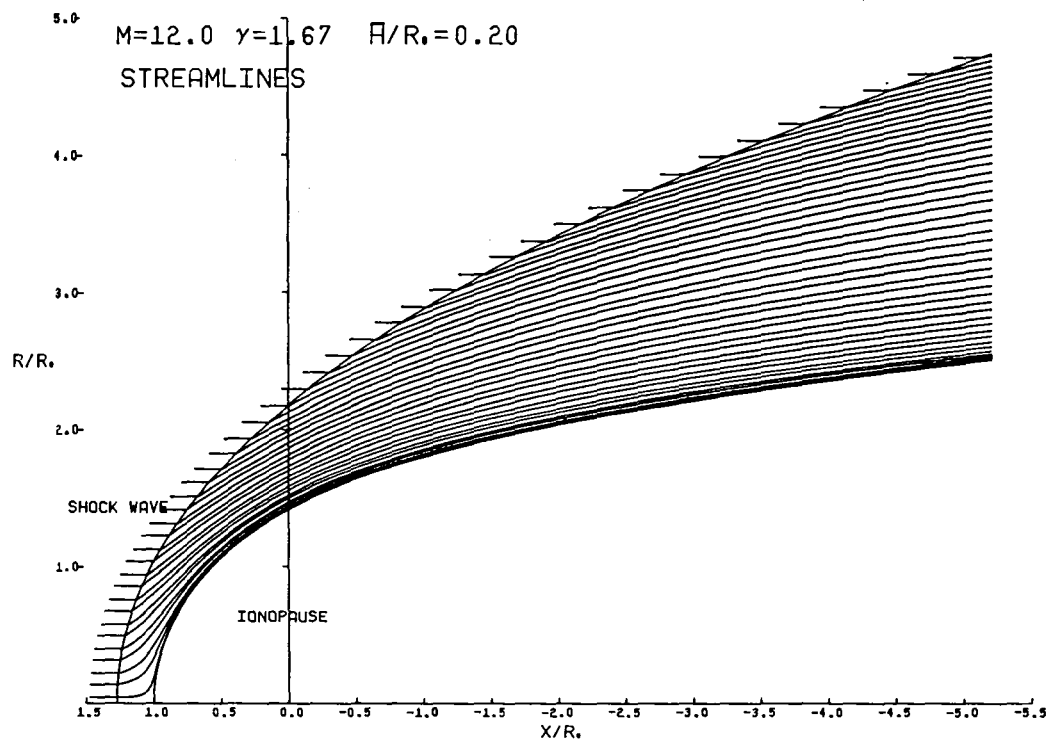


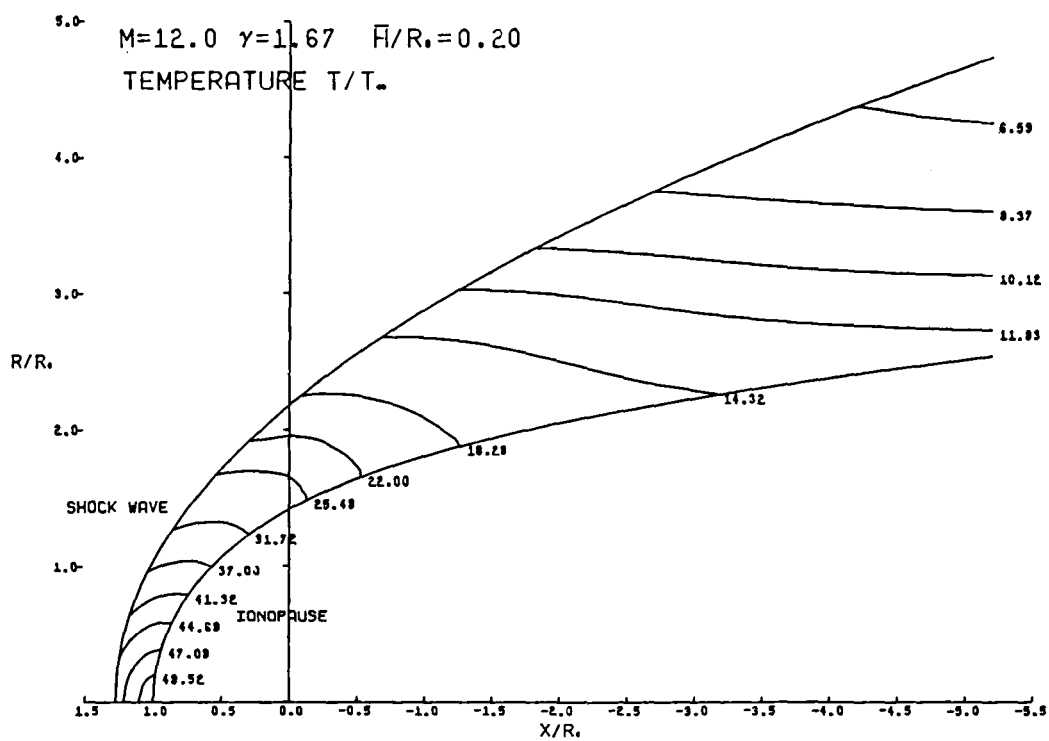
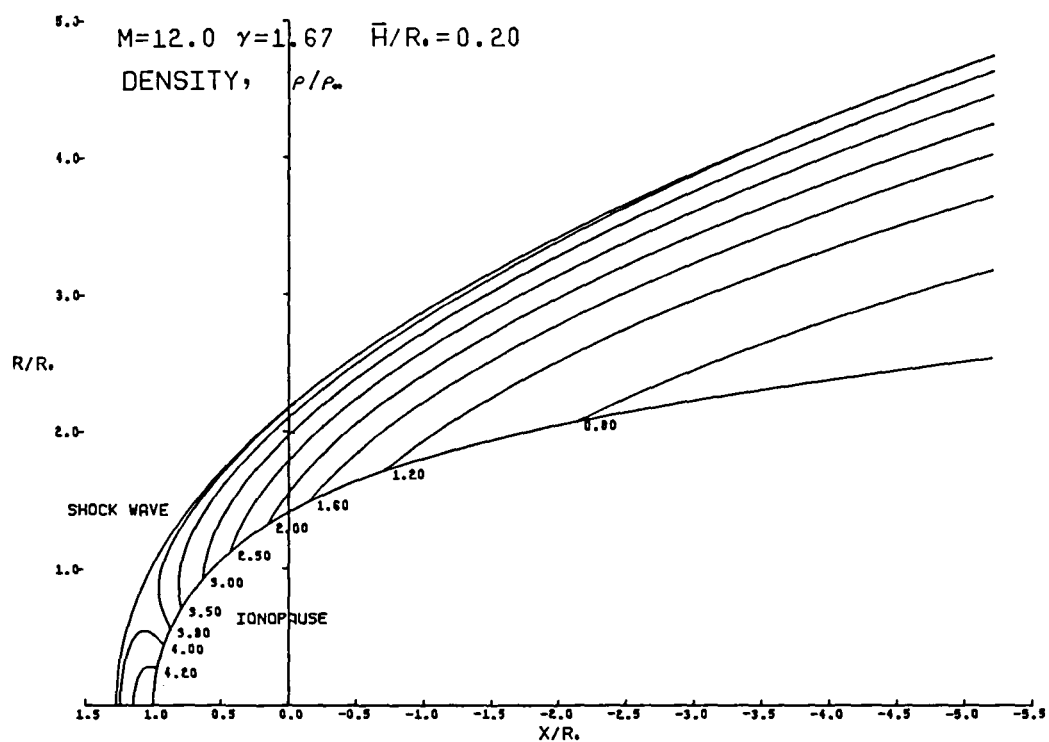


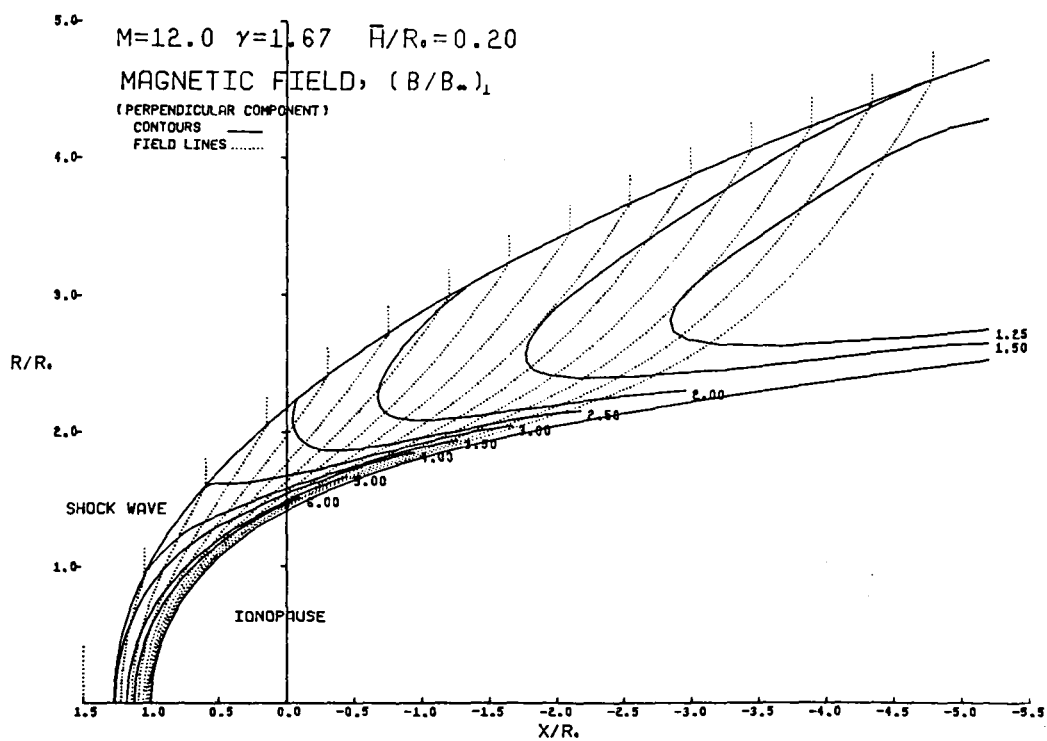
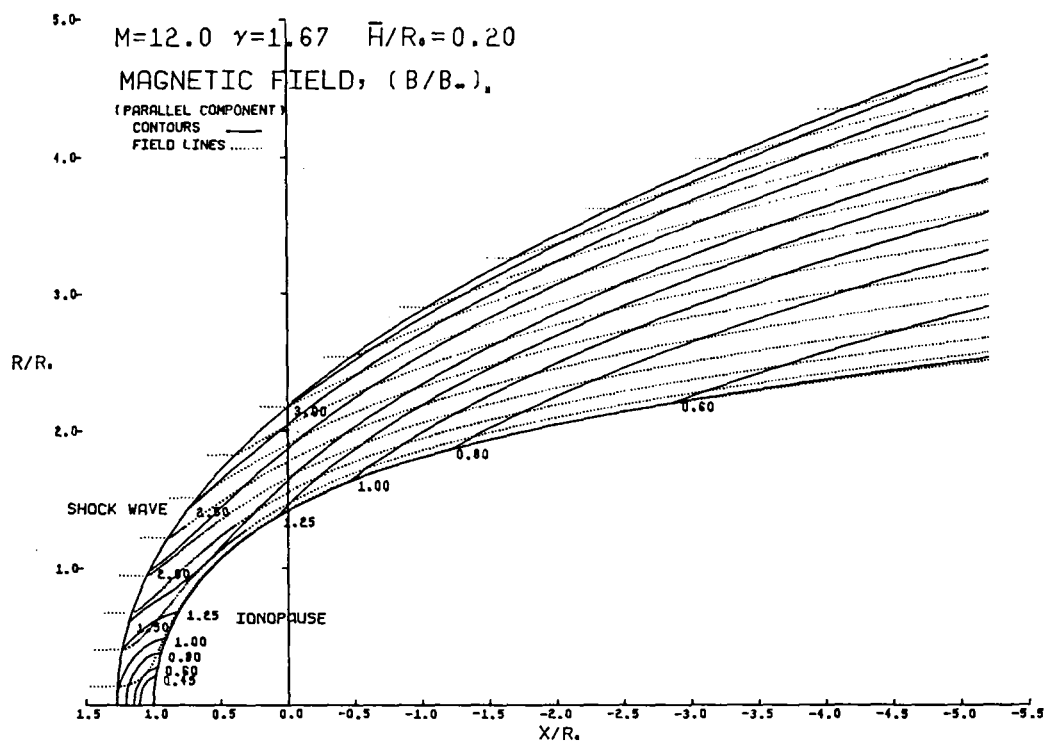


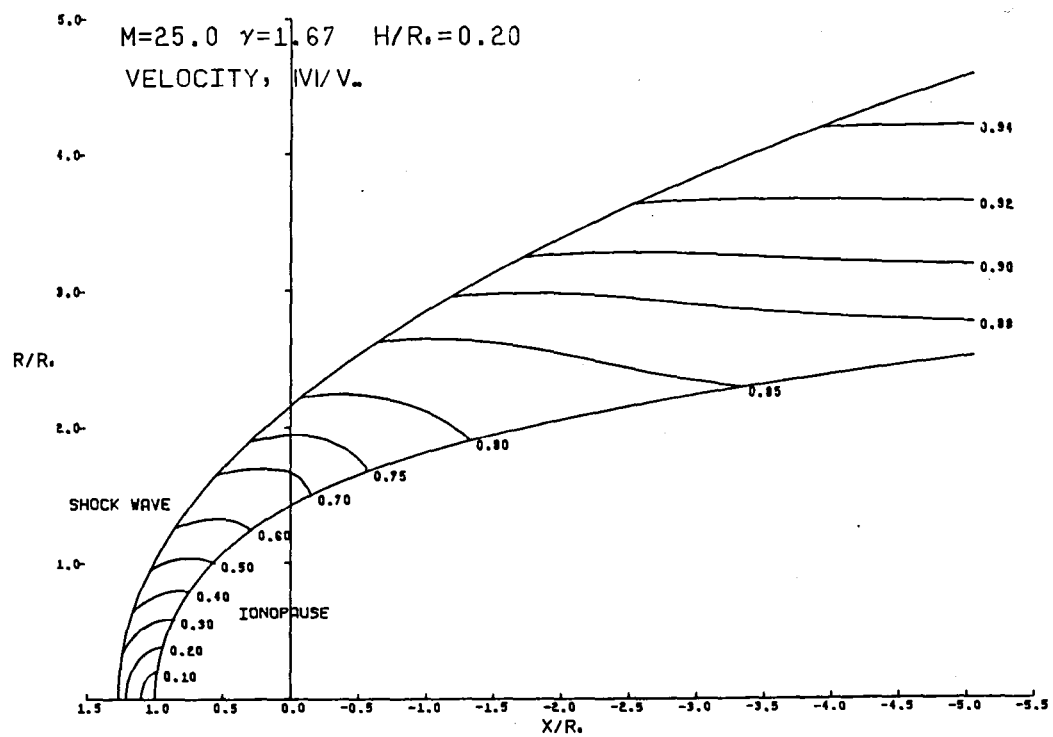
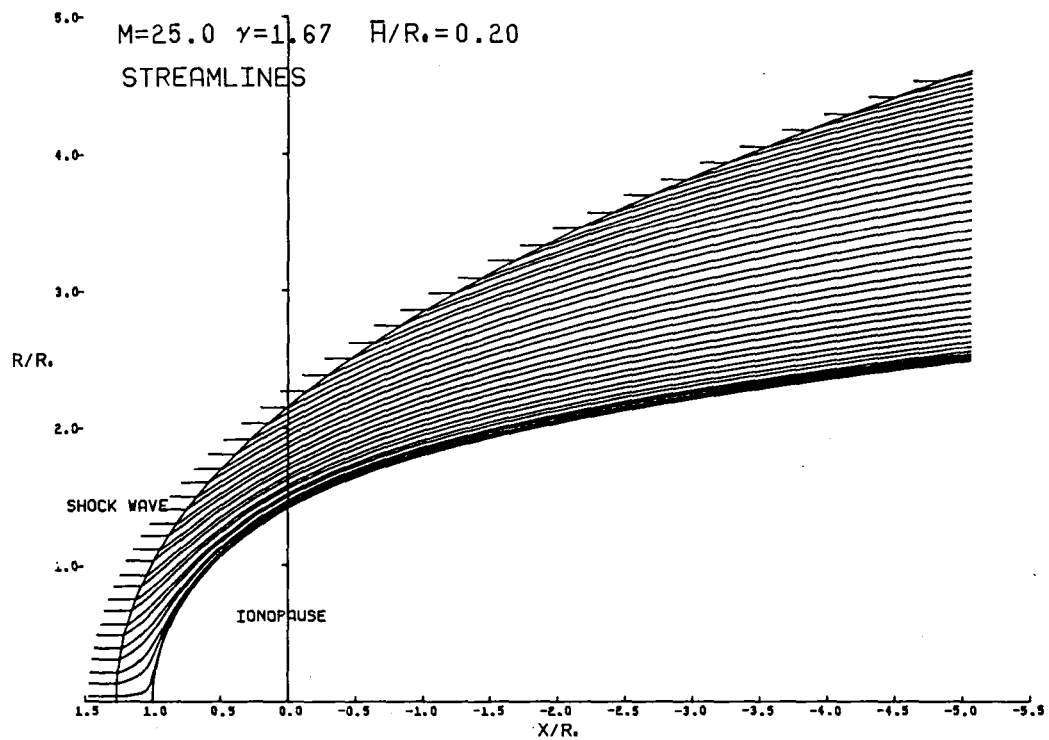


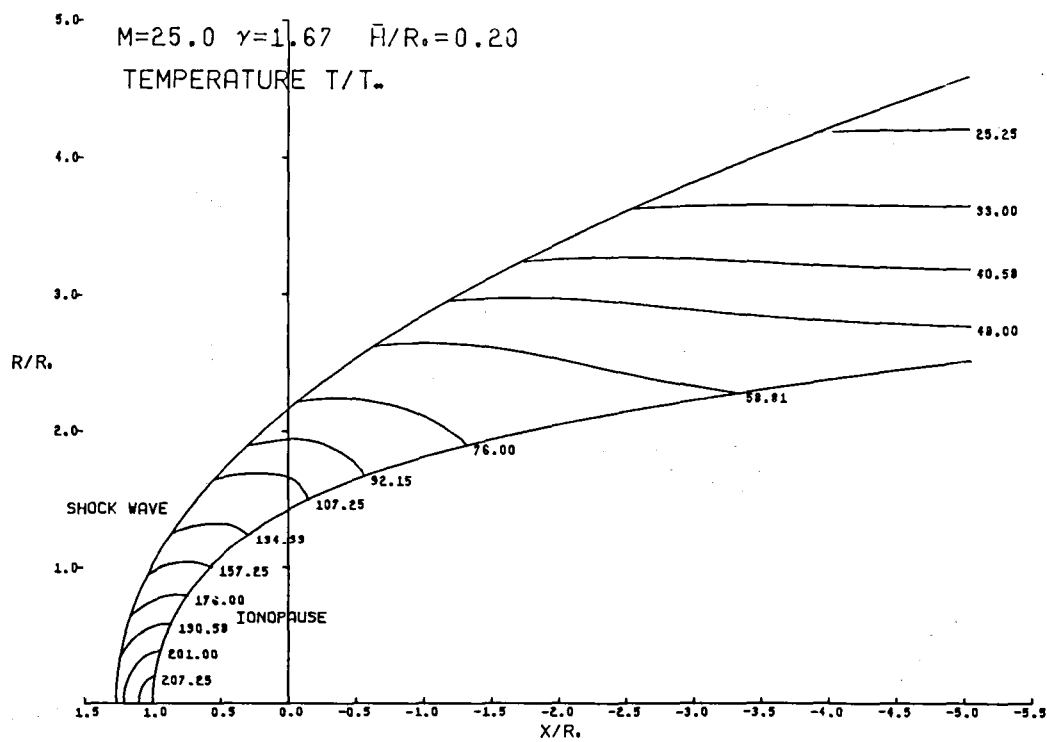
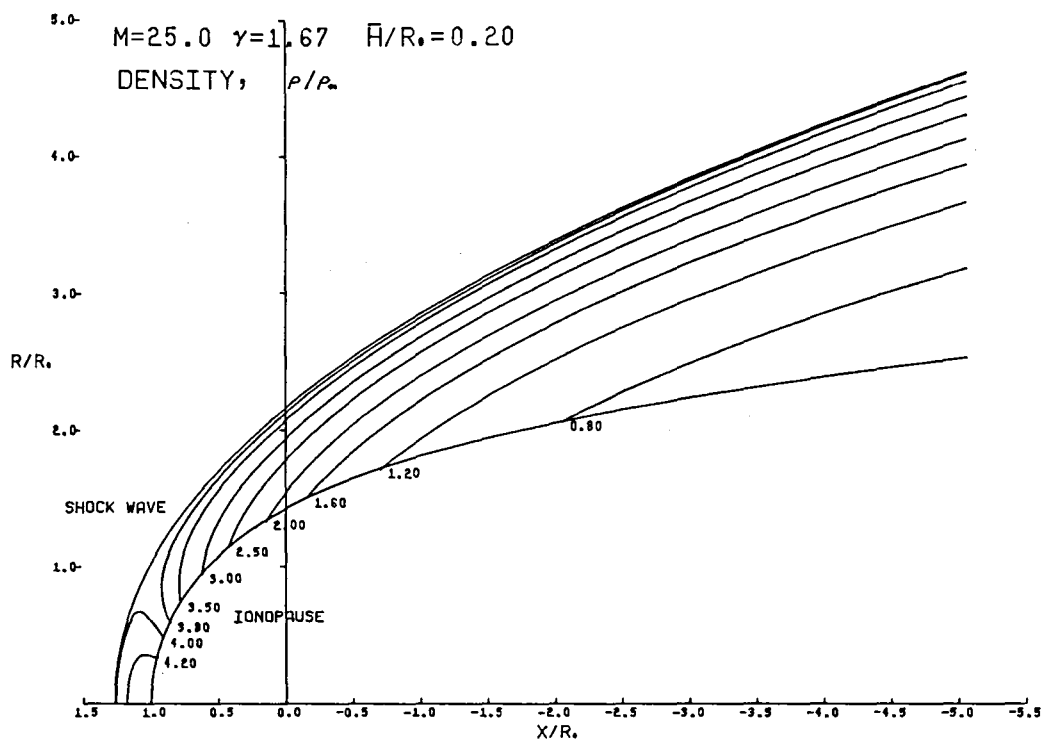


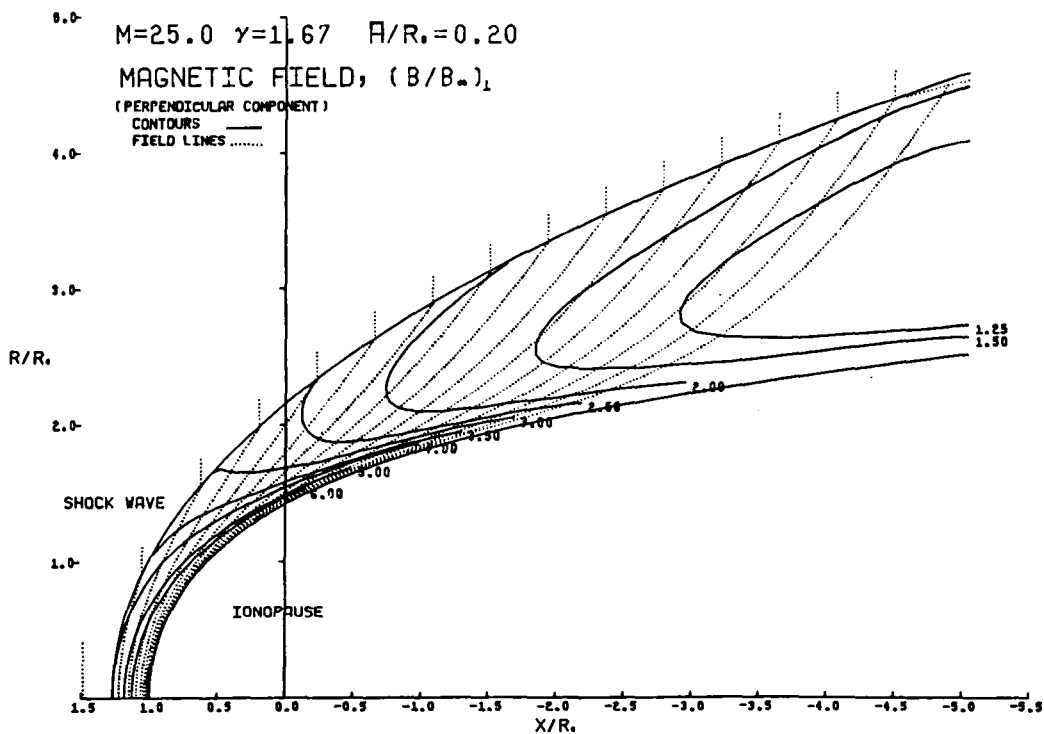
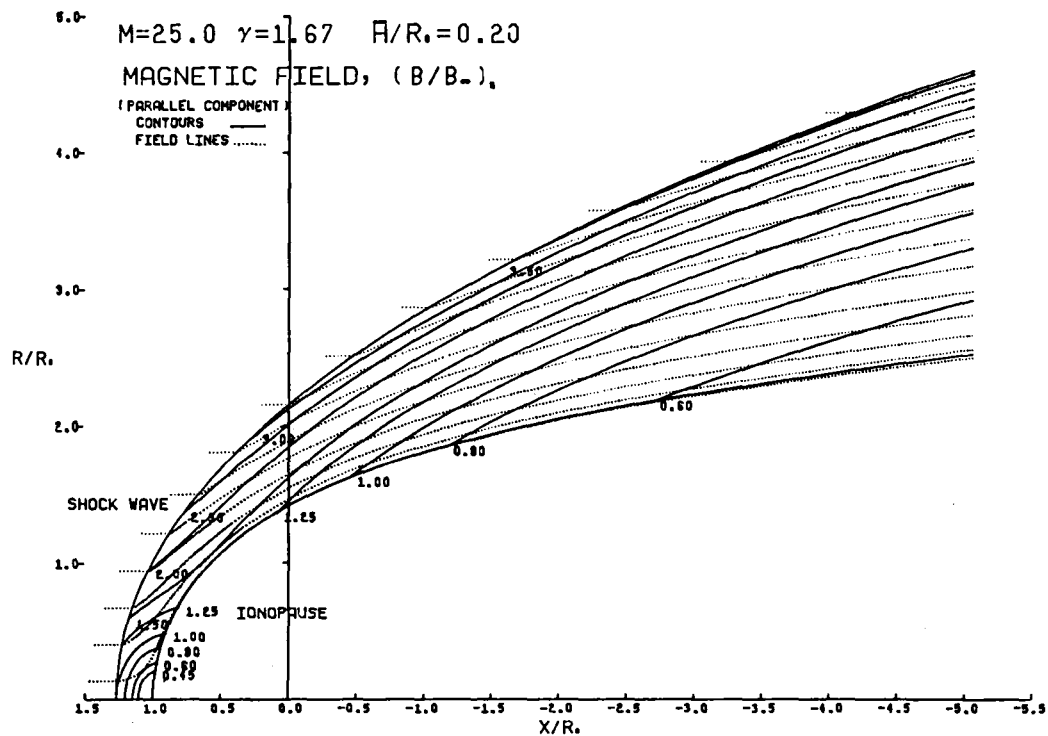


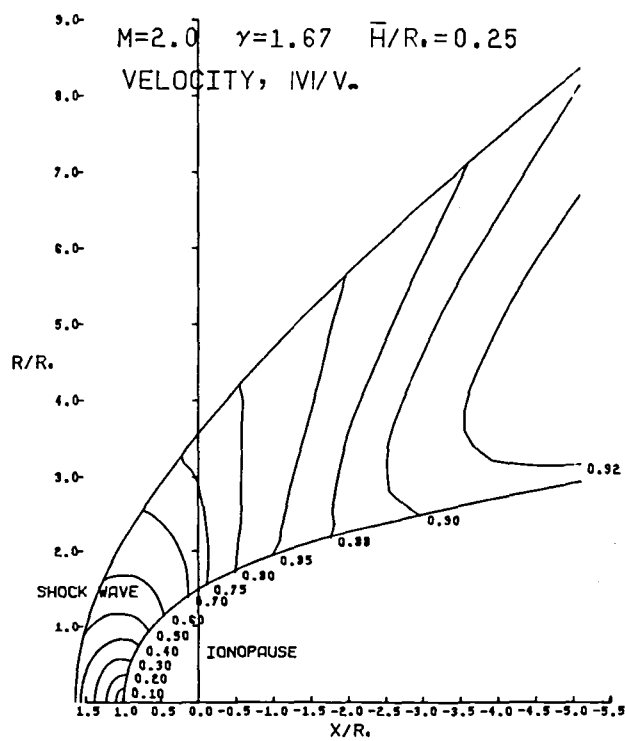
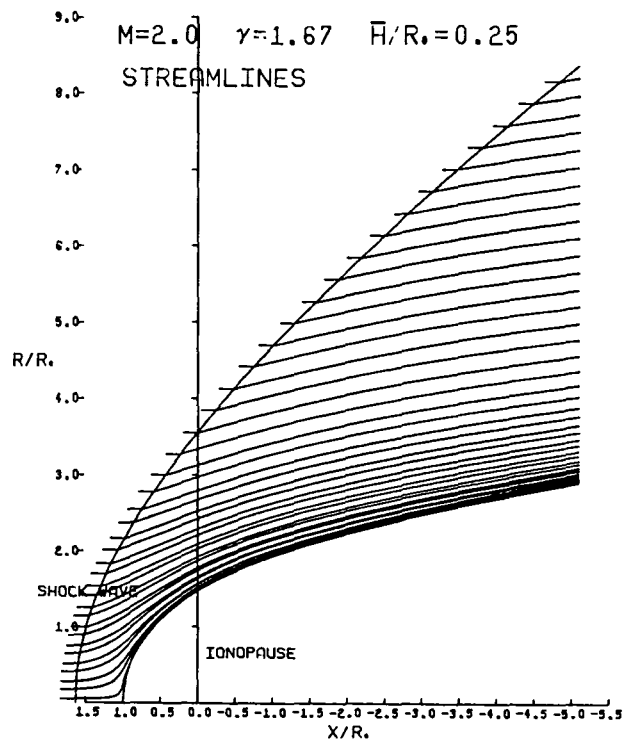


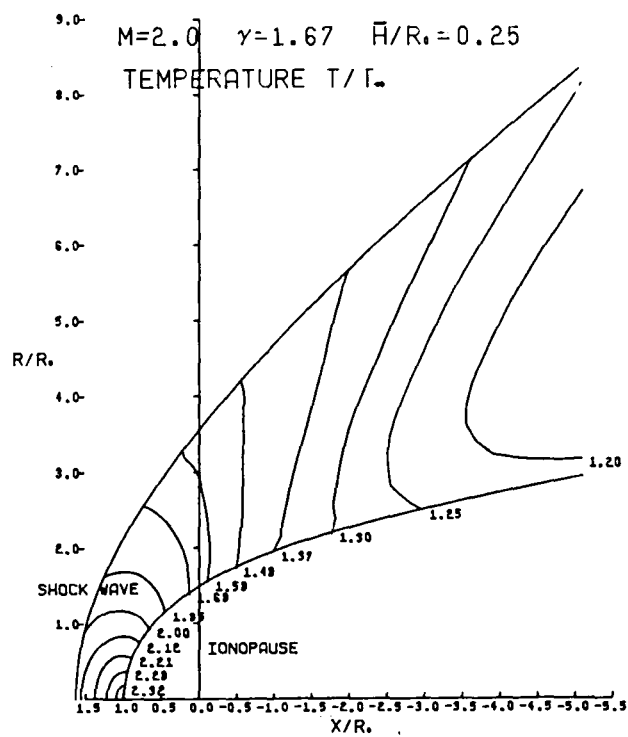
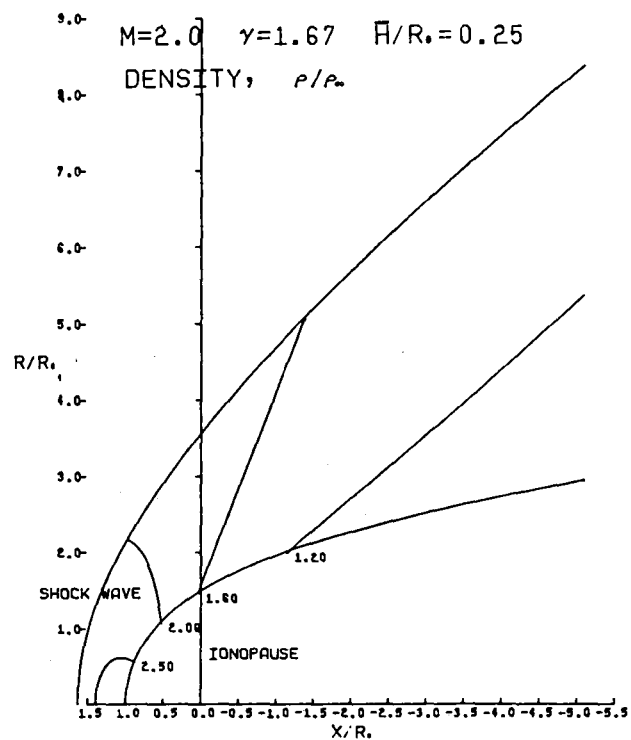


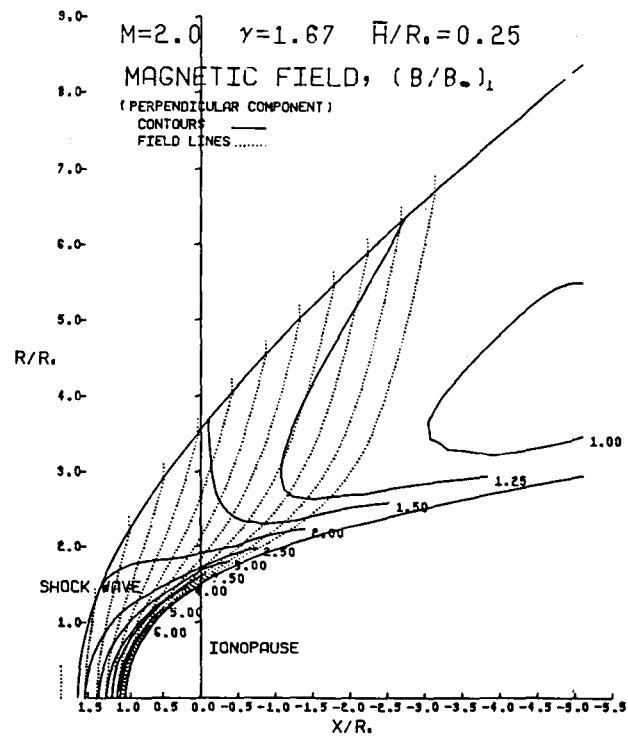
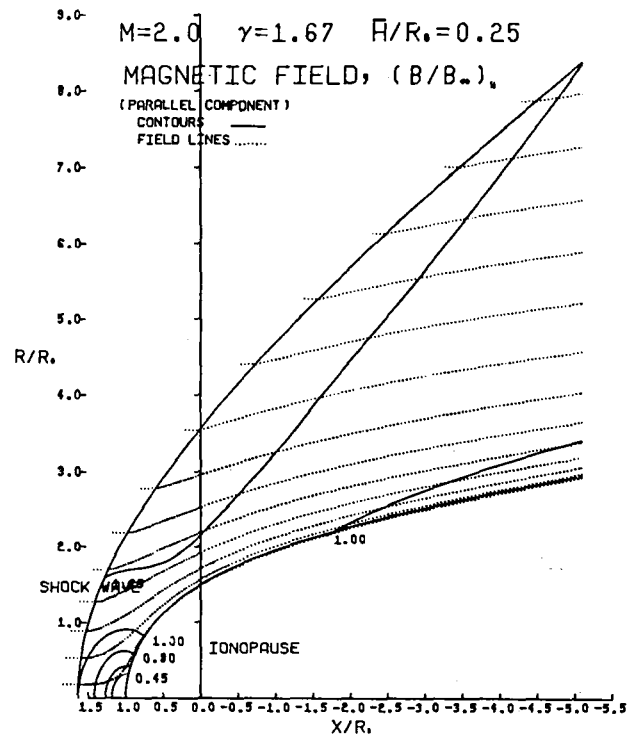


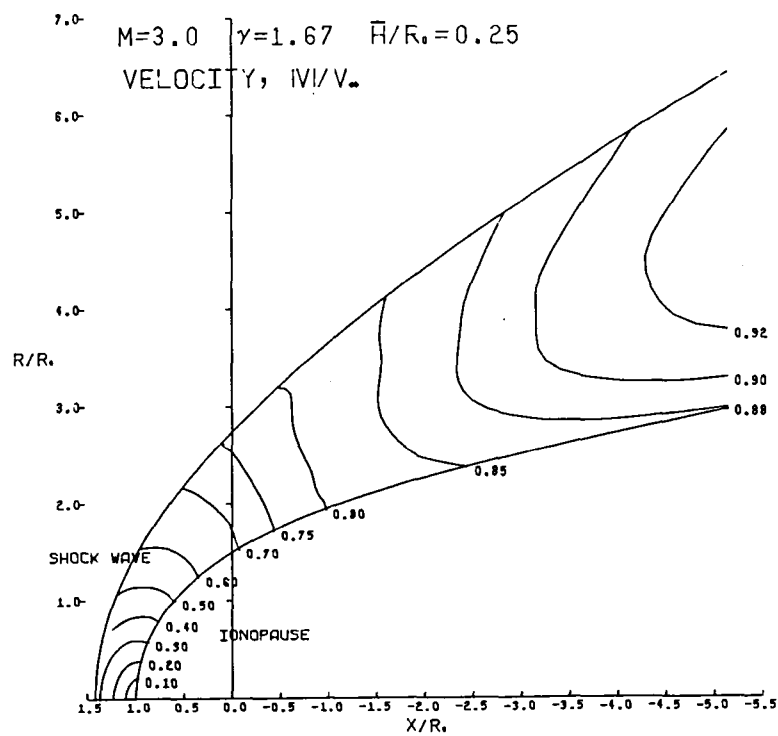
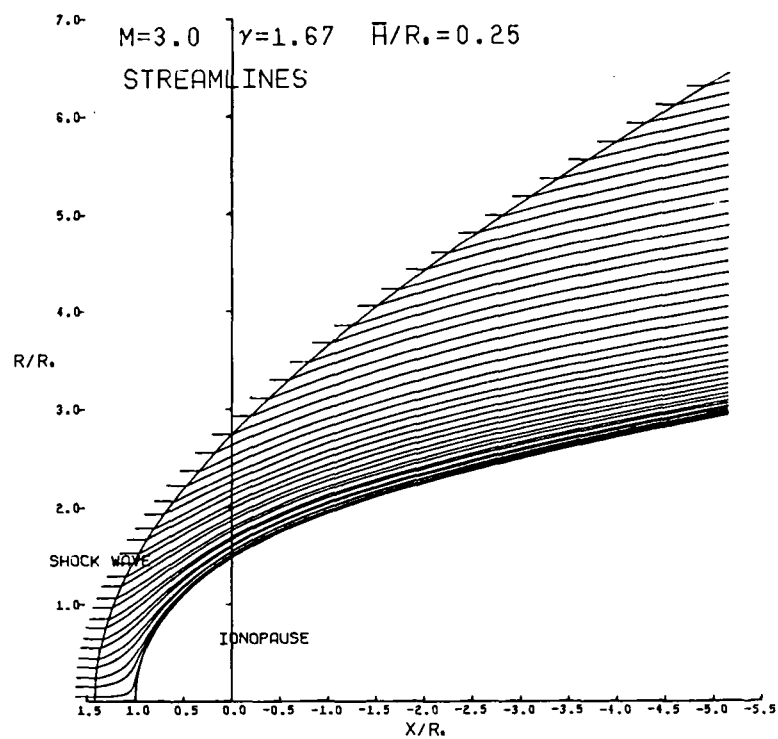


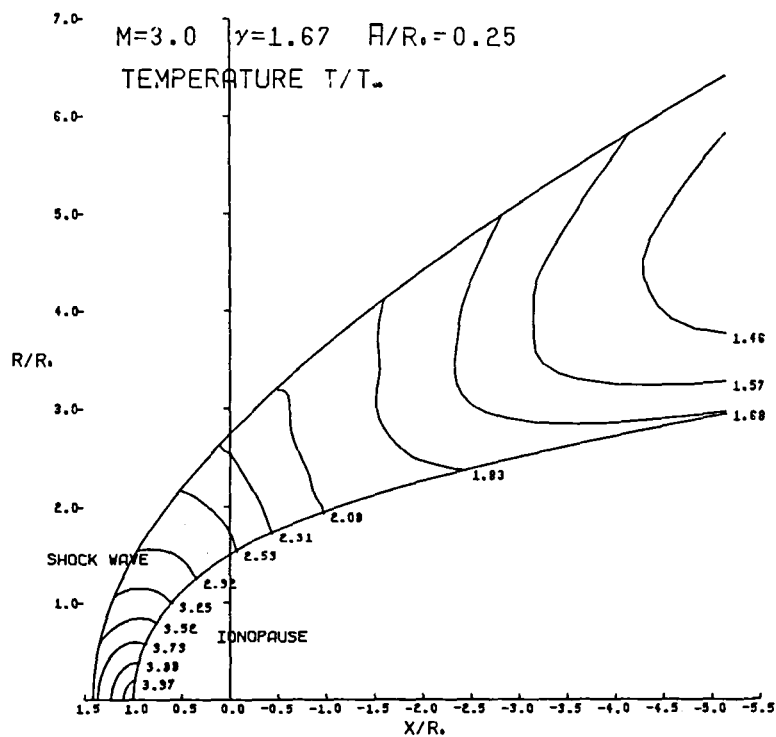
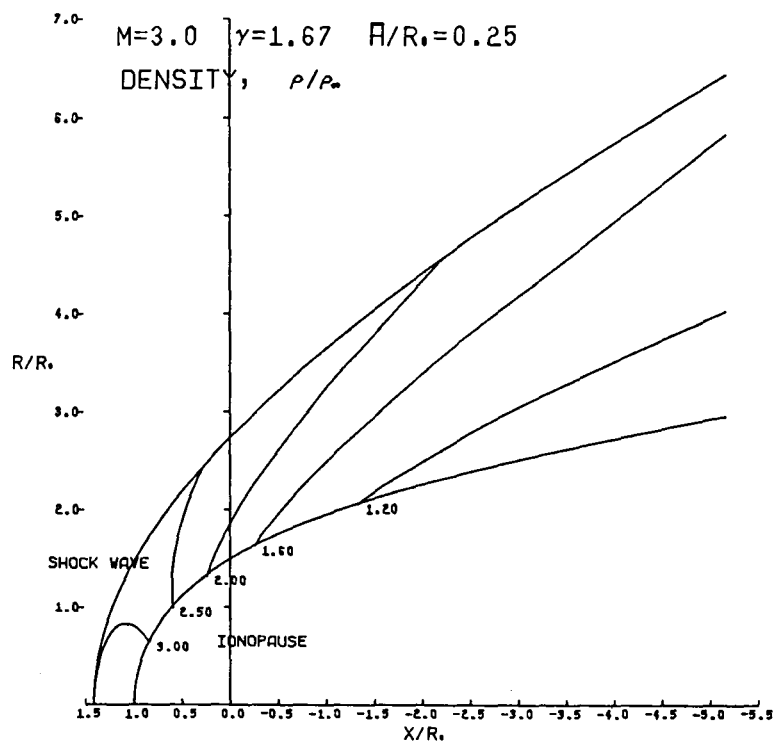


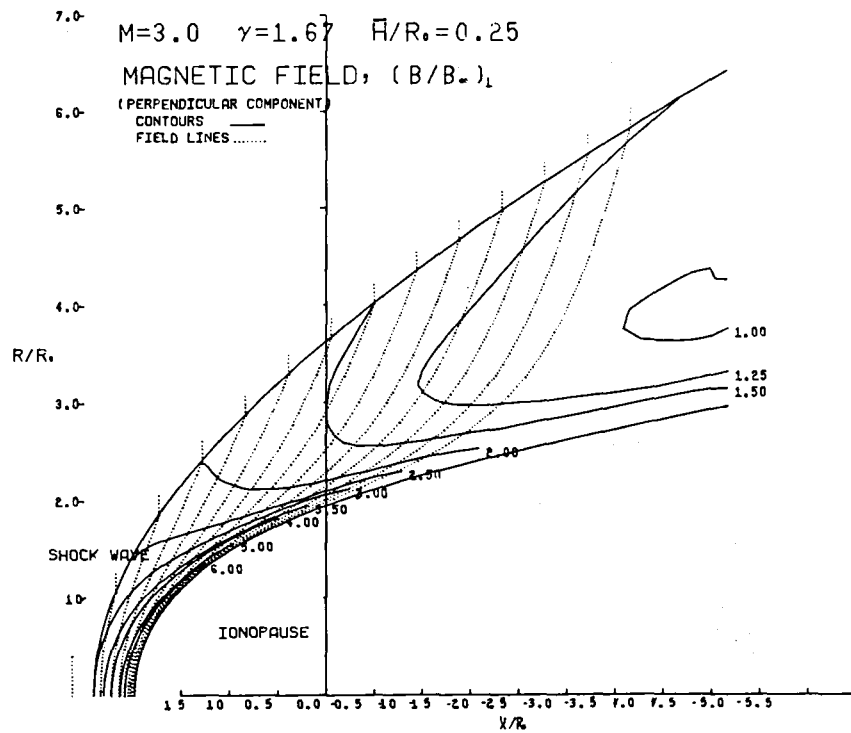
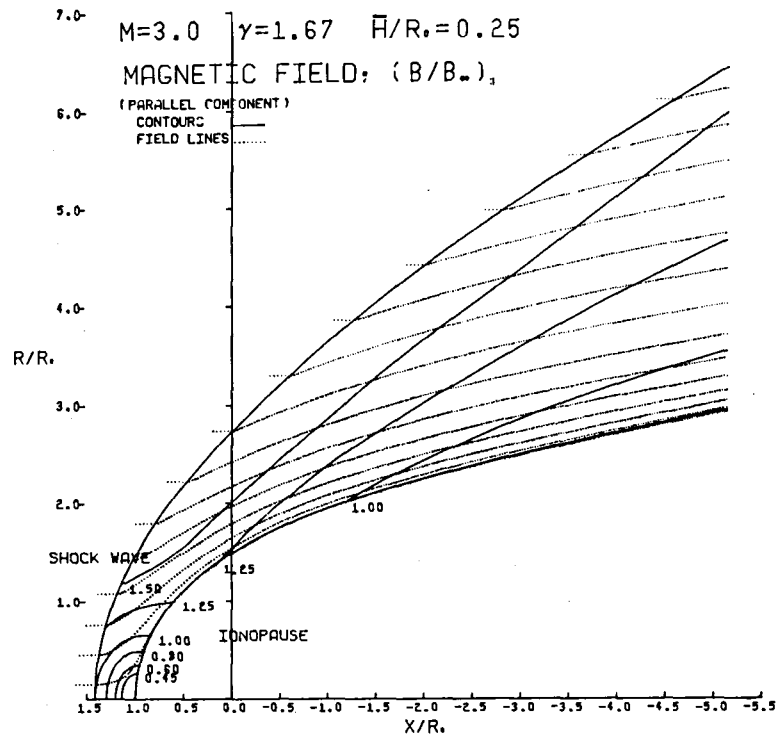


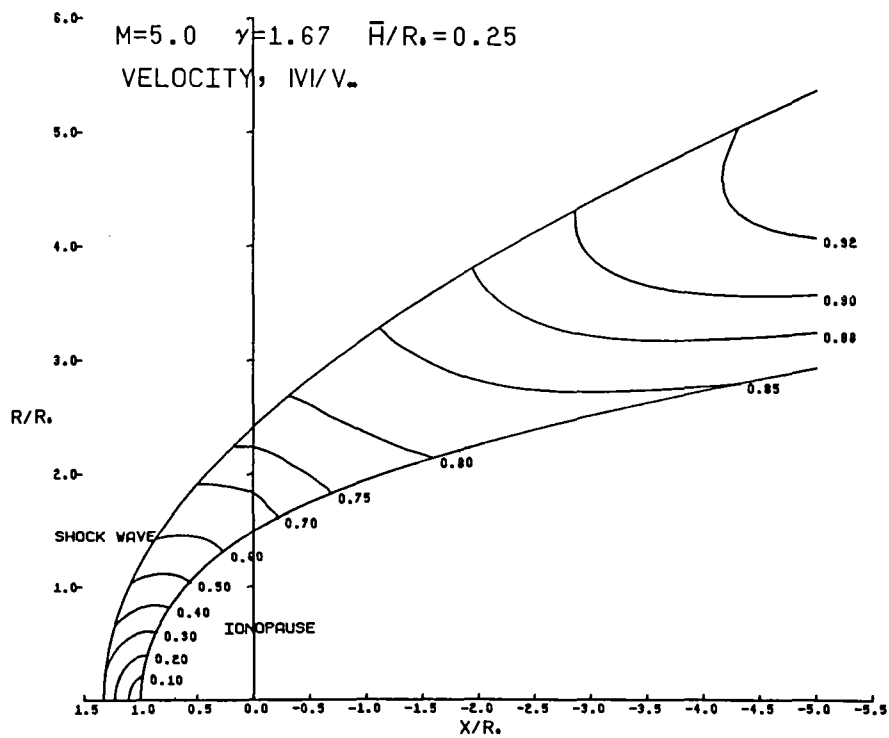
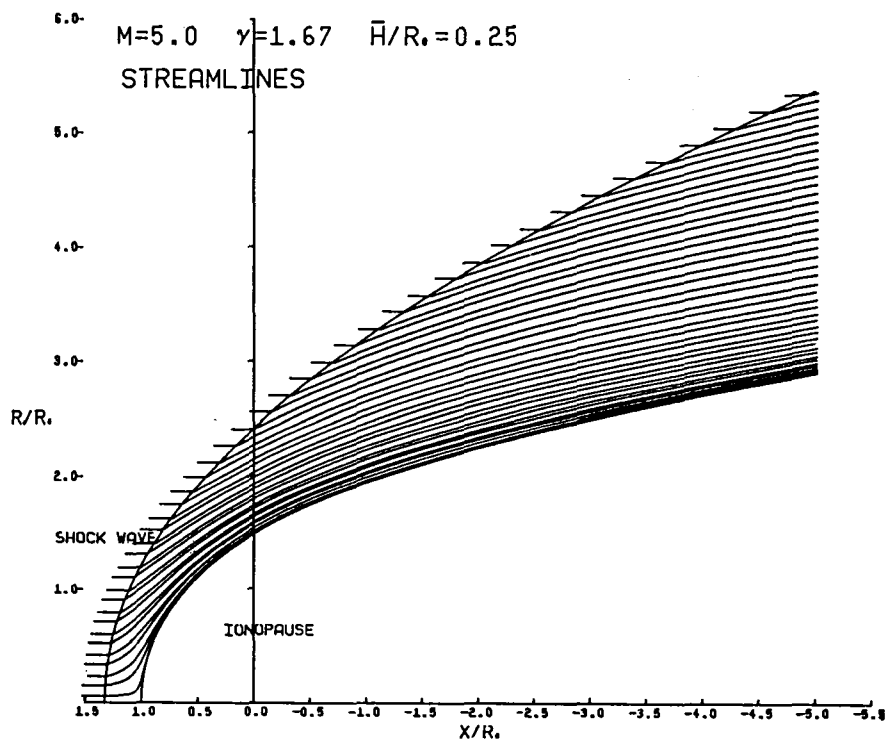


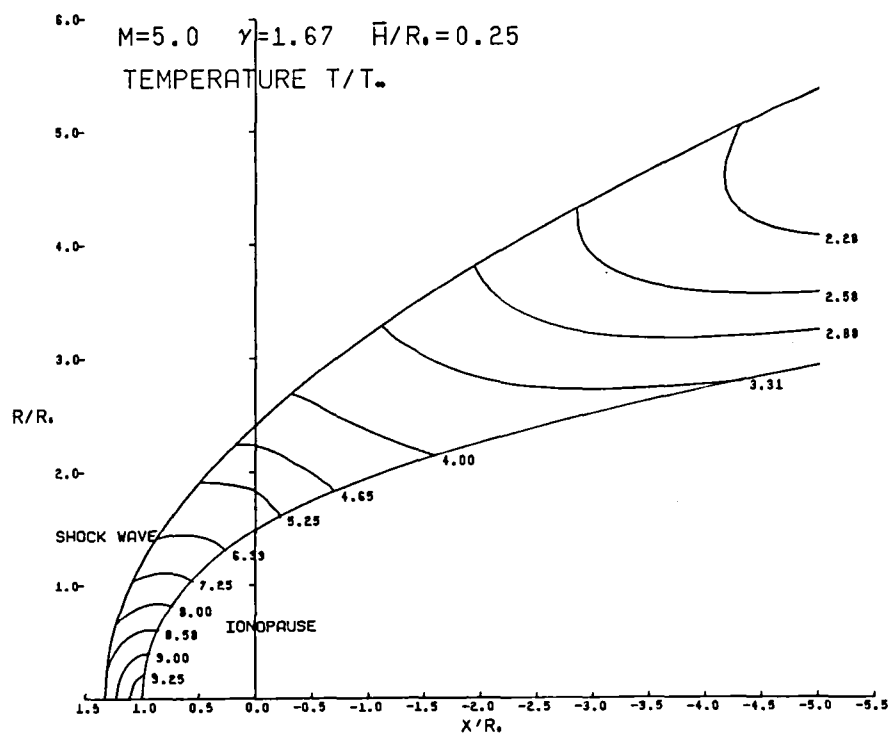
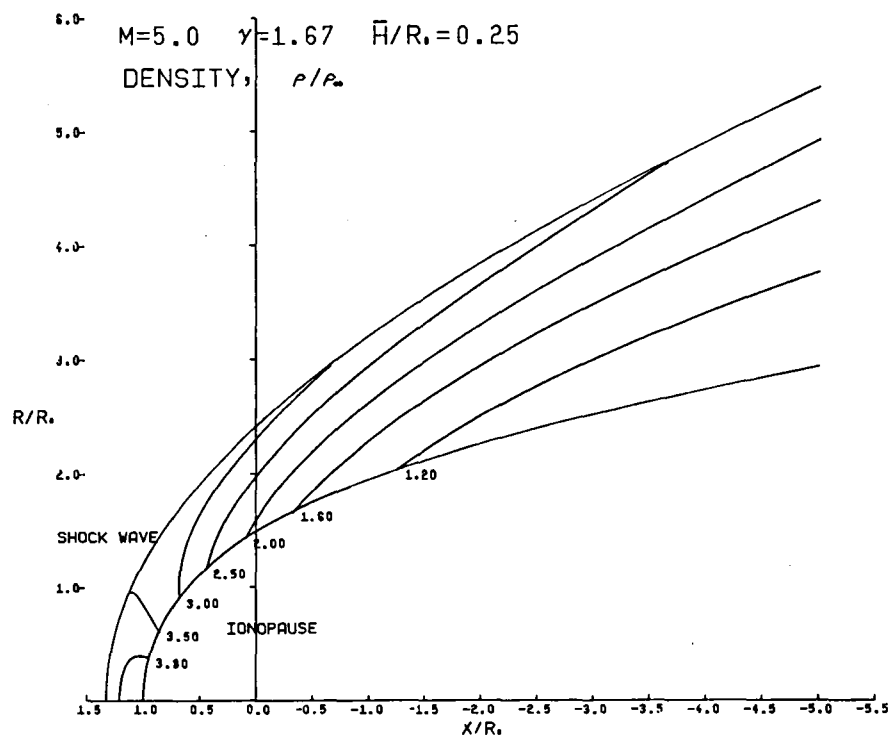


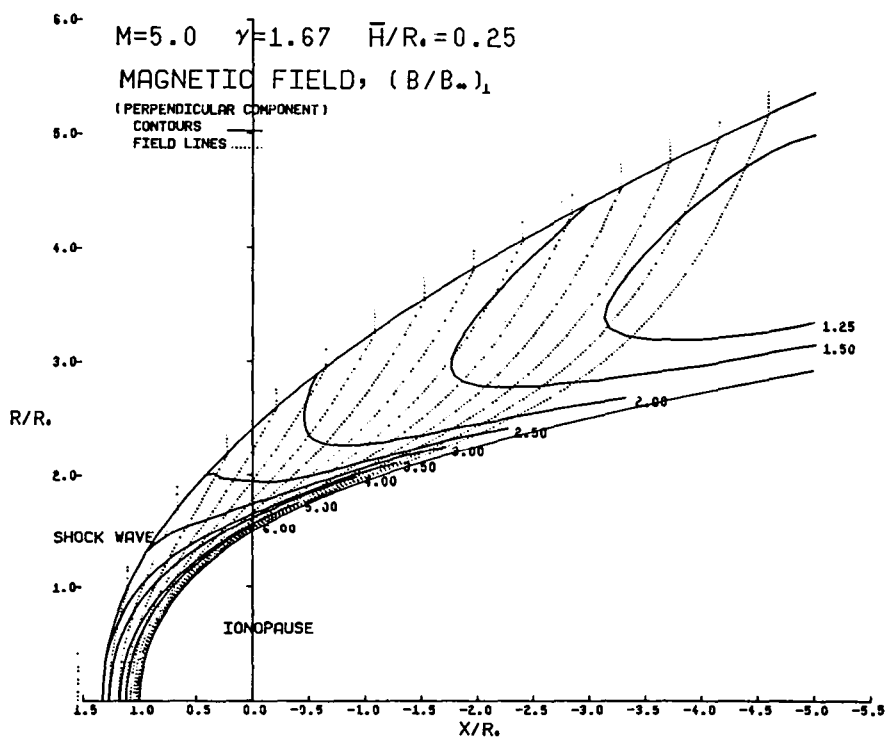
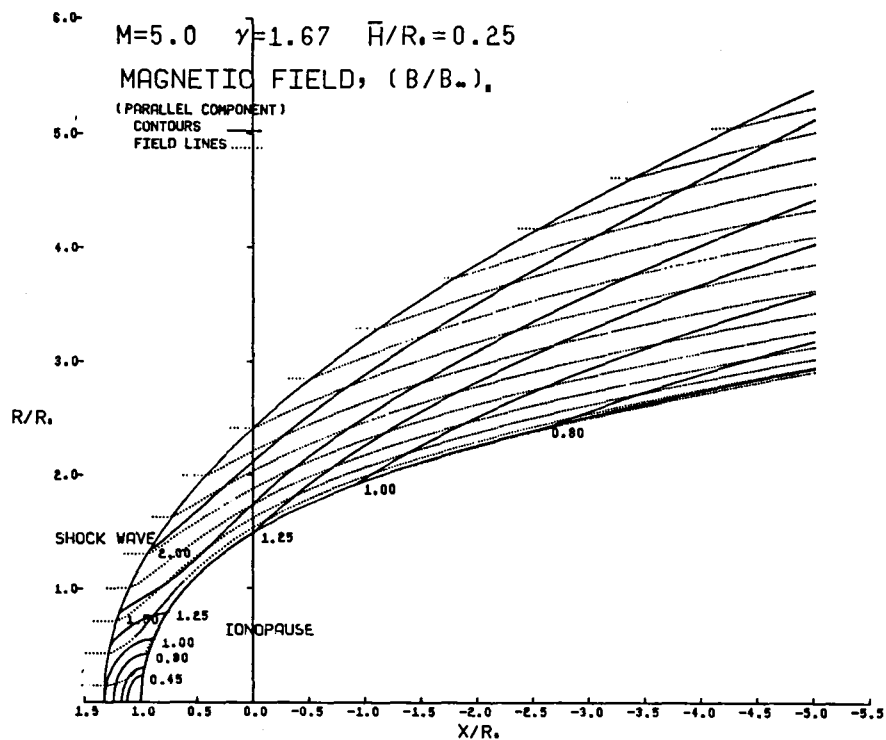


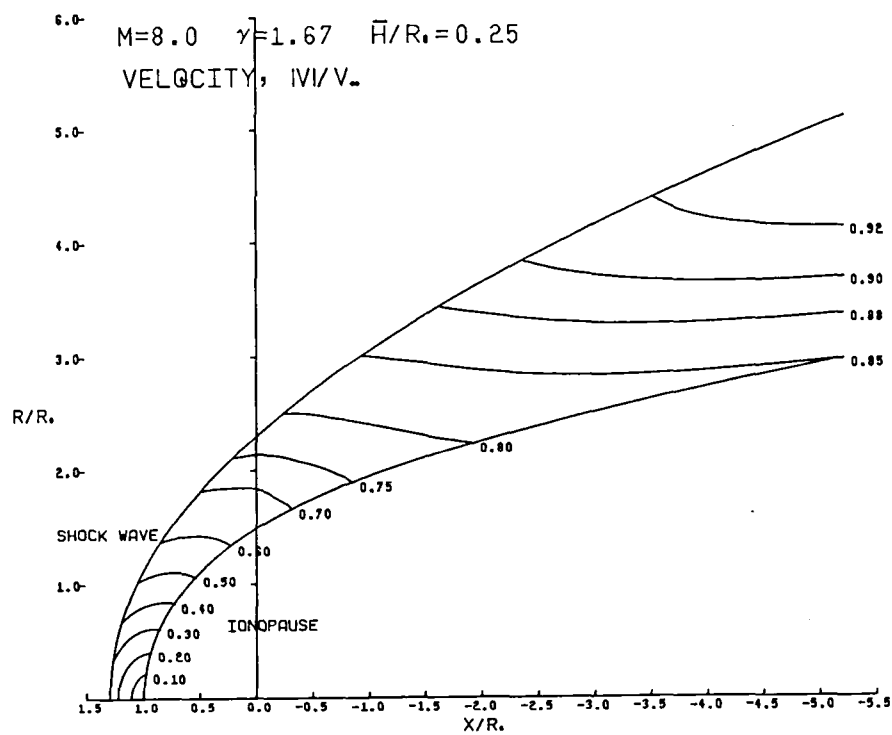
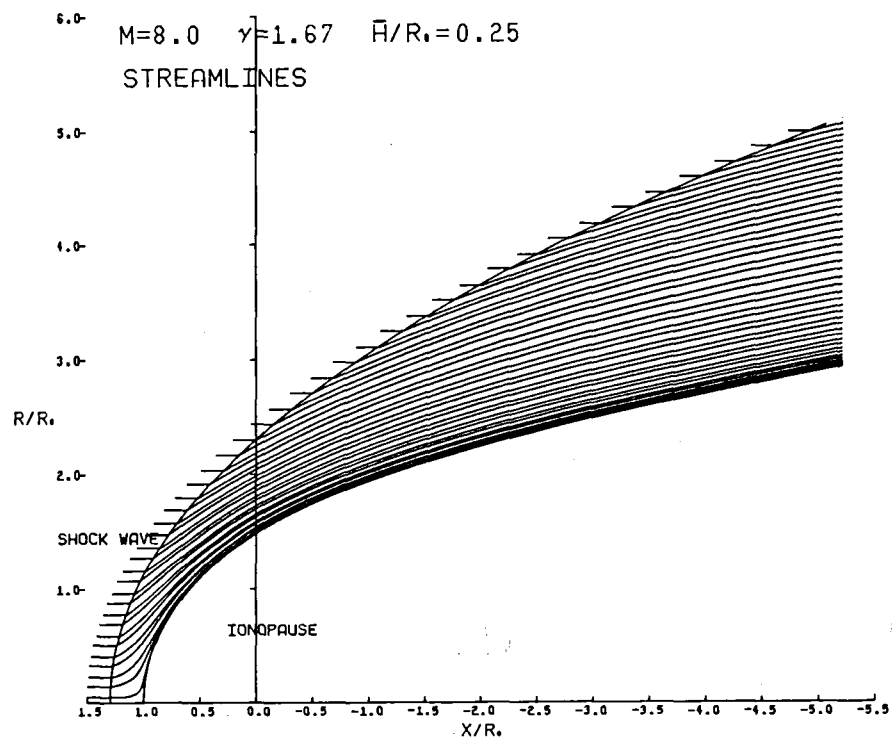


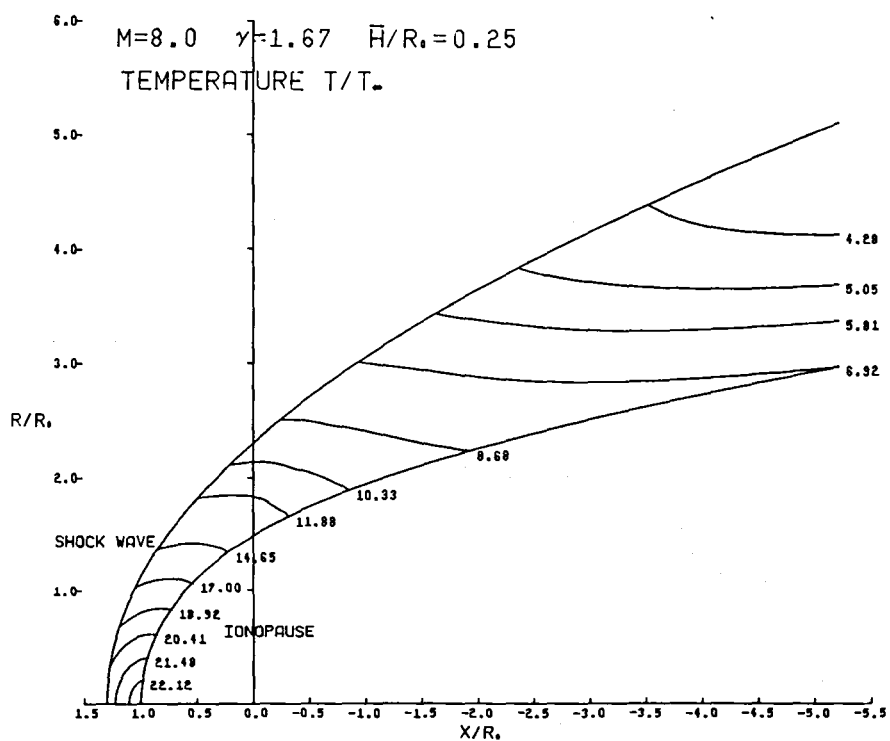
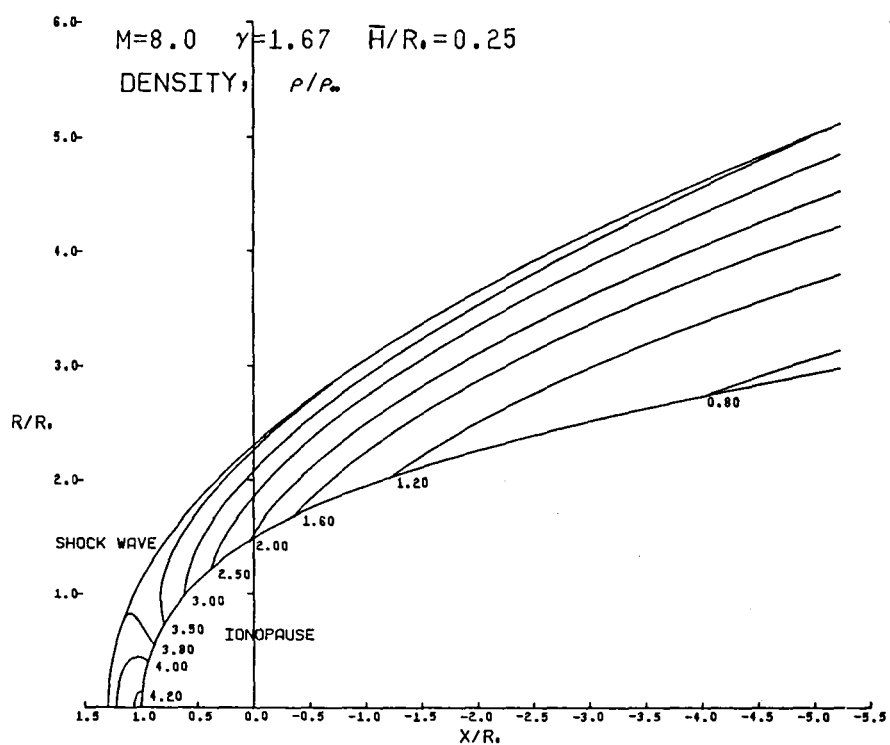


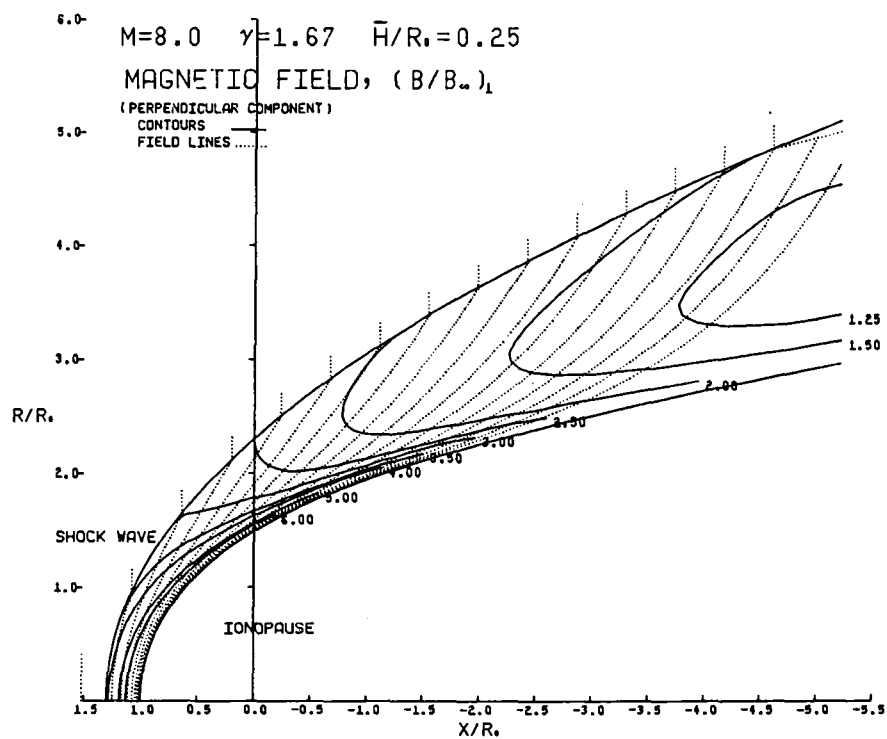
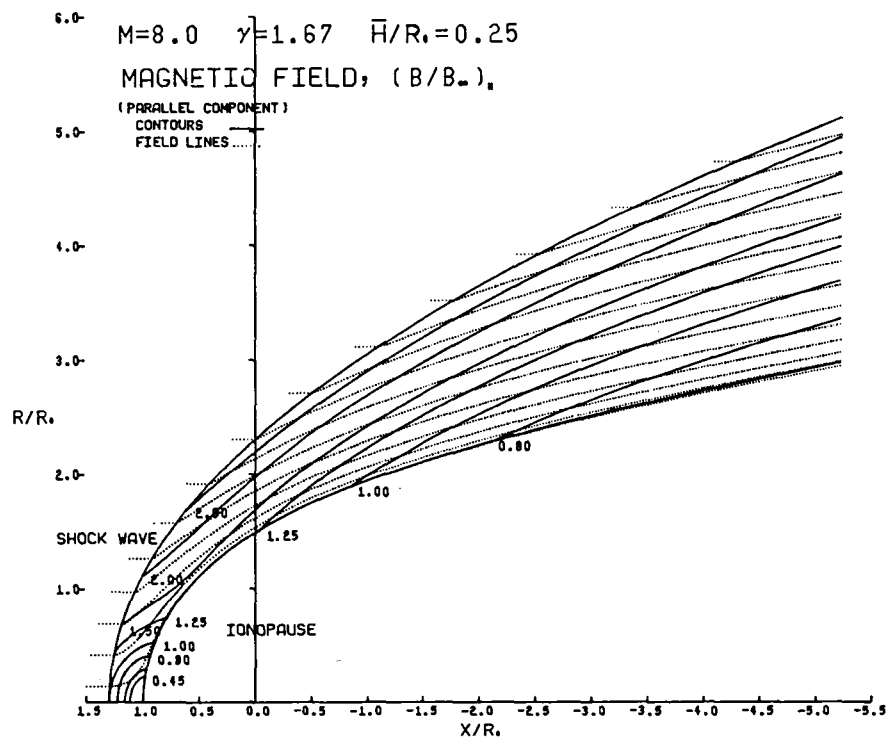


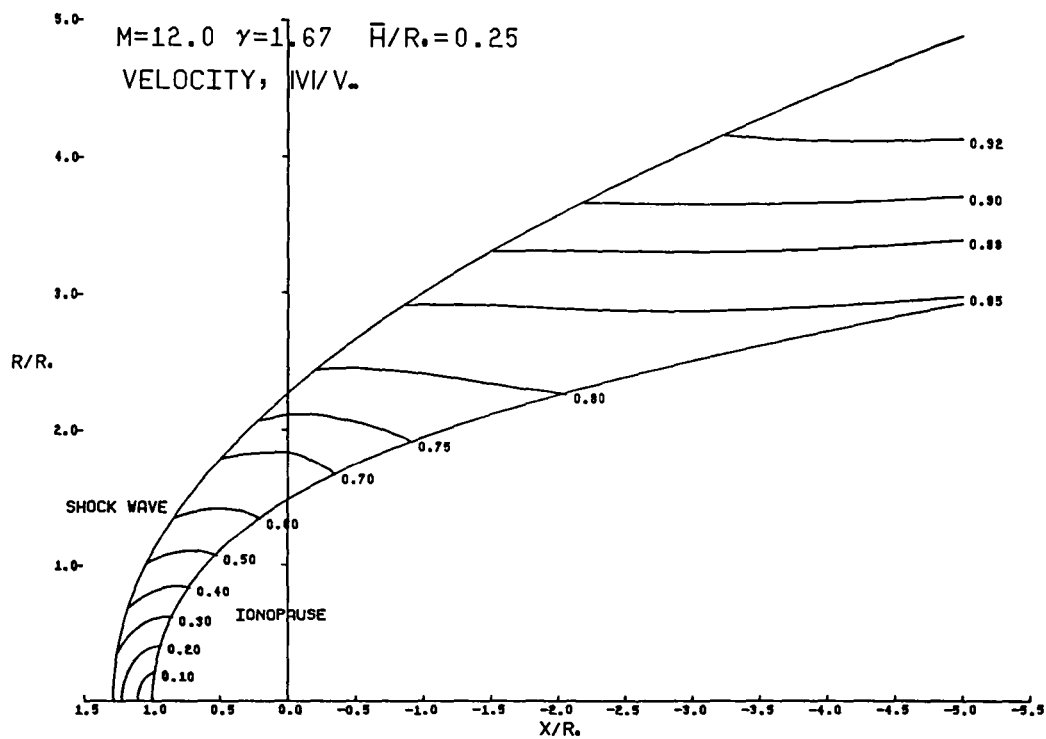
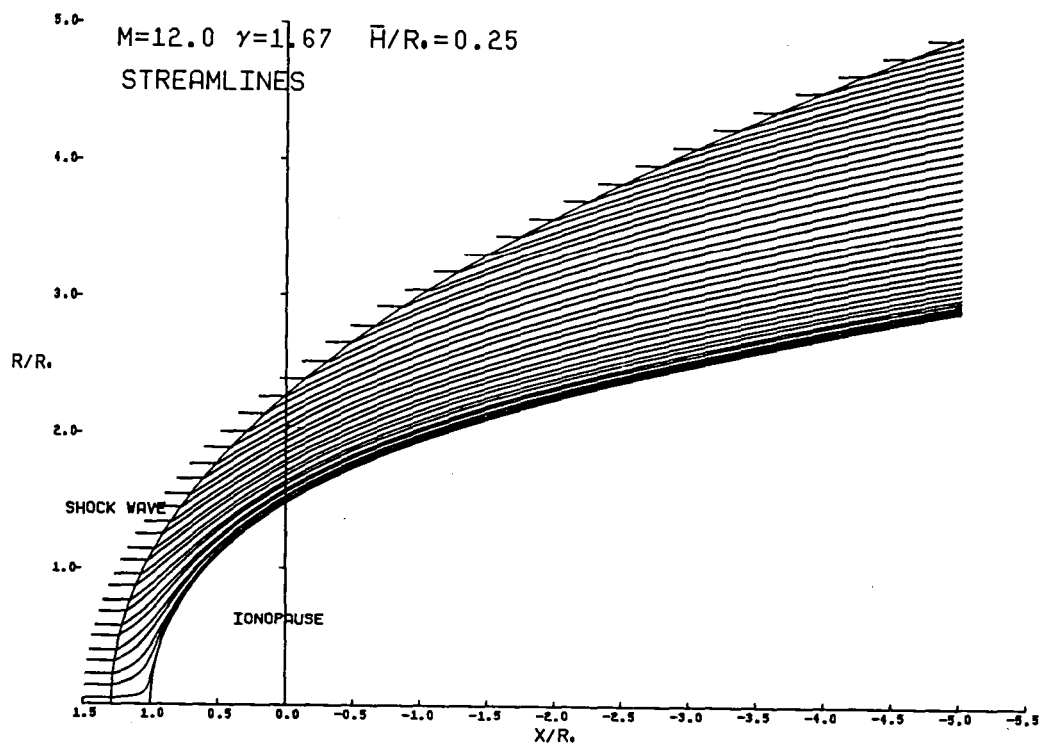


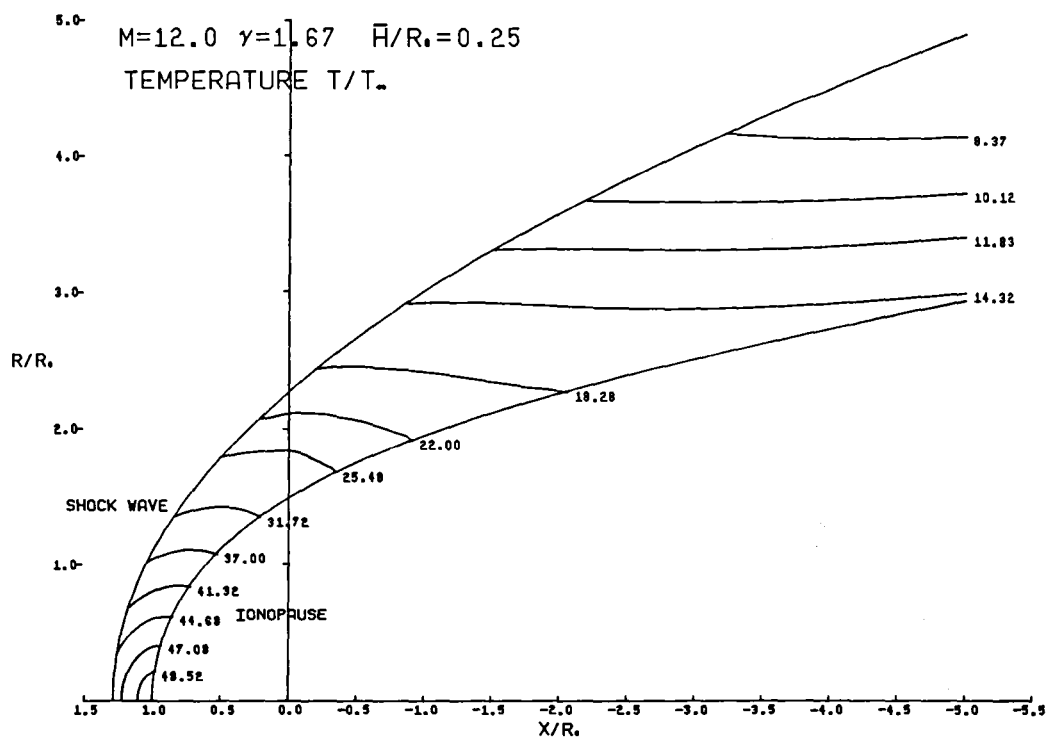
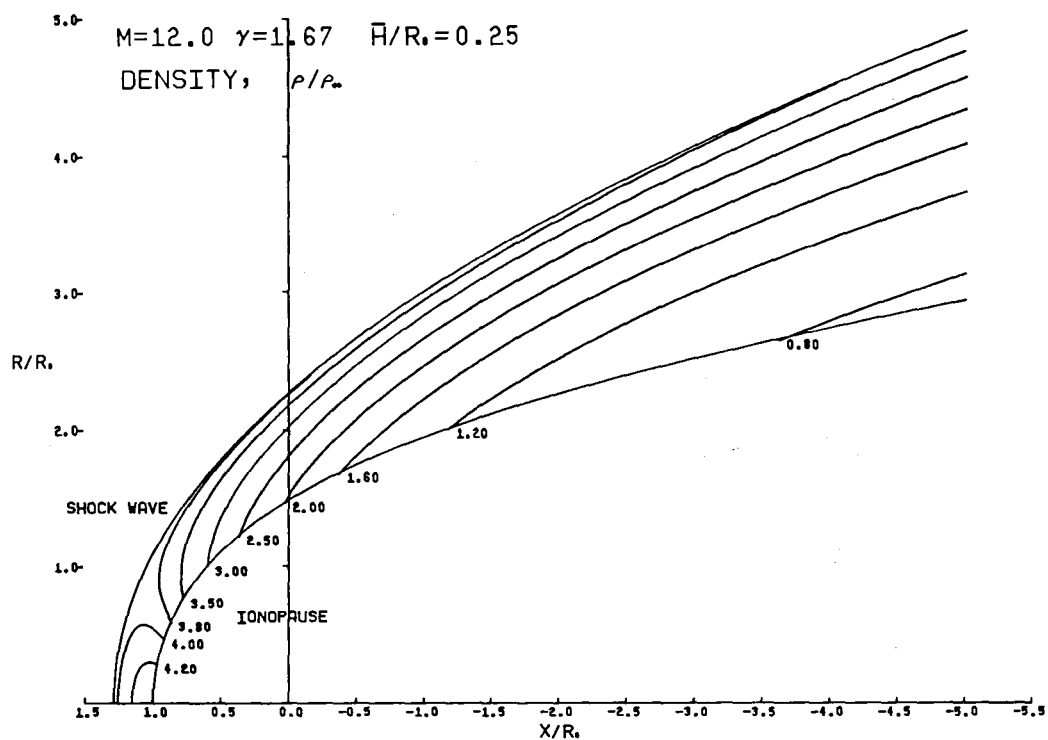


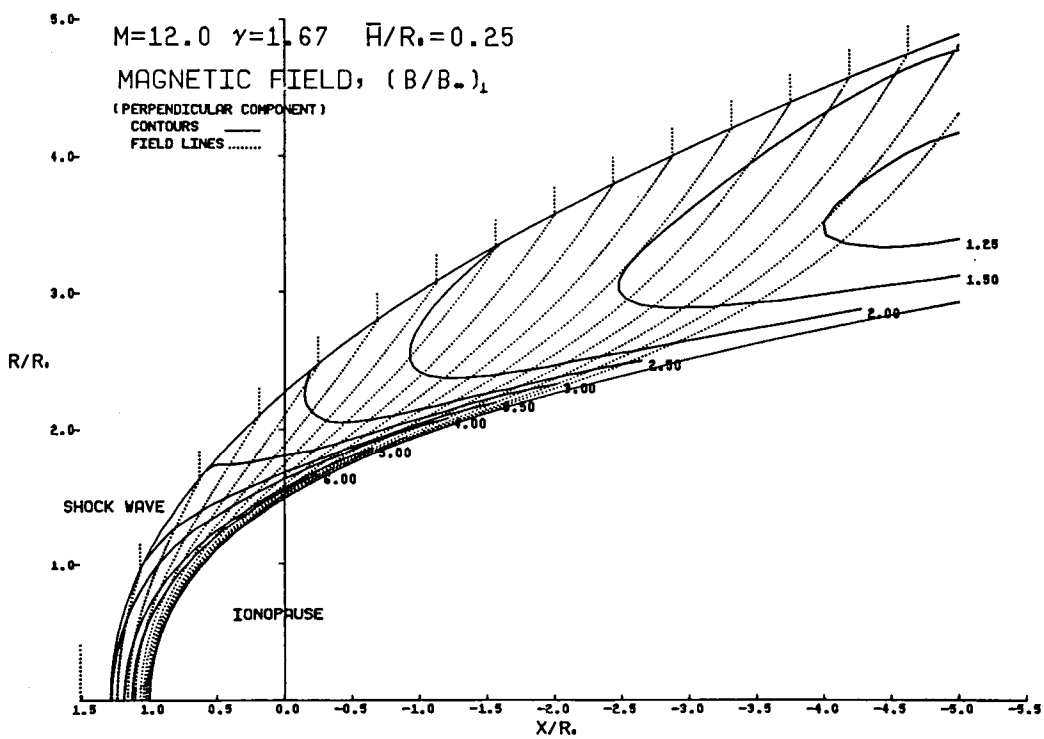
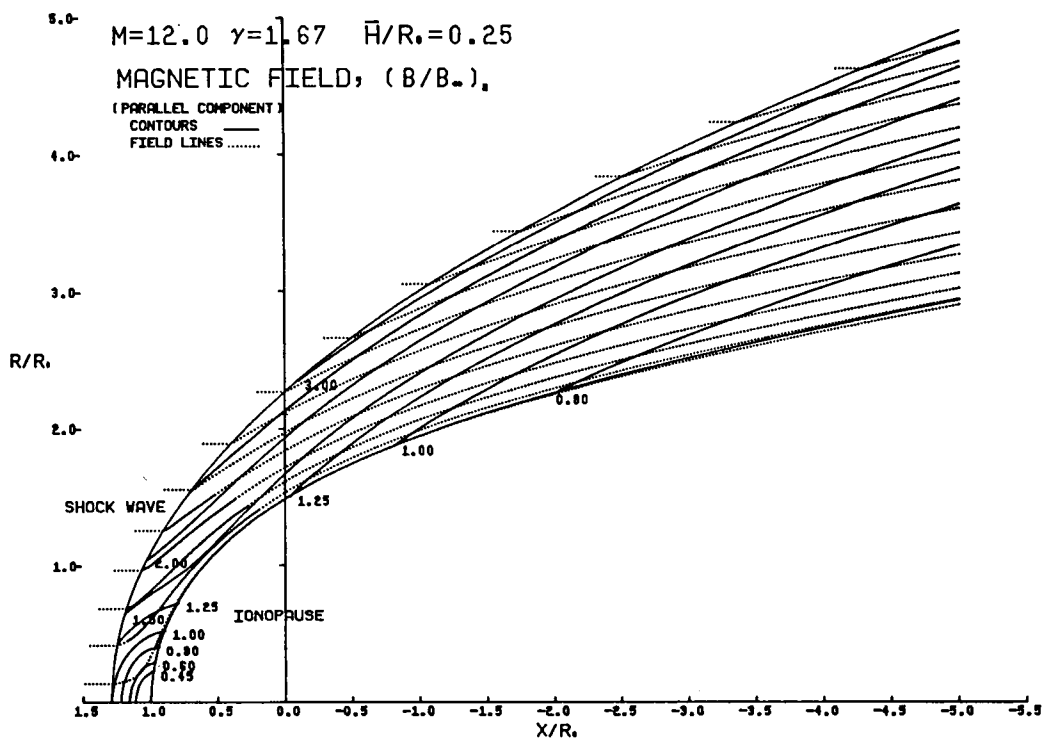


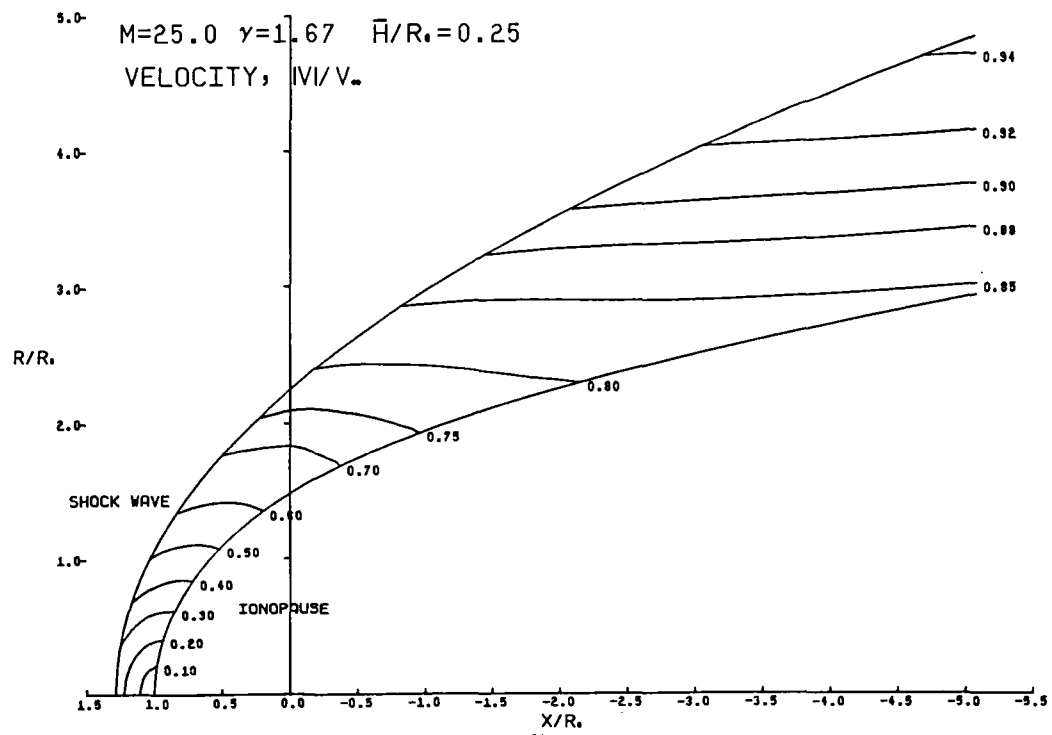
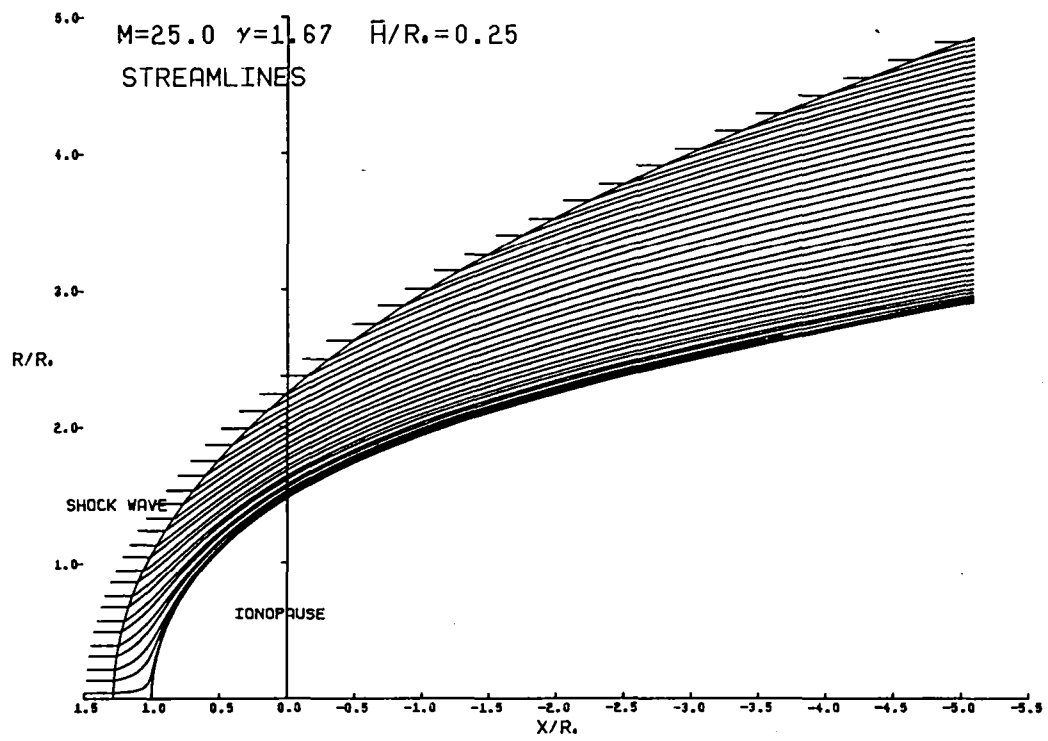


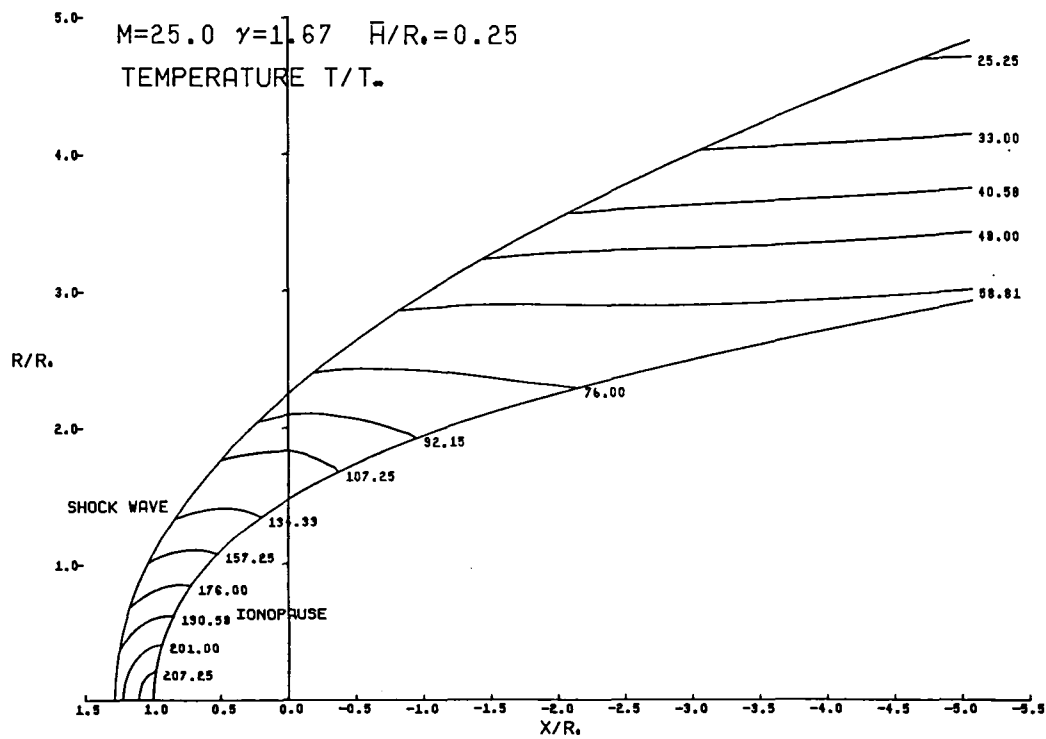
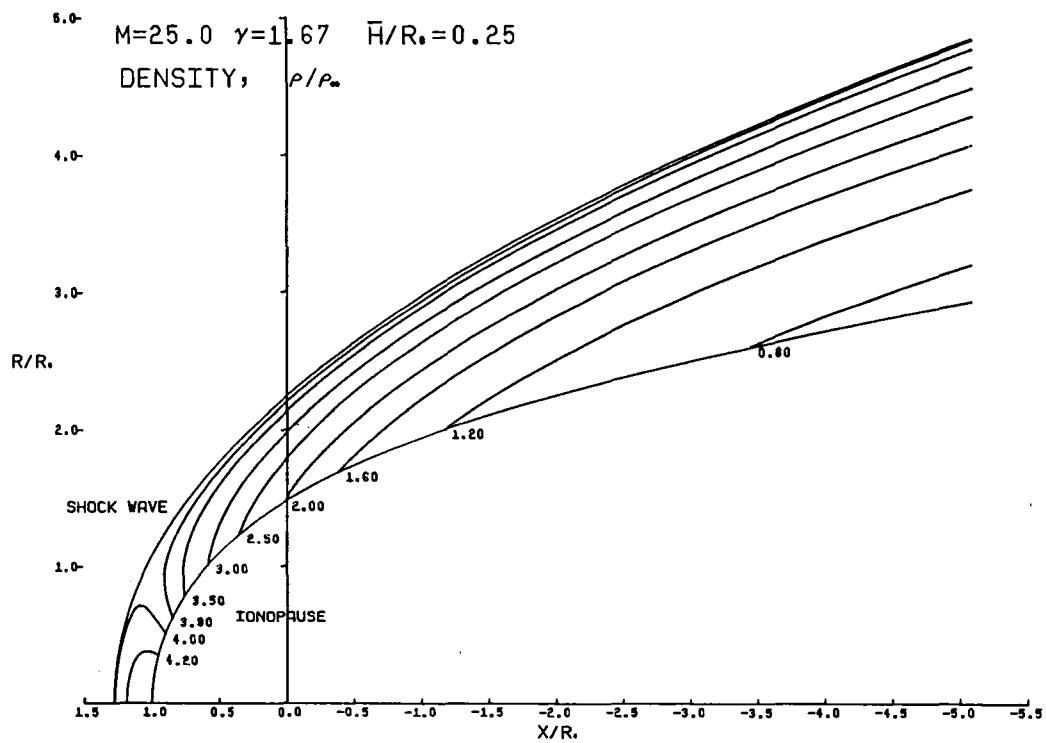


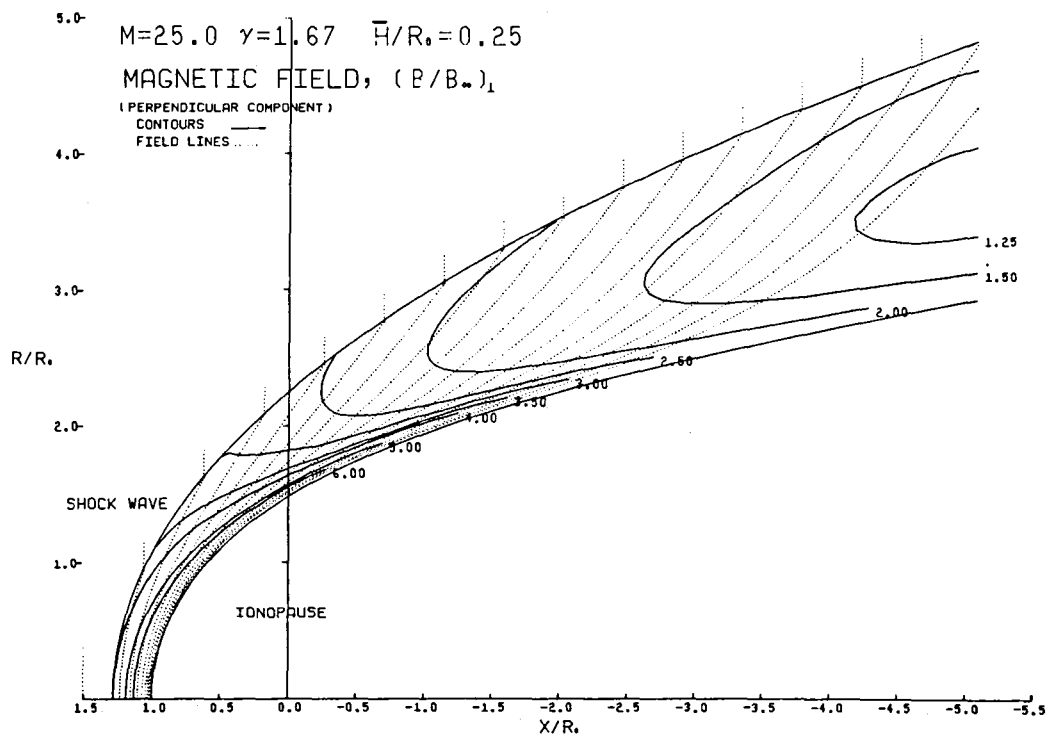
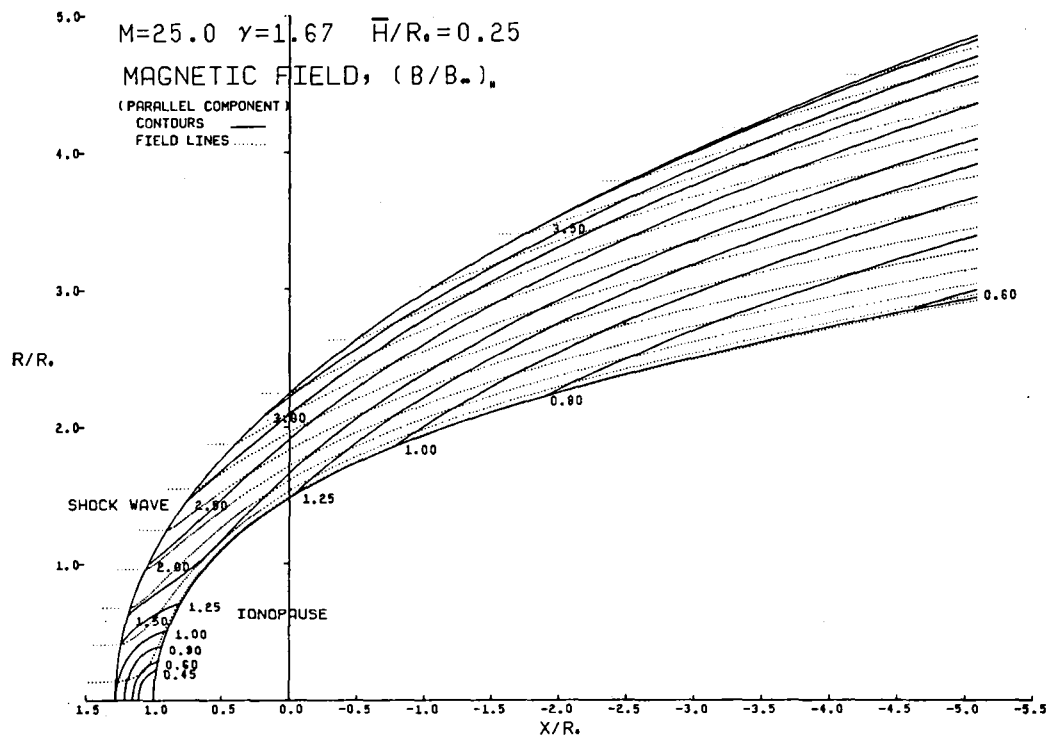












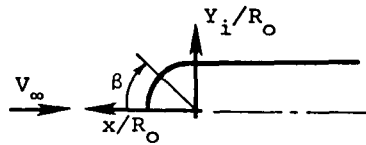
REFERENCES

1. Spreiter, J. R. and Jones, W. P.: On the Effect of a Weak Inter-planetary Magnetic Field on the Interaction Between the Solar Wind and the Geomagnetic Field. *J. Geophys. Res.*, Vol. 68, 1963, pp. 3555-3564.
2. Spreiter, J. R., Alksne, A. Y., and Summers, A. L.: Hydromagnetic Flow Around the Magnetopause. *Plan. & Space Sci.*, Vol. 14, 1966, pp. 223-253.
3. Dryer, M. and Faye-Petersen, R.: Magnetogasdynamic Boundary Condition for a Self-Consistent Solution to the Closed Magnetopause. *AIAA Journal*, Vol. 4, 1966, pp. 246-254.
4. Dryer, M. and Heckman, G. R.: Application of the Hypersonic Analogy to the Standing Shock of Mars. *Solar Phys.*, Vol. 2, 1967, pp. 112-120.
5. Spreiter, J. R., Alksne, A. Y., and Summers, A. L.: External Aerodynamics of the Magnetosphere. *Physics of the Magnetosphere* (Ed. R. L. Carovillano, J. F. McClay, and H. R. Radoski), D. Reidel Pub. Co., 1968, pp. 304-378 (also NASA TN 4482, 1968).
6. Spreiter, J. R., Summers, A. L., and Rizzi, A. W.: Solar Wind Flow Past Nonmagnetic Planets - Venus and Mars. *Plan. & Space Sci.*, Vol. 18, 1970, pp. 1281-1289.
7. Spreiter, J. R. and Rizzi, A. W.: Aligned Magnetohydrodynamics Solution for Solar Wind Flow Past the Earth's Magnetosphere. *Acta Astronautica*, Vol. 1, 1974, pp. 15-35.
8. Spreiter, J. R.: Magnetohydrodynamic and Gasdynamic Aspects of Solar-Wind Flow Around Terrestrial Planets: A Critical Review. *NASA SP-397*, 1975, pp. 135-150.
9. Stahara, S. S., Chaussee, D. S., Trudinger, B. C., and Spreiter, J. R.: Computational Techniques for Solar Wind Flows Past Terrestrial Planets - Theory and Computer Programs. *NASA CR-2924*, Nov. 1977.
10. Knudsen, W. C., Spenner, K., Spreiter, J. R., Miller, K. L., and Novak, V.: Thermal Structure and Major Ion Composition of the Venusian Ionosphere: First RPA Results from Venus Orbiter. *Science*, Vol. 203, No. 4382, Feb. 1979, pp. 757-763.
11. Knudsen, W. C., Spenner, K., Whitter, R. C., Spreiter, J. R., Miller, K. L., and Novak, V.: Thermal Structure and Energy Influx to the Day- and Nightside Venus Ionosphere. *Science*, Vol. 205, No. 4401, July 1979, pp. 105-107.
12. Kuhn, G. D., Goodwin, F. K., and Perkins, S. C., Jr.: User's Manual for Space-Shuttle Computer Programs. *NEAR TR 110*, Apr. 1976.

REFERENCES (Concluded)

13. Beam, R. M. and Warming, R. F.: An Implicit Finite-Difference Algorithm for Hyperbolic Systems in Conservation-Law Form. J. Comp. Phys., Vol. 22, No. 1, Sept. 1976.
14. Kentzer, C. P.: Discretization of Boundary Conditions on Moving Discontinuities. Proceedings of the Second International Conference on Numerical Methods in Fluid Dynamics, Lecture Notes in Physics, Vol. 8, M. Holt, ed., Berkeley, CA, 1970, pp. 108-113.
15. Thomas, P. D., Vinokur, M., Bastionon, R., and Conti, R. J.: Numerical Solution for the Three-Dimensional Hypersonic Flow Field of a Blunt Delta Body. AIAA J., Vol. 10, July 1972, pp. 887-894.
16. Kutler, P., Reinhardt, W. A., and Warming, R. F.: Numerical Computations of Multi-Shocked Three-Dimensional Supersonic Flow Fields with Real Gas Effects. AIAA Paper No. 72-702, June 1972.
17. Kutler, P., Reinhardt, W. A., and Warming, R. F.: Multi-Shocked, Three-Dimensional Supersonic Flow Fields with Real Gas Effects. AIAA J., Vol. 11, May 1973, pp. 657-664.
18. Chaussee, D. S., Holtz, T., and Kutler, P.: Inviscid Supersonic/Hypersonic Body Flow Fields and Aerodynamics from Shock-Capturing Technique Calculations. AIAA Paper No. 75-837, June 1975.
19. MacCormack, R. W.: The Effect of Viscosity in Hypervelocity Impact Cratering. AIAA Paper No. 69-354, 1969.
20. Alksne, A. Y. and Webster, D. L.: Magnetic and Electric Fields in the Magnetosheath. Plan. & Space Sci., Vol. 18, 1970, pp. 1203-1212.
21. Wolfe, J., Intriligator, D. S., Mihalov, J., Collard, H., McKibbin, D., Whitten, R., and Barnes, A.: Initial Observations of the Pioneer Venus Orbiter Solar Wind Plasma Experiment. Science, Vol. 203, No. 4382, Feb. 1979, pp. 750-752.
22. Intriligator, D. S., Collard, H. R., Mihalov, J. P., Whitten, R. C., and Wolfe, J. H.: Electron Observation and Ion Flows from the Pioneer Venus Orbiter Plasma Analyzer Experiment. Science, Vol. 205, No. 4401, July 1979, pp. 116-119.
23. Russell, C. T., Elphic, R. C., and Slavin, J. A.: Initial Pioneer Venus Magnetic Field Results: Dayside Observations. Science, Vol. 203, No. 4382, Feb. 1979, pp. 745-748.
24. Russell, C. T., Elphic, R. C., and Slavin, J. A.: Initial Pioneer Venus Magnetic Field Results: Nightside Observations. Science, Vol. 205, No. 4401, July 1979, pp. 114-116.

Table 1.- Ordinates of Various Ionopause Shapes



β	IONOPAUSE		IONOPAUSE		IONOPAUSE		IONOPAUSE		IONOPAUSE	
	$\bar{H}/R_o = 0.01$		$\bar{H}/R_o = 0.05$		$\bar{H}/R_o = 0.10$		$\bar{H}/R_o = 0.20$		$\bar{H}/R_o = 0.25$	
	x/R_o	y_i/R_o	x/R_o	y_i/R_o	x/R_o	y_i/R_o	x/R_o	y_i/R_o	x/R_o	y_i/R_o
0°	1.0000	0.0000	1.0000	0.0000	1.0000	0.0000	1.0000	0.0000	1.0000	0.0000
2°	0.9994	0.0349	0.9995	0.0349	0.9995	0.0349	0.9995	0.0349	0.9996	0.0349
6°	0.9946	0.1045	0.9950	0.1046	0.9953	0.1046	0.9958	0.1047	0.9960	0.1047
10°	0.9851	0.1737	0.9861	0.1739	0.9870	0.1740	0.9883	0.1743	0.9888	0.1744
14°	0.9709	0.2421	0.9727	0.2425	0.9746	0.2430	0.9771	0.2436	0.9781	0.2439
18°	0.9520	0.3093	0.9550	0.3103	0.9580	0.3113	0.9622	0.3126	0.9638	0.3132
22°	0.9285	0.3751	0.9330	0.3770	0.9374	0.3787	0.9435	0.3812	0.9459	0.3822
26°	0.9006	0.4393	0.9068	0.4423	0.9127	0.4451	0.9211	0.4492	0.9243	0.4508
30°	0.8684	0.5014	0.8764	0.5060	0.8840	0.5104	0.8949	0.5167	0.8991	0.5191
34°	0.8320	0.5612	0.8419	0.5679	0.8514	0.5743	0.8649	0.5834	0.8701	0.5869
38°	0.7916	0.6185	0.8035	0.6278	0.8148	0.6366	0.8312	0.6494	0.8374	0.6543
42°	0.7474	0.6729	0.7613	0.6854	0.7745	0.6973	0.7935	0.7145	0.8009	0.7211
46°	0.6995	0.7243	0.7153	0.7407	0.7303	0.7563	0.7520	0.7787	0.7604	0.7874
50°	0.6482	0.7725	0.6658	0.7934	0.6824	0.8133	0.7066	0.8421	0.7159	0.8532
54°	0.5937	0.8172	0.6128	0.8435	0.6309	0.8683	0.6571	0.9044	0.6673	0.9184
58°	0.5363	0.8582	0.5565	0.8906	0.5756	0.9212	0.6035	0.9657	0.6143	0.9831
62°	0.4761	0.8954	0.4971	0.9349	0.5168	0.9719	0.5456	1.0261	0.5569	1.0473
66°	0.4135	0.9287	0.4346	0.9761	0.4543	1.0203	0.4504	1.1147	0.4947	1.1744
70°	0.3487	0.9581	0.3691	1.0142	0.3882	1.0665	0.4163	1.1437	0.4274	1.1744
74°	0.2820	0.9833	0.3009	1.0492	0.3184	1.1103	0.3444	1.2010	0.3548	1.2374
78°	0.2135	1.0046	0.2298	1.0811	0.2448	1.1517	0.2673	1.2574	0.2764	1.3001
82°	0.1436	1.0219	0.1560	1.1098	0.1674	1.1908	0.1845	1.3130	0.1915	1.3628
86°	0.0724	1.0354	0.0794	1.1355	0.0858	1.2276	0.0956	1.3677	0.0997	1.4254
90°	0.0000	1.0454	0.0000	1.1583	0.0000	1.2620	0.0000	1.4218	0.0000	1.4883
94°	-0.0736	1.0523	-0.0824	1.1782	-0.0905	1.2943	-0.1032	1.4753	-0.1085	1.5516
98°	-0.1485	1.0566	-0.1680	1.1955	-0.1861	1.3244	-0.2148	1.5284	-0.2271	1.6156
102°	-0.2251	1.0591	-0.2572	1.2102	-0.2875	1.3524	-0.3361	1.5813	-0.3572	1.6807
106°	-0.3040	1.0603	-0.3506	1.2226	-0.3953	1.3785	-0.4686	1.6343	-0.5010	1.7472
110°	-0.3861	1.0607	-0.4488	1.2330	-0.5106	1.4027	-0.6142	1.6875	-0.6608	1.8156
114°	-0.4723	1.0609	-0.5527	1.2415	-0.6346	1.4253	-0.7753	1.7414	-0.8400	1.8866

Table 1.- Concluded.

β	IONOPAUSE		IONOPAUSE		IONOPAUSE		IONOPAUSE		IONOPAUSE	
	$\bar{H}/R_o = 0.01$		$\bar{H}/R_o = 0.05$		$\bar{H}/R_o = 0.10$		$\bar{H}/R_o = 0.20$		$\bar{H}/R_o = 0.25$	
	x/R_o	y_i/R_o	x/R_o	y_i/R_o	x/R_o	y_i/R_o	x/R_o	y_i/R_o	x/R_o	y_i/R_o
118°	-0.5641	1.0610	-0.6638	1.2484	-0.7690	1.4462	-0.9551	1.7963	-1.0427	1.9610
122°	-0.6630	1.0610	-0.7835	1.2539	-0.9159	1.4657	-1.1578	1.8529	-1.2746	2.0397
126°	-0.7708	1.0610	-0.9142	1.2583	-1.0782	1.4840	-1.3890	1.9118	-1.5434	2.1243
130°	-0.8903	1.0610	-1.0587	1.2617	-1.2597	1.5012	-1.6562	1.9738	-1.8598	2.2165
134°	-1.0246	1.0610	-1.2209	1.2643	-1.4654	1.5175	-1.9703	2.0403	-2.2393	2.3189
138°	-1.1783	1.0610	-1.4064	1.2664	-1.7027	1.5331	-2.3465	2.1128	-2.7047	2.4353
142°	-1.3580	1.0610	-1.6229	1.2679	-1.9817	1.5482	-2.8081	2.1939	-3.2913	2.5715
146°	-1.5730	1.0610	-1.8816	1.2692	-2.3176	1.5632	-3.3909	2.2872	-4.0570	2.7365
150°	-1.8377	1.0610	-2.1999	1.2701	-2.7338	1.5784	-4.1545	2.3986	-5.1025	2.9460
154°	-2.1754	1.0610	-2.6057	1.2709	-3.2686	1.5942	-5.2045	2.5384	-6.6208	3.2292
158°	-2.6262	1.0610	-3.1471	1.2715	-3.9884	1.6114	-6.7470	2.7260	-9.0300	3.6484
162°	-3.3654	1.0610	-3.9152	1.2721	-5.0210	1.6314	-9.2448	3.0038	-13.4322	4.3644
166°	-4.2564	1.0610	-5.1047	1.2727	-6.6450	1.6568	-13.9882	3.4877	-23.9161	5.9630
170°	-6.0204	1.0610	-7.2230	1.2736	-10.1609	1.7004	-26.3596	4.6480		
174°	-10.1111	1.0610	-12.1370	1.2758	-16.8192	1.7678				

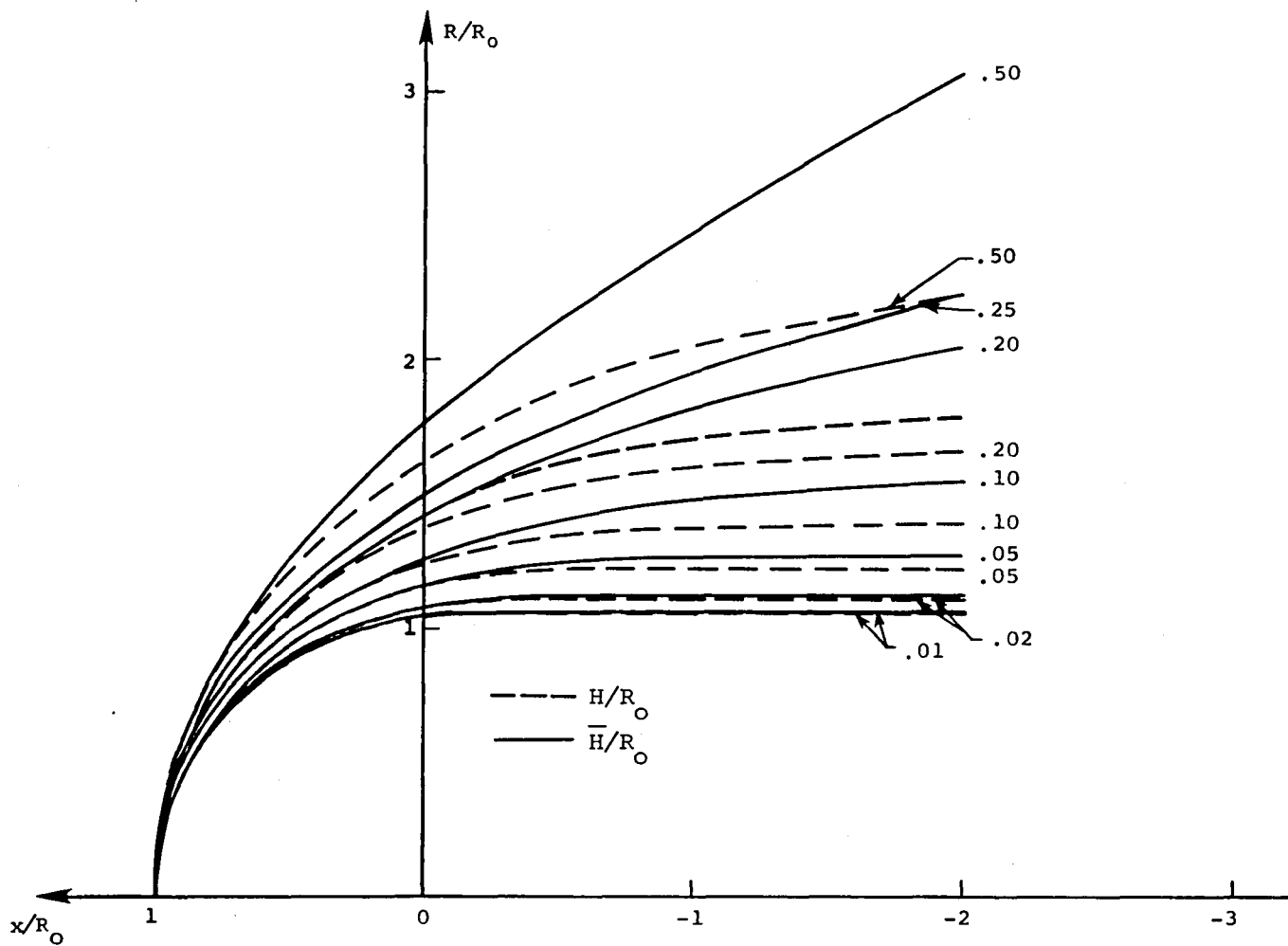
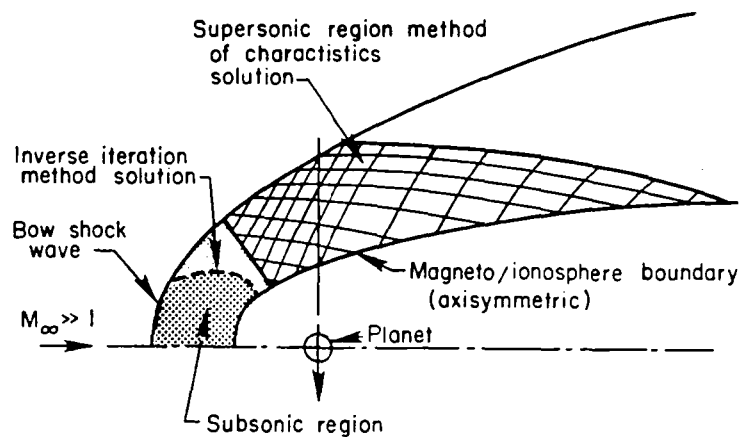
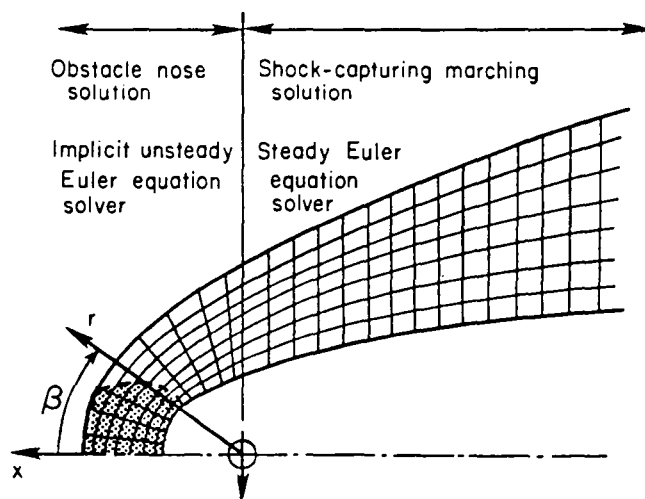


Figure 1.-Illustration of ionopause shapes for atmospheres with various
 (i) constant scale heights H/R_0 and (ii) gravitational variation
 included in the scale height H/R_0 .



(a) Former method.



(b) Present method.

Figure 2.- Comparison of former and present computational procedures for determining the gasdynamic flow properties of solar wind-magnetosphere/ionopause interactions.

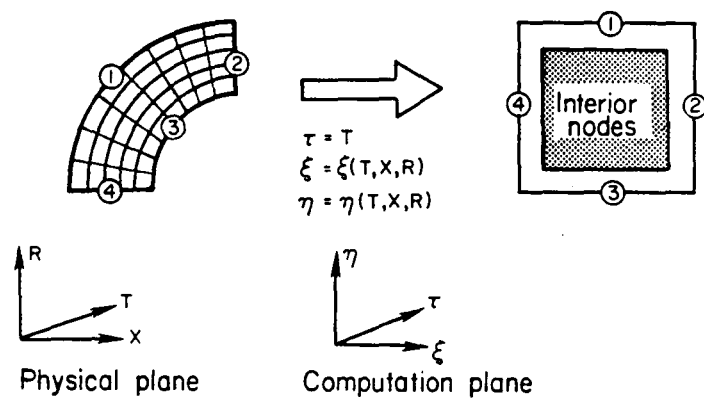


Figure 3.- Transformation from physical domain to rectangular computational domain.

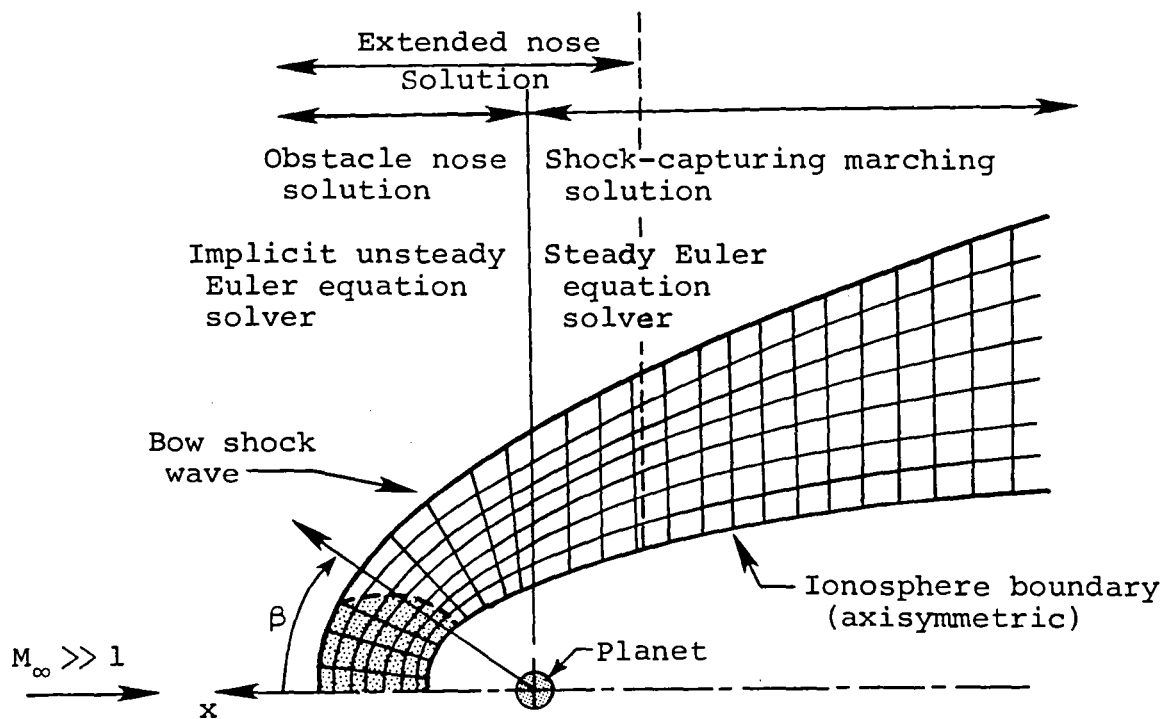


Figure 4.- Illustration of capability for providing an additional flow-field segment to the obstacle nose solution in the computational procedure for determining the gasdynamic flow properties of solar wind-ionopause interactions.

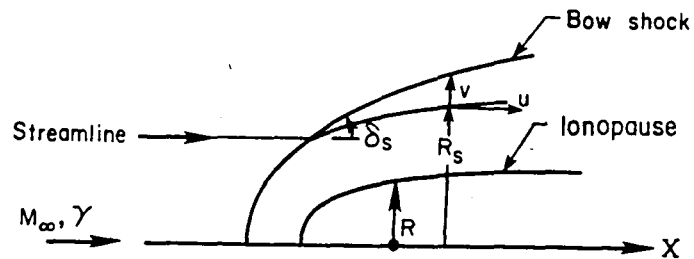


Figure 5.- Illustration of quantities used for streamline calculation.

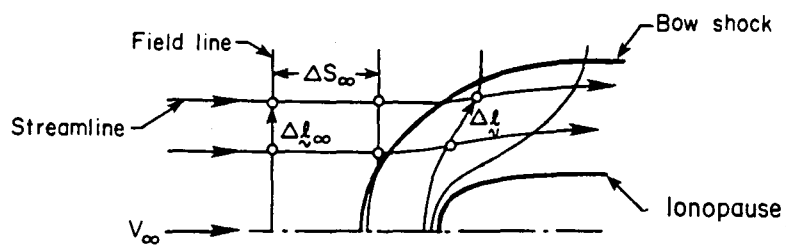


Figure 6.- Illustration of quantities used for magnetic field-line calculation in the plane of magnetic symmetry.

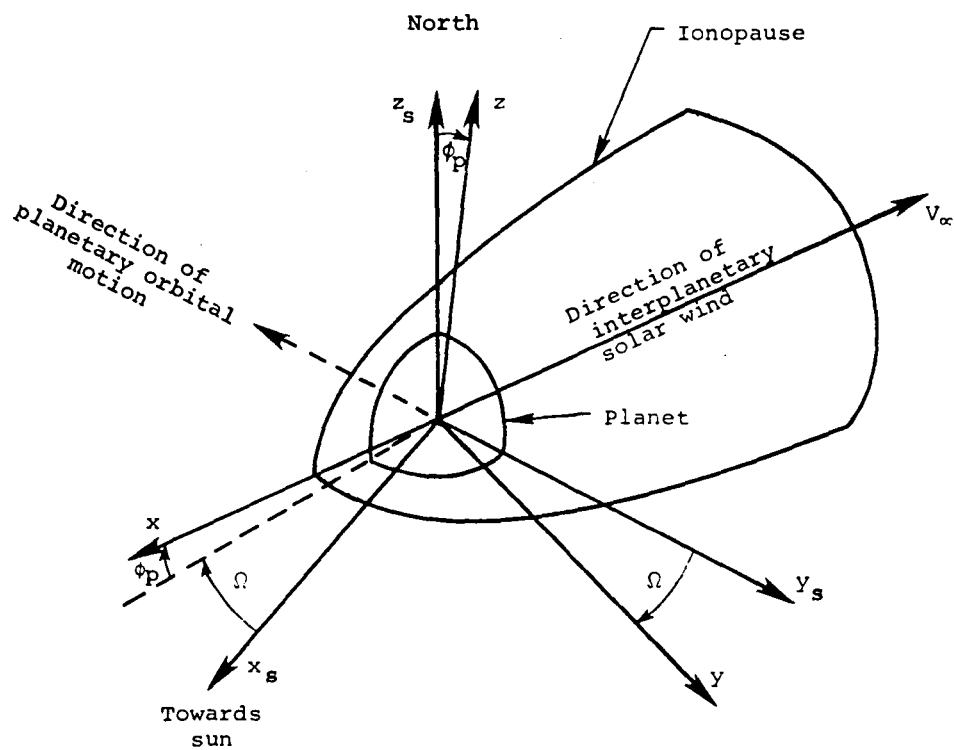


Figure 8.- Illustration of sun-planet (x_s, y_s, z_s) and solar wind (x, y, z) coordinate systems and the azimuthal (Ω) and polar (ϕ_p) solar-wind angles, both shown in a positive sense.

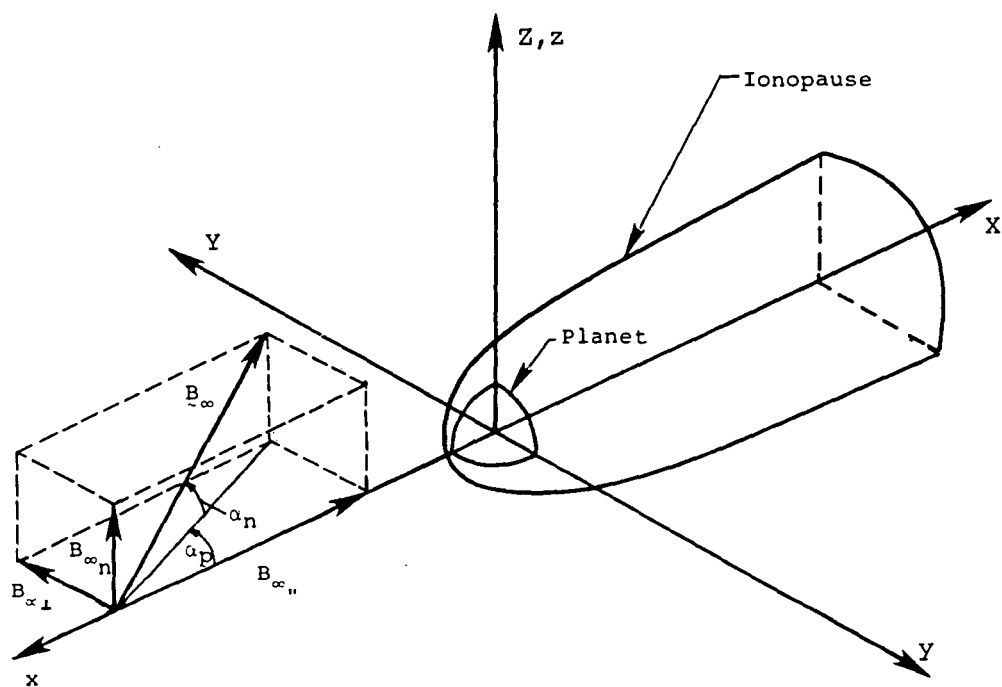


Figure 9.- Illustration of solar-wind (x, y, z) and (X, Y, Z) coordinate systems and the interplanetary magnetic field and magnetic-field angles (α_p, α_n) .

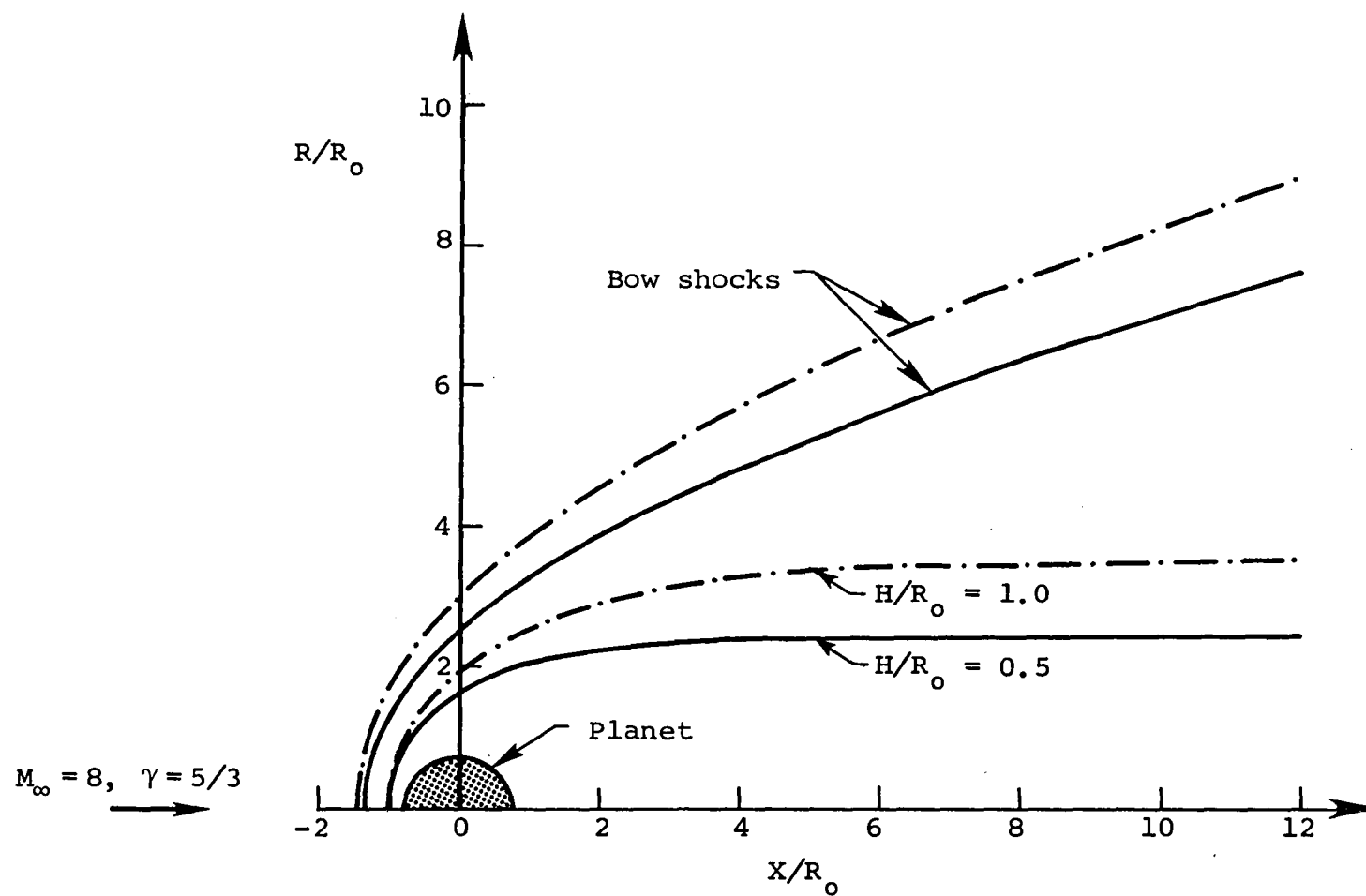


Figure 10.- Bow shock locations for $M_\infty = 8.0$, $\gamma = 5/3$ flow past constant scale-height ionopause shapes with $H/R_0 = 0.5$ and 1.0 .

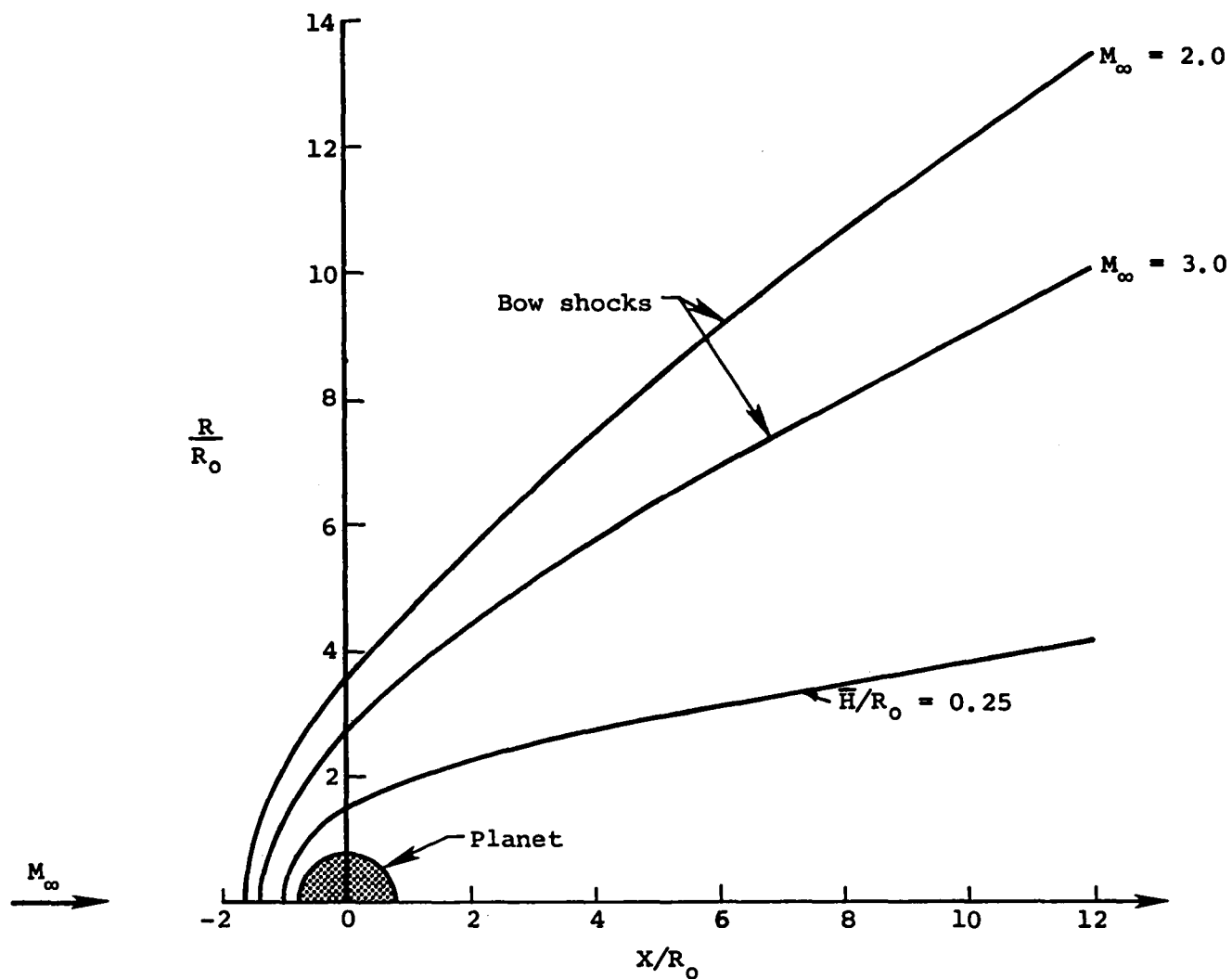


Figure 11.- Bow shock shapes for flow past an ionopause shape with gravitational variation included in scale height with $\bar{H}/R_0 = 0.25$, $\gamma = 5/3$ and $M_\infty = 2.0$ and 3.0 .

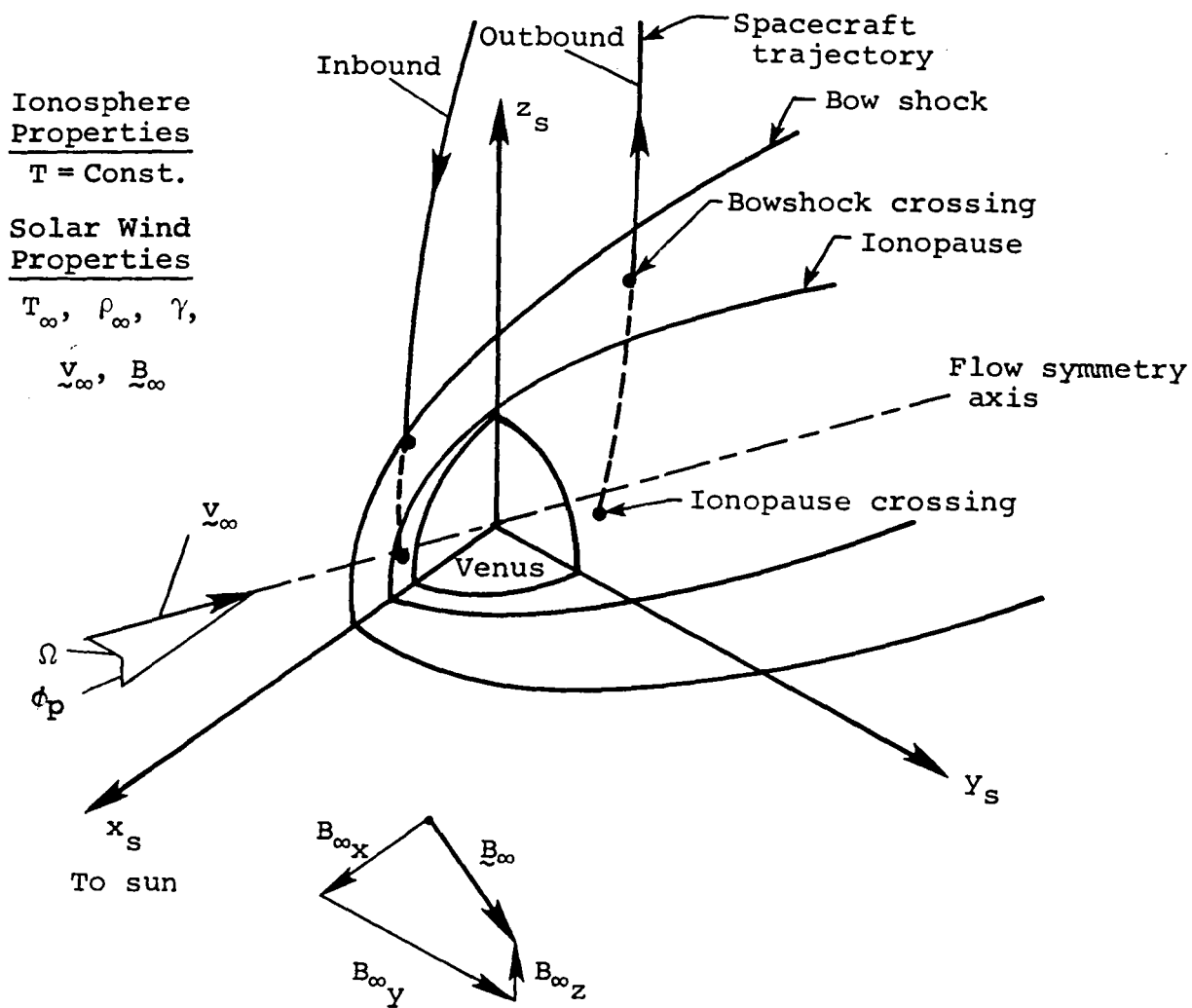


Figure 12.- Overall features of Pioneer-Venus orbiter trajectory crossings of solar-wind/Venus-ionosphere interaction region.

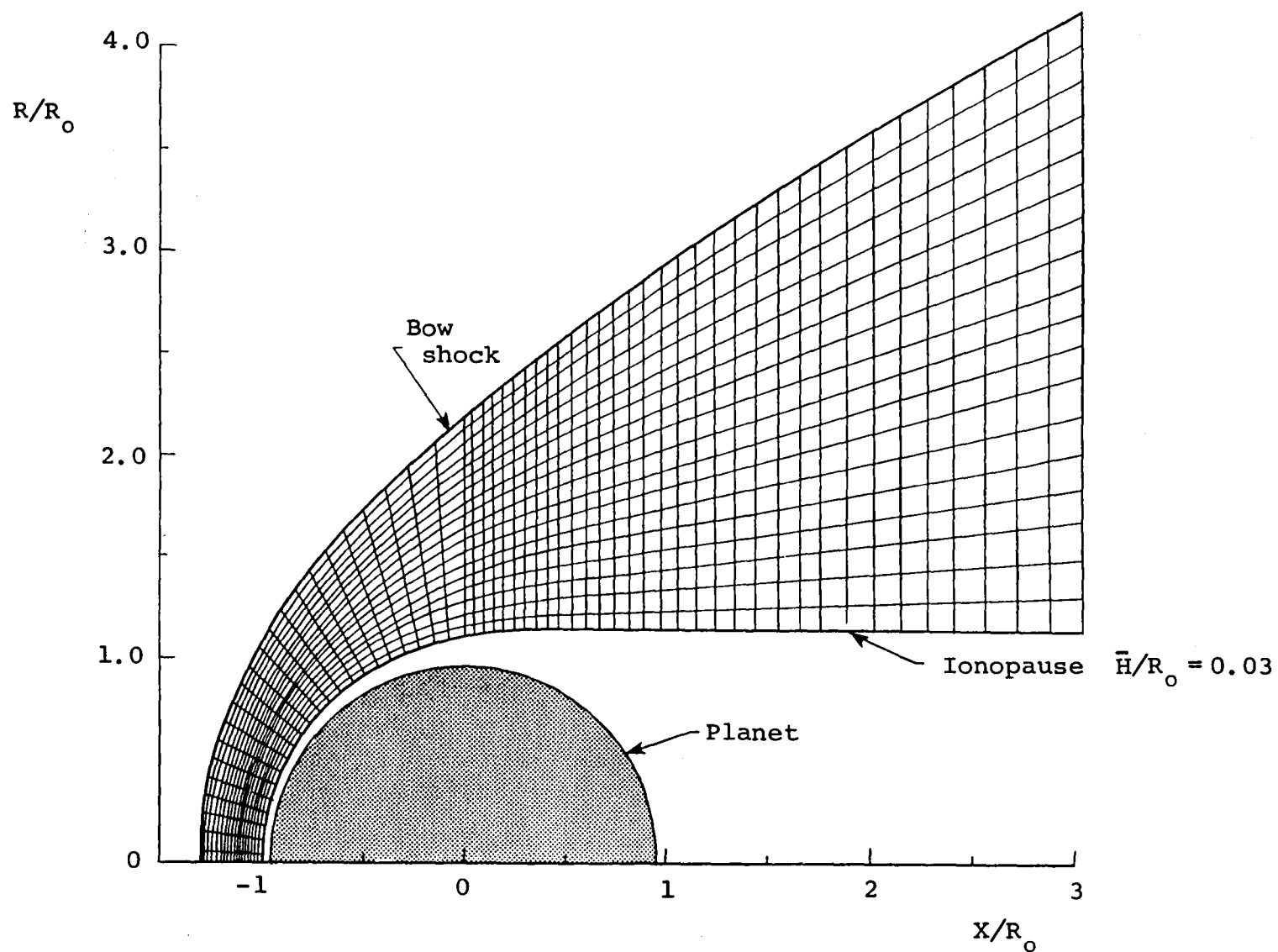


Figure 13.- Illustration of typical flow-field grid density for gasdynamic solution; $M_\infty = 3.0$, $\gamma = 5/3$.

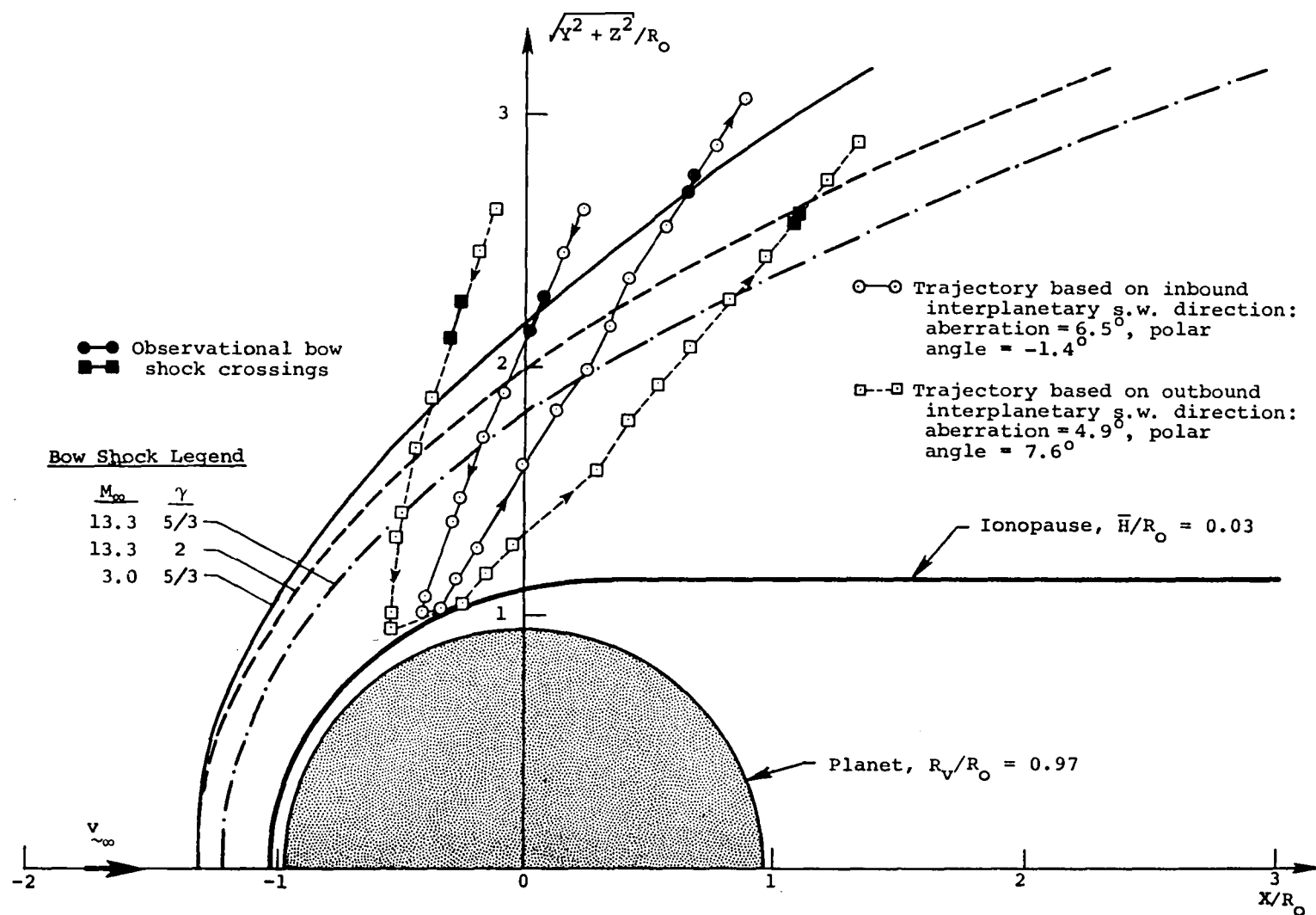


Figure 14.- P-V Orbit 6 trajectories and observational bow shock crossings as viewed in solar-wind coordinates based on inbound and outbound interplanetary solar-wind directions; also, various bow shock shapes for different interplanetary solar-wind conditions.

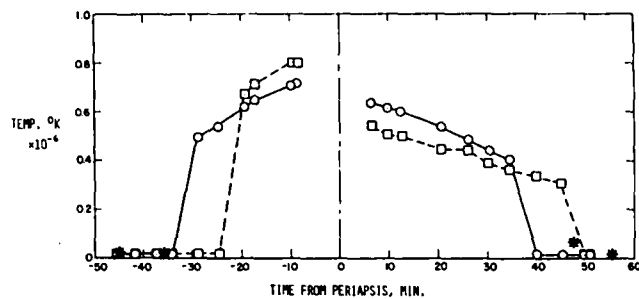
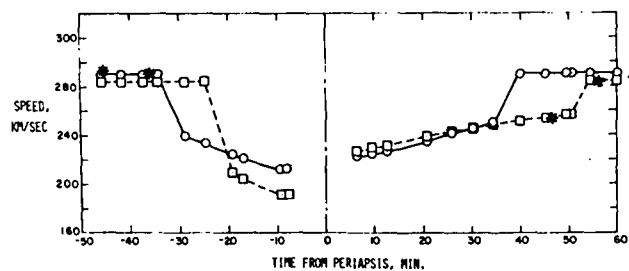
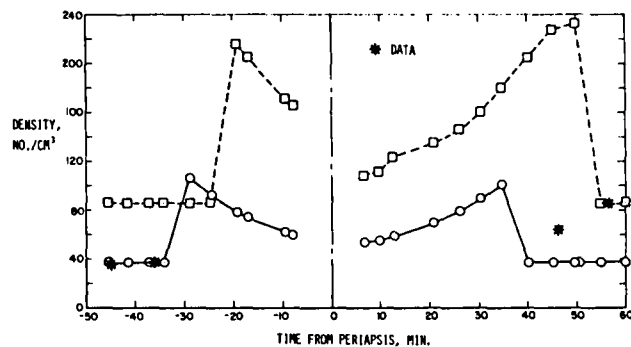
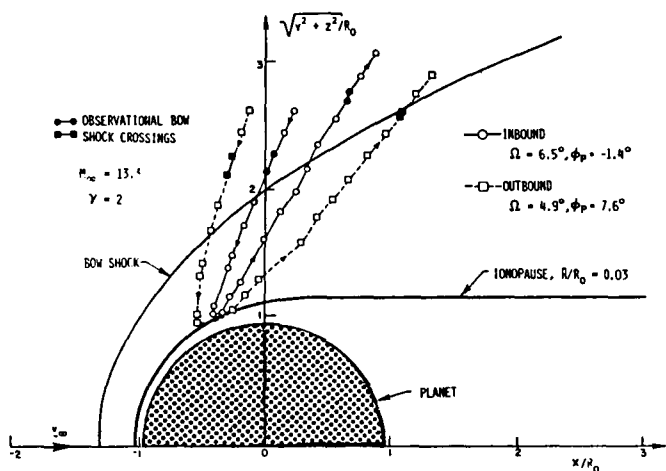


Figure 15.- Comparison of observed (OPA) and theoretical time histories of ionosheath plasma properties for P-V Orbit 6 based on inbound and outbound interplanetary solar-wind conditions using a gasdynamic solution for $M_\infty = 13.3$, $\gamma = 2.0$.

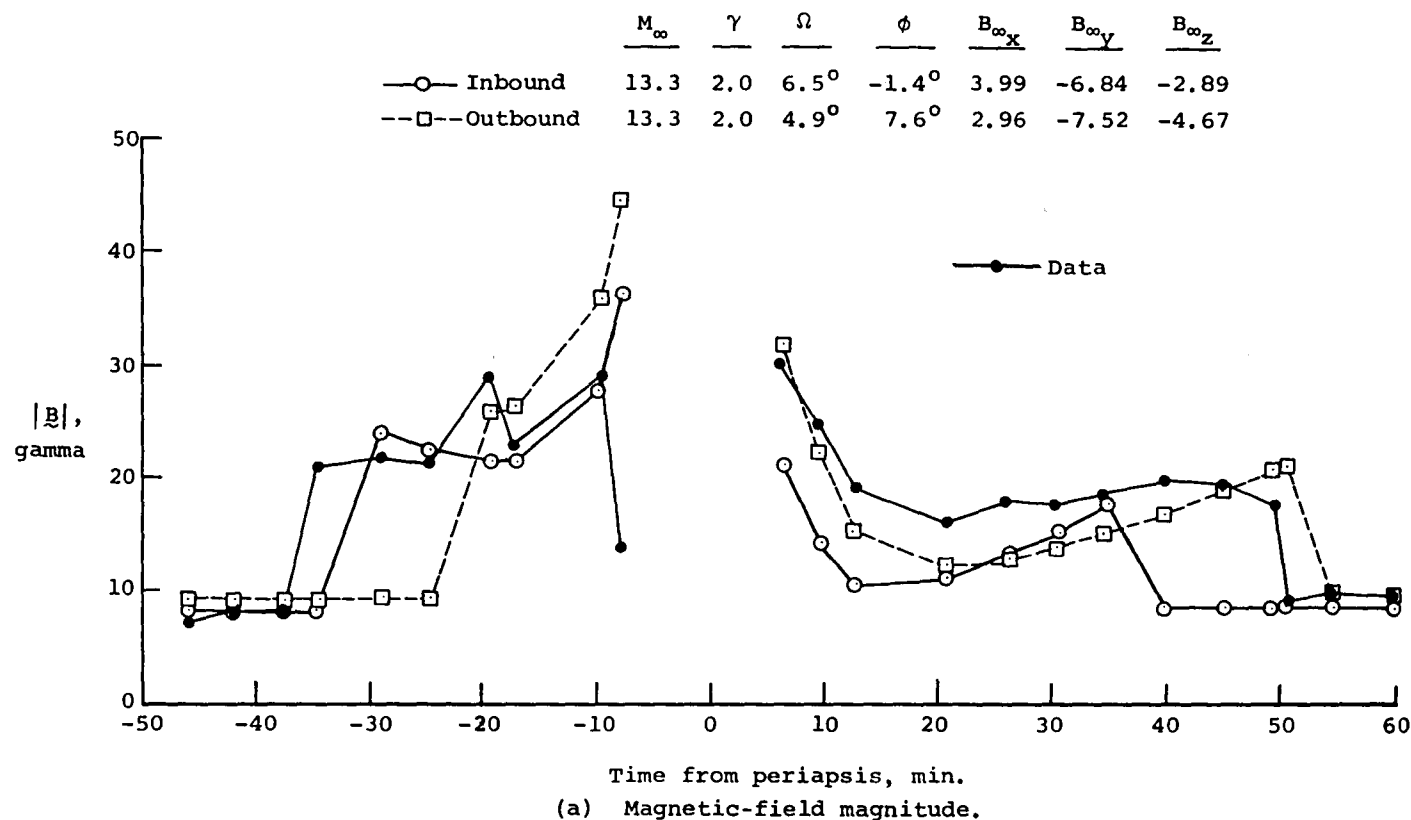
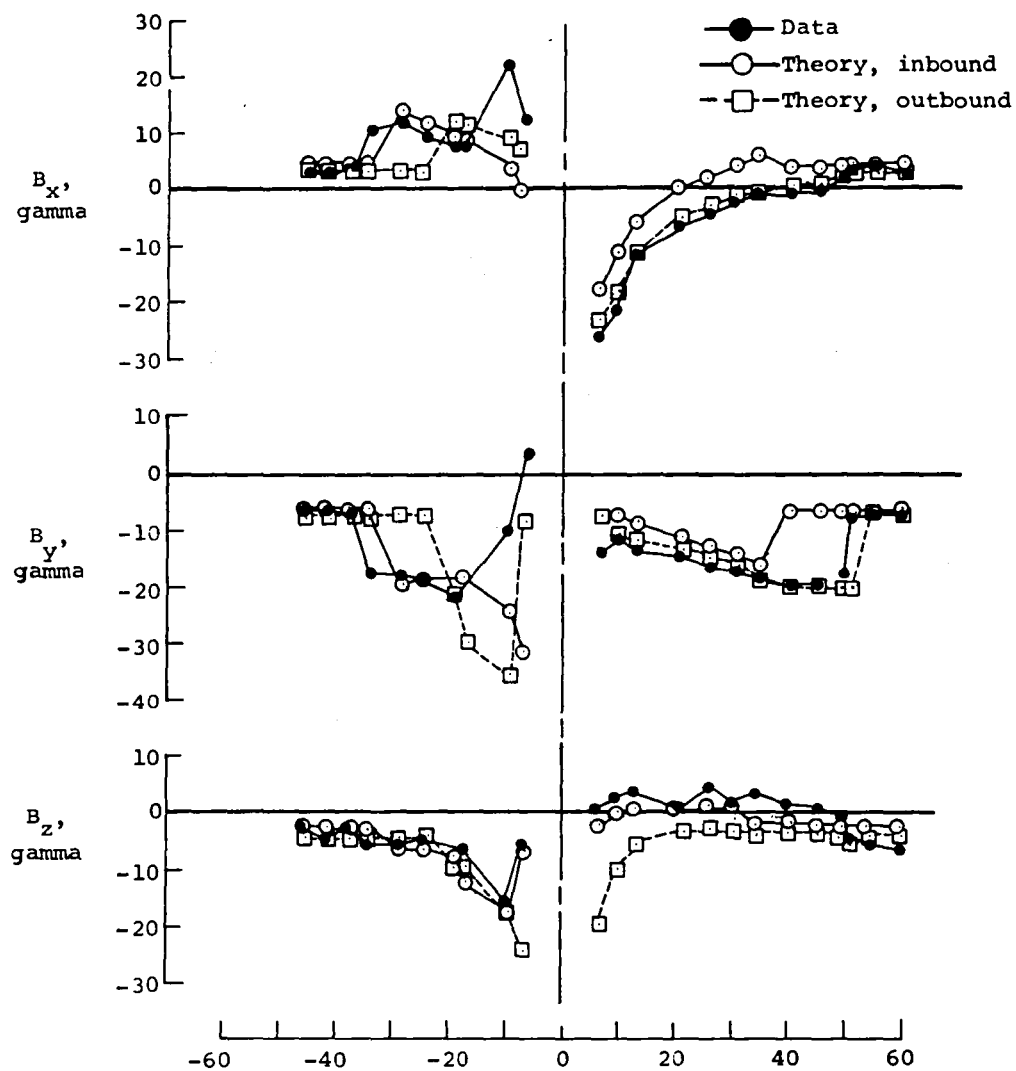


Figure 16.- Comparison of observed (OMAG) and theoretical time histories for the magnitude of the magnetic field for P-V Orbit 6 based on inbound and outbound interplanetary conditions using gasdynamic solution for $M_\infty = 13.3$, $\gamma = 2$.



Time from periapsis, min.
(b) Magnetic-field components.

Figure 16.- Concluded.

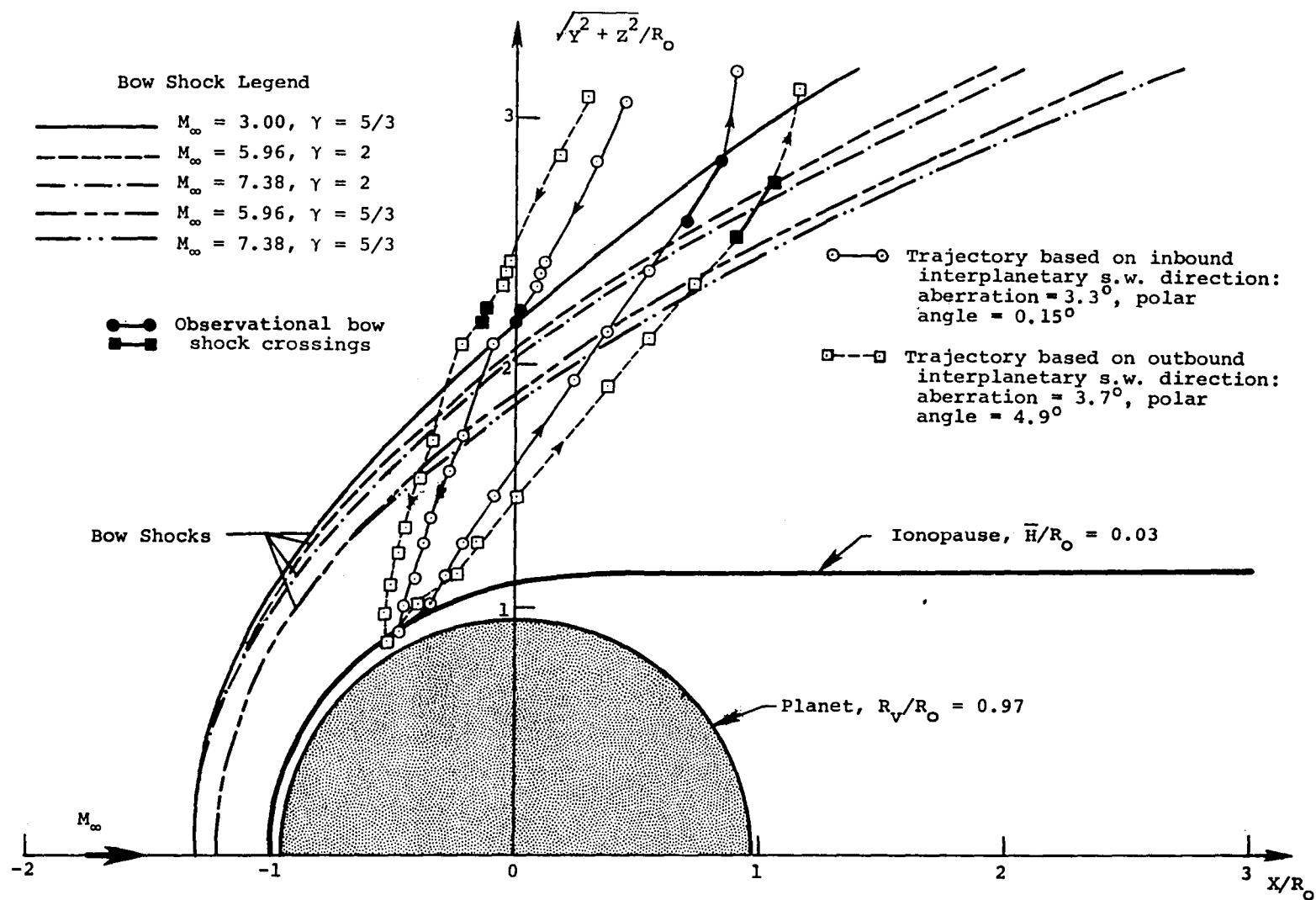


Figure 17.- P-V Orbit 3 trajectories and observational bow shock crossings as viewed in solar-wind coordinates based on inbound and outbound interplanetary solar-wind directions; also, various bow shock shapes for different interplanetary solar wind conditions.

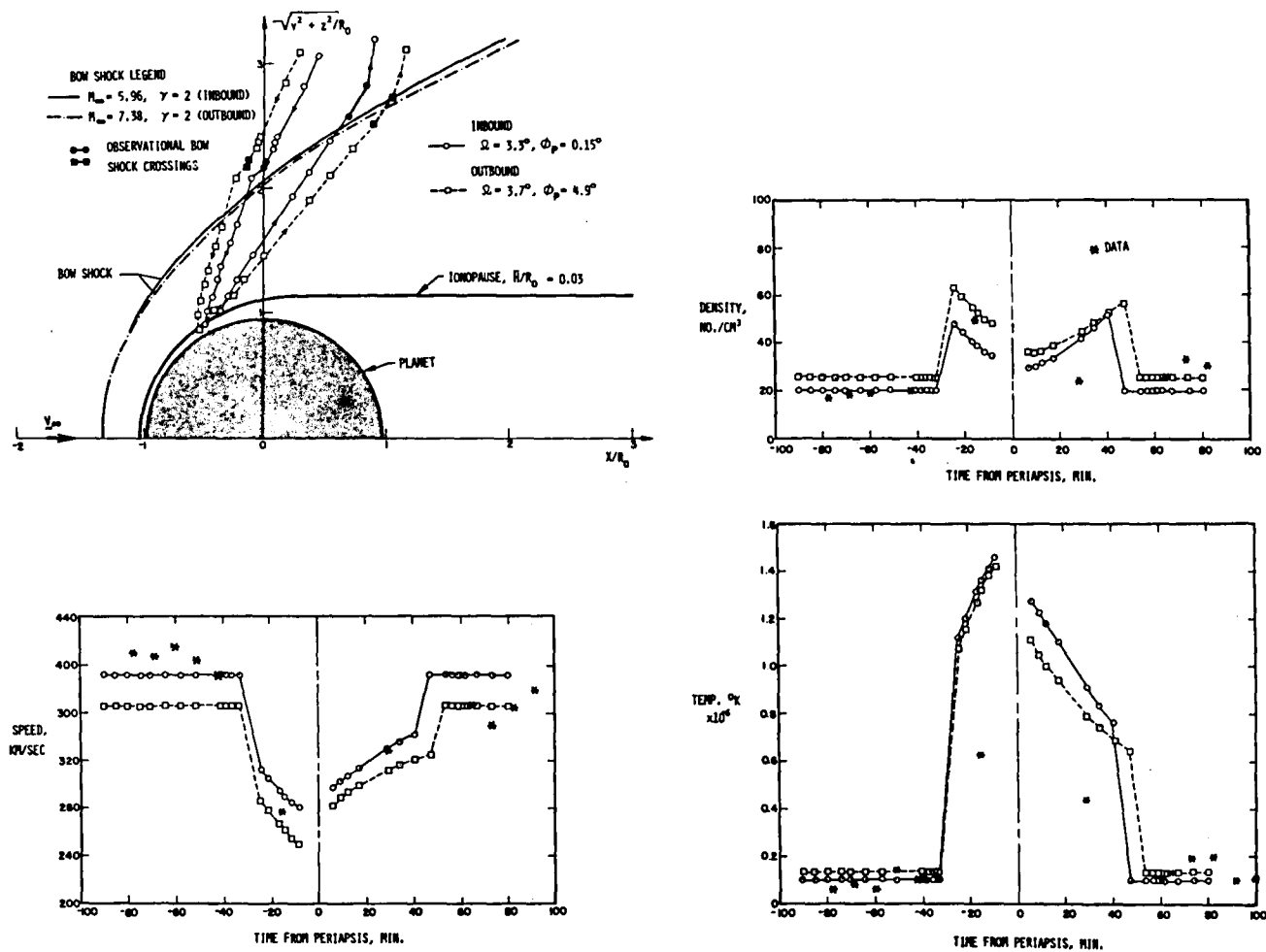
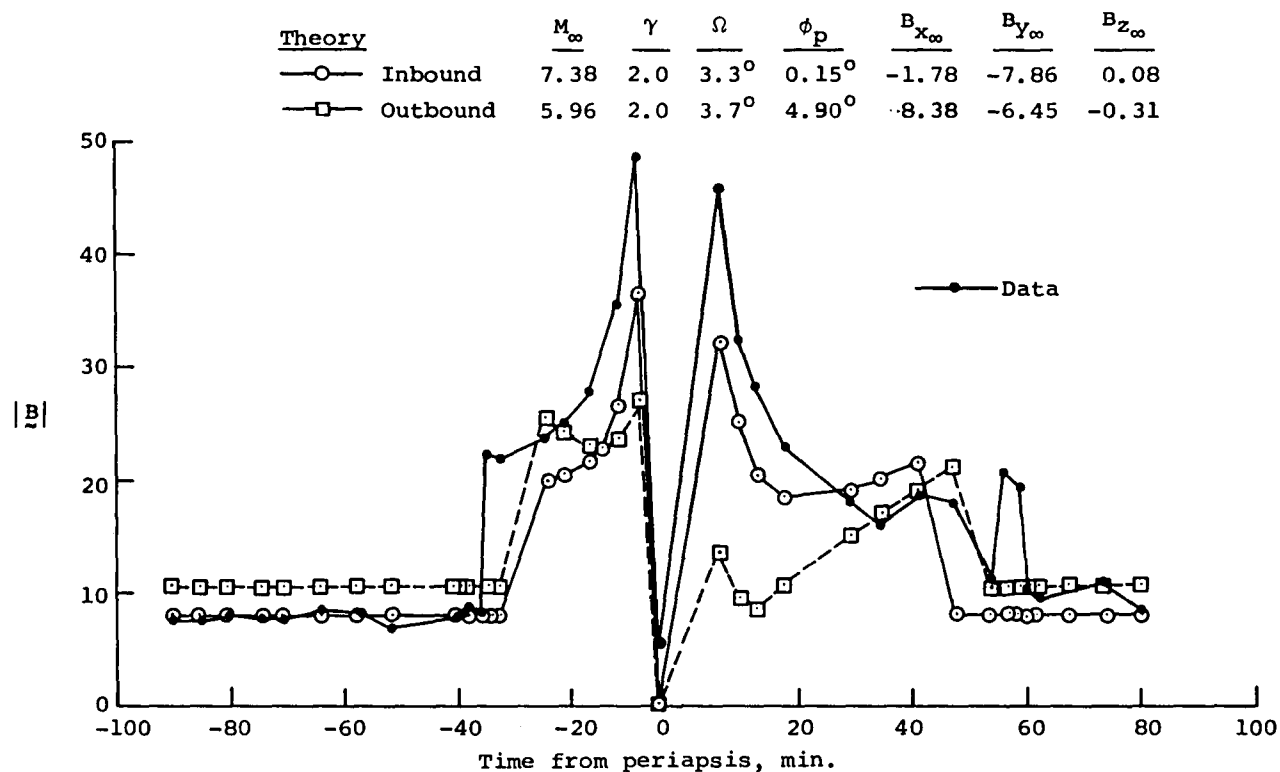
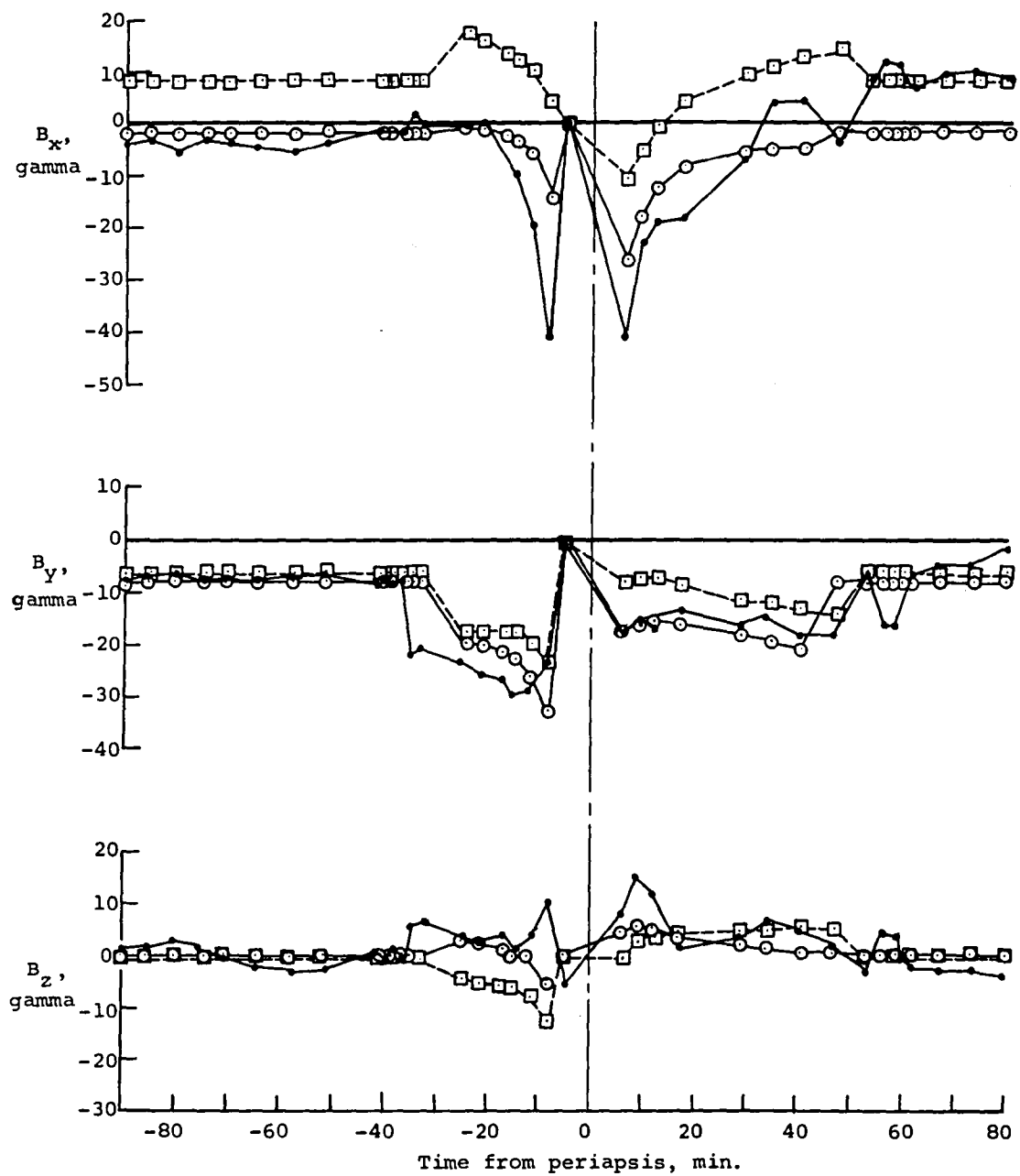


Figure 18.- Comparison of observed and theoretical time histories of ionosheath plasma properties for P-V Orbit 3 based on inbound and outbound interplanetary solar-wind conditions.



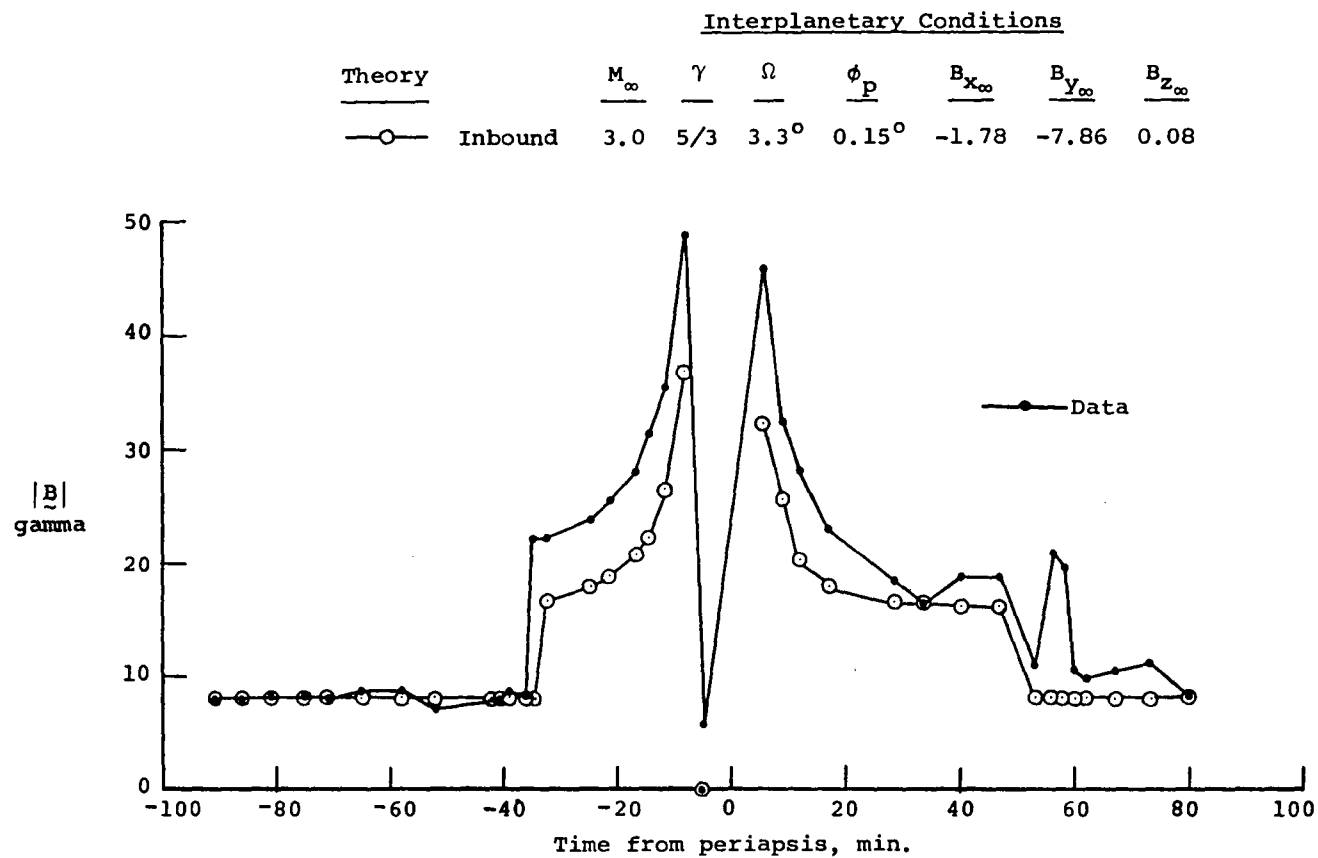
(a) Magnetic-field magnitudes.

Figure 19.- Comparison of observed (OMAG) and theoretical time histories for the magnetic field for P-V Orbit 3 based on inbound and outbound interplanetary solar-wind conditions using gasdynamic solutions $M_\infty = 7.38$, $\gamma = 2.0$ for inbound and $M_\infty = 5.96$, $\gamma = 2.0$ for outbound calculations.



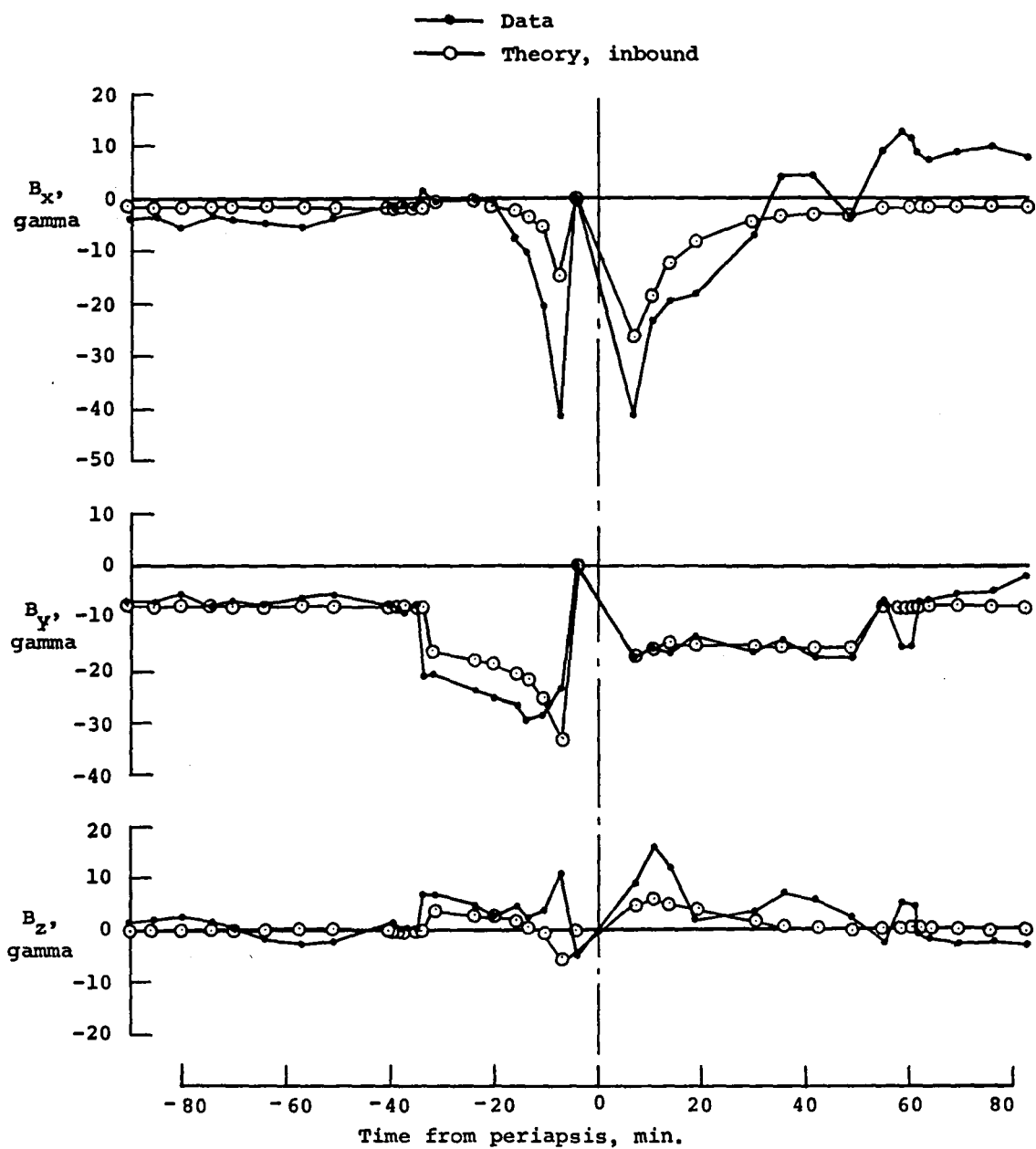
(b) Magnetic-field components.

Figure 19.- Concluded.



(a) Magnetic-field magnitude.

Figure 20.- Comparison of observed (OMAG) and theoretical time histories of the magnetic field for P-V Orbit 3 based on inbound solar wind interplanetary conditions using a gasdynamic solution for $M_\infty = 3.0$, $\gamma = 5/3$.



(b) Magnetic-field components.

Figure 20.- Concluded.

1. Report No. NASA CR-3267		2. Government Accession No.		3. Recipient's Catalog No.	
4. Title and Subtitle APPLICATION OF ADVANCED COMPUTATIONAL PROCEDURES FOR MODELING SOLAR-WIND INTERACTIONS WITH VENUS - THEORY AND COMPUTER CODE				5. Report Date May 1980	
				6. Performing Organization Code 498/C	
7. Author(s) Stephen S. Stahara, Daniel Klenke, Barbara C. Trudinger, and John R. Spreiter				8. Performing Organization Report No. NEAR TR 202	
9. Performing Organization Name and Address Nielsen Engineering & Research, Inc. 510 Clyde Avenue Mountain View, CA 94043				10. Work Unit No.	
				11. Contract or Grant No. NASW-3182	
12. Sponsoring Agency Name and Address National Aeronautics and Space Administration Washington, DC 20546				13. Type of Report and Period Covered Contractor Report 7/78 - 9/79	
				14. Sponsoring Agency Code	
15. Supplementary Notes NASA Headquarters Technical Monitor: Robert E. Murphy					
16. Abstract Advanced computational procedures are developed and applied to the prediction of solar-wind interaction with nonmagnetic terrestrial-planet atmospheres, with particular emphasis to Venus. The theoretical method is based on a single-fluid, steady, dissipationless, magnetohydrodynamic continuum model, and is appropriate for the calculation of axisymmetric, supersonic, super-Alfvénic solar-wind flow past terrestrial planets. The procedures, which consist of finite-difference codes to determine the gasdynamic properties and a variety of special-purpose codes to determine the frozen magnetic field, streamlines, contours, plots, etc. of the flow, are organized into one computational program which has been extensively documented and is presented in a general user's manual included as part of this report. Theoretical results based upon these procedures are reported for a wide variety of solar-wind conditions and ionopause obstacle shapes. Plasma and magnetic-field comparisons in the ionosheath are also provided with actual spacecraft data obtained by the Pioneer-Venus Orbiter. These results have verified the appropriateness of the basic theoretical model, and have indicated the importance of accounting for the variable oncoming direction of the interplanetary solar wind.					
17. Key Words (Suggested by Author(s)) Solar-Wind/Ionosphere Interaction Finite-Difference Methods Steady Flow Frozen Magnetic Field			18. Distribution Statement Unclassified - Unlimited Subject Category 92		
19. Security Classif. (of this report) Unclassified		20. Security Classif. (of this page) Unclassified		21. No. of Pages 316	
				22. Price* \$11.75	

End of Document